

AD-A083 203

ADVISORY GROUP FOR AEROSPACE RESEARCH AND DEVELOPMENT--ETC F/G 9/2
THE USE OF COMPUTERS AS A DESIGN TOOL.(U)

JAN 80

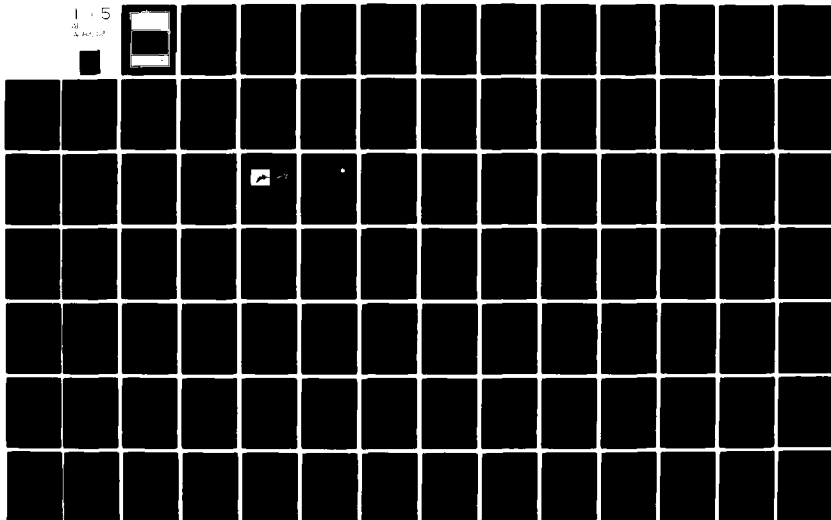
UNCLASSIFIED

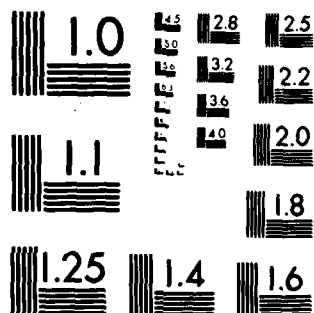
AGARD-CP-280

NL

1 5

W 100000





MICROCOPY RESOLUTION TEST CHART
NATIONAL BUREAU OF STANDARDS-1963-A

LEVEL II

12

AGARD-CP-280

AGARD-CP-280

AGARD

ADVISORY GROUP FOR AEROSPACE RESEARCH & DEVELOPMENT

7 RUE ANCELLE 92200 NEUILLY SUR SEINE FRANCE

ADA 083203

SELECTED
APR 17 1980
C

AGARD CONFERENCE PROCEEDINGS No. 280

The Use of Computers as a Design Tool

This document has been approved
for public release and sale; its
distribution is unlimited.

NORTH ATLANTIC TREATY ORGANIZATION



DISTRIBUTION AND AVAILABILITY
ON BACK COVER

80 4 14 106

FILE COPY
DEC

14 AGARD-CP-280

NORTH ATLANTIC TREATY ORGANIZATION
ADVISORY GROUP FOR AEROSPACE RESEARCH AND DEVELOPMENT
(ORGANISATION DU TRAITE DE L'ATLANTIQUE NORD)

DTIC
ELECTE
APR 17 1980

1 Conference proceedings.

AGARD Conference Proceedings No.280

6 THE USE OF COMPUTERS AS A DESIGN TOOL.

124491

11 Jan 80

This document has been approved
for public release and sale; its
distribution is unlimited.

Papers presented at the Flight Mechanics Panel Symposium on The Use of Computers as a Design Tool,
held in Neubiberg, Germany, 3-6 September 1979.

4100043

JAB

THE MISSION OF AGARD

The mission of AGARD is to bring together the leading personalities of the NATO nations in the fields of science and technology relating to aerospace for the following purposes:

- Exchanging of scientific and technical information;
- Continuously stimulating advances in the aerospace sciences relevant to strengthening the common defence posture;
- Improving the co-operation among member nations in aerospace research and development;
- Providing scientific and technical advice and assistance to the North Atlantic Military Committee in the field of aerospace research and development;
- Rendering scientific and technical assistance, as requested, to other NATO bodies and to member nations in connection with research and development problems in the aerospace field;
- Providing assistance to member nations for the purpose of increasing their scientific and technical potential;
- Recommending effective ways for the member nations to use their research and development capabilities for the common benefit of the NATO community.

The highest authority within AGARD is the National Delegates Board consisting of officially appointed senior representatives from each member nation. The mission of AGARD is carried out through the Panels which are composed of experts appointed by the National Delegates, the Consultant and Exchange Programme and the Aerospace Applications Studies Programme. The results of AGARD work are reported to the member nations and the NATO Authorities through the AGARD series of publications of which this is one.

Participation in AGARD activities is by invitation only and is normally limited to citizens of the NATO nations.

The content of this publication has been reproduced directly from material supplied by AGARD or the authors.

Published January 1980

Copyright © AGARD 1980
All Rights Reserved

ISBN 92-835-0256-6



*Printed by Technical Editing and Reproduction Ltd
Harford House, 7-9 Charlotte St, London, W1P 1HD*

PREFACE

This symposium, held in Neubiberg, Germany on 3-6 September 1979, was organised as a follow-on action of a previous Flight Mechanics Panel sponsored symposium on Aircraft Design Integration and Optimisation (Florence, October 1973, AGARD CP 147). The main objective was to present the latest developments in computerised aircraft design.

Thirty-two papers were presented in the following sessions:

- 1 - Specifications and Assessment of Requirements.
- 2 - Computer-Aided Design and Computer Graphics.
- 3 - Computational Aerodynamics and Design.
- 4 - Structural Analysis and Design.
- 5 - Propulsion and System Design.

Due to time limitations, the discussions following the presentations were relatively short, though compensated, at least partially, by the final round table discussion included "in extenso" in the Technical Evaluation Report (AGARD Advisory Report No.158). It appears that the presented papers and the discussions covered equally the positive and negative aspects of computerised aircraft design, the cost and technical effectiveness, the benefits, the difficulties and limitations of the whole process.

The following important general conclusions are proposed:

- The designer, as a human being, plays and will continue to play an outstanding role within the computerised aircraft design process.
- Large advances have been made in the last few years in each speciality in computer-aided design. However, an integrated multi-disciplinary detailed design process appears remote, and continues to require a substantial development effort.
- To meet the demands of various disciplines, principally computational aerodynamics, computers of increased speed and with new architectures are required.
- Due to the rapid evolution and advances in computer hardware and software it is highly desirable to bring together periodically design specialists, generalists and computer experts in order to develop and improve the communication among these groups.

J.CZINCZENHEIM
Dr J.M.KLINEBERG
Technical Programme Committee

Accession For	
NAME	DATE
DOC. NO.	DATE
Unpublished	Justification
By	
Distribution/	
Availability Code	
Dist.	Availand/or special
A	

CONTENTS

	Page
PREFACE	iii
	Reference
 <u>SESSION I – SPECIFICATIONS AND ASSESSMENT OF REQUIREMENTS</u>	
THE USE OF COMPUTER AIDED DESIGN METHODS IN AIRBORNE SYSTEMS EVALUATION by P.Ebeling and E.Pfisterer	1
CRITERIA FOR TECHNOLOGY by R.L.Haas	2
AN ACCEPTABLE ROLE FOR COMPUTERS IN THE AIRCRAFT DESIGN PROCESS by T.J.Gregory and L.Roberts	3
THE USE OF COMPUTER BASED OPTIMISATION METHODS IN AIRCRAFT STUDIES by B.Edwards	4
SOME FUNDAMENTAL ASPECTS OF TRANSPORT AIRCRAFT CONCEPTUAL DESIGN OPTIMIZATION by E.Torenbeek	5
 <u>SESSION II – COMPUTER AIDED DESIGN AND COMPUTER GRAPHICS</u>	
Survey Paper on COMPUTER AIDED DESIGN by D.Weinhauer	6
COMPUTER GRAPHICS AND RELATED DESIGN PROCESS AT MBB by V.Antl and W.Weingartner	7a
COMPUTER GRAPHICS, RELATED DESIGN AND MANUFACTURE PROCESS AT DORNIER by J.Nagel, L.Thieme and A.Harter	7b
COMPUTER GRAPHICS AND RELATED DESIGN PROCESSES IN THE U.K. by R.I.Hacking and B.Reuben	7c
DISTRIBUTED GRAPHICS SYSTEM FOR COMPUTER AUGMENTED DESIGN AND MANUFACTURE by A.N.Baker	8
LE ROLE DE L'INTERACTIVITE DANS LA CONCEPTION ET LA FABRICATION ASSISTEES PAR ORDINATEUR par M.Slissa	9
A FRAMEWORK FOR DISTRIBUTED DESIGN COMPUTING by A.W.Bishop	10
LIASSE ELECTRIQUE ASSISTEE PAR ORDINATEUR par J-P.Pauzat	11
 <u>SESSION III – COMPUTATIONAL AERODYNAMICS AND DESIGN</u>	
USE OF ADVANCED COMPUTERS FOR AERODYNAMIC FLOW SIMULATION by F.R.Bailey and W.F.Ballhaus	12
UTILISATION DE L'ORDINATEUR POUR LE DESSIN DE CONFIGURATIONS AERODYNAMIQUES par P.Perrier	13

WING DESIGN PROCESS BY INVERSE POTENTIAL FLOW COMPUTER PROGRAMS by L.Fornasier	14
THE ROLE OF COMPUTATIONAL AERODYNAMICS IN AIRPLANE CONFIGURATION DEVELOPMENT by B.Dillner and C.A.Koper, Jr	15
COMPUTATIONAL AERODYNAMIC DESIGN TOOLS AND TECHNIQUES USED AT FIGHTER DEVELOPMENT by P.Sacher, W.Kraus and R.Kunz	16
USE OF COMPUTERS IN THE AERODYNAMIC DESIGN OF THE HiMAT FIGHTER by R.D.Child, G.Panageas and P.Gingrich	17
NUMERICAL METHODS FOR DESIGN AND ANALYSIS AS AN AERODYNAMIC DESIGN TOOL FOR MODERN AIRCRAFT by W.Schmidt	18
 <u>SESSION IV – STRUCTURAL ANALYSIS AND DESIGN</u>	
MAINTENANCE OF NASTRAN AS A STATE-OF-THE-ART COMPUTER PROGRAM by J.L.Rogers, Jr	19
A COMPUTER BASED SYSTEM FOR STRUCTURAL DESIGN, ANALYSIS AND OPTIMISATION by A.J.Morris, P.Bartholomew and J.Dennis	20
STRUCTURAL OPTIMIZATION WITH STATIC AND AEROELASTIC CONSTRAINTS by D.Mathias, H.Röhrle and J.Artmann	21
APPLICATIONS OF MIXED AND DUAL METHODS IN STRUCTURAL OPTIMIZATION by G.Sander, C.Fleury and M.Geradin	22
ELEMENTS FINIS ET OPTIMISATION DES STRUCTURES AERONAUTIQUES par C.Petiau et G.Lecina	23
NEW COMPUTER APPLICATIONS FOR SPECIAL STRUCTURAL PROBLEMS by J.Massmann	24
 <u>SESSION V – PROPULSION AND SYSTEMS DESIGN</u>	
COMPUTER PROGRAMMES FOR THE DESIGN AND PERFORMANCE EVALUATION OF NACELLES FOR HIGH BYPASS-RATIO ENGINES by R.Smyth	25
COMPUTERIZED SYSTEMS ANALYSIS AND OPTIMIZATION OF AIRCRAFT ENGINE PERFORMANCE, WEIGHT, AND LIFE CYCLE COSTS by L.H.Fishbach	26
MATHEMATICAL MODELLING IN MILITARY AIRCRAFT WEAPON SYSTEM DESIGN by N.Mitchell	27
BACTAC – A COMBAT-WORTHY COMPUTERISED OPPONENT by I.Jones	28
INTERACTIVE AIDED DESIGN SYSTEM FOR AIRCRAFT DYNAMIC CONTROL PROBLEMS by W.J.Kubbat, G.Oesterheld and U.Korte	29
THE USE OF ADVANCED COMPUTER TECHNIQUES IN FLIGHT TEST EVALUATIONS by D.P.Maunder and R.E.Lee	30

THE USE OF COMPUTER AIDED DESIGN METHODS IN AIRBORNE SYSTEMS EVALUATION

P. Ebeling, E. Pfisterer
INDUSTRIEANLAGEN-BETRIEBSGESELLSCHAFT MBH
WEHRTECHNISCHE SYSTEME
OTTOBRUNN, FEDERAL REPUBLIC OF GERMANY

INTRODUCTION

Computerized aircraft design is a well-established tool in aircraft systems design, both civilian and military ones, manned or unmanned, as well as in all types of missile systems. Starting from very first feasibility investigations in early phases of weapon systems work down to detailed development efforts digital computer programs are used with increasing complexity and accuracy. They are applied for design studies both in the aircraft industry and in those government agencies concerned with weapon systems predesign and evaluation work. This paper mainly deals with the application of computer aided design methods for predesign and evaluation purposes of airborne systems, especially in early phases. In order to provide a rough survey on the enormous amount of work already completed in this field a list of references has been added to this paper containing an extract from various sources applicable. This list should not be considered complete, it might be helpful for readers especially interested in this topic in order to obtain additional details.

GENERAL DESIGN PROBLEM

First of all one has to analyze the general problem of systems design, i.e. the design sequence ranging from the predesign to the development phase and to isolate those parts of the procedure where the computer can relieve the design engineer from multiply repeated routine operations. These time consuming activities are implied in any systems design work unfortunately. The following objectives can be achieved by applying computer-aided design methods

- Considerable time savings
- Relief of qualified engineering personnel from routine work
- To enable the engineer to focus on his specific, innovative design contributions
- Better, i.e. thoroughly optimized solutions, especially if multi-dimensional optimization problems have to be analyzed
- Possibilities to perform parametric design work, in order to reduce the development risk (especially in early phases). For instance the effects of different technology assumptions on systems characteristics, performance and cost can be investigated in order to determine risk and cost.

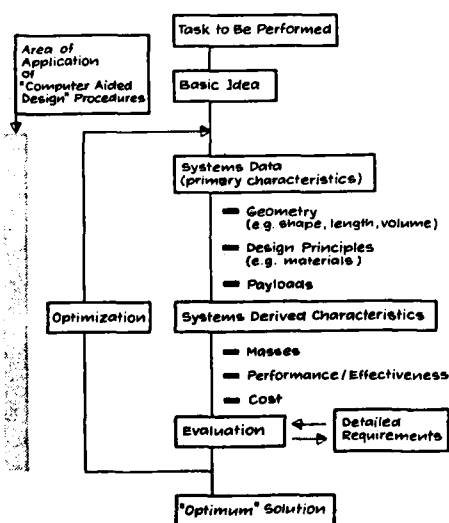


Fig.1 General Design Cycle of Systems

Figure 1 presents a general scheme how any system is conveyed. Normally it can be assumed that at the very beginning at least preliminary objectives are already available as far as application, tasks to be performed etc. are concerned. In systems realization the first step consists from the engineer's idea, defined in terms of a drawing, the definition of its main characteristics and principles and the selection of payloads, derived from the preliminary requirements. Within this step and the subsequent one of estimating effectiveness/performance/cost the engineer has to be aware of the technological state of the art on which his design can be based. This comprises the consideration of the development risk and the appropriate forecast of the relevant technologies. After the systems characteristics have been determined the evaluation step follows. This evaluation is based on the requirements, which will become more specific with increasing knowledge about the system. Subsequently -according to the results of this evaluation step- the system's characteristics are changed in order to improve the fulfillment of the requirements.

This general sequence will be run through for many times. Various methods which imply increasing accuracy of prediction as well as increasing manpower required are applied. At the end of the development phase hopefully an optimum solution can be achieved.

Computer aided design can be helpful in the areas hatched in Figure 1. Its application could start when the basic idea is established which the engineer has to describe. If computer aided design methods are used this basic solution has to be translated into an appropriate set of input data for the computer program. Such a program can be helpful in determining systems characteristics, especially if

- detailed requirements are not sufficiently fixed
- a large number of alternative solutions and parameter values have to be considered
- different technological assumptions have to be evaluated in their effects on the systems characteristics.

COMPUTER AIDED DESIGN METHODS FOR AIRBORNE SYSTEMS

In order to illustrate how the previously described scheme is followed in practice for computer aided design, two methods are presented in this paper. The first one is the aircraft design computer program APFEL (Reference 1) which is described in some detail. The second application is the missile design program PROFET (Reference 2). Both programs are extensively used within the Systems Engineering Division of IABG for predesign and evaluation work of aircraft and missile weapon systems. Typical applications including some results are presented in section 4.

AIRCRAFT SYSTEMS

The block diagram given in Figure 2 is more or less representative for the aircraft design procedure, it describes the different steps contained in the computer program. Provided that the payloads (weapons etc.) have been defined and the respective requirements on the target acquisition and fire control system are established, size and mass of the target acquisition sensors -properly matched to the weapons requirements- and of the avionics system are determined.

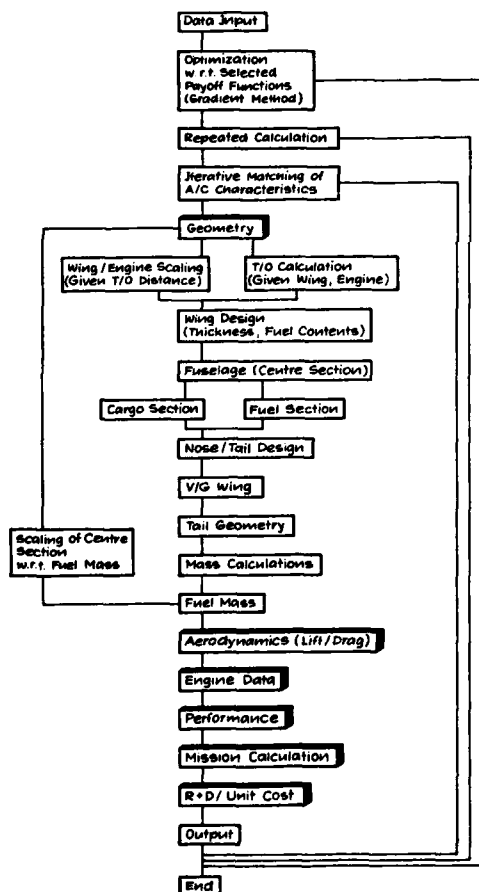


Fig. 2
Block Diagram for the Computer Program APFEL

Now a first drawing of the aircraft is made based on some rough assumptions on configuration, type of propulsion to be used, structural principles to be applied etc. This step can be done on the drawing board, highly sophisticated programs also utilize digigraphic displays. In this case the engineer directly communicates with the computer, providing the geometric input data to the program.

Starting with this first design, the overall take-off mass is estimated and all necessary input data are compiled. Advice is given to the computer whether an optimization with respect to a carefully selected pay-off function is intended, a parametric variation of basic variables should be performed or whether an iterative match of design characteristics has to be done in order to achieve prescribed performance values.

The next step consists of the geometric description of the aircraft. Its essential elements as available in the APFEL program are given in Figure 3. These different geometric options are used in formulating the input data. The computer program uses these data to calculate volumes, lengths, surfaces required by subsequent steps, and to perform scaling or other geometric changes if necessary. Wing geometry is treated first, thickness distribution, fuel volume and wing area are calculated. Similar steps are made for the centre, forward and aft fuselage sections respectively, including horizontal and vertical tail size required. If variable wing geometry is used the sweep axis is positioned properly. Based on the geometric characteristics and a number of other input variables (maximum structural load factor, speed etc.) a mass estimation of all subsystem is performed by statistical methods and the remaining fuel mass is calculated. If that fuel mass does not fit into the fuel volume available, both quantities are matched by scaling the centre section of the fuselage appropriately.

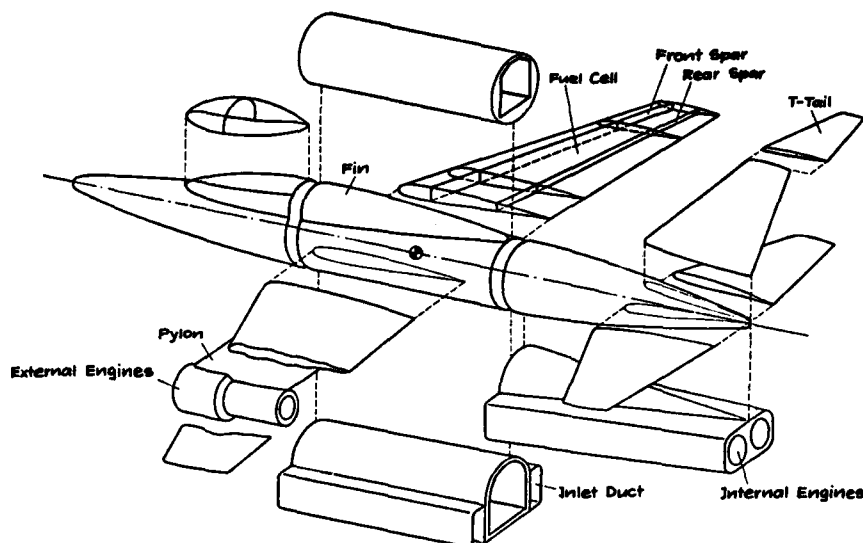


Fig.3 AIRCRAFT GEOMETRY

The aerodynamic characteristics (drag vs. lift, Mach number, altitude) are determined by a standard procedure (DATCOM) both for the clean and the external stores configuration. Installed engine data (thrust and specific fuel consumption) are scaled, if necessary. They are used for the subsequent performance and mission calculations. By means of a statistical cost model applying standard cost estimation relationships (CERs), unit cost are obtained.

These steps can be repeated as many times as necessary within very short time so that a lot of aircraft with different characteristics can be treated for design purposes. Typical applications are given in section 4.

MISSILE SYSTEMS

In a similar way computer programs can be used for missile synthesis. As a second example figure 4 presents the main portion of the IABG program PROFET in a simplified block diagram. A variety of different missile configurations (Figure 5) can be handled by the program with up to three pairs of surface, different types of controls, nose sections etc.

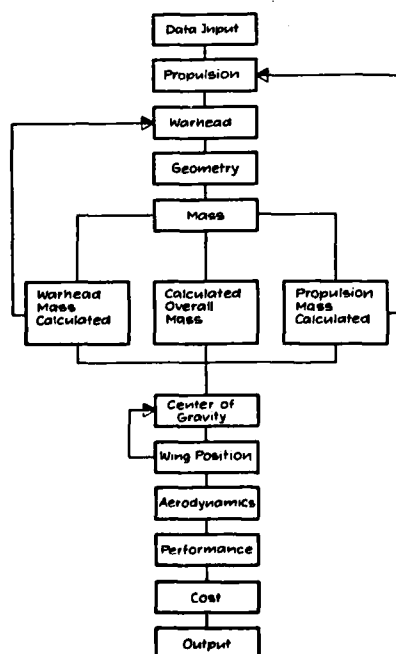


Fig.4
Block Diagram for the Computer Program PROFET

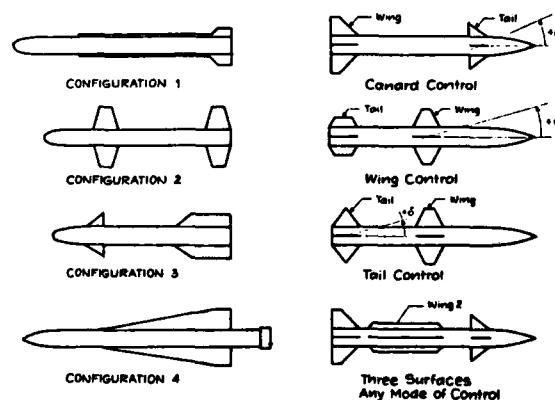
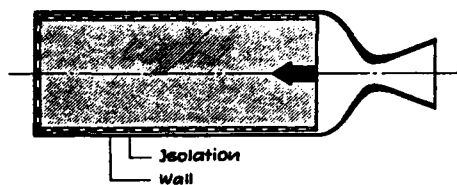


Fig.5 Selection of Missile Configurations (PROFET)

Cigarette Burner



➔ Burning Direction

Radial Burner

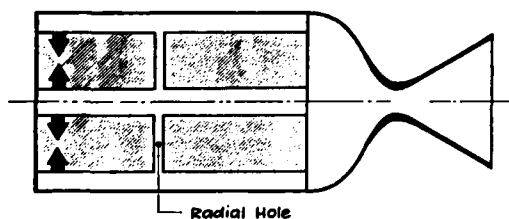


Fig. 6

Types of Rocket Engines (Examples)

The propulsion section accounts for various rocket engines, e.g. the conventional solid propellant rocket engine with cigarette or radial burner (figure 6). Thrust profile and total impulse are determined together with the proper nozzle design and other characteristics. A mass and centre of gravity balance including C.G. shift due to engine burn-out is established and the wing position is determined according to static margin limits. The aerodynamic data (lift, drag, pitching moment) are calculated using a semiempirical procedure of both theoretical and experimental back-ground information (Reference 48). If the target trajectory is prescribed and provided to the program, the missile performance in terms of the intercept volume is calculated by means of a modified 3 DOF simulation program. Different boundary criteria like maximum normal acceleration obtainable, speed, seeker limits etc. are checked. As far as guidance is concerned the program at this stage is employing the kinematic guidance law without considering the guidance and control loop in detail. Again the assumption is made that this subsystem of the missile, especially the forward sensor (if required) has been investigated prior to the application of the computer program. In future, however, this program section will be hopefully amended, same applies to the cost estimating part. This main portion of the design program is imbedded in different control loops, providing the capability for parametric design studies or multi-variable optimization applications.

APPLICATIONS AND RESULTS

So far the IABG computerized design methods have been explained, now some typical results will be shown. First of all it should be stated that IABG is not concerned with weapon systems development. As mentioned previously, however, one of the main tasks of our Systems Engineering Division consists of predesign and evaluation work for future airborne systems.

One typical kind of tasks which have to be treated in our agency are parametric design studies. Their main objectives are to assess the effect of different requirements on one hand or of variations in technology assumptions on the other hand on weapon systems characteristics. The results obtained provide the armament department of our MOD with the background information necessary for establishing requirements as well as for international talks. Furthermore these systems data serve as a first guess in terms of technical and cost inputs for operational studies. In a later stage when various systems proposals are available feasibility and relative value of these concepts have to be analyzed.

Extensive use of the design programs as described previously is being made.

A few examples and results of this work is illustrated in the following figures. Figure 7 shows the result of a design analysis for an existing fighter aircraft. Geometry and stationary flight envelopes are compared with manufacturer data, they provide an impression of the accuracy to be achieved by this method. Recently a new aerodynamic subroutine with increased accuracy has been incorporated.

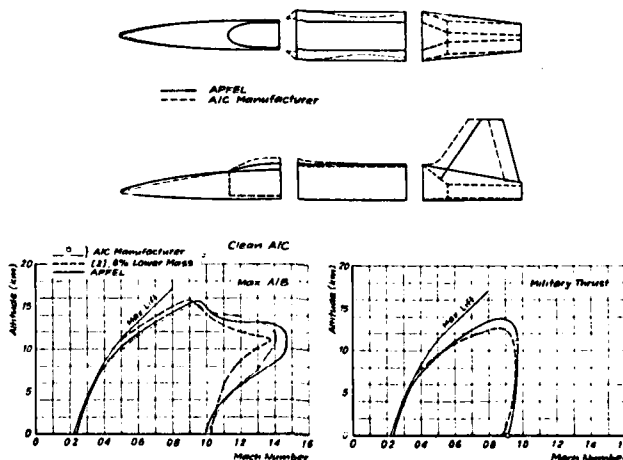


Fig. 7 Application of Computerized A/C Design on Existing A/C (Example)

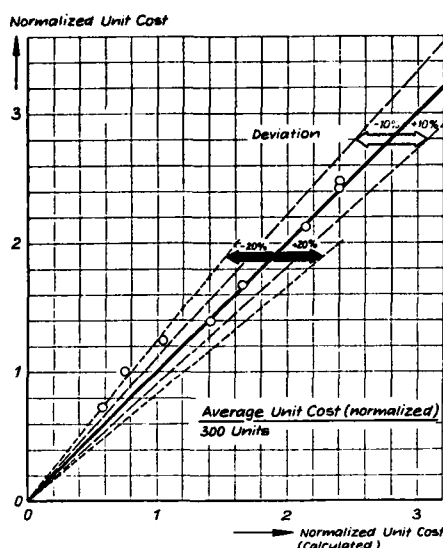


Fig.8 Comparison Between Real and Calculated Unit Cost

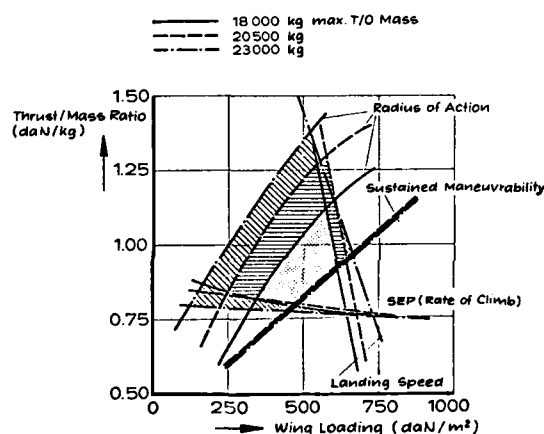


Fig.9 Parametric A/C Design (Example)

A comparison between real and calculated unit cost values for various fighter aircraft is given in figure 8. Bearing in mind that cost estimation is a very complex task because of a number of uncertainties (productivity, multi-source production etc.) this accuracy is sufficient for most design investigations during early phases in the life cycle, where these methods are applied to the greatest extent.

The result of a parametric design study for a heavy fighter aircraft is shown in the thrust/mass ratio vs. wing loading diagram (figure 9). In this case the whole area of the diagram has been covered by a large number of design points, varying engine size (thrust) and wing area at three constant T/O mass values. For each of these designs all performance parameters are available, so that lines of constant radius of action, maneuverability, rate of climb and landing speed respectively can be drawn. The hatched area in this picture represents those designs which fulfill all the requirements. Due to the major influence of aircraft mass on range this area is rapidly reduced with decreasing mass. The smallest aircraft just meeting the requirements will have approximately 15 500 kg of T/O mass, represented by the lowest corner in the diagram.

Figures 10 through 12 show a fighter aircraft optimization, starting from a basic solution (calculation step 0). The objective was to maximize a pay-off function composed from range R and sustained turn rate ω , with weights of a_1 , a_2 (see figure 12). The computer program was varying the following independent design variables:

- Sweep of the wing quarterline $\varphi_{0,25}$
- Wing area A_W
- Take-off gross mass $m_{T/0}$
- Wing thickness δ_{Root}

In addition the following constraints had to be taken into account

- Maximum mass less than 12.000 kg
- Maximum Mach number at least 0,85
- Positive sweep of the wing quarterline.

By means of the built-in gradient method the design had been optimized after about 180 calculation steps, leading to a straight wing (because of the low Mach number required), the maximum possible mass (due to the heavily weighed range requirement), a 10% thick wing and a nearly constant wing area of 16m². The configuration is sketched in figure 12.

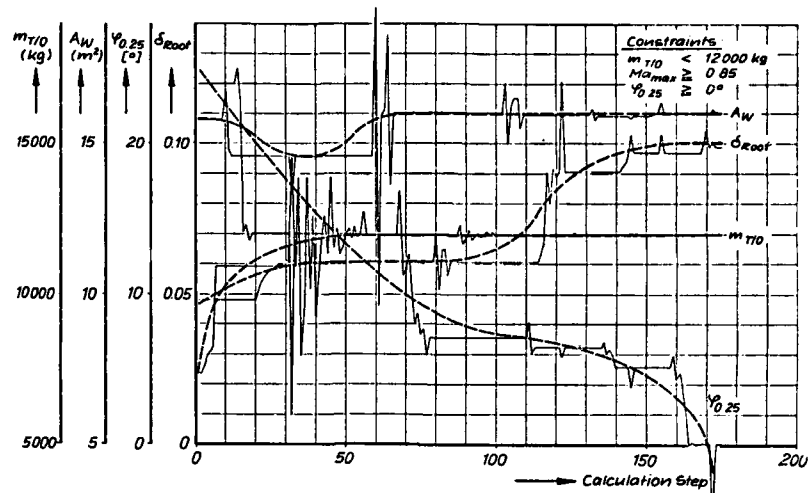


Fig.10

AIC Design Using the Gradient Method - Example
(Geometry, Mass)

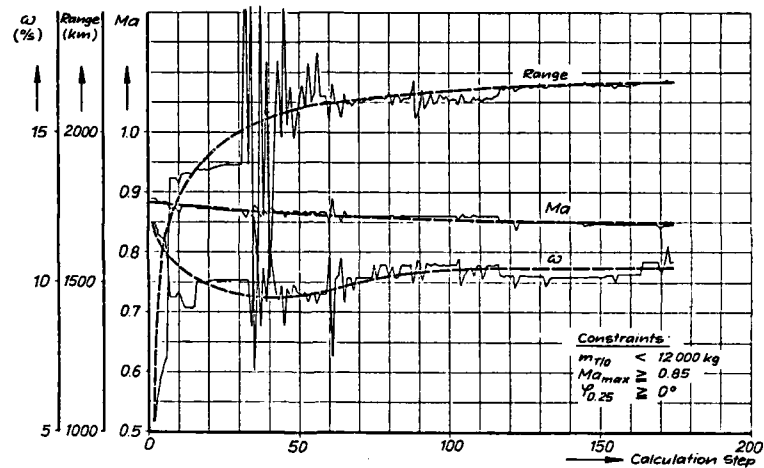


Fig.11

AIC Design Using the Gradient Method - Example
(Performance)

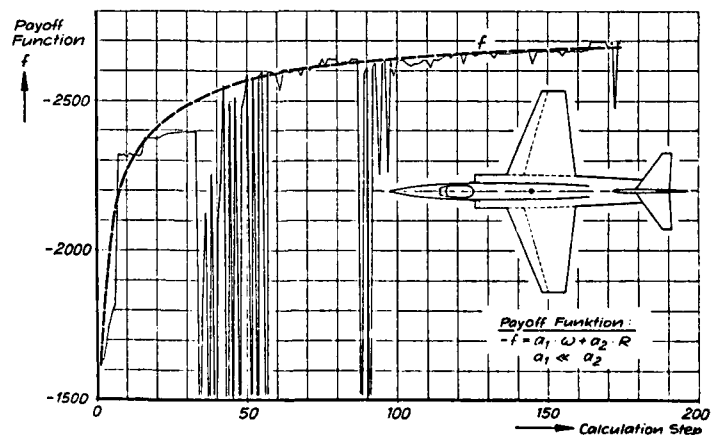


Fig.12

AIC Design Using the Gradient Method - Example

Some corresponding examples have been treated in the guided missile case using the missile design program PROFET.

Figure 13 gives a comparison between aerodynamic coefficients obtained by the computer program and experimental data. In general the agreement is good and substantiates the application of this method for other design purposes. The remaining discrepancies however have led us to a replacement of the aerodynamics subroutine by a more up-to-date version, which offers improved accuracy, especially in the high angle-of-attack and high Mach number regime.

Figure 14 shows a comparison of calculated intercept boundaries with data provided by the manufacturer, both obtained by similar simulation methods. Again quite close agreement is evident so that one can rely on this method for further applications.

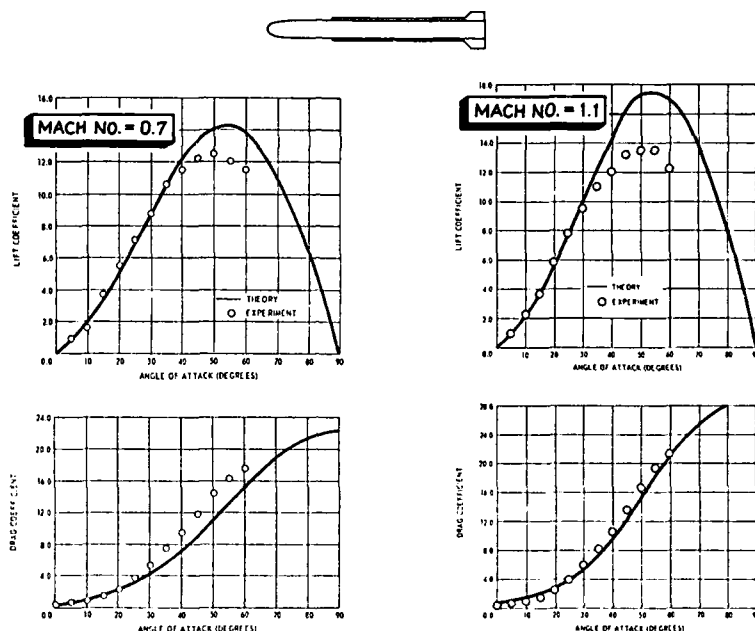


Fig.13 Comparison between Calculated and Experimental Aerodynamic Data

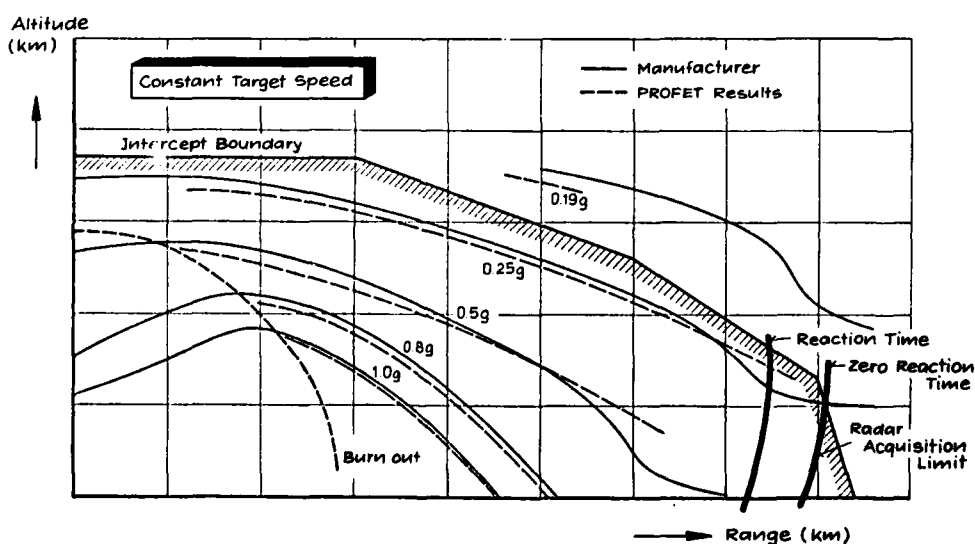


Fig.14 Maximum Normal Acceleration Limits (Example)

A parametric study has been done on an existing ground-to-air missile investigating the influence of wing size and thrust level (at constant total impulse) on altitude and down-range performance.

Figure 15 presents the results of this work showing that increased wing area improves altitude performance, while a reduced thrust level can be beneficial for increasing down range.

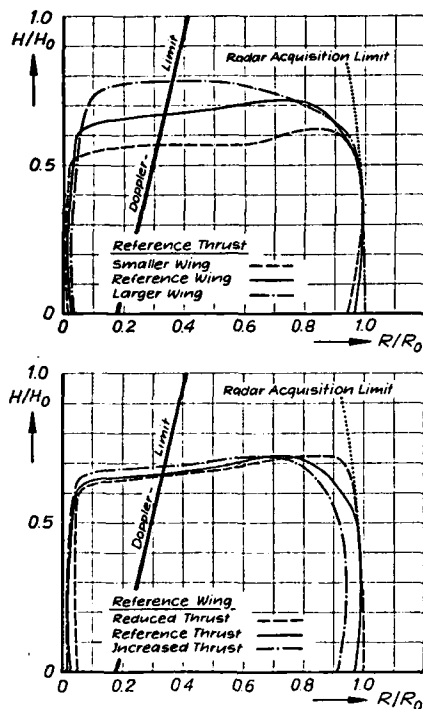


Fig.15 Firing Envelopes

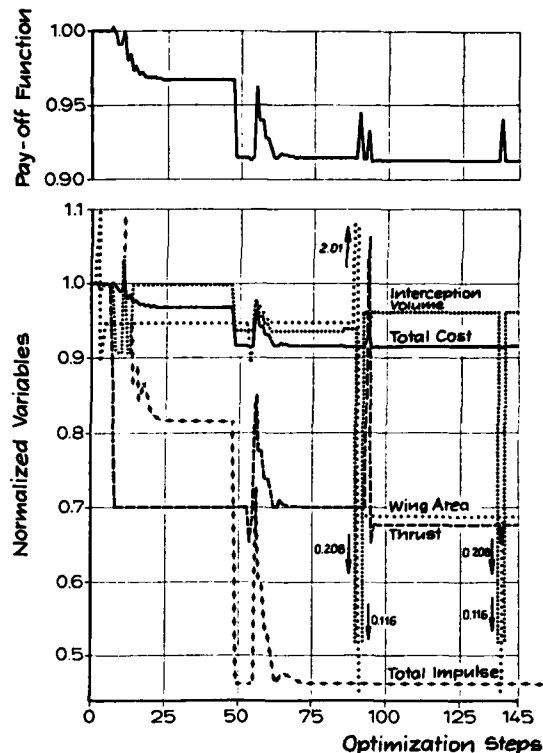


Fig.16

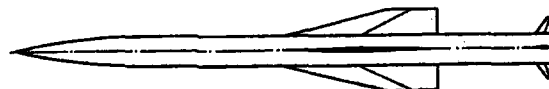
Variables and Pay-off Function versus Optimization Steps

Figure 16 shows a final example, where a pay-off function composed of intercept volume and unit cost had to be maximized using wing area, thrust level and total impulse as independent variables. The optimization resulted in a smaller and lighter missile design. The initial and the final missile configuration are presented in figure 17.



Initial Missile Configuration

Fig. 17



Final Missile Configuration after Optimization

CONCLUSIONS

As shown in this paper computer aided design methods are a helpful tool, if properly applied for engineering purposes during all phases of systems development, provided that the computer program is sufficiently accurate to be able to represent the effects to be investigated. Of course this degree of accuracy increases rapidly in later phases of systems development, leading to a large amount of computer software and calculation time required. The application of those methods, however can help to solve problems the engineer alone is not able to handle, especially in multidimensional optimization of designs. An enormous time saving is possible. By parametric variation of the important effects (especially technological assumptions) an increased confidence in the design results can be achieved and development risk for airborne weapon systems could be reduced.

REFERENCES

1. P. Ebeling et. al.:
Ein Digitalrechenprogramm für parametrischen Entwurf und Leistungsrechnung von Flugzeugen (APFEL)
IABG-Report B-WT 1205/01, June 1975
2. P. Ebeling, E. Pfisterer et. al.:
Ein Digitalrechenprogramm zu Entwurf und Optimierung von Flugkörpern.
IABG-Report B-WT 1207/01, June 1975
3. W. Stepniewski, C. Kalmbach:
Multivariable search and its application to aircraft design optimization
RAS Aero. Journal, Vol. 74, May 1970
4. M. Krzywoblocki, W. Stepniewski:
Application of optimization techniques to the design and operation of V/STOL aircraft.
International Congress of Subsonic Aerodynamics, New York, April 1967
5. W. Herbst:
Ein einfaches Bewertungsverfahren für Militärflugzeuge.
Luftfahrttechnik, Raumfahrttechnik 13, No. 3. March 1967
6. D. Hague, C. Glatt:
An introduction to multivariate search techniques for parameter optimization.
NASA CR - 73 200, April 1968
7. R. Boyles:
Aircraft design augmented by a man-computer graphic system.
Journal of Aircraft, Vol. 5 No. 5, Sept. 1968
8. J. Chuprun:
Solution of the optimization problem by the maximum principle.
J. Automation and remote control, Dec. 1963
9. S. Coons:
An outline of the requirements for a computer - aided design system.
Spring Joint Computer Conference, Vol. 23, 1968
10. D. Ross, J. Rodriguez:
Theoretical foundations for the computer - aided design systems.
Spring Joint Computer Conference, Vol. 23, 1968
11. V. Lee et. al.:
Computerized aircraft synthesis.
Journal of aircraft, Vol. 4, No. 5, Sept. 1967
12. H. Roland:
Parametric weight-sizing methods
General Dynamics Rept. MR - SS - 040, 1966
13. R. E. Wallace:
Parametric and optimization techniques for airplane design synthesis.
AGARD LS-56, March 1973
14. B. W. Boehm:
Keeping the upper hand in the man-computer partnership.
AIAA Astronautics and Aeronautics, April 1967, pp. 24-28
15. V. A. Lee et. al.:
Computerized aircraft synthesis.
AIAA Journal of Aircraft, Vol. 4, No. 5, September-October 1967, pp. 402-408
16. G.W. Klees:
Description and operating instructions.
Boeing Engine-Airplane Matching Program (Beam).
Boeing Doc. D6-20383, July 1968
17. G. J. Wennagel et. al.:
IDEAS - Integrated design and analysis system.
SAE Paper No. 680728, October 1968
18. R. E. Wallace:
Computing geometric airplane characteristics.
Paper in Education in Creative Engineering Seminar,
Massachusetts Institute of Technology, April 1969, pp. 163-182
19. P. D. Milliman et. al.:
Feasibility study of a computerized preliminary design process.
Boeing Doc. D6-23935, June 1969

20. D. I. Cook:
Preliminary engineering design system - design specification.
Vol. I, Boeing Doc. D1-81-0081, 8th May 1969
21. W. Herbst, H. Ross:
Application of computer aided design programs for the technical management of complex fighter development projects.
AIAA Paper No. 70-364, March 1970
22. J. Kondo:
Application of computer techniques to aircraft design problems. The Seventh Congress of the International Council of the Aeronautical Sciences.
ICAS Paper 70-28, September 1970
23. R. F. Greer et. al.:
Interactive preliminary design system - Vol. II - Director and file handler.
Boeing Doc. D 1-62-10347-2, 11th May 1971
24. V. Commisso:
Interactive preliminary design system - Vol. III -
The graphics processor.
Boeing Doc. D 1-62-10347-3, 11th May 1971
25. S. K. Landgraf:
Some applications of performance optimization techniques to aircraft.
AIAA Journal of Aircraft, March-April 1965, pp. 153-154
26. J. Kowalik, M. R. Osborne:
Methods for unconstrained optimization problems.
Elsevier, New York, 1968
27. D. A. Hague, C. R. Glatt:
An introduction to multivariable search techniques for parameter optimization (and program AESOP).
NASA CR-703200, April 1968
28. G. S. Schairer:
The challenge of optimizing synthesis and systems engineering.
1967 Daniel Guggenheim Medal Award Paper, Presented in June 1968 for the American Society of Mechanical Engineers
29. D. A. Hague, C. R. Glatt:
A guide to the automated engineering and scientific optimization program.
Boeing Doc. D2-114271-1, September 1968
30. D. A. Hague, C. R. Glatt:
Application of multivariable search techniques to the optimal design of a hypersonic cruise vehicle.
NASA CR-73202, April 1968
31. F. D. Schmitz:
Takeoff trajectory optimization of a theoretical model of a STOL aircraft.
AIAA Paper No. 69-935, August 1969
32. A. E. Bryson Jr. et. al.:
Energy-State approximation in performance optimization of supersonic aircraft.
AIAA Journal of Aircraft, Vol. 6, No. 6, November-December 1969
33. B. Silver, H. Ashley:
Optimization techniques in aircraft configuration design.
Department of Aeronautics and Astronautics,
Stanford University Report, SUDAAR No. 406, June 1970
34. S. A. Coons:
An outline of the requirements for a computer aided design system.
Proceedings of the Spring Joint Conference 1963, pp. 299-304
35. S. H. Chasen:
The introduction of man-computer graphics into the aerospace industry.
Proceedings of the Fall Joint Computer Conference, 1965, pp. 883-892
36. G. O. Gellert:
Geometric computing - Electronic geometry for semi-automated design.
Part I - The Method and its Application,
Machine Design, 18th March 1965, pp. 152-159;
Part II - Fields of Application, Machine Design,
1st April 1965, pp. 94-100
37. W. L. Johnson et. al.:
Analytical surface for computer aided design.
SAE Paper No. 660152, January 1966

38. S. H. Chasen, R. N. Seitz:
On-line systems and man-computer graphics.
AIAA Astronautics and Aeronautics, April 1967, pp. 48-55
39. D. L. Flannagan:
Surface molding - New tool for the engineer.
AIAA Astronautics and Aeronautics, April 1967, pp. 58-62
40. R. Q. Bowles:
Aircraft design augmented by a man-computer graphics system.
AIAA Journal of Aircraft, Vol. 5, No. 5,
September-Oktober 1968, pp. 486-497
41. B. W. Boehm et. al.:
Developing interactive graphic systems for aerospace applications.
AIAA Paper No. 69-954, September 1969
42. R. M. Naraharg:
Computer aided design.
Space/Aeronautics, December 1969, pp. 56-64
43. H. P. Y. Hitch:
The application of modern computer techniques to aeronautical design problems.
The Seventh Congress of the International Council of the Aeronautical Sciences,
ICAS Paper No. 70-27, September 1970
44. B. F. Saffell, M. L. Howard, E. N. Brooks:
A method for predicting the static aerodynamic characteristics of typical missile
configurations for angles of attack to 180 degrees.
Naval Ship Research and Development Center, Report 3645
45. M. Barrère et. al.:
Raketenantriebe.
Elsevier Publishing Company
Amsterdam - London - New York - Princeton 1961
46. Missile synthesis and performance computer program.
Final presentation brochure
Martin Marietta Corp. Orlando, Florida
47. DOD-Wide missile system costing.
Keith E. Marvin
OASD (System Analysis) Resource Analysis
48. W. R. Schmidt, H. W. Stock:
Ein Verfahren zur Berechnung der aerodynamischen Beiwerte von Flugkörpern im
Unter-, Trans-, Über- und Hyperschall, Teil I und Teil II.
Dornier Forschungsbericht 75/10B, April 1975
49. P. Ebeling:
Technische Bewertung fliegender Waffensysteme.
BMVg-FBWT 75-29, page 243 ff., 1975

CRITERIA FOR TECHNOLOGY

by

R. L. HAAS

AIR FORCE FLIGHT DYNAMICS LABORATORY (AFFDL)
WRIGHT-PATTERSON AFB OH 45433

ABSTRACT

The application of the computer to automation of the overall air vehicle synthesis process continues to grow. Beginning with machine tool process control, progressing through layout drawings, structural design and conceptual/preliminary design, the use of computers is now transitioning to and greatly expanding the scope of the technology of systems.

The ever expanding realm of computational power and software is supporting the transition of the application of computer aided design methodology to full system synthesis, with design representing only one element in the overall process. The objective is no longer simply a point design aircraft but rather a complete concept based on complex payoff functions having the nature of maximizing return on investment based on new approaches to defining criteria (measures of merit) for technology development and military capability.

A merger of operations research, mission need/definition, cost analysis and design as an iterative process is occurring in order to explore the relative merit of concepts, as a means of focusing development of technology and to initiate early definition and systems assessment of competitive alternatives.

This paper offers a perspective on the use of computers in an approach to technology program planning. It presents a rationale for cost benefit assessment of technology to form the foundations for the technology of systems. An approach is defined which builds on techniques associated with computer aided design capability and is analogous in form to process control. A description of the basic process applied to a tactical fighter problem is discussed.

Recent technology and systems programs have incorporated iterative computer aided design, mission analysis and cost analysis to assess payoff (return on investment) of concepts on a higher or global level of evaluation. Classical figures of merit for aircraft design such as range/payload, maneuverability and persistence and for technology such as L/D and structural weight fraction are being augmented with higher order criteria such as cost per target kill, exchange ratio, number of targets killed, and etc.

The problem of establishing the basic nature of system alternatives and selecting proper concept, aircraft design and technology requirements is made particularly difficult because the creation and validity of many options is strongly influenced by technology. The converse is also true; the benefit of many technology options is strongly influenced by problem definition.

Elements essential to the solution of this complex interdependent problem include:

1. A knowledge of the technological options available and the resultant opportunities available through development and application of technology.
2. An ability to assess the impact of requirements and technologies on basic characteristics (i.e., cost, effectiveness, survivability) and associated elements; the parametrics and sensitivities of the problem.
3. A measure of the benefit and the cost of any given element (e.g., maneuverability, cruise speed, size) referenced to survivability and effectiveness (e.g., target coverage, target kill probability) as a function of the problem definition.
4. A process for combining and assessing information at an appropriate level of military relevance or global context wherein the effects of various alternatives can be comparatively evaluated. The top level of assessment is overall military/economic victory or effective deterrence in probable confrontations. The level of assessment actually employed is a challenge to the decision maker but should be consistent with the problem and the objective.
5. An ability to transform (in both directions) cost/benefit information between the technology and military utility domains.

Sensitivities to various input assumptions, scenarios and other parametrics are determined as a function of technology and concept and identified in order to provide an understanding of the effect of analytical assumptions and possible changes in parametrics on the selected alternatives. The results are used both to create and to assess concepts and to provide guidance for the next iteration of criterial technology/design/mission/scenario selections.

Insight to the problem and the role of technology in resolution of the problem is the goal. Application of systems technology to identify viable alternatives including sensitivities to variations in parametrics is the approach.

INTRODUCTION

The opportunities and risks associated with the aggressive application of technology to (future) military needs are great. The long lead time required to transition a flight vehicle system from concept to operation results in great potential payoff if required technology can be identified and developed in a timely manner. Worked as part of the problem, technology itself can impact the evolution of requirement and help establish a balance between system capability, tactics, numbers, and etc.

Historically, the benefit of technology has been assessed through criteria (or measures of merit) directly associated with technology itself and has only been constrained in a broad sense by cost. For example, an advancement in aerodynamic technology may be quantified through an increase in L/D (efficiency) which in turn may be manifested in an improvement in maneuverability and range. Such criteria is invaluable for understanding accomplishment within a technological domain but does little to resolve the issue of real impact on military capability or to identify the relative payoff of investing in aerodynamic technology in lieu of, or in addition to structural technology (nor is the relative importance of each in providing a military capability identified).

The Air Force Flight Dynamics Laboratory is exploring the realm of the technology of systems and developing approaches to increasing the effectiveness of its technology development planning (investment strategy) through a direct cost/benefit analysis of the military utilization of technology. Utility is measured with some form of return on investment criteria (estimation of future payoff of technology and the required investment or cost). This approach begins with a generic definition of a problem and works toward alternative solutions as compared to the more standard approach of beginning with a technology and looking for an application (the two approaches are complementary and should be worked in parallel). The analysis is accomplished in a "global" sense which encompasses all relevant (subjectively determined) elements of a problem and is much broader in scope than classical aircraft performance (design) optimization. The argument for the global approach results from consideration of a system having multiple elements and the fact that optimization of the sum of elements (or whole system) is not equal to the sum of local optimizations for each element. For convenience and ease of understanding, cost/benefit assessment is viewed as a control process and the individual elements as blocks in that process. The process results in a measure of overall return (payoff) on overall investment (cost) and does not, for example, automatically result in emphasis on single airplane performance parameters such as speed, maneuverability or one on one kill ratio (which lead to higher complexity and cost per aircraft). However, the process inherently accommodates single element assessment.

The main purpose of any analysis is to provide sufficient information about the alternatives under study to make a rational decision. In this case the goal for the technologist is identification of strategies for maximization of return on investment where real quantification of return (payoff) increases as problem insight is improved as a result of working the analysis process. The approach in its simplest form is to address and understand the whole problem as an entity, each of the individual elements and the interactions between elements while establishing sensitivities to constraints and changes in parameters which exceed linear small perturbation variations. Insensitivity to change is frequently referred to as robustness.

The general objective of technology cost/benefit assessment is to provide insight into the high payoff technology areas and the associated system (aircraft, avionics and weapon) concepts and to provide initial planning for timely development. Cost benefit assessment is the foundation of the technology of systems and offers the following productivity:

- (1) provides the opportunity for technology to impact the initially perceived requirement,
- (2) stimulates the emergence of innovative concepts,
- (3) accommodates the identification of the probable set of competitive alternatives (and comparisons), i.e., systems options,
- (4) addresses the issue of whether the right problem was identified,
- (5) results in a parametric data base,
- (6) identifies the impact of constraints,
- (7) identifies the sensitivity to change in any element or any parameter,
- (8) ranks the dominance of parameters, and
- (9) identifies and prioritizes technology development needs.

APPROACH

The challenge is to properly define or project a problem in the military context and then to effectively apply technology to the resolution of the problem so that competitive alternatives emerge under conditions where perceived requirements and the problem definition itself are variables. This, by its nature, becomes a complex process which, somewhat analogous to optimization in the feedback control process, involves a search for the global solution and encompasses many variables, constraints and initial or starting conditions.

Conceptually, the process is simple, although the real problem is obviously far more complex because of the large numbers of interrelated parameters and issues to be faced. The approach involves looking at a large number of different design, technology, and mission alternatives and then conducting cost/benefit analysis deriving integrated cost, survivability and effectiveness measures for each, using the results of each successive pass through the (necessarily) iterative process to guide the selection of alternatives considered on the next pass. Finally, it inherently involves gaining insight to the nature of the parameters and sensitivity to change.

The output of the process forms a running account of the military relevant impact of technology which can be used to create and support technology development/transition programs and as a point of departure for solving specific system needs. The approach is easily investigated if it is viewed as a feedback control process with defined elements and a desired response for a given input (Figure 1). Then, because of its nature, cost/benefit analysis functions as an optimal control process (a process of optimization or

convergence maximizing return on investment) in which unique solutions are not expected.

The concept is an expansion of the familiar design loop iterations. Design itself becomes an element (or inner loop) in the overall system concept synthesis. Problem complexity is readily apparent when simple design convergence is viewed as a function of constrained parameters or performance goals (Figure 2, which shows characteristics as a function of specified acceleration and ground roll). Imagine the difficulty in convergence for the global problem.

The process lends itself to military relevant cost/benefit assessment of technology. Just as the basic computer aided design process allows rapid iteration between sub-elements, the overall technology assessment process is a massive iteration between the various elements including cost, benefit, system synthesis, mission and threat. Emphasis for the application of the process is on the identification of technology opportunities and benefits. The process is started with trial values and conditions which are based on an initial subjective assessment and unfortunately, can and often induce a bias (which also is true of the design process). It results in an overall closed loop approach to assessment and supplants the previous largely open loop approach which measured inner loop results as payoff without measure of overall payoff. The process leads to better defined, better understood alternatives along with the supportive rationale. It also defines sensitivity to variation in parameters and provides the ability to respond to the "what if" questions (what if the threat changes, what if the technology is not available, what if an assumption is incorrect, etc.). The projection of the cost benefits of individual technologies is dependent upon the success of other technologies and technology integration. The complexity of the process makes it largely dependent on extensive computational power as applied to analysis and synthesis techniques.

The problem structure itself is crucial and must be open to the whole spectrum of alternatives. For example, if the full capability being projected for long range air to air missiles is realized a thought process might conclude that increased acquisition and kill range (range advantage) results in first shot and multiple shot firing opportunities. The emphasis on technology is then shifted from that associated with high maneuverability to that associated with weapons and avionics. However, considering the opponent has the ability to reduce his detectability, the problem is more appropriately viewed as one of time advantage and the technology emphasis is not so clear. Full understanding of the contribution of new technology requires parallel consideration of the sensitivity to changes in parameters such as the effects of a variety of alternate performance goals and design concepts as they jointly influence operational effectiveness. The projections of benefits/costs of technology advancements with complex modern weapons systems are interdependent with (1) the way the technologies are applied in specific air vehicle designs, (2) the way the concept itself is militarily employed and (3) the choice of measure of merit (how benefit is measured). In essence, no part of the technology cost/benefit picture can be adequately evaluated in any relative or absolute sense without consideration of the relationship of each element to all other elements (for large variations in parameters).

To see why this is the case, it is useful to address a simple example. Consider the weight and hence the cost of a series of aircraft of different design types sized to meet different takeoff distance requirements, but with all other performance parameters held fixed.

Decreasing the design takeoff roll for each given type requires necessary increases in wing and engine size which cause the aircraft to become larger and more expensive (Figure 3). However, the variation of cost vs design takeoff distance is found to be different for each different basic type (CTOL, STOL, VTOL) of aircraft and, also, for the same basic type of aircraft but for alternate mission types. Furthermore, it is found that individual technologies can influence the location (on the takeoff distance axis) of the intersections that define which design concept is best for any given set of mission requirements. For example, an improved high-lift system will extend to shorter takeoff distances the region where a conventional aircraft is superior to the powered-lift approaches. A full iteration of the rationale for the requirement in the broader military sense may disclose different issues (lift and thrust not crucial). The basis for the ground roll requirement may involve unexpected elements such as semi-prepared site operations as the overriding military problem. Low speed control or some other parametric may then become the truly dominant technical characteristic.

What then, is the right way to apply technology and then as a result, how are the "highest payoff" technologies and concepts defined? Vectored thrust/powered lift may have no payoff at all on one set of mission rules but still yield significant gains on alternate missions that are relatively similar in nature. Can technology impact the requirement? The impact of technology is a function of the problem and the structure of the problem is a function of the technology. Both are a function of the measures of merit. If, for example, a breakthrough were made in Vertical Takeoff and Landing (VTOL) technology that could greatly reduce the associated cost and performance penalties, then mission concepts using VTOL technology would become much more attractive. Often, however, the technology will have the same relative impact on more than one concept. In the global sense, the absolute benefits obtained are strongly influenced by other variables such as the magnitude of the runway denial threat posed by potential adversaries. If the crucial problem turns out to be operations from semi-prepared sites, landing gear/footprint considerations along with simple solutions to deceleration and control will be key technical challenges while support, supply and maintenance become the operational detractors.

Thus, the selection of high return on investment aircraft technology or design concepts is impossible without at least some insight into the overall problem including the relationship between goals, design, technology, and military capability. The problem is closed loop: no rational decision in one area can be made without some knowledge of its influence on the other areas. Development of such insights into the interrelationships between elements of the process is a continuing objective and a continuing advantage of the process.

THE PROCESS

The simple control process perspective of cost/benefit assessment can be expanded in a number of ways. For the purpose of discussion, the process is divided into the elements discussed below. The elements and the interactions between elements are diagrammed in Figure 4. Each element is itself divided into sub-elements and so on. The basic elements of the concept and technology cost/benefit analysis process include:

1. Threat and scenario definition - Defines the overall problem context in which the candidate solutions are played. The element defines measures of merit and provides the structure for evaluation models in order to project the return on investment.
2. Mission Model - Covers the mission profile (range, maneuvers, etc.), payload, design requirements and etc. The element is treated as a variable and the process is initiated with best judgment values.
3. Candidate Technology - Identifies probable technology sets available to meet future mission and other requirements, defines status/availability, cost and time for development. The element provides the technical data base for concept definition.
4. Design Synthesis - Covers the methods employed to converge designs and corresponding characteristics including cost and needed technology. The element is composed of subelements which consist of aero, weights, stability and control performance, subsystem, structure, and etc.
5. Configuration tradeoffs - Includes identification of and performance/one-on-one type comparisons of alternative approaches to resolving the problem. The element encompasses the relative investment in and contribution of the air vehicle, the avionics and the weapons.
6. Analysis (effectiveness, survivability, cost) - Provides the global evaluation of achieved capability and the cost to accomplish.
7. Key Technology - Identifies high leverage technology and the relationship with concepts. The element utilizes the comparison of concepts to document technological tradeoffs, parametrics and sensitivities. The element leads the way for the next iteration and provides the technology of systems data base, including risk assessment.
8. Technology development plan/roadmap - Covers the accomplishment of plans for specific technology development, including schedules, costs and criteria for transition.

The interactions between elements (the essence of the technology of systems) determines the nature of and dominates the process (a feedback control process). Full understanding of these relationships is therefore essential. For example, a mission requirement for an $8g$ $P_g = 0$ maneuver at design condition might insure supremacy in a one on one dogfight but can result in excessive weight-cost penalty if the relationship between maneuver g and gross weight is particularly sensitive (Figure 5). If design goals are appropriately reduced, the savings (cost/benefit) can be applied in another manner such as the purchase of greater numbers of aircraft or weapons which in turn could have a greater overall military impact.

A better understanding of the structure of the process and the nature of results obtained can be gained from a brief review of the main considerations encountered in applying the process.

Development of the elements themselves leads to a major limitation of the process. Many of the elements and sub-elements are difficult to quantify. The credibility of the process becomes an issue as a function of confidence in the definition and understanding of the elements and the interactions between elements. The process has greatest payoff if fully understood but greatest efficiency if fully automated. The decision maker must consider both aspects and judgment based on experience predominates. The optimum level of manual interface should be based on whatever stimulates the most thinking. Insight, innovation and opportunity are the objectives. In other words, the decision maker is faced with the problem of determining to what degree computer results can (or should) be used to guide the decisions that must be made. The decision maker must judge the adequacy of the resulting numerical data as a representation of the real world. The role of the computer in any synthesis or analysis process is often challenged for lack of correlation and validation. The real world is far more subtle and complex than even the best computer models. Many models are trivial and the results are essentially known once the input is assembled. For a given air-to-air combat model, defining a missile with longer range capability than that of the threat, (technologies necessary to achieve high missile P_k are assumed), results in the obvious outcome, the longer range capability wins. The combination of a large number of questionable numbers still leads to questionable answers.

The computer can, however, fulfill several valuable functions. It can supply quantitative answers to a whole range of variations in parameters. It can, in particular, allow a wide range of assumptions to be systematically investigated on a consistent basis to provide guidance as to which factors are and are not important. It provides the opportunity for judgment and creative thinking to be directed at the right problems.

Direct answers can be supplied to many specific questions, particularly those relating to comparisons between well-defined physical characteristics of alternate systems. In many respects heavy reliance on computer use is the only way a quantitative "feel" can be gained for the relative sensitivities between potential investment areas, aerodynamic performance and avionics performance, for example. Further, in an indirect sense, the discipline involved in trying to quantify benefits and penalties in terms the computer can work with is often found to be a valuable contribution to clarifying important issues - the process itself is an important aid to understanding the problem.

As with any "optimal" process definition of the criteria for optimization (measures of merit) is most difficult. Fortunately, for technology assessment, identification of the "right" criteria is not essential (as it would be for a system development plan) and in fact much problem insight is acquired when the "technology criteria" itself is treated as a discrete variable. This is feasible as long as knowledgeable subjective selection of "trial" higher order criteria is accomplished.

Generation and understanding of measures of merit (MOM) to be applied to the process and constraints to be imposed on the process is an integral part of the analysis and results in enhanced insight to the problem. Optimization about a criterion can provide the system cost/benefit sensitivity to the criteria. Caution is essential when identifying trial criteria in order to insure effort is not wastefully expended on trivial or non-relevant problems.

Selection and generation of criteria to evaluate the payoff of technology (measures of merit) on the basis of return on investment equates to establishing a scoring procedure for measuring the importance ranking of technology. There are many ways to quantify benefit. Measures of aircraft performance have been the classical approach. Direct measures of military utility are the optimal or cost/benefit approach. Using air combat capability as an example, radius of action, sortie rate, exchange ratio, maneuverability, cost per target killed, targets killed per sortie, payload and targets killed per unit time are all measures of merit. Radius of action, maneuverability and payload relate to the classical approach. The remaining measures of merit relate to the optimal approach.

Since the orientation is towards return on investment, the investment required to achieve a given capability is always of major importance regardless of utilized MOM.

The credibility of cost projections is often an issue. Agreement on what "cost" encompasses and how it is defined is not universal. Accurate estimation of weapon system development and acquisition costs is difficult. Prediction of operational and maintenance costs over a reasonable life span is even more difficult.

The use of Life Cycle Cost (LCC), the total investment required over the peacetime life span of the system, is both convenient and common. The obvious drawback to LCC is that wartime "costs" are not accommodated. Also, there is temptation to ask the cost if a military capability or objective is not achieved. Rigid pursuit of an effectiveness goal can lead to unacceptable cost. Conversely, rigid pursuit of a cost goal can lead to an ineffective capability. Both are extremes and generally represent poor return on investment.

Any specified requirement by its nature effectively dictates the cost. For instance, a requirement for a probability of survival of .9999 against today's conventional weapon threat could result in the space shuttle as a solution. Unfortunately, a fleet of such vehicles would represent a very large investment. Imposing an additional requirement to effectively deliver a conventional weapon would greatly compound the problem and increase the cost. Payoff (return) must be balanced by reasonable investment in order for a solution to be realistic.

Probably the most difficult problem in deriving meaningful overall cost/benefit results lies in quantifying the threat system and defining its response to the large number of aircraft design and performance features that can be taken to evade or defeat it. Even against presently existing threats the problem is difficult, and it is greatly compounded when trying to evaluate systems designed to operate well in the future. All technology assessments depend on forecasts and judgments of technology in many areas, but technology development does not always progress as planned. This has been particularly a problem in the weapons area but it is also true of airframe and avionics related technologicals. If the problem is viewed as one of forecasting technology, the problem of forecasting the threat is the same as forecasting our own capability, for example, adequate definition of offensive missile weapon probability of kill (P_k) and the determination of overall sensitivity to that P_k is difficult in both cases.

One of the greatest difficulties in this regard is that advanced guided weapons tend either to work (in which case the target's probability of survival is near zero) or not to work (in which case the survival probability is near one). Whether or not the weapons do, in fact, work is typically a function of many factors - having or not having the right ECM, how much maneuver capability and threat warning time is available, the penetration Mach number and altitude, and etc. The role of tactics and the policy imposed for beyond visual range engagement are vital. The problem is particularly difficult in designing a system to be operated a decade or more in the future, because the threats can, at least in part, be responsive to aircraft design parameter improvements. For example, if aircraft are designed to overfly existing surface-to-air missiles, new missiles can be developed with higher altitude capability, or old ones can be upgraded by adding additional booster stage. For any system designed to operate 15 or 20 years in the future, it is, therefore, fundamentally impossible to put a high confidence level on any particular single answer concerning absolute survivability, no matter how "sophisticated" the analytical techniques.

But, analysis of the problem is not futile. It simply means that the analyses that are done must be placed in the proper context and directed at reasonable objectives. Even though future systems will face new threats, the nature of much of the threat will be relatively evolutionary with some possible revolutionary weapons, so current and recent historical experience can be used as a gross check on the validity of at least "singular case" results. The basic objectives of the analyses must be directed at gaining insight into regions of highest leverage in resolving the problem, rather than at obtaining highly detailed results for limited, specific, well-understood cases. The analyses also must establish whether or not the right problem was identified.

The process must operate within the framework of military fundamentals. Constraints are normally considered as fixed boundaries in an optimization process. As a result, the solution often lies on a constraint.

In the case of the cost/benefit analysis constraints are generally dictated by the mission to be accomplished and the scenario selected along with the threat environment in which the technology is applied and the concept must perform. Although parameters making up the mission, threat and scenario elements are often accepted by planners as fixed because of a perceived need and thus largely fixed for systems development synthesis/analysis (i.e., constrained), technology assessment by its nature stimulates variation of these elements (and parameters) for deeper understanding of the problem and identification of the opportunities for technology to impact the problem. Technology itself changes the constraints because it is always necessary to find a concept, tactic or technology to defeat a capability which the other combatant possesses. Hence, the technology assessment process can run unconstrained within practical limits. Constraints, however, can be far more subtle than a specified mission profile. A requirement to utilize a weapon (missile for example) on existing aircraft as well as the new aircraft for which it is to be designed, can result in severe restriction on design and carriage because of existing aircraft envelope constraints. The aircraft/store combination may induce unwanted reductions in range, speed and maneuverability over that exhibited by the basic aircraft. Store separation severely limits the launch envelope of most aircraft. Missile launch envelope is a complicated problem involving target speed, heading and maneuverability; aircraft launch speed, heading and angle of attack; missile seeker gimbal limits; radar detection range; target radar cross section; ground clutter; fuze time; and many other parameters. Blind adherence to a constraint such as a specific mission requirement may result in low return on investment and is indicative of not understanding the problem sensitivities. Also, a priori specification of constraints is an invitation to bias since part of the solution is already defined.

Problems of bias often result either from inevitable built-in preconceptions frequently manifested in starting conditions, baselines and overly restricted constraints including threat or scenario assumptions.

Even after a qualitative accounting of all the applicable constraints is accomplished, there is the difficulty of quantifying them. What level of survivability is acceptable? What is a probable level of investment to be allocated a new capability? Are numbers constrained? Real answers to such questions are not crucial for technology assessment but an understanding of the sensitivity to variations in the parameters is essential.

Results are very scenario dependent. The definition of the opposing capability and the environment in which the engagement is to occur drives the solution and may dominate it. The solution often lies on the constraint. Prioritization of missions and scenarios is not the domain of the technologist nor is threat definition. However, determination of the sensitivity of a technology assessment to variations in these elements is crucial to technological investment.

The general discussion should have made it apparent that the process is a familiar one to product oriented organizations and is based on familiar precepts. However, it should also be apparent that a great deal of input information and information processing is required. The application of the process by a technology oriented organization to focus investment is less familiar and the complexity of the process can be awesome. The risk is the potential for losing control of the process (relying on the process without understanding it). Much subjective judgment is required in problem setup and manual transfer of results from one element to the next. Often results from such analyses are used selectively to support a preconceived position and the objectivity of the process disappears.

The process is dependent upon availability of major tools including computer aided design, costing models and a variety of models measuring one-on-one and aggregate effectiveness and survivability. An enormous amount of data must be handled. The importance of proper information transfer between models cannot be overemphasized. A real danger for technology assessment is loss of single part benefit in the noise level. Each significant variation of mission, concept, or technology basically involves designing or sizing a new aircraft configuration, new weapons and new avionics resulting in further loop interactions, thereby avoiding or minimizing the problem of small disturbance or linear extrapolations being carried too far. Some results from a case study are presented as an example of the insight achieved for the potential application of technology to a generic problem area.

CASE STUDY

The basic military capability desired is autonomous night/all weather second echelon attack. The target set is comprised of both fixed and mobile elements. The problem is to identify technological payoff and associated concepts for an overall (military) maximization of return on investment. Initial figures of merit and the problem structure are postulated (Figure 6).

The numbers of aircraft delivering weapons over a specified period of time against a given target set will directly relate to the number of kills or effectiveness. It is postulated that total kills, sorties and kills per sortie are useful figures of merit. Hence, sortie generation is considered a key element in effectiveness and is a function at least of maintainability/repairability/serviceability, numbers available (impacted by initial buy, losses, etc.), weapons available and airbase condition.

Trends of the relationships between speed, maintenance hours per flight hour, initial numbers, cost and total missions flown per day are presented in Figure 7. The peaking in the missions per fleet day versus speed results from the reduction in mission time as speed increases, initially driving the missions up with increasing speed, and the significant increase in materials costs and required maintenance as speeds are increased beyond those currently employed finally driving the missions down again. The insight obtained is that the application of very high performance to solution of the survivability problem (in a fixed investment environment) is likely to result in a large reduction in sorties (fewer numbers, longer turn around times) which will correspondingly reduce effectiveness per unit time. Also, there is probably an optimum associated with a materials cost boundary.

Rather subtly, the issue of the relationship between effectiveness, survivability and numbers has been raised. Speed has been related to sorties (effectiveness) and cost. Next, the relationship between speed and survivability against an airborne intercept threat is considered. The issues of likelihood of encounter and of loss are addressed. Figure 8 presents a plot of encounter with airborne interceptor per sortie as a function of both penetrator and airborne interceptor speed. The curves are nearly asymptotic for conditions of the AI having the speed advantage and indicate that if the interceptor has a small speed advantage the probability of encounter is high but that if the penetrator has a significant speed advantage the probability of encounter is very low.

The loss rate summary chart shows trends in losses to an air intercept threat for Mach, altitude variations in the nominal speed and altitude range (Figure 9). The trend toward lower losses with increasing altitude and speed is expected. The combination of speed and altitude leads to consideration of areas of flight envelope sanctuary. It is expected that at very low altitudes the trend would reverse (with altitude) due to clutter (detectability) and maneuverability constraints but the emergence of lookdown, shootdown capability is to be reckoned with. The danger in adhering to a fixed threat is also apparent. The information does not indicate sensitivity to threat variation. Applying the trend information in an absolute sense implies zero loss rates are readily achievable at high altitude.

Consideration of the surface to air threat in the same manner (probability of encounter, probability of kill) leads to the conclusion that mid-altitudes and speeds are not the place to be. High and fast or low and fast may offer sanctuary. The issue of the relative cost to achieve a sanctuary vs that to deny it must be considered from an overall investment perspective.

Regardless of the absolute level of survivability, taken in isolation, it is not a full measure of military accomplishment. There is some form of offensive objective to be met. Usually, effectiveness is presented as a fixed value or a fixed rate one time assessment, (sorties per day, exchange ratio) but conditions can and do change with time in a non-linear fashion. The dynamic assessment of military capability provides additional problem insight. Figure 10 shows a comparison of targets killed as a function of time (in this case, days) for a high altitude/high speed penetrator, a very low altitude penetrator (with and without terrain masking) and a low observables penetrator. The initial high rate of kill for the high altitude penetrator is largely a result of a high sortie rate giving more initial missions. However, after a few weeks of warfare the losses which are higher than those for either the low altitude or low observables penetrator results in lower long term effectiveness. Note the very rapid decay in effectiveness for the low altitude penetrator without benefit of terrain masking. The sensitivity to terrain masking is pronounced. The zero day kill rates are high but very rapidly decrease to zero because of the high loss rate. It may be reasonable to conclude that for a very short war, kill rate is more important than loss rate and that as the war is lengthened, loss rate increases in significance. Get a lot of kills as early as possible.

The initial problem definition called for no particular prioritization of targets but target selection may be another parameter to which results are sensitive. Exploring this presents a perspective of cooperative effectiveness and survivability. It is expected that the survivability and the effectiveness for the penetrator will increase if a supporting force is used to suppress the opponents defenses. This leads to questioning the impact of applying early sorties of our penetrator force specifically to defense suppression (target prioritization) and then to attacking remaining targets. In Figure 11, attrition and accomplishment are shown as a function of time and the employment of defense suppression as the first task of the penetrator force. The trends are representative of the effect of defense suppression from either the use of additional forces applied to the defense suppression role or the timely dedication of a portion of the penetrator fleet to defense suppression. This can also be generalized to be representative of the trend of the effect of increasing survivability on effectiveness. Defense suppression pays off, particularly when applied early and when viewed for longer periods of time.

Having briefly addressed survivability and effectiveness, attention is now given to cost. We began by fixing the total cost so that cost is manifested in force effectiveness (but not single vehicle effectiveness) measured by capability achieved per dollar invested. The overall impact of technology is then directly measured by this factor and is seen in the numbers purchased, single vehicle capability and overall military effectiveness.

Cost per target kill was an initial figure of merit. Assessment of the impact of technology was a stated objective. Figure 12 presents trends resulting from the application of technology to the air vehicle part of the problem and shows improvement in cost/kill ratio as compared to an existing technology baseline. For the concept addressed, the cost of the weapon is the dominant parameter and working the aircraft technology in isolation does not have an overwhelming impact on cost. The "target" is actually a target mix which is dominated by mobile armor. A subset of the problem is shown in Figure 13 which presents trends in cost to kill a rail bridge with an inertially guided weapon as a function of target location error. In this case the target is fixed (non-mobile) and the weapon cost is not as high as the aircraft cost. Contrasting this to the previous aggregate cost per kill data provides insight to the difficulty in killing mobile armor and demonstrates the sensitivity of cost/kill to the selection of target set.

Additional consideration of the vehicle synthesis element and its role in the cost/benefit assessment is offered in Figure 14. For a fixed mission (range, payload) the sensitivity of takeoff gross weight to variations in penetration altitude and speed for a baseline supercruise configuration. The noteworthy points are that 36,000 pounds appears to be a minimum weight and that expanding the right hand side of the flight envelope (high dynamic pressure) will cause the expected weight penalty. The complexity of the analysis is better appreciated and additional insight acquired if one considered that the surface presented is a function of only two variables (speed and altitude) but that in reality takeoff gross weight is a function of many variables and an M dimension surface results. Adherence to a level of capability that is parametrically asymptotic is ill advised.

Trends in the impact of technology on air vehicle gross weight are presented (Figure 15) to show the potential for improvement in air vehicle efficiency. The comparison is sensitive to the selection of a baseline which is a result of subjective judgment.

The baseline chosen is based on perceived 1970 level technology which makes payoff (gross weight reduction) more sensitive to the application of advanced technology. The perspective to be gained in the air vehicle design iterations is that improvement resulting from combined advanced air vehicle technology is highly dependent on successful integration and design convergence/compromise and is at least as important as single technology improvement.

Nearly all new advanced air vehicle concepts being considered along with resultant projections of return on investment are highly dependent on the application of advanced composites to reduce size and cost to achieve a given capability. Figure 15 estimates a 25% reduction in TOGW for the application of advanced materials. A different perspective on the potential payoff for advanced composites is presented in Figure 16. Trends in weight and cost reduction through use of composites are shown with a useful limit identified (subjectively) at about the 50% level of incorporation. This perspective does not appear to offer as much promise of the previous one, but taken together the two offer a range of probable improvement. It is necessary to make the point that if a commitment to a new system were actually made today, the level utilized would be in the 10% range because the technology has not yet been transitioned. Thus, the results are also significantly impacted by technology availability (what technology will be used at what point in time).

The example case study was initiated with consideration of sortie generation to which we return from a different perspective as the closing step in the case study. A primary consideration in sortie generation is enemy action in opposition to that generation. The effectiveness of enemy action in deterring sorties will be a function of our air vehicles basing dependence and the operational condition of the base. One approach to reduction of sensitivity to enemy action is use of short field concepts for operations from both home base and from semi-prepared sites. Trends of air vehicle TOGW sensitivity are presented in Figure 17 as a function of ground roll for several approaches to short field capability. Proper identification of the real airbase/runway denial issues and all key technological elements is crucial. Synthesis may have to consider lift, acceleration, deceleration, rotation angle, low speed control, etc., and the dominant parameter is not self evident.

Full circle achieved. A summary of the problem insight is presented in Figure 18.

CONCLUSIONS

A change in technology planning strategy has occurred. The old perspective is now augmented and balanced by an additional one. New criteria for measuring the value of technology are being employed. The technology of systems will receive greater emphasis.

In the past, local area technology plans evolved from local area technology developments. Military payoff evolved in a random fashion. Prioritization was based on perceived opportunities to advance the technological state-of-the-art.

In the emerging scheme there exists a combination of planning inputs from both the opportunity for technological advancement and the opportunity for a military relevant prioritization for technology development. Prioritization is jointly based on advancing the state-of-the-art and opportunities available for technology to impact future requirements and capabilities.

The future will bring greater application and reliance on the cost/benefit process, but better understanding of rigor required as a function of objective is needed. A dilemma of more automation versus more understanding of basic principles will emerge.

The computer and associated analysis and synthesis methods are to blame and to credit.

REFERENCES

1. Nicolai, Leland M., Col, USAF: Changing Requirements in Aircraft Design, *Astronautics & Aeronautics Journal*, pp. 22-31, June 79.
2. New Strategic Airlift Concepts Study, AFFDL-TR-3051, Vols I-III, Boeing Aerospace.
3. New Strategic Airlift Concepts, AFFDL-TR-3062, Vols I-V, Douglas Aircraft.
4. B. I. Rachowitz, V. J. Pulito, M. Izzi: Modular Life Cycle Cost Model For Advanced Aircraft Systems Phase II, Vol I, Cost Methodology Development and Application, AFFDL-TR-78-40, Grumman Aerospace Corporation, dated April 1978.
5. S. C. Jensen, E. A. Barber and I. H. Rettie: The Role of Figures of Merit in Design Optimization and Technology Assessment, AIAA Paper 79-0234 presented at 17th Aerospace Sciences Meeting, New Orleans LA, January 15-17 1979.
6. P. G. Osterbeck, R. C. Sutton and L. D. Hawkins: Introducing Cost Effectiveness into the Tactical Airplane Design Cycle in a Cost Effective Manner, AIAA Paper 79-0235 presented at 17th Aerospace Sciences Meeting, New Orleans, LA, January 15-17 1979.

THE PROCESS

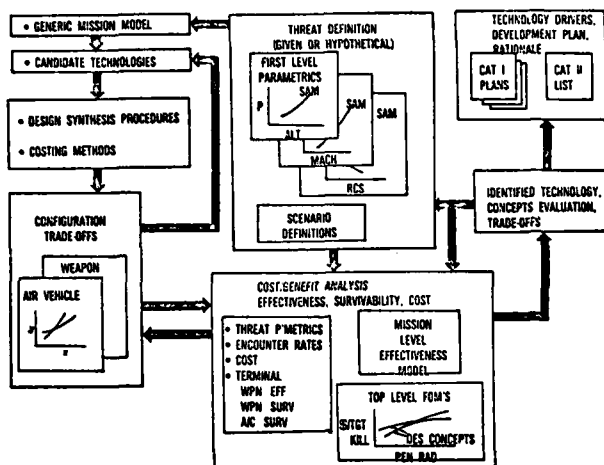


FIGURE 4 DIAGRAM OF THE PROCESS

PERFORMANCE-GROSS WEIGHT TRADEOFFS

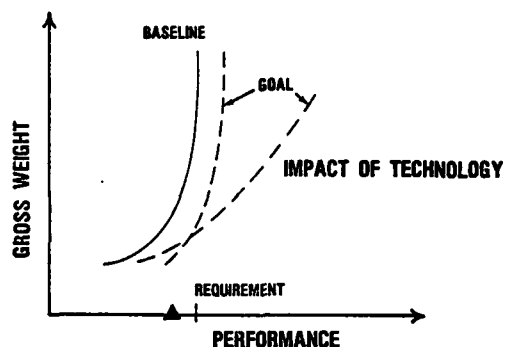


FIGURE 5 PERFORMANCE/COST SENSITIVITY

PROBLEM

AUTONOMOUS NIGHT ALL WEATHER SECOND ECHELON ATTACK

MEASURES OF MERIT

- COST PER KILL
- TOTAL KILLS
- SORTIES
- KILLS PER SORTIE
- LOSSES
- PROBABILITY OF SURVIVAL
- LIFE CYCLE COST

1. SURVIVABILITY

- HOW DO WE BEAT THE THREAT?

- DETECTABILITY
- SUPERCRUISE
- STANDOFF WEAPONS
- ECM
- ACTIVE DEFENSE

2. LETHALITY

- HOW DO WE FIND AND KILL THE RIGHT TARGETS?

- EXTERNAL AIDS
- SAR
- FLIR
- GUIDED WEAPONS
- UNGUIDED WEAPONS

3. EFFICIENCY

- HOW DO WE STAY WITHIN THE COST CONSTRAINT?

- UNDERSTAND TOTAL PROBLEM
- THE RIGHT DESIGN REQUIREMENTS
- THE RIGHT TECHNOLOGIES
- CONSCIOUS EFFORT

FIGURE 6 PROBLEM STRUCTURE

SORTIE RATE TRADES

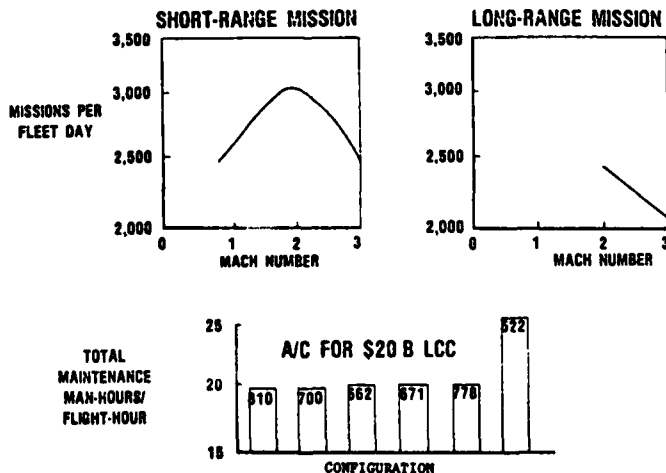


FIGURE 7 SORTIE RATES

TYPICAL ENCOUNTER-GENERATION SENSITIVITIES

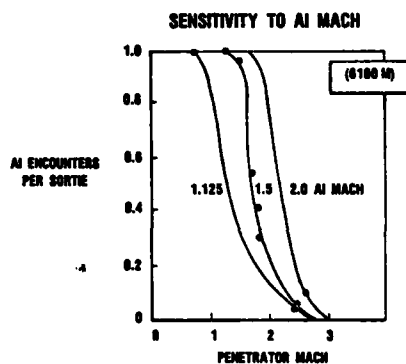


FIGURE 8 PROBABILITY OF ENCOUNTER

LOSS RATE SUMMARY - AI THREAT

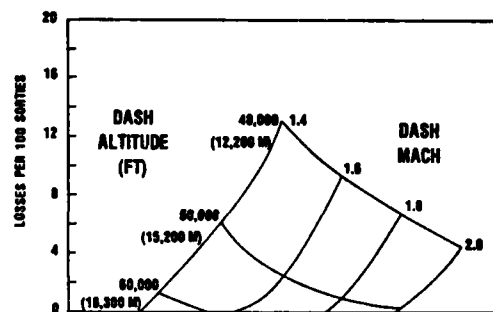


FIGURE 9 LOSS RATES

TARGET KILLS

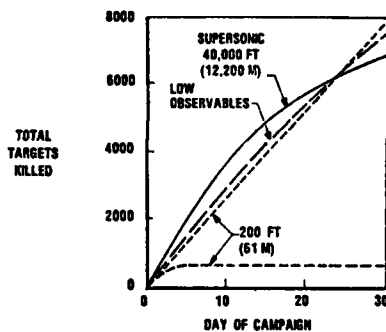


FIGURE 10 TARGETS KILLED

TYPICAL CAMPAIGN RESULTS

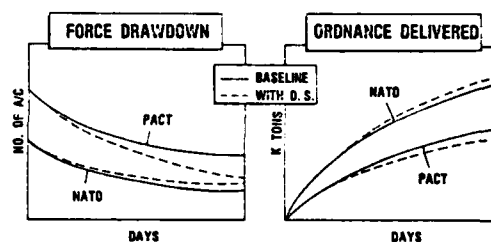


FIGURE 11 DEFENSE SUPPRESSION

COST PER TARGET KILL

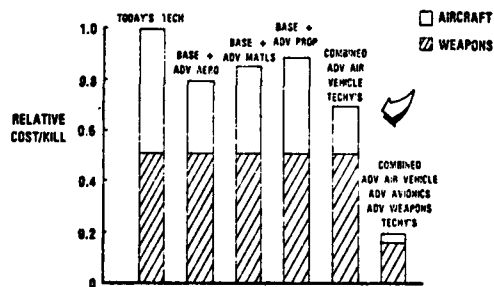


FIGURE 12 IMPACT OF TECHNOLOGY ON COST PER KILL

COST PER RAIL BRIDGE VS TARGET LOCATION ERROR

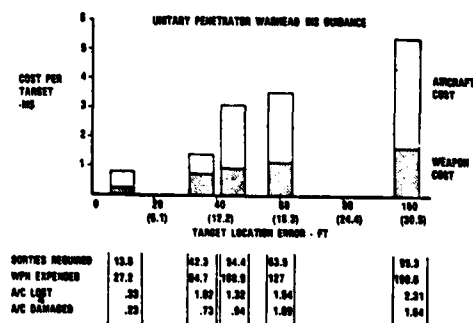


FIGURE 13 A SUBSET OF COST PER KILL

TOGW SENSITIVITY TO SPEED AND ALTITUDE

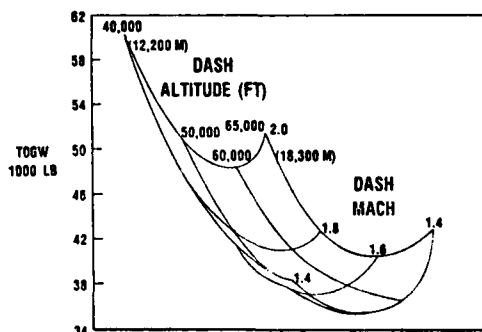


FIGURE 14 TAKEOFF GROSS WEIGHT SENSITIVITY TO DESIGN SPEED AND ALTITUDE

AIR VEHICLE TECHNOLOGY IMPACT ON TOGW

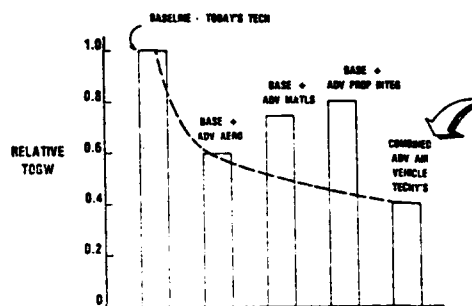


FIGURE 15 IMPACT OF TECHNOLOGY ON GROSS WEIGHT

SENSITIVITY TO COMPOSITES

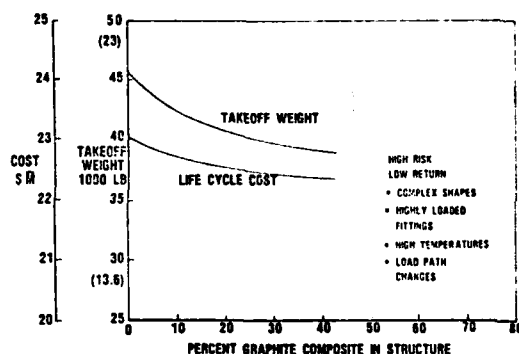


FIGURE 16 COST AND WEIGHT TRENDS WITH COMPOSITES

STOL SIZING TRENDS

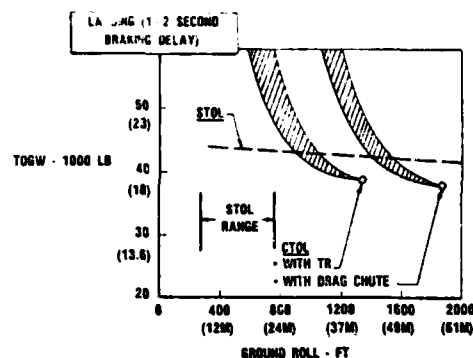


FIGURE 17 TAKEOFF GROSS WEIGHT SENSITIVITY TO LANDING GROUND ROLL

ANSWERS TO KEY QUESTIONS

SURVIVABILITY - AIR VEHICLE ALTERNATIVES, STANDOFF, ECM

LETHALITY - EXTREME DEPENDENCE ON WEAPONS, SAR

EFFICIENCY - CONCEPT IS THE COST DRIVER, TECHNOLOGY CAN MINIMIZE

ALTERNATIVES	TECHNOLOGY
HIGH & FAST	WEAPON SIZE SAR & ECM (SIGNATURE) SUPERCruise (WORKLOAD)
LOW & FAST	WEAPON SIZE SAR & ECM SIGNATURE T/F/T/A (WORKLOAD)
LOW SIGNATURE	WEAPON SIZE SAR & ECM AERO/SIGNATURE T/F/T/A (WORKLOAD)

IMPERATIVES AND OPPORTUNITIES

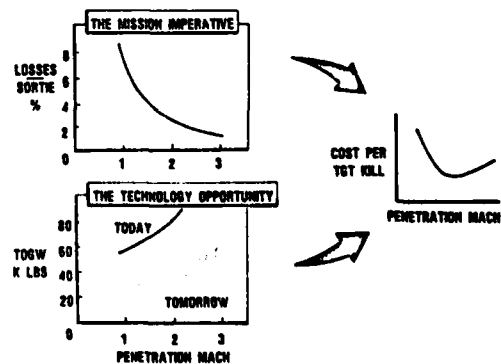


FIGURE 18 PROBLEM INSIGHT

AN ACCEPTABLE ROLE FOR COMPUTERS IN THE AIRCRAFT DESIGN PROCESS

Thomas J. Gregory

Chief, Aircraft Aerodynamics Branch

and

Dr. Leonard Roberts

Director, Aeronautics and Flight Systems

NASA Ames Research Center

Moffett Field, California 94035, USA

SUMMARY

The role of the computer in aircraft design appears to be increasing. And the role of the technical specialists and the aircraft designers who use computers significantly also appears to be increasing. This trend toward more computerization has not been wholly accepted, especially by those in decision-making or managerial roles who must rely on the computer-generated results. Many of these people have relied on measured data and other engineering approaches to design successful aircraft in the past.

Some of the reasons why this computerization trend is not wholly accepted have been explored for two typical cases: (1) computer use in the technical specialties and (2) computer use in aircraft synthesis. The factors that limit acceptance are traced, in part, to the large resources needed to understand the details of computer programs, the inability to include measured data as input to many of the theoretical programs, and the presentation of final results without supporting intermediate answers. Other factors are due solely to technical issues such as limited detail in aircraft synthesis and major simplifying assumptions in the technical specialties. These factors and others can be influenced by the technical specialist and aircraft designer. Some of these factors may become less significant as the computerization process evolves, but some issues, such as understanding large integrated systems, may remain issues in the future. Suggestions for improved acceptance include publishing computer programs so that they may be reviewed, edited, and read. Other mechanisms include extensive modularization of programs and ways to include measured information as part of the input to theoretical approaches.

INTRODUCTION

Computers are used extensively in the aircraft design process. However, the scope and effectiveness of their use are sometimes considered suspect, especially by managers and decision makers who must depend, to some extent, on computer-generated results. What causes this suspicion? Can it be allayed? Is there hope for better acceptance? Perhaps some insight can be gained into these questions by examining typical cases in aircraft design and noting faults in these non-ideal, but realistic, situations. Then it may be possible to postulate adjustments that overcome these faults and help improve the acceptance of computers in aircraft design.

There are two cases where large-scale computers are used extensively in aircraft design. The first is in the technical specialty areas where sophisticated theoretical methods have been combined with repetitive calculation powers of the computer. Computational aerodynamics (refs. 1-3), finite-element structural analysis (ref. 4), and trajectory optimization (ref. 5) are examples of fields where these tactics have given definitive technical detail. The second major area is in aircraft synthesis (refs. 6-8). Here the emphasis is on combining all the technical specialty areas so that an integrated design solution is achieved quickly and with low resource expenditure. These design synthesis programs are in use in practically every company and government agency.

An example of each of these areas will be discussed and the focus will be on the concerns in each case that lead to low acceptance by the users of the computer results. (The developers of computer programs are much more content with the results although they also have some similar concerns.)

Concluding remarks will attempt to forecast the evolution of computer use in aircraft design and suggest some ideas to improve acceptability in the future.

CASE 1 - COMPUTER USE IN THE TECHNICAL SPECIALTIES

The technical specialist contributes to the design process when the initial vehicle concept is defined - that is, when the aircraft overall size, shape, and relative placement of components are loosely known. However, there is still uncertainty about the details of the aircraft geometry, aerodynamic flow, and structural loads and deformations. In a typical case the specialist starts with an aircraft configuration that has some specific geometric boundaries but has considerable latitude with the geometric details between these boundaries. For example, the location of engine and landing gear cavities may dictate outer and inner contours as well as the main structural members at specific locations on the aircraft. However, the design specialist has considerable freedom in specifying the details at and between these locations.

At the present time, each specialist usually decides to use a major computer program to analyze the details in his discipline. The computer program usually requires extensive input information, especially the type that comes from other technical specialties. To a large extent, this input information is not specified by the designer or his drawing. The specialist spends substantial resources preparing this input either by computation or assumption. The computer program may be run several times with adjusted inputs so that an efficient design results. In many cases, it is also necessary to modify the programs to account for special features on the aircraft. For example, in the case of using potential flow programs it has been necessary to make major modifications to allow for wing-canard interactions on some of the new fighter designs.

The results from the first computer calculations are used to build test models, both aerodynamic and structural. The measured data from these tests are compared with computed results. The comparison information is used to modify and/or enhance the next configuration iteration.

The above description is typical, but fails to mention the shortcomings that reduce the acceptability of the results and the efficiency of the process. Some of these shortcomings are discussed next. First, the input to large computer programs is in many cases very rigid and demanding of resources. For example, in aerodynamic paneling programs, the needed geometry definition is quite detailed and must be specified in terms of three-dimensional coordinates at the corners of each panel element. Figure 1 shows a wind-tunnel model and its geometric representation which is made up of approximately 200 parametric cubic spline patches (ref. 9). Each curved patch contains many quadrilateral panels (not shown) that are used in aerodynamic paneling programs. Minor flaws in the geometric input usually cause the aerodynamic programs to fail without achieving the intended results. The substantial resources needed to supply the error-free input have caused many potential users to avoid extensive use of this particular computational approach.

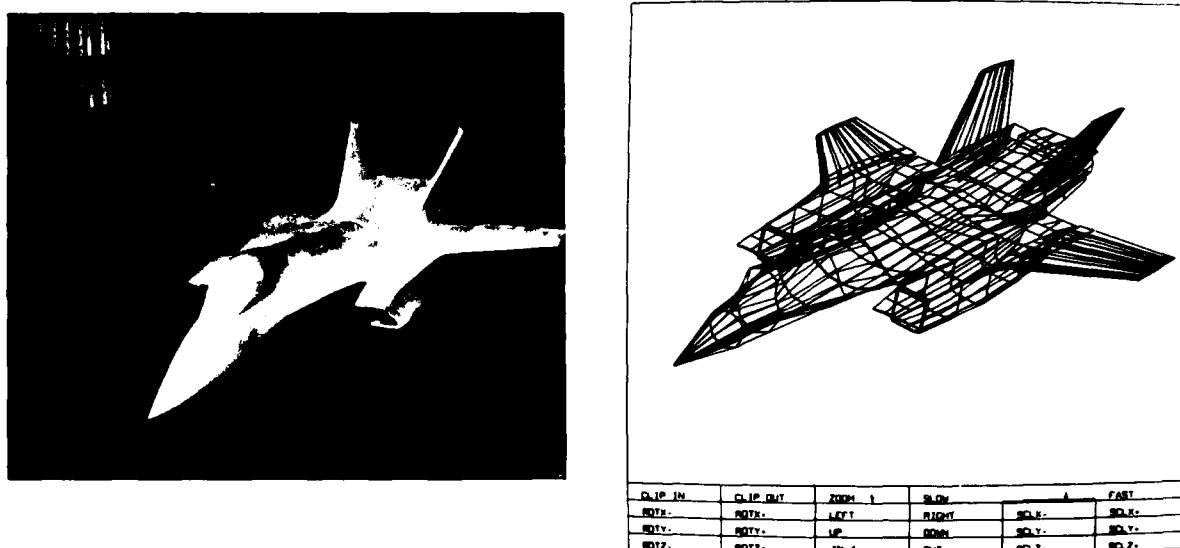


Fig. 1 VSTOL fighter model and geometric representation.

A second shortcoming is that numerous assumptions, often quite coarse, are needed to generate the input to make the geometry and aerodynamic programs operate on realistic cases. Often these assumptions overwhelm the fine detail that is inherent in the sophisticated methods. This is particularly true in the case of the flow-field geometry definition for aerodynamic calculations. Figure 2 shows the calculated leading-edge vortex location above a highly swept canard airfoil (refs. 10, 11). In the practical application of paneling methods, the effect of this major flow phenomenon is not included. (Current research (ref. 12) is addressing this topic.) Omitting this and other major flow phenomena reduces the utility and therefore the acceptance of these powerful approaches.

Computer results usually come in the form of voluminous listings that must be interpreted and digested. This effort, which can take considerable time, is most instructive to the analyst but adds little to the understanding needed by the end user or decision maker. The end user may have a general idea about the technique used in the computer program but it is the intermediate data from the calculations that give assurance that the final results are reasonable. It is particularly disturbing to have final answers that "look reasonable" but have intermediate ones that do not. An example (fig. 3) from potential flow calculations is the oscillation of calculated pressures from one paneling point to the next. These situations, which are caused by special geometric situations, may give good overall forces and moments, but are not acceptable in terms of satisfying the users that the computational process is sound. In this case, the analyst and/or specialist may have sufficient experience to overcome the difficulties by small adjustments of the geometric input. Or he may simply ignore the oscillations because he considers them to be insignificant or easily fixed. Again, the end user becomes uncertain about the acceptability of the results. (In the example shown, the theory has been reformulated in the development program (ref. 13) and the oscillations are not generated; in earlier programs, the possibility of an oscillation still exists.)

A key issue in the above discussion is that in many instances the input and intermediate data are not presented or discussed adequately. This omission is due to the typical way computed results are output — by large tabulated listings of intermediate quantities. This format is not amenable to summarization. In many cases, preparation time is not budgeted for summarizing intermediate results since the final results are of primary interest. The result is low acceptance of the answers.

As the design proceeds, usually there is new information in the form of test data. As this and additional information accumulates it is often difficult to integrate it with the purely theoretical technique that the computer programs are usually based on. Figure 4, for example, shows the VSTOL wind-tunnel model (ref. 14) with pressure orifices in key locations. The measured data from these orifices currently cannot be used as input to the previously described paneling program. Adjustment factors may be developed (or rationalized) to account for the discrepancies between the measured and calculated final results, but there is uncertainty whether these factors apply to the next configuration change. This uncertainty and the fact that the measured and calculated data cannot be easily combined often leave the project manager or designer

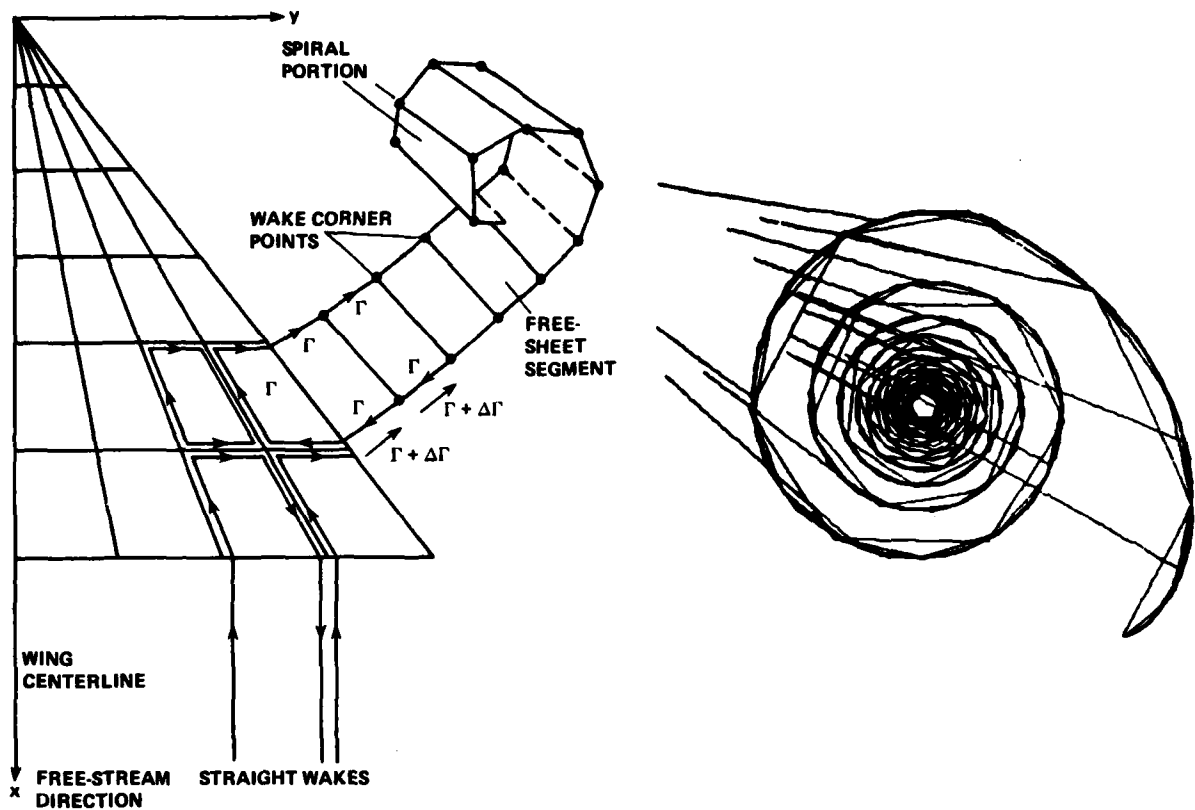


Fig. 2 Theoretical leading-edge vortex roll up.

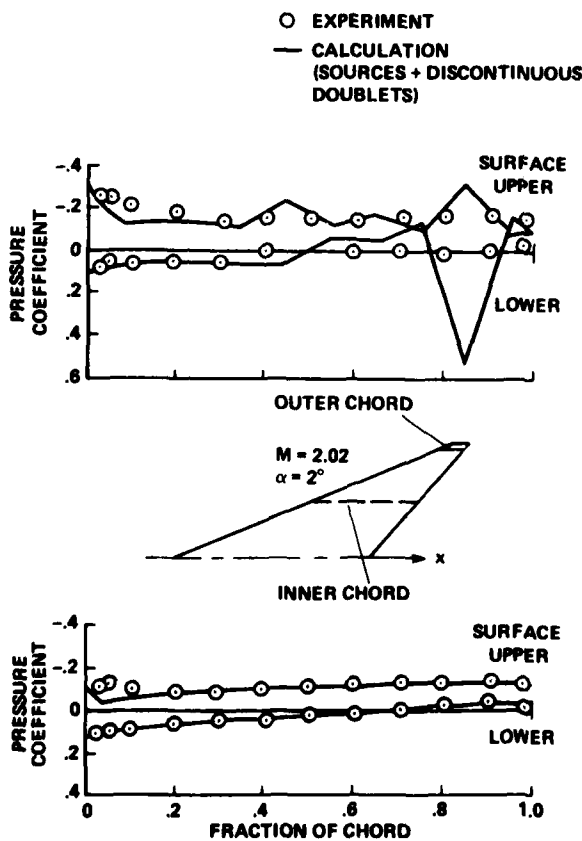


Fig. 3 Pressure oscillations in paneling programs.

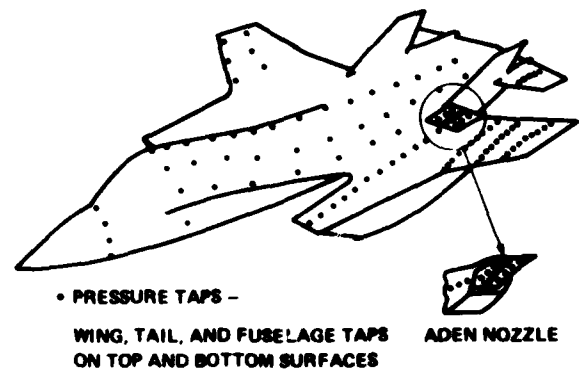


Fig. 4 Measured data on a VSTOL model.

with an uncomfortable choice. He usually elects to use the measured data as the basis for the design credibility. This means, in effect, that the computed results have lower acceptability.

Another factor that leads to low acceptance is the difficulty in checking the logic flow in large computer programs. In many cases, the general idea can be expressed easily, but when the details are studied the logic flow can be extremely difficult to follow. This is different than following a noncomputerized procedure for several reasons.

First, the computerized logic is usually implemented in a computer language, such as Fortran, that is cryptic to people not skilled in programming. Second, the name of variables may not be mnemonic, i.e., the variable name and computer language symbol do not easily correlate for the reader. Third, the logic flow in the programs can become extremely complicated and still work. In many instances, the logic has been developed by adopting a series of "fixes" or

"patches" after discovering a series of flaws during testing and use. These usually occur when special situations are encountered. The result is that the program will work for previously tested cases, but may not work or may not give correct answers for slightly dissimilar cases.

- **MASSIVE INPUT, CODE AND OUTPUT**
- **SIGNIFICANT SIMPLIFYING ASSUMPTIONS**
- **CODED AND COMPLEX LOGIC**
- **INTERMEDIATE RESULTS PRESENTATION**
- **LIMITED REVIEW AND APPROVAL**
- **SIGNIFICANT OPERATING COST**

Fig. 5 Acceptability factors in the technical specialties.

In addition, many technical specialty programs are extremely large; in some cases, they may have tens of thousands of coded statements. The investment needed to understand, implement, and/or operate the programs involves significant resources. If only a few groups have made this investment, then there is not a community of users that typically express opinions about its credibility, utility, concerns, etc. This leads to a general uncertainty about the program which lowers its acceptance.

The items above suggest that the program developer can trace logic through intermediate and final results, but others usually do not. Therefore, the end user depends solely on the program developer and has little means for adequately reviewing the work. These circumstances lead to lower acceptance of the computer-generated results.

Figure 5 summarizes several factors that affect the acceptance of computer-generated results in the technical specialties.

CASE II - COMPUTER USE IN AIRCRAFT SYNTHESIS

Large aircraft synthesis programs are used in the conceptual design phase to integrate all the disciplines and get a combined answer that indicates the overall feasibility of the project. In the usual case, it is necessary to simplify the computations in each of the discipline areas so that the computer program is manageable in terms of both the project team size and the available computer power. In aircraft synthesis, the inputs and outputs of each discipline are connected, and it is not as necessary as in the previous case to assume inputs from one discipline in order to make detailed computations in another. Figure 6 shows that typical synthesis programs are modularized by discipline and in some cases the sequence of calculations is controlled by a separate module. After the program has been developed and/or modified for the particular aircraft design case of interest, trade studies are conducted to find the best combination of design parameters that meet the mission specifications. This process, called optimization, can be done automatically (refs. 6, 15), but it is usually augmented by manual tradeoffs. The output from the aircraft synthesis process is quantitative information on which to select a preferred configuration for further design work.

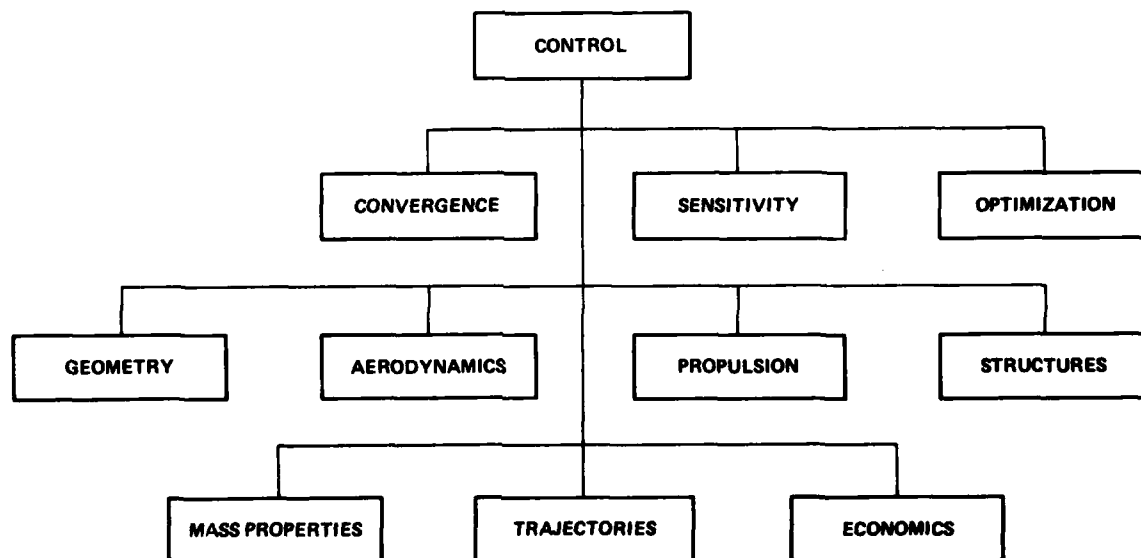


Fig. 6 Synthesis program functions.

A number of factors lead to low acceptance of this process. An important one is due to the technical specialist himself, who believes the simplifications used in the aircraft synthesis process are indeed oversimplifications. This attitude comes from an understanding of all the factors that go into each technical specialty and a general unawareness that many of these factors are accounted for by sweeping empiricism. This difficulty in acceptance again relates to the fact that intermediate results are not presented. In many cases, it is possible to allay the concern for oversimplification, if, in fact, test data from previous aircraft projects are compared with the calculated results. This usually shows that the simplifying algorithms used in the aircraft synthesis may, in fact, correlate well with historical data. Where the correlation is poor it is usually possible to show the sensitivity of the final result to the parameter in question. Again, the difficulty is in budgeting sufficient time for preparation and presentation of this intermediate data during briefings and reportings.

While the logic in the technical specialty programs is involved, the logic in most synthesis programs is even more so. The difficulty here is that the design process in aircraft synthesis is very iterative and there are multiple, nested-iteration loops that are needed to converge a design and perform tradeoff studies. The explanation of this looping process is usually unclearly written or described and leads many viewers or observers to doubt the credibility of the process. It is particularly unsatisfying when a reviewer asks for reasons why a configuration parameter has been selected and the answer is that an extensive iterative search was made to find the optimum value of the parameter. For the particular parameter in question, the aircraft synthesizer may not have graphic material that explains the basis for selecting the value of the parameter. Several parameters may be interrelated or be a function of several others. An example is shown in figure 7, which describes the sizing of both the propulsion system and the wing on a VSTOL fighter (ref. 16). In this case, the particular mission was specified and the best combination of wing size and engine size was the result of many iterated computer solutions. In the case of major parameters like wing size and engine size, design charts such as this are presented; however, for other parameters such as thickness-to-chord ratio, a chart such as this may not have been prepared or presented. In this case it is difficult for the aircraft synthesizer to explain the selection of the value of the thickness-to-chord ratio without such graphic information.

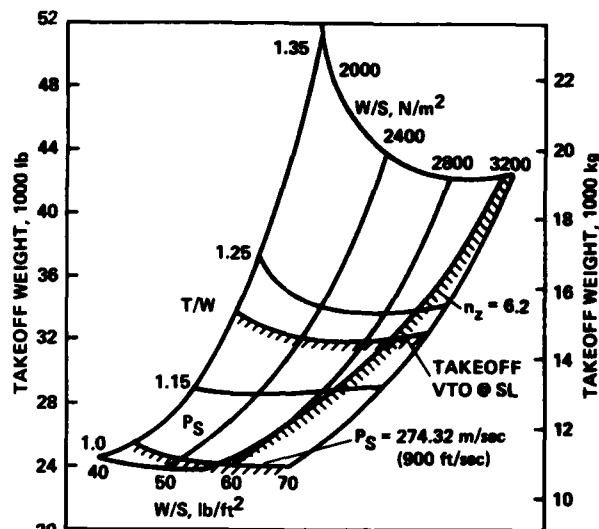


Fig. 7 Design results.

Another factor that relates to the ones above is the expectations of the reviewers or end users of the information. In many cases, reviewers or users want more technical depth in the aircraft synthesis process. Usually the depth is limited by the budgeted resources and/or the computer facility. In many cases, the users would like to have a detailed design or a very good preliminary design in place of the conceptual design that is the usual output from the synthesis process. Therefore, the primary factor that leads to low acceptability here is that the objectives of the process are not clear. That is, the objective of the aircraft synthesis process is to select aircraft design parameters that will permit a more detailed study in the detailed design or prototype design phases. Clear descriptions of the objective are crucial to acceptance. Figure 8 summarizes several factors that affect the acceptance of aircraft synthesis.

- TECHNICAL DEPTH
- COMPARISON WITH DATA
- SENSITIVITY TO UNCERTAINTIES
- INTERMEDIATE RESULTS PRESENTATION
- COMPLEX LOGIC FLOW
- OBJECTIVES CLARIFICATION

Fig. 8 Acceptability factors in aircraft synthesis.

PROJECTED EVOLUTION OF CASES I AND II

The obvious question at this point is: why aren't the detailed calculations in the technical specialties combined with the aircraft synthesis calculations? The answer is that, at the present, the computer power of even the largest computers is not adequate, but probably will be in the future. However, even with more powerful computers, some modifications to the present processes are anticipated. For example, the levels of detail will exceed the one or two levels implied previously, i.e., one level for synthesis and another in the technical specialties. It is expected that there will be several levels of detail in each discipline and that the aircraft synthesist and a technical specialist will work as a team. In the initial design phases, the levels may be appropriately quite simple and, as the vehicle definition becomes more detailed, the levels of technical computation will become more detailed. Figure 9 shows how the aerodynamics methods can range from simple empirical estimates from charts through several levels of aerodynamic calculations to measured wind-tunnel data. The other technical disciplines have similar levels.

The process of combining several levels will require more modularization of each of the technical specialties. The data communication between the disciplines may become more sophisticated. Fortunately, emerging computer technology in both hardware and software will aid this activity. Computer technology will also aid the display of intermediate results. However, the integration of the detailed technical levels will still be limited to some extent by the power of even the largest computers envisioned. Distributed computing facilities may alleviate this limit, but will tax the data base and communications technology.

Measured data at the present time and in the future will continue to be the most convincing element in the definition of the future airplane design. There is a need to find theoretical techniques in the technical specialty areas that include test data as an integral part of the calculated results. This is accomplished to some extent in the synthesis process by the modification of purely theoretical approaches by empirical or historical information. However, in the technical specialties, most of the purely theoretical approaches leave little opportunity to include test data as part of the input to these approaches (fig. 4). In the future, it may be possible to reformulate the theoretical approaches to accept test information as part of the input process.

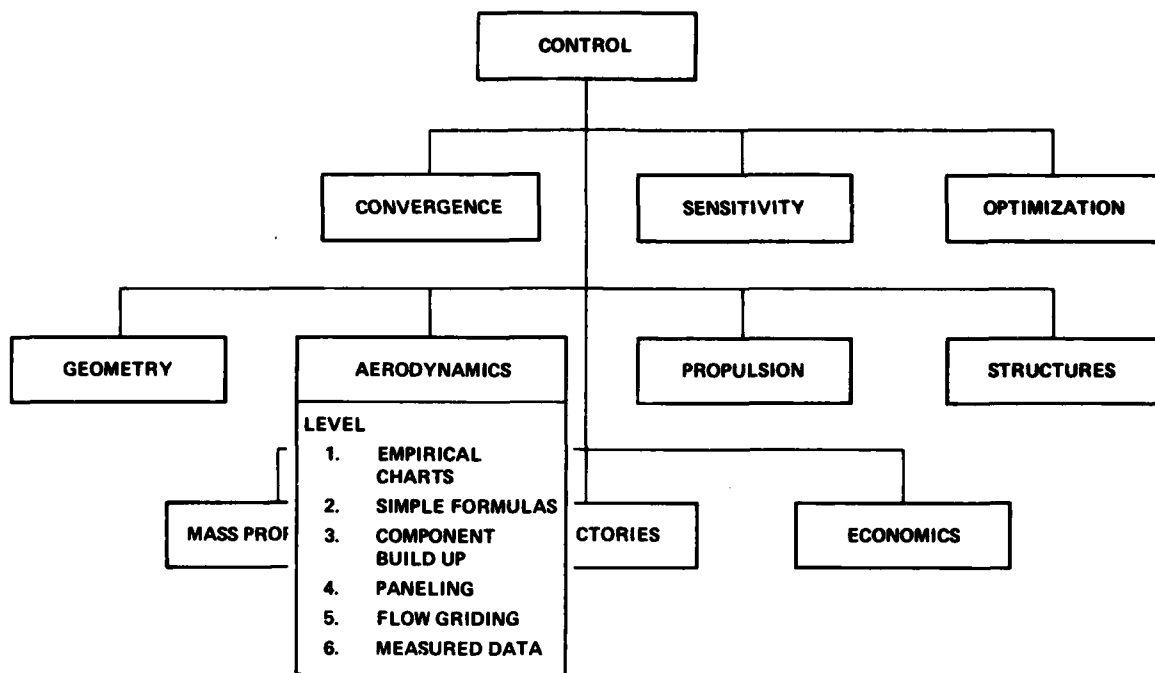


Fig. 9 Aircraft design functions and levels.

One of the key factors in the acceptance of computer-generated results will be whether the programs themselves are readable by the technical community. This calls for the development of computer codes that use standard programming languages, which in the future should be readable by all engineers. Computer programs that are documented within the code itself will be more readily accepted since reviewers can more easily spot check the logic, the algorithms, and the overall architecture of the computer programs. This is an entirely different prospect than in current practice. It will be important that the algorithms that describe technical computations be reviewed and edited much the way scientific journals are in the present. Just as any language can be written clearly, concisely, and with great readability, it is also possible to write with confusion, wordiness, and complexity. Before computer programs can be fully accepted it will be necessary that they be written clearly, reviewed, edited, and published. Then the intrinsic factor in acceptability — which is understanding — can be met.

Modularity, which has been discussed as an aid to understanding and implementing synthesis programs, also enhances their readability. It is also extremely effective in clarifying the discipline computations that specialists understand. In fact, people with good engineering backgrounds should be able to read modular programs. If modularity is accomplished, the data communications between separate discipline modules become the key to understanding. It becomes imperative to know what is input for one module and what is output for another, and where the origin of all parameters is located. Understanding how the data is communicated is almost impossible in large nonmodularized programs.

Finally, it will be important to expend much more effort on defining and explaining some of the very complex and highly original algorithms currently in use to conduct matrix computations and complicated convergence loops. In many cases, fluid dynamicists, structural analysts, etc., do not describe these iteration processes well enough since they often are more appropriate for computer science or numerical analysis papers than for papers in fluid dynamics or structures. Consequently, this extremely important part of the engineering process is sometimes lightly covered during reporting.

- **EXTENSIVE MODULARIZATION**
- **INTEGRATE MEASUREMENTS WITH THEORY**
- **PRESENT INTERMEDIATE RESULTS**
- **PUBLISH PROGRAMS**

Fig. 10 Acceptability improvers.

In summary, the acceptance of computer-generated results in the future will depend on several items, including: integration of measured data and theory, presentation of intermediate results and assumptions, and good programming practice and review process (fig. 10).

CONCERNS FOR THE FUTURE

Even if computer usage in the technical specialties and in aircraft synthesis evolves as described above, and even if the prospective enhancements are adopted, there will continue to be concerns about the use of computers. One expected concern stems from the prospect of integrating the synthesis process and the technical specialties. This concern is that the complexity of the process will become so enormous that even the most astute computer scientists and designers on the team will not be able to adequately understand the total process. While modularity and good programming practice will certainly aid understanding, there is a point at which the scope and depth of the potential computational system of the future will be beyond the capabilities of a single individual or even small groups of individuals.

Another concern stems from the prospect of combining measured and calculated information in the design of an aircraft. While the proper use of both measured and calculated data will certainly give aircraft design the most credibility, it may be difficult to discern the extent to which the airplane is based on test data, empirical information, or totally theoretical approaches. At this point, it may be difficult to assess the risk in taking the airplane to production or flight test. The measure of risk may be based largely on the record of the computational system in predicting the performance capability of existing aircraft. As the computational systems evolve, they may develop success records much the way design teams have in the past.

REFERENCES

1. Rubbert, P. E., and Saaris, G. R.: "Review and Evaluation of Three Dimensional Lifting Potential Flow Analysis Program for Arbitrary Configurations," AIAA Paper 72-188, Jan. 1972.
2. Woodward, F. A.: "Analysis and Design of Wind-Body Combinations at Subsonic and Supersonic Speeds," *J. Aircraft*, Vol. 5, No. 6, Nov.-Dec. 1968, pp. 528-534.
3. Hess, John: "Calculation of Potential Flow About Arbitrary 3-D Lifting Bodies," Douglas Report MDCJ-5679-01.
4. Butler, T. G., and Michel, D.: "NASTRAN-A Summary of the Functions and Capabilities of the NASA Structural Analysis Computer System," NASA SP-260, 1971.
5. Hague, D. S., Jones, R. T., and Glatt, C. R.: "Combat Optimization and Analysis Program," Vols. 1-4, USAF-AFFDLTR 71-52, May 1971.
6. Gregory, T. J.: "Computerized Preliminary Design in the Early Stages of Vehicle Definition," AGARD-CP-147, Vol. 1, June 1974.
7. Oman, B. H.: "Vehicle Design Evaluation Program," NASA CR-145070, Jan. 1977.
8. Meyer, D. D.: "Development of Integrated Programs for Aerospace Vehicle Design (IPAD)-Reference Design Process," NASA CR-2981, March 1979.
9. Roland, D. P.: "Parametric Cubic Surface Representation," Paper presented at the NASA Ames Workshop on "Aircraft Surface Representation for Aerodynamic Computation," March 1-2, 1978.
10. de Silva, B. M. E., and Medan, R. T.: "Vortex Effects for Canard Wing Configurations at High Angles of Attack in Subsonic Flow," NASA TM 78543, Dec. 1978.
11. de Silva, B. M. E., and Medan, R. T.: "User's Manual for Interfacing a Leading-Edge Vortex Rollup Program With Two Linear Panel Methods," NASA TM 78564, April 1979.
12. Johnson, F. T., and Tinoco, E. N.: "Recent Advances in the Solution of Three Dimensional Flows Over Wings with Leading-Edge Vortex Separation," AIAA Paper 79-0282, Jan. 1979.
13. Ehlers, F. E., Epton, M. D., Johnson, F. T., Magnus, A. E., and Rubbert, P. E.: "A Higher Order Panel Method for Supersonic Flow," NASA CR-3062, May 1979.
14. Nelms, W. P.: "Studies of Aerodynamic Technology for VSTOL Fighter/Attack Aircraft," AIAA Paper 78-1511, 1978.
15. Vanderplaats, G. N.: "Automated Optimization Techniques for Aircraft Synthesis," AIAA Paper 76-909, 1976.
16. Brown, S. J.: "Study of Aerodynamic Technology for VSTOL Fighter/Attack Aircraft-Horizontal Altitude Concept," NASA CR-152130, May 1978.

THE USE OF COMPUTER BASED OPTIMISATION METHODS IN AIRCRAFT STUDIES

by

Brian Edwards

Aerodynamics Department, Royal Aircraft Establishment,
Farnborough, Hampshire, GU14 6TD, England

SUMMARY

The paper is about multivariate optimisation (MVO) computer programs in the field of aircraft design. The constitution of such programs, which embody an optimisation method as well as a mathematical model of aircraft design and operation comprised of aircraft design synthesis and performance analysis methods, is discussed in general terms. The main part of the paper is concerned with some techniques for using MVO programs and seeks to show how the optimisation method can be used to explore the model and cultivate an insight into its characteristics. The paper concludes with a discussion of some possible applications for MVO programs.

NOTATION

A	wing aspect ratio
BTAA	flap angle during approach to landing
CLA	lift coefficient during approach to landing
CLCR	lift coefficient at start of cruise
COF	compound objective function
DOC	direct operating cost
ELES	slat chord/wing chord
ETE	flap chord/wing chord
HCR	height at which aircraft is designed to cruise
HCR1, HCR2	particular values of HCR
MENG	installed mass of engines
MSSCR	aircraft mass at start of cruise
MTO	aircraft mass at take-off
OF1, OF2	particular simple objective functions
PFUEL	price of fuel
QCR	dynamic pressure in cruise condition (VCR, HCR)
RATING	an engine re-rating parameter which maintains constant time between overhauls
S	wing reference area
SFIN	fin area
SFIN1	fin area required for weathercock stability
SFIN2	fin area required to cope with engine failed case
SWP	angle of sweepback
TC	wing thickness/chord
VCR	speed at which aircraft is designed to cruise
WLD	wing loading at take-off
Δ	an increment due to cruise height being HCR2 instead of HCR1
ϵ_{OF}	error in objective function
ϵ_{SV}^i	maximum error in selected variable
n	weighting parameter

1 INTRODUCTION

This paper is about multivariate optimisation (MVO) computer programs in the field of aircraft design. More specifically it is concerned with MVO programs that can be used to determine, though only in broad outline, the design of the best aircraft for a chosen role and specified performance. An MVO program of this kind was described by Kirkpatrick and Larcombe in a paper presented at an earlier meeting in this series (Florence, Italy, 1973). The purpose of such a program is to suggest the best values for the most significant aircraft design parameters, thus furnishing a rudimentary description of the optimum

aircraft and its capabilities. For convenience this rudimentary description will be termed a design, but it is, of course, only a design in an embryonic sense, and it would not even be wise to adopt it as the starting point for the detailed design of a new aircraft without first undertaking exploratory investigations in much greater depth.

The paper begins with a general survey of the constitution of MVO programs of the type characterised above. This survey provides the basis for an extended examination of some MVO program results illustrating how the complex interactions involved in the design process may be traced and how an improved understanding of the working of the mathematical model can be achieved. If experience shows that the model is a good one, the improved understanding of the model is potentially capable of providing new or improved physical insights into the design of real aircraft. The paper concludes with an example and some further suggestions for the exploitation of MVO programs.

2 THE CONSTITUTION OF AN MVO PROGRAM

An MVO program embodies design synthesis and performance analysis methods and, in addition, an optimisation method. The design synthesis and performance analysis methods are combined to create an aircraft design and operations model, and the optimisation method is used to explore and exploit the possibilities presented to it by the model.

The user of an MVO program should make every effort to acquire an insight into the working of its model, and advantage should be taken of every opportunity to deepen and extend this insight. Thorough appraisal of the results of related optimisations performed using the same MVO program is the means to this insight but an intimate knowledge of the model itself is an essential prerequisite. To this end the user should be familiar not only with the methods embodied in the model but also with the precise way in which they have been formulated.

Considerations connected with the optimisation method will have influenced the formulation of the model. These considerations include the facilities provided by the optimisation method and also any susceptibilities which may adversely effect its interaction with the model in the presence of some particular model characteristics. Apart from being aware of these aspects of the optimisation method the user does not need to know in detail how the optimisation process works. However, part of the printout indicates how the optimisation has proceeded and how the optimisation method has functioned, and it is desirable for the user to be able to interpret this information.

In a mathematical model the aircraft and performance descriptions are in terms of a number of measurable quantities. The quantities may be dimensional and non-dimensional. There are geometric quantities such as wing span, wing sweep, wing taper ratio, fuselage length, fuselage maximum cross sectional area. There are mass quantities such as the take-off mass of the aircraft, the mass of its payload, the mass of the fuel it consumes, the masses of its structural components, power plant, furnishings, and so on. There are also quantities relating to the aircraft's aerodynamic characteristics, principally lift and drag coefficients. These of course are interrelated quantities even for a given aircraft design and moreover their relationship changes during flight with changes in aircraft configuration (flap setting and whether the undercarriage is extended or retracted). Other quantities relate to the aircraft's performance. Examples of these are cruise speed, cruise altitude, approach speed, take-off field length. The performance quantities of interest depend to some extent on the type of aircraft being considered. For a combat aircraft they would include such measures of performance as specific excess power and sustained rate of turn. There are also price quantities, for example the price of the aircraft, the price of its airframe, the price of its engines, the cost of spares, the cost of maintenance, the cost of the fuel consumed. There may be measures of aircraft productivity. As well as containing quantities relating directly to the aircraft of the model there are quantities such as those which define the standard atmosphere. The foregoing examples are only a small selection from the host of diverse quantities that are involved in the construction of a model. Some of these quantities are of greater, or at least more regular, interest than others, perhaps because more meaning attaches to them or because their significance is easier to appreciate. Other quantities are of little interest in themselves and perhaps only serve as convenient intermediate values in the progress of the design and performance calculations. In between there are quantities that are of occasional interest.

The quantities are all interrelated by equations and inequations which, more than anything else, characterise the model. Some of these are of a fundamental nature but a few are likely to be wholly empirical and many more semi-empirical. In some instances the model may include relationships implied by tabulated data, but then the formulation of the model will of necessity include interpolation subroutines. This is effectively the same as if empirical relationships had been embodied in the program.

The selection of the quantities that are to be included in a model involves many choices that are related to the detail to be included in the model. In making these choices the purpose for which the model is to be used should be kept clearly in mind. In practice the model will not be immutable but will evolve as experience is gained and shortcomings are recognised and perhaps also because the need arises to use the model for a purpose that was not originally envisaged. When this happens it is important to review the level of detail in the various parts of the model to guard against any serious degree of imbalance. The selection of the equations and inequations which express the inter-relationships between the quantities involves judgements that are mainly concerned with

the level of approximation that should be accepted. Here the problem is to maintain a reasonable balance between the disadvantages of greater complexity and the benefits of greater accuracy.

A model in the terms described above is a conceptual model but still not a usable model. It is necessary to arrange the quantities and equations in some coherent manner so that the model can be used and 'explored' by the optimising method. This process of formulating the model so that it can be embodied in an MVO program involves assigning roles to all of the quantities. In what has been referred to as the conceptual model, some of the quantities are constants but most are variables. Examples of constants in the conceptual model could be the acceleration due to gravity, or the temperature lapse-rate in the troposphere of the standard atmosphere. In the formulation of the model for an MVO program some of the variable quantities of the conceptual model may be assigned to the role of constants (an example might be stage length in the formulation of a model for studying transport aircraft). The assignment of a truly variable quantity to the role of a constant in the formulated model reduces the freedom of the optimisation method to explore the model but it does not prejudice the true character of the quantity. The reason for treating a variable quantity in this way may be connected with the envisaged way of using the MVO program, or it may be associated with a compromise that has been accepted in order to avoid unduly complicating the program. Among the remaining truly variable quantities it is necessary to assign some to the role of independent variables and the rest to the role of dependent variables. These assignments are necessary to enable the formulation of the model, i.e. to convert the conceptual model into a usable model, but, as in the case of the assignment of variable quantities to the role of constants, they do not change the fundamental character of the variable quantities concerned. Thus when an individual optimum aircraft design is being considered the distinction between the variable quantities that have been assigned to the role of independent variables and those assigned to the role of dependent variables within the MVO program has no significance and the distinction can be disregarded. It can however be useful to retain the distinction when the results of a sequence of related designs, generated by means of the same MVO program, are being examined to gain a better insight into the model with the aid of the optimisation method.

Variable quantities should be selected for the role of independent variables with the joint aims of simplifying the formulation of the model and saving computing time. But the number of possible alternative formulations is very large indeed and the one finally evolved is likely to be one of a large number of satisfactory formulations of practically indistinguishable merit.

After the model has been formulated there is some scope for reassigning roles. It is an easy matter to fix the value of a quantity assigned to the role of an independent variable in the formulation of the model, thus effectively reassigning it to the role of a constant. It is also possible to perform a sequence of optimisations with one of the variable quantities that has been assigned to the role of a constant being given a different value for each member of the sequence of optimisations. The quantity thus reverts to a variable role but only outside the MVO program. A variable quantity used in this way may be described as having been assigned to the role of an 'external' independent variable to distinguish it from the independent variables within the MVO program. In the remainder of the paper phrases such as "the variable quantity assigned to the role of independent variable/dependent variable/external independent variable" will be abandoned in favour of the more concise terminology "independent variable (IV)/dependent variable (DV)/external variable (EV)", but the phrase "variable quantity assigned to the role of ..." will nevertheless be implied.

The inclusion of inequations in both conceptual and formulated models has already been mentioned, but so far no indication has been given of the way in which they arise. An example will now be given. A conceptual model for studying transport aircraft, including passenger carrying aircraft, might include the philosophy that fuel should be excluded from the fuselage and carried in the wing instead in order to enhance the prospects for passenger survival in accidents culminating in a fire. This philosophy would exclude from the model any aircraft design in which the wing is too small to accommodate all of the fuel and would give rise to the following inequation:

Volume required to accommodate maximum fuel ∇ space available for fuel in wing .

In this example, it is probable that the quantities on both sides of the inequality symbol would be dependent variables but this is not the only possibility. In general dependent variables, independent variables and constants may be involved. Inequations that involve an independent variable and a constant present no difficulty since the optimisation method can readily be programmed in such a way that the value of each independent variable may only be chosen from within a limited range of values. The inequation can then be enforced by setting the appropriate bounding value (i.e. either the upper or lower bound) for the relevant independent variable equal to the constant in the inequation. To cope with inequations in which one of the quantities is a dependent variable, or where both of the quantities are dependent variables, an optimisation method with the facility to deal with inequality constraints is needed.

There are more ways than one of providing such a facility. From the MVO program user's point of view, two categories of inequality constraint can be discerned. In one of these categories (barrier function methods) the constraints are satisfied at all stages of an optimisation from beginning to end. Aircraft designs that comply with all of the

constraints are termed 'feasible' designs and designs that fail to comply with one or more of the constraints are termed 'infeasible'. It is generally necessary for the user to supply data that can be used in the program to define an aircraft design which serves as the point of departure for the optimisation. For methods in the category already mentioned this first design must be a feasible one. It is not reasonable to put the onus on the MVO program user for ensuring that the first design, based on the data supplied, will be a feasible one, and consequently barrier function methods require an additional process which can modify an infeasible first design and convert it into a feasible one before the optimisation process commences. With a complex set of constraints this can present serious difficulties and the need for this additional process is a drawback. Methods in the other category do not encounter this difficulty because they are not limited to working with feasible designs. These methods have the capability of 'learning' how to choose sets of values of the independent variables so as to reduce any violations of the inequations. The inequations originally conceived in the form

$$A \geq B \quad \text{or} \quad B \leq A$$

are expressed in the form

$$C \leq 0 \quad \text{where} \quad C = B - A.$$

The quantities C , which are always dependent variables, are called constraint residuals. When the constraint residual of an inequality constraint is negative it is called a constraint violation. The inequality constraints corresponding to constraint violations are used to reduce the magnitude of the constraint violations in successive designs. They work by providing incentives which influence the choice of values for the independent variables. The inequality constraints that are acting in this manner are said to be active. The set of active constraints can change during the course of an optimisation and commonly does so, especially in the early stages. Since the individual inequality constraints can change from being active to being inactive and vice versa during the course of the optimisation it is sometimes useful to be able to distinguish the ones that are active in the case of the final (optimum) design, and for this purpose the term binding constraints may be used. It is not necessary to make this distinction in the present paper because reference will only be made to the optimum designs and therefore the terms active and inactive will be used. At the outset of an optimisation some large constraint violations may occur, but during the course of the optimisation the magnitude of the violations are progressively reduced until, by the end of the optimisation, any constraint violations are contained within a very small tolerance which may be specified so that for all practical purposes compliance with the inequations is achieved.

The model may include concepts which may be expressed in the form of one or the other of the following statements,

$$A \text{ is equal to the greater of } B \text{ and } C,$$

or

$$G \text{ is equal to the lesser of } H \text{ and } J.$$

The optimisation process involves numerical differentiation procedures and these statements, which result in a discontinuity in the rate of change of A or G with respect to at least one of the independent variables, can disturb the steady progress of an optimisation. The contingency can be avoided by providing a smooth transition confined to a rather small region in the vicinity of the intersection of B and C or G and H . This cannot be done without introducing a small error but the error can be made so small that it is of no practical importance. Although sufficient to obviate difficulties with the optimisation method, the transition is too localised to be detected by the user of the MVO program to whom the original gradient discontinuity will appear unchanged. As far as the user is concerned the effects near the intersection of B and C or H and J are similar to the effects in the vicinity where an inequality constraint changes between being active and being inactive, and to the effects in the vicinity where an independent variable changes from being a variable to being a constant because it has encountered either its upper or lower bound.

The interrelationship between some quantities in a model may be such that an analytic solution either does not exist or else it is perhaps unduly cumbersome. The normal way of dealing with this situation is to solve by iteration. But some optimisation methods embody an equality constraint facility which can be used instead. An equality constraint facility functions in a very similar way to the inequality constraint facility already described. An equation, normally in the form $P = Q$, which is to be dealt with by an equality constraint is re-expressed in the form

$$C = 0 \quad \text{where} \quad C = P - Q.$$

As for an inequality constraint, C is called a constraint residual but, in the case of an equality constraint, the constraint residual is a constraint violation regardless of its sign, and an equality constraint is always active. It is not possible to generalise about whether it is more economical to use an iteration or to employ an equality constraint. It all depends on the particular case. However in one respect the use of an equality constraint can show a clear advantage. Sooner or later the possible desirability of extending an existing model by incorporating some new features may be mooted. By the use of the equality constraint facility it may be possible greatly to simplify changes to the existing program and perhaps avoid the need to rewrite it extensively. Even if the resulting program turns out to be less efficient the use of equality constraints can save program

redevelopment time and enable the effect of changes to the model to be determined more rapidly.

For an MVO program, whose model includes inequations, an optimisation method with an inequality constraint facility is a virtual necessity. To have an equality constraint facility as well is an advantage. These capabilities have been discussed simultaneously with the formulation of the model on account of the vital part that they play in the formulation. One important aspect of the interrelationship between the model and the optimisation method remains to be discussed and that is the way in which the optimisation method is to gauge the relative merits of different designs. The optimisation method requires a measure and this must be selected by the MVO program user. The measure is termed the objective function and it is conventionally defined so that a smaller value indicates a better design. Since it may be desired to consider different design aims at different times provision may be made for several alternative objective functions from which any one may be chosen for a particular optimisation. Another possibility for which provision should be made is the use of objective functions compounded from two, or even more than two, simple objective functions with adjustable individual weightings. The utility of such compound objective functions will be discussed later in the paper. Which-ever objective function is chosen for a particular optimisation, whether simple or compound, it is probable that it will be a dependent variable. There is no fundamental reason why this should be so, it is merely a reflection of the fact that an objective function is generally a complicated quantity such as aircraft weight, or aircraft first cost, or cost of ownership, or direct operating cost. It is hardly likely that any of these quantities would be an independent variable since their adoption as such would not be likely to lead to a simple formulation of the model. However it is not impossible to imagine a simple quantity being an objective function. For example it would be possible to conceive circumstances in which there might be interest in finding the aircraft with the smallest possible wing span compatible with the attainment of some stipulated performance requirement. In such a case the same quantity could be an independent variable and the objective function at one and the same time.

3 USING AN MVO PROGRAM

It might be thought that an optimisation study involving a single optimisation, *ie* one application of an MVO program, would be quite usual. In fact it is quite exceptional. Some reasons for this will perhaps become self evident when possible ways of exploiting MVO programs are discussed in the final section of this paper. But there is one reason that underlies all of the others. It is that it is possible to learn so much more from repeated applications of an MVO program than from a single application.

3.1 Examining the results of a systematic study

In this section of the paper some MVO program results will be used to demonstrate how the results of a systematic study may be examined, and how the MVO program can, if necessary, be used in order to develop a more complete and coherent understanding of the original results. Along the way the principle phenomena that can occur in constrained optimisation studies will be encountered, and before the end is reached a systematic approach to the investigation of 'peculiar' results will have emerged. It is emphasised that the results are not presented as they would be if they themselves were the subject of the paper, and that they are, in fact, only introduced to serve the purposes of the demonstration.

The results come from part of a study of conventional swept-wing transport aircraft. The MVO program used in the study had 15 independent variables, 9 inequality constraints, and 2 equality constraints. Two of the independent variables were fixed so that as used in the study there were 13 independent variables (see Table 1). The study aircraft were all optimised with direct operating cost as the objective function. All of the results considered here are for twin-engined aircraft having the same payload capacity, able to carry their capacity payload over the same stage length, able to take-off and land within the same prescribed distances, and able to comply with the same engine failed ceiling requirement.

The two independent variables that were fixed in the MVO method were the cruising speed (VCR) and the cruising height (HCR). These two quantities were used as external variables. Only two values of cruising height were considered and they will be called HCR1 and HCR2, the latter being the greater one. In the first place five equally spaced values of cruising speed were chosen and optimisations were performed at each of these speeds and at both heights. For present purposes it will be supposed that interest centres on the way in which the change in cruising height from HCR1 to HCR2 affects the design of optimum aircraft at the various cruising speeds, and also how the direct operating costs are affected. Of the many variables that could be considered only a few can be dealt with here. For preliminary purposes a representative selection has been made. It includes the objective function, three other dependent variables, and one independent variable. The objective function is the direct operating cost (DOC). The three other dependent variables are the aircraft mass at take-off (MTO), the aircraft wing loading at take-off (WLD), and the aircraft span loading (WLD/A)*. The independent variable is the total installed mass of the engines (MENG). For the pair of altitudes considered in the study the effect of designing for the greater cruising height is to increase the direct operating cost, take-off mass, and installed engine mass, and to decrease the wing loading and span loading.

* A = aspect ratio so $WLD/A = \text{take-off weight/span}^2$.

Points representing the differences in these variables are plotted in Fig 1. The purpose of the figure is to show how the differences vary with cruising speed. The actual values of the differences are not relevant to the present discussion. The scales and their origins were chosen so as to separate the sets of points and spread them evenly over the figure, and, to avoid confusing the figure they are not shown. However a consistent convention has been adopted for all of the quantities and the magnitude of a positive quantity increases up the figure whilst the magnitude of a negative quantity decreases up the figure. No attempt has been made to draw curves through the sets of points but successive points have been connected by straight lines. It would be easy to draw smooth curves through the top three sets of points, i.e. those for ΔDOC , $\Delta MT0$, and ΔWLD . But some difficulty could be experienced in attempting to draw smooth curves through the lowest two sets of points, i.e. those for $\Delta(WLD/A)$ and $\Delta MENG$. With the object of clarifying the shape of the last two curves four more pairs of optimum aircraft were therefore generated at cruising speeds which equally divide each of the original four speed intervals. With nine points in each set it might be expected that the curves would be adequately defined. The augmented sets of points are plotted in Fig 2 which shows that the expectation is not fulfilled. The fourth and fifth sets of points can be seen to exhibit definite irregularities which make it impossible to interpolate their curves with any confidence. What is more, the third set of points now shows clear signs of irregularity, and in the second set of points a suspicion of irregularity may be detected. Only in the case of the first set of points do the four new points blend in with the original five points.

What is the meaning of this result? Is it an indication of the quality of the results produced by the MVO program? Why do the results for some quantities exhibit more irregularity than others? Is it perhaps significant that the most regular set of results are those for the objective function? Well yes, as a matter of fact it is! A justification for this assertion will be given almost immediately. But another question that could be asked is as follows. Are there any grounds for expecting the curves to be continuous or to exhibit continuity of slope? The answer to this question will emerge in the course of this section of the paper. Returning to the question whether it is significant that the most regular set of results are those for the objective function, consider the following proposition. Suppose that following an optimisation any one variable, independent or dependent but excluding the objective function, were to be singled out for special consideration. This variable will be referred to as the selected variable. Its optimum value would be known (see Fig 3). Suppose that the optimisation were to be repeated with one difference, namely with the selected variable forced to take a value differing from its optimum value. The value of the objective function for the new design should not be less than the value for the design generated in the original optimisation because in the second optimisation a degree of freedom has been given up. Very exceptionally the second optimisation could yield the same value for the objective function as did the original optimisation but usually a higher value would be obtained. In the second optimisation all of the other variables would be free to assume new optimum values to make the new value of the objective function a minimum with the prescribed value of the selected variable. Suppose that an ideal optimisation method were to be available so that perfectly error-free results could be produced in both of the foregoing optimisations. Now a real, as opposed to an ideal, optimisation method embodies a procedure whose purpose it is to terminate the optimisation when the true optimum has been sufficiently closely approached. This involves the acceptance of an error (although it is an error that can be made very small). Suppose that the original problem with the selected variable free were to be tackled using the real optimisation method and that on account of its termination procedure it stopped with precisely the same solution as found in the second optimisation with the ideal optimisation method. The difference between the values found for the variables (including the objective function) and those found in the first optimisation using the ideal method would now be errors caused by the termination of the optimisation. If the real optimisation had terminated with the same value of the selected variable but with a different value for one or more of the other variables the error in the objective function would have been greater. This means that a constant error contour for the objective function must be shaped as shown in the diagram (see Fig 3), and it shows that if the difference between the original and second ideal optimisations are regarded as errors due to an optimisation termination procedure, then the difference between the values of the selected variable is the *maximum* error in the selected variable that can be associated with an error in the objective function equal to the difference in the values of the objective function.

By prescribing a series of values for the selected variable, ranging from below to above its optimum value, and performing an optimisation with each value, a curve relating the objective function and selected variable could be determined. Its shape could be of the kind shown in Fig 4. Interpreting this curve in the light of the foregoing discussion it can be seen that, in the vicinity of the true optimum, the relationship between the error (ϵ_{OF}) in the objective function and the *maximum* error (ϵ_{SV}) in the selected variable could be closely approximated by an equation

$$\epsilon_{OF} = (\epsilon_{SV}^1/k)^2$$

where k is a coefficient whose value would depend on which of the many variables had been selected. Consequently

$$\epsilon_{SV}^1 = \pm k\sqrt{\epsilon_{OF}}$$

The error in the objective function can only be positive but the error in the selected variable may be positive or negative. If with a given probability the scatter in the values of the objective function is within a range ϵ_{OF} , then the scatter for the selected variable would be within a range $2k\sqrt{\epsilon_{OF}}$. This shows that if the optimisation termination procedure were to be made more stringent, then the scatter exhibited by any of the variables other than the objective function would decrease more slowly than would the scatter exhibited by the objective function itself. It is to be expected that the objective function scatter would be made minimal, but this might not be sufficient to ensure that the scatter would be imperceptible for every variable.

On the basis of the foregoing discussion of the errors that could arise as a consequence of the optimisation termination procedure, the possibility that the irregularity in some of the sets of points plotted in Fig 2 might be due to scatter could not be excluded. But it is only fair to reveal that the apparent irregularity in some of the results has very little to do with scatter. This will be demonstrated by determining the true shape of the curves. To accomplish this, and to provide a satisfactory explanation, it will be necessary to examine the results closely. Another reason for pursuing this course is to dispel any impression there may be that it is very difficult, or perhaps even impossible, for the user of an MVO program to gain a satisfactory insight into the reasons why a particular design emerges from an optimisation. In fact, with proper techniques, using an MVO program can be at least as instructive as, for example, engaging in parametric studies where the parameters are varied one at a time.

In order to show how the designs evolve as the specified cruising speed is increased, and to indicate some of the factors that influence and mould the changing design, some results have been extracted from the computer printout, which contains comprehensive information about each design and its performance. The sequence of designs for the lower cruising height HCR1 is dealt with first in rather considerable detail, and then the sequence of designs for the greater cruising height HCR2 is briefly considered. Finally, with the insight gained into both sequences of designs, the way in which a change of cruising height from HCR1 to HCR2 affects the design of optimum aircraft is again considered.

Readers who are interested in the techniques that may be used to investigate sequences of designs, but who are not so interested in following the detailed changes in the particular design sequences examined here, will find that they can scan fairly rapidly through most of the following discussion.

3.2 Examination of the sequence of aircraft designs for the lower cruising height HCR1

For aircraft A, which is the optimum design for the lowest cruising speed considered in the study, the printout reveals that two inequality constraints are active. They are the inequality constraints designated IC2 and IC4, both of which are concerned with aspects of aircraft performance with an engine failed. IC2 ensures that a safe climb gradient can be attained following take-off, and IC4 ensures that the net ceiling is not below a specified value. In addition, although the inequality constraint IC1 is not active, the value of its constraint residual is small and this suggests that IC1 may be active for a design not far removed from aircraft A. A look at the results shows that IC1 is active in the case of aircraft B, the optimum design at the next higher cruising speed. The inequality constraint IC1 ensures that aircraft are capable of complying with the take-off field length specified. It appears that at a cruising speed somewhere in the interval between the cruising speeds of aircraft A and aircraft B there is a change in the state of the inequality constraint IC1. To investigate how the optimum design evolves through the cruising speed interval two supplementary optimisations were performed, one at each end of the speed interval. The aim was to achieve a new aircraft design at the speed of aircraft B which has the same active constraints as aircraft A, and to achieve a new aircraft design at the speed of aircraft A with the same active constraints as aircraft B. The new design at the speed of aircraft B was optimised with the constraint IC1 suppressed and, after checking that it had the same active inequality constraints as aircraft A, it was designated aircraft B₁. The new design at the speed of aircraft A was optimised with IC1 made into an equality constraint and after checking that it had the same active constraints as aircraft B it was designated aircraft A' (see footnote). The aircraft A' and B₁ although properly optimised are not legitimate aircraft, as are aircraft A and B, because the requirements they have been made to fulfil have been distorted. But the affinity between aircraft A and B₁ on the one hand and between aircraft A' and B on the other hand is of assistance in interpolating legitimate designs in between aircraft A and B. In addition, by studying the trends of design change firstly between aircraft A and B₁, and subsequently between aircraft A' and B, the effects of the inequality constraint IC1 becoming active can be seen.

The increase in cruising speed VCR (the external variable), between aircraft A and aircraft B₁ is 2.85%.

3.2.1 With IC1 inactive (aircraft designs A and B₁)

It is found that the increase in cruising speed results in block speed increasing by 2.53%. The consequent increase of aircraft productivity dominates the other cost changes and results in direct operating costs being lowered by 1.44%. The increase in the cruising speed VCR is associated with an increase in the airflow dynamic pressure QCR

* In addition to having the same active constraints there are other requirements relating to the independent variables which are explained later.

amounting to 5.78%. The take-off mass is increased by only 0.43%. The fuel consumption is increased by a relatively greater amount (1.44%) and consequently the landing mass increases by a relatively smaller amount (0.24%). The fuel fraction used before reaching cruising height is slightly greater for the faster aircraft (2.84% instead of 2.80%) and consequently the increase in the aircraft mass at the start of cruise MSSCR is only 0.38%. Since the cruise dynamic pressure QCR is increased by 5.78% and the mass at the start of cruise is only increased by 0.38% it follows that the product of the lift coefficient at the start of cruise CLCR and the wing area S must decrease since

$$MSSCR/QCR = CLCR \times S$$

It is found that the cruise lift coefficient CLCR is reduced by 2.69% and the wing area S is reduced by 2.44%. It is of interest to notice that the wing aspect ratio A is reduced by 2.47% which is less than the reduction in cruise lift coefficient since this indicates that the ratio of lift-induced drag over aircraft weight is improved being reduced by 0.23%. This follows from

$$\text{lift-induced drag} \div \text{aircraft weight} \propto \left(\frac{CLCR^2}{\pi A} \right) / CLCR$$

The installed engine mass is increased by 2.59% to enable the prescribed net ceiling to be attained with an engine failed (constraint IC4).

However, because RATING is reduced by 2.42% the static thrust available for take-off is increased by a mere 0.10% and the static thrust/weight available for take-off is actually reduced by 0.32%.

The reduction of RATING is of some interest because it illustrates how searching the computer optimisation process is. An increase of RATING results in a proportionate increase in the thrust available at take-off from an engine of given size and installed mass. It also results in a reduction in the cruise thrust available, this reduction being graded to balance the adverse effect of the higher take-off rating on engine life. Thus the effect of varying RATING is to vary the take-off thrust available and the cruise thrust available from an engine of given size and mass without affecting engine life and hence engine maintenance costs. RATING does not affect the thrust available to maintain net ceiling with an engine failed. The question arises therefore, what advantage is to be gained in reducing RATING when the aircraft is not cruise thrust limited, i.e. when the size of engine installed is not influenced by the thrust required for the cruise? To answer this question it is necessary to consider how the fin is sized. SFIN is in effect the greater of SFIN1, the minimum fin size required for weathercock stability, and SFIN2, the fin size required to counteract the worst yawing moment with one engine failed. In the present case SFIN2 is greater than SFIN1, and SFIN2 depends on the maximum thrust the engines can develop. As long as the installed engine size remains unchanged therefore, reducing RATING will result in reducing fin size with consequent weight and drag savings. As RATING is reduced with constant installed engine size the thrust available for take-off distance and take-off climb is reduced. By suppressing IC1 we have suppressed the take-off distance requirement and RATING is reduced until the aircraft becomes take-off climb gradient limited (IC2).

The increased masses at take-off and landing combined with the reduced wing area result in higher take-off and landing wing loadings:

Take-off wing loading is increased by 2.99%
Landing wing loading is increased by 2.79%

Since a constant approach speed is specified, the increase in landing wing loading is matched by an equal increase in approach lift coefficient:

CLA increased by 2.79%

This increased approach lift coefficient is attained with smaller slat and flap chords (ELES and ETE) but increased approach flap angle (BTAA). This curious result is a consequence of complex interactions between the component weights of the wing structure and flap operating systems and their combined effect on the mass and price of the airframe. Although the resulting interplay between flap and slat chord and flap angle is of some interest it would not be profitable to pursue it further in this account.

However one consequence of the diminishing slat chord is that the available take-off lift coefficient is reduced. The optimising program has not found any benefit from deflecting the trailing edge flaps for take-off but deploys the leading edge device. The consequence of changes in wing geometry (mainly reducing slat chord) is to reduce available take-off lift coefficient CLTO by 5.82%. This reduced take-off lift coefficient together with the higher take-off wing loading causes the take-off speed to be increased by 4.57%.

The higher take-off speed together with the reduced thrust/weight available at take-off leads to an increased take-off distance and in fact to a take-off distance in excess of the limit stipulated in the original requirement. This excessive take-off distance could not have occurred if IC1 had not been suppressed.

3.2.2 With IC1 active (aircraft designs A', B, C and D₁)*

It is found that the speed increase between aircraft A' and B is accompanied by a direct-operating-cost reduction of 1.37% (cf 1.44% when IC1 was suppressed) so, although direct operating cost is still decreasing with increasing cruising speed, it is not decreasing so rapidly, ~~is~~ the restoration and activation of the constraint has resulted in a small direct-operating-cost penalty.

The increase in VCR now leads to an increase in the take-off mass of only 0.36% (cf 0.43% with IC1 suppressed). Despite the take-off mass at the increased speed being less than with IC1 suppressed the first price of the aircraft is 0.32% greater than with IC1 suppressed.

The fuel consumed at the higher speed is increased by 1.16% (cf 1.44% with IC1 suppressed) and the landing mass increases by 0.22% (cf 0.24% with IC1 suppressed).

The fuel fraction used before reaching cruising height is now slightly less for the faster aircraft (2.79% instead of 2.80%) and so the increase in the mass at the commencement of cruise is 0.37% (~~is~~ 0.01% greater than the percentage increase in MTO).

The 5.78% increase in QCR together with the 0.37% increase in initial cruise mass means that the product of CLCR and S must decrease by 5.12%. In fact

	Aircraft A' to B	Aircraft A to B ₁
CLCR is reduced by	2.55%	2.69%
and S is reduced by	2.64%	2.49%

The aspect ratio is reduced by 2.19% (cf 2.47% with IC1 suppressed), so $\frac{CDI}{CL} = \frac{CLCR}{A}$ is reduced by 0.37% (cf 0.23% with IC1 suppressed).

	Aircraft A' to B	Aircraft A to B ₁
The installed engine mass is increased by	2.27%	2.59%
but RATING is only reduced by	0.02%	2.42%

(RATING remains practically constant above the speed just exceeding A where IC1 becomes active). With a higher take-off thrust being required, to enable take-off within the specified distance, reducing RATING further would result in heavier engines being required and there would not even be any savings in fin size and weight to offset against the heavier engines.

The combined effect of the changes in engine size and RATING is to increase the thrust available for take-off by 2.25% (cf 0.10% with IC1 suppressed). The consequence of this thrust increase and the proportionately smaller increase in the take-off mass is that the thrust/weight ratio at take-off increases by 1.88% whereas it decreased by 3.25% when IC1 was suppressed.

The increased masses at take-off and landing combined with the reduced wing area result in higher take-off and landing wing loadings:

	Aircraft A' to B	Aircraft A to B ₁
Take-off wing loading increased by	3.08%	2.99%
Landing wing loading increased by	2.93%	2.79%

With the constant approach speed specified the increase in landing wing loading is matched by an equal increase in approach lift coefficient:

CLA increased by 2.93% (cf 2.79% with IC1 suppressed)

This increased approach lift coefficient is attained with increased slat chord ratio ELES and smaller flap chord ratio ETE (though not as small as with IC1 suppressed) and with larger approach flap angle BTAA (though not as large as with IC1 suppressed).

These changes in the dependence of ELES, ETE and BTAA on VCR, together with the changed dependence of RATING, which has already been discussed, are the most striking consequences of the constraint IC1 becoming active.

The changed dependence of ELES, ETE and BTAA on VCR are closely connected and it appears reasonable to regard the changed dependence of ETE and BTAA as secondary to the changed dependence of ELES. The reason for this is that the change from ELES decreasing to ELES increasing with increasing VCR is the major factor enabling the available take-off lift coefficient to be increased so that take-off can be accomplished within

* Initially the changes between aircraft A' and aircraft B will be compared with the changes between aircraft A and aircraft B₁. Then the subsequent evolution of the family of designs containing aircraft A' and B will be traced through aircraft C and D₁.

the specified distance, despite the increasing take-off wing loading, with lighter engines than would otherwise be required.

With the increased cruise speed the take-off lift coefficient available is increased by 1.33% instead of being reduced by 5.82% as when ICL was suppressed.

With this increased take-off lift coefficient the increase in take-off speed is held to 0.86% despite the increase in take-off wing loading (of 4.57% increase in take-off speed with ICL suppressed).

Take-off within the specified distance at this increased take-off speed can be achieved by virtue of the higher thrust/weight available at take-off.

If the cruise speed VCR is further increased it is found that the aircraft designs evolve smoothly until a speed just above the third discrete value considered and then one of the independent design variables encounters its upper bound. To facilitate detailed consideration of the effect of this encounter, the upper bound of the affected independent variable may be raised sufficiently to obviate its being encountered before the next discrete speed is reached. The aircraft design generated with this upper bound raised is not designated aircraft D but aircraft D₁ since, although it is a member of the family of designs that includes aircraft A', B and C, it is not a legitimate design.

It has already been noted that in the interval between the first two cruise speeds considered the product of CLCR and S must decrease because the increase of dynamic pressure is proportionately much greater than the increase in the aircraft mass at the commencement of the cruise. This remains broadly true for the first three cruise speed intervals on which attention is now focussed.

Table showing percentage change (increase positive) in interval

Aircraft:	A'	B	C	D ₁
VCR	+2.85	+2.77	+2.70	
QCR	+5.78	+5.62	+5.47	
MSSCR	+0.37	+0.62	+0.87	
(MSSCR/QCR) \propto CLCR \times S	-5.12	-4.73	-4.36	
CLCR	-2.57	-2.80	-3.53	
S	-2.62	-1.99	-0.86	

However the table shows that whereas in the first speed interval the reduction is more or less equally shared between CLCR and S, successive reductions of CLCR increase in magnitude whilst the accompanying reductions of S decrease in magnitude. In seeking a cause for this phenomenon it is necessary to beware of oversimplifying the possibly complex underlying interactions. It could be supposed that further reductions in S are being more strongly inhibited by take-off or landing considerations. These possibilities could of course be investigated by generating additional designs with the take-off and landing requirements relaxed in turn. In the present instance it is probable that increasing compressibility drag is having a significant effect.

Although the sequence of optimum aircraft have increasing sweep (SWP) and reducing thickness-chord ratio (TC) and CLCR, their compressibility drag, expressed as a fraction of total drag, increases progressively with each increase of cruising speed and Mach number.

Aircraft:	A'	B	C	D ₁
Compressibility drag/total drag %	+4.36	+5.04	+5.94	+6.88
% change in interval:				
VCR, MCR	+2.85	+2.77	+2.70	
SWP	+6.80	+7.30	+6.82	
TC	-4.04	-4.27	-5.02	
CLCR	-2.57	-2.80	-3.53	

This suggests that compromises involving compressibility drag may be at least partly responsible for putting the brake on further reductions in wing area and perhaps for reversing the trend.

Successive aircraft in the sequence penetrate further into the compressible flow regime and the penalty of increased compressibility drag appears not to be a sufficient deterrent because the aircraft for the fourth discrete cruise speed considered (aircraft D₁) penetrates further than the design synthesis model would normally permit.

The design synthesis model employed in the study being discussed incorporates a quantity which is intended to be a measure of the degree of penetration into the compressible flow regime. This quantity is used to indicate aircraft which would cruise too close to, or even beyond, the buffet boundary and thus encounter or risk encountering unacceptable compressibility effects. It can therefore be used to exclude such aircraft from consideration.

The design synthesis could have been formulated with this quantity a dependent variable in which case an inequality constraint would have been required. In fact the

particular design synthesis being used was formulated with this quantity as an independent variable IV6 and the upper bound on this independent variable takes the place of an inequality constraint. Raising the upper bound, to enable aircraft D₁ to be generated, is equivalent to relaxing a constraint. Restoring the upper bound to its normal value is equivalent to reinstating a constraint.

The effect of restoring the upper bound on IV6 to its normal value so as to limit penetration into the compressible flow regime will be considered next and it will be seen that further growth of the compressibility drag fraction is inhibited and that the resulting aircraft D exhibits a bigger reduction of CLCR and a smaller reduction of S than in the case of aircraft D₁. This lends support to the hypothesis that the restraining effect of increasing compressibility drag fraction played a significant role in retarding the continuing decline in the wing area of successive aircraft in the sequence. To facilitate comparisons with the family that includes aircraft A', B, C and D₁, the new family will include a member C' which can be generated by fixing the value of IV6 at the value of its upper bound.

3.2.3 With IV6 on its upper bound (aircraft designs C', D, E and F₁)

It is found that the speed increase from aircraft C' to aircraft D causes the compressibility drag fraction to rise from 5.94% to 6.08% instead of to 6.88% which is the value for aircraft D₁.

The smaller compressibility drag fraction of aircraft D compared with that of aircraft D₁ at the same cruising speed and Mach number is of course due to its more limited penetration of the compressible flow regime under the restraining influence of the restored upper bound on IV6. The imposition of this upper bound results in the following changes between aircraft C' and D compared with those found between aircraft C and D₁:

	Aircraft C' to D	Aircraft C to D ₁
Sweep increases by	8.22%	6.82%
TC reduces by	5.26%	5.02%
CLCR reduces by	4.31%	3.53%

The mass at the commencement of cruise is increased by 0.91% (cf 0.87%) so that aircraft D and D₁ are practically identical in this respect.

Aircraft D's bigger reduction in CLCR is associated with a smaller reduction in wing area (only 0.01% compared with 0.86%).

As well as the effects already discussed it is interesting to observe that another consequence of IV6 encountering its upper bound is that RATING resumes a downward trend. This is consistent with the earlier discussion of its interaction with the constraint IC1. The increased wing area of aircraft D compared with that of aircraft D₁ could be expected to lead to a reduction of RATING by making it easier to comply with the take-off distance requirement. It appears that the effect on RATING is a secondary consequence of IV6 encountering its upper bound.

If the cruise speed VCR is still further increased the aircraft designs evolve smoothly along their new course until, at a speed in between the fifth and sixth values (i.e. between aircraft E and F), the inequality constraint IC9 becomes active. To facilitate detailed consideration of the effect of the activation of this constraint as well as to establish more clearly the trend of development when it is not active it will be suppressed, thus enabling an unconstrained aircraft F₁, belonging to the same family as D and E, to be generated. For present purposes the family will be represented by aircraft C', D, E and F₁. Of these four designs only D and E are optimum aircraft generated by the normal program. Aircraft F₁ does not comply with inequality constraint IC9 and has a lower direct operating cost than aircraft F which does comply with the constraint. Aircraft C' having been generated with independent variable IV6 fixed on its upper bound has a higher direct operating cost than aircraft C for which the program was free to optimise the value of IV6. However aircraft C' is very similar to aircraft C whose optimum value of IV6 is very close to the upper bound value. This is a consequence of the cruise speed of aircraft C and C' being only marginally below the cruise speed for which the optimum value of IV6 just equals the normal value of the upper bound on IV6.

Although successive percentage increments of QCR become smaller and successive percentage increments of aircraft mass become larger, the increments of dynamic pressure continue to be proportionately greater than the increments of aircraft mass through the third, fourth and fifth intervals (i.e. between aircraft C', D, E and F₁). Consequently the product of CLCR and S must continue to fall (see first part of following table).

Aircraft:	C'	D	E	F ₁
% change in interval				
VCR	+2.70	+2.63	+2.56	
QCR	+5.47	+5.32	+5.18	
MSSCR	+0.91	+1.19	+1.45	
MSSCR/QCR \propto CLCR \times S	-4.32	-3.93	-3.55	
CLCR	-4.31	-4.65	-4.89	
S	-0.01	+0.75	+1.42	
QCR \times CLCR \propto MSSCR/S	+0.92	+0.42	+0.04	

However, with further penetration into the compressible flow regime being restrained by the upper bound on IV6, the increments of cruise Mach number that are associated with the increments in cruise speed result in wing sweep increasing more rapidly and TC and CLCR decreasing more rapidly than was the case for the family of aircraft A', B, C and D₁ considered previously.

Aircraft:	C'	D	E	F ₁
Compressibility drag/total drag %	+5.94	+6.08	+6.24	+6.42
% change in interval				
VCR, MCR	+2.70	+2.63	+2.56	
SWP	+8.22	+8.35	+8.81	
TC	-5.26	-5.51	-5.76	
CLCR	-4.31	-4.65	-4.89	

In the first interval the reduction of MSSCR/QCR is almost entirely balanced by the reduction of CLCR, and S is very nearly constant. In the ensuing intervals the reduction of CLCR becomes greater than the reduction of MSSCR/QCR and consequently the wing area S has to increase. In the last interval (between aircraft E and F₁) the reduction of CLCR almost balances the increase in cruise dynamic pressure QCR, whilst the increase in wing area S almost balances the increase in the mass at the start of cruise MSSCR (see last part of table at foot of previous page).

Although the aspect ratio decreases it does so proportionately less rapidly than does CLCR, and so CLCR/A and hence also induced drag/weight continues to fall at a rate varying between 0.95% in the interval between aircraft C' and D, and 0.79% in the interval between aircraft E and F₁.

RATING falls slowly but the installed engine mass increases more rapidly and the installed thrust at take-off rating increases faster than does take-off mass. Consequently the ratio of available thrust/weight for take-off increases. As already shown the wing area begins to increase and in the last interval (between aircraft E and F₁) its rate of growth nearly matches the rate of growth of take-off mass. Consequently although take-off wing loading continues to increase its value is nearly constant in the last interval. In any case the take-off thrust/weight ratio increases faster than does the wing loading and so the take-off lift coefficient required for take-off decreases. Even so, to compensate for the effect of increasing sweep an increasing slat chord is required (see following table).

Aircraft:	C'	D	E	F ₁
% change in interval				
MTO	+0.91	+1.19	+1.45	
S	-0.01	+0.75	+1.42	
RATING	-0.23	-0.30	-0.33	
Engine mass	+2.64	+2.99	+3.25	
Take-off thrust	+2.40	+2.68	+2.90	
Take-off thrust/weight	+1.48	+1.47	+1.42	
Take-off wing loading	+0.91	+0.43	+0.04	
Take-off lift coefficient	-0.43	-0.91	-1.25	
Sweep	+8.22	+8.35	+8.81	
Slat chord ratio	+4.47	+3.86	+3.99	

From aircraft A through aircraft F₁ each increase of cruise speed has resulted in wing thickness-chord ratio decreasing, and the rate of decrease has accelerated with increasing cruise speed and Mach number. The particular design synthesis program used in this study incorporates an inequality constraint, IC9, which exercises an overriding control over wing thickness-chord ratio and excludes from consideration aircraft with wings which are too thin.

The reasons for incorporating such an inequality constraint are peripheral to the subject of this paper and it would not be appropriate to discuss them in any depth. But it is perhaps worth digressing to the extent of mentioning one possible reason for such a constraint, namely, to confine the search conducted by the optimisation program to a region in which the methods embodied in the design synthesis may be considered reliable. If such a constraint were to be regularly activated it would be necessary to consider the desirability of improving the methods embodied in the design synthesis so that its range of application could be extended and the inequality constraint could then be relaxed. Before embarking on this course however it would be worth relaxing the constraint experimentally to explore the design synthesis model. The results might suggest that the optimum design is only just outside the confines of the original search and that the value of the objective function cannot be significantly improved. One possibility is that another inequality constraint may be activated and that this limits further excursions from the confines of the original region perhaps by making them unprofitable in terms of the value of the objective function. In the present instance, for example, further reductions of wing thickness will at some stage result in aircraft whose wings have internal volumes which are too small to accommodate the fuel required for maximum range. In the design synthesis which produced the results being examined, consideration of such aircraft would be excluded by another inequality constraint (IC5) whose purpose is to ensure that the wings can accommodate fuel tanks with sufficient capacity.

The effect of reinstating the inequality constraint IC9 will be considered next. Plotting the constraint residuals (with IC9 suppressed if necessary to prevent its being activated) shows that activation of the inequality constraint should occur with aircraft cruising speeds greater than a value about three-quarters of the way between the cruising speeds of aircraft E and F_1 . To facilitate comparisons with the family which includes aircraft C', D, E and F_1 , the new family will include a member E' which can be generated by making the constraint IC9 an equality constraint.

3.2.4 With IC9 active (aircraft designs E', F, G, H and J_1)

The reduction of wing thickness-chord ratio in the fifth speed interval is much less than with IC9 suppressed. To compensate for the smaller reduction of thickness-chord ratio it is necessary for sweep to increase more and/or for the reduction of CLCR to be greater. Changes between aircraft E' and F are compared with changes between aircraft E and F_1 in the following table.

	Aircraft E' to F	Aircraft E to F_1
TC reduces by	1.73%	5.76%
SWP increases by	12.89%	8.81%
CLCR reduces by	6.94%	4.89%

The reduction of CLCR between aircraft E' and F is greater than the increase of QCR and so the increase of wing area must be proportionately greater than the increase of aircraft mass, and wing loading must be reduced:

% change in interval	Aircraft E' to F	Aircraft E to F_1
CLCR	-6.94	-4.89
QCR	+2.56	+2.56
MSSCR	+1.37	+1.45
S	+3.58	+1.42
MTO	+1.39	+1.45
MTO/S	-2.11	+0.04

The table shows that, as a consequence of the constraint IC9 being active, wing loading begins to fall rather abruptly.

This is a reasonable point at which to consider the shape of curves showing the dependence of the objective function on external variables especially in the vicinity of an event such as when an inequality constraint changes its status (becomes active or inactive) or when an independent variable encounters or leaves either of its bounds. A value of an external variable which coincides with an event will be referred to as an event value (see Fig 5). Of particular interest is the way in which the curve for all legitimate aircraft is composed of segments (each of which corresponds to the legitimate segment of the curve for one family of aircraft), and the conditions where one segment ends and another commences. This will be illustrated by considering what happens in the fifth speed interval where the inequality constraint IC9 becomes active (an event). The objective function is direct operating cost and the external variable is cruise speed. Fig 5, which is diagrammatic, illustrates the topography of an event and how it is related to the objective function curve.

On account of the constraint IC9 being active its residual is ideally zero for every aircraft belonging with aircraft E' and F to the fourth family. The residual of constraint IC9, for aircraft belonging with aircraft E and F_1 to the third family, changes from being positive to negative as the cruise speed is increased from that of aircraft E to that of aircraft F_1 . One member of the family between aircraft E and F_1 has zero IC9 residual. This aircraft is at an event point and its cruise speed is an event value of cruise speed. As well as being the last (i.e. the highest cruise speed) legitimate member of the third family it is also the first (i.e. the lowest cruise speed) legitimate member of the fourth family of aircraft. This can be tested by generating additional aircraft with the appropriate cruise speed.

The last member of one segment is always potentially the first member of the following segment (in the present case the last legitimate member of the third family is potentially a member of the fourth family because like members of the fourth family its IC9 residual is zero). Exceptionally, with another kind of event which will be discussed later, the last aircraft of one segment is different to the first aircraft of the following segment. Even in this exceptional case the two aircraft have the same value of objective function and the objective function versus external variable curve although composed of a series of segments does not exhibit discontinuities of value.

Returning to the particular example, the next observation is that for any value of cruise speed in the vicinity of the event value, whether greater or lesser, the direct operating cost of the aircraft belonging to the fourth family cannot be less than, and will generally be greater than, that of the aircraft belonging to the third family, since a degree of freedom has been lost in the optimisation of the former aircraft on account of constraint IC9 being active. It follows that the curves of direct operating cost for the two families do not intersect but that they touch at the event value of the external variable where they share a common tangent.

The difference between the values of the objective function for the two families of aircraft is therefore an even function of the difference between the value of the

external variable and its event value. It is plausible to suppose that in the immediate vicinity of the event value of the external variable the objective function difference will vary approximately as the second power of the external variable difference. Thus the direct operating cost of aircraft E' should be higher than that of aircraft E, and the direct operating cost of aircraft F should be higher than that of aircraft F₁. Moreover, since the value of the external variable for aircraft E and E' is about three times as far removed from the event value as is the value of the external variable for aircraft F₁ and F, it is to be expected that the objective function difference of aircraft E and E' will be about nine times as great as for aircraft F₁ and F. In fact both of these predictions are realised in practice as shown by the following:

$$\frac{\text{Direct operating cost of aircraft E'}}{\text{Direct operating cost of aircraft E}} = 1.000228$$

$$\frac{\text{Direct operating cost of aircraft F}}{\text{Direct operating cost of aircraft F}_1} = 1.000025$$

$$\frac{\text{Direct operating cost difference for aircraft E' and E}}{\text{Direct operating cost difference for aircraft F and F}_1} = 8.8$$

Having discussed in some detail the case of an inequality constraint becoming active it is only necessary to point out that the consequences of an inequality constraint becoming inactive may be deduced by following the external variable of the foregoing description in the reverse direction. The consequences of an independent variable encountering either of its bounds are similar to the consequences of an inequality constraint becoming active, whilst the consequences of an independent variable leaving either of its bounds are similar to the consequences of an inequality constraint becoming inactive.

If still higher cruise speeds are considered it is found that the aircraft design evolves smoothly along its latest course and the fourth family of aircraft continues through aircraft G and H, but in the eighth interval of cruising speed one of the independent variables (IV9) encounters its upper bound. To establish more clearly the trend were this not to happen, and to clarify the effect of the encounter, the bounding value may be experimentally increased, thus enabling the fourth family of aircraft to be extended to a member J₁:

Aircraft:	F	G	H	J ₁
%change in interval				
MTO	+1.69	+1.95	+2.16	
S	+3.26	+3.06	+3.18	
RATING	-0.35	-0.33	-0.29	
Engine mass	+2.78	+3.27	+3.41	
Take-off thrust	+2.42	+2.92	+3.11	
Take-off thrust/weight	+0.72	+0.95	+0.93	
Take-off wing loading	-1.52	-1.07	-0.99	
Take-off lift coefficient	-2.15	-1.93	-1.83	
Sweepback angle	+12.32	+10.53	+8.48	
Slat chord ratio	+5.50	+7.42	+7.61	

The table comparing aircraft F, G, H and J₁, shows that wing area and take-off thrust increase more rapidly than take-off weight as cruise speed is increased. It follows that wing loading falls whilst simultaneously the thrust-weight ratio available for take-off increases, and consequently the lift coefficient required at take-off decreases. Even so, the wing sweepback angle increases at such a high rate that successive aircraft require an increase in slat chord ratio. Slat chord ratio is the independent variable IV9, and the normal upper bound value is attained at about three-tenths of the speed interval between aircraft H and J₁. The need for enforcing an upper bound on the independent variable IV9 in the particular design synthesis which produced the results being examined is not a primary concern of this paper. However, the comments already made concerning the need for the inequality constraint IC9 are relevant to the need for an upper bound on IV9.

The effect of restoring the upper bound on IV9 to its normal value is considered next. As well as the legitimate aircraft J, an additional member H' of the fifth family has been generated by fixing the value of slat chord ratio and making it equal to the upper bound value.

3.2.5 With IV9 on its upper bound (aircraft designs H' and J)

It is found that the speed increase from aircraft H' to aircraft J is accompanied by the changes given in the following table. The corresponding changes between aircraft H and aircraft J₁ are also listed in the table for comparison

	Aircraft H' to J	Aircraft H to J ₁
Take-off lift coefficient decreases by	3.27%	1.83%
Sweepback angle increases by	6.42%	8.48%
Take-off mass increases by	2.18%	2.16%
Wing area increases by	4.79%	3.18%
Take-off thrust increases by	3.10%	3.11%
Engine mass increases by	3.72%	3.41%
RATING decreases by	0.60%	0.29%
Take-off thrust/weight increases by	0.89%	0.93%
Take-off wing loading decreases by	2.49%	0.99%

It can be seen that there is a bigger loss of take-off lift coefficient despite a smaller increase of sweepback angle. The increase of take-off mass is greater but only slightly so. Adverse effects on take-off performance are compensated by a greater increase in wing area. It is interesting to see that although the increase in the thrust available for take-off is hardly affected it is produced by relatively bigger engines. These are required to enable the specified net ceiling to be attained with an engine failed. The engines are rerated to reduce take-off thrust to the level required and to avoid the penalty of a bigger fin.

This concludes the detailed examination of the set of results for cruising height HCR1. It has been included in the paper to indicate how MVO results may be scrutinised and how an MVO program can be used to produce a clear picture of the implications of the model. It would of course have been possible to examine the results in much greater detail if that had been desired.

Fig 6 summarises the events and also shows the families of related results already discussed. It shows how the families overlap one another, also a system of notation which may be used to designate the members of families, *i.e.* with a prime to indicate members to one side of the legitimate ones and a suffix to denote members to the other side of the legitimate ones. Clearly this event table could have been constructed from a cursory examination of the original nine optimisations and would have indicated very clearly what additional optimisations were required to extend the families beyond their legitimate span to produce overlapping results.

If the results for any chosen quantity were to be plotted versus cruising speed (the external variable) the curve for all the legitimate results would be found to consist of a number of segments, each of which would correspond to the legitimate segment of the curve for a particular family. In the present case, legitimate curves for variables other than the objective function exhibit discontinuities of slope at the event points where the curves for two families intersect. The curve for the objective function is better behaved, the curves for each pair of families being tangential at the event points where they meet so that the slope of the curve of (legitimate) results is continuous. But this is not always the case as will appear presently.

3.3 Examination of the sequence of aircraft designs for the greater cruising height HCR2

Optimum designs were generated for the nine equally spaced values of cruising speed already adopted for the aircraft with lower cruising height. Fig 7 is an event table based on a survey of the results. In the event table for the lower cruising height HCR1 (Fig 6) none of the speed intervals contained more than one event, but in the table for HCR2 there is a speed interval that contains two events, namely interval E-F where an independent variable leaves its upper bound and an inequality constraint becomes active. These two events could be separate events occurring at different speeds within the same speed interval, but it is also possible that they may be a double event, *i.e.* they may occur together at the same speed. An attempt could be made to determine whether the two events are separate or not by subdividing the speed interval, or, more generally, the interval in the external variable, into smaller parts and generating additional optimum designs at the new speeds. Using this procedure it may be possible to establish either that the events are separate, or else that the separation between them is so small that, for practical purposes, they can be regarded as a double event. The stage at which the attempt to separate events, which have already been shown to be quite close to one another, should be terminated, depends on the circumstances of the particular case. But in some instances, even when the separation between two events is very small, valuable enlightenment may be gained from the discovery that one event precedes, and perhaps also triggers, the other. However in the case of the events in the interval E-F an examination of the results reveals an additional complication on account of which it is more difficult to locate the events as closely as might be desired. To understand the nature of this difficulty it is necessary to reconsider what happens in the vicinity of an event.

The values of the objective function for adjoining families of designs are equal at the event point which coincides with the last legitimate design of one family and the first legitimate design of the next family. However, for the kind of events discussed earlier, where one design is common to both families at the event point, the curves of objective function versus external variable for the two families do not intersect but are tangential to one another at the event point. Consequently the construction of such curves is not an altogether satisfactory way of locating such an event point. A more satisfactory method is to construct the curves for the affected independent variable, or, in the case of an inequality constraint, the constraint residual, versus the external variable since these curves for the two families of designs actually intersect at the

event point and so locate its position with greater certainty. Adopting this course for the speed interval E-F discloses a new state of affairs. The curves do not intersect. There must therefore be a jump in value at the event point whose position can only be located by finding the value of the external variable where the value of the objective function is the same for both families of designs. The curves of objective function versus external variable for the adjacent families of designs are not generally tangential to one another at this kind of event point where the adjacent families of designs do not share a common member. Instead, they are likely to intersect. However, the intersection may be a very shallow one, in which case the location of the event point will be only poorly defined. For this reason, the prospect of demonstrating that two events that are close to one another are separate events and not a double event is diminished.

Since for the new kind of event the last legitimate design of one family differs from the first legitimate design of the next family, *ie* the adjacent designs at the event point are not identical, it could be expected that they may differ from one another in many respects and that there may be a jump in the value of many of the independent and dependent variables including the constraint residuals. There is therefore a likelihood that an event involving jumps may be a double or even a multiple event. Consequently if the event table discloses that two or more events lie within one interval of the external variable the possibility should be considered, not only that they may constitute a double or multiple event, but also that they may constitute a double or multiple event involving jumps. But jumps will not show up at all in the event table unless they result in an independent variable being taken onto or off one of its bounds, or unless they result in an inequality constraint becoming active or inactive.

The probability of jumps occurring tends to increase with the complexity of the model. But the greater the complexity of the model, the more independent variables and inequality constraints it is likely to include and so the more likely it is that a jump will result in an event of the kind that appears in the event table. Nevertheless the possibility exists that there may be hidden events which are of the new kind discussed above but which do not result in any independent variable encountering or leaving a bound, or in any inequality constraint being activated or inactivated. This is a disturbing prospect, but there is some comfort in the realisation that the likelihood that an event involving jumps will remain hidden is related to the size of the jumps themselves, and that events involving large jumps are less likely to remain hidden than events involving only small jumps.

The kind of topography that gives rise to a hidden event is depicted in the map at the top of Fig 8. To construct such a map the results of normal optimisations at a number of values of the external variable would be combined with the results of additional optimisations at a network of values of the external variable and the independent variable, the latter also being treated as an external variable for the purpose. Thus a considerable volume of work is entailed. The construction of such a map is an interesting exercise, but its only purpose is to build up confidence in, and also to develop a feel for, the optimisation process, and it would not normally be undertaken in an MVO study. These comments also apply to the other maps that will be discussed. At the lowest values of the external variable shown in the figure there is one family of optimum designs denoted 'family n'. At a somewhat higher value of the external variable a second family of optimum designs, denoted 'family n+1', appears and coexists with the original family n. At a still higher value of the external variable family n dies out and family n+1 remains on its own. At the event value of the external variable the optimum designs of both families have equal values of objective function. The range of values of the external variable where the two families of designs coexist is a region of suboptima. At values of the external variable within the region of suboptima but below the event value the designs of family n+1 are suboptimum designs. Within the region of suboptima but above the event value the designs of family n are suboptimum designs. The behaviour of the objective function is shown in the middle section of Fig 8.

An optimisation at a value of the external variable within the region of suboptima may generate a design of either family and consequently a suboptimum design may be produced. In practice MVO programs seem to exhibit a preference for one or the other of the families of designs and, if optimisations are performed at a sequence of values of the external variable within the region of suboptima, the designs generated switch from one family to the other at a value of the external variable that differs from the event value. This is depicted in the lower part of Fig 8. The characteristic shape of this figure is worth bearing in mind when examining plots of values of the objective function versus an external variable since it may lead to the detection of a hidden event. A suboptimum value of the objective function may only differ from the true optimum value by a small amount, but relatively bigger errors may be experienced in the values of the independent and dependent variables if a suboptimum design is not recognised as such.

An event involving a jump to a bound is illustrated in Fig 9. The map in the upper half of the figure depicts the topography for an independent variable that encounters its upper bound, whilst the map in the lower half of the figure depicts the topography for one of the other independent variables. Both maps relate to the same event, and contain the same optimum and suboptimum designs at the same values of the external variable. Both maps would be constructed by the method already described in connection with Fig 8 and if it were not for the bound their topography would resemble that of Fig 8. The imposition of the bound directly limits the size of the jump of the independent variable it acts on. It also changes the location of the jump, *ie* it changes the event value, and the range of values of the external variable within which suboptimum designs exist.

In addition it exercises a restraining influence on the size of the jump of the other independent variables as indicated on the lower map.

For every point on the lower map there is an optimum value of the independent variable of the upper map, and so contours showing the optimum values of the upper map independent variable could be superimposed on the lower map. One such contour must therefore correspond to the value of the upper bound imposed on the upper map independent variable. This contour divides the lower map into two zones and may be called a zone frontier. In one zone the imposition of the upper bound has no effect since the optimum values of the upper map independent variable are everywhere less than the bound value. In the other zone though, a new set of optimum designs are required that do not violate the upper bound. Since a degree of freedom has been lost the new optimum designs inevitably have larger values of objective function and this shows in the new objective function contours. These new contours merge smoothly with the original contours for the zone at the frontier between the two zones, and hence they merge into the unchanged contours of the other zone, i.e. the values and slopes are equal on either side of the frontier.

The map for a jump event in which an inequality constraint is activated is similar to the lower map in Fig 9. In such a case one of the zones would correspond to the inequality constraint being active (zero constraint residual) and the other zone would correspond to the inequality constraint being inactive (positive constraint residual).

A detailed study has not been undertaken to determine whether or not the two events in the interval E-F are separate events, but it appears probable that they are not separate and that, at least for practical purposes, they may safely be regarded as a double event. There is certainly an event in the interval that involves jumps and this supports the view that the two events are combined. The topography for such an event is more complex than those depicted in Figs 8 and 9. The map for the independent variable that leaves its bound would have two zones, with a frontier where the inequality constraint changes between being inactive and being active. The map for any of the other independent variables would have two frontiers, one associated with the inequality constraint and one with the bound. The latter maps would therefore have at least three zones, and even more if the frontiers were to intersect.

The double event in the interval E-F appears not to be the only event involving a jump. The event in the interval G-H also exhibits a jump though only a weak one. The events in the intervals A-B and C-D are of the kind already discussed in connection with the aircraft designed for the lower cruising height HCR1.

3.4 The effect of designing for cruising height HCR2 instead of for cruising height HCR1

Having analysed the results for the two cruising heights HCR1 and HCR2 separately, it is possible to construct curves through the sets of points showing the effect of the increase of altitude on direct operating cost (ΔDOC), take-off mass (ΔMTO), take-off wing loading (ΔWLD), take-off span loading ($\Delta(WLD/A)$), and engine mass ($\Delta MENG$), which were originally plotted in Fig 2. It was the irregularities exhibited by some of these sets of points that engendered some perplexity about the MVO results, or, alternatively, misgivings about their accuracy, and provided an incentive for the detailed analysis that has been undertaken. This analysis has disclosed a number of what have been termed 'events' with which are associated various kinds of discontinuities, namely, discontinuities of curvature or possibly of slope in plots of the objective function, and discontinuities of slope or even of value in the case of the other variables. These discontinuities, which are the visible consequences of the events, explain the seeming irregularities to be seen in some of the sets of points. Fig 10 lists the events in the order in which they occur as cruising speed is increased, gives their approximate locations, and indicates where jumps may be found. The curves showing how the increments in direct operating cost (ΔDOC), take-off mass (ΔMTO), take-off wing loading (ΔWLD), take-off span loading ($\Delta(WLD/A)$), and engine mass ($\Delta MENG$) vary with cruise speed VCR, each with the original set of nine points, are contained in Fig 11. Results from the extended families of designs were used to plot additional points used in the construction of the curves, but these points have been removed from the figure presented, and the curves themselves have been cut back so that the figure does not contain information relating to any designs that are not legitimate ones. No extrapolation was involved in drawing any of the segments of the curves.

The curves in Fig 11 display more features than would normally be the case. Being the difference between two sets of results means that each curve is likely to include double the number of discontinuities, but also, because each of the plotted values is the relatively small difference of two large quantities, the discontinuities are far more pronounced than they would otherwise be. For the same reason any random errors in the results would also be easier to discern. In fact, no scatter was perceptible in the complete sets of results, including the results for the illegitimate designs generated to extend the families of legitimate designs.

The results support the view that by using an MVO program it is possible to generate aircraft designs that accurately reflect the characteristics of the model employed in the MVO program. The challenge therefore is to create models which are sufficiently realistic for the purposes they are intended to serve. It can be asserted with confidence that it is already possible to create models that are adequate for many useful applications of MVO, and it is to be expected that, in the course of time, further advances will enable the development of MVO programs for use in a broader field of applications.

4 APPLICATIONS FOR MVO PROGRAMS

Having described the essentially dual nature of an MVO program (model plus optimisation method), and having considered some techniques for exploiting this duality (making use of the optimisation method to explore the model), it remains to discuss applications for MVO programs. The possibility to use an MVO program in the earliest stages of the consideration of a new aircraft design was mentioned in the introduction. In this application the MVO program serves to provide an embryo aircraft design which can be taken as the starting point for more detailed investigations. In addition, by providing consistent and extensive information about the consequences of making changes to the performance requirements, it may assist designers to evolve aircraft designs which, by appealing to more operators, offer the prospect of sales in greater numbers and consequently increase the probability of success. Opportunities such as these for the use of MVO programs by aircraft designers are surely easy enough to identify and so there is little need to discuss them here. Instead, the use of MVO programs in studies undertaken with the specific aim of helping to establish the best combination of performance requirements for a particular aircraft operator will be considered. This application is of some interest to major airlines but the need is greater in the framing of requirements for military aircraft. For this reason much of the ensuing discussion will be based on a study relating to a possible military requirement.

It has been implied that it is more difficult to decide on the requirements for a new military aircraft than it is to specify the requirements for a new civil transport aircraft. It is certain that, at least in some respects, the formulation of a model for military aircraft presents greater difficulties than does the formulation of a model for civil transport aircraft. The diversity of military tasks gives rise to a great variety of aircraft configurations including aircraft with variable sweep as well as other forms of variable geometry, and also aircraft with provision for deflecting the thrust of their engines. Of course a model may be formulated to deal with only one type of configuration. Even so it may have to take into account the carriage of stores externally, possibly only on certain missions, and even then only during part of the flight if the store is released. Packaging, that is to say the positioning of the crew, all of the equipment, the power plant and the fuel in acceptable locations, and the definition of an envelope shape that will enclose them all, is more complicated than for a civil transport aircraft. The range of flight conditions that has to be considered is greater extending well into the supersonic regime and including high g manoeuvres. And the range of engine operating conditions is broader, including performance with and without reheat. On account of factors such as these the MVO program used in the example to be discussed embodies a model which is in some respects more complex than that embodied in the transport aircraft MVO program that produced the results used in the last section of the paper. But in other respects the model is simpler and it is formulated with a smaller number of independent variables. The same optimisation method is employed in both programs.

The requirement to which the program has been applied is for a strike aircraft. The sortie involves take-off and climb to a moderate altitude where the aircraft cruises at an economical speed before descending to commence, at a specified radius, a low-level high-speed (subsonic) dash to the target area. The distance penetrated in this dash is treated as an external variable. On reaching the target area the aircraft commences a search which is allowed for by flight at a specified speed and normal acceleration for a specified period of time after which the aircraft is assumed to release its weapons. The aircraft then repeats the stages of its outward flight but in reverse order, commencing with the low-level high-speed dash followed by climb, economical cruise, descent, and landing at the base from which it started. Reheat is not employed in the basic mission. The thrust available during the dash out and back, and during the search, is limited to the maximum dry thrust of the engines. All of the fuel required for the complete sortie (including reserves) is to be carried internally. The objective function chosen for the study is aircraft unit production cost.

Some results from the study are shown in Figs 12 to 15 which contain curves relating unit production cost, engine size, wing area, and fuel used to the penetration distance. The curves labelled A are for aircraft which have only to fulfil the basic sortie requirement. Among the complete results for these aircraft is information on their airfield performance. A perusal of this information suggests that a better standard of airfield performance is desirable to enable operations from short runways or from usable sections of longer runways that have been damaged by enemy action. The curves labelled B are for aircraft which, as well as fulfilling the requirements of the basic sortie, comply with upper limits imposed on their take-off and landing distances, the use of reheat being permitted during take-off. It was necessary to introduce two additional inequality constraints to limit the take-off and landing distances which, as the model is formulated, are both dependent variables. For the aircraft with the shortest penetration distances the inequality constraint concerned with landing distance was active but for the rest of the designs generated this constraint was inactive and the constraint concerned with take-off distance was active instead. The event where the status of these two inequality constraints changes is shown most clearly by the slope discontinuity near the left-hand end of the curve labelled B in Fig 14. Clearly it would be possible to consider more than one level of airfield performance, and instead of one family of designs several families of designs could be generated. Then, instead of one curve B in each figure, there would be a separate curve for each family of aircraft designs, ie one for each specified level of airfield performance. A decision on the level of airfield performance to be demanded in the ultimate requirement could then be taken with the benefit of an indication of the likely consequences in terms of aircraft unit production cost.

It could be of interest to determine the consequences of broadening the requirement so that it would result in an aircraft capable of fulfilling other, possibly subsidiary, roles. The curves labelled C show the effect of adding a requirement that the clean aircraft should be capable of attaining a specified high speed in level flight at a specified high altitude. The values of speed and altitude could be chosen to ensure a reasonable escape and pursuit capability. The formulation of the model is such that the altitude could be entered as data but because attainable speed is a dependent variable a further inequality constraint is required. The results show that, for the particular combination of speed and altitude considered, the inequality constraint is not active if only a short penetration distance is required. This means that the low penetration distance aircraft associated with the curves labelled B are capable of fulfilling the additional requirement. The curves labelled D and E show the effect of adding requirements first for a high specific excess power at an intermediate altitude, which would enable the aircraft to climb rapidly for interception, and then, in addition, for a high sustained rate of turn at a high altitude and a specified speed, which would ensure some desired level of manoeuvrability for air combat. Between them, the additional requirements involved in going from the curve labelled B to the curve labelled E involve specifying the values of seven quantities. These could all be treated as external variables to generate more information which could be of assistance in determining the best set of requirements. However another approach may be followed.

As a general rule, a good principle to adopt in MVO studies is to allow the optimisation method as much freedom as possible to find the optimum solution. An example of the benefit that may be derived will be given. It is possible to define a parameter which is a good overall measure of the air combat capability of an aircraft. Several such parameters have been defined and used. They are all functions of such quantities as specific excess power, sustained rate of turn, and maximum instantaneous rate of turn under defined conditions of altitude and speed. Two aircraft having equal values of such a parameter would be expected to be more or less equally matched in combat with one another. Adopting one such parameter it was found that all of the aircraft designs corresponding to the curves labelled E in Figs 12 to 15 have practically the same value. This is not too surprising since the aim in generating these aircraft was to give them an equal air combat capability. However, the aircraft were generated specifying a minimum level for both specific excess power and sustained rate of turn, under defined conditions, by means of two inequality constraints. A further set of designs was generated replacing these two inequality constraints by one which was used to stipulate that the aircraft designs could attain a minimum level of the selected air-combat parameter equal to that attainable by the aircraft associated with the curves labelled E. The curves labelled F are for the resulting aircraft, which have the same level of air combat capability as do the aircraft associated with the curves labelled E, but lower unit production costs. By using the air combat parameter, instead of using specific excess power and sustained rate of turn, unit production cost is cut by an amount varying between 3½% at the shortest penetration distance and 7% at the longest penetration distance. This advantageous result was possible because the optimisation method was free to explore the various possibilities presented to it by the air combat parameter, trading between the various quantities embodied in it, instead of being tied to the attainment of fixed values of two quantities which yield the same air combat capability.

In a study, like the strike aircraft study, where the object is to investigate the consequences of various requirements, attention would be focussed on the value of the objective function rather than on the details of the aircraft generated in the study. However other interesting information may be contained in the rest of the results which should not be completely neglected. Giving the strike aircraft an air combat capability increases the unit production cost (the objective function) by about 7% in this particular instance (see Fig 12). But Fig 15 shows that it would also increase the fuel used in the strike role by between 8% and 16% which could be an important drawback from a logistics point of view. But, of course, fuel consumption as such is not within the compass of the objective function used in the study. This suggests that insufficient emphasis may have been placed on the importance of keeping down fuel consumption, and points to a possible shortcoming in the objective function used in the study. Observations such as this can lead to the development of improved objective functions.

The broadening of the strike aircraft requirement to include additional requirements giving a measure of air combat capability is a simple example of a promising field of application for MVO methods, namely to study the penalty incurred by combining various roles. The advantages of multi-role aircraft are not difficult to appreciate and they have, of course, been recognised for many years. It may be possible to combine some roles with only minor consequences but other combinations of roles may involve conflicting requirements and consequently a heavy penalty may be incurred. Whilst it may be possible to judge when a serious conflict may arise, to quantify the penalty is not so easy and the use of an MVO program to investigate the various possibilities could be beneficial.

The small number of events displayed in the results of the strike aircraft study appears remarkable when compared with the many events that occurred in the transport aircraft study results considered in the previous section of the paper. The following discussion arises from the observation. Some requirements may be specified precisely but there are generally others that specify the attainment of a minimum level without excluding a margin of over-attainment. Some examples of the former type of requirement taken from the transport and strike aircraft studies are cruising speed, cruising height, payload and stage length, dash speed, dash altitude, stores load and penetration distance. Examples of the type of requirement in which a margin of over-attainment is not excluded are take-off field length, specific excess power, and sustained turn rate. The latter

type of requirement is, of course, applied by means of an inequality constraint. An optimum design usually has at least one active inequality constraint but probably also has several inactive inequality constraints. An inequality constraint that is inactive is associated with a margin of over-attainment the existence of which may confer some advantage on the aircraft, though any such advantage is not taken into account in its value of objective function. However, if a way could be found to reduce or even eliminate the margin of over-attainment it might be possible to improve (i.e. reduce) the objective function. The greater the number of independent variables the more scope there is for the optimisation method to mould the solution so that the capabilities of the optimum design that emerges are better matched over the spectrum of requirements as a whole. For this reason, optimum designs found using a model with a greater number of independent variables are likely to be superior to the corresponding designs generated with a model that has a smaller number of independent variables. One way of improving a model is to study the margins of over-attainment of optimum designs produced by the model, and to try to envisage the best way of elaborating the model so as to improve the scope for reducing the margins. Margins of over-attainment cannot always be converted into improvements in the value of the objective function but the possibility should always be contemplated. Dedication to reducing margins of over-attainment whenever they can be exchanged for any improvement in the objective function, however small and despite the consequent loss of any advantage they confer, is entirely logical because the objective function is supposed to be the true measure of the merit of a design. If there are any doubts about the current objective function thought should be given to evolving a better one. A greater number of independent variables generally makes it possible for more inequality constraints to be active simultaneously, but as the value of an external variable changes so does the membership of the group of active inequality constraints, and it appears that the more numerous the group the more frequently its membership changes. This accounts for the greater number of events in the results from the transport aircraft studies.

From time to time circumstances arise in which the use of a compound objective function may be helpful. A compound objective function is a weighted mean of two, or exceptionally more, distinct quantities, at least one of which is potentially an interesting objective function. The following equation is for the case when the compound objective function COF is a weighted mean of two potential objective functions OF1 and OF2:

$$\text{COF} = (1 - \eta) \times \text{OF1} + \eta \times \text{OF2} \quad 0 \leq \eta \leq 1$$

A compound objective function can be used to generate a sequence of designs by changing the value of the weighting parameter η so that a curve such as that shown in Fig 16 can be constructed. One possible application would be to determine the smallest penalty in the direct operating cost OF1 of a transport aircraft due to reducing its noise footprint area OF2. Another possible application would be to investigate the range of possibilities between the minimum direct operating cost OF1 aircraft and the minimum fuel consumption OF2 aircraft. This is an interesting case because the cost of the fuel is one component in the direct operating cost. It follows that there exists a level of fuel price which would lead to the same aircraft being generated in a simple optimisation with direct operating cost as the objective function. This can be shown as follows.

The part of the direct operating cost due to the cost of the fuel is equal to the product of the price of fuel PFUEL and the fuel consumed and so the direct operating cost can be written

$$\text{DOC} = \text{DOC1} + \text{PFUEL} \times \text{FUEL CONSUMED}$$

where DOC1 is the part of the direct operating cost that is not associated with fuel consumed. The combined objective function is therefore

$$\begin{aligned} \text{COF} &= (1 - \eta) \times \text{DOC} + \eta \times \text{FUEL CONSUMED} \\ &= (1 - \eta) \times \text{DOC1} + \{(1 - \eta) \times \text{PFUEL} + \eta\} \times \text{FUEL CONSUMED} \\ &= (1 - \eta) \times \left\{ \text{DOC1} + \left(\text{PFUEL} + \frac{\eta}{1 - \eta} \right) \times \text{FUEL CONSUMED} \right\} \end{aligned}$$

Within an optimisation η , and hence also $(1 - \eta)$, does not vary and so the same aircraft design would be generated with a simple objective function equal to

$$\text{DOC}' = \text{DOC1} + \text{PFUEL}' \times \text{FUEL CONSUMED}$$

where $\text{PFUEL}' = \text{PFUEL} + \eta/(1 - \eta)$. Although the same aircraft design would be generated its direct operating cost would be higher on account of it being calculated with the higher fuel price PFUEL'. If the direct operating cost of the aircraft were to be recalculated with the original fuel price it would be found to have the value originally obtained. This shows that every design produced by the compound objective function is a minimum direct operating cost design at a different fuel price level (see Fig 17). The minimum direct operating cost design tends towards the minimum fuel consumption design as the price of fuel tends to become infinitely great. Curves such as those in Figs 16 and 17 define a boundary between a region in which designs do not exist and a region where designs do exist. But the designs on the boundary are the only ones that are potentially

interesting. By providing a rapid means for finding such designs a compound objective function can serve a useful purpose.

Among the applications for MVO that have not been discussed is its use for assessing the likely benefits that could result from advances in technology. Most advances can best be exploited by using them to further the evolutionary development of recognised types of aircraft. MVO is well suited to the preliminary study and evaluation of such evolutionary developments. A simple example is to be found in Ref 1.

5 CONCLUSIONS

Complex models of aircraft design and operation can be explored with great facility using computer based optimisation methods in MVO programs. An MVO program should not be regarded as a means to produce isolated optimum designs but as a versatile tool which can be used to assemble comprehensive sets of consistent data. By systematically examining such sets of data a deep and thorough understanding can be gained of the interaction between the contending effects within the model. Applications for MVO programs are not confined to indicating starting points for aircraft design studies. Other important applications include helping to provide a better basis for drafting requirements for future aircraft.

Acknowledgments

I should like to thank Mr D.A. Lovell for supplying Figs 12 to 15 (discussed in section 4 of the paper) from his strike aircraft study. I should also like to acknowledge the debt I owe to Mrs Joan Collingbourne who has been my co-worker in MVO pursuits generally over a long period of time.

Table 1

QUANTITIES IN MVO PROGRAM USED IN STUDY REFERRED TO IN SECTION 3

Independent variables:

IV1	Wing area	} Independent variables defining overall wing geometry
IV2	Aspect ratio	
IV3	Sweepback	
IV4	Taper ratio	
IV5	Thickness-chord ratio	
IV6	Compressibility drag parameter	} Independent variables defining engines
IV7	Engine mass	
IV8	Engine re-rating parameter	
IV9	Slat chord ratio	
IV10	Flap span ratio	} Independent variables defining high lift system
IV11	Flap chord ratio	
IV12	Flap take-off setting	
IV13	Flap landing setting	
EV1	Cruise speed	} Potentially independent variables but fixed, \therefore constants, and used as external variables
EV2	Cruise altitude	

Inequality constraints:

IC1	Take-off field length \geq specified field length
IC2	Take-off climb gradient \leq airworthiness requirement
IC3	Cruise thrust \leq cruise drag
IC4	Net ceiling with engine failed \leq specified value
IC5	Fuel volume available \leq fuel volume required
IC6	Aspect ratio - sweep function \geq specified value
IC7	Throttle setting during approach \leq specified value
IC8	Body angle at landing \leq specified value
IC9	Thickness-chord ratio \leq function of sweep

Equality constraints:

EC1	Approach speed ratio = 1.3
EC2	Thickness-chord ratio = calculated thickness-chord ratio

REFERENCES

- 1 D.L.I. Kirkpatrick, M.J. Larcombe: Initial design optimisation on civil and military aircraft. AGARD-CP-147 (1974)
- 2 A.G. Purcell: The development of quasi-Newton methods for unconstrained minimisation. RAE Technical Report 77132 (1977)
- 3 A.G. Purcell: Fortran programs for constrained optimisation. RAE Technical Report 77142 (1977)

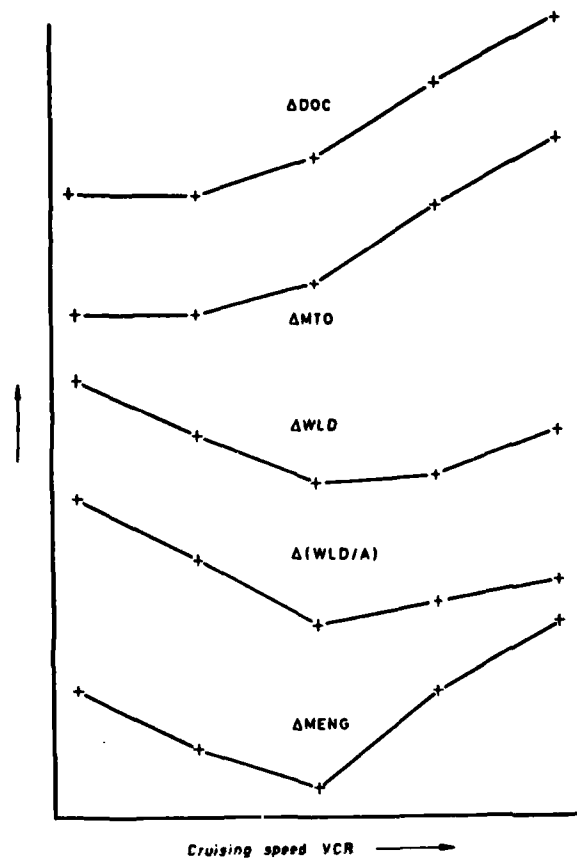


Fig 1 Effect of increasing cruise height (original set of results)

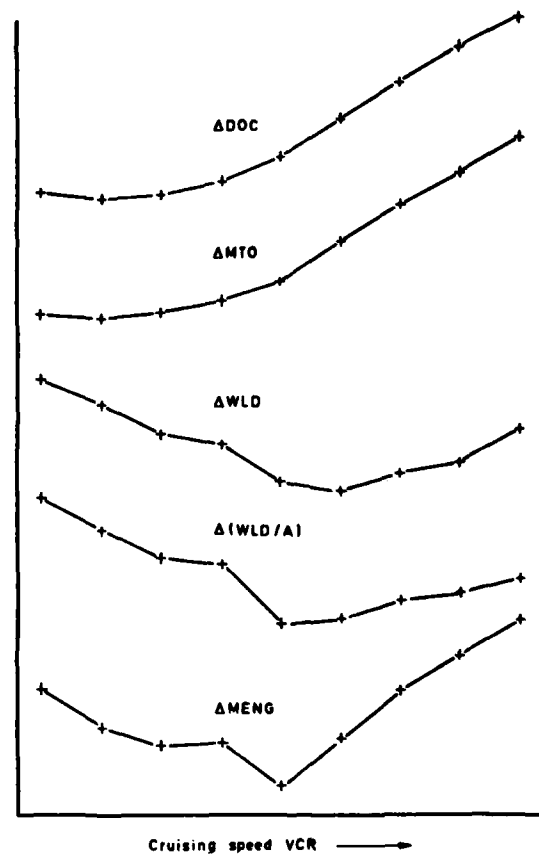


Fig 2 Effect of increasing cruise height (augmented set of results)

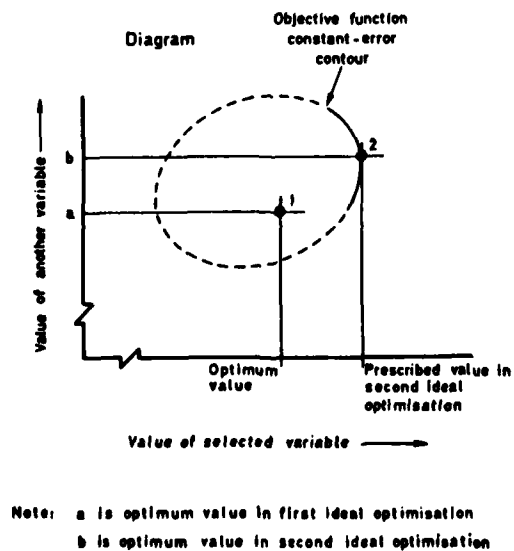


Fig 3 Objective function error contour

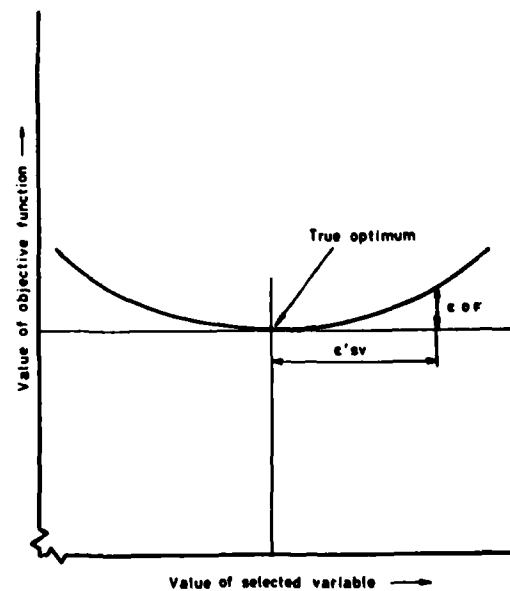
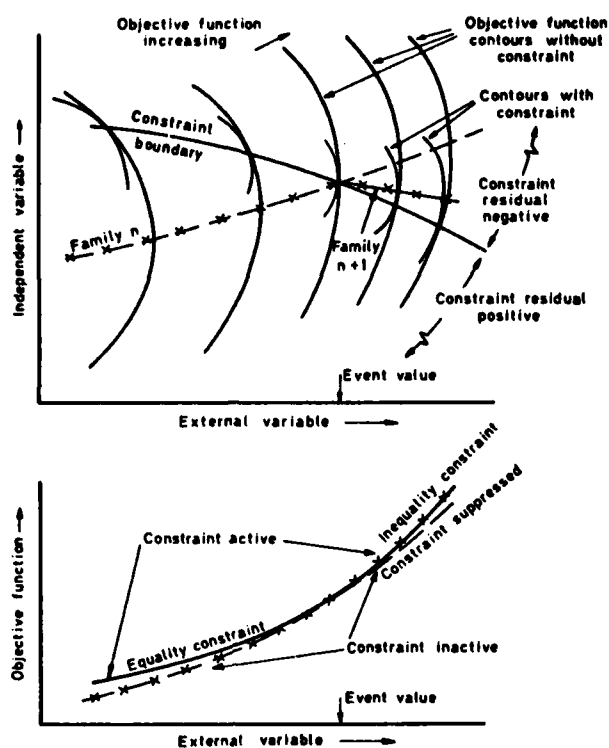


Fig 4 Relationship between error in objective function and maximum error in a variable



Crosses indicate values for legitimate designs

Fig 5 Topography of an event in which a constraint becomes active

Original set of results		A	B	C	D	E	F	G	H	J
Inequality constraints	IC 1		Active							
	IC 2									
	IC 3									
	IC 4									
	IC 5									
	IC 6									
	IC 7									
	IC 8									
	IC 9						Active			
Independent variables	IV 1									
	IV 2									
	IV 3									
	IV 4									
	IV 5									
	IV 6				Upper bound					
	IV 7									
	IV 8									
	IV 9									
	IV 10								Upper bound	
	IV 11									
	IV 12									
	IV 13									
Families of results	1	A	B	C	D	E	F	G	H	J
	2	A	B	C	D	E	F	G	H	J
	3	A	B	C	D	E	F	G	H	J
	4	A	B	C	D	E	F	G	H	J
	5	A	B	C	D	E	F	G	H	J

Fig 6 Event table for HCR1 results

Original set of results		A	B	C	D	E	F	G	H	J
Inequality constraints	IC 1						Active			
	IC 2									
	IC 3									
	IC 4									
	IC 5									
	IC 6									
	IC 7									
	IC 8									
	IC 9				Active					
Independent variables	IV 1									
	IV 2									
	IV 3									
	IV 4									
	IV 5									
	IV 6		Upper bound							
	IV 7									
	IV 8									
	IV 9									
	IV 10		Upper bound							
	IV 11									
	IV 12									
	IV 13									
Families of results	1	A	B ₁	C	D ₁	E	F ₁	G	H ₁	J
	2	A'	B							
	3			C'	D					
	4					E'	F			
	5							G'	H	

Fig 7 Event table for HCR2 results

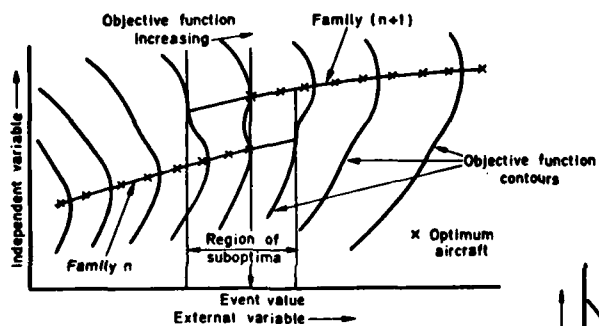


Fig 8 Topography of a hidden jump event

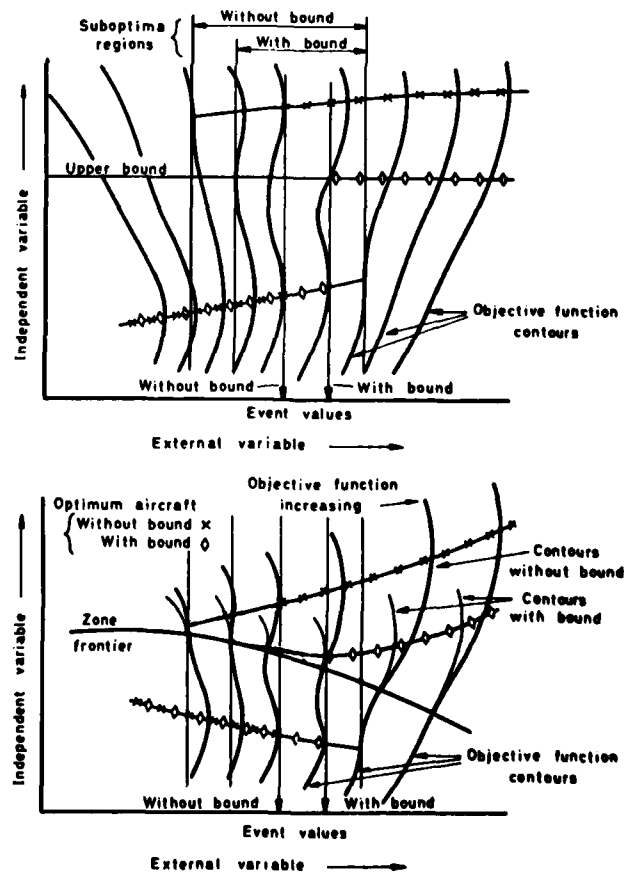


Fig 9 Topography of a jump event with a bound being encountered

Cruising speed interval	Cruising height	Event location within cruising speed interval	Comments
A-B	HCR1	Close to A	Double event, strong jump
A-B	HCR2	50% from A	
C-D	HCR1	20% from C	
C-D	HCR2	Close to D	
E-F	HCR1	20% from F	
E-F	HCR2	A little indefinite but near F	
G-H	HCR2	Indefinite but nearer to H than to G	
H-J	HCR1	20% from H	
			Weak jump

Fig 10 Combined event sequence

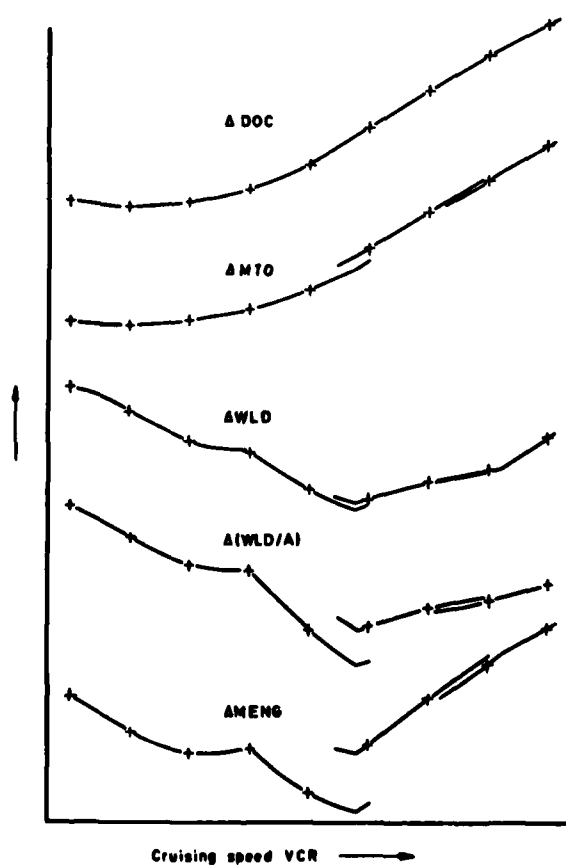


Fig 11 Effect of increasing cruise height (final curves)

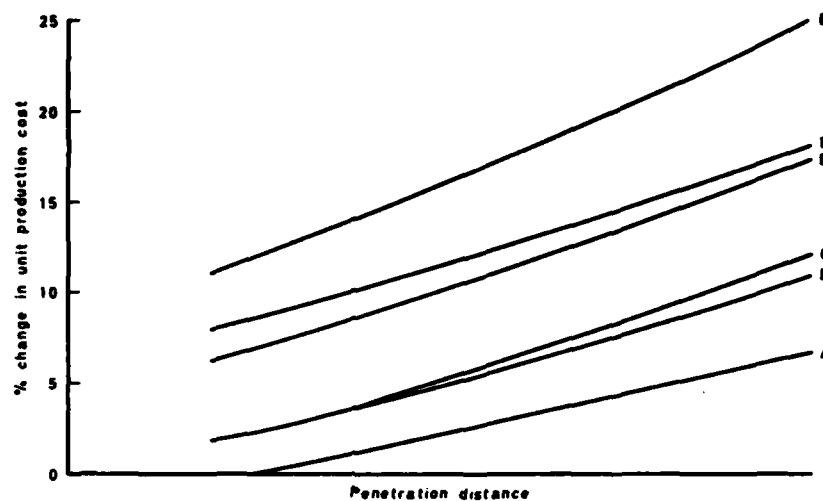


Fig 12 Strike aircraft study results - unit production costs

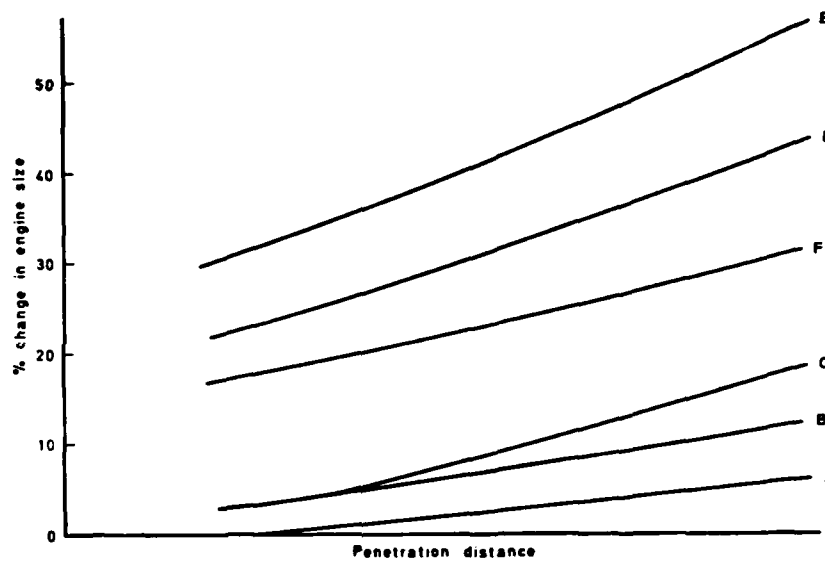


Fig 13 Strike aircraft study results - engine size

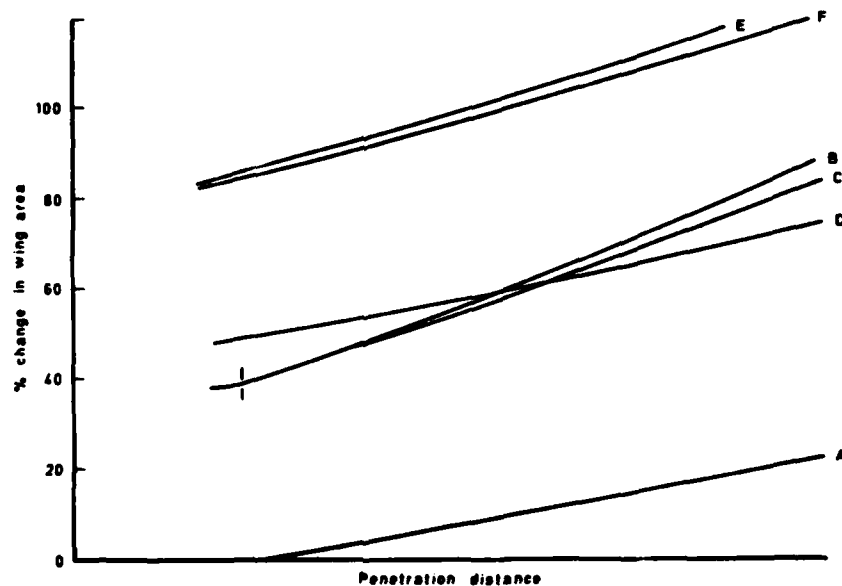


Fig 14 Strike aircraft study results - wing area

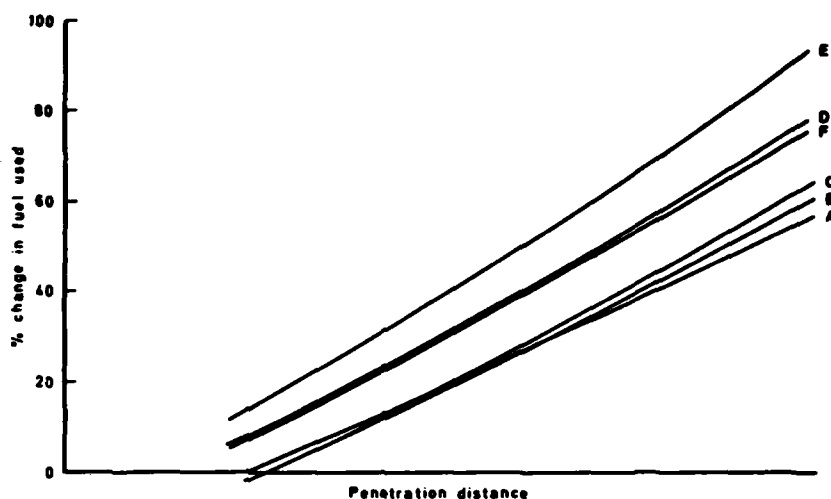


Fig 15 Strike aircraft study results - fuel used

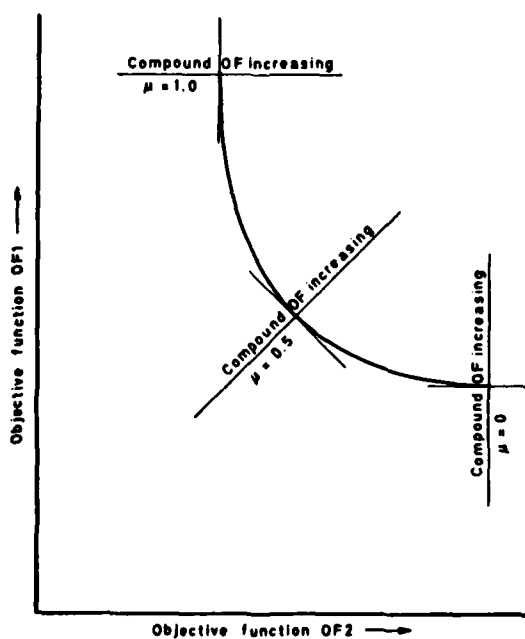


Fig 16 Results with compound objective function

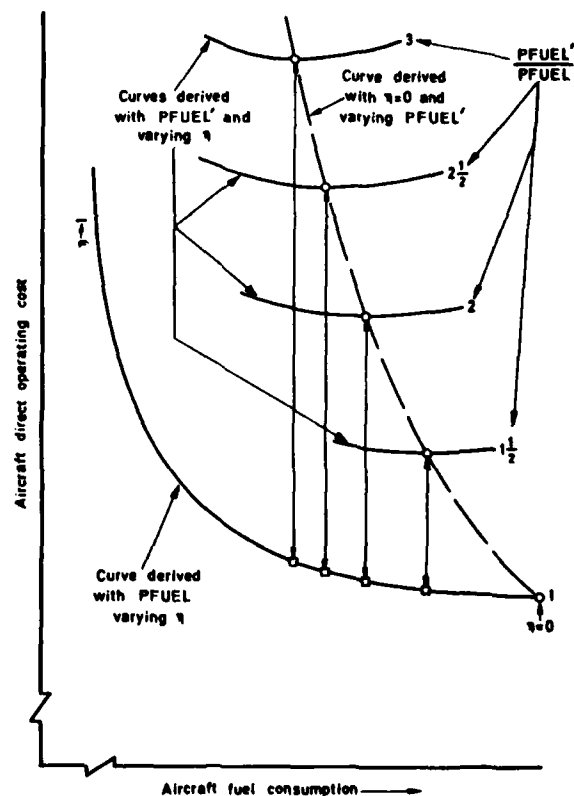


Fig 17 Effect of minimising direct operating costs with different fuel prices

SOME FUNDAMENTAL ASPECTS OF TRANSPORT AIRCRAFT CONCEPTUAL DESIGN OPTIMIZATION

by E. Torenbeek
Senior Lecturer Aircraft Design
Delft University of Technology
Department of Aerospace Engineering
2629 HS Delft - the Netherlands
August 1979

SUMMARY

Various design merit functions and program structures are discussed and program elements common to most design exercises are analyzed. Criteria are presented for optimum cruise conditions for aircraft with or without Mach number dependent drag polars and arbitrary propulsion systems. Constrained and unconstrained optima for design cruise speed and altitude, engine thrust, wing loading and aspect ratio are presented in the form of generalized analytical expressions. They are based on closed-form equations for the payload weight fraction. A Powerplant Merit Function is proposed, which can be used for assessing propulsion systems in the project study phase in isolation from the aircraft design.

The method gives clear insight into the design problem structure and is adaptable to arbitrary ground rules and different data bases. The trade-off between mission requirements, technological factors and (optimum) design characteristics is evident from the criteria presented.

NOMENCLATURE

A	- aspect ratio; unconstrained optimum point
a_0	- velocity of sound at sea level, standard atmosphere
B	- constrained optimum point
b	- wing span; factor in DOC formula
C_D	- aircraft drag coefficient (\bar{C}_D airframe drag coefficient)
C_{D0}	- zero-lift drag coefficient
C_{D0}^o, C_{DM}	- logarithmic derivatives of C_D w.r.t. C_L and M, resp.
\bar{C}_D^o, C_{DL}^o	- equivalent profile drag coefficient $d(C_D S)_{wet}/dS$
C_{LP}	- lift coefficient; $C_{L_{ref}}$: C_L for min. wing - associated drag; $C_{L_{MD}}$: C_L for minimum drag
C_{L2}	- lift coefficient at take-off safety speed
C_P	- turboprop engine ESFC
C_T	- turbojet and -fan TSFC
C_t	- powerplant specific weight
C_η	- factor relating η , η_M and M: $C_\eta = \eta/(\eta_M M)$
D	- drag; D_p : powerplant installation drag
E	- ratio of $C_L^2/\pi A$ to the total C_D at V_2 (take-off)
e	- Oswald factor
F	- fuel burnt per unit time
F_D	- fixed drag area
F_P	- Powerplant Merit Function
g	- acceleration due to gravity
H	- specific calorific value of fuel (J/kg)
h_{to}	- reference height in take-off analysis
k_{run}	- factor of proportionality in take-off analysis
L	- lift
M	- Mach number; M_{MD} : minimum drag Mach number
m	- mass (contribution); indices: "fix" for fixed, "F" for fuel, "P" for powerplant, "pl" for payload, "oe" for operating empty, "to" for take-off, and "var" for variable
N_e	- number of propulsion engines installed per aircraft
P_{br}	- brake horsepower (P_{eq} : equivalent HP)
p	- atmospheric static pressure; p_0 : at sea level standard
q	- dynamic pressure
R	- range; \bar{R} : equivalent design range

R_H	- range-equivalence of H : $R_H = H/g$
S	- wing area
S_{air}, S_{run}, S_{to}	- air distance, run length and total field length for take-off
T	- net thrust; T_{to} : static thrust at sea level, ISA ; T_{MD} : thrust at MD alt.
t	- time; t_b : blocktime
V	- true airspeed; V_b : blockspeed; V_2 : take-off safety speed
W	- weight; indices: "a" for airframe, "F" for fuel, "P" for powerplant, "pl" for payload and "to" for MTOW ; no index: aircraft weight
γ	- ratio of specific heats of atmospheric air
δ	- relative atmospheric pressure
η	- total engine efficiency; $\bar{\eta}$: referred to $T-D_p$; η_p : propeller efficiency
η_T, η_M	- logarithmic derivatives of η w.r.t. T/δ and M , resp.
η	- propeller efficiency
θ	- relative atmospheric temperature
λ	- normalized drag/lift ratio at V_2
μ	- mass ratio
ρ_{to}	- atmospheric density during take-off
τ	- normalized T/W ratio at V_2
σ_A, σ_S	- empty mass sensitivity parameters w.r.t. A and S , resp.
ϕ	- induced drag factor for wing design - C_L
ω	- normalized span loading used in take-off analysis.

1. INTRODUCTION

Until about 1955-1960 conceptual aircraft design studies were generally based on relatively simple criteria and methods. Although published contributions (e.g. Refs. 4, 5, 11) have not always been representative of industrial practice, they do indicate that early parametric studies were made on a limited scale, frequently by highly competent and experienced designers with a thorough insight into what could be considered as realistic optimization opportunities in the conceptual design process.

The situation changed drastically when high-speed digital computers were introduced, enabling the designer to analyze a virtually unlimited number of parametric variations. The application of interactive graphics tools has considerably enhanced Computer Aided Design (CAD), and all major aircraft factories nowadays use CAD in certain phases of the design process. A fundamental problem inherent to any computer-assisted effort is that the designer's mind tends to be detracted towards optimizing a mathematical model instead of designing the best aircraft. A solution here is to keep the structure of the design problem apparent through flexible and modular programs. However, recent publications by Kirkpatrick (1971) and Keith Jackson (1977) indicate that useful help can also be expected from analytical methods to interpret and check the results of complex multi-variate programs. The present contribution can be interpreted to belong to this category. Contributions to design optimization have been made long before the CAD era. Göthert (1939) made one of the first comprehensive attempts to optimize the span and wing area of propeller aircraft (1939). Pearson (1949) gave an elementary derivation of the optimum engine thrust and Mach number for long-range jet aircraft. Ashkenas (1948) studied optimum cruise conditions for constant engine ratings and devised an aerodynamic criterion for the optimum wing area. Backhaus (1958) attempted a comprehensive optimization of jet transports, that is still worth reading. Sanders (1961) made various analytical studies involving wing weight variation, and demonstrated the importance of differences in the figures of merit. Bagly and Anderson (1965) isolated the engine optimization problem from the overall airplane design cycle. Küchemann and Weber (1968) made an important contribution to the optimization of cruise altitude and engine thrust, based on maximum payload fraction.

The basic problem of applying these contributions is that they cannot be related to each other, because the aircraft categories considered and the optimization criteria are different. In addition, the omission of compressibility effects and SFC variation with speed renders many contributions obsolete.

The present paper describes a basically analytical approach to conceptual design optimization, intended to enhance the understanding of the basic design problems of transport aircraft and to contribute to certain classes of practical design studies. An introductory chapter deals with the choice of a suitable merit function and the structure of different design problems. Criteria are presented in Chapter 3 to find the optimum cruise conditions applicable to given aircraft with arbitrary type of powerplant and drag polars including a drag rise. Chapter 4 forms the basis to select optimum cruise conditions for a given airframe shape in which turbofan engines have to be installed. The minimum thrust required to take an aircraft out of a given airfield is derived from approximate take-off analysis. Chapters 5 and 6 deal with criteria for optimum wing aspect ratio, wing loading, lift coefficients, cruise altitude and thrust-to-weight ratio for engines sized for cruising and field performance, respectively.

2. THE GENERAL DESIGN OPTIMIZATION PROBLEM

2.1 Figures of merit

The choice of a suitable criterion on which to base the assessment of an aircraft design (Fig. 1) is essential and unavoidable, particularly in the case of CAD. For transport aircraft, ROI or profit margin theoretically appear to be the most comprehensive of the various criteria, but there are restrictions, as illustrated hereafter.

a. Optimum block speed

The effects of block speed variation, for example, indicate that for a given annual utilization and depreciation period the optimum block speed can be markedly different when fuel usage, DOC or ROI are compared (Fig. 2). This is caused primarily by a different weighing of productivity, resulting in significant differences in the optimum block fuel load variation with block speed for given range:

$$\text{minimum fuel cost} : \frac{d W_F}{d V_b} = 0 \quad (2-1)$$

$$\text{minimum DOC} : \frac{d \log W_F}{d \log V_b} = \frac{\text{DOC/trip}}{\text{fuel cost/trip}} - 1 \quad (2-2)$$

$$\text{maximum ROI} : \frac{d \log W_F}{d \log V_b} = \frac{\text{mean income/trip} - \text{trip IOC}}{\text{fuel cost/trip}} - 1 \quad (2-3)$$

where $d \log W_F / d \log V_b$ is the logarithmic derivative of the block fuel w.r.t. block speed, effectively the ratio of relative fuel change with relative speed increment. Trip OC refers to the indirect operating cost directly proportional to the number of trips, such as landing fees, local maintenance, aircraft and traffic servicing, passenger servicing and food, flight administration and sales, etc. The economic value of speed is emphasized most when ROI is considered. Aircraft with appreciably different cruising speeds and/or productivities must therefore not be compared on a basis of DOC only. The conditions of constant annual utilization and depreciation period, however, are questionable. Aircraft may be designed for a given service life or total number of trips; hence an increment in block speed does not necessarily materialize in a proportional increase in the total earnings. The annual utilization will therefore tend to decrease with increasing block speed.

Since for long-range operation the condition $d W_F / d V_b = 0$ is effectively related to the drag rise ($d C_D / d M$), the block speeds for minimum DOC and ROI are sensitive to the shape of the drag rise. Optimization of the best Mach number is therefore possible only when the aerodynamic design is well established.

b. Effects of field length constraints

Fig. 3 illustrates that field performance requirements have a marked effect on DOC. The "design field length" is the take-off distance required with the maximum number of passengers and MTOW under critical atmospheric conditions. Aircraft A is optimized for cruising flight, but fails to satisfy the field constraint. Since it has to unload passengers on all but the longest routes, its economics are inferior for operators with critical field limits. Design B just meets the field performance criterion at the design range, resulting in the lowest attainable operating cost. This design has the lowest operating cost, provided the required fields length decreases with shorter ranges at least as fast as the available field length. Design C satisfies the field requirements on all ranges, but at higher cost. Since operators tend to have widely divergent field performance requirements, one should be careful in compromising to cope with an extremely critical requirement. It may well be advantageous to propose different versions of the same basic design, e.g. the VFW-Fokker F-28 aircraft family with different wing designs.

c. Importance of the payload fraction

The various weight fractions mentioned in Fig. 1 can be combined into an approximate expression for the design sensitive DOC (per seat - km, given range):

$$\text{DOC} = \frac{1}{V_b W_{pl}} \left(\frac{a}{t_b} W_F + b W_a + c W_{to} + d T_{to} + \dots \right) \quad (2-4)$$

where the various factors have the following meanings:

- a: specific fuel price; t_b : block time
- b: hourly depreciation, interest, insurance, maintenance and spares cost per unit of airframe less powerplant weight;
- c: hourly maintenance, personnel and flight crew cost per unit of MTOW;
- d: hourly powerplant depreciation, maintenance and spares cost per unit of total take-off thrust.

The simplified DOC expression can be evolved into:

$$\text{DOC} = \frac{b}{V_b} \left[\frac{m_{to}}{m_{pl}} \left(1 + \frac{c}{b} \right) + \frac{m_F}{m_{pl}} \left(\frac{a}{b t_b} - 1 \right) + \frac{m_E}{m_{pl}} \left(\frac{d}{b C_t} - 1 \right) + \dots \right] \quad (2-5)$$

where C_t denotes the specific powerplant weight. Taking representative numerical values for the constants in (2-5), it can be shown that the payload fraction m_{pl}/m_{to} forms the most significant contribution. It is therefore justified to concentrate on the condition

for maximum payload fraction or, when block speed variations are involved, on the maximum of $V_b m_{pl}/m_{to}$, provided annual utilization and depreciation period are not affected. Only for different designs where these criteria are almost equal does it become worthwhile to consider m_{pl}/m_{to} and m_{pl}/m_{to} as secondary criteria. Those comparisons are particularly sensitive to specific fuel prices and engine cost per unit take-off thrust.

2.2 The structure of aircraft design problems and ground rules

The subdivision into specified characteristics, parameters or free variables, dependent variables and constraints is different in almost any conceivable design problem. The following summary of design options encompasses most problem structures.

OPTION 1

Optimum cruise conditions for a given aircraft: cruise altitude and Mach number combinations, resulting in the lowest fuel consumption or cost per km, for variable or fixed engine ratings. This performance problem is not only common to most design studies, but is also a general aspect of operational and cost studies of existing aircraft.

OPTION 2

Engine selection for given airframe geometry: the engine selection procedure is based on the rule that for the lowest flying cost the engines should be sized for cruising. The engine thermodynamic cycle and the cruise altitude can be optimized in order to obtain a maximum payload fraction for each Mach number. The condition for minimum DOC is obtained from the block speed times the maximum payload fraction, for either unconstrained or constrained lift coefficient and Mach number combinations. The optimum take-off weight and thrust thus obtained have to be compared with the thrust and weight based on field and/or climb performance criteria. In case of a major discrepancy the engine cycle or the number of engines should be adapted.

OPTION 3

Airframe optimization for fixed engines, to be achieved in several steps.

- Constant design-payload and range, constant Mach number: optimum wing area, aspect ratio and altitude are calculated, based on max. m_{pl}/m_{to} , considering fuselage geometry, wing section t/c, sweep angle and taper invariant.
- Constant design payload and range, variable Mach number: the previous step is repeated for several Mach numbers, resulting in an extremum of $V_b (m_{pl}/m_{to})_{max}$. For each Mach number the wing aerodynamic design is matched.
- Variable payload and range, constant wing design: a case referring to fuselage stretching and/or range extension studies. Field and climb performance constraints will set an upper limit to the MTOW. For each payload and fuselage design optimum cruise performance is obtained (Option 1). The resulting design missions are assessed on a basis of cost and operational suitability.
- Variable payload and range, variable wing design: for each design mission steps 3(a) and (b) are repeated and optimum configurations are compared with regard to cost and operational suitability.

OPTION 4

Optimization of aircraft/engine combinations. Similar to Option 3 the solutions for given mission and constant or variable Mach number are developed: steps 4a and 4b respectively. For each step the engine selection procedure follows Option 2. If the wing geometry is fixed (step 4c), the engine for each design mission is selected according to Option 2. In the case of variable design missions, with the aim of obtaining an optimum aircraft/engine combination for each mission, steps 4a and 4b will be repeated for each design mission. The variable mission designs have to be assessed not only on the basis of cost, but primarily on their operational suitability.

The following basic design elements are underlying all options:

- Fuselage design for given design payload.
- Aerodynamic wing design (section shape, sweep angle, taper) for given area, aspect ratio, and design C_L and M combination.
- Performance optimization for minimum fuel or cost.
- Sensitivity of the mass breakdown to design variations.
- Variation of the payload fraction (given airframe) with engines sized for cruising at different altitude and Mach number combinations.
- Calculation of the minimum thrust level required for specified field and climb performance.
- Calculation of the payload fraction (given payload and range) as affected by wing area, aspect ratio and cruise altitude variation. Engines are either specified or sized for cruising.
- As (g), but engines sized for field or climb performance.
- Assessment of design mission variations w.r.t. operating cost and operational suitability.

The items (a), (b) and (i) are considered to be outside the scope of the present paper. All other items form elements of the following chapters.

3. MAXIMUM SPECIFIC RANGE FOR GIVEN AIRCRAFT

Due to the recent sharp rise in fuel prices, this subject described under "Option 1" in the previous section has aroused new interest recently. Analytical conditions for maximum range (or minimum fuel) are known for many years; an overview is given in Ref. 1. The weakness of these criteria in practical cruise performance analysis is due to the basic

assumptions underlying most derivations:

- (a) the drag polar is parabolic,
- (b) compressibility drag is neglected,
- (c) total engine efficiency is constant (propeller a/c) or proportional to Mach number (jet a/c, corrected TSFC constant).

Neither of these assumptions is valid for turbofan-powered aircraft. The classical criteria result in an optimum cruise altitude only in the case of thrust-limited flight but numerical performance analysis generally indicates the max. specific range to occur at reduced engine ratings. For given W/δ (i.e. $C_M^2 = \text{constant}$) the TSFC variation has a marked effect at all speeds; compressibility at high speeds invalidates the classical criteria almost completely. The generalized criteria presented next apply to subsonic aircraft with and without compressible drag polars and arbitrary propulsion system characteristics. Their relation to classical criteria will be shown.

3.1 The range parameter

The range parameter $\eta L/D$ is related directly to the specific range V/F , since in horizontal flight ($T = D$):

$$\eta \frac{L}{D} = \frac{W}{H} (V/F) = \frac{d(R/R_H)}{d(m_F/m)} \quad (3-1)$$

where $R_H = H/g$ is the range-equivalence of the specific heat content of the fuel, approx. 4400 km^H for jet fuel. The total engine efficiency,

$$\eta = \frac{\text{useful propulsive power}}{\text{heat added per unit time}} = \frac{TV}{H d m_F/dt} \quad (3-2)$$

works out as follows in the range parameter.

Jet aircraft: since η is related to corrected TSFC and Mach number,

$$\eta \frac{L}{D} = \frac{a_o}{H} \frac{ML/D}{C_T/\sqrt{\theta}} \quad (3-3)$$

The corrected thrust and TSFC are both functions of M and the corrected RPM; hence by elimination of the RPM.

$$\eta = \eta(T/\delta, M) \quad (\text{variable RPM}) \quad (3-4)$$

A typical plot (Fig. 4) shows that over a wide range of T/δ values η is primarily affected by M , while T/δ variation is of secondary importance. A log-log scale has been used here for the reason to be explained in section 3.2.

Propeller aircraft

The total efficiency is the product of the propeller and engine efficiencies:

$$\eta = \eta_p \frac{P_{eq}}{H d m_F/dt} = \frac{\eta_p}{H C_p} \quad (3-5)$$

where C_p is the SFC referred to ESHP. The range parameter becomes:

$$\eta \frac{L}{D} = \frac{\eta_p}{H C_p} \frac{L}{D} \quad (3-6)$$

For turboprop engines both η_p and C_p are functions of M and $P_{br}/\delta\sqrt{\theta}$. Since shaft power and useful propulsive power are interrelated via η_p , it can be shown that (3-4) also applies to propeller aircraft and is therefore completely general.

Maximum lift/drag ratio

For high-subsonic aircraft $C_D(C_L, M)$ and the L/D -ratio are no longer unique functions of C_L . For a given Mach number, L/D -max is defined by:

$$\left. \frac{d \log C_D}{d \log C_L} \right|_M = C_{D_L} = 1 \quad (M \text{ constant}) \quad (3-7)$$

Horizontal cruising at a given aircraft weight (more generally $W/\delta = \text{constant}$) is equivalent to $C_L M^2 = \text{constant}$, and it can be shown that for maximum L/D :

$$2 C_{D_L} - C_{D_M} = 2 \quad (W/\delta \text{ constant}) \quad (3-8)$$

$$\text{where } C_{D_M} = \left. \frac{d \log C_D}{d \log M} \right|_{C_L} \quad (3-9)$$

In the drag rise $C_{D_M} \neq 0$ and (3-7) compared with (3-8) results in different C_L and L/D -max values. Plotting the drag polars on a log-log scale (fig. 5) yields the numerical values of C_{D_L} and C_{D_M} directly from the local slopes of $\log C_D$ vs $\log C_L$ and $\log M$, resp. Equation (3-8) can also be constructed in the polars and its intersection with curves: $\log C_L + 2 \log M = \text{const.}$ defines L/D -max. for constant W/δ , which is appreciably below the value for constant M (cf. also Ch. 11 of Ref. 10).

3.2 Maximum range parameter for variable engine rating

In (quasi-) horizontal flight $T/\delta = D/\delta$ (C_L, M) and it follows from (3-4) that:

$$\eta \frac{L}{D} = \eta \frac{L}{D} (C_L, M) \quad (3-10)$$

Differentiating w.r.t. the two degrees of freedom C_L and M yields the conditions shown in Fig. 6. The logarithmic derivatives of C_D w.r.t. C_L and M are related to the propulsion derivatives, defined as follows:

$$\eta_M = \frac{d \log \eta}{d \log M} \Big|_{T/\delta} ; \quad \eta_T = \frac{d \log \eta}{d \log (T/\delta)} \Big|_M \quad (3-11)$$

These characteristics are manifest in Fig. 4 as the local slopes of $\log \eta$ vs $\log M$ and $\log T/\delta$, resp. Since normally η_T is close to zero, the derivative η_M is most important as it plays a dominant role in all optimizations involving Mach number variation. Its numerical value is generally between 0 and 1, but it can become slightly negative for propeller aircraft at high speeds. The classical analytical criteria assume $\eta_M = 0$ (η constant) for propeller aircraft and $\eta_M = 1$ ($C_T/\sqrt{\delta} = \text{constant}$) for jet aircraft. Typical values for high-bypass engines are between 0.5 and 0.8, but flight speed has an effect on these figures. Furthermore, η_M can be related to useful approximations for the corrected TSFC of turbofans:

$$\left. \begin{array}{l} \text{for } C_T/\sqrt{\delta} = C_1 + C_2 M \rightarrow \eta_M = \left(1 + \frac{C_2}{C_1} M\right)^{-1} \\ \text{for } C_T/\sqrt{\delta} = C M^n \rightarrow \eta_M = 1 - n \end{array} \right\} \quad \text{for both cases: } C_\eta = \frac{\eta}{\eta_M} = \text{constant}$$

Values for "n" are given in the ESDU Data Sheets (Ref. 1). It is to be noted that in Figures 4 and 5 the base of the log. is 10.

It is concluded from Fig. 6 that for $\eta_T \ll \eta_M$ the condition $C_{D_M} \approx \eta_M$ always results in optimum cruising conditions to be in the drag rise, for both specified C_L and the unconstrained case. For example, if $M = 0.8$, $C_D = 0.032$ and $\eta_M = 0.63$, the result is $dC_D/dM = 0.025$. The optimum cruise Mach number for given C_L is thus below the drag-critical Mach number ($dC_D/dM = 0.10$).

The unconstrained optimum for altitude and Mach is obtained by intersection of the first two conditions of Fig. 6. In the drag polar this point can be located directly, provided values of η_M and η_T are known. For $\eta_T \approx 0$, the optimum is simply defined by the intersection of $C_{D_L} = 1$ with $C_{D_M} = \eta_M$, but more accurate solutions can be found by graphical procedures most readily when log-log plots are being used.

3.3 Constrained optima

(a) Constant W/δ

A constraint on W/δ , usually interpreted as a specified altitude for given W , leads to $C_L M^2 = \text{constant}$. The table in Fig. 6 shows that a combination of C_{D_L} and C_{D_M} defines the constrained optimum Mach number, and a solution is now also found for $C_{D_M} = 0$. Since for a parabolic drag polar:

$$C_{D_L} = 2 \frac{\text{induced drag}}{\text{total drag}} = \frac{2(C_L/C_{L_{MD}})^2}{1 + (C_L/C_{L_{MD}})^2} ; \quad C_{L_{MD}} = \sqrt{\frac{C_{D_0}}{d C_D/d C_L^2}} \quad (3-12)$$

the optimum C_L and M are found for $\eta_T = 0$ as indicated. The classical criteria below can be derived directly from this result:

propeller aircraft: $\eta_M = 0 \rightarrow C_L = C_{L_{MD}}$

jet aircraft : $\eta_M = 1 \rightarrow C_L/C_{L_{MD}} = 1/\sqrt{3}$, and $M/M_{MD} = \sqrt[3]{3}$

For a typical turbofan-powered aircraft with $\eta_M = 0.6$, we find, however:

$$C_L = 0.733 C_{L_{MD}}, \text{ and } M = 1.17 M_{MD}.$$

(b) Constant T/δ

A constraint on T/δ (or $C_M^2 = \text{constant}$) can be interpreted for jet aircraft as a limit on the engine rating in the case of stratospheric flight, provided Mach number effects on thrust are neglected. The simple optimum condition for parabolic polars (no drag rise),

$$\frac{C_L}{C_{L_{MD}}} = \frac{1}{\sqrt{1 + \eta_M}} \quad (3-13)$$

again compares directly to the classical result $C_L/C_{LMD} = 1/\sqrt{2}$ for $C_T/\sqrt{\theta} = \text{constant}$ ($\eta_M = 1$), but (3-13) is more general.

3.4 Operational cruise conditions

The relative flatness of the $\eta L/D$ curves near the optimum allows operators to pick up a worthwhile gain in cruise speed for only small fuel penalties. The long-range cruise Mach number is usually defined as the highest M for which the specific range is 99% or 99.5% of its maximum value.

In view of the economic value of speed (cf. Section 2.1a) the cost-economical speed is in excess of the long-range cruise condition. Using (2-2), for example, the drag rise for minimum DOC is defined as follows:

$$C_{D_M} = \eta_M + \frac{\text{DOC/trip}}{\text{fuel cost/trip}} - 1 \quad (3-14)$$

For example, if the DOC is three times the fuel cost per trip and $\eta_M = 0.6$, the result is $C_{D_M} = 2.6$. For typical cruising conditions this is equivalent to $d C_D/dM \approx 0.10$, i.e. the usual definition of the drag-critical Mach number. The recent developments in super-critical wing technology, resulting in a pronounced and narrow "compressibility drag bucket", will bring the various optimum operating conditions as defined by (2-1) through (2-3) closer together.

It will be obvious that operational constraints, such as speed stability, buffet margins, climb potential and max. cruise ratings, have to be respected in the final choice of operational cruise conditions. For short ranges, the cruise altitude will be compromised to reduce the extra fuel lost in climb and descent.

4. TURBOFAN ENGINE SELECTION FOR GIVEN AIRFRAME GEOMETRY AND PAYLOAD

The basic approach to engine selection is summarized as "Option 2" in Section 2.2 above. The conceptual design problem, as visualized in Fig. 7 can be broken down into the following questions:

- How many engines?
- What type of engine cycle and engine scaling laws?
- How sensitive are the empty mass and drag to engine thrust level variations?
- What is the best design cruise altitude and speed?
- What is the minimum thrust required for given field or climb performance?

The designer's problem differs from the performance analyst's primarily because of the variations in the mass breakdown and drag polar when engine thrust levels are sized to match the cruise drag variation with altitude and Mach number. The present analysis will be restricted to aircraft with turbofan engines, but may be adapted readily to propeller aircraft.

4.1 Aircraft mass variation; the Propulsion Figure of Merit

For podded engine installations the basic airframe geometry can be considered independent of the powerplant variations. The grouping of masses into fixed and variable components,

$$m_{to} = m_{fix} + m_{var} + m_{pl} \quad (4-1)$$

yields an expression for the payload fraction:

$$\frac{m_{pl}}{m_{to}} = \frac{1 - m_{var}/m_{to}}{1 + m_{fix}/m_{pl}} \quad (4-2)$$

The variable masses are:

- Engines and associated installation provisions (nacelles, thrust reversers, etc.):

$$W_p = C_t T_{to} \quad (4-3)$$

with C_t typically of the order 0.25 to 0.30. This expression implies that the engine scaling laws allow a linearization of the engine weight vs thrust, which is usually true for exponential scaling laws.

- Fuel:

$$m_F = \frac{\bar{R}/R_H}{\bar{\eta}} \frac{\bar{C}_D}{C_L} m_{to} \quad (4-4)$$

where \bar{C}_D is the airframe less pod installation drag coefficient, $\bar{\eta}$ the powerplant total efficiency, based on the pod thrust (i.e. net thrust minus installation drag, $T - D_p$) and \bar{R} the equivalent design range. The latter can be derived from the actual range by means of various corrections allowing for the cruise procedure, take-off, climb, descent, reserve fuel, etc.

- Variation of the empty mass (less powerplant) caused by take-off mass variations, equal to μm_{to} .

When the engines are sized for cruising at a given rating, the variable mass fraction is found by adding items (a), (b) and (c) above:

$$\frac{m_{var}}{m_{to}} = F_P \frac{\bar{C}_D}{C_L} + \mu \quad (4-5)$$

where the Propulsion Figure of Merit (PFM) is defined as follows:

$$F_P = C_t \frac{T_{to}}{T - D_P} + \frac{\bar{R}/R_H}{\eta} \quad (4-6)$$

Since for given flight conditions and payload the minimum PFM results in a maximum for the payload fraction, it can be used as an effective criterion for the engine cycle selection, weighing the relative importance of:

- . installed η (or TSFC),
- . powerplant installation weight, including nacelles,
- . thrust lapse with altitude and speed,
- . powerplant installation drag.

The PFM does not explicitly account for the number of engines installed. Therefore, when engines are sized for engine-out performance an additional assessment is necessary.

4.2 Effects of cruise conditions on the payload fraction

As soon as an engine cycle has been selected (provisionally), the PFM and \bar{C}_D/C_L ratio and hence the first term of (4-5) can be calculated for each flight condition; a typical result is shown in Fig. 8. Analytical optima can be derived resulting in either a conditional maximum m_{pl}/m_{to} for given M , C_L or W/δ , or in the unconstrained maximum. The results are summarized in Figures 8 and 9. All local optima appear to be related to the ratio of the powerplant installation mass to the fuel mass,

$$\mu_{PF} = \frac{m_P}{m_F} = C_t \frac{T_{to}}{T} \frac{\eta}{\bar{R}/R_H} \quad (4-7)$$

The most intriguing and simple of all criteria is the unconstrained optimum for Mach numbers below the drag rise:

$$\frac{m_P}{m_F} = \frac{1}{2} \bar{\eta}_M \quad ; \quad C_L/C_{L_{MD}} = 1/\sqrt{1 + \bar{\eta}_M} \quad (\text{max. } \frac{m_{pl}}{m_{to}}) \quad (4-8)$$

where

$$\bar{\eta}_M = \eta_M - 2 \frac{D_P}{T} / (1 - D_P/T) \quad (4-9)$$

This result is in accordance with Pearson's criterion (Ref. 12) -derived for $C_T/\sqrt{\theta} = \text{constant}$ ($\eta_M = 1$)-stating that the optimum cruising flight for jet aircraft is found at an altitude and speed where the engine weighs half the fuel load. However, equation (4-8) is more general and more realistic as regards the numerical value. It is also noteworthy that the corresponding C_L is very similar to the criterion found in Section 3.3 for given T/δ . Nevertheless, the criticism is valid that the maximum payload fraction is not a very useful criterion here since speed and productivity variations are involved.

The condition of optimum cruise altitude and C_L for given M (Fig. 9a) is most significant. This defines a trade-off between engine thrust^L (and mass) increasing with altitude and fuel mass which is minimum at the altitude for minimum drag. The best altitude is therefore always below that for minimum drag. Provided the drag polar (with or without compressibility) is parabolic, the optimum powerplant-to-fuel mass ratio is obtained from:

$$\frac{\mu_{PF}}{(\mu_{PF})_{MD}} = (1 + 2 \mu_{PF})^{-1/2} = \frac{C_L}{C_{L_{MD}}} \quad (4-10)$$

Fig. 9a gives the general solution of this equation, defining the optimum airframe drag coefficient, and the optimum engine thrust is accordingly:

$$\frac{T_{to}}{W_{to}} = \frac{T_{to}}{T_{MD}} \frac{\bar{C}_D}{C_{L_{MD}}} \quad (4-11)$$

Repetition of the calculation for different Mach numbers results in $m_{pl}/m_{to} - \text{max.}$ vs M and the condition for $(V_b m_{pl}/m_{to}) - \text{max.}$ is readily obtained. The optimum cruise C_L for given M has also been derived by Küchemann and Weber (Ref. 9). In spite of the different derivation - their solution is not presented in closed form - the results are numerically close to the present (Fig. 9b). Finally, the "optimum" C_L and M for given altitude (cf. Fig. 8 and 9b, curve III) may be of some use if the thrust is based on the take-off since lines of constant altitude are roughly equivalent to constant take-off T/W ratio.

4.3 Minimum engine thrust for given take-off and climb performance

Engines may be sized by a one engine-out service ceiling requirement. The T/W ratio is then determined directly from the minimum drag condition at the ceiling, and the ratio of engine thrust available (with engine failure) at altitude to the take-off thrust (all

engines). Although a simplified take-off analysis is not always necessary, the following results form a useful starting point for optimization of the wing design when the engines are sized by take-off distance and climb criteria. When engines are to be sized for take-off, a distinction is made between cases when the take-off flap design and setting are specified, and the case when optimum values for the take-off lift coefficient can be chosen for each condition.

(a) Fixed C_L at V_2

The minimum thrust generally occurs when the one engine-out climb gradient equals the minimum second segment climb gradient. In this case the airdistance approaches a more or less constant value, and the lift-off speed is almost equal to the take-off safety speed. The take-off run length may therefore be related to the kinetic energy at the screen height:

$$S_{to} - S_{air} = k_{run} \frac{V_2^2/2g}{(\bar{T}/W) - 0.04} \quad (4-12)$$

where k_{run} is a factor of proportionality, \bar{T} is the mean thrust (at about $0.7 V_2$) and the constant 0.04 allows for ground friction and air drag during the run. The T/W ratio is thus obtained from:

$$\frac{\bar{T}}{W} = 0.04 + k_{run} \frac{m_{to}/S}{\rho_{to} (S_{to} - S_{air}) C_{L2}} \quad (4-13)$$

Values for S_{air} and k_{run} may be obtained from actual performance data. A check should be made on the engine-out climb performance.

(b) Optimum C_L at V_2

Assuming the engine failure to occur at the rotation speed, the take-off distance may be approximated by:

$$S_{to} = k_{run} \frac{m_{to}/S}{\rho_{to} (C_L T/W)_{V_2}} + \frac{h_{to}}{\left(\frac{N_e - 1}{N_e} T/W - C_D/C_L \right)_{V_2}} \quad (4-14)$$

where the numerical value of k_{run} is different from that in (4-12), e.g. $k_{run} = 1.40$. The factor h_{to} is a reference altitude, equal to 35 ft plus an additional amount for the flare-up, e.g. $h_{to} = 0.01 S_{to}$. Assuming the drag coefficient at V_2 for variable flap setting to be represented as follows:

$$\left(\frac{C_D}{C_L} \right)_{V_2} = \frac{C_{L2}}{\pi A E} \quad (E \approx 0.60 - 0.65) \quad (4-15)$$

it is found that (4-14) can be re-arranged as a relation between three non-dimensional parameters:

$$\omega = \tau \lambda \left(1 - \frac{1}{\tau - \lambda} \right) \quad (4-16)$$

where ω , τ and λ are defined in Fig. 10. The optimum lift/drag ratio for minimum T/W is found from $\lambda_{opt} = \tau - \sqrt{\tau}$, or:

$$\left(\frac{C_D}{C_L} \right)_{V_2} = \frac{C_{L2}}{\pi A E} = \frac{N_e - 1}{N_e} \left(\frac{T}{W} \right)_{V_2} - \left[\frac{h_{to}}{S_{to}} \frac{N_e - 1}{N_e} \left(\frac{T}{W} \right)_{V_2} \right]^{\frac{1}{2}} \quad (4-17)$$

on the condition that the last term exceeds the minimum specified climb gradient. The T/W ratio at V_2 required for a specified field can be approximated by $\tau = 2 + 1.15 \sqrt{\omega}$, or

$$\left(\frac{T}{W} \right)_{V_2} = 2 \frac{h_{to}}{S_{to}} \frac{N_e}{N_e - 1} + 1.15 \left[\frac{N_e}{N_e - 1} \frac{k_{run}}{\pi E} \frac{m_{to}/b^2}{\rho_{to} S_{to}} \right]^{\frac{1}{2}} \quad (4-18)$$

The following conclusions can be drawn from (4-13), (4-17) and (4-18).

- For fixed flap setting (and C_L at V_2) the T/W ratio is either determined by the aspect ratio, or by the wing loading, whichever condition climb gradient or take-off distance is critical.
- For optimum C_L at V_2 the T/W ratio depends primarily on the span loading m_{to}/b^2 . Many other detailed design studies confirm this observation.
- A high C_L is not always desirable for take-off: equation (4-18) emphasizes the importance of a high lift-dependent drag factor E . Obviously, it should be verified that the optimum C_L according to (4-17) is compatible with the high-lift system performance limits.
- The optimum C_L at V_2 does not necessarily correspond to the condition where the minimum engine-out climb gradient forms the limit.

5. WING AREA AND ASPECT RATIO VARIATIONS FOR TURBOFAN AIRCRAFT

The subject of this chapter refers back to step (a) of options 3 and 4 dealt with in Section 2.2. The design cruise Mach number will be assumed invariant in the following analysis. This allows us to concentrate on the payload fraction as the Figure of Merit, and to assume that the wing sweepback, thickness/chord ratio variation and taper ratio are constant.

5.1 The lift/drag ratio

Wing area (or wing loading) and aspect ratio variations are directly felt in the drag polar, the lift coefficient, and hence in the fuel load. Associated variations are required in the tailplane design in order to maintain a desirable level of stability and controllability, and in the nacelle drag. For limited excursions from a baseline design the drag polar variation may be represented as follows (Ref.14, Ch. 7).

$$C_D = \bar{C}_{D_p} + \frac{F_D}{S} + \frac{C_L^2}{\pi A \phi} \quad (5-1)$$

\bar{C}_{D_p} is primarily wing profile drag (including drag rise), but it includes also the tailplane drag area proportional to wing drag area. The fixed drag area F_D is primarily the fuselage drag area plus the invariable tailplane drag area that is considered dependent on the fuselage size. In the case of specified engines the nacelle drag area is included in F_D , for variable engines eq. 5-1 represents the airframe drag only while powerplant installation drag is accounted for as an effective thrust and efficiency loss (Section 4.1). The last term of (5-1) represents the induced drag at the design C_L , assuming that wing camber, twist and wing setting are optimized for each C_L . Fig. 11 shows the variation of L/D with wing loading and altitude for an example airliner design. For specified altitude and Mach number (hence q) the maximum L/D is obtained for:

$$\frac{W/S}{q} = C_{L_{ref}} = \sqrt{\bar{C}_{D_p} \pi A \phi} \quad (5-2)$$

defining the maximum L/D value,

$$\left(\frac{L}{D}\right)_{max} = \left[2 \sqrt{\bar{C}_{D_p} \pi A \phi} + \frac{1}{2} \gamma \delta M^2 \frac{F_D P_0}{W} \right]^{-1} \quad (5-3)$$

The optimum induced drag coefficient appears to be equal to \bar{C}_{D_p} , and the higher the aspect ratio, the higher L/D. An optimum altitude is not found from (5-3) but in the case of fixed engines the cruise altitude is limited, and the highest L/D thus achievable amounts to:

$$\left(\frac{L}{D}\right)_{max} = .5 \sqrt{\frac{\pi A \phi}{\bar{C}_{D_p}}} \left(1 - \frac{F_D}{T/q} \right) \quad (\text{thrust limit}) \quad (5-4)$$

The related "optimum" wing area follows from:

$$\bar{C}_{D_p} S = \frac{1}{2} (T/q - F_D) \quad (5-5)$$

and the maximum altitude is given by:

$$q_{min} = 2W \sqrt{\bar{C}_{D_p} / \pi A \phi} / (T/q - F_D) \quad (5-6)$$

Fig. 11 shows that the "optimum" wing loading for the thrust limited case decreases with increasing T/W ratio available, while the L/D ratio is more sensitive to the wing loading than in the case of a specified altitude. Due to the cancelling effects on $C_{L_{ref}}$ and on the cruise altitude of aspect ratio variation the wing area according to (5-5) is not affected by the aspect ratio, as opposed to the trend indicated by (5-2). In any wing optimization study the cruise altitude is therefore an essential parameter. Totally different conclusions can be obtained when the cruise altitude is specified or variable, or when the engines are either specified or scaled up to match the drag.

5.2 Aircraft mass breakdown

(a) Empty mass variation

The sensitivity of the empty mass can be obtained from a detailed account of all relevant elementary contributions for a baseline or reference design with known (estimated) mass breakdown. Most variations can be linearized w.r.t. A and S, provided the variations from the baseline are not too large. A typical result for the operating empty mass is:

$$m_{oe} = m_{ref} + m_{to} \left[\mu + C_t (T/W)_{to} + \phi_S / (m_{to}/S) + \phi_A A \right] \quad (5-7)$$

The max. cruise altitude does not appear in this expression, but may be accounted for by addition of a term proportional to the cabin pressure differential. The term m_{ref} comprises most of the fuselage and vertical tailplane structure, systems, payload accommodation and operational items, and a contribution originating from the wing structural mass linearization. Its magnitude will appear to be insignificant for the present optimization study. The first bracketed term of (5-7) summarizes elements of the structure with masses proportional to the MTOW, such as the undercarriage. Wing structure is sensitive to the Zero Fuel Weight (ZFW) and its mass variation can be accounted for by adding terms proportional to m_{pe} and the maximum payload. The second bracketed term is the powerplant installation and nacelle mass, while the last two terms reflect the sensitivity to wing area and aspect ratio variation of the wing and tailplane structural mass:

$$\phi_S = \partial m_{oe} / \partial S ; \phi_A = \partial (m_{oe} / m_{to}) / \partial A \quad (5-8)$$

Typical values are 80% of the specific wing mass (kg/m^2) for ϕ_S and 0.012 to 0.015 for ϕ_A , for conventional structural design.

(b) Fuel mass

The fuel can be subdivided into quantities required to cancel the fixed drag area and the wing-associated drag over the equivalent range \bar{R} :

$$m_F = \frac{\bar{R}/R_H}{\eta} \left\{ F_D q/g + m_{to} [\bar{C}_{D_P}/C_L + C_L/(\pi A \phi)] \right\} \quad (5-9)$$

6.3 Optimum wing for given altitude

The payload fraction is obtained by adding the payload mass to (5-7) and (5-9):

$$\frac{m_{pl}}{m_{to}} = \frac{1 - \left\{ \mu + \phi_S/(m_{to}/S) + \phi_A A + F_P [\bar{C}_{D_P}/C_L + C_L/(\pi A \phi)] \right\}}{1 + m_{ref}/m_{pl} + F_P \frac{F_D}{m_{pl}} q/g} \quad (5-10)$$

where the engines are assumed to match the cruise drag.

Equation (5-10) shows the effects of all variables involved. Curves of constant payload fraction in the C_L - A field can be calculated directly with it, as exemplified in Fig. 12. Instead of the wing loading, the parameter C_L/C_{Lref} according to eq. 5-2 has been used, which makes the figure symmetrical on a log-log scale about a vertical axis given by the first criterion in the table. This table also summarizes the expressions for the optimum aspect ratio (given C_L) and for the unconstrained optimum C_L and aspect ratio. The latter is conveniently summarized in the form of an optimum ratio of induced drag to lift:

$$\frac{C_{Lopt}}{\pi A_{opt} \phi} = \frac{\phi_A A_{opt}}{F_P} = \frac{q}{q \pi \phi} (m_{to}/b^2)_{opt} = \left[\frac{\phi_A}{\pi \phi F_P} (\bar{C}_{D_P} + \frac{\phi_S q}{F_P q}) \right]^{1/3} \quad (5-11)$$

A simple result is then obtained for the maximum payload fraction for given cruise conditions:

$$\frac{m_{pl}}{m_{to}} = \frac{1 - \left[\mu + 3F_P C_{Lopt}/(\pi A_{opt} \phi) \right]}{1 + m_{ref}/m_{pl} + F_P \frac{F_D}{m_{pl}} q/g} \quad (5-12)$$

with C_{Lopt} and A_{opt} defined by (5-11). The following conclusions are now evident:

- The optimum variable mass of structure, powerplant and fuel associated with wing design variation is equal to three times the fuel and engine mass required to balance the induced drag.
- For given altitude the wing design can be optimized without regard to the reference mass and the fixed drag area.

Some other conclusions that can be found from numerical examples are:

- The unconstrained optimum C_L is almost independent of the range, contrary to A_{opt} , which increases considerably with range.
- The payload fraction is much more sensitive to non-optimum choice of wing area than it is to aspect ratio.
- Practical limits on m_{to}/S , C_L and A associated with buffet margin limits, wing volume requirements for fuel, low-speed performance limits and aero-elastic effects lay more emphasis on the partial optima for C_L and A as indicated by the boundaries in Fig. 12.

5.4 Cruise altitude variation

Equation 5-10 provides the basis for determining the sensitivity to design altitude. Fig. 13 gives an example of calculated payload fraction contours for given aspect ratio and variable altitude and C_L . Contrary to Fig. 12 the gust load factor is considered variable with mainly the wing loading, resulting in different numerical values for ϕ_S in the cases of critical manoeuvre and gust loads. From the general unconstrained optimum solution it is concluded that:

- the optimum C_L is not very sensitive to range, size of the aircraft, etc.;
- the best wing loading decreases with increasing range, and therefore the optimum altitude will increase;

- (c) large aircraft (with high m_{to}/F_D) should have high wing loadings;
- (d) high Mach numbers and high aspect ratio wings require high cruise lift coefficients, wing loadings, and altitudes;
- (e) reductions in wing profile drag, structural mass and engine specific weight result in lower optimum wing loadings, unless they are applied in combination with higher aspect ratios.

A numerical example (Fig. 14) illustrates that aspect ratio variation does not pay as much as wing loading optimization. The unconstrained optimum is, however, not sensitive to altitude and usually an aerodynamic limit on C_L constrains the practical design.

5.5 The case of specified engines

All the results given in Sections 5.3 and 5.4 are still valid, provided:

- (a) the powerplant installation and nacelle mass are added to the reference mass,
- (b) the engine efficiency refers to the net installed thrust,
- (c) the powerplant installation drag area is included in F_D ,
- (d) C_t is taken equal to zero everywhere, hence

$$F_P = \frac{\bar{R}/R_H}{\eta}$$

The results summarized in Fig. 12 can be combined in order to find the unconstrained optimum. Since the engine rating is variable, it has to be verified that the drag does not exceed the max. cruise thrust. This can be translated into:

$$\frac{C_L}{C_{L_{ref}}} \leq \left[\frac{m_{to}/S}{\bar{C}_{Dp}} \left(\frac{2g}{\gamma P_0 M^2} \frac{T_{cr}/\delta}{W_{to}} - F_D/m_{to} \right) - 1 \right]^{\frac{1}{2}} \quad (5-13)$$

The optimum wing loading and aspect ratio are lower than in the case of a variable engine size.

5.6 Engines sized for take-off performance

The payload fraction for this case is given by:

$$\frac{m_{pl}}{m_{to}} = \frac{1 - \left\{ \mu + \phi_S/(m_{to}/S) + \phi_A A + C_t (T/W)_{to} + \frac{\bar{R}/R_H}{\eta} [\bar{C}_{Dp}/C_L + C_L/(\pi A \phi)] \right\}}{1 + m_{ref}/m_{pl} + \frac{\bar{R}/R_H}{\eta} \frac{F_D}{m_{pl}} q/g} \quad (5-14)$$

The T/W ratio is given by (4-13) or (4-18).

Figures 15a and 15b show contours for constant payload fraction for fixed and optimum C_L at V_2 resp. Apart from the usual constraints, the maximum recommended cruise thrust must not be exceeded. This condition is given by eq. 5-13.

The following conclusions can be drawn from Fig. 15.

(a) Constant C_L at V_2

Conditions for optimum C_L , m_{to}/S and A - summarized in Fig. 15a - are all lower than in the case of engines sized to cruising because the engine thrust increases progressively with the wing loading when field performance is fixed.

(b) Optimum C_L at V_2

Fig. 15b shows that the unconstrained optimum wing loading is higher, and the optimum cruise altitude lower than in the previous case, although the difference in the payload fraction for the constrained optimum is insignificant for the present example. Therefore other considerations may become important, such as difference in installed engine thrust, cruising rating, and altitude. Optima for C_L and the wing loading can be derived from (5-14) by means of geometric programming techniques; they will not be presented here. The optimum aspect ratio for given C_L and wing loading is obtained from:

$$\phi_A A^2 - \frac{\bar{R}/R_H}{\eta} \frac{C_L}{\pi \phi} = 0.575 C_t \frac{T_{to}}{T_{V_2}} \left(k_{run} \frac{N_e}{N_e - 1} \frac{A}{\pi E} \frac{m_{to}/S}{\rho_{to} S_{to}} \right)^{\frac{1}{2}} \quad (5-14)$$

Comparing this result with Fig. 12 (curve II) it is found that a higher optimum value is obtained as compared to the case of engines sized for cruising. Aero-elasticity limits may well impose decisive constraints.

6. CONCLUDING REMARKS

- (a) Although the examples in this paper are based on a specific baseline design, all criteria presented are completely general and applicable to any transport aircraft. The large variations in the parameters shown are not realistic, but they have been maintained in order to demonstrate the trends.
- (b) The equations for the payload fraction and the local optima can be refined, if necessary, without setting up the formulae presented. For example, the effects of aspect ratio variation on the wing profile drag coefficient (through Reynolds number variation) appears to be equivalent to an increase in the factor ϕ_A and a reduction of \bar{C}_{Dp} . For the example in Fig. 12 the unconstrained optimum A is then reduced by about 25%.
- (c) All relationships presented can be manipulated easily to suit most of the feasible program structures. Besides the payload fraction, criteria can be derived for minimum fuel or maximum production for given engines, etc. This enables one to find the sensitivity of the conceptual optimum design to variations in the specification items, technological advances and different merit functions.

- (d) A simple, flexible, and effective computer program for conceptual design can be based on it, which optimizes aircraft by solving a set of simultaneous algebraic equations. Such a program can be used as a first iteration step for more complex programs, as a subroutine for interactive graphics CAD systems, or as a stand-alone program for top-desk mini-computers.
- (e) It is concluded that the proposed methodology gives a clear insight into the design problem structure, is adaptable to arbitrary design ground rules and different data bases, and as such is truly a designer's approach. Since the trade-off between cost and technological advances is present in the equations, management decisions can be supported by its use.

7. REFERENCES

1. Anon.: Engineering Sciences Data Unit "Performance", Vol. 5, "Estimation (range and endurance)", Sheet No. 73019, Oct. 1973.
2. Ashkenas, I.L.: "Range performance of turbojet airplanes", J. of Aeronautical Sciences, Vol. 15, 1948, pp. 97-101.
3. Backhaus, G.: "Grundbeziehungen für den Entwurf optimaler Verkehrsflugzeuge", Jahrbuch der WGLR, 1958, pp. 201-213.
4. Cherry, H.H., and, Croshere Jr., A.B.: "An approach to the analytical design of aircraft", S.A.E. Quarterly Transactions, Jan. 1948, Vol. 2, No. 1, pp. 12-18.
5. Driggs, I.H.: "Aircraft design analysis", J. of the Royal Aeron. Soc., 1950, Vol. 54, pp. 65-116.
6. Göthert, B.: "Einfluss von Flächenbelastung, Flügelstreckung und Spanweitenbelastung auf die Flugleistungen", Luftfahrtforschung, Vol. 6, 1939, pp. 229-250.
7. Keith Jackson Jr., S.: "Propulsion system sizing" Aircraft Design Short Course, Dayton, Ohio, U.S.A., August 1977.
8. Kirkpatrick, D.L.I.: "Review of two methods of optimizing aircraft design", AGARD Lecture Series No. 56, April 1972 (paper no. 12).
9. Küchemann, D., and Weber, J.: "An analysis of some performances of various types of aircraft designed to fly over different ranges at different speeds", Progress in Aeronautical Sciences, Vol. 9, Pergamon Press, 1968, pp. 329-456.
10. Miele, A.: "Flight Mechanics", Vol. 1, Theory of Flight Paths, Addison-Wesley Publishing Company, Inc. 1962.
11. Millicer, H.K.: "The design study", Flight, 17 Aug. 1951, pp. 201-205.
12. Pearson, H.: "The estimation of range of jet-propelled aircraft", The Aeronautical Quarterly, Vol. I (1949), pp. 167-182.
13. Sanders, K.L.: "Aircraft Optimization", SAWE Paper No. 289, May 1961.
14. Torenbeek, E.: "Synthesis of subsonic airplane design", Delft University Press, May 1976.

OVERALL ECONOMICS:

- RETURN ON INVESTMENT (ROI)
- PROFIT MARGIN
- LIFE CYCLE COST (MILITARY)
- PROFIT POTENTIAL/PRODUCTIVITY*

OPERATING COST:

- DIRECT OPERATING COST (DOC)
- TOTAL OPERATING COST (DOC+IOC)

WEIGHT FRACTIONS:

- PAYLOAD/MTOW
- PAYLOAD/OEW, OR OEW/MTOW
- FUEL USED PER KM/PAYLOAD, OR FUEL/MTOW
- PAYLOAD/TAKE-OFF THRUST, OR T/W

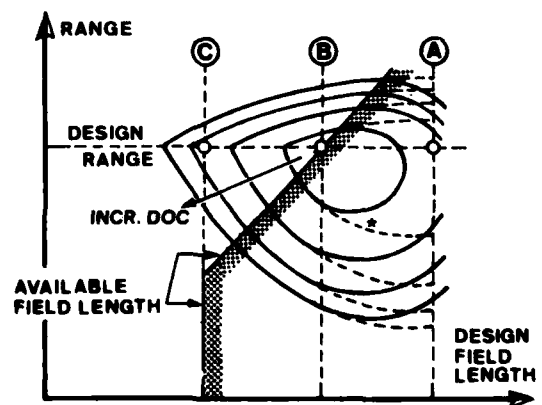
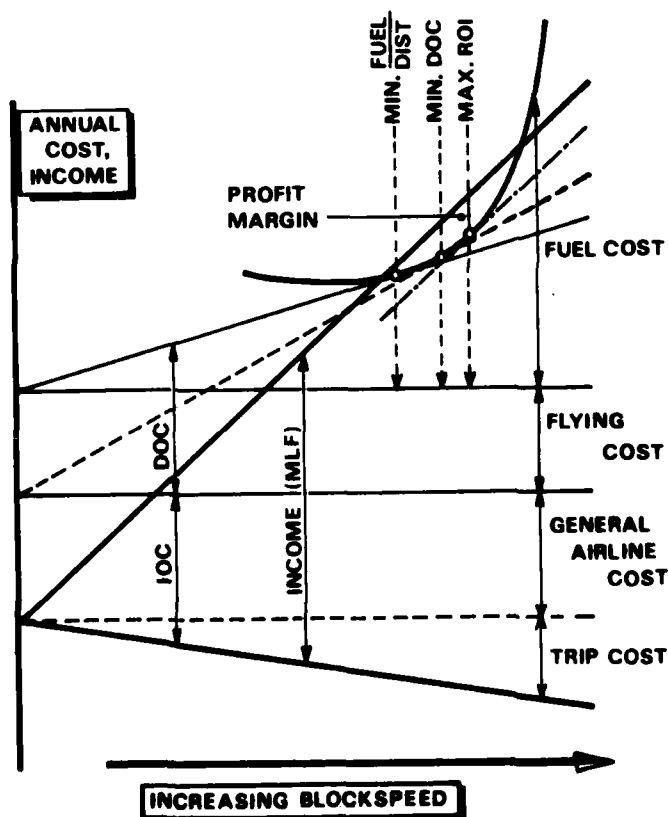
OTHER CRITERIA:

- PERFORMANCES (MISSIONS, FIELD LENGTH,)
- EXTERNAL NOISE
- COMPOUND CRITERIA**

* sometimes referred to as "economic efficiency"

** example: $DOC + \text{factor} \times \text{field length}$

Fig. 1: Figures of merit in aircraft design



* dotted DOC curves: no field constraint

Fig. 3: Effect of field length constraint on DOC

Fig. 2: Economic value of blockspeed

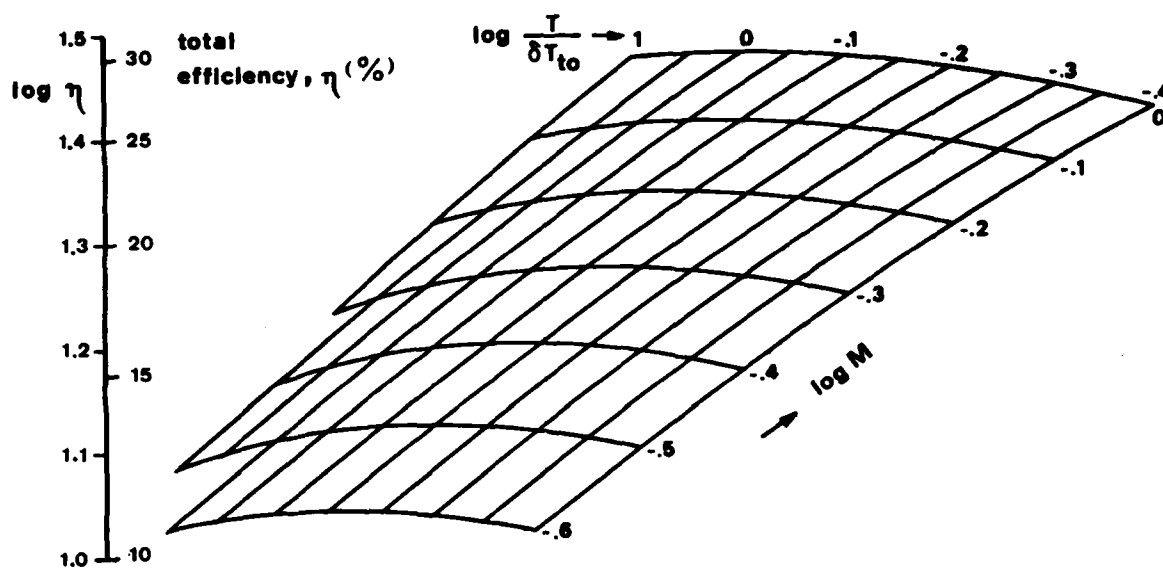


Fig. 4: Engine efficiency curves for a low bypass engine

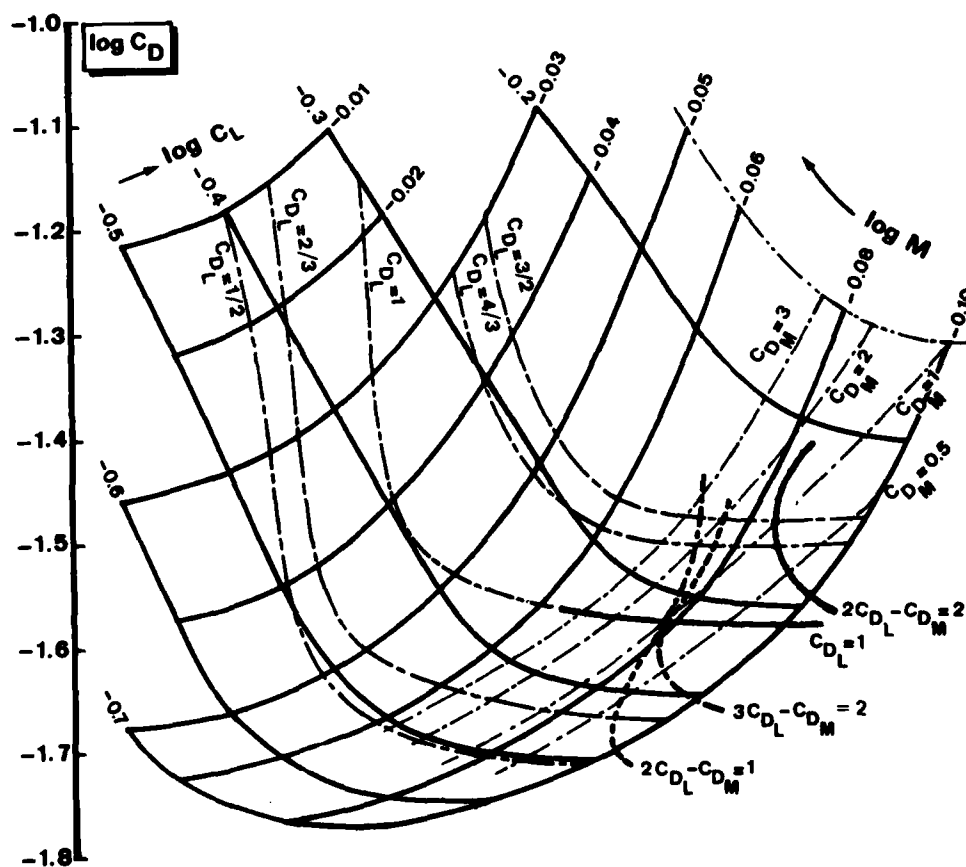
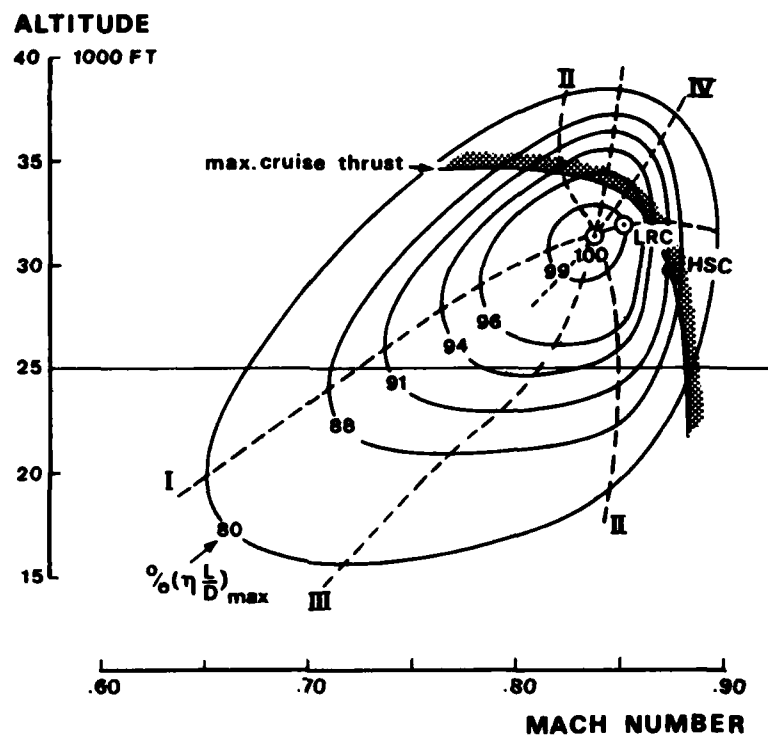


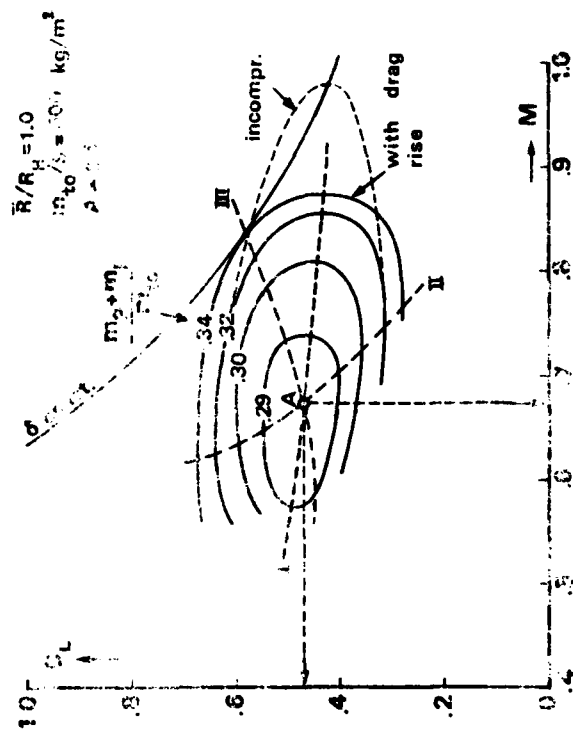
Fig. 5: The drag polars and logarithmic derivatives C_{D_L} and C_{D_M}



CURVE	CONSTANT	CONDITIONS FOR MAXIMUM $\eta L/D$		
		general	no drag rise * ($C_{DM}=0$; $\eta_T=0$)	
			C_L/C_{LMD}	Mach number
I	M	$C_{DL} = (1 - \eta_T)^{-1}$	1	-
II	C_L	$C_{DM} = \frac{\eta_M + 2\eta_T}{1 - \eta_T}$	-	-
III	W/δ	$2C_{DL} - C_{DM} = 2 - \frac{\eta_M}{1 - \eta_T}$	$\left(\frac{2 - \eta_M}{2 + \eta_M}\right)^{1/2}$	$\left(\frac{2W/\delta}{\gamma P_o S C_{LMD}} \sqrt{\frac{2 + \eta_M}{2 - \eta_M}}\right)^{1/2}$
IV	T/δ	$C_{DL} (2 + \eta_M) - C_{DM} = 2$	$(1 + \eta_M)^{-1/2}$	$\left(\frac{2T/\delta}{\gamma P_o S C_{D_o}} \frac{1 + \eta_M}{2 + \eta_M}\right)^{1/2}$

* drag polar: $C_D = C_{D_o} + \frac{dc_D}{dc_L^2} C_L^2$; $C_{LMD} = \sqrt{C_{D_o} / \frac{dc_D}{dc_L^2}}$

Fig. 6: Effect of operational conditions on the range parameter



CURVE	CONSTANT	CONDITIONS FOR MAXIMUM PAYLOAD FRACTION, ENGINES SIZED FOR CRUISING			
		general	h_{PF}	C_L/C_{LMD}	parabolic point, no drag rise (except curve I) (each number)
I	M	$\bar{C}_{DL} = (1 + h_{PF})^{-1}$	eq. 4-10 Fig. 3a.	$(1 + 2h_{PF})^{-1/2}$	-
II	C_L	$\bar{C}_{DM} = \frac{\bar{h}_M}{1 + \frac{h_{PF}}{h_M}}$	h_{PF}	-	$N \left(\frac{\bar{h}_M}{C_L} \right)^{1/2}$
III	ALT.	$2\bar{C}_{DL} - \bar{C}_{DM} = 2 - \frac{h_{PF}}{h_M}$	$\frac{h_{PF}}{h_M}$	$\left(\frac{h_{PF}}{h_M} + \frac{h_{PF}}{h_M} \right)^{-1/2}$	$N_{MD} \left(\frac{C_L}{C_{LMD}} \right)^{1/2}$
UNCONST. OPTIMUM (POINT A)		$\bar{C}_{DL} (2 + \bar{h}_M) - \bar{C}_{DM} = 2$	h_{PF}	$(1 + \bar{h}_M)^{-1/2}$	$N_{MD} \left(\frac{\bar{h}_M}{C_L} \right)^{1/2}$

* conditions at tropopause (11,000 ft): $\bar{C}_L = C_L \bar{V}_M / V^*$; $\bar{C}_M = \bar{h}_M / (\bar{h}_M + 1)$ is constant

$$\bar{C}_{DL} = \frac{d \log \bar{C}_D}{d \log C_L M} ; \bar{C}_{DM} = \frac{d \log \bar{C}_D}{d \log M} \cdot C_L$$

Fig. 8: Variable mass fraction variation for fixed airframe geometry

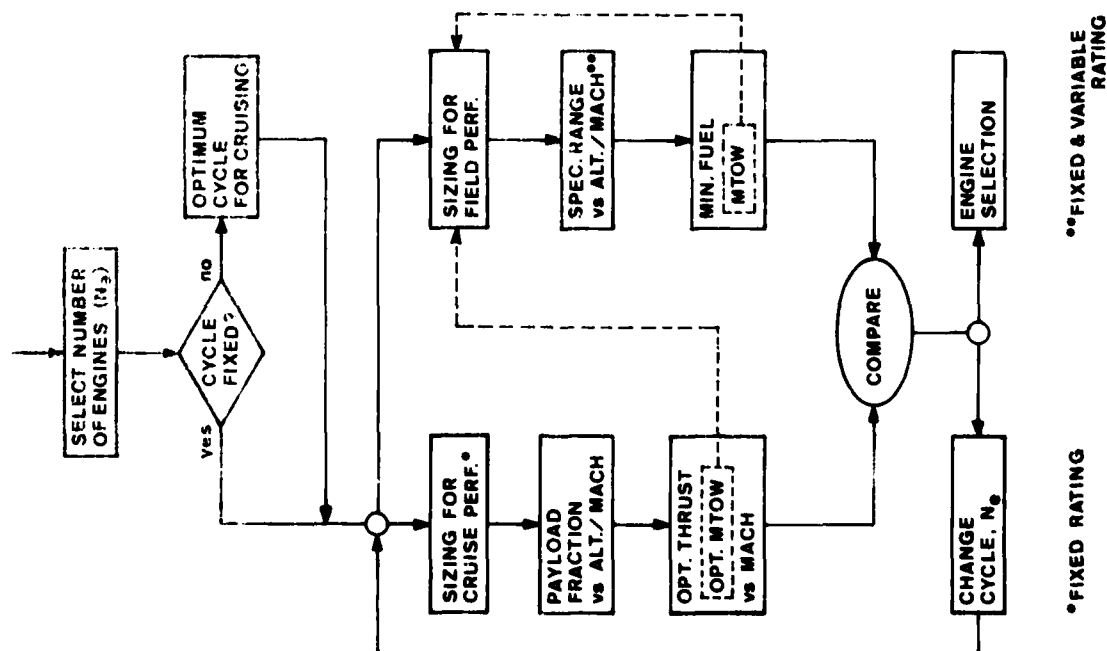


Fig. 7: Engine selection procedure for fixed airframe geometry and mission

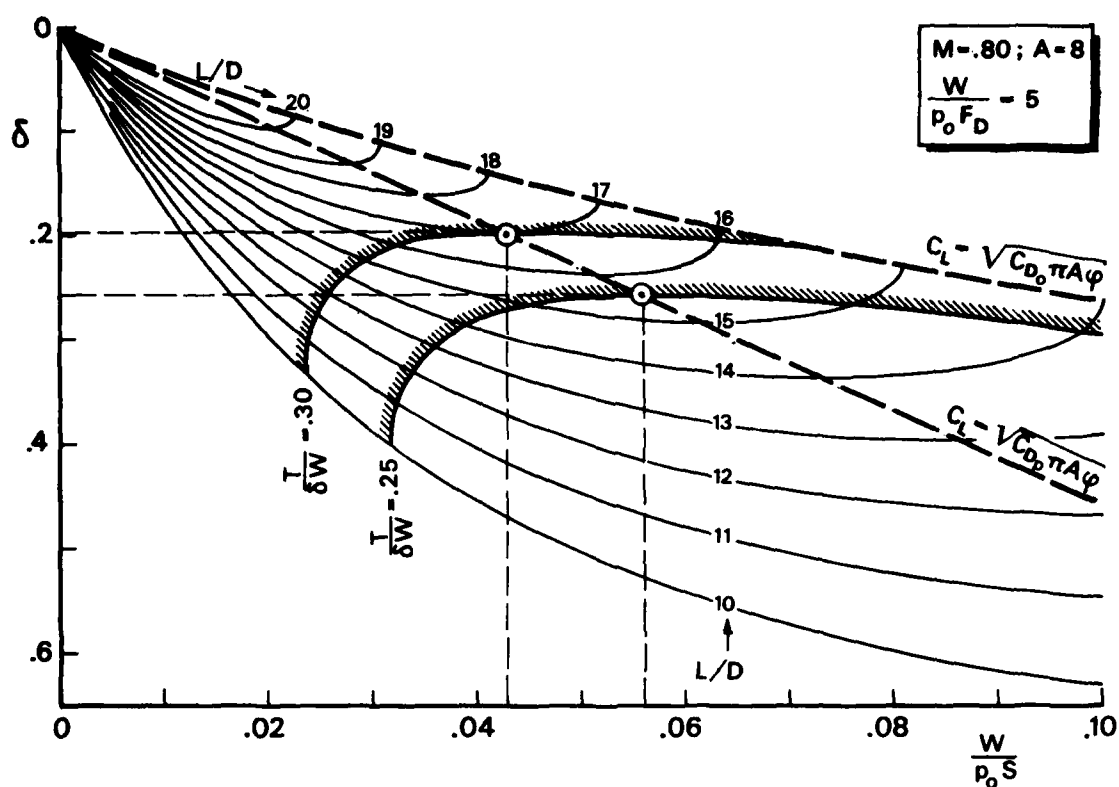


Fig. 11: Altitude and wing loading effects on the lift/drag ratio

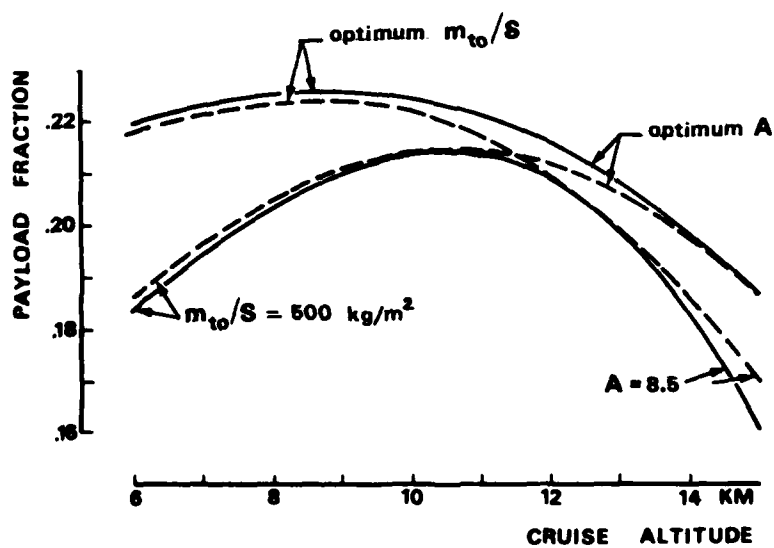
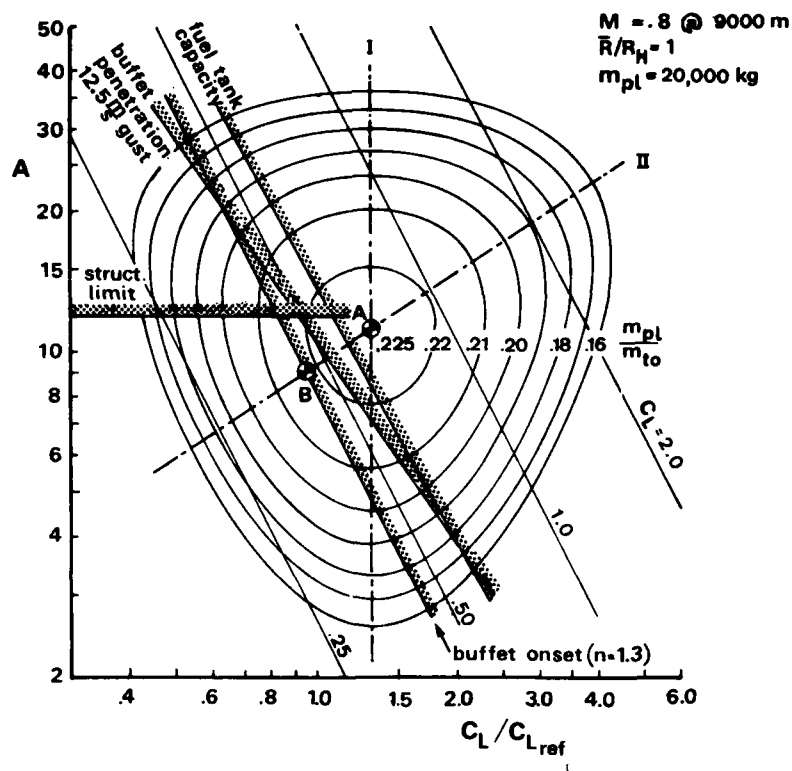


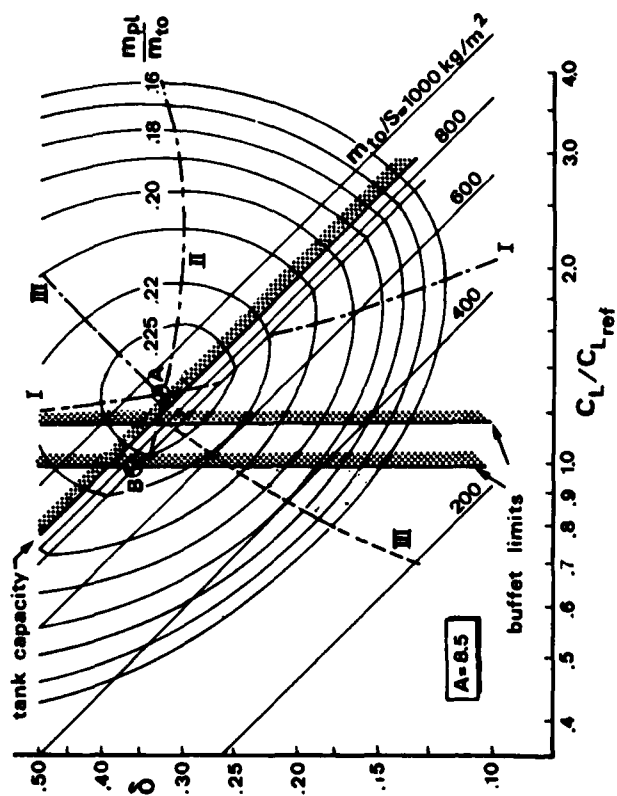
Fig. 14: Constrained and unconstrained optimum cruise altitudes



CURVE	CON- STANT	CONDITIONS FOR MAXIMUM PAYLOAD FOR GIVEN ALTITUDE AND M	
		engines sized for cruising	fixed engines
I	A	$\frac{C_L}{C_{Lref}} = \left(1 + \frac{\phi_S g}{F_P q \bar{C}_{Dp}}\right)^{1/2} = \left(\frac{\bar{C}'_{Dp}}{\bar{C}_{Dp}}\right)^{1/2}$	$\frac{C_L}{C_{Lref}} = \left(1 + \frac{\phi_S g \eta}{\bar{R}/R_H q \bar{C}_{Dp}}\right)^{1/2} = \left(\frac{\bar{C}''_{Dp}}{\bar{C}_{Dp}}\right)^{1/2}$
II	C_L	$A = \left(\frac{C_L F_P}{\pi \phi \phi_A}\right)^{1/2} \quad (\text{POINT B})$	$A = \left(\frac{C_L \bar{R}/R_H}{\eta \pi \phi \phi_A}\right)^{1/2}$
UNCON- STRAINED OPTIMUM (POINT A)		$C_L = \left[\left(\bar{C}'_{Dp}\right)^2 \frac{\pi \phi F_P}{\phi_A}\right]^{1/3}$	$C_L = \left[\left(\bar{C}''_{Dp}\right)^2 \frac{\pi \phi \bar{R}/R_H}{\eta \phi_A}\right]^{1/3}$
		$A = \left[\left(\frac{F_P}{\phi_A}\right)^2 \frac{\bar{C}'_{Dp}}{\pi \phi}\right]^{1/3}$	$A = \left[\left(\frac{\bar{R}/R_H}{\eta \phi_A}\right)^2 \frac{\bar{C}''_{Dp}}{\pi \phi}\right]^{1/3}$

Notation: $q = \frac{1}{2} \gamma p M^2$; $C_{Lref} = \sqrt{\bar{C}_{Dp} \pi A \phi}$; $F_P = \frac{\bar{R}/R_H}{\eta} + C_t T_{to}/(T-D_P)$

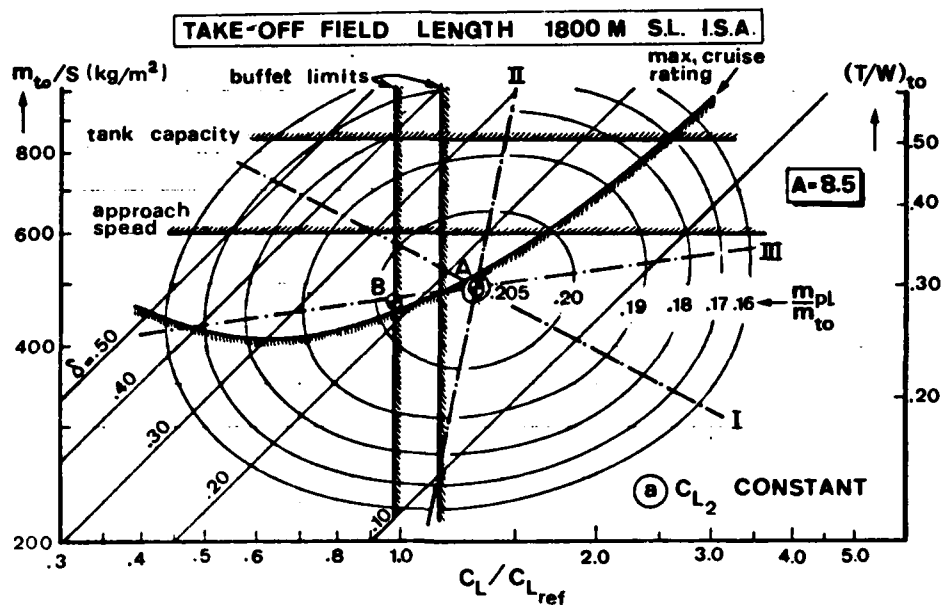
Fig. 12: Payload fraction affected by wing loading and aspect ratio



CURVE	CON- STANT	CONDITIONS FOR MAXIMUM PAYLOAD FRACTION, GIVEN ASPECT RATIO	
		engines sized for cruising	fixed engines
I	ALT.	CF. FIG. 12 CURVE I	CF. FIG. 12 CURVE I
II	C_L	$\frac{m_{to}}{S} = \left\{ C_L \frac{m_{to}}{F_D} \frac{\bar{n}}{\bar{R}/R_H} \left[\phi_S + \frac{C_t}{g} \frac{T_{to}}{T/q} \left(\bar{C}_{D_p} + \frac{C_L^2}{\pi A \phi} \right) \right] \right\}^{\frac{1}{2}}$	$\frac{m_{to}}{S} = \left(C_L \frac{m_{to}}{F_D} \frac{\bar{n}}{\bar{R}/R_H} \phi_S \right)^{\frac{1}{2}}$
III	$\frac{m_{to}}{S}$	CF. FIG. 8 CURVE I	$C_L = C_{L_{MD}}$
UNCON- STRAINED (POINT A)	APPROXI- MATE SOLUTION	$\frac{C_L}{C_{L_{ref}}} = 1 + \frac{1}{2\bar{C}_{D_p}} \left(1 + 2 \frac{C_t}{\phi_S} \frac{T_{to}}{g} \frac{T/q}{\bar{R}/R_H} \right)^{-1} \left(\frac{F_D}{m_{to}} \frac{\bar{n}}{\bar{R}/R_H} \phi_S C_{L_{ref}} \right)^{\frac{1}{2}}$	$\frac{C_{L_{opt}}}{C_{L_{ref}}} = 1 + \frac{1}{2\bar{C}_{D_p}} \left(C_{L_{ref}} \frac{\bar{n}}{\bar{R}/R_H} \phi_S \right)^{\frac{1}{2}} \frac{F_D}{m_{to}}$
		$\frac{m_{to}}{S} = 1.1 \left[C_{L_{ref}} \frac{m_{to}}{F_D} \frac{\bar{n}}{\bar{R}/R_H} \left(\phi_S + 2.5 \bar{C}_{D_p} \frac{C_t}{g} \frac{T_{to}}{T/q} \right) \right]^{\frac{1}{2}}$	$\frac{m_{to}}{S} = \left(C_{L_{opt}} \frac{m_{to}}{F_D} \frac{\bar{n}}{\bar{R}/R_H} \phi_S \right)^{\frac{1}{2}}$

F_D' : F_D with pod drag area included

Fig. 13: Payload fraction affected by wing loading and altitude



CURVE	CONSTANT	CONDITIONS FOR MAXIMUM PAYLOAD FRACTION; GIVEN MACH NUMBER; CONSTANT C_L @ V_2
I	Alt., A	$\frac{C_L}{C_{L_{ref}}} = \left[\left(1 + \frac{\phi_S g}{q C_{D_p}} \frac{\bar{n}}{\bar{R}/R_H} \right) \left(1 + c_t \frac{\bar{n}}{\bar{R}/R_H} \frac{T_{to}}{\bar{T}} \frac{k_{run}}{\rho_{to} S_{run} C_{L_2}} \frac{q}{\rho_{to} g S_{run} C_{L_2}} \frac{\pi A \phi}{C_{L_2}} \right)^{-1} \right]^2$
II	m_{to}/S , A	$C_L = C_{L_{MD}}$
III		$\frac{m_{to}}{S} = \sqrt{\phi_S} \left(c_t \frac{T_{to}}{\bar{T}} \frac{k_{run}}{\rho_{to} S_{run} C_{L_2}} + \frac{\bar{R}/R_H}{\bar{n}} \frac{F_D}{m_{to} C_L} \right)^{-1/2}$ (point B)
-	C_L	$A = \left(\frac{C_L}{\pi \phi \phi_A} \frac{\bar{R}/R_H}{\bar{n}} \right)^2$

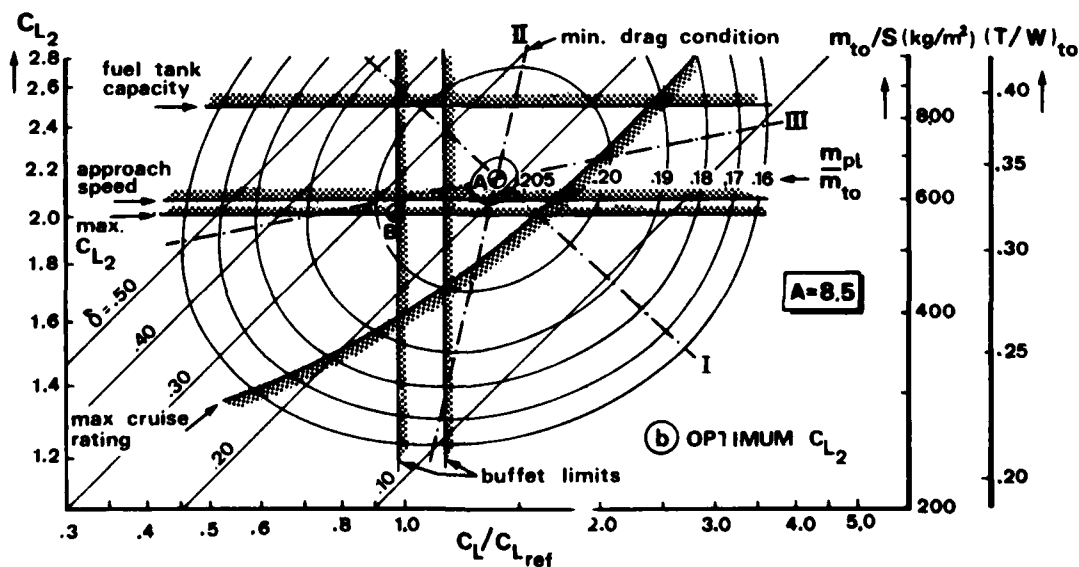


Fig. 15: Payload fraction affected by wing loading and altitude, engines sized for take-off/climb

Survey Paper on COMPUTER AIDED DESIGN

Review of the S.M.P. Specialists' Meeting on
"Computer Aid in the Production Design Office"

by

D. Weinhauer
Chief of airframe design
VFW-Fokker GmbH
Postfach 107845
2800 Bremen 1
West Germany

This paper has been entitled - Survey Paper on Computer Aided Design - but it is purely a Survey and Review of the S.M.P. Specialists Meeting on "Computer Aid in the Production Design Office". As to me, it seems to be nearly impossible to reach a total survey about the theme of CAD/CAM today.

Even though this rather young development is, at least on the European scene, on its real way to become a - state of the art - tool for designers, the short period of about 10 to 15 years has already been long enough to distribute, split and verify software development so widely that it is hardly possible to get an overlook.

At the S.M.P. we have had some pilot papers to find out the topic to be handled during the Specialists Meeting. According to a paper presented by Mr. W. Norman, McDonnell Douglas Aircraft Corp., St. Louis, USA, the situation in the USA seems to be such that CAD, CAM already represent the state of the art design methodology widely spread all over the main aircraft manufacturers. Compared to that, we have the impression that the European market shows quite a different picture. Therefore the S.M.P. Specialists Meeting has been outlined mainly to show up what is going on in Europe, especially due to the fact that all main aircraft developments in Europe (as e.g. MRCA, Jaguar, Alpha-Jet and Airbus) are of multi-national character. In order to this data exchange, design commonality and international cooperation are of quite an interest.

We have had papers from France, England, Italy and Germany. Specialists and/or representatives from well known companies as

- Aérospatiale, Marignane
- Avions Marcel Dassault
- British Aerospace
- British Computer Aided Design Centre, Cambridge
- Aeritalia
- Messerschmitt-Bölkow-Blohm
- VFW-Fokker

reported about their individual position reached up to date. I don't want to record details or summaries. All papers have been printed and published in January 1979 by AGARD CONFERENCE PROCEEDINGS No. 250 and may be reread from this publication.

As a conclusion of the Specialists Meeting I just want to highlight some results, statements or perspectives of common interest.

- a. In many places in Europe remarkable steps in developing and introducing of CAD/CAM have been taken by companies on their own initiative. The level reached so far varies highly and the degree of commonality in the sense of the NATO-common defence posture and the common benefit of the NATO community is poor!
- b. There is no doubt about the need for this new Design Methodology as a multifunctional tool for decreasing lead times and cost as well. Despite this fact, it has to be realized up to now that a broad and genuine breakthrough has not taken place.
- c. There is no question about the efficiency of CAD/CAM in general. Even though there are no, or only a few precise figures or results of investigations available so far, drawing time itself can generally be cut, but it was well understood by all participants that beside this the main impact is achievable downstream of the design process. Mr. Dyson from British Aerospace formulated it like this: "The return from computer systems in the conceptual design phase is not likely to result in lower costs, but will result in improved designs that provide a better position for the company in competition for new development. Less time spent in non-creative tasks presumably means more resources for creative tasks."

In individual cases

- design cost can be reduced
- design and product performance improved
- productivity enhanced and
- lead time for design of prototypes, pre-production and production reduced.

These gains result both from improved efficiency within each phase and from the fact that the output from the process supporting one design phase is used as input to the next phase. This ability to cascade computer systems is of the greatest significance.

- d. Also a lot of discussion time was spent on the questions dealing with 3-D-Systems and the opinions about host computer versus distributed design computers. A final statement or trend analysis was not reached! The discussion is still going on! The software specialists seem to be well prepared to take the next steps ahead before the state of the art reached by now is fully adopted by the majority of the users who are just about to check the possibilities and potentials of this new design tool offered to them. (This statement is related indeed to the European situation only.)
- e. Authors and participants at the S.M.P. Specialists Meeting expressed their interest and readiness for follow-on activities for which especially AGARD forms an outstanding platform because of its non-competitive status.

Therefore, as a result of the meeting, the following proposals for future activities have been raised in order to reach a higher degree of commonality within the NATO countries in this field.

1. The common development of a specification for a realistic 3-D-System related to the users' requirements.
It seems that in various places activities are just being started. It could be of interest as well as of assistance to those people engaged in this work to get an international crosscheck.
2. Common development of an interface specification to enable data transfer between design offices of different nations and/or companies.
This should be done without touching the already existing company internal basic systems and/or individual modules.
3. Common development of a specification for design-specific data bases (e.g. standards).
Everybody needs it and every one grudges the expense. This could perhaps be overcome by sharing the job between a number of partners and putting together the results.

Nevertheless it has been decided at the S.M.P. Panel to wait for the results of the todays F.M.P. Specialists Meeting and not to start new actions before checking weather or not there are common interests and to be frank and open for hopefully common interpanel activities.

Computer Graphics and related Design Process at MBB

by

Volkmar Antl

and

Werner Weingartner

Messerschmitt-Bölkow-Blohm

Postfach 80 111 09

8000 München 80

Germany

Summary

This paper is a short description of the complex CAD/CAM process how it is realized at MBB. First there are given some examples of using computer graphics, then a brief description of the main system functions and at last a survey of the entire MBB-CAD/CAM concept.

Contents

1. Preface - what is GEOLAN
2. Examples of using GEOLAN on realized projects
 - 2.1 Airbus A 300
 - 2.2 BO 105
 - 2.3 BK 117
 - 2.4 DNW
 - 2.5 WEA
 - 2.6 Fighter
3. Description of GEOLAN
 - 3.1 Characterization of functions
 - 3.2 A complete example
4. Utilization of results
 - 4.1 Design office
 - 4.2 Manufacturing
5. GEOLAN within MBB's CAD/CAM concept

1. Preface

At MBB GEOLAN is used in all cases of sculptured surface problems. This program-system was developed in our company and is permanently expanded and improved.

GEOLAN means: GEometric LANguage.

GEOLAN

- is largely analogous to APT (Automatic Programmed Tool) in syntax and logic
- is meantime programmed in FORTRAN (FORMula TRANSLation) and so easy to implement in most of the EDP-systems (already used on IBM and DEC)
- is able to immediately display geometric objects by using a graphic storage tube (TEKTRONIX)

GEOLAN is used at MBB in the three divisions military aircraft, civil aircraft and helicopters

GEOLAN is able to

- define geometric objects (e. g. points, lines) largely similar to APT, but with considerably extended 3-dimensional facilities
- execute several operations with the pre-defined objects:
 - o sliding and rotating in space
 - o smoothing lines, change point-spacing
 - o combine and part of lines and surfaces
 - o intersect surfaces with planes and other surfaces
 - o display the objects on a graphic screen and produce plots; for example in a perspect view or only parts of the geometric objects
 - o output of surface data in an APT-Canon format
 - o output all results in an desirable format on punched cards or magnetic tape
 - o extract data for finite-element and aerodynamic calculations

2. Examples of using GEOLAN on realized projects

GEOLAN is already in use since some years. Depending on the different jobs there have been cases, where a whole aircraft, and other cases, where only a surface for a wing was developed.

The following examples shall be briefly described.

2.1 Airbus A 300 - see Picture 1

By developing of the first European wide-body-jet, the Airbus A300, CAD was used in a high degree and from the beginning.

One of the most typical application was the scale 1:1 drawing of the frame-segments including clips, stringers and skin-overlappings. The principle of the clip-contour was always the same, but the size depending on the position of the stringers was different, see Picture 2

These drawings have been completely plotted and this was the first important use of a large flatbed-plotter at MBB in 1970.

The clips have been manufactured direct from the lofted foil.

2.2 BO 105 - see Picture 3

The BO 105 is a light multi-purpose helicopter in the class around of 2 tons with 5 seats and is used for transport of seriously injured people for example. Within the continuous running series of types it was necessary to re-design the hull of the backwards-(upper)fuselage, because of using new (stronger) engines. In this case the most important problem was the exact accommodation onto the existing fuselage-contour and a convenient aerodynamic covering of the varying devices. - see Picture 4

2.3 BK 117 - see Picture 5

The multi-purpose helicopter BK 117 was developed in cooperation between MBB and Kawasaki Heavy Industries. It can be equipped with up to 11 seats and has a payload of around 1200 kg. The first flight was on 13th June, 1979. The aerodynamically important stabilizer-system was designed by using GEOLAN. - see Picture 6

A special difficulty was in this case, that the vertical stabilizer fin had been taken original from BO 105 and the other parts (of different shape) had to be accommodated. Furthermore a large number of design-details had been defined numerically, for example tips and fillet radii between vertical and horizontal stabilizers.

2.4 DNW - see Picture 7

DNW is a cooperation project between Germany and the Netherlands. There is built a large low-speed windtunnel in the Netherlands and therefore a complex-shaped airscrew-blade was needed. - see Picture 8

The definition of the geometry had been developed with GEOLAN from the beginning. Of special importance was the correct aerodynamic shape. It was constructed from different wing-profiles with a non-linear law of the shift-angles.

For the manufacturing in carbon-fibre-compound the fullscale drawings had been plotted, and for adjusting of fixtures and control-measurement a lot of point-coordinates had been calculated.

2.5 WEA - see Picture 9

In the case of a wind energy converter there was reached a new class of extension for wing-shaped objects. This two-blade rotor of around 150 metres diameter shall be able to produce an electric power of 3 Megawatts.

This project is sponsored by the German Ministry of Research and Technology and shall be installed in the vicinity of Hamburg. It will be used for exploration of new pollution-free energy production systems.

Additionally to the very large dimensions and the complex shape of the wing-blades the problem of developing the surface arose in this case, since the production-fixtures will be built from parts of metal sheets. This problem has been solved by new generated CAD-methods. - see Picture 10

2.6 Fighter

The military aircraft Division at MBB Ottobrunn is working on several studies for new fighters.

Starting with simple drawings scale 1:10 there have been developed several fuselage- and wing-lofts by means of GEOLAN. By using foreground-time-sharing operation and interactive graphic display, it was possible to produce drawings for the pre-design in a very short time.

Furthermore - first time in this case - geometric data defined by GEOLAN had been converted to an APT-CANON and then with CAM-I-APT there was produced a scale 1:7 windtunnel model of a complete wing.

At present this project is in further development. Herewith problems arose, which have been unknown until today; for example the calculation of a development-curve of a small (fiber-) tape on a sculptured surface. Such problems can be solved in a comparatively short time with the already working software-production team.

3. Description of GEOLAN

3.1 Characterization of Functions

The logic execution of GEOLAN is similar to APT, i. e. the operations are controlled by statements within the input data stream, which are executed sequentially.

The statements are of the following forms:

1. name = expression
2. keyword / parameter (parameter ...)
3. name = Keyword / parameter (parameter ...)

For example:

L1 = SPSCS / 50, 30, 0, 100, 50, 0, 150, 100, 0

- L1 is the name of the geometric object, here a spline.
- SPSCS is the keyword which is used to define the type of object and the method of description, here a spline by points, slopes and cross-slopes.
- 50, 30, 0 ... are the parameters, in this case the point coordinates to build up the spline.

The type 1 of statement is used for arithmetical calculations.

The type 2 switches on or off some distinct functions, for example additional output of results at the terminal.

The type 3 is the most used from and serves as definition-statement for all types of objects and also for operations therewith. The geometric object gets the name of the character string left from equal-sign and is defined to be a type depending on the keyword. The parameters are interpreted using a law derived also from the keyword. The data results of this operation are stored for later use by specifying simple the name of the object within another statement's parameterlist.

GEOLAN user for storage of the geometric data two so-called workfiles (on disc) and optional several archive-files (discs or tapes). As source of input data stream there is mainly used a file on a disc which is created by using some edit methods. Usage of punched cards and other data carriers are dependent on the available hardware.

At MBB GEOLAN is preferable used under time sharing operation system direct on a screen. With this foreground-processing it is possible to watch the proceeding and to immediately recognize any errors.

Furthermore it is possible to enter the GEOLAN-statements in an interactive way on the screen, look for the result, and then decide what to do next.

GEOLAN is also able to produce graphic display of geometric objects. To do this, a suitable statement (for example PROJEC) is used to produce a close spaced sequence of points in two dimensions out of the three-dimensional objects.

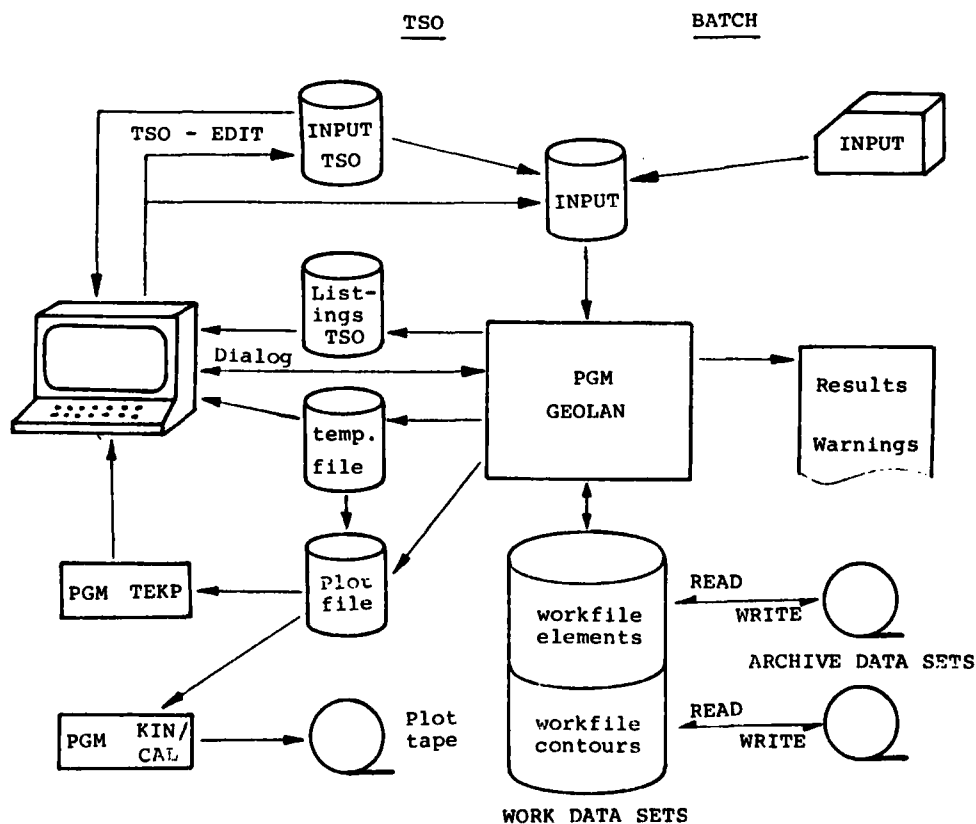
These picture data are stored on a disc-file and it is further possible to produce some types of output by using a postprocessor for:

- drum plotter (CALCOMP)
- flatbed plotter (KONGSBERG)
- graphic storage tube (TEKTRONIX)

Another feasibility is to use the graphic screen for inputting the GEOLAN statements direct via the keyboard and then not only achieve calculated results, but also graphic display everytime when a picture-producing statement is used. These pictures are stored on a temporary file and within the following proceeding it is possible to add some (partials) to a complete picture or to erase others. Finally it can be decided whether to store the pictures on a permanent file or not. The complete flow in- and output data as well as the possibilities of used hardware are shown on schema 1.

Schema 1

GEOLAN data flow



3.2 A complete example

The following example of a entire GEOLAN-run will be described to explain the main functions.

```

1) PARTNO AGARD-EXAMPLE
2) $$
3) L1 = SPSCS / 10 , 10 , 10 , 100 , 10 , 30 , $
      200 , 10 , 120
      $$
4) L2 = SPSCS / 10 , 150 , 20 , S, 0.3 , 0 , 1 , 100 , 200 , 120 , $
      250 , 170 , 140
      $$
5) S1 = MSCS / L1 , 2 , 0 , 1 , 1 , 6 , L2 , 3 , 0 , 2 , 1 , 0.7
      $$
6) D1 = MA02Y / 0 , 0 , 0 , Z , 0.2 , 0.1 , 1 , X , 0.5 , -1 , 0
      $$
7) COSYS / D1
      $$
8) I1 = POIPLM / Y , 80 , S1
      I2 = POIPLM / Y , 150 , S1
      COSYS / BASIC
9) U1.2 = SPCM / S1 , U , 1.2
      U1.4 = SPCM / S1 , U , 1.4
      .
      .
      .
      $$
10) TRASET / 0 , 0 , 0 , 300
      PROJEC / YZ , S1
      TRASET / 0 , 0 , 300 , 300
      PROJEC / XZ , S1
      TRASET / 0 , 0 , 300 , 0
      PROJEC / XY , S1
      $$
      COSYS / D1
      NOCROS
      TRASET / 0 , 0 , 150 , 0
      PROJEC / XZ , S1 , I1 , I2 , U1.2 , U1.4 , U1.6 , U1.8 , $
      V1.2 , V1.4 , V1.6 , V1.8 , V2.2 , V2.4 , V2.6 , V2.8

```

Description of the statements

1. PARTNO ...
Title of job; the text following 'PARTNO' is used as headline on the printed output pages
 2. Double Dollar-sign: serves as comment-line, no program function
 3. Definition of a spline using three points built up from three coordinates each
 4. Spline as before with addition of a slope on point one
 5. Creation of a mesh-surface by using the previously determined two splines; cross slopes are added on the second point of the first spline and the third point of the second spline
 6. Definition of a secondary coordinate system (matrix) out of origin and two axis vectors
 7. Switch on the new system
 8. Intersection of the surface with 2 y-constant-planes in the new system
 9. Derivation of some intermediate lines on the surface for better display
 10. Projection of surface in three different views and of surface, intersect line and the intermediate lines in an inclined view, using the above named matrix
See picture No. 12
4. Using of GEOLAN-results in design office and manufacturing.

When the lofted surfaces and the system lines are numerical defined by GEOLAN, all needed informations for design and manufacturing can be obtained from this base.

4.1 Design office

For the design of parts there are mainly needed drawn loft-lines on foil. These are usually intersection lines between the concerned surfaces and some system planes. Very often the thickness of skin is to be subtracted and so an offset from the outer contour is to be drawn.

Furthermore some other parallels to loft-lines are needed (for example for centre lines of holes) and also core-lines (for example of stringers and spars) have to be drawn. By producing developments of sheets additionally to the intersection line also the bevel-angle is to be calculated and to be quoted.

For indicated measures and other purposes sometimes the coordinates of points are explicitly needed.

Always when loft-dependant information is needed, the designer will call support of loft-department. Here he will be advised which types of information may be suitable for his problem. Then this drawing will be produced by using GEOLAN and the result is delivered into design office.

By using time-sharing foreground jobs, plotter and graphic screen, it is generally possible to do a normal task in one to three days.

4.2 Manufacturing

The geometric data created with GEOLAN are also used for manufacturing, but for this purpose there are often needed other and/or more information as for design. To provide these informations, each drawing bears a note which points to the concerned surfaces. The necessary data for manufacturing are demanded from the loft-department, when the drawing reaches the factory.

For normal manufacturing often some additional intersect lines are required; sometimes it is possible to replace parts of surfaces by planes or cylinders. The factory and the loft-department cooperate to clarify, where such simplification is possible; then the data for measure the planes etc. are generated.

For parts from metal-sheet additional lofted foils are often needed. These drawings are plotted and can be photo-copied on the metal sheet. This may be used as master for production.

For NC (Numerical Control) manufacturing it is possible to output intersect data as row of points but also entire surfaces as APT-CANON. This geometry is given on a data carrier to the factory, where it will be used to create NC-programs by using APT or CAM-I-APT.

For control measurement and other purposes often explicit point coordinates are calculated.

Occasionally for special production methods or fixtures some extra surfaces must be created.

All of the needed informations and data are produced by using the original GEOLAN-data.

5. GEOLAN within the CAD/CAM concept at MBB

GEOLAN is only a part of a CAD/CAM (Computer aided design/computer aided manufacturing) project at MBB, which is planned for EDP support of the design office and a few special manufacturing departments.

5.1 Contents of CAD/CAM concept

In this CAD/CAM-project a lot of problems which have geometric aspects are gathered until now. The main topics are:

- Master dimension: development of GEOLAN and interface to other systems using loft-data
- CADAM: implementation, adaption and development of Lockheed's CADAM-system for production of drawings
- NC: development of systems for the use of geometric data derived from design for Numerical controlled manufacturing (based on CADAM, APT, CAM-I-APT)
- CADAM-EL: Data transfer from CADAM drawings
 - o to administrative design data systems
 - o to special calculating routines (for example areas of wire-sections, lack of electrical tension)
 - o to support of automated manufacturing (wire plate press, cable bundle device)
- ST: development of finite element structures from design data

- 3D-GEO: numerical representation of general three-dimensional objects used as a data base for:
 - o investigation of collision of movable parts and devices to be built-in
 - o design of high-grade complex parts (for example NC-frames)
 - o Process planning
 - o calculating of volumes, areas and intersections

The connection of these geometric topics is shown on the schema 2.

5.2 Examples of applications

Some of the CAD/CAM projects and their interfaces have reached a stage of production and so the following examples can be shown.

5.2.1 GEOLAN-NC

The pictures show:

Pic. No. 13: the numerical defined surface (patches), created by GEOLAN

Pic. No. 14: the NC-milled windtunnel-model, made out of this data

5.2.2 GEOLAN-CADAM

The pictures show:

Pic. No. 15: the surface patches of the BO105 helicopter fuselage, created by GEOLAN

Pic. No. 16: also GEOLAN-derived intersection lines

Pic. No. 17: accomplished drawing by CADAM.

5.2.3 GEOLAN-ST

The pictures show:

Pic. No. 18: Perspective view of a proposal for a new fighter

Pic. No. 19: from the wing-geometry derived finite element structure (Input for NASTRAN)

AD-A083 203

ADVISORY GROUP FOR AEROSPACE RESEARCH AND DEVELOPMENT--ETC F/6 9/2
THE USE OF COMPUTERS AS A DESIGN TOOL.(U)
JAN 80

UNCLASSIFIED

AGARD-CP-280

NL

2 5

2 5

2 5

2 5

2 5

2 5

2 5

2 5

2 5

2 5

2 5

2 5

2 5

2 5

2 5

2 5

2 5

2 5

2 5

2 5

2 5

2 5

2 5

2 5

2 5

2 5

2 5

2 5

2 5

2 5

2 5

2 5

2 5

2 5

2 5

2 5

2 5

2 5

2 5

2 5

2 5

2 5

2 5

2 5

2 5

2 5

2 5

2 5

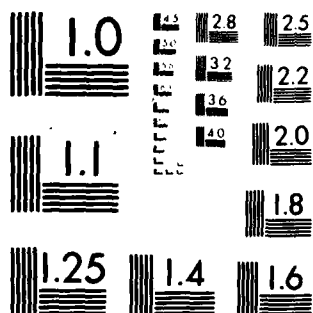
2 5

2 5

2 5

2 5

2 5

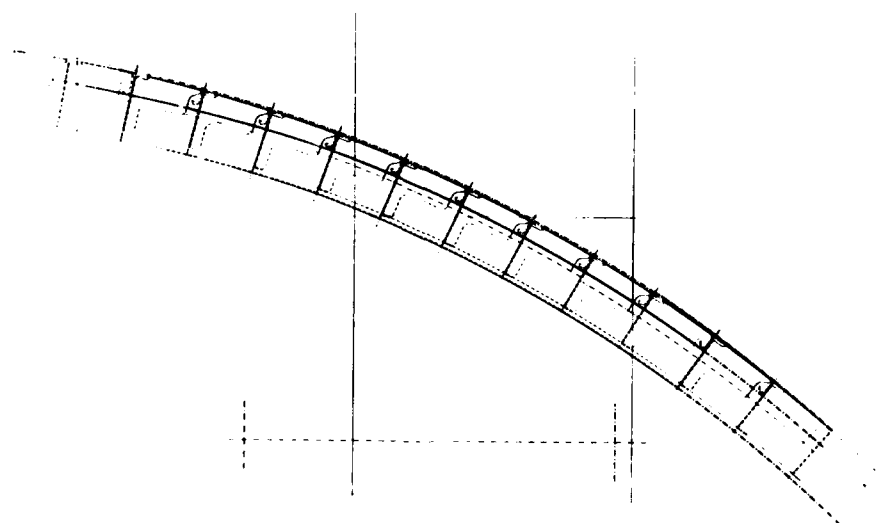


MICROCOPY RESOLUTION TEST CHART
NATIONAL BUREAU OF STANDARDS 1963-A

Picture 1 Airbus A300



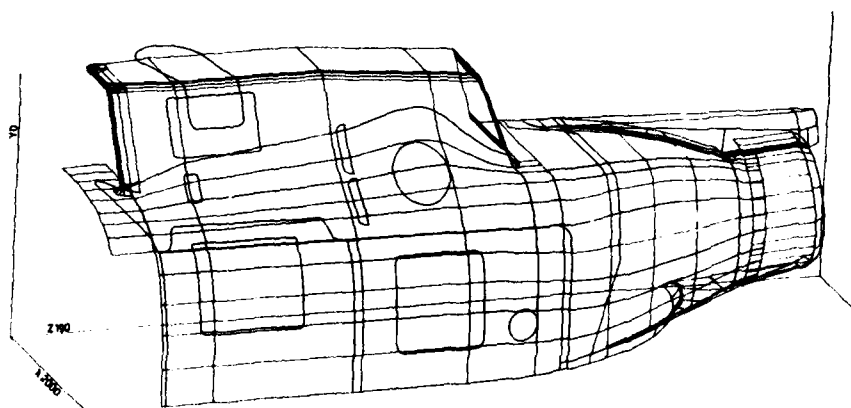
Picture 2 Airbus frame computer drawing



Picture 3 BO105



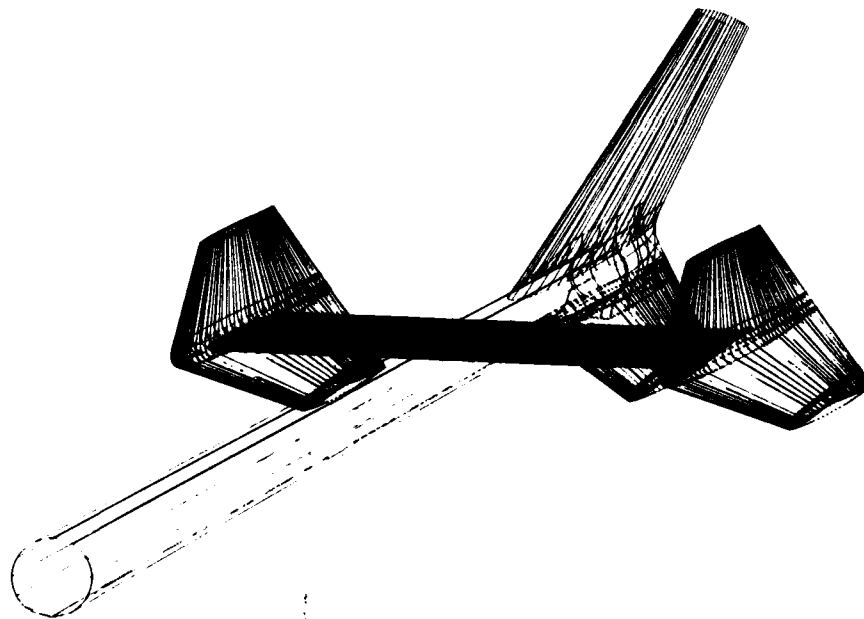
Picture 4 BO105 rear fuse computer drawing



Picture 5 BK117



Picture 6 BK117 rear stabilizer system plot



Picture 7 DNW windtunnel fan

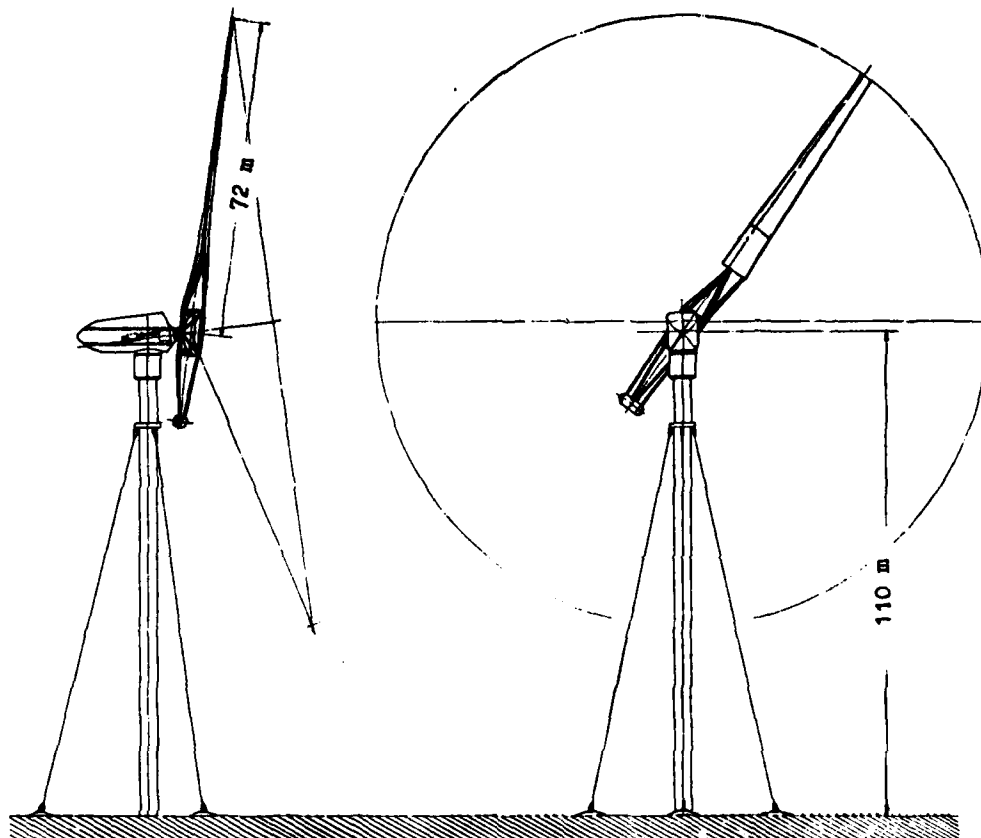


Picture 8

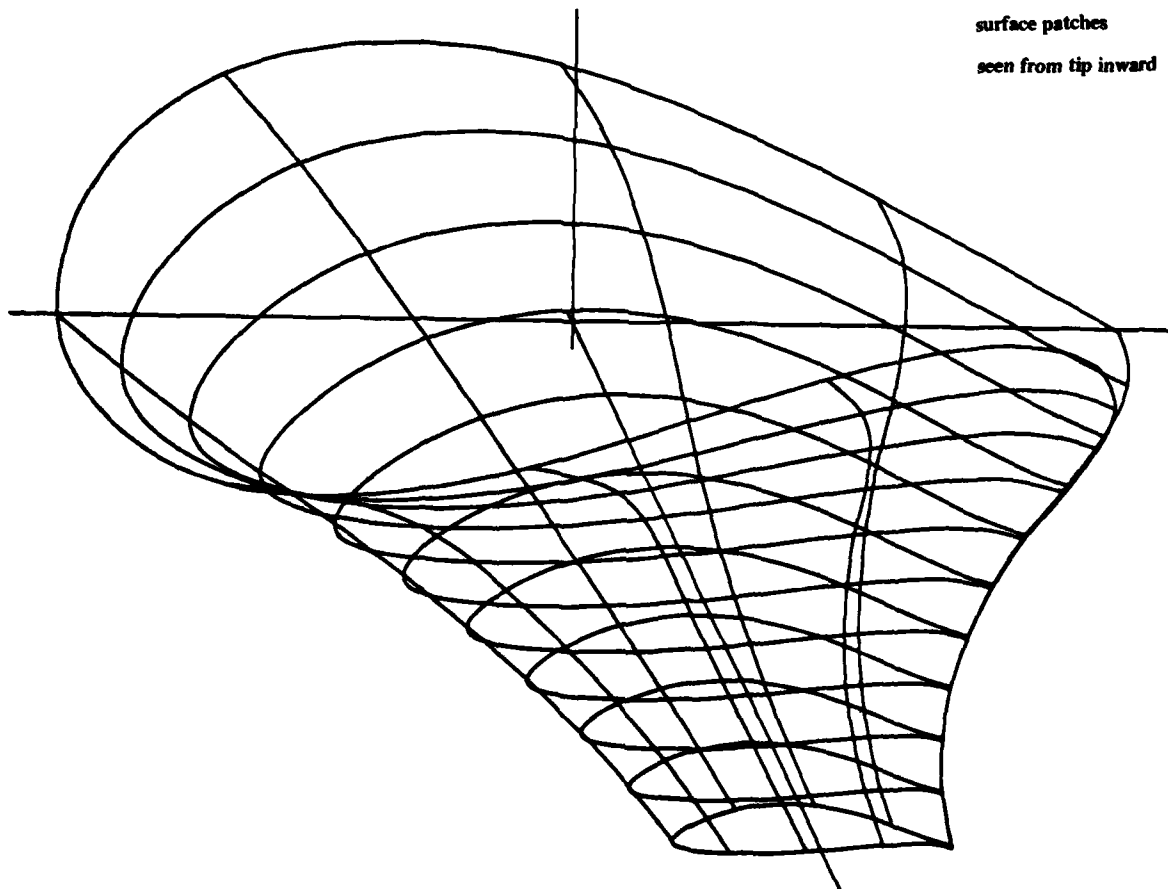
DNW airscrew blade



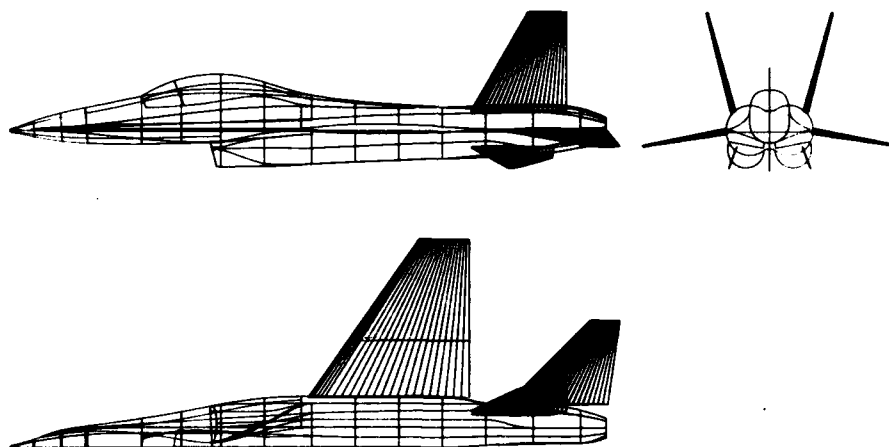
Picture 9 WEA wind energy converter project



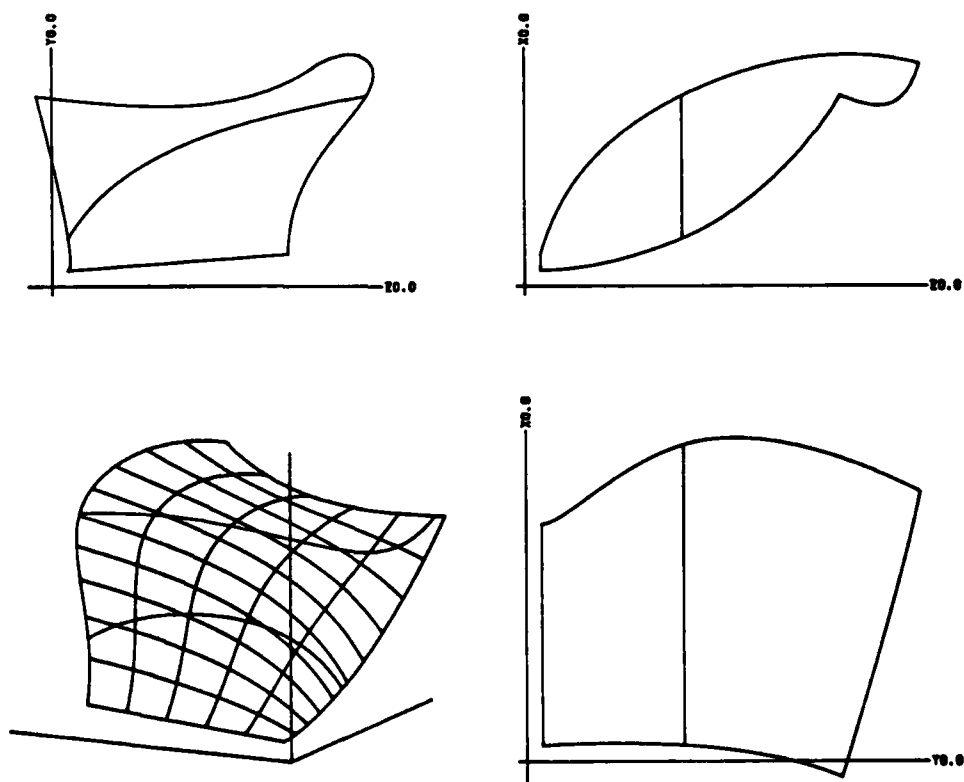
Picture 10 WEA rotor blade
surface patches
seen from tip inward



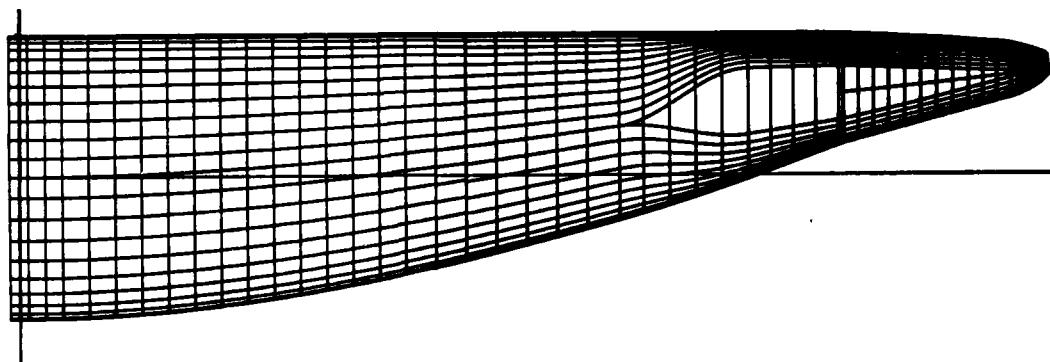
Picture 11 Fighter computer drawing of 3-side views



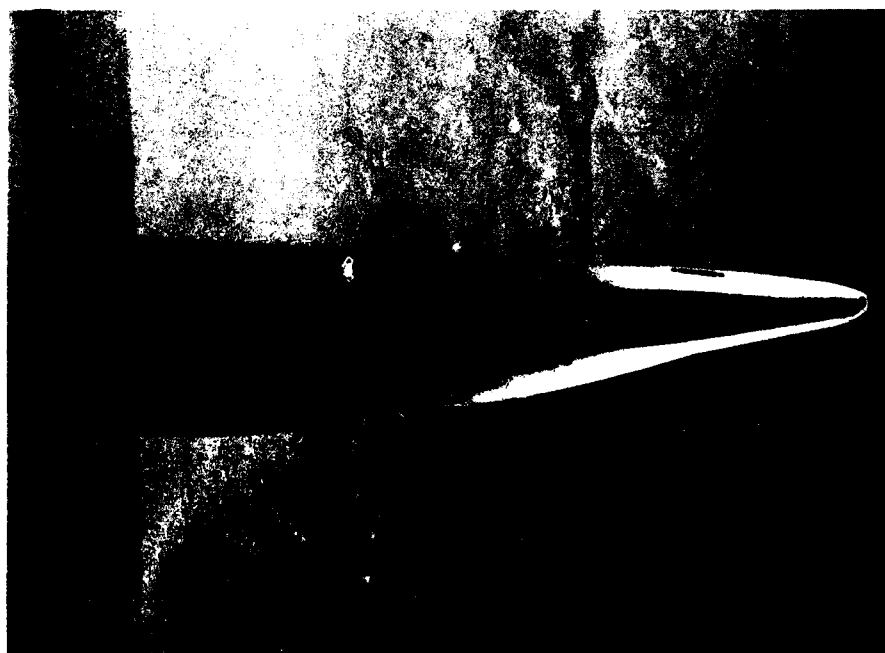
Picture 12 GEOLAN - AGARD - Example



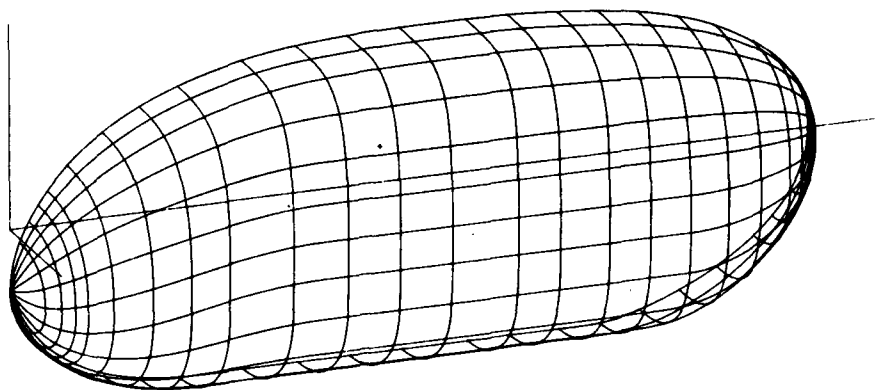
Picture 13 Airbus rear fuse patches



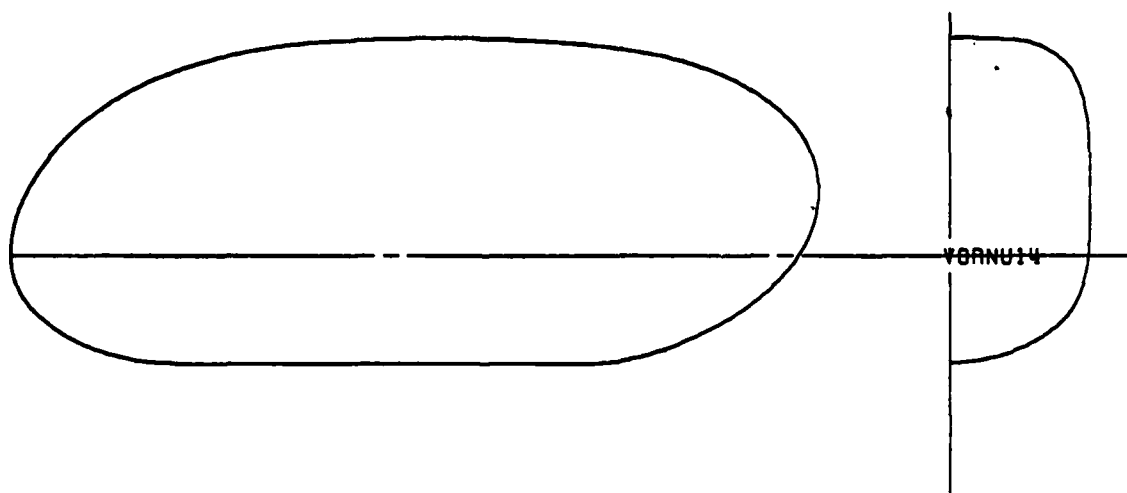
Picture 14 Airbus rear fuse NC-milled model



Picture 15 BO105 fuselage patches



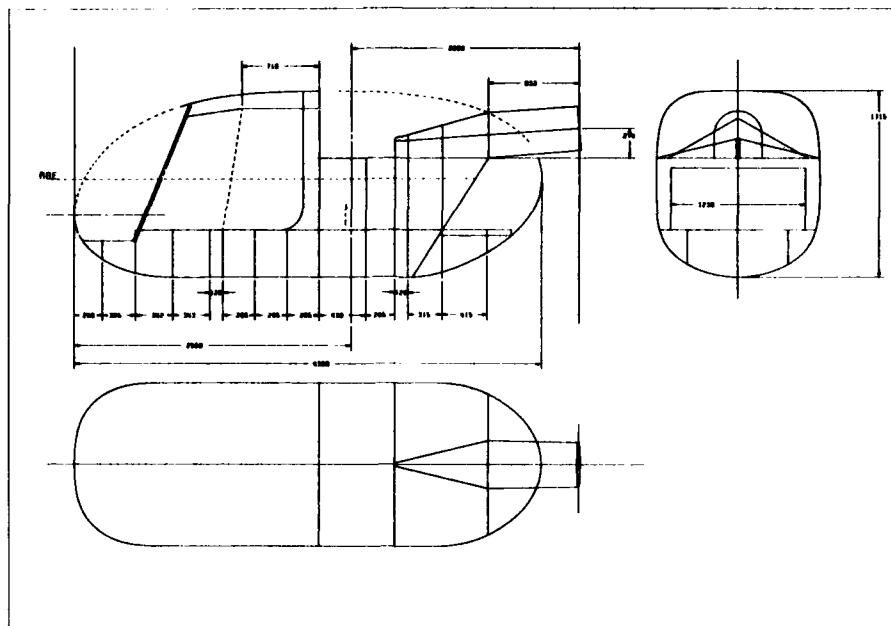
Picture 16 BO105 fuse intersects



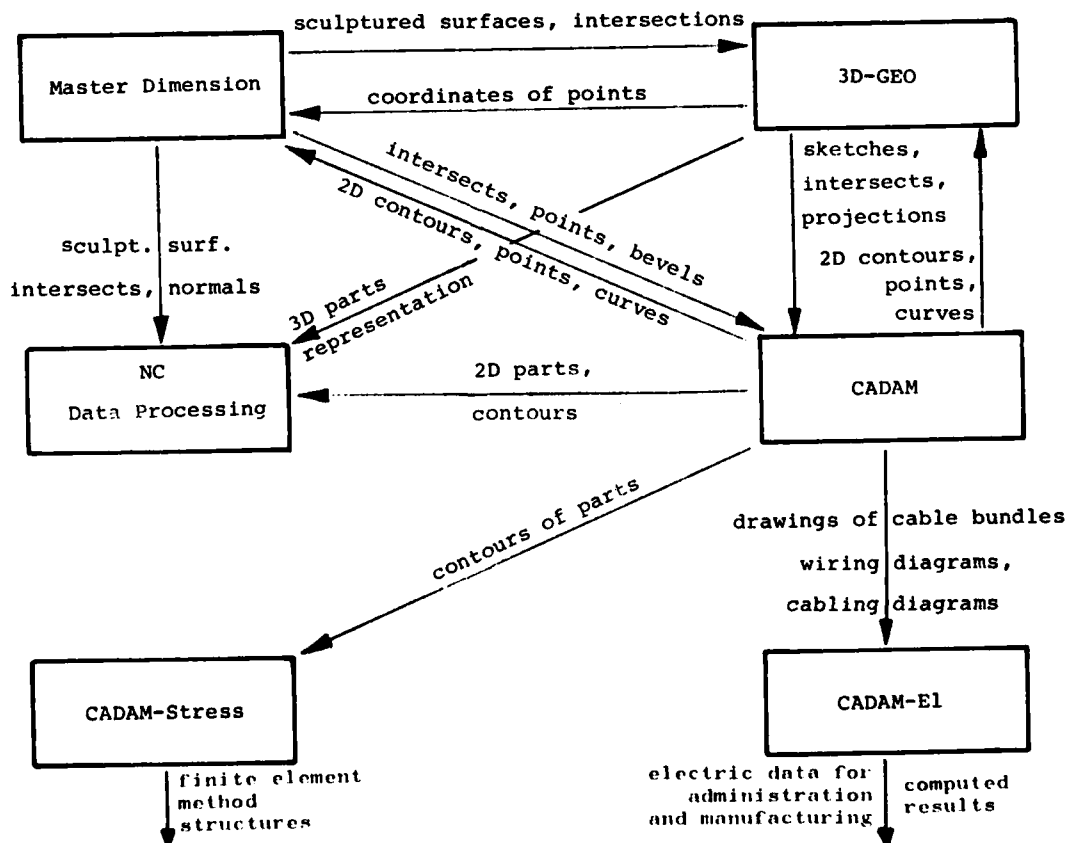
GEOLAN STRAK BO105 MIT CADAM GEZEICHNET



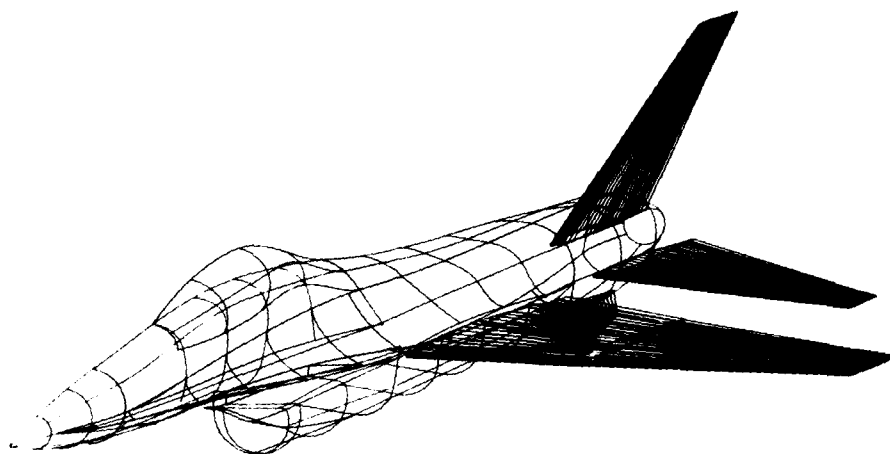
Picture 17 BO105 CADAM drawing



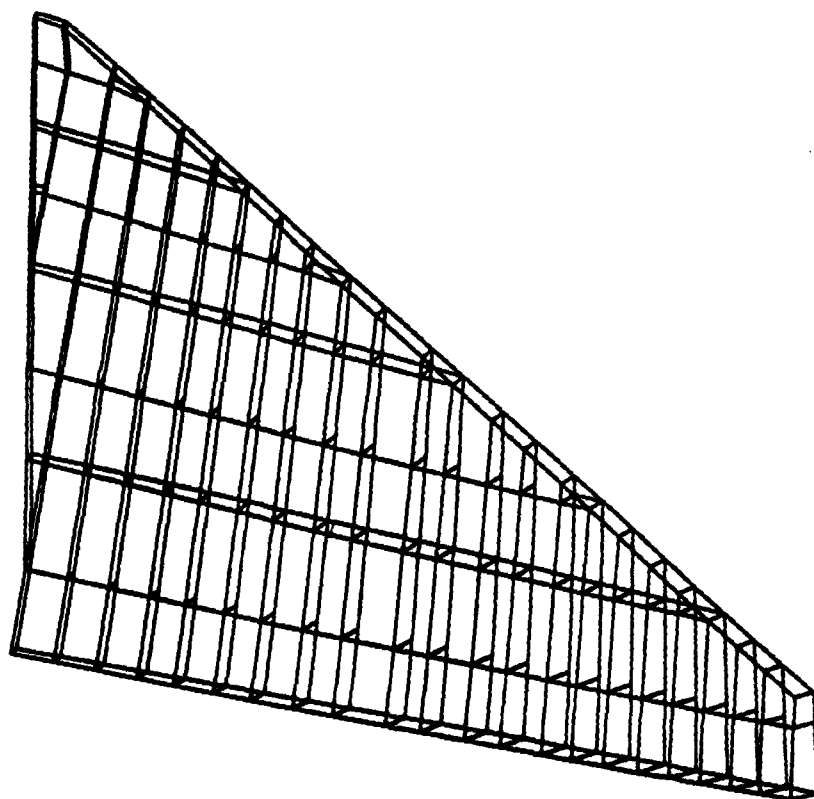
Schema 2 connections of topics within
CAD / CAM project



Picture 18 Fighter perspective computer drawing



Picture 19 Fighter wing FEM structure



COMPUTER GRAPHICS, RELATED DESIGN AND
MANUFACTURE PROCESS AT DORNIER
J.NAGEL, L.THIEME, A.HARTER

Dornier GmbH
Postfach 1420
D7990 Friedrichshafen 1

1. General View

The outer contour of aircraft cannot be represented by simple mathematical functions. For this reason it was formerly generated graphically.

With the progressive development of the computers numerical methods could be developed and introduced.

Dornier has developed a program system, which, besides the APT possibilities, attaches great importance to the definition and machining of general surfaces.

2. Substantial Processor Features

- Programming in FORTRAN IV
- Syntax and semantics similar to APT
- Data input and formal error control on ON-LINE screens
- Program run on IBM/370 in batch
- APT-compatible output (CLDATA)
- Various outputs (see fig. 1)
- Application for 5 years.

3. Application in all stations of a project

3.1. Aerodynamic calculations

- Input of the data in the computer in the form of coordinates or functions
- Modification and smoothing of the profiles or surfaces
- Transfer of the data for aerodynamic calculations
- NC data for wind tunnel models (fig. 2: Alpha-Jet fuselage on NC machine, fig. 3: SKF model with fuselage). The calculation of the cutter offset along the intersection of two surfaces is possible.

3.2. Outline, preliminary design

- Supply of all surface data
- Calculation and NC drawing of intersections (fig. 4: Light Transport Aircraft drawing)
- NC milling of templates (fig. 5: LTA model)
- General calculations:
 - mounting investigations
 - investigations with regard to the field of vision (Fig. 6: LTA)
 - system dimensions.

3.3. Design

- Calculation and NC drawing of any kind of intersections and unrollings
- Partial design drawings (fig. 7: nose rib)
- Calculation of contour-dependent dimensions.

3.4. Tools

- NC drawn foils for light-controlled machine (fig. 8: tool and plate)
- NC punched tapes for master models, jigs and tools (fig. 9: air intake).

3.5. Manufacture of components

- NC punched tapes (example: finishing milling of a complete wing: fig. 10).
- Surface data in the APT format for further use in the APT.

3.6. Inspection

- NC milled inspection templates (fig. 11)
- Inspection lists (Surface data).

The main field of application for the geometry processor are parts with difficult contours and a relatively simple technology. (Item 3.4.)
The cutter offset path is generated automatically with the build-up of the surface according to certain key words and parameters. Drive instructions are not required.
Program example for the NC milling of a surface: see fig. 12.

The change-over of the processor from the batch mode to a graphically interactive mode (Tektronix screen with APL) is programmed and presently tested in operation.

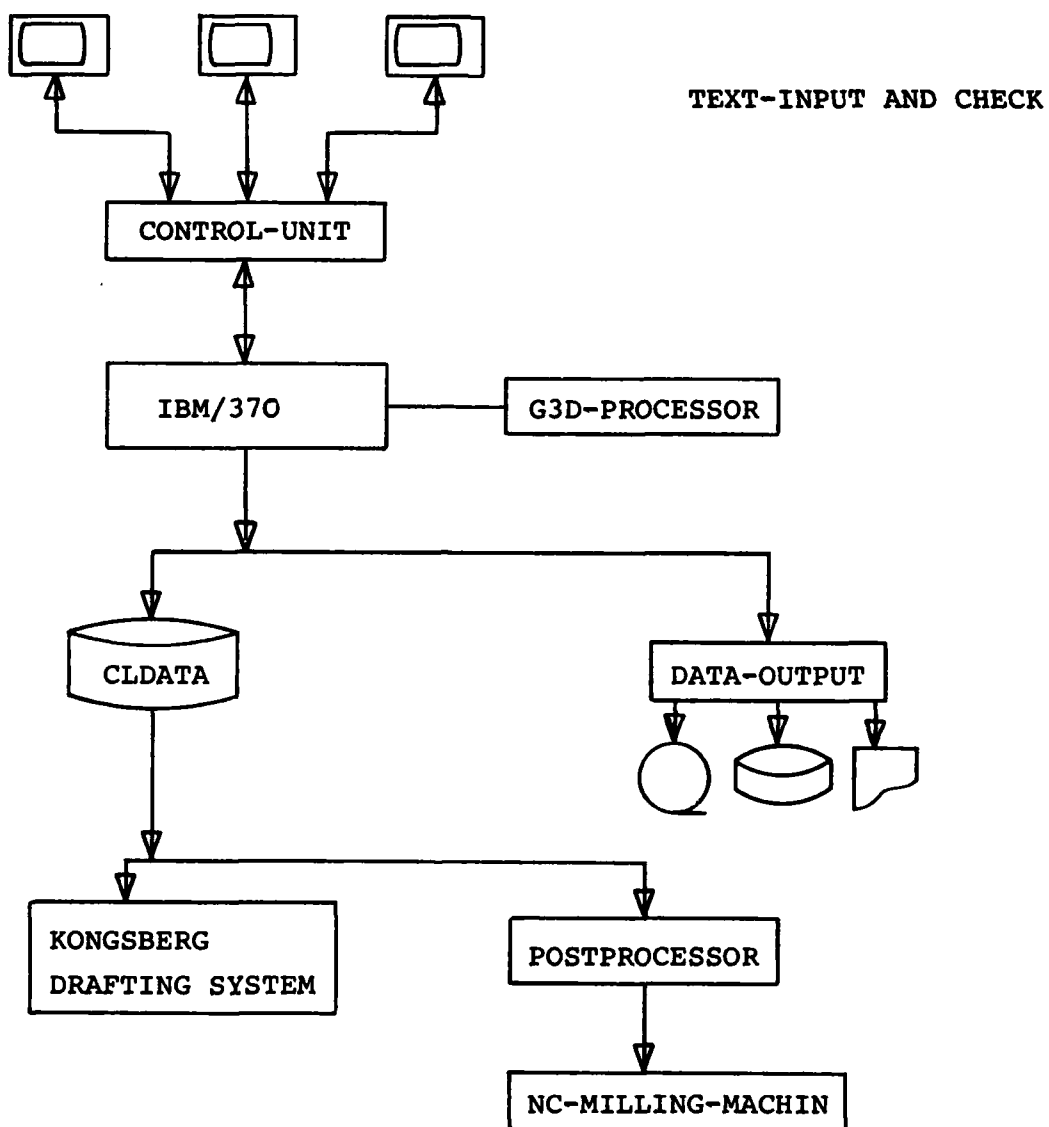
FLOW DIAGRAM G3D

Figure 1

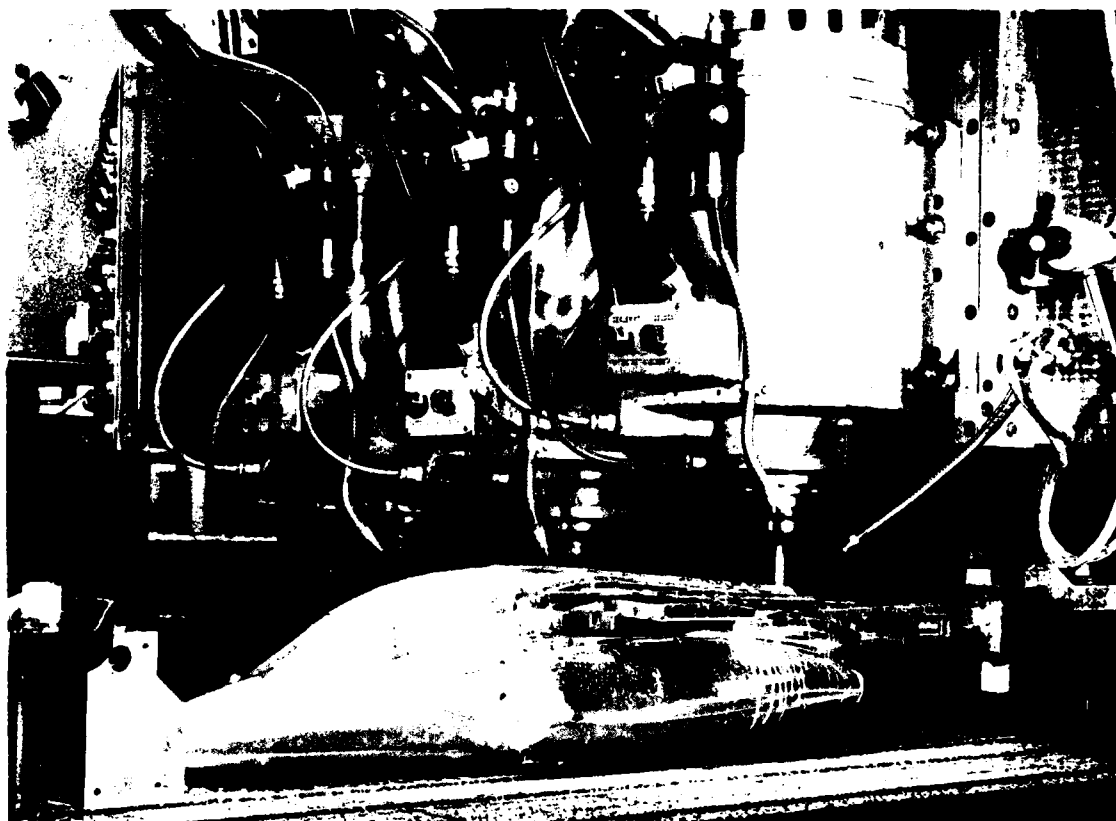


Figure 2

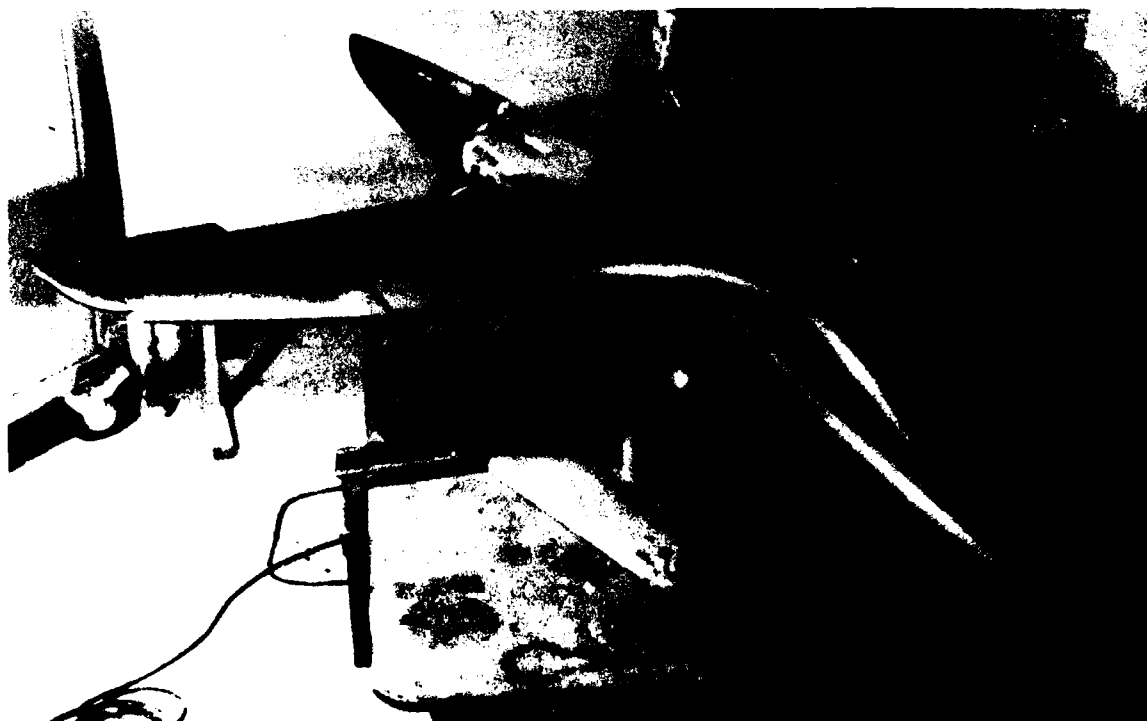


Figure 3

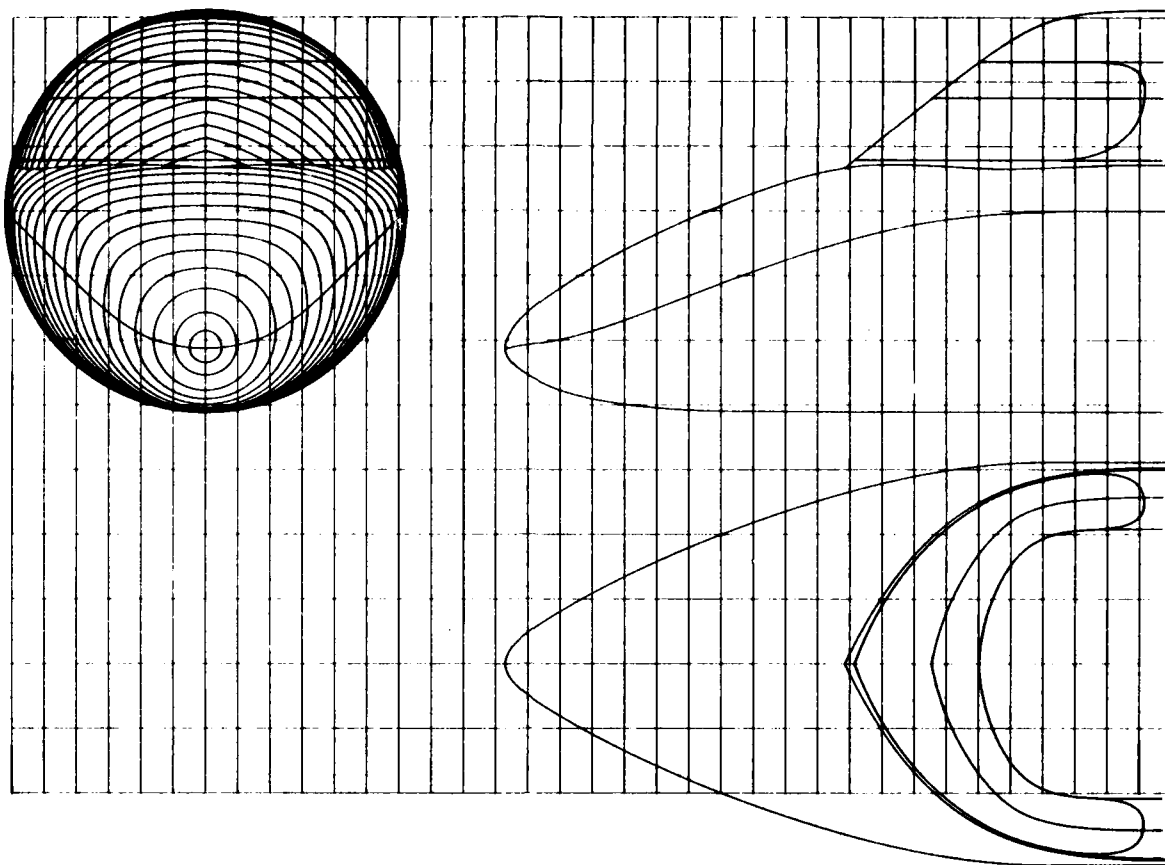


Figure 4



Figure 5

X = 4250

Y = -550

Z = 3170

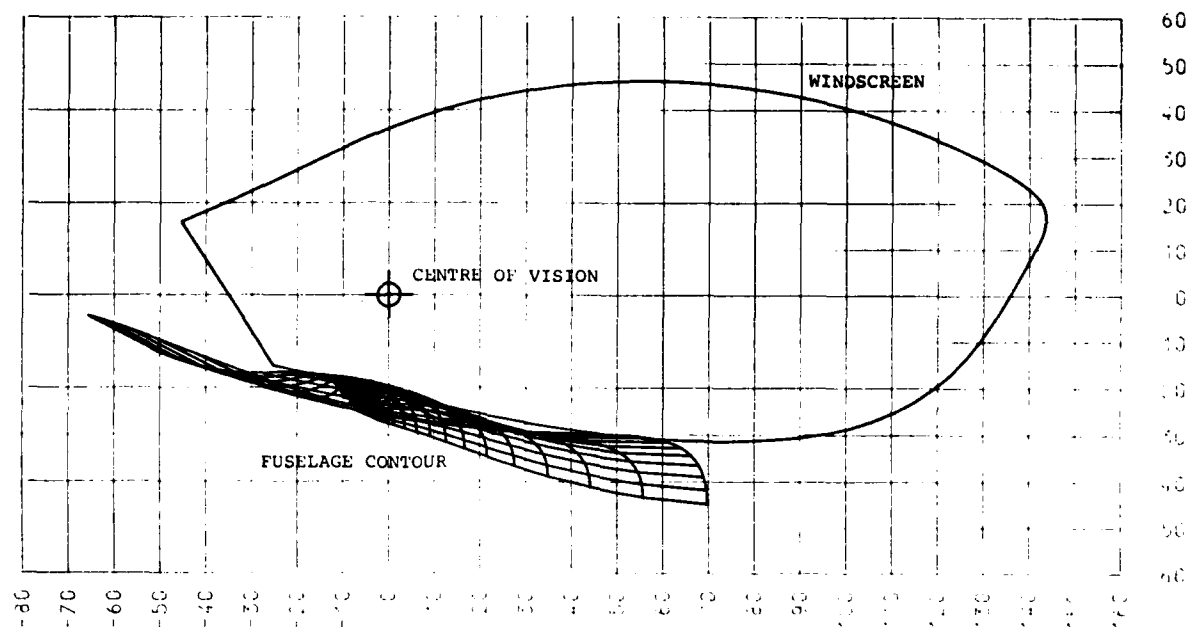


Figure 6

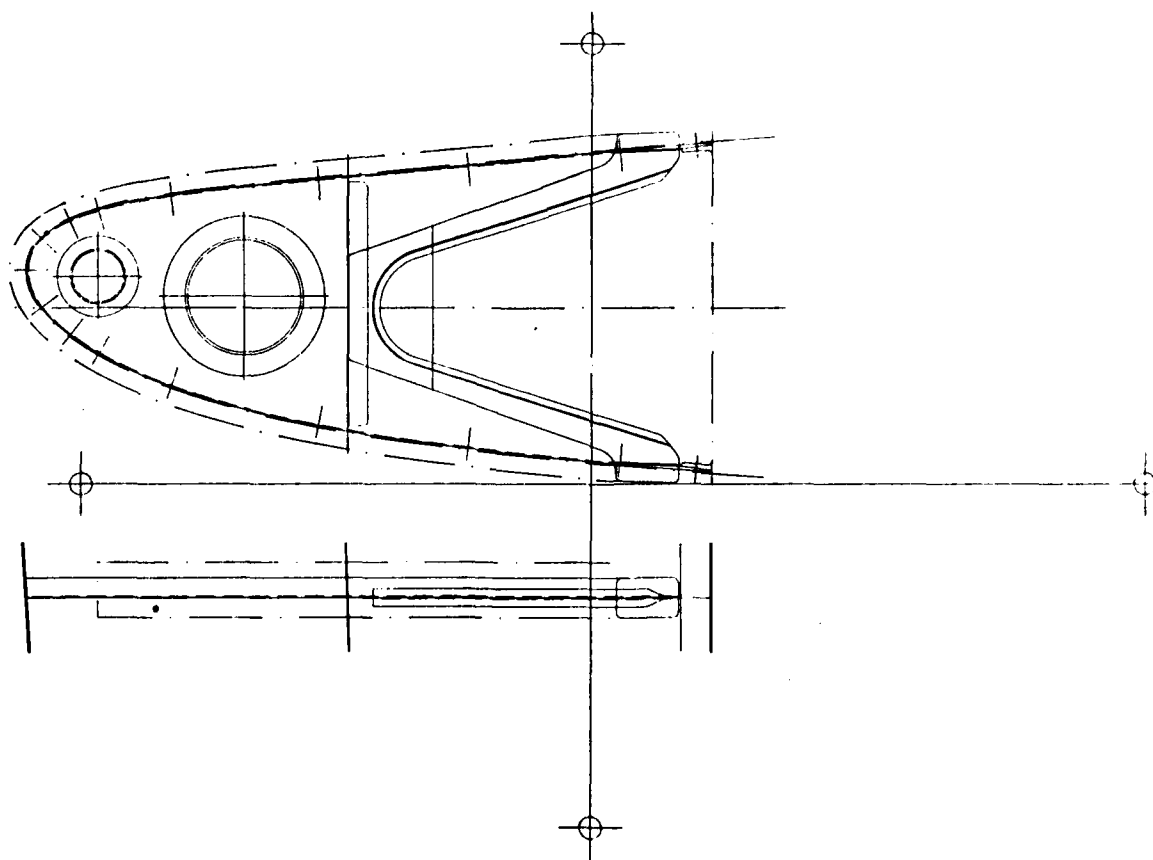


Figure 7



Figure 8



Figure 9

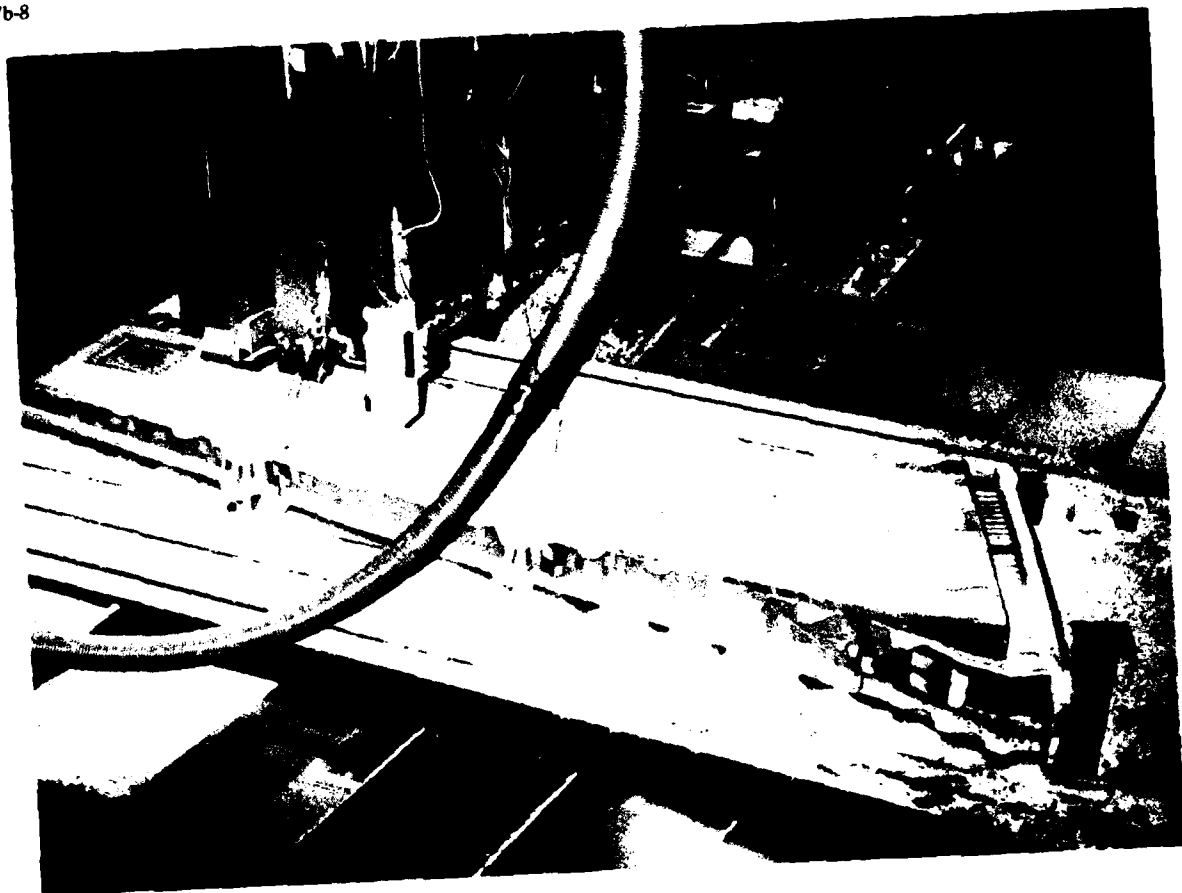


Figure 10

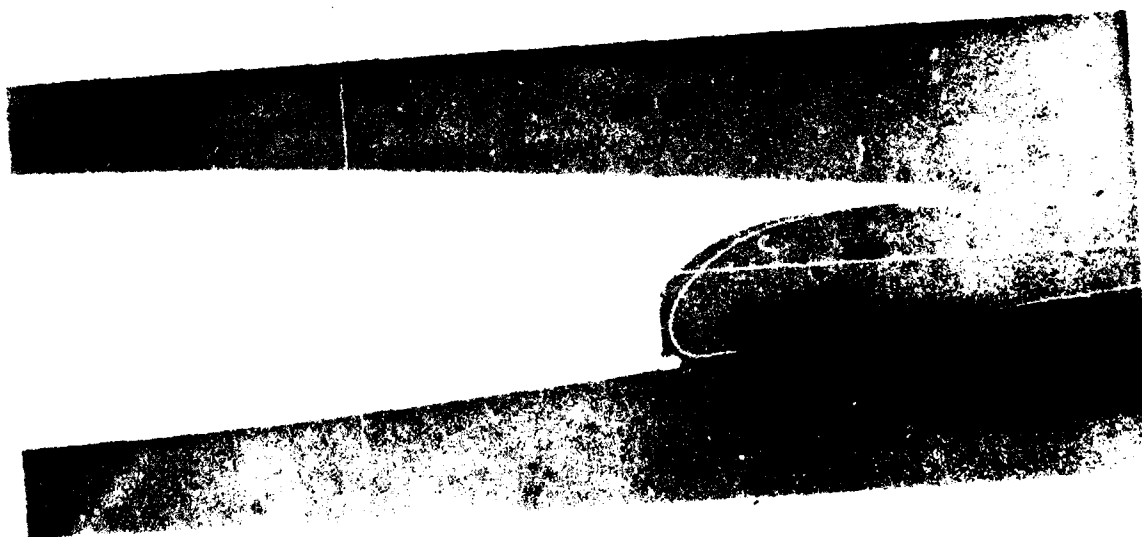


Figure 11

EVEL 2.0 (JAN 76)

G3C - SOURCE LIST

DATE 2. 8.79

PAGE 1

***** PROGRAMMER : THIEP

***** REFERENCE : PSAGAP *****

```

LN   1   C   ***** E X A M P L E   G 3 C *****
LN   2   C   GC-PROGRAM TO FILE A SURFACE LINE BY LINE
LN   3   C   POSTPROCESSOR=CALL
LN   4   C   FACHIN/'RISCH',15435
LN   5   C   FUNCTIONS TO BE INSERTED
LN   6   C   10 RAPTIZ/
LN   7   C   11 GUEFLTA/100,17ANG,200
LN   8   C   P/100/11EXT1
LN   9   C   STR=PC11/150,100,200
LN  10   C   FUNCTIONS WITH LABEL 10 AND 11 INSERTED
LN  11   C   ASSEMBLY/10,11
LN  12   C   SURFACE START WITH SURFACE OFFSET 2.5 MM
LN  13   C   PARTSURF/100,2.5
LN  14   C   NO. OF LINES AND DIRECTIONS
LN  15   C   MILESORE/100,300,STZIG/AC,1,SPLINE
LN  16   C   STARTING POINT
LN  17   C   FROM/STR
LN  18   C   FEED RATE, SPINTEL SPEED, COOLANT
LN  19   C   FEEDRAZ/1500, SPINTEL/6300, COOLANT/100
LN  20   C   CUTTER WITH SIGN
LN  21   C   CUTTER/-50, -1.6
LN  22   C   3-D LIMITATION OF THE ORIGINAL CURVES BY A ROTATED PLANE
LN  23   C   FROMCUBZ/100,11,153,12,98,17ANG,5.8
LN  24   C   OPER. DATA CASE
LN  25   C   INPUT/12
LN  26   C   DATA CALL TO A LUMP
LN  27   C   CU/30,1,1,15
LN  28   C   30 DATA/1XSEAT,1
LN  29   C   LIMITATION OF THE CUTTER-OFFSET PATH BY A RULED SURFACE
LN  30   C   FROMCEST/100,SEAT,1,CURVE,1,CURVE,2
LN  31   C   TERMINATE PARTIAL SURFACE, IF NECESSARY, FURTHER
LN  32   C   PARTIAL SURFACES
LN  33   C   CENERZ/
LN  34   C   GUEFLTA/100,200
LN  35   C   RAPTIZ/
LN  36   C   CUT/STR
LN  37   C   COOLANT/FEED, SPINTEL/FEED, STOP/
LN  38   C   PARTSURF/FEED
LN  39   C   END/

```

Figure 12

COMPUTER GRAPHICS AND RELATED DESIGN PROCESSES IN THE U.K.

by

R.I.Hacking - BAe Warton
and B.Reuben - BAe Brough1) Introduction

We are now poised on the threshold of the 1980's with some 20 years of widespread computer usage behind us.

The pace of developments in computer hardware has, on the whole, been astounding. In areas such as integrated circuitry and disk drives, the change has been most marked with improvements of 100 fold over the last ten or so years. In other areas the pace has not been so intense. In particular the development of graphics display devices has been relatively slow over the last decade.

On the software side, progress has been more steady, not exhibiting the erratic development rate seen in the hardware field. The most striking observation is that the size of the total problem increases exponentially. Each subsystem in computer aided design has become more complex and refined in itself and at the same time requires more powerful links into parallel subsystems. This is compounded by the lack of higher level concepts which would eliminate the need to consider the fine detail of these large systems. That is to say, CAD is attacking problems on a broader and broader front and yet each factor has to be considered in a more refined manner.

This complexity of the overall task has meant that the development rate of a CAD program - as with most other computer programs is very difficult to predict.

Both these factors, the erratic nature of hardware development and the unpredictability of software improvements, have not prevented the introduction of many aids to aircraft design. Computer solutions to many problems in aircraft design and manufacture have been developed and as time has passed these applications have been expanded in capability and scope to become large scale computer systems. In so doing the areas where computers have had little impact have become high lighted, especially in the area of information transfer between different disciplines. It is in these areas that major gains are to be made and to which mammoth projects such as NASA's IPAD seek a solution. This coming together of major computer systems will be referenced in this paper, not least in the consideration of geometrical systems for the description and analysis of flying surface shape.

2) Geometry

The task of making computer aided design into an effective design tool is being attacked on two distinct fronts. In one case we are interested in the shape of individual components and in the other case we are interested in the gross shape of the aircraft. In time the division between these 2 activities will disappear with the introduction of the total geometric configuration description. Whilst this is a general statement of activity in this field there is noticeable differences in emphasis and technique being employed by the various companies.

To explain the current situation within British Aerospace, the two activities will be described beginning with the description and analysis of aircraft gross shape.

3) The Description of Aircraft Gross Shape Using the Numerical Master Geometry System

This is indeed a wide subject and can only be covered in out-line. Firstly a short history of NMG is appropriate, then I will explain the usage of NMG in 3 typical situations. That is:-

- a) Improved data output to detail design
- b) System usage by manufacturing
- c) Transfer of data to aerodynamics and structural engineering departments

3.1 History of NMG

This shape description technique came into existence in 1965 and was first used in production in 1968 on the Concorde project. It has been the subject of continuous extension and development which has striven to keep pace both with the developments in computer hardware and with the engineering demands of more facilities for the minimum of manpower.

It was conceived as a batch processing system relying on data storage on magnetic tapes but has been transferred into an on-line facility to match the new computer hardware and operating systems. This development has been soundly based within the requirements of the Tornado design and production programme. Each new feature or method of usage has had to pass the test of producing answers within the available timescale and with a high degree of reliability and integrity. However, whilst Tornado is important, NMG has been used extensively on 5 BAe civil projects and several other military projects. This has generated a flexibility in the system which is demonstrated by its adoption by a major car manufacturer as a shape definition and manufacturing system.

3.1.2 Recent developments

Up until recently NMG has concentrated on very good representation of aircraft shape. This has been attained by the usage of unique mathematics and refined algorithms. Examples of the system capability are shown on Fig.1. These examples depict the flexibility of a single patch equation and demonstration that transitions from square corners to circular sections and reversals of curvature are readily handled. Note in particular that all the cuts through the surface are smooth and engineeringly desirable. Normally such a patch forms a small element in a whole surface representation on NMG and the aircraft will comprise many such surfaces (Fig.2.)

However geometry is an essential input to many engineering tasks and recent NMG developments have addressed the interfaces to these related tasks. Fig.3. shows the more important users of master geometry information.

A major obstacle in the usage of NMG by occasional users has been the difficulty of knowing what information is required in a particular situation. For example, aerodynamics assessment of the wing on the 50th aircraft requires that user to know the surface names which represent the various surfaces which made up the wing and flaps, etc, for that particular aircraft.

In the past this has been achieved by a general arrangement drawing which illustrates the various surfaces and their NMG identifiers for each batch of aircraft. This presentation of information is not easily understood or accessed by some classes of user and has led to difficulty in using NMG data.

Now a recent extension to the NMG system, known as the structures facility, enables the whole of a particular aircraft to be treated as a single structure which can be intersected as though it were a single surface.

This has a twofold effect, firstly it enables the occasional user to quickly find the information he requires, and secondly it means that the geometric model can be far more detailed and may be used to represent internal structure and fittings without becoming cumbersome to operate and use.

3.2 Let us quickly consider some typical users of the NMG system.

3.2.1 Supply of section drawings for component design.

The design organisation requires a plot on plastic film, and in addition they may require the significant curves to be stored for subsequent use in detail drafting or NC manufacture.

Using the NMG structure facility cuts through the aircraft can be plotted showing the space available for a new or modified component. The more complete the NMG model is, then the more informative are the sectional plots, but it is envisaged that components will not be represented in fine detail - only in gross shape. For instance, an undercarriage leg is represented by several cylinders and prisms but the detail geometry of nuts, fittings, etc, is omitted.

From such sectional plots a designer can position a component with the desired access and clearance, or perhaps locate a hydraulic pipe, etc. In the case of running pipework, 3 dimensional presentation can be a useful aid to design.

Primarily the designer is using the plotted information and as such the relationships between that data are less important than in the subsequent examples. Also he does not need to know which equipment is located in the design vicinity because the computer can determine this from the aircraft identification and the geometric model of that aircraft.

3.2.2 Use of NMG data by manufacturing

The range of users for NMG in manufacturing span from the smallest wind tunnel model to the largest wing skin and in all cases the benefits derived are essentially the reduction in hand-finishing, the improved dimensional accuracy and the consistency of the product.

During the early stages of a project, many configurations of the aircraft will be investigated and a fair number will be tested in the tunnel. Such models can be rapidly manufactured by NMG on numerical control machine tools using semi-automatic techniques. For each aircraft configuration a number of loading cases is considered, representing various flight conditions. Typically for the simulation of a high 'g' turn, the wing is subjected to twist and bending within the NMG system to produce a wind tunnel model of the deformed wing. The aerodynamic properties of the deflected wing can then be studied. The models themselves are normally constructed from steel in many pieces, so that again the effect of differing wing sweep, etc., may be studied by fitting the various wings onto the available fuselages.

After investigating many configurations, hopefully one is chosen for the project, but the data gleaned in the extensive wind tunnel tests may be of use several years later. At British Aerospace we are currently validating a number of aerodynamic theories against wind tunnel tests performed some years ago. To perform the theoretical calculations, NMG is required to retrieve and produce data relating to obsolete surfaces, which have been discarded several years previously.

Fortunately, in the design of the NMG system we recognised the need to retain old designs for many years, and such retrievals can be easily performed. Some typical wind tunnel models are illustrated in Fig.7.

Manufacturing proper receive a large amount of information from design, which has been extracted from the NMG system, in some cases the information is supplied by the drawing office, such as coordinate information for inspection purposes, but often, as in the case of NC manufactured parts, the NMG data is used directly. Certain types of parts, such as form blocks, may be manufactured in a similar manner to wind tunnel models, but often a greater degree of control is required. Then a computer program, such as APT140 (a part of the NMG system), is required with full capability to control the cutting conditions and geometry. One of the more complicated parts we have produced in this manner is the Tornado wing pivot bearing, which was produced by directly machining the NMG surfaces, using the APT140 machining program. (Fig.8). These parts are being manufactured on 5-axes CINCINNATI milling machines from titanium forgings.

3.2.3 Transfer of information to Aerodynamics and Structural Engineering Groups

Aerodynamics require geometric information for analysis by a variety of computer programs. There is still a requirement for 2-dimensional information on wing streamwise sections, but more and more the demand is for 3 dimensional data, for use in generalised fluid flow computer programs. These 3 dimensional programs require an approximation to the outer envelope of the aircraft, but of course, on the NMG system, the information is much more detailed. The NMG representation of a wing will comprise basic wing, flaps, etc., but Aerodynamics require only the outermost shape of this assembly. There again is a use for the NMG structure facility, which assists in the obtaining of a single outer shape. In a similar manner a single shape can be derived for a fuselage at each required station. (fig.9).

However, the information generated within the NMG system is not directly usable by the aerodynamics programs. The minimum requirement is that the information be re-formatted into the format required by the particular aerodynamics analysis which is to be used. In many cases there is an additional requirement for a data reduction function to be performed; that is to say, data has to be selected from the mass of data available. One technique available within the NMG system is designed to assist in the construction of a mesh of quadrilateral patches, which approximate to the aircraft shape. This mesh of 'flat' patches is then used in 3D sub-sonic analysis. The technique is illustrated in Figs. 10 & 11.

The demand for geometric data for stress analysis purposes arises later in a project than the aerodynamic requirements. Because it is concerned with the stress and strain in a real structure, the information required from the NMG system is more detailed. Usually data is supplied in a suitable form for the Nastran analysis program, but before the analysis can be performed, a large amount of structural idealisation data must be added to the basic geometric information. This all represents a mass of detailed information, much of it generated manually, which leads to a considerable problem with erroneous data. Consequently, before doing the analysis, the data is extensively checked using graphic displays and plots. Figs. 12 & 13 show the structural idealisation of a fairing, displayed for checking purposes on a graphic display or paper plot.

4

The description of Individual Components

Several years ago an evaluation was made of the design computing requirements in the 1980's. It was seen that data transfer between the various disciplines could be made advantageously using computers, the basic data handled by all

these disciplines being geometry. Consequently a decision was taken to introduce a system to allow the capture of geometric data by a computer as early as possible in the design process, i.e. at the scheming or detail drawing stages. The system had therefore to be useable by draughtsmen, most of whom had no previous computer experience, and not be specialists trained specifically to operate the system.

In the consideration of the system capabilities, the following requirements emerged:-

- . Unified geometry to allow transfer to and from other user disciplines.
- . Easy to use.
- . Easy to learn.
- . Easy to access.
- . Secure data.
- . Ease of system modification.
- . Cost effective.

These requirements were evaluated against commercially available systems, some of which ran on mainframe computers with refresh graphics displays while others ran on mini-computers with storage displays. None satisfied our original requirements, therefore, a new system should be developed.

4.1 System concepts

Consideration of the two requirements for ease of use and ease of learning led us to the conclusion that the system should be, as far as possible, self-tutorial. Accordingly at any stage during the construction of a command the system should prompt the user with a set of options applicable only at that stage. In other words a constantly changing display was required presenting the user with messages and commands appropriate to the current working condition. A need to be able to rapidly scale and translate the displayed geometry, and to delete parts of it was also recognised. In consequence a decision was made to use refresh graphics displays rather than the storage type.

A second decision was that in order to maintain adequate response to the user, a dedicated mini-computer was essential, perhaps controlling 4 - 8 terminals. With the downward trend in mini-computer hardware this also provided a cost effective solution.

4.2 System development

4.2.1 User Interface

The first phase of system development falls into what might be called the user interface. This was developed in the first instance on a refresh tube using a light pen alpha-numeric keyboard for user interaction, and later using a data tablet and stylus in place of the light pen.

The interface developed consists of the following information displayed on the screen (as well as the geometric information being constructed):-

- . a vertical menu at the right hand side of the screen which changes according to the command being built.
- . instructions to the user on the left side (e.g. pick menu, or input radius value).
- . a command line at the top of the screen showing the user the stage he has reached in building the command.
- . error messages or results or analytical interrogations at the bottom of the screen.

Interaction, using the light pen, is achieved by either:-

- a) pointing the light pen at the menu which causes the item pointed at to be underlined. This choice is confirmed by pressing the keyboard space bar at which time the system takes the appropriate action.

b) pointing the light pen at a geometric item causing a cross to be displayed on the item at the approximate position of the pick. This is again confirmed by pressing the space bar which causes the geometry item to be returned to the computer together with the position of the pick which is used to resolve ambiguities. (E.g. When drawing a line tangential to two circles the picks or the circles determine which of the four possible mathematical solutions is the one required).

c) keying in dimensional information or text from the keyboard. This is sent to the computer using the keyboard return key.

Interaction using the data tablet and stylus is similar. Menu or geometric items are picked by positioning a cursor on the screen corresponding to the stylus position on the data-tablet, but confirmation is achieved in this arrangement by depressing the tip switch on the stylus - a one handed rather than two handed operation.

At any time during the construction of a command the geometry displayed may be scaled, translated or rotated. In the light pen implementation this is performed by the use of specified keys, and in the data tablet implementation by using areas of the tablet designated for these functions.

4.2.2 Applications

The second phase of the development was, and still is, the implementation of application routines. These started as a set of two dimensional routines allowing the creation of points, lines, circles and circular arcs, giving the draughtsman an equivalent system to paper, pencil, squares, compasses etc. in which any projections had to be performed in a similar way to manual methods. Later work has made the system into a pseudo 3-dimensional one enabling true three dimensional points, lines, curves and planes to be created, but circles and arcs only being allowable in a z-plane.

Other facilities have also been built in. For instance:-

- . to allow sets of geometric items to be copied as groups.
- . to allow flanges to be developed into the flat.
- . to allow points to be equally pitched linearly, or around a circle, arc or curve.
- . to produce linear dimensions.
- . to interrogate geometry to obtain distances between geometry items, areas or centres of area.
- . to work in imperial or metric units.

4.3.3 The Present and the Future.

The system developed to date, known as MAXIS (Multiple AXis Interactive System) has been used extensively by draughtsmen at the Brough site of BAe. mainly, so far, in a lofting environment to produce templates for production purposes, and to create input geometry for an N.C. system. User reaction to the system has been excellent with new users able to produce useful work after about a one hour introduction to the system.

The type of work produced so far has been limited by the availability of only two screens because of software limitations in the Mk.1. system, but a Mk.2. system capable of controlling four screens via an improved software driver is almost complete, at which time the system will be implemented at other BAe. sites. Further development work is aimed at increasing the number of screens so that eventually a ratio of one screen per eight to ten draughtsmen is achieved. In parallel with this, developments are planned to include such items as:-

- . full 3-D geometric modelling capability.
- . creation of drawings to the same standard, in terms of content, to manually produced drawings.
- . improvement to the data base to include relationships between geometry items, and hence to produce a "live" mechanism modelling capability.
- . a drawing control system to parallel the present manual system.

- . a capability to produce geometry for the description of the part in a way suitable for N.C. machining.
- . the incorporation of the surface design and interrogation features available within NMG into the highly interactive environment created for detail part description.

5) Conclusion

All airframe manufacturers are experiencing a widening of the scope of computer aided design especially in the recent past.

Simultaneously we, at British Aerospace, are coping with the process of integration of the parent companies of BAe and the rationalization in their working methods.

It is our intention to bring together the various facets of CAD, some of which have been described in this paper and to combine the best features of the existing systems.

The resultant system will, we believe, be a major aid to the design and production of advanced technology aircraft in the next decade.

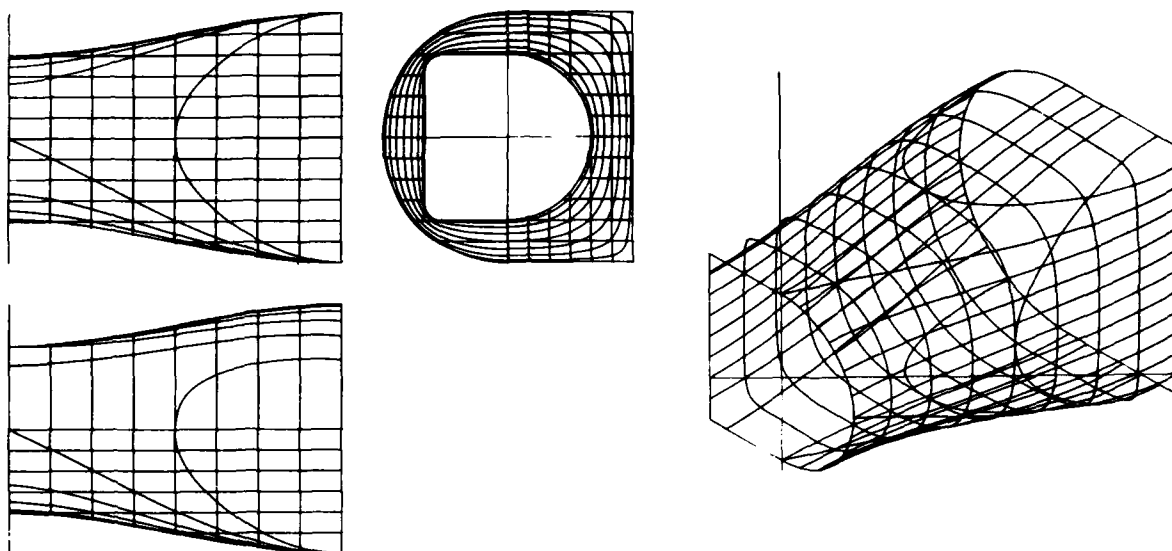
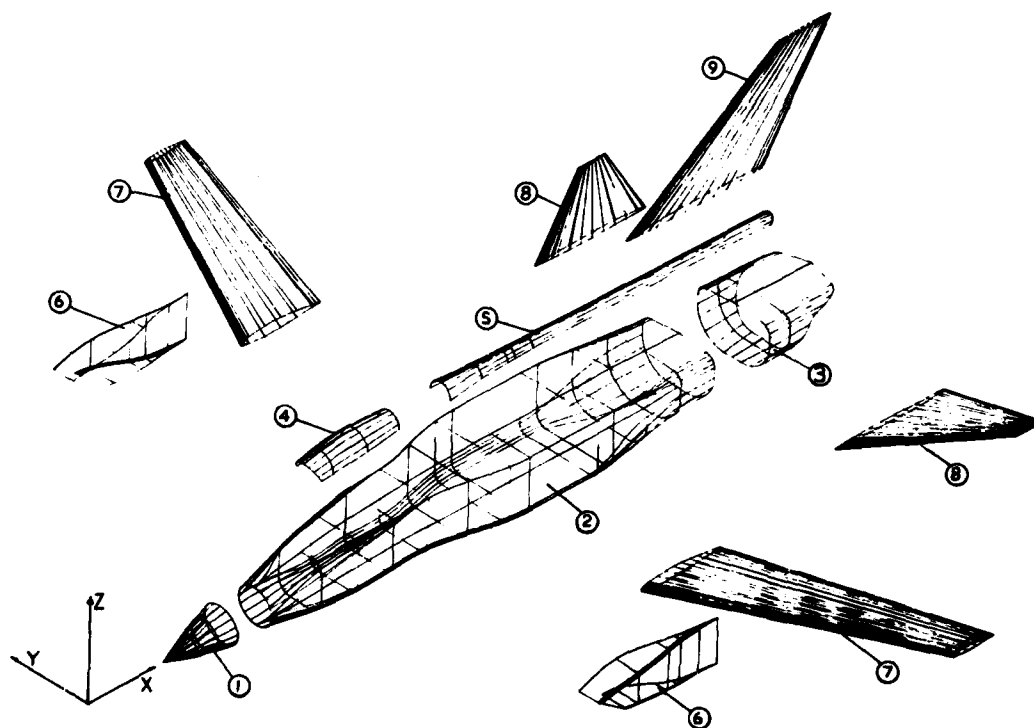


Fig 1. Shape transition of a single NMG patch.



ISOMETRIC VIEW OF TYPICAL AIRCRAFT SURFACES

Fig. 2.

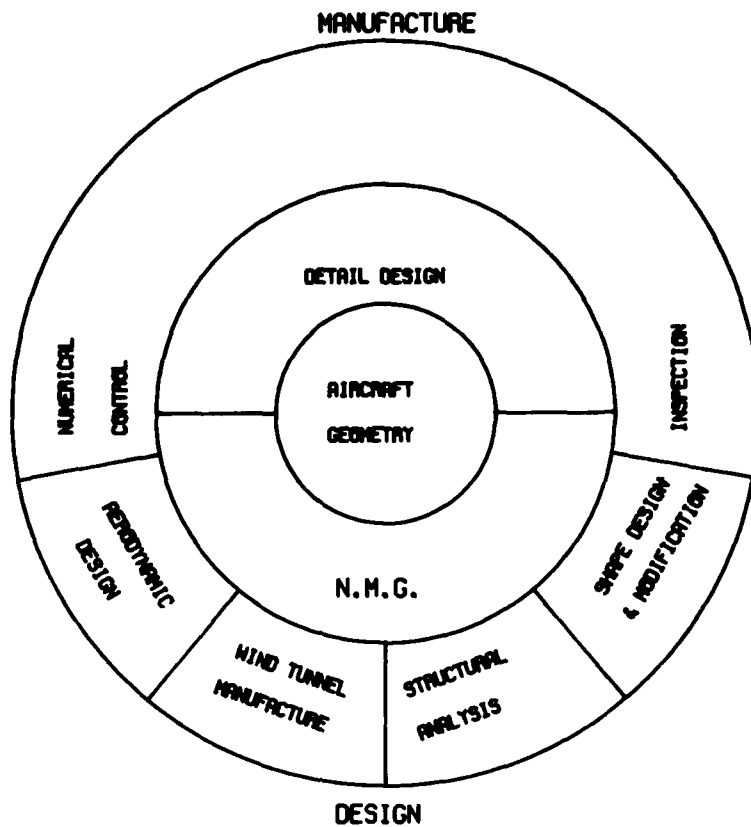


Fig 3. Users of geometry information.

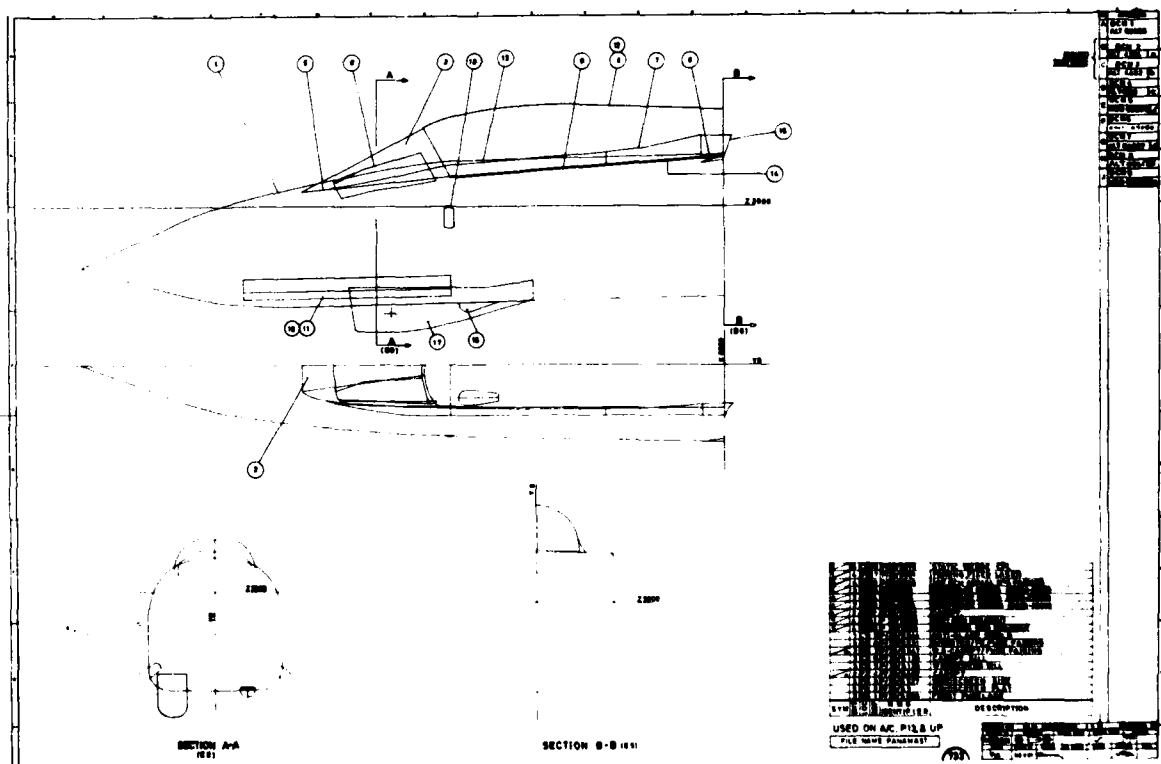


Fig 4. Key diagram of the front fuselage.

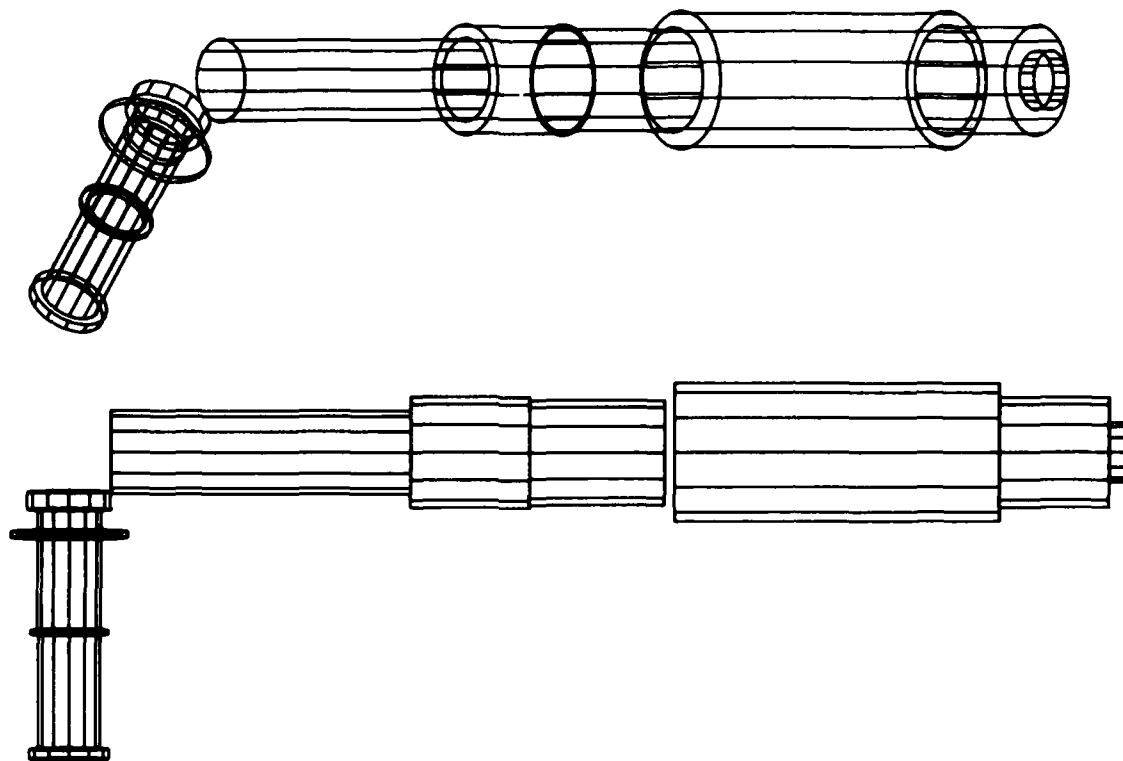


Fig 5. Modelling of an undercarriage leg.

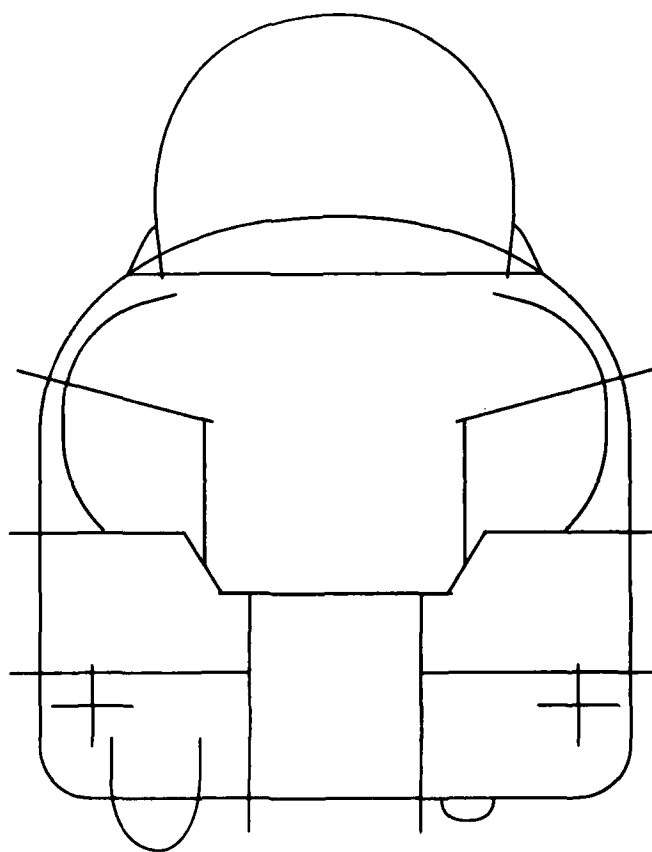


Fig 6. Aircraft section showing internal structure.



ROUGH MACHINED FUSELAGE
CUTTER FOLLOWS SURFACE GENERATOR LINES



ROUGH MACHINED WING



FINISHED WING

Fig.7 N/C produced wind tunnel model components



Fig 8. Tornado wing pivot manufacture.

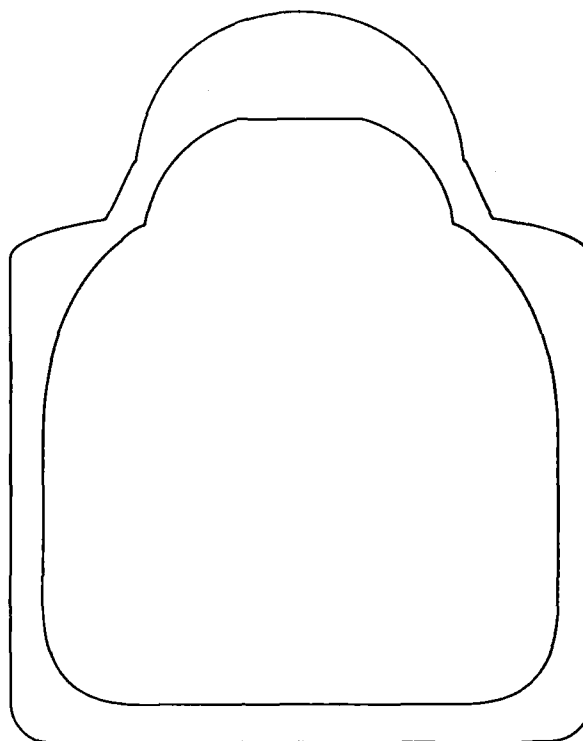


Fig 9. External shape sections of the aircraft.

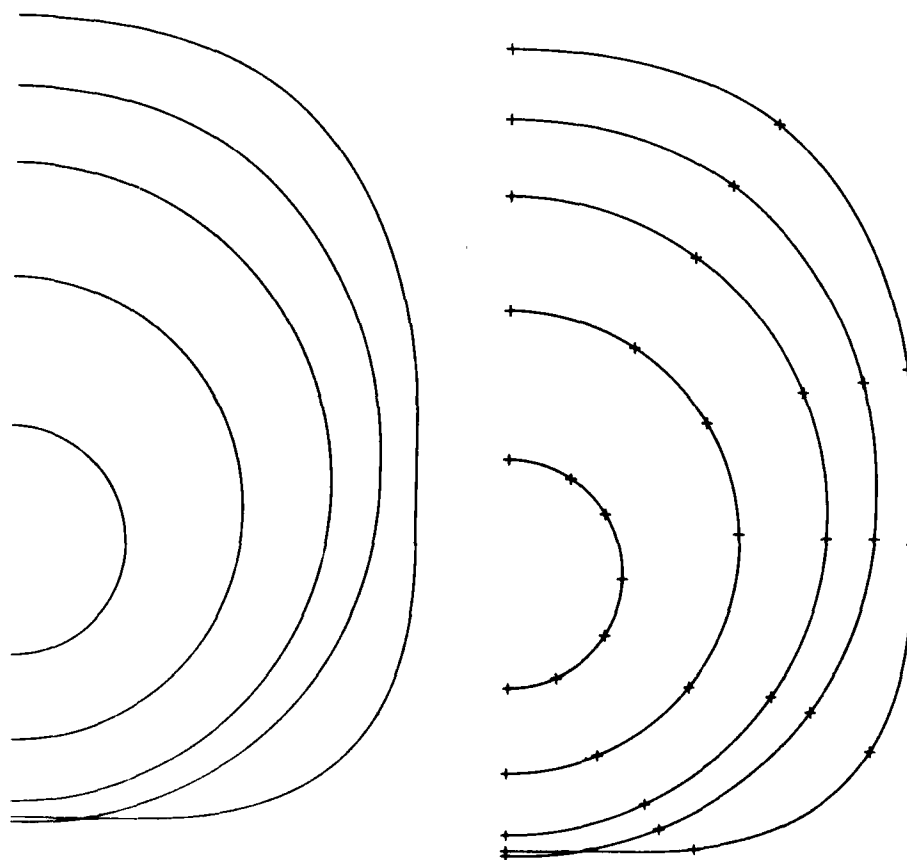


Fig 10. Aerodynamics data extraction (1) .

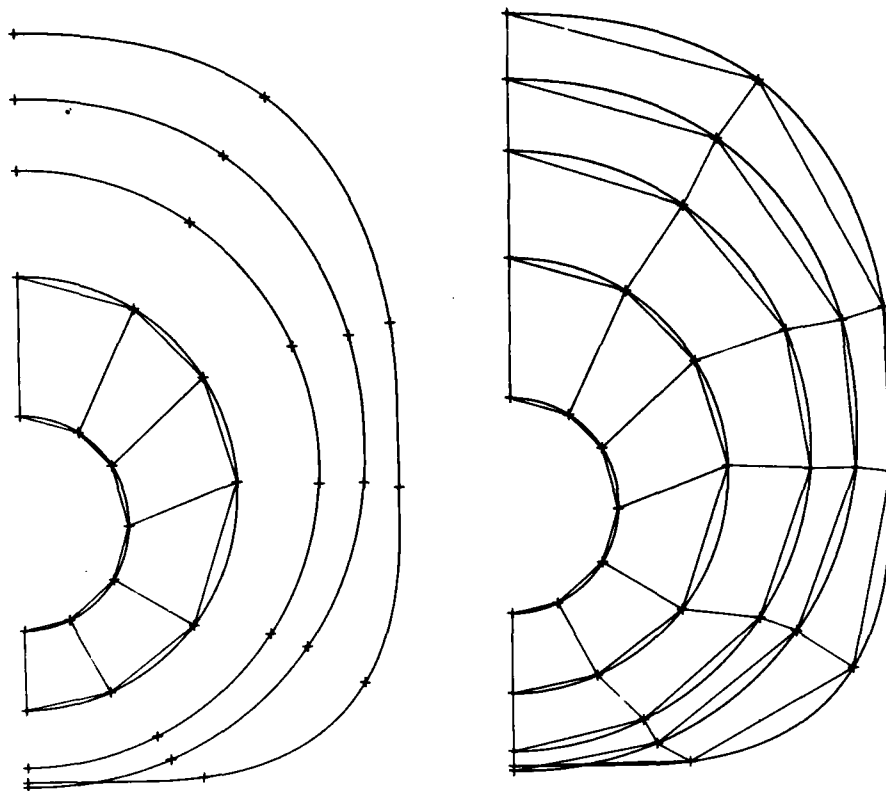


Fig 11. Aerodynamics data extraction (2).

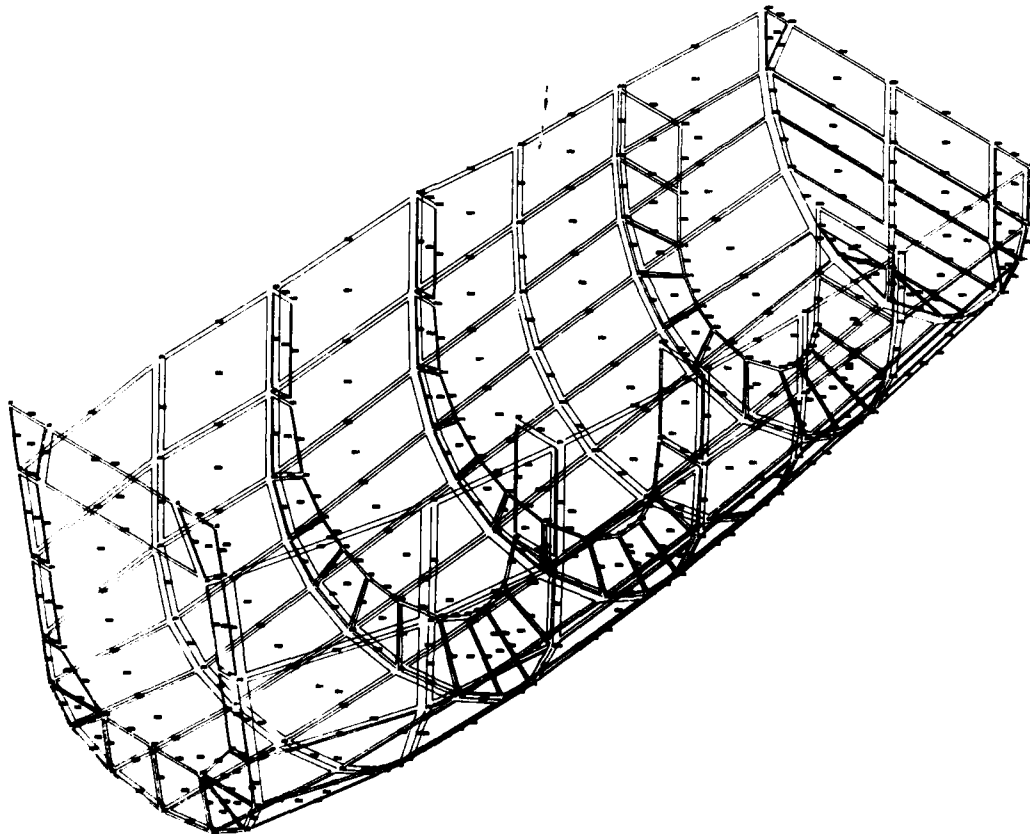


Fig 12. Structural analysis model of a fairing.

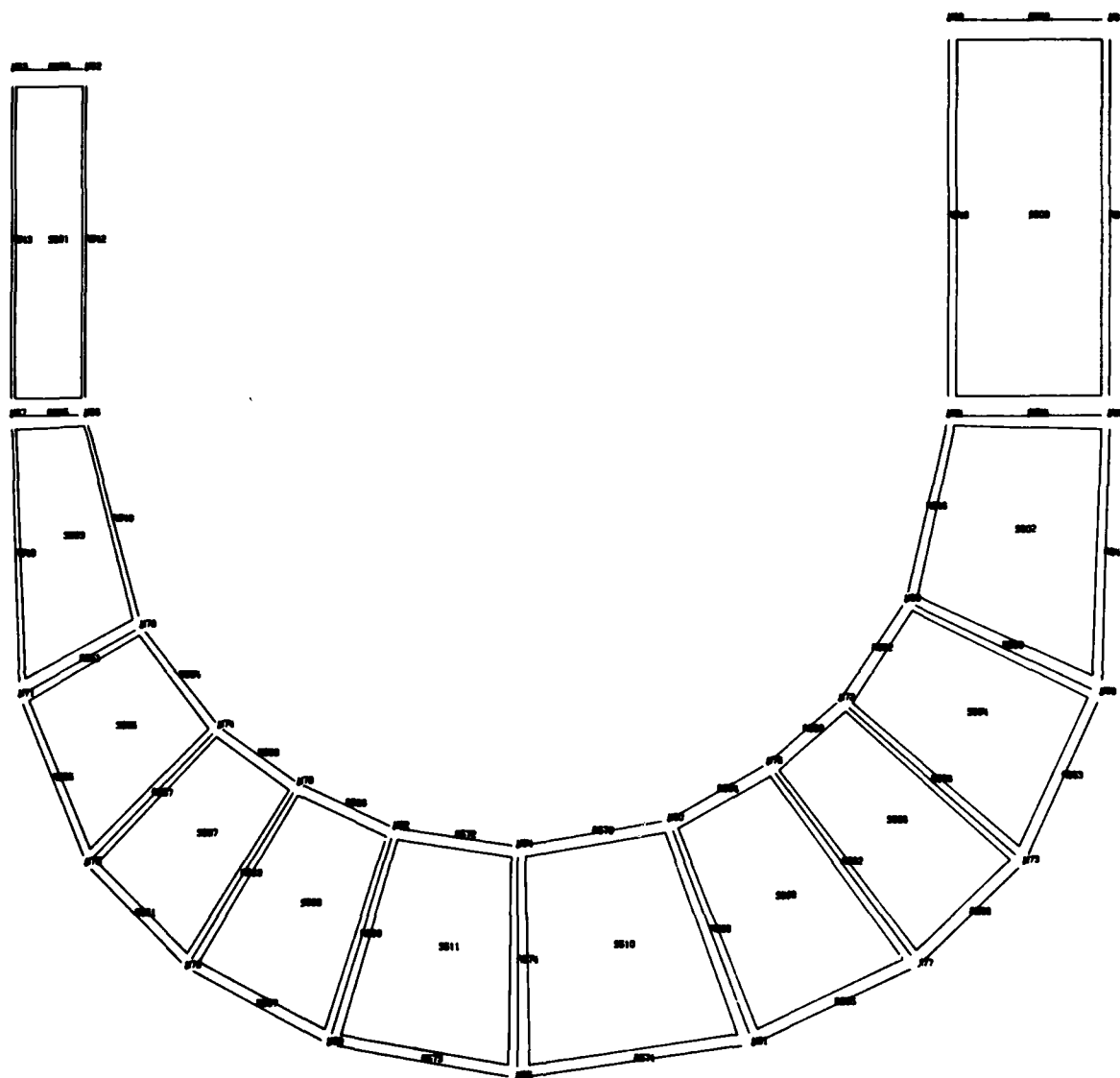


Fig 13. Section of the structural analysis model.

DISTRIBUTED GRAPHICS SYSTEM FOR COMPUTER AUGMENTED DESIGN AND MANUFACTURE

by

A.N. BAKER
Lockheed-California Company
Burbank, California, U.S.A.

INTRODUCTION

Interactive computer graphics systems are a powerful tool for use in the analysis, design, and manufacture of complex structures such as aerospace vehicles. The ability to interact directly with the computer in a timely fashion greatly enhances the effective use of a computer by an engineer. Graphical display units allow visualization of the output of the computer. Interactive graphics systems compound the effectiveness of each element of the system. Because of their effectiveness, interactive computer graphics systems are playing an increasingly important role in many aspects of engineering and manufacturing.

A number of interactive computer graphics systems for computer-aided design and computer-aided manufacture have been developed throughout the world. These systems comprise both the particular hardware configuration and the application software programs; they vary widely in terms of their size, complexity, and application. One system, called Computer-Graphics Augmented Design and Manufacture with the registered trademark CADAM, is in use at many plants in the United States as well as in other NATO nations and Japan. The hardware portions of the system include a large central host computer for data management and interactive graphics calculations and a number of local terminals with graphic display units tied to the host computer by high data rate communication lines.

A new distributed graphics system has been developed that expands the usefulness and range of applications of CADAM. The characteristics of both the central and distributed forms of CADAM are described as representative examples of the current state of the art. Future trends for interactive computer graphics are forecasted on the basis of anticipated developments in software and hardware.

CADAM DESCRIPTION

The development of the CADAM system was started in 1966. Recognizing that a major benefit of a computer-aided system is the reduction in man-hours required for a given task, the CADAM system is directed primarily at design drafting applications for optimum cost benefit. The system is a high-function, general purpose, design package containing analytical and conceptual design aids. The fundamental architecture is based upon bounded numeric geometry and employs the methodology of classical descriptive geometry.

Functionally, CADAM can be divided into an interactive, or real-time, portion and a batch portion. The interactive portion allows a console operator to construct geometry and text to be stored in a large data base. This geometry may later be input to batch routines to produce output in the form of hardcopy for virtually any hardcopy device currently available, or to produce a tape to run digitally driven devices such as numerical control machines. In addition, the batch routines perform required data management functions on the data base.

Both two- and three-dimensional shapes may be represented, using construction and development techniques familiar to the conventionally trained designer. Lines, circles, ellipses, and curves are rapidly created under the direct control of the user. A matrix transformation feature assists the designer in the development of oblique and isometric views.

Design models may be retrieved immediately from the data base. Individual views may be stacked, juxtaposed, separated, or otherwise located within the arbitrarily defined drawing perimeter. Interfacing components, subassemblies, or drawing details may be shown simultaneously to assure compatibility. Conversely, an assembly can be broken down into separate details to develop exploded views. Sizes and dimensions may be changed rapidly. Error-detecting logic reduces the incidence of human and configuration errors. Precision to at least six digits is obtainable.

CADAM is also designed to assist the N/C programmer in developing a sequence of operations directing a specific machine tool to produce a part. The N/C part programming capability utilizes the displayed geometry of the part as the reference for creating the N/C program. Using the geometry already in the data base, a direct, accurate, analytical solution to the required tool path can be obtained. Program checking is facilitated by dynamic motion (animation) in the display to represent the tool path and cutter depth. The tool centerline data, as graphically displayed, may be selectively modified. Machine control data are produced by processing through widely available APT post-processor programs.

The hardware portions of the CADAM system require a central host computer, such as an IBM 360/370 series, and a number of interactive graphics display terminals, such as the IBM 2250, with associated controllers. The display is a refresh-type, vector-generating,

cathode ray tube with light pen, alpha-numeric keyboard, and function keyboard. High data rate communication lines connect with the central processor, placing a practical limitation on geographical separation of the terminals from the processor of approximately three kilometers.

The CADAM system is strongly user-oriented. An important objective of the system was to provide the user with a faster, more accurate, and more convenient way of doing what he is accustomed to doing, rather than requiring him to adhere to a drastically new method. New functions are available as well; such as the ability to merge, overlay, or juxtapose separate drawings in real time.

The central data base can be quite large, making available to the user a wide range of information. Standard hardware permits storing of as many as a million typical engineering drawings in a single machine unit with on-line retrieval and storage. A comprehensive data management system permits efficient dissemination of data to all users of a given system.

CADAM UTILIZATION

The use of CADAM as a drafting tool is straight forward. Aircraft three-view general arrangement drawings, various layouts, and production drawings are being developed on CADAM and used as released data. This has resulted in a drawing data base which is readily available to analysis engineers using finite element techniques.

CADAM provides for the automatic extraction of data for the structures, loads, flutter, aerodynamics, and parametric analysis functions using some form of finite element-type modeling. This modeling is used for displaying data grids on the screen, or the data may be extracted for processing in analysis batch computer programs. The loads, flutter, and advanced design parametric analysis organizations have other graphics subroutines which extract non-finite element geometric-type data from CADAM produced drawings.

The CADAM system presently contains six subroutines related specifically to solving analytical problems. These programs were developed to complement the basic drafting tools already present in the package. The programs are to be used to help evaluate a drawing as to its structure or analytical acceptability. They are very basic in concept and are not meant to give detailed answers to complex analytical evaluations, but to provide a quick guide to a given design problem. The routines include section properties analysis, weights analysis, torsional stiffness analysis, crippling analysis, lug analysis, and fluid flow delivery analysis.

Productivity improvements using CADAM are a strong function of the type of design being performed. Typical tests show improvements compared to manual methods of 4:1 for mechanical installation drawings and up to 17:1 for design changes. High productivity occurs with the use of repetitive construction entities, drawings with symmetry, and those requiring analytical geometry calculations.

Since a drawing's geometric data, as well as alpha-numeric data, are stored in the computer files, it is not always essential to produce a hard copy of a drawing. For example, the data can be recalled on the terminal and used by a CADAM parts programmer for the preparation of numerically controlled machine tool tapes.

Centralized CADAM has limitations in addition to the geographical separation restrictions noted earlier. All of the many designers using the system at the same time have access to the central computer and are dependent on it. If the computer goes out of operation, none of the designers are able to continue their work until the computer is functioning again. Also, all of the designers have the same set of tools. Special requirements are placed on the computer in order to mix the more demanding analytical tasks that are required by a fraction of the designers into the centralized CADAM system. For these reasons, and others, a complementary approach to the problem has been taken.

DISTRIBUTED GRAPHICS

A new distributed graphics system has been developed and is in experimental use within Lockheed. The key new hardware feature of the system is a remote graphics terminal comprising a minicomputer, local storage, graphics display unit, and other accessories.

The CADAM software has been reconfigured so that the interactive graphics calculations are done in the remote terminal while the data handling and batch processing are done in the large central host computer. New software has been designed to control the input/output functions and interfaces with the central operating system.

An analysis of all the functions to be performed and the associated data rates led to the new distribution of functions. The interactive graphics calculations and associated analytical calculations require high data rates and are done locally. Recall of drawing data and transmission of output data for batch processing can be done at lower data rates and are done through telecommunication channels to the central host computer. Local storage of data offers additional flexibility in the partitioning of functions.

The local disk storage has sufficient capacity to retain all the data necessary for a full day's work. The transfer of batch data or of entire drawing files between the central host computer and the distributed graphics terminal can be accomplished at a slower data rate, using existing telephone lines. Thus, the distance limitation between graphics

terminal and host computer no longer exists. The semi-permanent process of installing a graphics terminal at some location is changed to where the terminal becomes, truly, a remote terminal and a movable terminal. The distributed graphics terminal is effectively a stand-alone minicomputer based system. Its operational status is not affected by the status of the host computer nor does it affect the host computer. The only limitation to portability is the environmental conditions which must be provided for the terminal, i.e., adequate power and air conditioning. The host computer retains those functions for which it is best suited economically to retain; namely, mass storage, batch processing, and plotting.

The basic distributed graphics terminal as presently configured includes a Vector General scope and its supporting electronics, the Interdata 7/32 minicomputer with 512K bytes of core memory, a CDC disk with 80M bytes capacity (removable pack), the Dataphone MODEM, and the work station cabinetry. Additional storage is available through a magnetic tape or additional disk unit, or both, as required by the application.

The work station has been designed to maximize operator performance. The experience gained in operation of the standard CADAM system plus the results of various man-machine interface experiments were used in determining the configuration of the equipment and the layout of the operating controls.

Use of a higher capability minicomputer, such as the Interdata 8/32, and additional local storage allows operation of the remote unit for analytical graphics use as well as CADAM applications. This system is more efficient in its use of the host computer than current analytical systems. Operational convenience and computational efficiency are substantially improved. The analytical graphics units are used for a large number of demanding calculations that use the geometrical information from the CADAM data base. Typical examples include continuous system modeling programs, structural analysis, wave drag, and wing optimization calculations.

DISTRIBUTED GRAPHICS UTILIZATION

The new distributed graphics system has a number of advantages over a centralized CADAM system. Response times are similar to the central system and essentially independent of the number of remote terminals. Geographical dispersion, security protection, and ease of adding or subtracting remote units provide substantial operational convenience. If the central computer goes out of operation, the remote units can continue functioning for an extended period. The new system performs all of the CADAM applications in preliminary and production design and numerical control machining. Analytical graphics capability can be selectively included where required without overburdening the central computer. However, for those applications involving numerous work stations in the same general location doing design jobs, the centralized CADAM system is usually more cost effective than the new distributed graphics system.

Twelve distributed graphics units have been produced and are in use in five different plants at Lockheed with geographical separations from the central computer of up to fifty miles. In addition to use in preliminary and production design, remote operation allows new users to access the CADAM system. Tool design and wind tunnel model design are being performed on the distributed units. Factory liaison can call up engineering drawings and rapidly make corrections and changes to the drawings.

The operational experience gained on these first twelve units will direct any modifications and improvements to be made to either the software or hardware portions of the system. After incorporation of the improvements in the design, additional units will be produced for use in a number of plants at Lockheed.

INTERACTIVE COMPUTER GRAPHICS EXPERIENCE

Utilization of interactive computer graphics is rapidly expanding and is being used in a wide variety of engineering and manufacturing applications. From the experience of developing and using the CADAM system, a number of conclusions can be drawn.

An interactive computer graphics system must be designed considering the viewpoint of the user. The user must see the system as his tool rather than as a large computer system to which he has access. For example, the response time of the system for routine commands should be at least as fast as the response time of a skilled operator. This requires fast and efficient algorithms for the commands and calculations. The system must have operational logic and error correction modes that allow effective utilization by less experienced operators. At the same time it must have the capability to allow highly experienced operators to work at their full capacity.

The system must have high reliability in order to gain broad acceptance. A designer must have sufficient confidence in the computer graphics system to make design release date commitments. Otherwise, he will continue to use the slower, but predictable, manual methods.

Sufficient attention must be paid to the management of this special resource. This is particularly important during the introduction phases of the system. Details of operation in a mixed mode where some of the work is done on the graphics system and the rest by traditional methods should be carefully considered to insure compatibility. Conversion of existing manual drawings into computerized form may be done in those design areas where significant change may occur later.

Use of a major interactive graphics system has longer range implications in the total operation of the organization. A central computerized data base is created. This data base can be used for many functions besides the original design function that created the data base. Appropriate design, utilization, and management of the central data base are demanding tasks that should be taken on by the organization. An integrated approach to data base management is required.

FUTURE TRENDS

The costs of computing power are rapidly decreasing and should continue to decrease for at least another decade. This allows greater use of powerful local computers such as in the distributed graphics system described above. Similarly, the costs of memory have decreased, thereby allowing very large central data banks as well as local data banks to be economically justified as compared with those that would have been considered economically prohibitive only a few years ago.

A major cost in the interactive graphics system is attributed to the vector-generating refresh cathode ray tubes. To avoid this cost, storage tubes have been used in some analytical graphics systems because of their lower initial cost. Development of an interactive raster scan graphics tube with sufficient accuracy and resolution for design use will offer major cost reductions in the hardware, but at a penalty of some increased complexity in software.

The applications of interactive computer graphics seem to be without limit. Future software systems must be designed to allow ready addition of applications programs to the existing core programs that operate the graphics system and manage the data base. The applications programs can then be written in a high order language that is machine independent. The core programs may still be partially machine dependent in order to gain maximum speed and efficiency of operation. Alternatively, the speed and capacity of the computer may increase sufficiently to allow use of machine independent language in the core programs.

At present, the major portion of the CADAM system uses a quasi-three-dimensional construction because of the rapid calculational speeds associated with this approach, and because it is most similar to the design methodology favored by the designer-draftsman. A true three-dimensional subset of the CADAM system is provided for those design tasks which require this capability. Some other graphics design systems are based entirely on a true three-dimensional architecture. Unfortunately, the calculation algorithms in such systems are necessarily complex and the resultant demands on the central computer resources limit the number of remote users and makes for long response times. Development of new approaches to three-dimensional descriptions may lead to more efficient computation schemes that allow broader uses of a three-dimensional approach.

A significant future trend is the distribution of processing power into user working locations. The current trends in improved telecommunications and computer networking are an essential corollary of this. Development of network systems of data management will greatly enhance distributed computer graphics as a useful tool. It will also lead to large integrated programs for analysis and design.

Interactive computer graphics will become a major tool in engineering analysis and design. It combines the computer's computational power and memory, an understandable and timely display of information, and an ability to directly interact with the system in a man-machine tool that fully exploits the capabilities of all elements of the system. Distributed graphics systems, such as described above, have additional advantages of which the most significant is the ability to locate this powerful tool directly in the user's working location.

LE ROLE DE L'INTERACTIVITE DANS LA CONCEPTION
ET LA FABRICATION ASSISTEES PAR ORDINATEUR

PAR

Monique SLISSA

Ingénieur Civil de l'Aéronautique
S.N.I. AEROSPATIALE - MARIGNANE
Division Hélicoptères
(France)

RESUME :

La Conception et la Fabrication Assistées par Ordinateur nécessitent la mise en oeuvre de techniques conversationnelles alphanumériques et graphiques pour supporter le dialogue "Homme-Machine" dans le processus de création d'un produit.

La définition du poste de travail, au sens le plus général, est très importante, par exemple dans le cas de la conception des formes tridimensionnelles, où l'interactivité permet le choix en temps réel.

Ces principes ont été retenus dans les études et les développements faits à l'Aérospatiale Marignane et spécialement dans le Système Systrid .1 de Conception d'objets tridimensionnels et dans le programme Sigma de l'Aérospatiale Toulouse, utilisé pour la création de formes géométriques.

1 - INTRODUCTION :

La Conception et la Fabrication Assistées par Ordinateur peuvent être définies au sens le plus général des termes comme l'utilisation d'un ordinateur pour créer un produit en :

- abaissant les cycles de définition
- diminuant les coûts de réalisation
- facilitant les modifications en réduisant le délai entre la naissance d'une idée et sa réalisation, un délai trop important provoquant souvent l'abandon du projet.
- permettant de réaliser une certaine optimisation en balayant des solutions différentes sans s'arrêter à la première solution valide trouvée.

Pour résumer, il s'agit d'obtenir un produit meilleur, à coût moindre dans un délai plus bref.

2 - LES TECHNIQUES MISES EN OEUVRE :

Ces techniques touchent plusieurs domaines :

- la création des données qui décrivent le produit à concevoir
- la manipulation de ces données pour obtenir une forme achevée de conception
- la génération des informations nécessaires à la fabrication de ce produit, à partir des données de description de la conception, stockées dans l'ordinateur.
- les techniques interactives, graphiques et alphanumériques, pour supporter le dialogue "homme-machine" dans le processus de conception et de réalisation d'un produit

Ce dernier point est tout à fait essentiel.

La nouveauté introduite par la Conception et la Fabrication Assistées par Ordinateur est que l'ordinateur ne travaille plus "en aveugle". Pour effectuer le travail, l'homme est constamment en dialogue avec lui, pour choisir la solution qui lui semble la mieux adaptée, jugée bien souvent selon des critères difficilement chiffrables, voire non transmissibles (l'expérience) et donc impossibles à enseigner à la machine, dans l'état actuel de ses possibilités.

Dans ce travail en symbiose, l'ordinateur apporte sa capacité à effectuer très rapidement des opérations fastidieuses, mais bien définies, sans risque d'erreurs, ni manifestations de fatigue.

Divers types de poste de travail peuvent être envisagés : écrans conversationnels avec photostyle, écrans à rafraîchissement assortis ou non de tablettes, tables à digitaliser dites interactives etc... Il est sans intérêt de faire une évaluation comparative de ces différents matériels, actuellement disponibles sur le marché : il n'existe pas aujourd'hui de poste de travail parfait du point de vue ergonomique, adapté à tout type d'application, et dans tout type d'entreprise. Certains conviennent mieux à une application qu'à une autre et même selon les phases d'une même application (conception ou exploitation par exemple) des postes de travail différents peuvent être envisagés, avec, actuellement, un certain avantage financier.

Il reste néanmoins fondamental que, pour les travaux de conception, toutes les solutions possibles (matérielles et logicielles) doivent être recherchées pour accélérer le "temps de réponse" et alléger la tâche du créateur.

3 - LES DOMAINES D'APPLICATION :

Des domaines très divers d'application peuvent être envisagés dans une entreprise : le calcul scientifique, les câblages électriques, les circuits hydrauliques, la gestion d'une liasse de dessins, la conception et la fabrication des formes simples et complexes etc....

En fait, ces domaines et bien d'autres sont liés dans la chaîne que constitue la vie d'un objet industriel ; elle peut être divisée en trois phases :

- la conception ou création du produit
- la fabrication ou production industrielle
- la maintenance avec des activités d'après-vente, de stockage, de réparation et de révision

Le moyen privilégié de communication dans ce processus était traditionnellement le plan.

L'introduction de l'informatique peut être faite à diverses fins :

- l'élaboration des plans eux - mêmes
- la présentation graphique de résultats de calculs
- l'automatisation des travaux répétitifs
- l'aide à la conception et à la fabrication des objets

Sur ce dernier point, l'expérience de la Société Nationale Industrielle Aérospatiale peut être décrite à titre d'illustration. Au sein de la Division Hélicoptères, des études et des développements poursuivis depuis 1972, ont conduit à l'élaboration et à la mise en oeuvre de Systrid .1 (Système tridimensionnel 1ère version), Système de Conception et de Fabrication d'objets tridimensionnels. La Division Avions a mis en place à partir de 1975 un logiciel, ayant les mêmes concepts de base, mais sur du matériel différent, Sigma (Système Interactif de Géométrie Assistée).

4 - SYSTRID .1, LE SYSTEME DE CONCEPTION ET DE FABRICATION D'OBJETS TRIDIMENSIONNELS, DE LA DIVISION HELICOPTERES DE L'AEROSPATIALE :

C'est donc le domaine des formes tridimensionnelles, simples et complexes qui a été choisi, en premier lieu, à Marignane, au sein de la Division Hélicoptères, pour mettre en valeur les techniques de Conception et de Fabrication Assistées par ordinateur. C'est un domaine éminemment créatif, fondamental dans l'élaboration du produit Hélicoptère. C'est aussi un domaine où l'interactivité permet le choix en temps réel (contrairement au Calcul des structures par exemple). Systrid .1 est donc un ensemble de programmes permettant :

- de créer et de modifier de manière conversationnelle
- d'exploiter (par des tracés-grandeur, des dessins à l'échelle désirée, la détermination d'outillages la génération de bandes pour l'usinage sur machines - outils à commande numérique)
- de calculer (caractéristiques géométriques et mécaniques) n'importe quelle forme tridimensionnelle simple ou complexe.

Ce système a été mis en exploitation en 1974, dans les services d'Etudes et de Fabrication de l'entreprise. Actuellement plus de soixante personnes ont été formées à l'utilisation de Systrid .1. Ce sont selon les problèmes traités, des ingénieurs de haut niveau, des projecteurs, des dessinateurs, des traceurs et des programmeurs de machines outils à commande numérique.

Les plans de formes de tous les nouveaux hélicoptères sont conçus et tracés en utilisant le système de conception de formes Systrid .1. Par ailleurs, les moules des pales et des entrées d'air réalisées en matériaux composites, sont créés et usinés à l'aide du système.

Ces comparaisons sont faites avec les méthodes traditionnelles. Elles s'avèrent très favorables aux nouvelles techniques. Des bilans établis pour la conception et le traçage de plans de formes pour des utilisateurs du système dans l'entreprise permettant d'afficher les gains suivants :

- les gains en coût sont toujours supérieurs à 25 % et atteignent, dans divers cas, 50 à 70 %, compte tenu, bien sûr des frais informatiques.
- les gains en délais sont supérieurs à 50 % et atteignent dans certains cas 90 %

Ces gains variables selon le type d'applications, sont particulièrement importants dans le cas de problèmes algorithmiques

Voici à titre d'exemple, les résultats constatés sur l'étude du fuselage, de l'ensemble des capots, du carénage de train et leur exploitation pour la définition d'outillages de fabrication d'une récente version du Dauphin bi-moteur.

Temps estimé pour l'exécution par les méthodes conventionnelles :

12 150 heures

Temps passé en utilisant Systrid .1 :

4273 heures

Gain : 64,8 %

Coût estimé pour l'exécution par les méthodes conventionnelles :

1.093.500 f

Coût constaté en utilisant Sysrid .1 (frais de personnel et frais informatiques cumulés) =

728.840 f

gain : 33,3 %

De plus, un tel outil apporte une rapidité de modification et une souplesse d'emploi qui permettent de balayer de nombreuses solutions en un temps très court, voire d'étudier des cas marginaux qui auraient été laissés dans l'ombre en son absence. Par là même, il y a gain de qualité du produit.

Afin de donner une idée plus précise de Sysrid .1, deux points peuvent être évoqués :

- les concepts de base :

les entités connues par le Système ont une représentation unique, paramétrique polynomiale, ce qui assure la notion d'objet tridimensionnel. Cela lui confère une maintenance aisée et une grande souplesse de développement.

- les fonctions disponibles

Elles peuvent être ainsi classées

- les fonctions de création d'entités (courbes et surfaces), de reproduction (lissage avec ou sans contraintes); de raccordements d'entités entre elles, d'extraction de formes à partir de formes déjà créées, de génération algorithmique de formes (formes parallèles, formes développables...)
- Les transformations géométriques : translation, rotation, symétries, homothétie, transformation quelconque, produit de transformations.
- Le traitement ensembliste des entités : transformation d'un ensemble d'objets....
- Des calculs sur les objets créés : aire, centre de gravité, inerties, longueur d'une courbe, rayon et centre de courbure en un point d'une courbe, angle de deux courbes, divisions égales sur une courbe...
- Des fonctions de contrôle et d'exploitation des formes créées, interaction courbe-courbe, courbe-surface, surface-surface.
- Des utilitaires comme l'affichage de valeurs numériques
- La sortie des tracés
- La préparation des bandes d'usinage

Il convient de citer à part, les fonctions qui permettent de réaliser l'interactivité graphique du système :

- Les fonctions donnant la possibilité de modifier rapidement les objets créés (déformation en continu par poursuite au photostyle).
- Les fonctions de gestion de l'image sur l'écran : sauvegarde automatique, régénération, remise à blanc, effacement d'une entité de l'écran avec possibilité de la régénérer ultérieurement, destruction définitive d'une entité, possibilité de désignation de n'importe quelle entité sur l'écran.
- Des utilitaires liés à la visualisation graphique : définition d'axes, modifications d'échelles, recadrage, perspectives, projections, tracés d'entités.

5 - CONCLUSION :

Sysrid .1, actuellement diffusé par le Centre de Recherches de l'Institut Battelle à Genève, constitue le noyau géométrique de base d'un système général de Conception et de Fabrication Assistées sur Ordinateur vers lequel tendent les études et développements de l'Aérospatiale Marignane.

Trois points fondamentaux sont à retenir pour un tel système :

- La possession d'une banque de Connaissances
- La mise en oeuvre d'un dialogue "homme-machine" agréable
- La possibilité d'introduire de nouvelles fonctionnalités.

A FRAMEWORK FOR DISTRIBUTED DESIGN COMPUTING

A W Bishop
British Aerospace - Aircraft Group Headquarters,
Richmond Road, Kingston Upon Thames, Surrey, KT2 5QS, England.

Large, geographically dispersed design teams are now the norm in manufacturing industries. Computer systems are potentially useful for data storage, communications, interactive design, administrative functions and numerical calculations. The work described provides a framework for the support of such applications systems in a dispersed environment, against a background of rapidly changing hardware.

1. INTRODUCTION

The manufacturing industry today requires ever more design effort to define each new article for production, in order to remain competitive and to satisfy myriad regulations and constraints.

Historically designers have used a large amount of computing power, but mostly for individual calculations - rarely as a means of communication, data management or 3D design. However, in the large (and often geographically dispersed) design teams which are now necessary in a number of industries these are the major problems. Designers spend most of their time finding, transforming and disseminating data, and all too little actually designing the product.

The work described here is designed to provide all the basic facilities needed to implement applications systems which have to meet these design needs. It is being applied to a number of new British Aerospace computer systems.

2. THE FRAMEWORK CONCEPT

Design computing systems (indeed all computing systems) have the basic structure shown below:

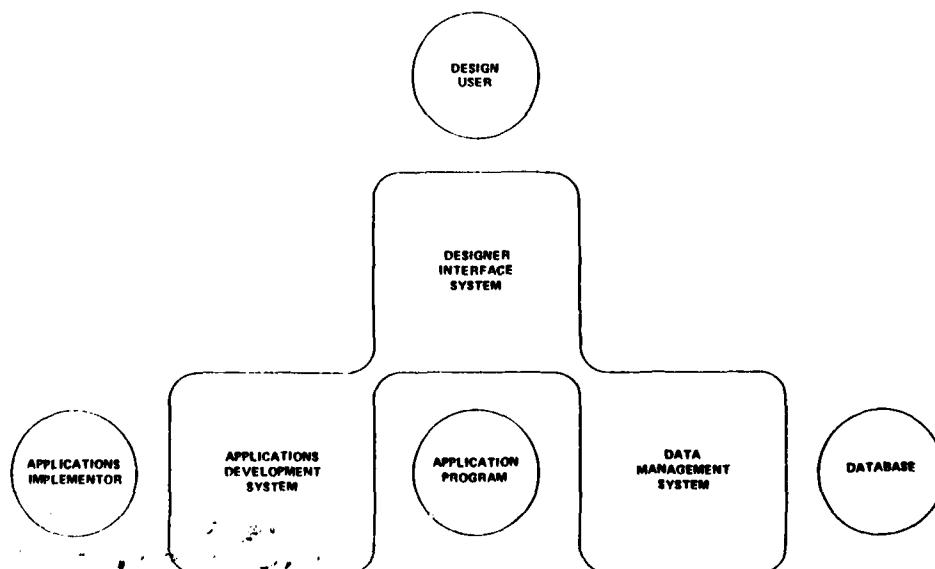


Figure 1 The Framework Concept

The user communicates with the computer using a command language, which is processed by interface software to execute the necessary internal tasks and to generate responses to the user.

The internal tasks are mainly applications programs, which need to communicate with stored data via a data management system.

The applications programs are created by people who need a variety of facilities for designing, coding, testing, documenting and modifying programs.

No external supplier provides the necessary facilities on BAe's range of computers, and thus an internal group has been established to fulfil the requirement. Where possible, software is being purchased to reduce timescales and costs, but where necessary new software is being implemented. The complete set of software will bridge the gap between the manufacturers' computer systems and the needs of BAe's applications teams.

In addition, by providing this framework independently of the manufacturers, we can make our applications programs essentially hardware independent. Portability of applications code is now essential in today's fast changing hardware environment.

This is now a widespread concept, having been recognised by the designers of PDMS (1), OXSYS (2) and others - but these are all restricted in scope of application. The only known system which aims at the same broad area of applicability is the NASA/Boeing IPAD project (3).

It is expected that such a framework will:

- cut the development time and cost of a new application by 20%, by avoiding the creation of basic software for each application.
- cut the time and cost of conversion to new hardware or operating systems by 80% by providing standard interfaces between the application code and other software.
- increase the benefits accrued by each application, due to the wider range of facilities which can be provided in a common framework.

This philosophy involves the creation of general purpose software for all applications, rather than special purpose software for each. In our case this brings a high pay-off, because of the large number of applications involved (about 30). It also offers efficiency advantages on modern computers on which general purpose code can be shared between many applications. Even if this were not the case, the rapidly falling cost of hardware compared to software encourages this approach.

The cost of such a framework is substantial. The NASA IPAD project is estimated at 120 man years - our own at 30 man years. But even when used only in-house, where we have 350 applications analyst/programmers, the return on investment is very high. The smaller organisation will not, of course, so easily be able to justify such developments. However, the potential market is large, and the products of larger organisations will no doubt be marketed to smaller ones.

3. THE DESIGNER INTERFACE

The key to the user's acceptance of the computer lies in his interface with it. And if we are to build an information system upon which the organisation depends, then we must be able to satisfy the full spectrum of requirements. This ranges from the 'T.P. enquiry' - a simple and well defined instruction with a standard screenful of output - to the most complex three dimensional graphical design task. In between lies the bulk of technical usage with relatively complex commands intermingled with ad hoc arithmetic and data references.

The designer interface system (figure 2) must handle teletype, character VDU, storage tube and refreshed graphics displays. Input of commands and data may be by keyboard, function buttons, cursor, tablet, lightpen, etc.

These inputs are accepted by a device input handler (one for each terminal type) which will transform them into a standard internal format.

The input controller may then queue the user, switching user data stacks as necessary. The command interpreter will then unscramble the input into 'command atoms' and check their validity. With the aid of data describing possible commands and their effect, it will generate a list of actions to be satisfied within the computer, and may generate a menu for display at the terminal. The list of actions is scheduled by the actioner, and may involve the execution of applications programs, utility programs and the generation of terminal or hard copy output via the output controller and a device output handler.

Whilst the basic commands will relate directly to applications code to be executed, the user will also want to be able to group commonly occurring sets of commands together as macros. During these processes, lightpen hits must be turned into useful addresses. Expressions and command pseudonyms will be resolved where these are allowed.

The user interface is also responsible for controlling all error feedback. In most cases the feedback depends on the style of use - in particular whether the error occurs during online or batch execution.

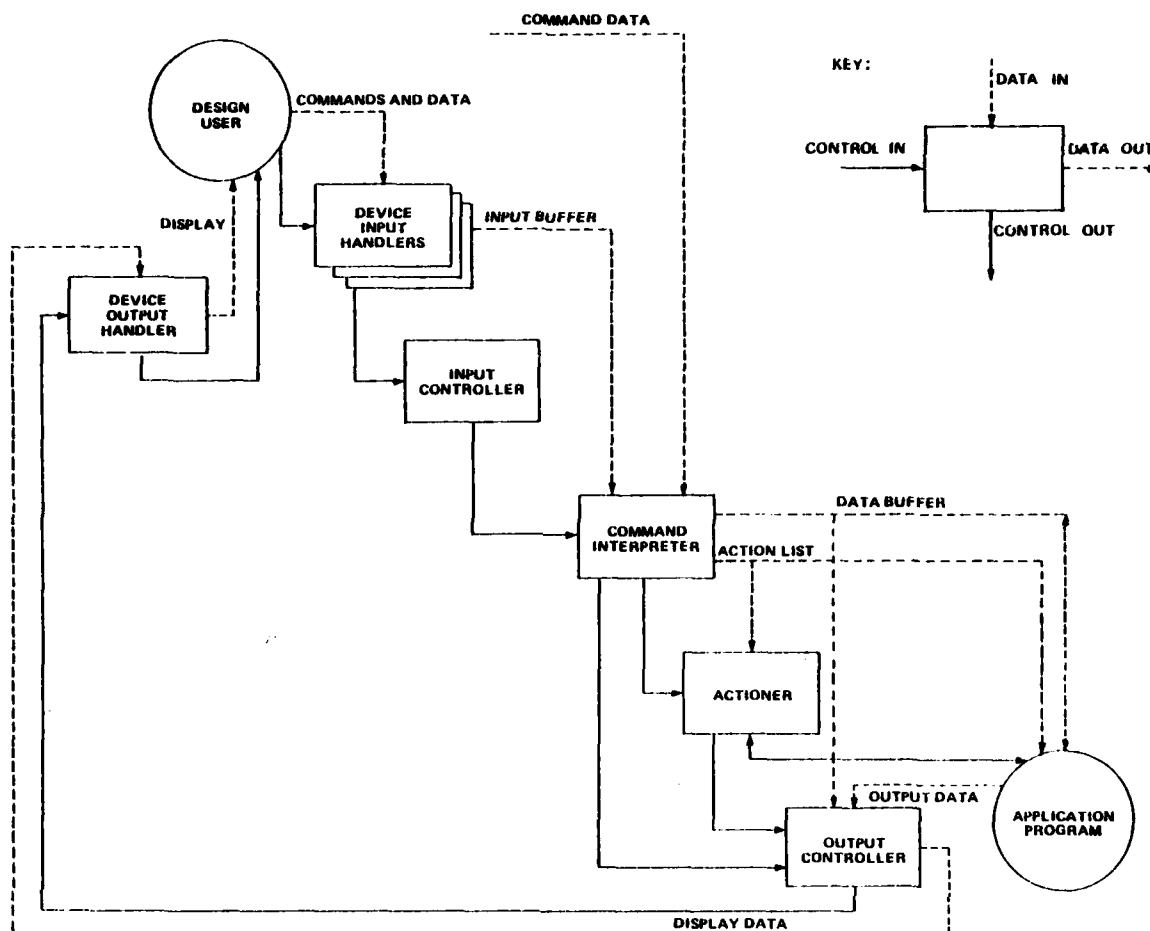


Figure 2 The Designer Interface

The commands, together with related data input and subsequent actions, are modelled as a state transition network. This technique provides a powerful, explicit and flexible means of defining a language, and enables a problem orientated language to be defined for each application. It is simple to modify (essential during application development) and the user can extend it using macros.

All command/action data is held on the data management system - such facilities are required because of the complex data structure and the volume of data (the volume for a complex application is of the order of 50 Kilobytes).

It is most important that a designer, who may use several computers in the course of a design task, can use this common language throughout. He should not be faced with the various JCLs and editors normally required to support applications.

This specification is not, of course, easy to meet. Current implementations have usually been biased heavily towards a particular part of the spectrum - usually the simpler part as that has been the major market area. But if computers are to be useful in the heart of manufacturing industry, we must aim to catch geometric data at source - ie. partially replace the drafting board by a terminal device. This becomes a major part of the market, and is the area which, above all, must be served. Hence our solution is biased in this direction while still satisfying wider requirements.

4. DATA MANAGEMENT

The efficient provision of interactive design facilities leads us to the distribution of micro/mini/midi computers throughout the design team. Working data must be similarly distributed, and so to maintain the integrity of data we have evolved the following approach:

- For each project, shared data will be stored centrally. This must be supported at very high standard of privacy and integrity. The volume of data supported will be of the order of 10,000 Megabytes.

- Each local computer has access to this central data via a communication network, and (given appropriate access controls) can write information to it or read from it. Typically, a designer will extract data created by other specialists prior to performing his own activity. When his piece of design work is complete, the resulting data will go through several approval processes before being made available for access by other designers as appropriate. Local database will be of the order of 1 to 10 Megabytes.
- All the privacy data (who can access what) and who has read what is stored centrally. This latter data is used to notify designers of changes to their input data. Also stored is data pertaining to the history of the design process - ie. which input data, in association with which application program was used to generate which output data. This is vital for recovery from design problems, accidents, etc.

The support of this approach involves three elements:

- Throughout the network of computers, data must be stored in the same logical format, ie. a common database design.
- On each computer this data must be supported in the same style, and with the same interface to applications programs.
- There must be a means of unloading, transporting and reloading data between databases.

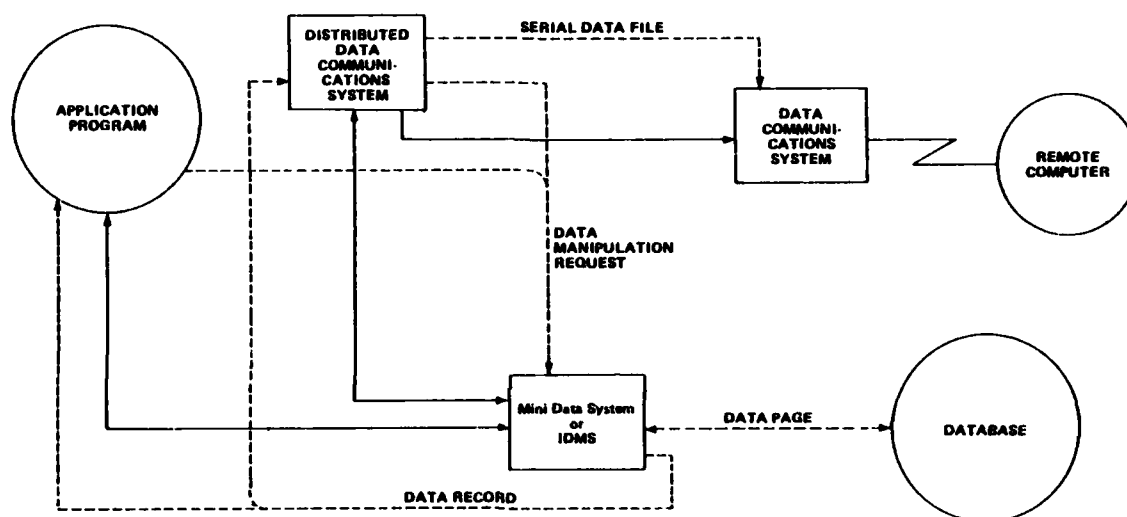


Figure 3 Data Management System

The international Codasyl standard for data management systems has been adopted. A data dictionary system is used to store both a high level (logical) database description and a lower level (physical) description. IDMS (4) is being used to support the central data and a 'Mini Data System' has been implemented to a subset of the Codasyl specification to support data in a highly interactive environment. A 'Distributed Data Communications System' (DIDAC) is being implemented to move data between Codasyl databases using the existing communications network with standard RJE protocols.

The Mini Data System provides a high performance data access system on the small local databases which support command language definitions and display files as well as design data. Pathlengths are reduced by excluding costly integrity procedures (which are not vital except on the central databases) and disc accesses are reduced by allowing an application to lock in core the most sensitive pages. Together with standard Codasyl techniques such as the clustering of related records, this provides a very high level of performance.

DIDAC consists of two major elements. The first unloads data under the direction of a selection language, turning it into a standard character representation of the data which is independent of any particular database. External references are held by name in a dictionary. This data can be 'posted' to any other computer where a load program adds it to an existing database. This process also is directed by a language which can transform data within records. The necessary field changes to suit local word lengths and data representations are performed automatically.

On the central data will be stored all the technical data necessary to describe the product, including geometry and associated design data, assembly and modification data (including the modifications to each specific aircraft being assembled) and derived properties of the aircraft ranging from overall aerodynamic qualities to the internal strength and the mass of each component. In addition project management and access control data will be stored. There will thus be direct interfaces to the production, financial and commercial databases which are being developed in parallel.

5. IMPLEMENTATION OF APPLICATIONS

Traditionally, many designers in BAE have produced their own applications programs. Over half the development effort is provided this way, the rest coming from computer departments at the design sites.

Whilst we have standardised on hardware, operating systems, languages and documentation, we have not previously used a consistent approach to the design and implementation of systems, nor have we used a single software framework. By adopting and teaching a particular approach, we aim to make the implementation of new applications much simpler, especially for the non-computing professional. The intention is that staff who are developing applications can concern themselves far more with satisfying user requirements, and far less with choosing or writing framework software and developing a style of design and implementation.

A particular benefit of this approach is that we can afford to provide carefully tailored documentation for those working in this environment - leaving out the mass of irrelevancies that the computer supplier inevitably pours forth.

The important elements of the approach are:

- 1) Above all, to enable the implementor to thoroughly design an application before he goes near the computer, by giving him:
 - a standard, structured technique for recording current activities and data flows within the relevant part of the organisation, so as to identify the requirements of a new system.
 - a similar technique for defining systems and programs. This definition appears later in the source code as primary documentation.
 - sizing data, so that performance can be accurately estimated during the system and program design phases.

The design will be vetted by third parties, particularly by those responsible for the framework software and the overall database design co-ordination.

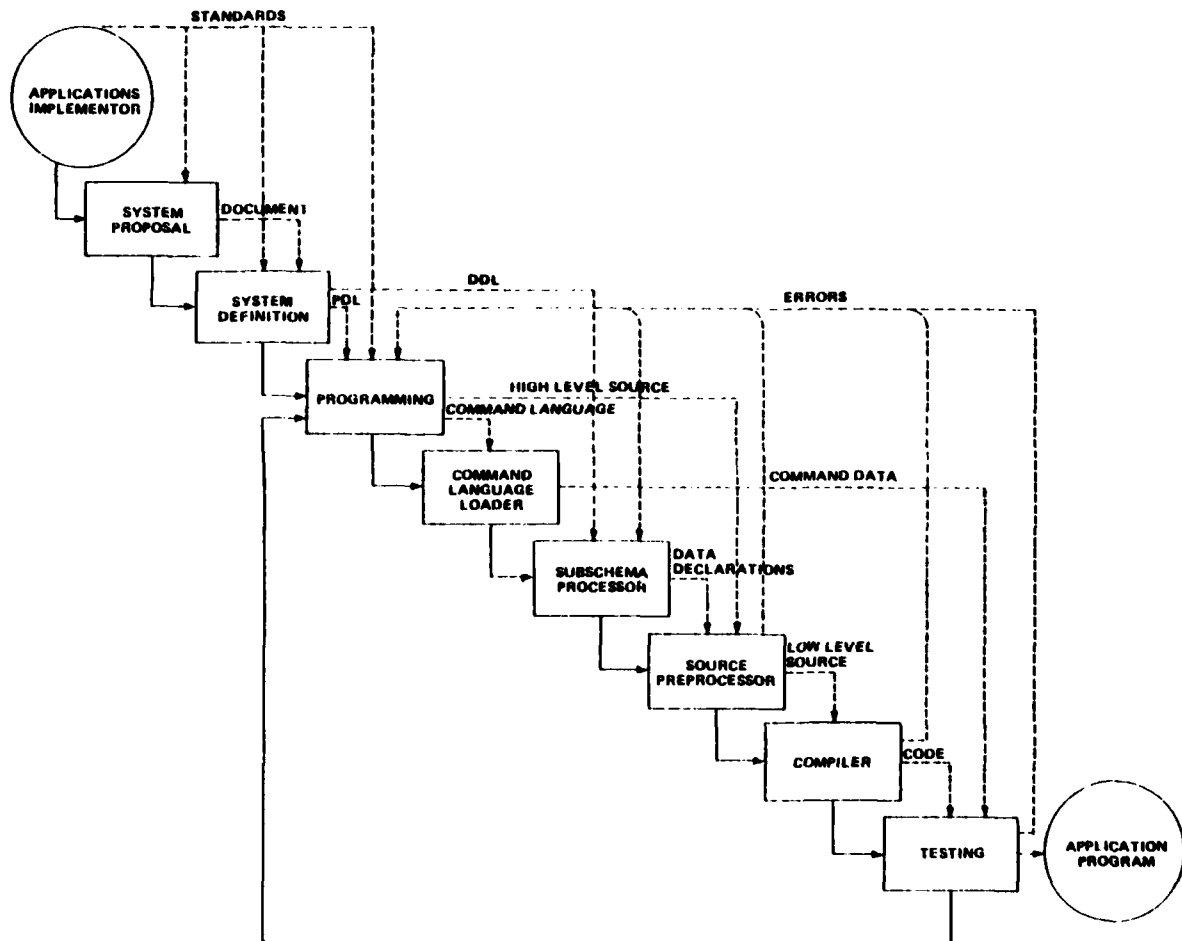


Figure 4 Applications Development

ii) Additional techniques to ensure efficient coding, testing and subsequent maintenance and modifications:

- a definition of the data management and designer interface systems.
- a data dictionary system, which stores the logical and physical design of the database and applications.
- a library system for documentation, code etc.
- a test envelope for top-down implementation and testing.

In establishing the requirements of a system and the high level system design, a diagrammatic representation of processes and data structure is used to aid communication. Figures 2,3 and 4 represent such process diagrams in a simple form; extensions cater for cross-referencing of diagrams at several levels of detail etc. The data structure diagram is that introduced by Bachman (5).

At the system definition level these structures are converted and extended to program and data definition languages (PDL and DDL).

Programming involves the addition to the PDL of the 'flesh' of the program, including references to the data manipulation language (DML). The PDL, DML and DDL can then all be processed automatically into the target source language such as FORTRAN or COBOL producing, respectively, the major control instructions, database CALL statements and data declarations.

To establish the user's command language, the definitions of commands, associated data and subsequent actions are input to a program which loads the command interpreter database.

6. FRAMEWORK IMPLEMENTATION

This framework is being implemented initially on the PDP 11 computer range by a team of 10 people. This is being followed by a VAX11 implementation.

The expertise needed to design such software is, of course, considerable, and we have used consultants and built various software prototypes to acquire this expertise.

Several critical elements are in use by applications teams including the Mini Data System and a prototype command interpreter.

While the application program interfaces will be standard, there are of course areas where the framework has to interface with the operating system. These must be rewritten for each computer type.

The framework naturally has a highly modular structure so that it can be tailored to particular needs. The mainframe would normally support all facilities, but at the other extreme we might configure a single user machine with core only data management.

Software being implemented by BAe is written in the RTL/2 language, chosen for its efficiency and portability.

ACKNOWLEDGEMENTS

The work reported in this paper is the outcome of the effort and involvement of many people within British Aerospace which has made such a demanding project feasible.

I acknowledge the permission of British Aerospace to publish this paper, but the views and opinions expressed are personal, and not necessarily those of the Corporation.

REFERENCES

1. Richens, P. 'New developments in the OXSYS system', CAD76 Proceedings, pp 44-50/. IPC Science and Technology Press Ltd., Guildford, UK, 1976.
2. Miller, R.E. and Fulton, R.E. 'IPAD Objectives, Scope, Implementation, Status'. Presentation to Interactive Design System Conference, Stratford-upon-Avon, UK, 1977.
3. Schubert, R.F. 'Integrated Database Management System'. Presentation to B.C.S. Symposium on Implementations of Codasyl Database Management Proposals, London, UK, 1974.
4. Bachman, C.W. 'The Evolution of Storage Structures', Communications of the ACM, pp 628-634, 1972.
5. Newell, R.G. et al. 'The Design of Systems for CAD' Presentation to IFIP. W.G. 5.2 Working Conference, University of Texas, Austin, USA, 1976.

LIASSE ELECTRIQUE ASSISTEE PAR ORDINATEUR

par

Jean-Pierre Pauzat
Ingénieur Bureau d'Etudes
Aérospatiale, Division Avion

1- QUE CONTIENT UNE LIASSE ELECTRIQUE ?

1.1- Pour un avion du type AIRBUS (après environ 9 ans d'exploitation), la liasse électrique comprend :

16.500 plans, répartis en :
 - 7.000 schémas de câblages (43%)
 - 5.000 listes d'équipements (30%)
 - 4.500 répertoires (27%)

1.2- Les informations traitées dans ces plans peuvent être estimées à environ (pour toutes les validités) :

. 80.000 Définitions concernant les câbles et leurs branchements,
 . 20.000 Définitions concernant les équipements,
 . 3.000 Définitions concernant les modifications,
 . 40 Validités standards, non affectés ou clients.

2- SYSTEME "G.I.C.E." :

Le système "G.I.C.E." (Gestion Informatique des Câblages Electriques) a pour but :

- 1- d'assister le Service Electricité dans la définition, la réalisation et la diffusion d'une liasse électrique ;
- 2- de prendre en compte les besoins des services extérieurs utilisant la liasse électrique : Préparation, Production, Contrôle, Après-Ventes.

2.1- Le Système "G.I.C.E." assiste le Service Electricité :

2.1.1- Le Système "G.I.C.E." assiste le service électricité dans la définition de la liasse au niveau :

- de la réservation des branchements sur tous les semi-équipements communs à plusieurs circuits (prises de raccordement, barrettes, splices) : 48.000 pour une liasse (40 versions actuellement pour l'AIRBUS) ;
- de la mise à jour de ces réservations après l'élaboration des schémas de câblages : 1250 schémas pour une liasse (1 avion).

Cette procédure informatique s'effectue à l'aide de plusieurs consoles alphanumériques installées au sein du service, parmi les dessinateurs. Ces derniers ont à leur disposition, plusieurs programmes conversationnels chargés de les guider pour effectuer ces travaux.

Cette procédure informatique ne supprime pas le travail de réservation des branchements mais fournit un outil de travail plus évolué qui permet :

- d'éliminer les registres tenus manuellement : 60 classeurs de 400 fiches correspondant à toutes les versions ;
- d'éliminer le travail de vérification des enregistrements pour chaque schéma de câblages : 1h par plan ;
- de déceler une partie des erreurs ou incompatibilités introduites dans la liasse électrique au niveau des repérages.

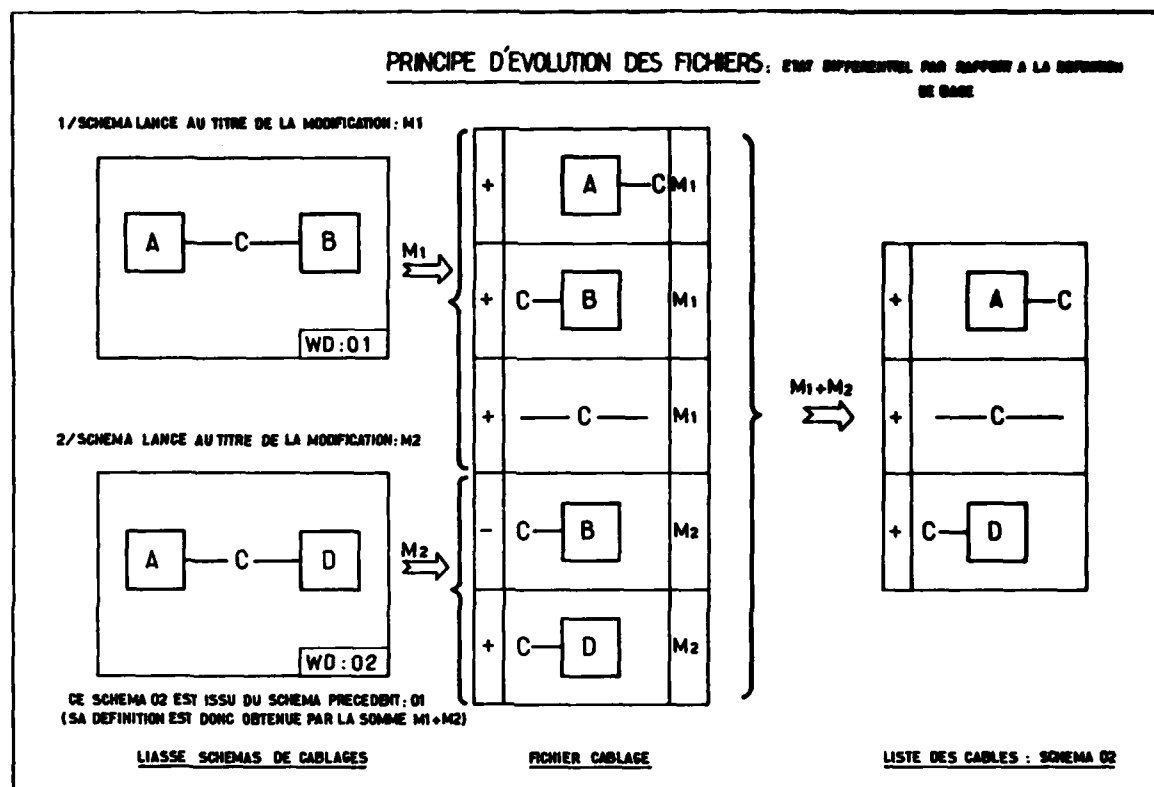
2.1.2- Le Système "G.I.C.E." assiste le service électricité dans la réalisation de la liasse :

- en prenant en compte l'ensemble des définitions câblages, équipements et validités dans des fichiers distincts d'accès direct (introduction classique par bordereaux et cartes perforées) ;
- en faisant évoluer ces fichiers au fur et à mesure de l'introduction des modifications, uniquement par états différentiels ; cette procédure a pour avantage de diminuer le volume d'informations à revalider manuellement, l'ordinateur se chargeant de faire la synthèse de l'ensemble pour chaque validité (voir fig.1- Page 2-).
- en donnant à chaque instant aux dessinateurs, la liste complète (pour toutes les validités) de tous les conducteurs, les équipements, les branchements, les plans, les modifications, les avions et leurs validités.

2.1.3- Le Système "G.I.C.E." assiste le service électricité dans la diffusion de la liasse :

- tout le processus de diffusion est informatisé : une série de programmes permettent, à partir de critères de validité issus des fichiers "avion" et "modifications", d'extraire de chaque fichier de base les éléments relatifs à la validité demandée (voir fig. 2- Page 3-).
- la cascade des plans pour une validité donnée est ainsi obtenue par un programme particulier. Ce dernier rend un service appréciable en supprimant une charge de travail très importante qu'il était difficile d'assurer dans des délais raisonnables.
- du fait de l'informatisation de la liasse, la cascade a été considérablement simplifiée : la majorité des ensembles supérieurs ont été supprimés et les documents restants sont en grande partie des listes de sortie ordinateur : (voir fig.3- Page 4-)

environ 2.350 répertoires et 2.800 listes d'équipements seront ainsi supprimés pour les liasses A.300 B2/B4 (et remplacés par 2 listes de sortie ordinateurs en ce qui concerne les équipements).



- Fig. 1 -

2. 2- Le Système "G.I.C.E." prévoit de prendre en compte les besoins des services extérieurs utilisant la liasse électrique :

PREPARATION, PRODUCTION, CONTROLES, APRES-VENTES.

La somme des informations "câblages, équipements et validités" qui constituent la BANQUE DE DONNEES BUREAU D'ETUDES peut être mise à la disposition des Services Extérieurs. Ceci permet en particulier d'éviter la duplication des travaux au niveau de la saisie des données "électricité" et garantit l'unicité de la définition de chaque information. Les différentes applications actuellement prévues concernent :

- la diffusion au Service Préparation des fichiers câblages et équipements pour une validité donnée pour la définition des faisceaux ;
- la diffusion au Service Approvisionnements de l'expression des besoins par validité des différents types d'équipements ;
- la diffusion au Service Contrôles des documents de référence "Bureau d'Etudes" ;
- la diffusion au Service Production des états différentiels "câblages et équipements" pour rattrapage sur avion ;
- la diffusion au Service Après-Ventes des fichiers complets reflétant l'état définitif de chaque avion.

NOTA : Ces diffusions sont prévues sous forme de bandes magnétiques ou microfiches.

2. 3- Conclusion :

Le Système "G.I.C.E." permet donc : d'améliorer le processus d'élaboration de la liasse électrique, d'éviter aux services extérieurs au Bureau d'Etudes de reprendre la saisie des informations "électricité".

Ceci s'avère très important au moment où l'augmentation des demandes clients et donc de la cadence de sortie des avions en chaîne implique une manipulation d'un volume d'informations de plus en plus important dans un délai très court.

Seule l'informatisation complète du processus peut permettre de traiter ce problème. En ce qui concerne le Bureau d'Etudes, cette étape finale sera réalisée grâce à la mise en place du Système "C.A.O.C.E.", basé sur l'utilisation du matériel à dessiner interactif, complément naturel du Système "G.I.C.E."

ORGANIGRAMME DU SYSTEME "G.I.C.E."

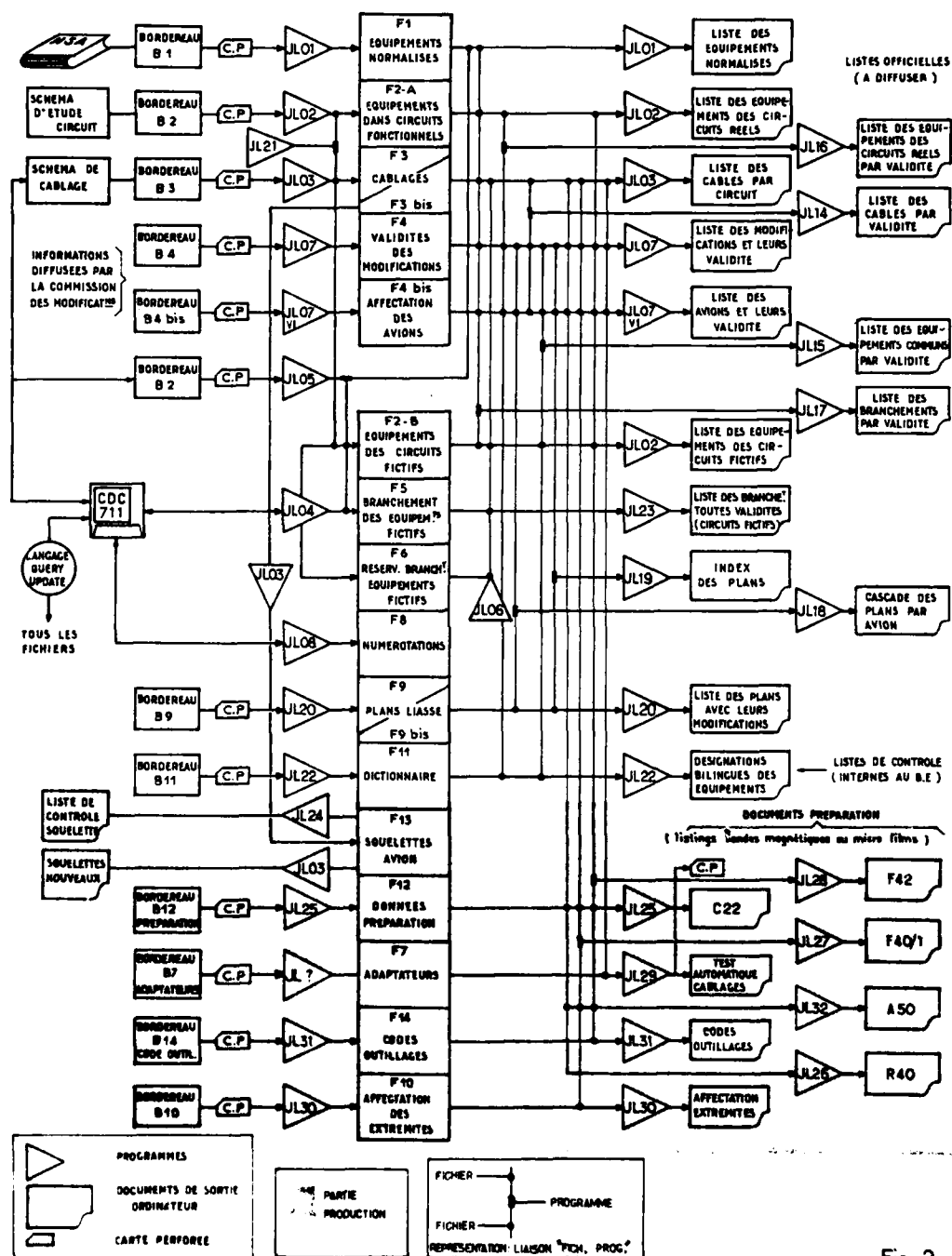
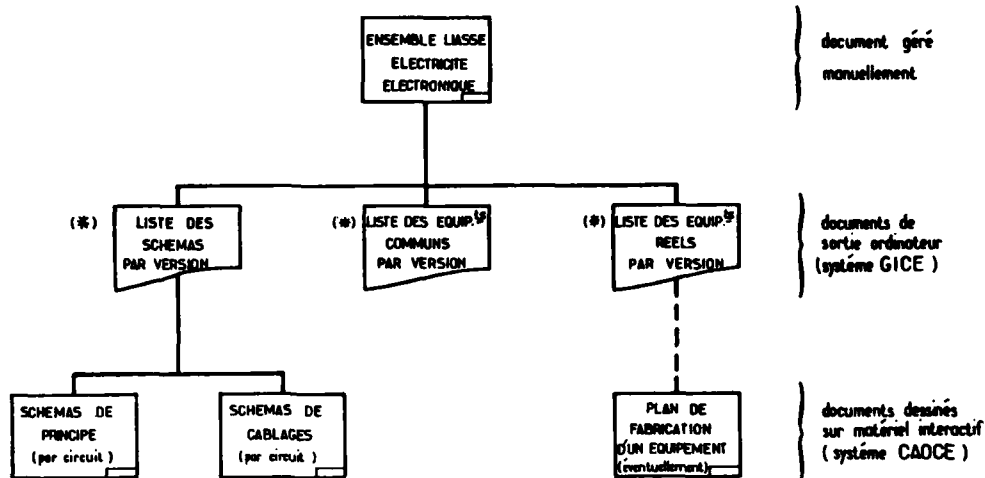


Fig. 2.

aérospatiale



CASCADE LIASSE ELECTRIQUE



(*) : Chacun de ces documents est diffusé pour une version donnée par tranche de 10 avions (classement par circuit)

APPLICATION des SYSTEMES 'GICE' et 'CAOCE'

- Fig. 3 -

3- SYSTEME "C.A.O.C.E."

Le Système "C.A.O.C.E." (Conception Assistée par Ordinateur des Câblages Electriques) a pour but de prendre en compte le dessin des schémas électriques sur du matériel interactif et de permettre la saisie au niveau informatique de toutes les données qui alimentent les fichiers de base du Système G.I.C.E.

3.1- Matériel et Logiciel

Le choix s'est porté sur un système vendu "Clefs en main" : système local fonctionnant sur un mini-ordinateur où le logiciel est fourni avec le matériel. De ce fait il a été inutile de prendre en compte l'écriture de ce logiciel, seule la liaison fonctionnelle avec le Système "G.I.C.E." travaillant sur un ordinateur C.D.C. (CYBER 172) doit être programmée.

Cette solution permet au Système "C.A.O.C.E." d'être indépendant de la charge de travail de cet ordinateur. Elle permet aussi d'utiliser directement un logiciel important et performant fonctionnant déjà par ailleurs pour des besoins similaires (BOEING).

La configuration actuelle qui représente la phase expérimentale est représentée ci-dessous : (voir fig.4-Page 5-).

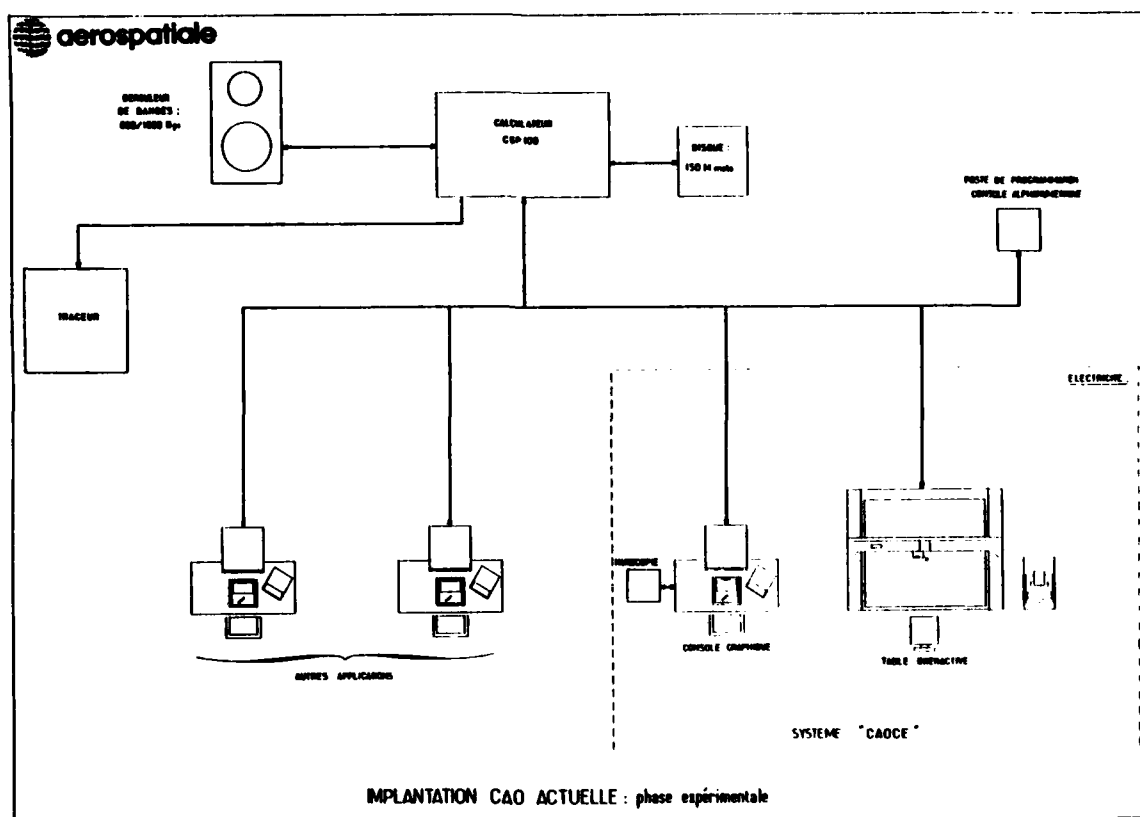
En phase opérationnelle environ 20 postes de travail sont prévus pour "traiter" une liasse électrique d'un avion type AIRBUS. Si l'on ajoute les besoins Après-Ventes ce chiffre monte à 30 postes de travail, la majorité étant des consoles graphiques.

3.2- Principe d'utilisation

NOTA : le principe n'est pas encore entièrement défini.

Deux critères importants devront cependant être pris en compte :

- 1) Assurer la saisie des données "câblages et équipements" au niveau "C.A.O.C.E." et supprimer ainsi la rédaction des bordereaux et la perforation des cartes au niveau "G.I.C.E."
- 2) Permettre au Service Après-Ventes de disposer de la liasse électrique du B.E. sans avoir à la redessiner entièrement, la duplication se faisant au niveau informatique (C.A.O.C.E.).



- Fig. 4 -

- Le principe qui avait été envisagé initialement est le suivant : (voir fig.5- Page 6-)

1- Pour une version de base ou tous plans nouveaux :

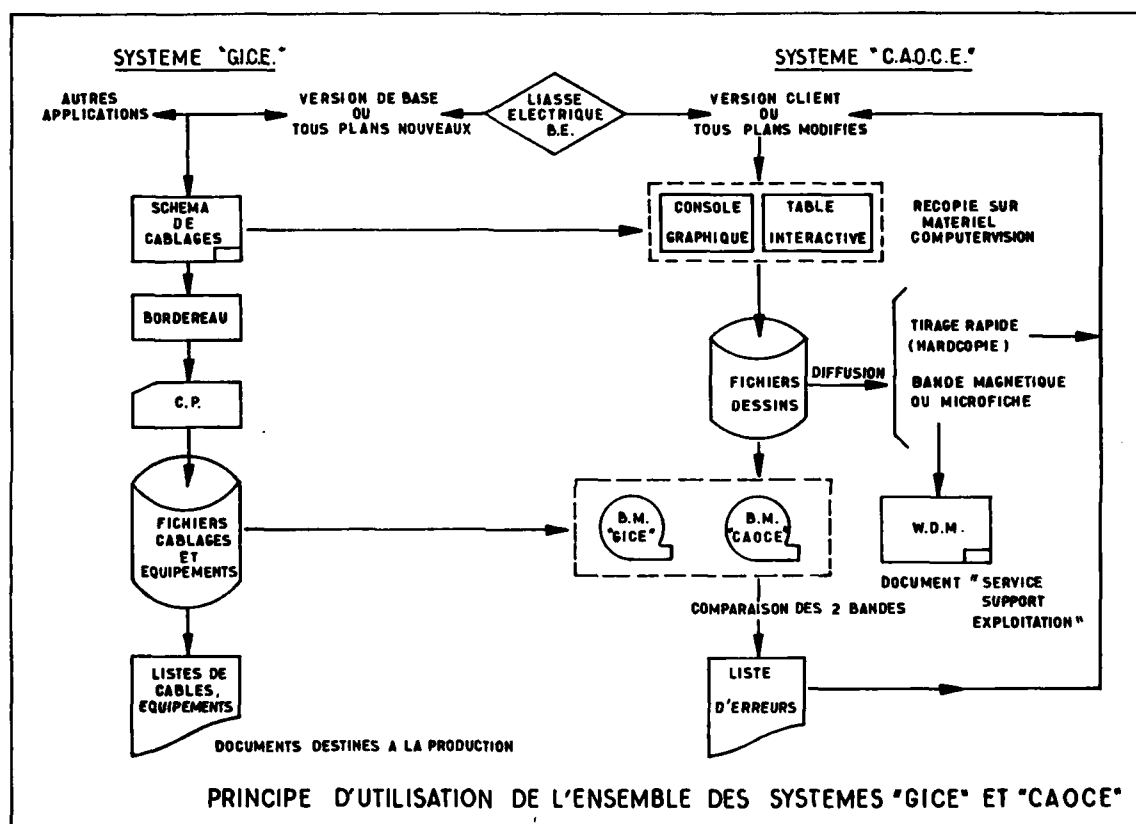
- de recopier les schémas de câblages sur la table à dessiner interactive ;
- de récupérer directement les informations "câblages" et "équipements" correspondants ;
- de vérifier pour chaque validité les fichiers ainsi créés avec ceux obtenus par le système "G.I.C.E." et de déceler ainsi toutes les anomalies entre les deux types de fichiers ;
- de donner à l'Après-Vente une liasse électrique directement exploitable pour les besoins de la documentation technique (WDM, etc ...) et en concordance parfaite avec la liasse B.E., ceci dans un délai très court.

2- Pour une version client et tous plans modifiés :

- d'appliquer directement les modifications sur la liasse archivée par le système soit sur table interactive dans le cas de modification importante, soit sur console graphique dans le cas de modification mineure ;
- de supprimer la rédaction des bordereaux et la perforation des cartes correspondant à la phase "saisie des données" dans le système "G.I.C.E." ;
- de donner à l'Après-Ventes la liasse électrique B.E. directement exploitable pour les besoins du W.D.M.

Remarque :

La comparaison précédente entre les 2 types de fichiers obtenus par les deux systèmes est devenue inutile puisque la liasse est un tronc commun où les erreurs dues aux bordereaux et à la perforation des cartes n'existent plus.



- Fig. 5 -

USE OF ADVANCED COMPUTERS FOR AERODYNAMIC FLOW SIMULATION

F. R. Bailey
 Ames Research Center, NASA
 Moffett Field, California 94035
 and
 W. F. Ballhaus
 Aeromechanics Laboratory
 U. S. Army Research and Technology Laboratories (AVRADCOM)
 Ames Research Center
 Moffett Field, California 94035

SUMMARY

The current and projected use of advanced computers for large-scale aerodynamic flow simulation applied to engineering design and research is discussed. The design use of mature codes run on conventional, serial computers is compared with the fluid research use of new codes run on parallel and vector computers. The role of flow simulations in design is illustrated by the application of a three-dimensional, inviscid, transonic code to the Sabreliner 60 wing redesign. Research computations that include a more complete description of the fluid physics by use of Reynolds averaged Navier-Stokes and large-eddy simulation formulations are also presented. Results of studies for a Numerical Aerodynamic Simulation Facility are used to project the feasibility of design applications employing these more advanced three-dimensional viscous flow simulations.

INTRODUCTION

In the past decade, the simulation of aerodynamic flows by numerical modeling on computers has become increasingly acknowledged as a valuable tool for aerodynamics research. This interest in flow modeling is a result of the remarkable progress that has been made in developing efficient solution procedures for a hierarchy of approximations (Refs. 1, 2) to the compressible Navier-Stokes equations governing fluid motion and from the progress in the development of large-scale, advanced computers. These advances have coupled to provide important new technological capabilities that have added a new dimension to the partnership of theory and experiment (Ref. 2). In the past, experimental programs were largely directed toward obtaining aerodynamic characteristics for point design and obtaining systematic data for configurations and flow-field data not amenable to analysis. The improved capability of numerical simulations and the limitations imposed by most experimental programs are placing increased emphasis on tests specifically designed to check theory at a few critical points or to generate data for improved theoretical flow models. Once the numerical analysis is proved adequate, it provides the capability to explore other geometries or flow conditions for which test data do not exist.

Advances in numerical methods and computers have also coupled to provide economic improvements. Historically, computer speed and memory have increased with time at a much greater rate than computer cost. Similarly, the computational efficiency of numerical algorithms is continually improving. This is illustrated in Fig. 1 (from Ref. 1) in which the trend in relative computation cost due to computer price/performance improvement alone is compared with the corresponding trend due to algorithm improvements alone. The two trends have combined to bring about an extraordinary cost-reduction trend in computational aerodynamics.

Although the technological and economic advances in computational aerodynamics have been remarkable, the full potential for application to engineering design has yet to be realized. Several numerical modeling issues are still being addressed (Ref. 3), including: algorithm efficiency, numerical resolution, accuracy and stability, computational grid generation, and turbulence modeling. In addition to these issues are computer speed and memory limitations that need to be addressed to effect substantial improvements in the configuration complexity and modeling accuracy needed to advance the role of computational aerodynamics in engineering design. In this paper, we briefly discuss present computer capabilities, their application to engineering design and research simulations, and projected capabilities for more advanced simulations.

ADVANCED COMPUTER RESOURCES

Historically, increases in computer speed and storage have had a major effect on the development of computational aerodynamics as well as on computational physics in general. Figure 2 shows the growth trend in computer speed (measured in millions of floating point operations per second, mflops) as typified by the introduction of increasingly advanced systems. The IBM 704, IBM 7090, CDC 6600, CDC 7600 and their contemporaries are conventional designs based primarily on the serial computing concept. In these systems a computer instruction is required to initiate each arithmetic operation such as a floating point addition or multiplication. Large increases in computing speed were primarily due to substantial improvements in electronic circuitry as technology progressed from vacuum tubes to integrated circuits. Similarly, storage capacities have improved with the transition from ferrite cores to semiconductor memories.

Conventional computers have been the principal tools used for linear and nonlinear inviscid and boundary-layer method development over the past two decades. Presently, most aerodynamic design applications use a wide assortment of conventional computers with codes based on these methods. The more advanced conventional computers have also been heavily used in the development of more complex models, such as those treating flow separation and turbulence with the Reynolds averaged approximation to the Navier-Stokes equations. Unfortunately, speed and memory constraints of these computer systems have inhibited the full exploration of these methods in three dimensions and have made their design use too costly.

In the 1960s it was recognized that the rate of increase in speed of conventional computers was being severely restricted by speed-of-light and heat dissipation limits on electronic circuitry. New design approaches were developed based on the concept of a single instruction initiating the execution of several identical arithmetic operations. This led to the introduction of parallel and vector computers, including ILLIAC IV, CDC STAR-100, TI ASC, and CRAY-1.

The ILLIAC IV (Ref. 4), developed by the University of Illinois and Burroughs Corp., implements this concept with 64 identical processing elements. The processors operate in parallel in a lock-step fashion so that one instruction can initiate the simultaneous execution of as many as 64 identical arithmetic operations (128 in half-word mode). The STAR-100, developed by Control Data Corp. (Ref. 5), and the ASC, developed by Texas Instruments Corp. (Ref. 6), use a pipeline approach. Here an arithmetic unit is segmented with each segment corresponding to one of several stages, each of equal time duration, that make up an arithmetic operation. An instruction initiates a stream of operands into the pipeline, so that when it is full several operands are being simultaneously processed, each at a different stage of completion. Much as in an assembly line operation, results appear at the rate needed to complete only a single stage. Because one instruction causes an operation to be performed on numerous operands, this type of processing is essentially the same as parallel processing. Pipeline operation is most efficient on long operand strings that aid in minimizing the effect of pipeline start-up and shutdown. The operand string is analogous to a vector so these computers are often called vector computers. Note that the ILLIAC IV operates on data strings (64 in length) and thus may also be thought of as operating on vectors.

The CRAY-1 (Ref. 7), also a vector computer, utilizes several specialized pipelines and registers that are optimized for vectors of length 64 or multiples of 64. Pipelines may also be "chained" together to produce a longer pipeline performing more complex operations, such as an addition followed by a multiplication. The result of this combined operation appears at the single-stage rate. In addition, the CRAY-1 addresses the overhead penalty for scalars (single element strings) and very short vectors by including a separate scalar unit. Thus the machine is sometimes viewed as a conventional computer with additional vector processing capability.

The new vector approach to computing has significantly affected simulation methodology. Although fluid dynamic approximations are largely amenable to simultaneous execution over large domains of discrete (grid) points, researchers have had to adjust their approach in algorithm structure and coding techniques to realize the potential of these advanced computers. Such new techniques are being developed at an accelerating rate, however, as the need for increased computing capability is realized. In particular, more emphasis is placed on data organization (Ref. 8) because of the parallel and vector computer's higher data bandwidth demands between memory and processing units. As researchers have become more familiar with these recently introduced computers, their use in aerodynamic simulation has grown, particularly in the areas of fluid dynamic research and advanced modeling studies. Examples include research computations using transonic potential (Refs. 9-13), Reynolds averaged Navier-Stokes (Refs. 8, 14-16), and turbulent eddy simulation (Ref. 17) approximations. In the next two sections, examples are given of the use of advanced conventional computers for design and the use of ILLIAC IV for fluid dynamic research applications.

DESIGN APPLICATIONS

A fundamental goal of computational aerodynamics is to provide cost-effective tools for design exploration. Aerodynamic codes typically used in design applications must meet three key criteria. The first is that the code not consume inordinate amounts of computer time and memory. For example, in the authors' experience with three-dimensional transonic flow simulation, one of the first successful attempts (Ref. 18) at transonic wing simulation required about 12 hr on the IBM 360/67 computer. This reduced the rate of development of the code and made it unattractive for use in design applications. The subsequent availability of the CDC 7600, with approximately 25 times the computing rate of the IBM 360/67, offered substantially shorter turnaround time and led to accelerated development. Typical runs on the faster machine were reduced to substantially less than an hour. This usually afforded at least two turnarounds during prime shift, and the code became attractive for use in engineering applications.

The second criterion is that the code adequately simulates flows about geometries that are sufficiently realistic and that it captures the physical phenomena that are essential to the design study. Since complex flows are highly three-dimensional, the most useful simulations are those closely approximating the dominant three-dimensional aspects of complex geometries. Although substantial progress has been made in numerical modeling of complex turbulent flows, the three-dimensional applications have been limited by computer resources to simple shapes. This has restricted three-dimensional design simulations to those involving inviscid linear, inviscid nonlinear, and attached boundary-layer models.

The third criterion is that the code be reliable and predictable. This generally implies that the code is based on a relatively mature methodology and that it has gone through a lengthy process of algorithm and model development, pilot code construction, test and evaluation, and subsequent refinement and documentation. As a consequence of this process, which usually spans several years, most design simulations are presently done on conventional computers, such as the CDC 7600, introduced a decade ago.

Because of limitations imposed by the above criteria, design simulations have not reached the point where they can be relied on for the full spectrum of performance data. Nevertheless, some present design analysis codes are being used to provide key guidance; they have fostered a new approach to aerodynamic design. This approach is typified by the Raisbeck group's program (Ref. 19) to improve the Rockwell Sabre-liner wing.

The objective of the program was to substantially improve the range capability of the aircraft without sacrificing its low-speed performance. The key to achieving this objective was redesign of the wing. The requirements were that: (1) the wing fuel carrying capacity be increased to carry an additional 1200 lb; (2) climb and cruise drag be improved; (3) takeoff and landing field lengths be reduced; (4) stall characteristics not be degraded; (5) the wing box contours be unchanged along the entire lower surface and along the upper surface outboard of midspan; (6) the existing ailerons be maintained to meet the cruise

requirement; and (7) retrofit be accomplished at a reasonable cost. The Raisbeck group elected to make heavy use of aerodynamic simulations and chose the Bailey-Ballhaus code (Refs. 20, 21) for three-dimensional transonic simulations during the wing redesign effort to improve high Mach number capability.

The redesign procedure consisted of three basic steps. The first step was to calibrate the code by comparing computed wing surface pressures with flight-test data for the original configuration. The resulting correlation, shown in Fig. 3 (from Ref. 22) provided the designers with confidence that the code could simulate the essential physics in the flow field, which in this case was the strength, location, and extent of the embedded shock wave on the wing upper surface.

The second step was to modify the wing geometry in the computer model using the code as a guide that the aerodynamicists could use to reduce the strength and extent of the shock wave. Results of this step are shown in Fig. 4 (from Ref. 19) where the computed surface isobars for the modified wing (Sabre 60 Mark Five) are compared with those for the original wing (Basic Sabre 60). The comparison shows that the modified wing has eliminated the shock wave in the inboard region and reduced its strength outboard. The outboard shock wave could not be completely eliminated because of geometrical constraints imposed by low-speed performance requirements.

The third step was to flight test the new wing to evaluate performance gains. Results are summarized in Fig. 5 (from Ref. 22); they show a 25% reduction in takeoff and landing field length, an 8% improvement in fuel efficiency, and a 27% increase in range.

The above example clearly demonstrates two key assets of the current design simulation capability. The first is the ability to study in detail the major flow phenomena governing aerodynamic performance near the design point. The second is the ability to rapidly investigate the design space and to literally "cut and file" on the computer. Presently, computer codes are limited in their ability to predict complete performance data for complex configurations. However, the availability of more accurate simulation models coupled with increased computer capability will allow future aerodynamicists to produce better designs even more quickly and economically. In the next section we look at some of the research activities aimed at meeting this objective.

RESEARCH APPLICATIONS

The goal of computational aerodynamics research is twofold: (1) the development of more accurate and efficient numerical models that capture increasingly detailed flow-field behavior and (2) the use of modern numerical techniques to gain an understanding of the underlying mechanisms of fluid physics and to explore questions still unanswered by experiment and simplified theory. An active area of research involves the simulation of fully turbulent viscous flows. Two approaches are of particular interest: Reynolds averaged Navier-Stokes and large eddy simulation approximations to the full Navier-Stokes equations.

Reynolds Averaged Navier-Stokes Equations

In this approximation the Navier-Stokes equations are averaged over a time interval that is long compared to turbulent eddy fluctuations but small compared to large-scale flow variations. The averaging process introduces terms representing the time-averaged transport of turbulent momentum and energy. Such terms must be modeled and it is the modeling of turbulence that introduces the principal inaccuracy of this approach. However, in many cases this approximation provides realistic simulations of separated flows, for example, unsteady flows with buffeting, and is capable of total drag prediction (Ref. 23). This promising approach, when fully exploited, should make it possible to use numerical simulations for actual performance prediction over a broad range of flow conditions and geometries.

A particularly interesting application of the Reynolds averaged Navier-Stokes equations is the numerical simulation of unsteady flows that are triggered and sustained by viscous mechanisms. The first demonstration of this capability was the simulation of transonic buffeting about a circular-arc airfoil by Levy (Ref. 24). This was soon followed by the computation of buffeting forces near and beyond maximum lift for a supercritical airfoil in a high Reynolds number transonic flow (Ref. 23).

Very recently, Steger and Bailey (Ref. 15) simulated aileron buzz using the ILLIAC IV. In 1947, during wind-tunnel tests of a semispan wing from the P-30, it was discovered (Ref. 25) that the severe aileron vibrations that had been encountered in flight were manifestations of a one-degree-of-freedom flutter. This phenomenon was characterized by shock-wave motion that produced a phase shift in the response of the hinge moment to the aileron motion; it was found to occur for certain combinations of Mach number and angle of attack. This classical experiment was simulated two-dimensionally by simultaneously integrating in time both the governing flow equations and a simple differential equation for aileron motion.

The simulation results are shown in Fig. 6 and reveal good agreement with the experimentally determined buzz-onset Mach number. Simulated histories of aileron deflection show that for an initial 4° deflection angle, the aileron returns to zero deflection for a free-stream Mach number of 0.79. When the Mach number is increased to 0.82, however, a limit cycle oscillation is reached. Figure 7 shows Mach number contours near the upper and lower limit of the buzz cycle and illustrates the severe shock-wave motion.

It is interesting to note that when the viscous terms in the governing equations were neglected, either stable or divergent aileron oscillations occurred; no aileron buzz was observed in the inviscid case. Furthermore, the computer code without adjustment automatically produced the appropriate steady and unsteady flows.

Only in the past year has the Reynolds averaged Navier-Stokes approximation been applied to simulations of three-dimensional flows. Due to computer limitations of even the most advanced computers these flows are still relatively simple in geometry. The first such simulation (Ref. 26), obtained on the CDC 7600, was for a three-dimensional swept shock wave interacting with a turbulent boundary layer. Recently,

Shang et al. (Ref. 27) simulated transitional and fully turbulent corner flows and obtained further results (Ref. 16) on the CRAY-1 computer for shock-wave boundary interaction in a wind-tunnel diffuser. In addition, Pulliam and Lomax (Ref. 8) simulated flow about a hemisphere cylinder at angle of attack using ILLIAC IV. Their results, given in Fig. 8, show a complex flow pattern, also studied experimentally (Ref. 28), involving three types of flow separations on the body. These include a separation bubble on the nose, a primary separation on the sides and a secondary separation embedded within the primary separation along the leeward surface.

Large Eddy Simulations

This approximation is based on the concept that in turbulent flow it is the large eddies that absorb energy from the mean flow. These eddies are highly anisotropic, vary according to Reynolds number and type of flow, and transport the principal turbulent momentum and energy. The small eddies, on the other hand, dissipate energy, tend toward isotropy, are nearly independent of Reynolds number and flow type, and transport relatively little turbulent energy or momentum. The numerical approach calls for the direct simulation of the large eddies while the small eddies, which are smaller in scale than the numerical grid (subgrid scale eddies), are modeled. The direct computation of the large eddies necessary for these simulations is very demanding of computer memory and storage. However, given sufficient computer resources this approach promises to provide simulations of phenomena such as aerodynamic noise, laminar-turbulent transition, and other turbulent characteristics from theoretical first principles. In addition, it provides a means for conducting numerical experiments to develop improved turbulence modeling for the less demanding Reynolds averaged approach.

Although large eddy simulation is still in a primitive stage, significant progress is being made (Ref. 1). The increased need for resolution makes this method a prime candidate for the most advanced computers. Particularly noteworthy is the work of Wray (unpublished results communicated to the author, 1979) which has been described by Chapman (Ref. 1). Previous simulations have been incompressible, but Wray recently conducted turbulent eddy simulations on the ILLIAC IV using 500,000 grid points (requiring approximately 7 million data words) for compressible flow in shear layers and round jets. Vorticity contours for a two-dimensional shear layer, shown in Fig. 9, illustrate the experimentally observed (Ref. 29) vortex pairing. Figure 10 shows that an initial three-dimensional disturbance develops irregular three-dimensional structure which is more commonly observed (Ref. 30).

FUTURE COMPUTER CAPABILITY

Although the growth in computer capability has been remarkably rapid there is reason for concern regarding continued growth. In fact, the computer speed trend shown in Fig. 1 indicates that a leveling-off in speed improvement has already occurred. A major contributing factor is that the initial defense-oriented drivers in electronics and computing are giving way to consumer oriented products, such as calculators, digital watches, minicomputers, and microcomputers. Although computers were once nearly all government-owned, private business today owns 97% of the computers in the United States. Through the mid-1960s, large-scale computers made up nearly 100% of the market; today, they account for only a small percentage of the market and it is projected that there will be even further decreases in that percentage in the future (Ref. 31). Furthermore, the emphasis on advanced high-speed computers shared by many users is switching to the concept of distributing slower computers among the users.

In the early years of computer development the U.S. government was a strong sponsor of numerical computing engines for defense needs; there is no such driving sponsorship today. It is concluded that as a result of these changes, supercomputers are no longer the focus for new electronic component technology developments, and no large economic incentive exists for major private capital investments in supercomputer development. It has also been concluded by some (Ref. 32) that the Federal government should resume its earlier role of sponsoring the development of supercomputers. In recognition of these circumstances and in recognition of the growing needs of computational aerodynamics, Ames Research Center has undertaken studies to investigate the feasibility of developing a Numerical Aerodynamic Simulation Facility (NASF). The purpose would be to provide, by the mid-1980s, a major new computational capability for aerodynamics that could be a pathfinder for other scientific computers to follow. The goal would be to achieve a two order-of-magnitude performance gain over conventional computers to provide an advanced computing tool for simulating three-dimensional viscous flows for both design and research applications. Several key results of the feasibility studies are discussed below.

The NASF is viewed as a unique computational system tailored for the numerical simulation of large-scale aerodynamic and other fluid dynamic flows. The facility would support all phases of large-scale aerodynamic simulation tasks, including code development, input data preparation, code execution, result editing and display, data storage/management, and other ancillary support activities. Results of the studies indicate that this can be best implemented by a distributed computing approach calling for the distribution of the various aerodynamic simulation tasks among hardware and software systems best suited to perform a given function. The implementation developed consists of the three-level hierarchy of systems shown in Fig. 11.

At the top level is the flow model processor (FMP) which is a very high-speed processor for simulating large-scale, three-dimensional flows by processing the appropriate fluid dynamic equation approximations cast in the form of numerical flow models. This system consists of specially designed processing, memory, and control elements fabricated from advanced, high-speed, high-density integrated circuit technology components. In addition to these hardware elements, the FMP would include a compiler for a high-level programming language (based on the well-known FORTRAN language), an operating system, and other required software elements.

The middle level is the support processing system (SPS) which consists of processing, storage, and peripheral devices configured as a "front-end" system to support FMP simulation tasks. This is a system of standard off-the-shelf hardware and software elements providing three major functions: (1) file storage for programs and data, (2) management of tasks and file movement to and from the FMP, and (3) interactive processing for source generation, compilation, input data preparation and result editing.

The bottom level in the hierarchy is the user interface system. It consists of that equipment and of those hardware/software subsystems that provide the means of interface between the FMP/SPS and the researcher. This system consists of three subsystems: graphics display, work-station, and data communication. The graphics display subsystem provides the important result-display function and includes three-dimensional display units with local computer system support. The work-station is an intelligent terminal unit device consisting of keyboard, low-resolution color graphics, local file storage, and some local processing capability. Work-stations will serve as the principal means of user communication with the FMP/SPS. The data communication subsystem provides high-bandwidth communication links to off-site researchers.

Most of the emphasis during the studies was placed on investigating concepts for the flow model processor. A major conclusion was that the performance goals could be attained only by exploiting parallelism, a conclusion also shared by others (Ref. 31). Furthermore, the time required for development and associated technological risks would be minimized by using state-of-the-art electronic components. Two concepts were developed, based on these premises, one by Control Data Corp. (Ref. 33), the other by Burroughs Corp (Ref. 34).

The Control Data concept (Ref. 33) is based on a vector approach implemented by four lock-step parallel pipelines that support up to triadic operations (e.g., $(A+B) * (C+D)$) often found in aerodynamic simulation models. The machine architecture includes special mapping units for assembling and disassembling contiguous vector streams from the noncontiguous memory patterns associated with three-dimensional array accesses, also found in many models. The system is highly distributed, allowing high-speed concurrent operation of these units as well as a scalar unit, I/O, and three levels of memory.

The Burroughs approach (Ref. 34) departs from the vector concept by providing 512 individual processors, each with its own working memory and instruction decoding unit. All processors operate concurrently, executing their own programs with coordination facilities to enable them to bear on a single problem. The independence of the processors allows simultaneous execution of different arithmetic operations as well as the same (i.e., vector) operation. Flexibility in memory access is provided by a connection network between the processors and a two-level, main memory. This network allows processors to concurrently access random memory locations with only minor performance degradation due to data interference.

The approach used to develop the above concepts consisted of matching computer technology to projected computational aerodynamics requirements. One of the fundamental requirements is a significant increase in grid-point capability which translates directly into memory capacity. Figure 12 shows a plot (Ref. 1) of the maximum number of grid points used in various years as reflected by publications in the fields of atmosphere dynamics and aerodynamics. The trend is indicative of both increasing computational domain size and finer grid resolution. It is of interest to note that the point shown at 1979 is for the large eddy simulation results (Ref. 1) (Figs. 9, 10) discussed in the last section.

Results of the feasibility studies are also shown in Fig. 12, based on a requirement of 30 words of memory per grid point, which is an approximate value for three-dimensional Reynolds averaged simulations that employ a complex turbulence model. Two points are indicated. The lower point corresponds to approximately 40 million words of random access memory (RAM) holding grid point data, miscellaneous arrays, and code. The upper point corresponds to this memory plus approximately 260 million words of block access memory implemented by charge-coupled devices (CCD). Based on the projections by Chapman (Ref. 1), the RAM memory alone is sufficient for Reynolds averaged simulations about wings and should suffice for more complex geometries when used in conjunction with so-called zonal methods that combine inviscid, boundary-layer, and Reynolds averaged domains. The additional CCD storage expands the memory capacity to treat more complex flows, including Reynolds averaged simulations about wing-body combinations. However, according to Chapman's estimates, this large memory capacity is still not sufficient for large eddy simulations beyond the airfoil stage. Increases by several more orders-of-magnitude are needed before this approach will be practical for complex shapes.

The other fundamental requirement of computation aerodynamics is increased computing rate to match the memory growth. In this case, the studies accounted for the algorithmic and data flow structure of three-dimensional simulation models (Ref. 35). Two models were studied in detail: a fully implicit (Ref. 36) and a mixed implicit-explicit (Ref. 37) approach to Reynolds averaged simulations. Both methods showed a very high degree of parallelism, due largely to their three-dimensional nature. The projected performance of these models for both computer concepts was studied in detail. Results of these analyses using timing simulations of actual code sequences gave a range of approximately 800-1,000 mflops on real code. This corresponds to about 200 times the execution rate of the CDC 7600 on the same codes scaled down to fit in that machine. More general capabilities of the two concepts were investigated by estimating performance for a Global Circulation Model supplied by the NASA Goddard Institute for Space Studies. In this case, the performance range was a respectable 500-700 mflops.

The projected capability of NASF in relationship to current capabilities and future requirements for advanced simulations is summarized in Fig. 13. This plot, again taken from Chapman (Ref. 1), shows the computer memory and speed requirement in millions of floating point operations per second corresponding to simulation of a steady flow with a 1-hr run using 1978 numerical methods. The range in requirements is representative of nonlinear inviscid simulations of transonic flows using the full potential formulations, Reynolds averaged Navier-Stokes simulations over a broad range of Reynolds numbers and compressor/turbine blade stages, and large eddy simulations in which the viscous sublayer is modeled. The domain shown for NASF projects a simulation capability for transonic inviscid flows about aircraft configurations and Reynolds averaged flows about airfoils, inclined bodies, compressor blades, and turbine blades using only the RAM. Careful use of buffering between RAM and CCD memory offers simulation capability that includes helicopter rotors and simple aircraft-like shapes. In addition to these capabilities, practical application can be made of sophisticated numerical optimization techniques for complex shapes and three-dimensional unsteady, viscous transonic flow studies. The projections for large eddy simulation restricts this approach to longer solutions about simple shapes. However, based on projected (Ref. 1) computer technology trends and continued advances in numerical methods, the practicality of this approach could be realized before the end of this century.

CONCLUSIONS

To meet the ever pressing demands of computational physics for increased processing speed, computer designers have implemented new architectures based on parallel processing principles that represent a significant departure from the previous conventional approach. The coexistence of two distinct computer types leaves large-scale computational aerodynamics in a period of transition. Engineering design simulations are presently conducted on conventional computers using mature models. These models are proving to be very useful in providing design guidance, but their accuracy limitations require that the bulk of the desired performance data be generated experimentally. Meanwhile, the new parallel computers are being increasingly utilized for simulation research aimed at overcoming these limitations. Constraints on electronic technology improvements indicate that parallel computers are here to stay and that they will be the computing resource for improved, large-scale, engineering design applications of the future. The NASF feasibility studies have shown that by the mid-1980s, the parallel computing approach can provide the computer resources that when coupled with advanced numerical techniques will make a broad spectrum of three-dimensional, viscous flow simulations practical for engineering design applications.

REFERENCES

1. Chapman, D. R.: Dryden Lectureship in Research-Computational Aerodynamics Development and Outlook. AIAA Paper 79-0129, Jan. 1979.
2. Gessow, G. and Morris, D. J.: A Survey of Computational Aerodynamics in the United States. NASA SP-394, 1977.
3. Future Computer Requirements for Computational Aerodynamics. A Workshop held at NASA Ames Research Center, Oct. 4-6, 1977, NASA CP-2032.
4. Illiac IV Systems Characteristics and Programming Manual. Burroughs Corporation, NASA CR-2159, 1972.
5. Control Data STAR-100 Computer Hardware Reference Manual. Control Data Corporation, Publication NR 60256000, 1974.
6. The ASC System Central Processor. Texas Instruments Inc., Publication Nr. 929982-1, 1975.
7. Cray-1 Computer System Hardware Reference Manual. Cray Research Inc., Publication Nr. 2240004, 1978.
8. Pulliam, T. H. and Lomax, H.: Simulation of Three Dimensional Compressible Viscous Flow on the Illiac IV Computer. AIAA Paper 79-0206, Jan. 1979.
9. Smith, R. E., Pitts, J. I., and Lambiotte, J. J.: A Vectorization of the Jameson-Caughey NYU Transonic Swept-Wing Computer Program FLO-22-VI for the STAR-100 Computer. NASA TM-78665, Mar. 1978.
10. Keller, J. D. and Jameson, A.: A Preliminary Study of the Use of the STAR-100 Computer for Transonic Flow Calculations. AIAA Paper 78-12, Jan. 1978.
11. Redhead, D. D., Chen, A. W., and Hotovy, S. G.: New Approach to the 3-D Transonic Flow Analysis Using the STAR-100 Computer. AIAA Journal, vol. 17, no. 1, Jan. 1976, pp. 98-99.
12. Hafez, M. M., Murman, E. M., and South, J. C.: Artificial Compressibility Methods for Numerical Solution of Transonic Full Potential Equation. AIAA Paper 78-1148, July 1978.
13. South, J. C., Keller, J. D., and Hafez, M. M.: Vector Processor Algorithms for Transonic Flow Calculations. AIAA Paper 79-1457, July 1979.
14. Holst, T. L.: Numerical Solution of Axisymmetric Boottail Fields with Plume Simulators. AIAA Paper 77-224, Jan. 1977.
15. Steger, J. L. and Bailey, H. E.: Calculation of Transonic Aileron Buzz. AIAA Paper 79-03134, Jan. 1979.
16. Shang, J. S., Bunning, P. G., Hankey, W. L., and Wirth, M. C.: The Performance of a Vectorized 3-D Navier-Stokes Code on the Cray-1 Computer. AIAA Paper 79-1448, July 1979.
17. Rogallo, R. S.: An Illiac Program for the Numerical Simulation of Homogeneous Incompressible Turbulence. NASA TM-73203, 1977.
18. Lomax, H., Bailey, F. R., and Ballhaus, W. F.: On the Numerical Simulation of Three-Dimensional Transonic Flow with Application to the C-141. NASA TN D-6933, 1973.
19. Timmons, L. M.: Improving Business Jet Performance: The Mark Five Sabreliner. SAE Paper 790582, Apr. 1979.
20. Bailey, F. R. and Ballhaus, W. F.: Comparisons of Computed and Experimental Pressures for Transonic Flows about Isolated Wings and Wing-Fuselage Configurations. NASA SP-347, 1975.
21. Ballhaus, W. F., Bailey, F. R., and Frick, J.: Improved Computational Treatment of Transonic Flow About Swept Wings. NASA CP-2001, 1976, pp. 1311-1320.
22. Kirk, P. S.: Summary of Wing Design Modifications for the SABRE 60 Executive Airplane. ASTLC Engineering Company, Renton, Wash., Report No. AEC-TRG-5, May 1977.

23. Delwert, G. S. and Bailey, H. E.: Prospects for Computing Airfoil Aerodynamics with Reynolds Averaged Navier-Stokes Codes. NASA CP-2045, 1978, pp. 119-132.
24. Levy, L. L., Jr.: An Experimental and Computational Investigation of the Steady and Unsteady Transonic Flow Field about an Airfoil in a Solid-Wall Test Channel. AIAA Paper 77-678, June 1977.
25. Erickson, A. L. and Stephenson, J. D.: A Suggested Method of Analyzing for Transonic Flutter of Control Surfaces Based on Available Experimental Evidence. NACA RM-A7F30, 1947.
26. Hung, C. M. and McCormack, R. W.: Numerical Solution of Three-Dimensional Shock Wave and Turbulent Boundary Layer Interaction. AIAA Paper 78-161, Jan. 1978.
27. Shang, J. S., Hankey, W. L., and Petty, J. S.: Three-Dimensional Supersonic Interacting Turbulent Flow Along a Corner. AIAA Paper 78-1210, July 1978.
28. Hsieh, T.: Low Supersonic, Three-Dimensional Flow About Hemisphere-Cylinder. AIAA Paper 75-836, June 1975.
29. Brown, G. L. and Roshko, A.: On Density Effects and Large Structures in Turbulent Mixing Layers. J. Fluid Mech., vol. 64, pt. 4, 1974, pp. 775-816.
30. Chandrsuda, C., Mehta, R. D., Weir, A. D., and Bradshaw, P.: Effects of Free-Stream Turbulence on Large Structure in Turbulent Mixing Layers. J. Fluid Mech., vol. 85, pt. 4, 1978, pp. 693-704.
31. Best, D. R.: Technology Advances and Market Forces: Their Impact on High Speed Performance Architectures. NASA CP-2032, 1978, pp. 343-353.
32. Tittsworth, J. V.: The Future of Super Computers in the U.S. Proceedings of VIM-28, Albuquerque, New Mexico, Apr. 1978, pp. 191-193.
33. Numerical Aerodynamic Simulation Facility. Control Data Corp., NASA CR-152286-89, 1979.
34. Numerical Aerodynamic Simulation Facility-Feasibility Study. Burroughs Corp., NASA CR-152284 and CR-152285, 1979.
35. Bailey, F. R. and Hathaway, A. W.: Numerical Aerodynamic Simulation Facility. NASA CP-2059, 1978, pp. 15-30.
36. Pulliam, T. H. and Steger, J. L.: On Implicit Finite-Difference Simulations of Three Dimensional Flow. AIAA Paper 78-10, Jan. 1978.
37. Hung, C. M. and McCormack, R. W.: Numerical Solution of Supersonic Laminar Flow Over a Three-Dimension Corner. AIAA Paper 77-694, June 1977.

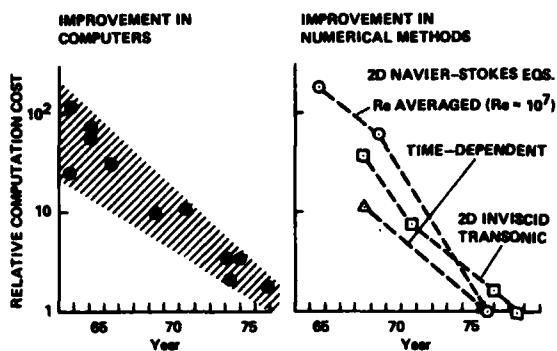


Fig. 1. Cost effectiveness improvements in computer hardware and numerical methods (Ref. 1).

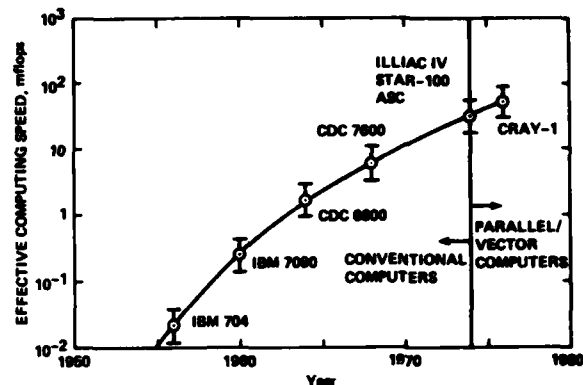


Fig. 2. Trends in effective computing speed for representative advanced computers.

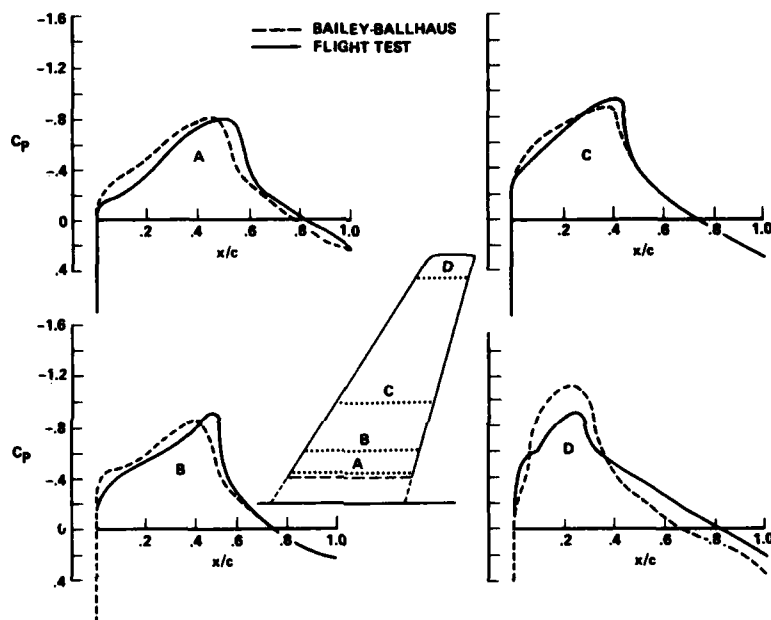


Fig. 3. Baseline comparison of upper surface pressures determined by computations and by flight test for the Sabreliner 60 (Ref. 22).

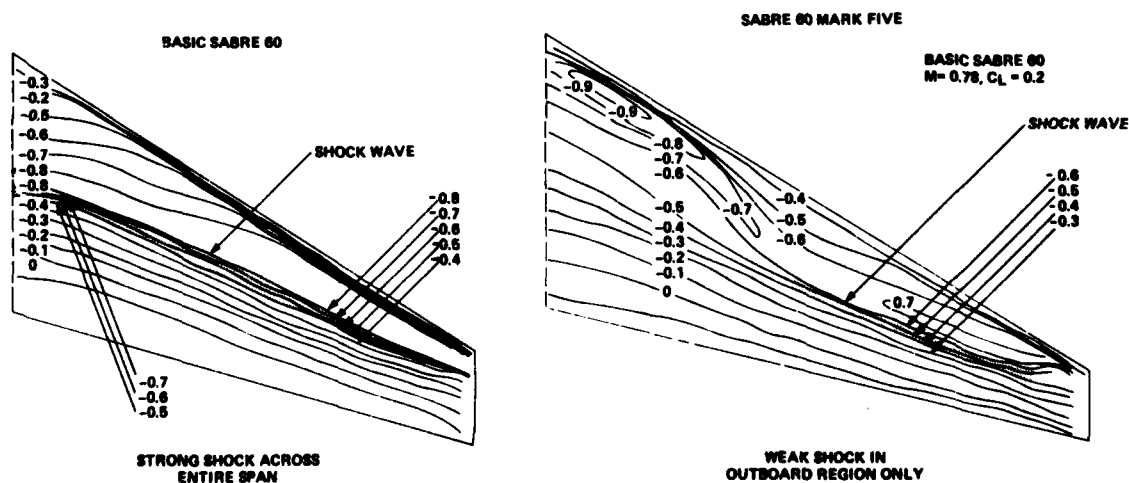
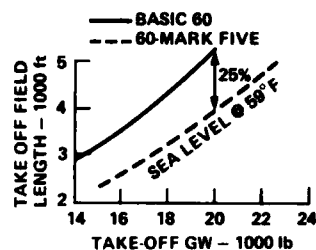
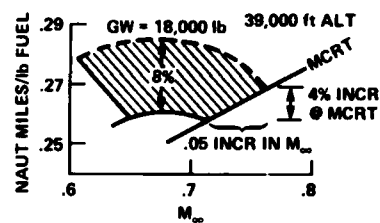


Fig. 4. Comparison of computed isobars for Sabreliner 60 and Sabreliner 60 Mark Five wings: $M = 0.78$, $C_L = 0.27$ (Ref. 19).

- SHORTER TAKE OFF AND LANDING FIELD LENGTHS OR INCREASED FUEL LOAD



- 8% IMPROVEMENT IN FUEL EFFICIENCY AT OPTIMUM CRUISE M_{∞} (OR 4% IMPROVEMENT WITH UP TO .05 INCR IN CRUISE M_{∞})



- 27% INCREASE IN RANGE (UP TO 61% INCREASE FOR SOME TAKEOFF AND FUEL RESERVE LIMITATIONS)

BASIC 60	1540 N.M.
60-MARK FIVE	1980 N.M.

Fig. 5. Summary of results of Sabreliner modification (Ref. 22).

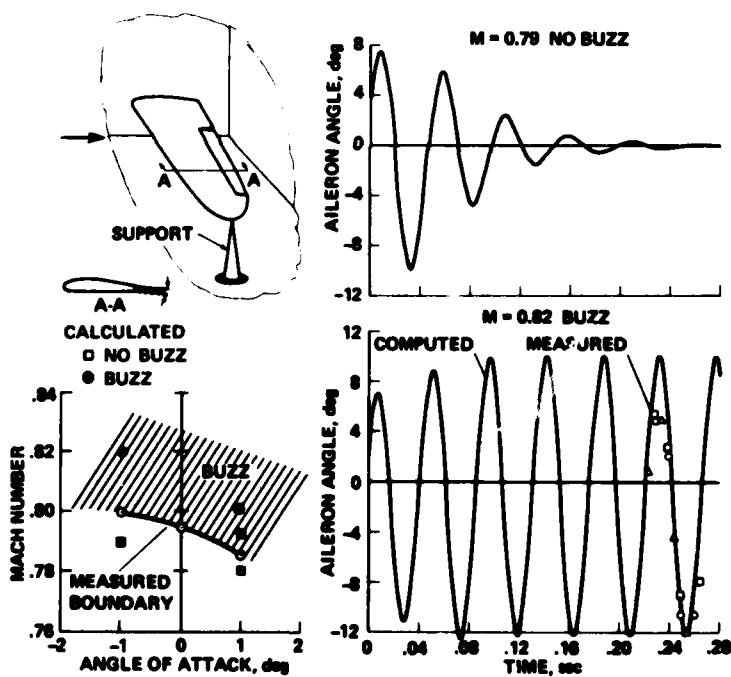


Fig. 6. Reynolds averaged Navier-Stokes simulated and measured characteristics of transonic aileron buzz (Ref. 15).

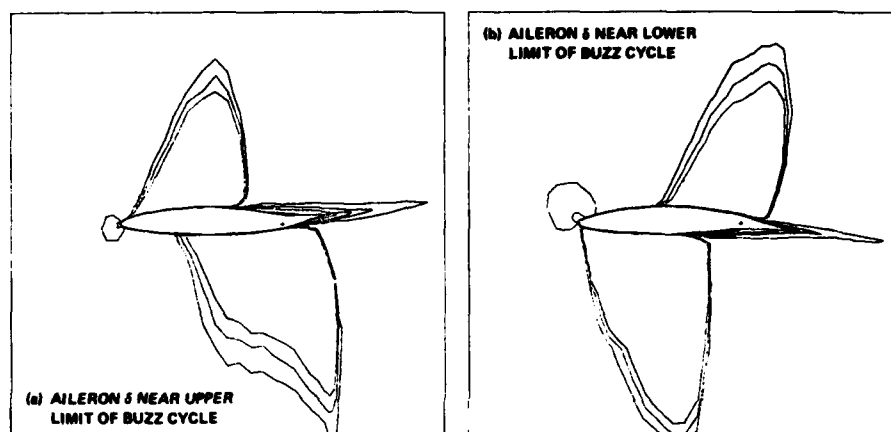


Fig. 7. Reynolds averaged Navier-Stokes simulated flow-field Mach number contours for transonic aileron buzz: $M_\infty = 0.82$, $\alpha = -1^\circ$ (Ref. 15).

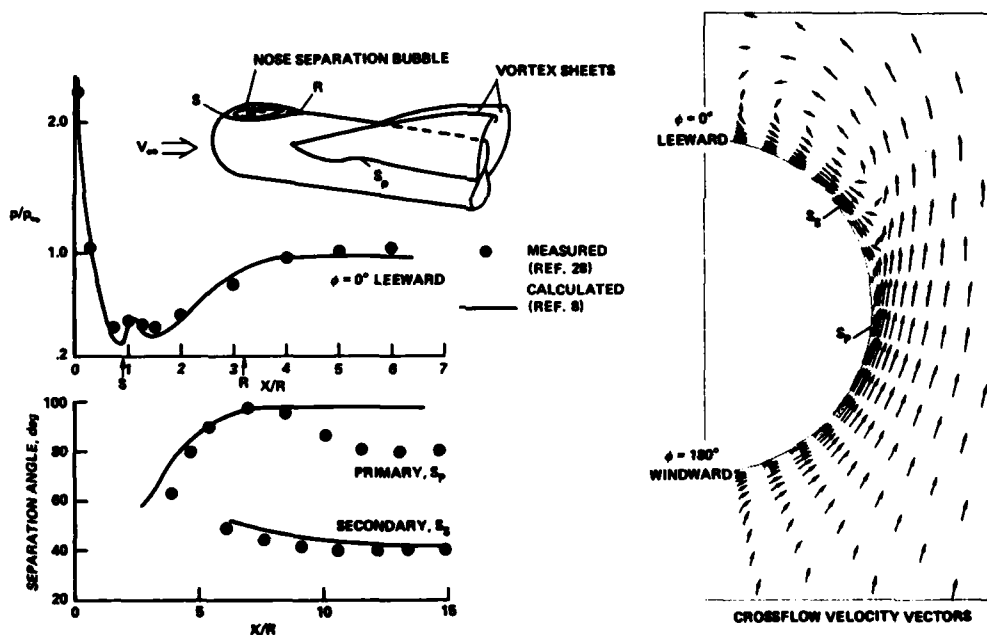


Fig. 8. Reynolds averaged simulated and measured flow characteristics for inclined hemisphere-cylinder body: $M_\infty = 1.2$, $\alpha = 19^\circ$, $Re_D = 445,000$ (Ref. 8).

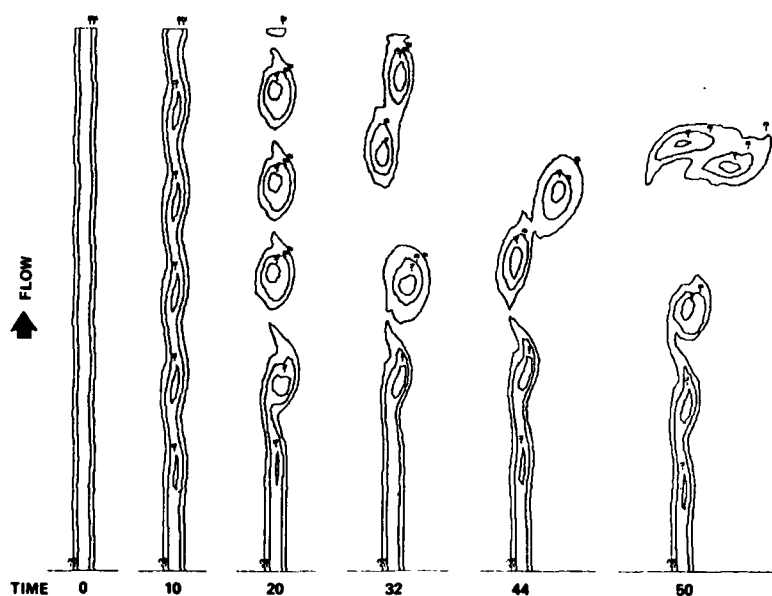


Fig. 9. Large eddy simulation of free-shear layer with 2-D initial disturbance: $M = 0.5$, unpublished results of A. Wray (1979).

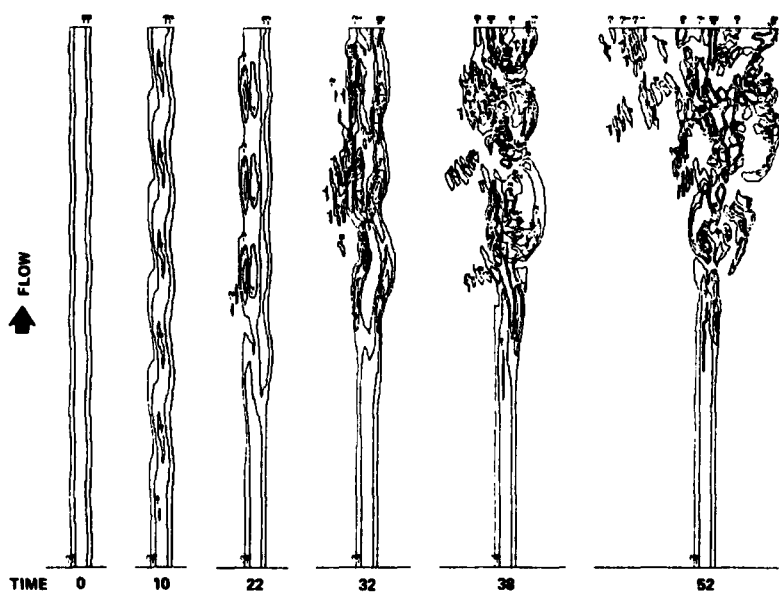


Fig. 10. Large eddy simulation of free-shear layer with 3-D initial disturbance: $M = 0.5$, unpublished results of A. Wray (1979).

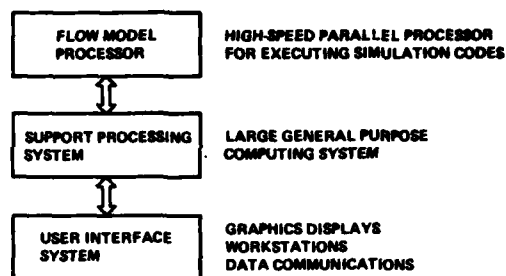


Fig. 11. Numerical Aerodynamic Simulation Facility distributed system hierarchy.

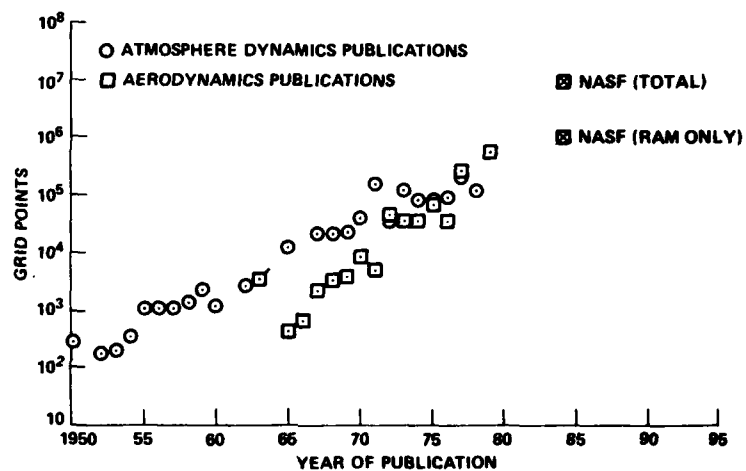


Fig. 12. Growth in maximum number of grid points used in computational publications (Ref. 1).

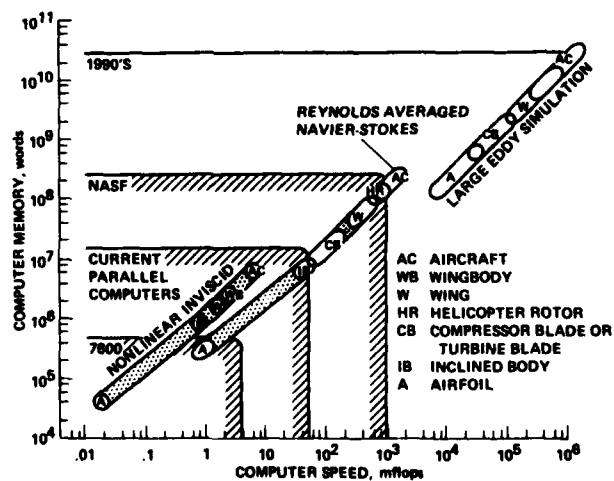


Fig. 13. Computer speed and memory requirements for aerodynamic simulations compared with large computer capabilities (Ref. 1).

UTILISATION DE L'ORDINATEUR POUR LE DESSIN DE CONFIGURATIONS AERODYNAMIQUES

par

Pierre PERRIER

Chef du Département des Etudes Théoriques Aérodynamiques

Division des Etudes Avancées

AVIONS MARCEL DASSAULT-BREGUET AVIATION

78, quai Carnot - 92214 ST CLOUD (France)

0. INTRODUCTION

0.1 - Le dessin des formes extérieures, pour des raisons de conception aérodynamique, a un rôle extrêmement important dans la conception de l'avion parce que la peau extérieure contient l'ensemble des équipements et, par ailleurs, que cette peau est la partie résistante de l'avion. Par conséquent, un changement important dans la définition des formes aérodynamiques de l'avion peut correspondre à une dépense très élevée. Aussi, y aura-t-il deux raisons pour réaliser au mieux ces formes aérodynamiques, d'une part pour obtenir les performances souhaitées du véhicule aérien et, d'autre part, comme assurance contre les erreurs de conception qui coûteraient très cher, en prix et délais, dans le développement du programme correspondant.

0.2 - Pour acquérir la définition aérodynamique de l'avion, on utilisait autrefois des raisonnements et des calculs très simples, associés à des essais en soufflerie de maquettes. L'utilisation systématique de l'ordinateur dans la conception aérodynamique des avions est relativement récente ; elle résulte de l'amélioration des puissances de calcul des ordinateurs et du développement de méthodes de calcul numérique adaptées.

Nous remarquerons qu'il faut nettement séparer les problèmes de conception et d'identification d'une configuration aérodynamique qu'on identifiera aussi comme problèmes d'optimisation et d'évaluation. Dans ces deux cas, l'ordinateur apporte une aide considérable avec, cependant, des efficacités très différentes et des méthodes d'emploi également très différentes.

On insistera sur le fait que ces opérations d'optimisation et d'évaluation ne sont pas équivalentes à des opérations d'analyse et de synthèse auxquelles on fait allusion habituellement dans le développement d'un projet d'avion ; l'analyse est plus typiquement une recherche et une compréhension des phénomènes en cause et des moyens à apporter pour remédier aux déficiences aérodynamiques relevées et la synthèse est davantage une intégration globale du produit en général. On la réalise par une adaptation de paramètres globaux simples entre des points extrêmes qui ont été eux-mêmes étudiés dans une étude systématique (surface, flèche moyenne, ...).

0.3 - Nous allons présenter successivement dans ce rapport les principes de conception et la terminologie employée pour la conception et l'identification, avec les différents niveaux de calcul associés qui sont d'usage systématique aux AVIONS MARCEL DASSAULT-BREGUET AVIATION pour concevoir les nouveaux prototypes.

Nous présenterons ensuite deux exemples concrets relativement simples, relatifs à des avions civils et militaires, permettant de voir ce qu'apporte l'introduction de l'ordinateur dans cette conception aérodynamique, puis nous montrerons comment ces principes sont généraux et font l'objet de méthodes tout à fait générales de conception aérodynamique assistée par ordinateur qui sont effectivement en service dans notre Société.

Enfin, on indiquera les développements qui peuvent être prévus dans les années à venir, compte tenu de l'amélioration des possibilités de calcul qui est envisageable.

1. REMARQUES GENERALES ET TERMINOLOGIE

1.1 - Le développement continu

Pour concevoir tout produit industriel, un bureau d'étude procède suivant deux démarches complémentaires. Une démarche traditionnelle qui est une amélioration du produit par sélection successive des meilleurs compromis. Dans le cas où un produit industriel a une longue tradition de développement antérieur et où le nombre de variantes du produit est relativement élevé, le processus du bureau d'étude consiste à corriger les défauts qui ont été remarqués dans la production antérieure et à déplacer le compromis dans le sens qui améliorera les qualités les plus remarquables du produit ou les qualités qui font l'objet d'un déficit par rapport à la concurrence.

Ceci suppose un développement continu des connaissances et c'est la démarche qui assure la plus grande sécurité, y compris dans le développement général des configurations aérodynamiques d'avions. Ce type de développement est employé systématiquement par le bureau d'étude des AVIONS MARCEL DASSAULT-BREGUET AVIATION et constitue une base saine et nécessaire de tout nouveau projet.

1.2 - La conception en vue d'objectifs nouveaux

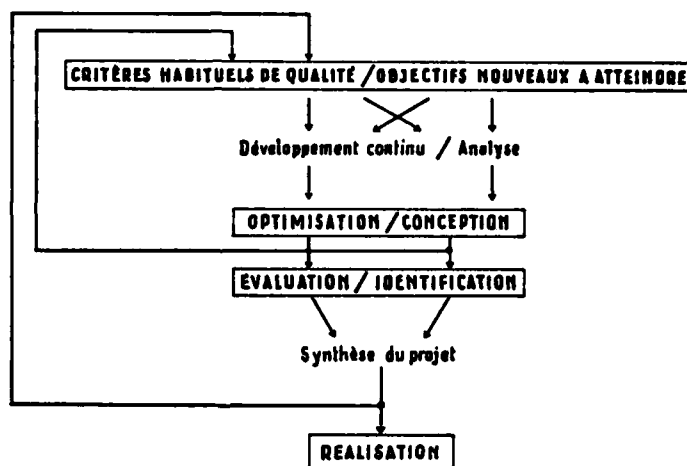
Par ailleurs, en plus de cette gestion par sélection et par amélioration des produits précédents, une conception complémentaire doit être faite en fonction des objectifs à atteindre. En effet, le choix des objectifs à atteindre changeant sur le nouveau produit, il est important de concevoir le nouveau produit en fonction des nouveaux objectifs. Dans la mesure où ces nouveaux objectifs ne sont pas recouverts par les anciens produits, et dans la mesure où ces objectifs sont nouveaux par rapport aux anciens produits, la conception sera nouvelle et l'ensemble des moyens à mettre en oeuvre au point de vue étude, recherche et développement, portera sur un nouveau problème. Il est souhaitable que la part de la conception attachée à satisfaire des objectifs nouveaux soit limitée dans un nouveau projet, de sorte que la part qui ne bénéficie pas d'une grande expérience soit limitée et fasse l'objet d'une évaluation précise.

1.3 - L'identification finale

L'identification du produit final ne se fera, en fait, qu'en essais en vol sur l'avion définitif, mais on peut imaginer un certain nombre d'étapes intermédiaires à base d'essais en soufflerie de la maquette la plus grande possible et la plus représentative possible et de calculs à l'aide du maillage le plus serré possible.

Dans la phase d'identification, le souhait sera de reconstituer le mieux possible les qualités et les bases de calcul du nouveau produit, alors que dans la phase de conception le but sera, sur un certain nombre de points objectifs, de réaliser le meilleur dessin aérodynamique possible, c'est-à-dire de supprimer des décollements ou de réduire des intensités de choc par exemple.

A partir de la définition de ces formes aérodynamiques, il sera possible, quand elles seront finalisées, de passer à la réalisation du produit industriel et là nous rentrerons dans une phase de conception des différents éléments structuraux et de réalisation proprement dite de l'avion. Dans cette phase, peut être comprise, en partie, la réalisation de maquettes grandeur ou de maquettes de taille importante destinées à l'identification en soufflerie ou à l'identification en essais statiques de l'avion.



1.4 - L'interaction avec le bureau d'étude

Cependant, il est important de noter que l'itération sur la conception aérodynamique des formes est beaucoup plus en liaison avec l'itération de type aérodynamique générale et calcul de performances qu'avec le détail de la réalisation des pièces qui constitueront le produit, alors que l'identification de l'avion suppose une définition de détail complète et suppose donc que le dessin de la structure et l'aménagement soit très avancé.

Comme la forme aérodynamique contient l'ensemble de la structure de l'avion et les équipements de l'avion, il y aura une interaction continue entre le groupe de conception des formes aérodynamiques et le responsable du projet et de son intégration en général, qui doit jouer à plein son rôle d'architecte du projet, en orientant l'ensemble des choix en fonction des objectifs qui ont pu être identifiés comme étant, soit difficiles à atteindre, soit impossibles, soit trop faciles à atteindre. Pour cela, il est nécessaire, pour le responsable du projet, de définir, avec de plus en plus de précision, ses demandes au fur et à mesure de l'élaboration des formes aérodynamiques et de leur évaluation détaillée.

L'obligation d'introduire des données précises dans l'ordinateur conduira finalement à une bien plus grande somme de réflexions rationnelles que dans le processus classique où le concepteur général ne pouvait qu'étudier un nombre limité de variantes et n'avoir qu'une évaluation globale pour un nombre limité d'itérations de conception aérodynamique résultant des essais en soufflerie.

1.5 - Les rôles fondamentaux de l'ingénieur dans une conception assistée par ordinateur

On insiste sur le fait que le rôle de l'homme est beaucoup plus important dans un système de conception assistée par l'ordinateur des formes aérodynamiques que dans un système classique d'itérations sans usage de l'ordinateur. Car, d'une part, les questions posées à l'architecte sont beaucoup plus précises sur les objectifs à atteindre et sur les valeurs relatives des différents objectifs à atteindre ; d'autre part, les demandes à satisfaire, au point de vue aérodynamique, sont beaucoup plus précises puisque résultant d'une analyse plus complète du problème et, par conséquent, nécessitent une réflexion plus importante sur les meilleurs moyens à mettre en oeuvre pour avoir des formes efficaces sur l'ensemble des points de vol retenus.

On insiste sur les éléments de compromis qui sont fournis par une série de calculs en ordinateur et qui devraient permettre d'accéder à une meilleure qualité globale du produit. On pourra ainsi distinguer deux niveaux très différents d'intervention : un niveau où on jouera directement sur le paramètre, qui a été reconnu comme devant être travaillé, et un niveau où on jouera sur des quantités plus analytiques et élémentaires. Par exemple, pour une étude de traînée de profil en transsonique, la demande correspondra systématiquement à un certain niveau de traînée et on pourra, soit optimiser directement cette traînée si elle est accessible au programme de calcul élémentaire ou, au contraire, remonter à une évaluation plus simple correspondant, par exemple, à une minimisation d'intensité de choc ou à un écoulement non décollé élémentaire.

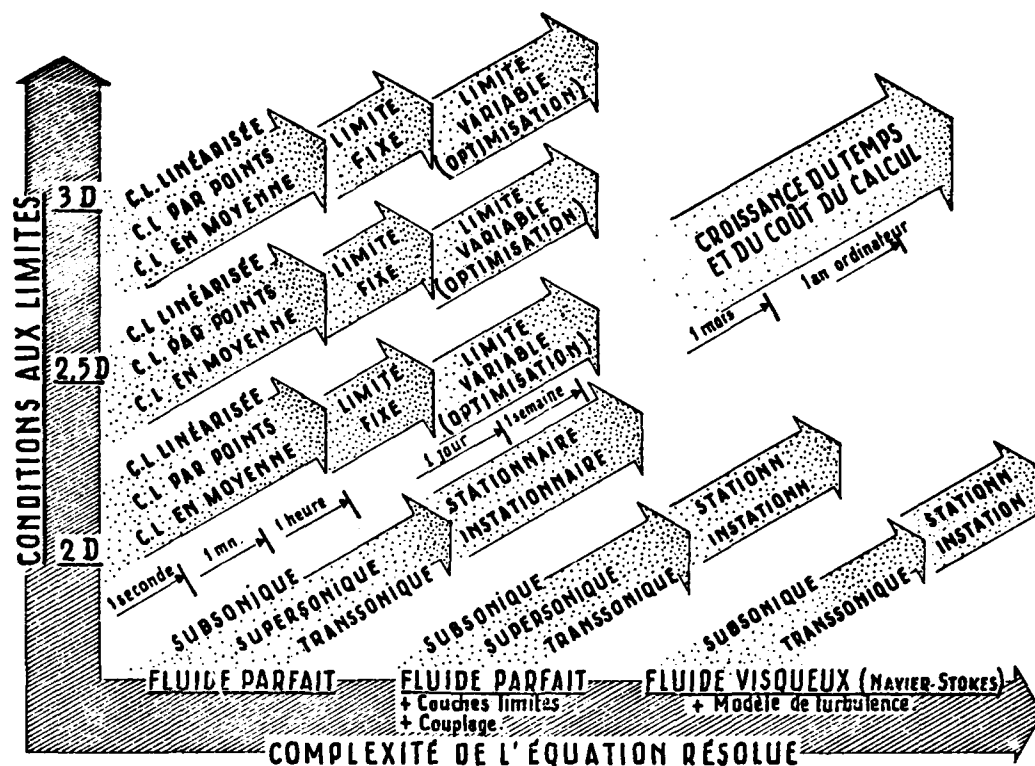
Suivant les cas, le choix sera plus ou moins économique en temps de calcul ordinateur et, par conséquent, on voit la très grande importance de l'ingénieur dans les boucles de conception des formes par ordinateur, puisque le choix des meilleurs moyens à mettre en oeuvre et des moyens en calcul par ordinateur sera primordial sur le coût et le délai nécessaire pour obtenir une convergence du processus de conception aérodynamique de l'avion.

Cette importance de l'ingénieur responsable de l'aérodynamique sera développée par l'expérience qu'il acquerra, et dans la connaissance des phénomènes aérodynamiques de base et dans leur application sur différents avions, et dans l'application des méthodes d'écoulement qui sont retenues pour le travail sur ordinateur.

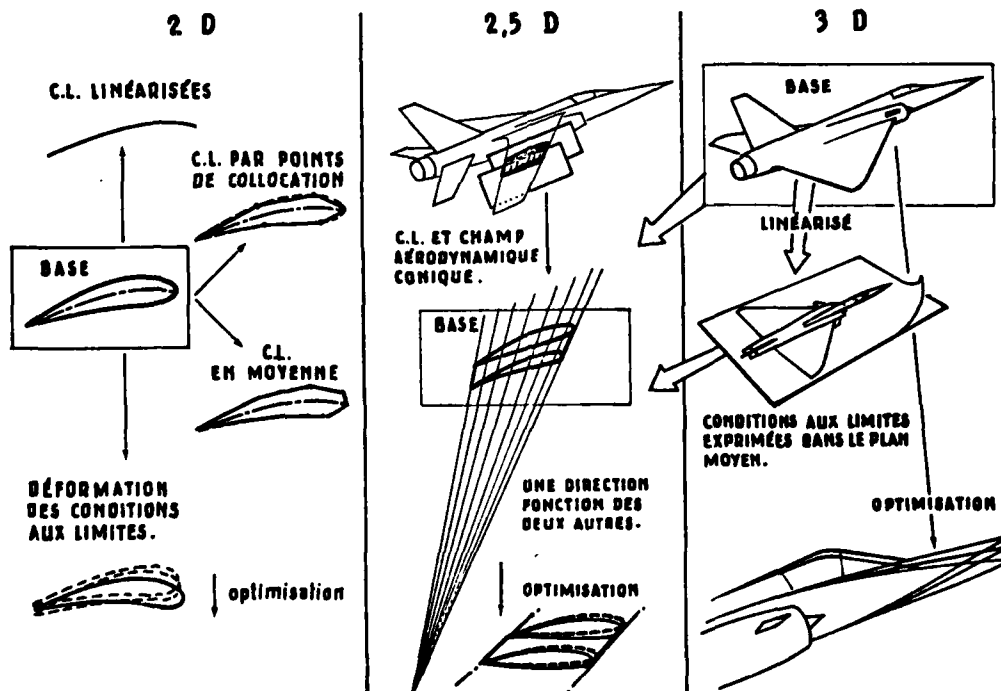
De toute façon une étude systématique d'influence des principaux paramètres est nécessaire pour que l'ingénieur soit aidé dans son bon sens et son intuition ; au cours de la recherche du meilleur compromis global il pourra ainsi sans perdre sur les performances critiques bien évaluées se placer au mieux pour satisfaire à des critères non évaluables mathématiquement de simplicité, accessibilité aux équipements, etc...

1.6 - Les méthodes de calcul et le compromis coût-précision

Avec un peu d'entraînement un ingénieur pourra choisir le meilleur compromis coût-efficacité pour avoir la réponse à un problème aérodynamique, mais de plus il devra pouvoir évaluer la relation coût-précision qui est fondamentale à cause des simplifications souvent nécessaires qu'il faut effectuer pour rendre calculable un écoulement complexe. Par exemple, si l'on veut faire une optimisation en traînée d'onde d'un avion nouveau en transsonique on peut se contenter dans un premier temps d'utiliser un programme linéarisé de traînée d'onde d'un corps de révolution équivalent. Ce programme a un temps de calcul extrêmement court et peut donc être rendu interactif ou mieux être optimisé directement, ce qui fournira les points sensibles de la loi des aires et les zones peu coûteuses. Pour aller plus loin dans la précision de calcul on pourra remplacer le fuselage seul par un corps de révolution équivalent et la voilure par une plaque linéarisée avec un programme d'interaction. On pourra enfin calculer l'avion complet sans linéarisation des conditions aux limites et en fluide parfait ou en tenant compte des couches limites et sillages ou même des zones décollées. La gradation en complexité et en coût de calcul dépend ainsi et de la qualité de résolution des équations et de la qualité de la représentation géométrique de l'avion. Cette dépendance est schématisée dans la figure 2 ci-dessous. Les temps de calculs passeront de quelques centièmes d'heure à des centaines d'heures avec les ordinateurs actuels si on a été trop ambitieux sur le nombre de degrés de liberté et la valeur maximale du nombre de Reynolds équivalent dans une résolution des équations complètes de Navier-Stokes.



Nous avons séparé dans ce tableau les conditions aux limites en fonction de la dimension de l'espace 2, 2,5, 3D avec limites fixes ou variables. Les calculs bidimensionnels (2D) et tridimensionnels (3D) sont bien connus et couvrent aussi bien les cas axisymétriques ou les cas à topologie simple (description possible par une surface à deux paramètres sans singularité tel le cas d'une aile seule) ou complexe (description impossible par une surface à deux paramètres mais multiples points ou lignes singulières pour un avion complexe quelconque). Par contre, la solution peut souvent être approchée très valablement par une fonction de deux coordonnées seulement, la dépendance vis-à-vis de la troisième étant explicite. C'est par exemple le cas d'un profil d'aile d'allongement élevé pour lequel les caractéristiques aérodynamiques varient peu en fonction de l'envergure bien que l'écoulement ne soit pas bidimensionnel par suite des flèches de bord d'attaque et de bord de fuite, ou de la variation de circulation en envergure ; on parlera alors de calculs 2,5D cf. figure 3 ci-dessous.



1.7 - Les degrés de liberté et les contraintes nécessaires

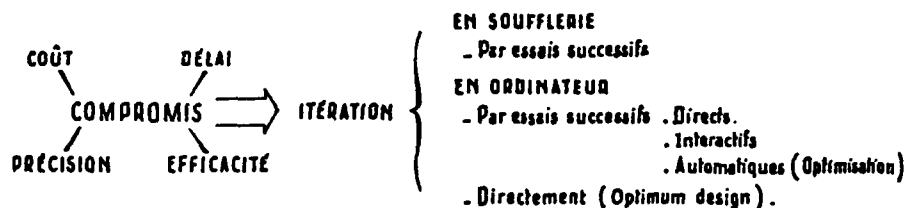
Les calculs aérodynamiques conduisent l'ingénieur responsable à modifier les formes aérodynamiques au mieux des objectifs visés. Mais en fait sa liberté est assez limitée par suite des nombreuses contraintes de conception non liées à l'aérodynamique mais liées à la résistance des matériaux, à l'aéro-élasticité ou plus simplement au volume requis pour les équipements ou le carburant ou pour la fabrication. Ces contraintes pourront s'exprimer par des points de passage obligés ou par des raccordements déterminés ou par l'existence de surfaces réglées ou de révolution. On pourra aborder deux stratégies opposées pour tenir compte de ces contraintes, soit les mettre dans les pénalisations que l'on ajoute à la fonction coût principale d'optimisation (la traînée dans un cas de calcul par exemple) sous forme de coûts additifs dépendant de l'écart entre contrainte désirée et réalisée (écart de volume de caisson de voilure par exemple pour le carburant à une valeur de référence souhaitée) ou bien en limitant les degrés de liberté de façon à satisfaire la contrainte (famille des déformations acceptables de profil passant toutes par les mêmes points d'épaisseur de longeron avant par exemple).

La deuxième procédure est plus économique car elle n'introduit pas de degrés de liberté inutiles, par contre elle n'est pas générale car les contraintes sont souvent complexes.

Nous verrons que ces demandes conduisent à une définition géométrique spécifique des formes que nous décrirons au paragraphe 3.3.1 ci-dessous, ou bien à un maillage de l'espace lors des déformations possibles qui permette la prise en compte de déformations acceptables.

1.8 - Optimisation manuelle, interactive, automatique

On distinguera dans la suite les optimisations interactive et automatique dans le processus de conception assisté par ordinateur par opposition à l'optimisation manuelle. Une optimisation interactive consiste en une série de calculs de temps unitaires assez courts et dont les résultats peuvent être présentés de façon suffisamment claire sur un écran de visualisation graphique pour que les paramètres d'un nouveau calcul puissent être très rapidement évalués et réintroduits dans l'ordinateur, qui donnera une nouvelle réponse ; et ainsi de suite jusqu'à satisfaction de critères moyens analogiques exprimés sur les chiffres, les courbes et graphiques présentés en sortie sur l'écran. Un temps élémentaire de calcul de quelques secondes et une réflexion inférieure à la minute sont des chiffres corrects dans une utilisation de ce type. Au-delà ou en-deçà le problème est trop simple ou trop complexe pour être étudié interactivement et il vaut mieux employer un processus automatique. Celui-ci suppose l'évaluation d'un critère de qualité ou de coût et la possibilité de modifier correctement les paramètres d'entrée du calcul. Citons comme exemples caractéristiques de programmes interactifs d'usage courant aux AMD-BA : lissage de courbes, optimisation de traînée, de portance, de décollements sur des profils, de répartition en envergure, d'équilibre longitudinal de l'avion etc... La figure 4 montre un exemple d'utilisation interactive d'un écran à photostyle d'entrée dans le 4e exemple ci-dessus.

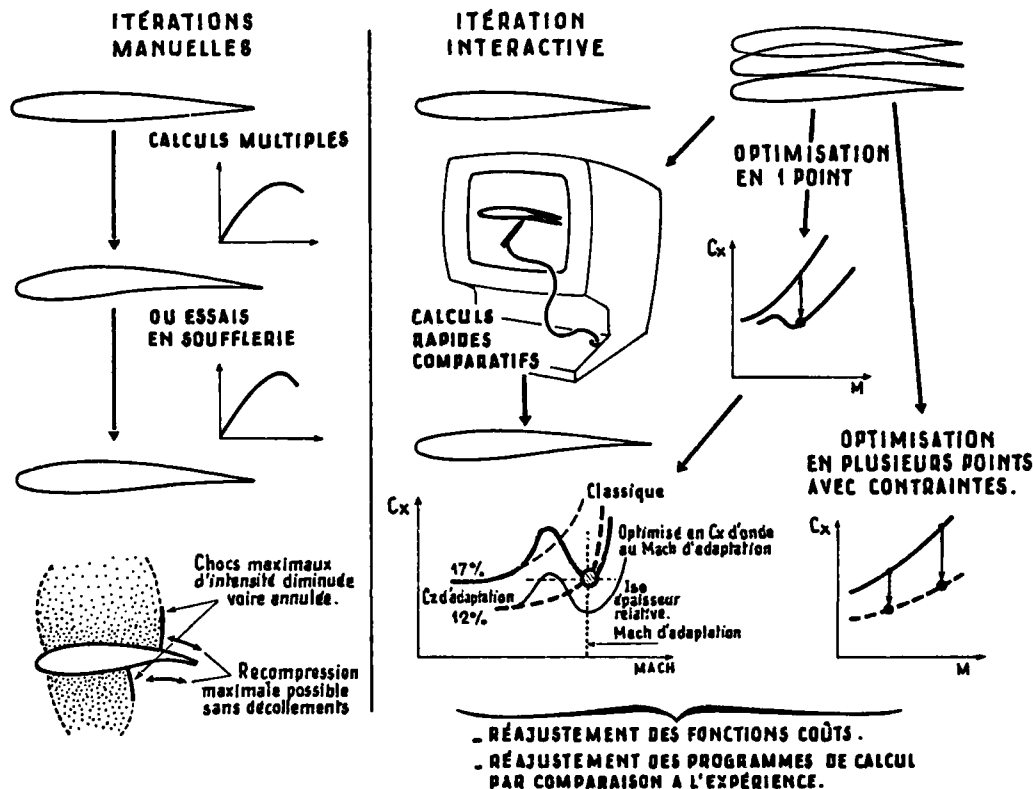


2. EXEMPLES DE CONCEPTION AERODYNAMIQUE

2.1 - Pour montrer les processus nouveaux de conception qu'il est possible d'utiliser grâce à l'introduction systématique de l'ordinateur nous allons retenir deux exemples élémentaires. L'un correspond au dessin d'un profil en transsonique et l'autre au dessin d'intégration d'une entrée d'air en supersonique. Les deux exemples ne seront pas étudiés ni explicités en détail, mais seulement pour un nombre restreint de cas de calcul de façon à mettre en évidence la nouveauté de la méthodologie plus que la façon exacte dont on l'emploie dans une étude industrielle.

2.2 - Etude d'un profil

Nous avons résumé dans la planche ci-dessous les points caractéristiques de la conception directe ou aidée par ordinateur d'un profil en transsonique.⁽⁶⁾



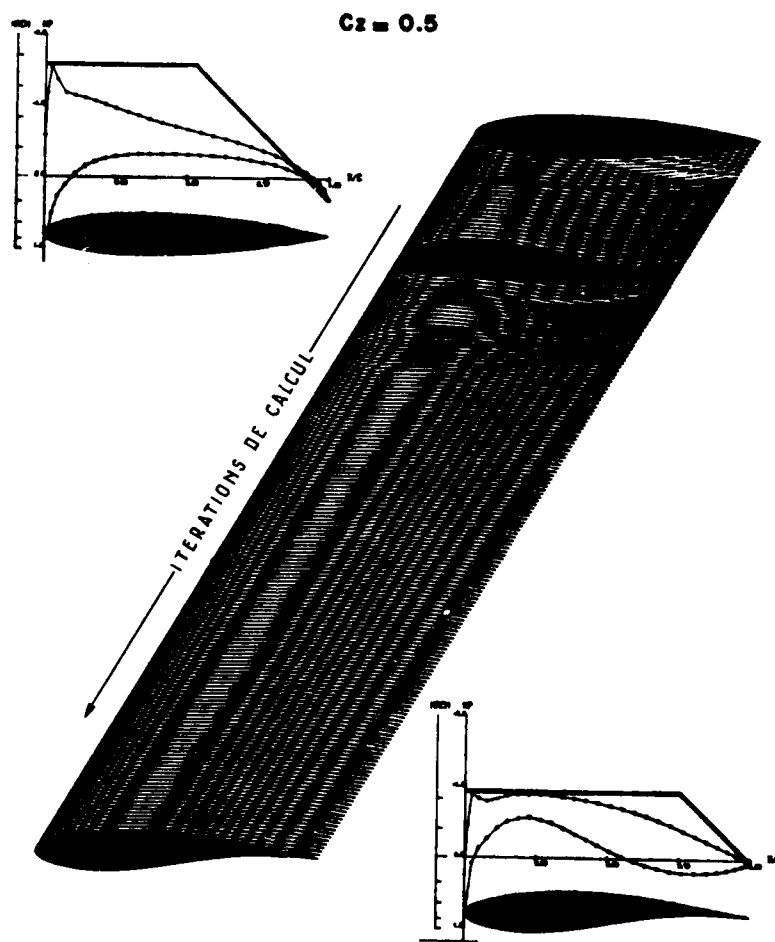
- EXEMPLE DE CONCEPTION DE PROFIL

Dans la conception directe un certain nombre de dessins sont faits manuellement et des calculs simples ou des recueils de résultats expérimentaux permettent de sélectionner quelques profils de qualité probable. Une série d'essais expérimentaux comparatifs permet de sélectionner les courbes de caractéristiques acceptables, excellentes ou inacceptables. Par comparaison on pourra choisir de nouveaux dessins, les redéfinir manuellement et les essayer.

Dans une conception interactive, on effectuera une partie des comparaisons de façon directe et en balayant par le calcul un certain nombre de profils on pourra orienter les choix vers les meilleurs dessins. Ce processus est l'occasion de l'apprentissage très rapide des points sensibles mais peut être moins précis que le procédé manuel direct. En fait on essaie d'optimiser ainsi en un point par essais successifs. On rappelle cependant qu'un tel travail est beaucoup plus risqué que le processus d'itération complet en soufflerie puisque la modélisation doit être sommaire pour avoir des temps de calculs restreints et on n'obtient pas d'information sur les points non optimisés ; ainsi a-t-on couramment des améliorations locales impressionnantes associées à des détériorations de qualité au voisinage de l'optimum. Une façon habituelle d'améliorer ces résultats trop ponctuels est d'étendre l'optimisation à plusieurs points voisins définissant des zones à améliorer. En compensation on retiendra souvent des critères d'optimisation assez simples pour être facilement interprétables. Le résultat d'optimisation entièrement automatique de ce type est souvent excellent et conduit économiquement à des dessins de bonne qualité, que l'on précisera ensuite en faisant appel à des programmes de calcul plus complets et surtout à des optimisations multiples.

On donne ci-dessous un exemple d'optimisation simple où des contraintes d'épaisseur relative au longeron et d'angle minimum au bord de fuite ont été introduites, le calcul est effectué en sub-critique par méthode d'éléments finis, le maillage étant réajusté à chaque itération, et la fonction coût ou la figure de mérite fait intervenir la survitesse maximale et les pentes maximales de recompression des couches limites. On distingue nettement la phase initiale de recherche des influences de base des formes autorisées par les degrés de liberté de définition (phase au cours de laquelle sont balayées même quelques configurations très éloignées du dessin initial ou final caractérisées par une ligne moyenne en S marquée du profil). Après la phase initiale de recherches la descente vers la solution est assez régulière et est limitée par la précision de calcul^⑤

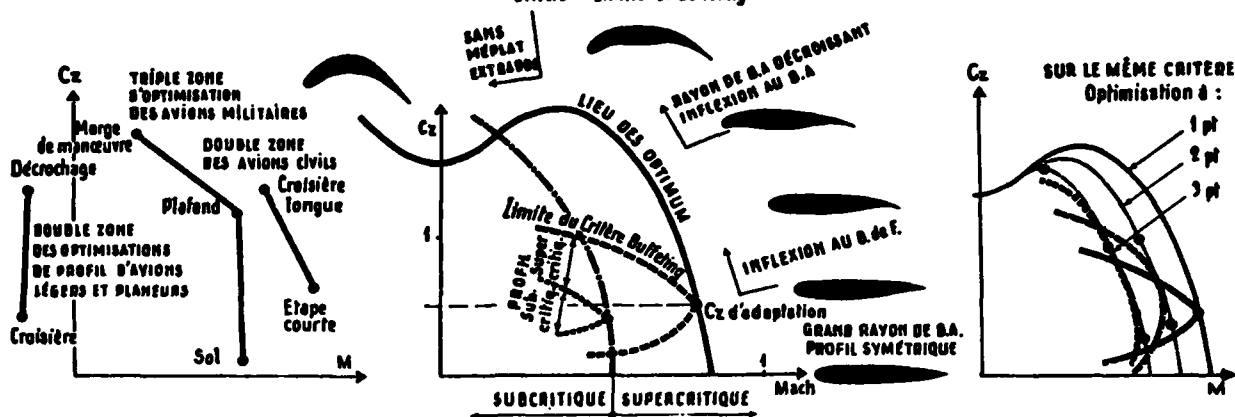
OPTIMISATION D'UN PROFIL PAR UNE MÉTHODE D'ÉLÉMENTS FINIS



Si l'on prend comme critère d'optimisation la traînée d'onde seule et comme contrainte l'épaisseur relative on peut rechercher dans un diagramme portance nombre de Mach la forme des profils optimaux adaptés en chaque point. Ces profils ne sont pas définis dans la zone subcritique, par contre quand le Mach et la portance ont des valeurs suffisamment élevées il n'est plus possible de trouver des solutions sans chocs en transsonique et il existe une forme optimale ayant une traînée d'onde fixée pour chaque point du domaine, si du moins les conditions ne sont pas trop extrêmes, zones où les programmes transsoniques ne convergent plus et n'ont d'ailleurs pas de valeur car les cas réels sont décollés. On peut tracer ainsi une famille de profils : depuis les profils symétriques jusqu'aux profils à grande portance et faible nombre de Mach. Tous sont optimisés ou supercritiques mais ont des formes très variables. On peut penser que de telles familles de profils permettraient de renouveler les vieux catalogues de profils. En fait il n'en est rien car leurs qualités hors adaptation sont souvent mauvaises alors qu'une forme relativement voisine serait acceptable. Aussi doit-on optimiser en deux ou plusieurs points pour garder des qualités pas trop pointues aux profils retenus. Le choix de plusieurs conditions d'adaptation, de plusieurs critères de qualité voire de plusieurs types de contraintes d'épaisseur conduira à une telle variété de profils que l'on renoncera à les cataloguer.

DOMAINE D'OPTIMISATION EN SUPERCRITIQUE

Exemple : épaisseur donnée - Optimisation 1 paramètre
Critère : Limite de buffeting



Nous donnons ci-dessous une comparaison des organigrammes de conception de profils que l'on a utilisé effectivement aux AMD-BA pour la conception de profils nouveaux. On a séparé dans ce tableau l'ancienne conception manuelle, la conception assistée en usage il y a quelques années et la conception par optimisation que nous utilisons systématiquement actuellement. On voit une diminution importante des étapes manuelles de conception. Notons cependant que, si l'intervention de l'homme est moins fréquente, elle est beaucoup plus délicate et exigeante qu'auparavant comme nous l'avons indiqué au chapitre précédent ; notons également que le processus retenu actuellement utilise une combinaison des optimisations interactive et directe et que les procédés d'itération sur les caractéristiques complètes sont justifiés non par des essais de soufflerie bidimensionnels mais par recoupement avec des essais de recherche très détaillés qui servent à évaluer le degré de confiance à accorder aux outils de calcul. On a ainsi repéré les phases de réflexion ou d'intervention manuelle artisanale par le signe ●, les phases de recoupements expérimentaux par les signes E, EX, EXX suivant qu'il s'agit d'expériences globales de pesées, d'expériences avec mesures de pressions et visualisations pariétales, ou d'expériences avec mesures détaillées de champs de vitesse ou couches limites ; les calculs sur ordinateurs sont repérés en calculs directs Δ, inverse ∇ et calculs non aérodynamiques X ou de fabrication en commande numérique. Les calculs d'optimisation où l'ordinateur effectue automatiquement les itérations à partir des indications des fonctions coûts successives sont indiqués par 0 en opposition aux méthodes interactives I. Celles-ci sont actuellement une part décroissante mais non négligeable ni complètement réductible du processus complet. Rappelons que l'on n'indique ci-dessous que le processus de conception aérodynamique et que cette conception sera un mélange des trois types ci-dessous suivant les possibilités de calcul et le cas étudié.

Conception manuelle	Conception assistée	Conception/optimisation
<ul style="list-style-type: none"> ● Choix des conditions de conception ● Choix de critères expérimentaux ● Evaluation des squelettes/épaisseur ● Compromis sur les formes ● Maquettage pour soufflerie E Essais extensifs en soufflerie ● Exploitation des essais ● Modifications squelette/épaisseur ● Choix de la solution ● Maquettage soufflerie E Identification en soufflerie ● Traçage pour fabrication 	<ul style="list-style-type: none"> ● Choix des cond. ● Choix des pressions souhaitées ∇ Calcul inverse ● Compromis sur les formes Δ Calcul direct transsonique ● Comparaison transs./subs. ● Maquettage EX Soufflerie sur qq. profils ● Exploitation des essais I Amélioration de dessin ● Choix de la solution X Maquettage C.N. EX Identification soufflerie * Fabrication 	<ul style="list-style-type: none"> EXX Essais de recherche ● Choix des cond. ● Choix des critères/coûts Δ Recalcul de cas voisins ● Choix des points d'opt. ○ Optimisation autom. Δ Identification calcul ● Exploitation calcul X Calculs non aérody. I Améliorations locales ● Choix X Maquettage C.N. EX Identification soufflerie * Fabrication

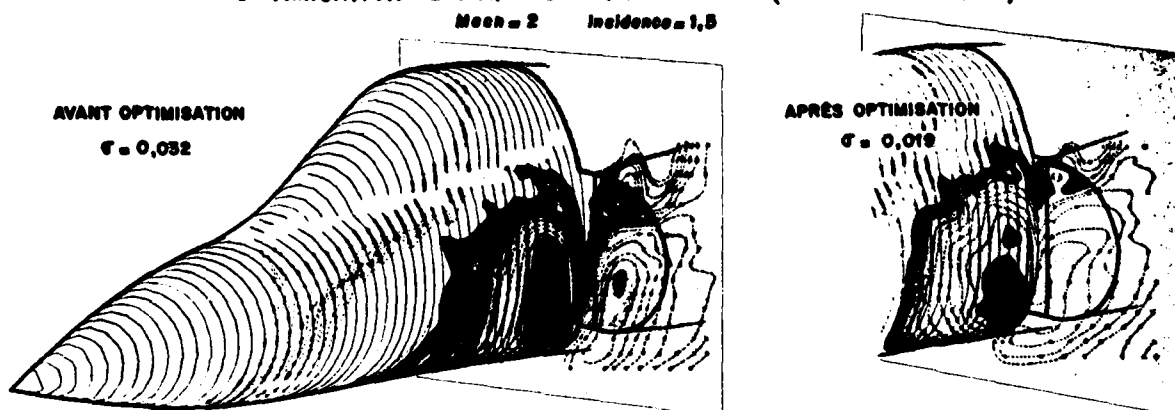
2.3 - Etude d'un élément de surface d'avion

On pourrait développer en détail la conception d'un élément de surface suivant une procédure analogue mais des problèmes nouveaux sont posés par la complexité du maniement des surfaces et également par la difficulté de définir nettement les fonctions et les critères de qualité à attendre de cette portion de surface. Nous montrerons cependant sur un exemple sans ambiguïté que l'optimisation^① peut remplacer avantageusement dans certaines parties de l'avion un processus d'essai et erreur classique ; beaucoup de travail d'analyse reste encore nécessaire pour clarifier les choix des formes optimales de la plus grande partie du fuselage et de l'interaction des choix aérodynamiques, structuraux et de dessin général.

Considérons une entrée d'air montée sur un fuselage en écoulement supersonique. Pour optimiser les distorsions dans le plan d'entrée d'air il est nécessaire de modifier les formes fuselage en amont pour assurer dans plusieurs conditions d'incidence et de vitesse à l'infini amont des fluctuations en grandeur et direction de vitesse dans le plan de l'entrée d'air aussi faibles que possible. On pourra prendre comme critère d'optimisation l'écart-type de la fluctuation par rapport à la valeur moyenne ou toute autre mesure de la distorsion moyenne ou extrême et comme contraintes les contraintes de fabrication habituelles ou de raccordement de cabine. On donne ci-dessous un exemple d'un tel calcul ; le gain obtenu sur la distorsion est de près de 40 % pour des modifications mineures du fuselage.

EXEMPLE DE CONCEPTION DE FUSELAGE OPTIMISATION DE CARTE D'ENTRÉE D'AIR (EN SUPERSONIQUE)

Mach = 2 Incidence = 1,5



Une chaîne de conception assistée sur ordinateur peut être mise en place comme pour un profil ; son organigramme est présenté dans les mêmes conditions ci-dessous, avec les mêmes signes schématisés, dans les cas d'optimisation manuelle, interactive ou d'optimisation pour permettre une évaluation comparée de même type. On notera l'introduction d'une phase de maquetage non pour essais mais pour évaluation directe à l'oeil du résultat de l'optimisation, par suite des difficultés de représentation graphique des formes générées par l'ordinateur.

Conception manuelle	Conception interactive	Conception/optimisation
<ul style="list-style-type: none"> • Choix des conditions de conception • Dessin d'un plan de forme • Tracé du pl. de f. • Maquetage manuel • Retouches de pl. de f. • Maquetage pour soufflerie E Essais soufflerie, visualisations • Exploitation des essais • Modifications en soufflerie • Choix de la solution E Identification en soufflerie • Tracé pour fabrication 	<ul style="list-style-type: none"> • Choix des cond. • Dessin du pl. de f. ▽ Calcul inverse I Entrée/lissage Δ Maquetage C.N. I Retouches pl. de f. Δ Calcul d'identification • Exploitation calcul Δ Maquetage C.N. soufflerie E Essai de qq. formes • Exploitation des essais I Améliorations locales • Choix du meilleur dessin Δ Maquetage C.N. soufflerie EX Identification soufflerie ★ Fabrication 	<ul style="list-style-type: none"> EXX Essais de recherche • Choix des conditions • Choix critères/coûts Δ Recalcul de contrôle • Dessin d'un pl. de f. I Entrée/lissage Δ Maquetage C.N. Δ Optimisations locales Δ Ident. calcul aéro. • Exploitation calculs I Modifications locales • Choix du meilleur dessin Δ Maquetage C.N. pour souff. EX Identification souff. ★ Fabrication

3. METHODOLOGIE GENERALE

3.1 - Les outils de calcul aérodynamique

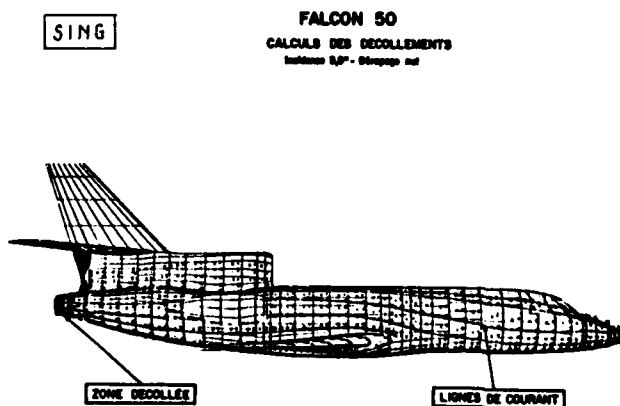
Pour pouvoir utiliser efficacement les procédures de conception assistée par ordinateur il faut en fait bénéficier de toute une gamme de méthodes de calcul dont la durée et le coût (combinaison de la durée et de la taille du programme et de ses fichiers et des coûts d'exploitation en entrée sortie) soient très variables. Les plus rapides (conditions aux limites et équations linéarisées, dimension réduite à 2 ou 2,5) serviront aux boucles d'itérations rapides d'optimisation directe ou interactive, les plus longs aux analyses complètes d'écoulements ou aux calculs d'identification, et ne pourront être utilisées en optimisation que pour des fonctions coût dérivables et optimisables mathématiquement (optimum design).

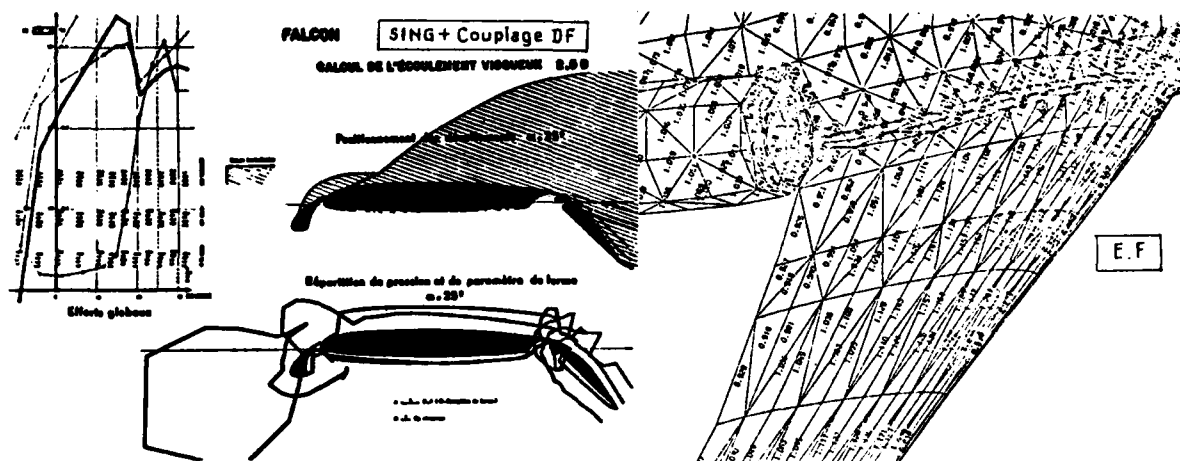
Nous n'insisterons pas sur les programmes bidimensionnels soit plans soit axisymétriques utiles dans les petites itérations nécessaires en début de projet et d'usage habituel dans l'industrie aéronautique. Par contre les outils tridimensionnels sont indispensables pour concevoir effectivement un avion dans le détail. Ils doivent pouvoir être utilisés soit en 3D pur soit en 2,5 D (cf. § 1.6 et Pl. 2) pour avoir accès à des temps de calcul plus courts ou à des discrétisations plus serrées. On rappelle que le calcul en 2,5 D peut être par exemple effectué avec la dépendance suivant la direction de conicité de la voilure ou du fuselage approchée par la dépendance calculée sur une discrétisation grossière. Un calcul préalable permet d'estimer le gain de précision que l'on peut atteindre en faisant une simple influence de taille des maillages.

Les outils en service continuels doivent couvrir les besoins de calcul aux grandes portances, aux petites portances et aux grandes incidences; les premiers calculs correspondant aux conditions de décollage et d'atterrissage portent sur le dessin des hypersustentateurs, les seconds sur le dessin en croisière ou en grande vitesse, les derniers aux calculs des configurations à grande incidence. Les méthodes de calcul font appel aux méthodes de singularités (SING), de différences finies (D.F.) ou d'éléments finis (E.F.). Pour le cas des AMD-BA les choix retenus en 3 D/2,5 D sont les suivants :

Type	Grandes portances hypersustentation	Petites et moyennes portances			Grandes incidences
Régime	Subsonique	Subsonique	Transsonique	Supersonique	Transsonique
Equations	Fluide parfait + couplage	F.P. + couplage	F.P. + couplage	F.P.	Navier-Stokes + modélisation
Méthode	Sing 2,5 D + équi- librage 3 D ①②③	Sing. ①	D.F. ⑦ E.F. ⑧⑨	D.F. ②	E.F. ③④

Nous donnons ci-dessous des exemples de calcul typiques qui permettent de voir l'emploi caractéristique des différents programmes de calcul. Pour le détail des méthodes employées on renvoie aux références citées dans la bibliographie ; un tableau général est donné en annexe.





3.2 - Les outils d'optimisation

Les méthodes d'optimisation directe par l'ordinateur, comme base des évaluations précises de formes, nécessitent deux types d'outils numériques suivant que l'on peut exprimer, ou non, mathématiquement les dérivées des fonctions coûts et le problème physique résolu. Si ce dernier est représenté par une équation aux dérivées partielles, et que le coût est exprimé mathématiquement, alors on doit développer les outils efficaces qui en tiennent compte et qui expriment l'optimisation de la fonction coût vis à vis des modifications des points du maillage qui correspondent aux formes libérées; cette optimisation viendra comme boucle extérieure dans les boucles de contrôle optimal utilisées pour résoudre le problème direct.

Si au contraire le problème physique est complexe et représenté par des équations de couplage fluide parfait, fluide visqueux, ou des formes approchées et si la fonction coût est complexe et non différentiable, alors on utilisera une recherche itérative des minima de la fonction-coût à l'aide de programmes de minimisation et l'on sera limité par le nombre de degrés de liberté. Le programme de minimisation étant général il devra être conçu de façon à accepter n'importe quel programme aérodynamique comme sous-programme. On pourra ainsi optimiser au choix un nombre de Mach maximum en transsonique ou une traînée à portance donnée, ou un paramètre de forme de couche limite etc

Notons que la minimisation de l'écart de la répartition de pression à une répartition voulue, constitue le problème inverse de distribution de pression pour lequel aucun programme particulier n'est ainsi nécessaire.

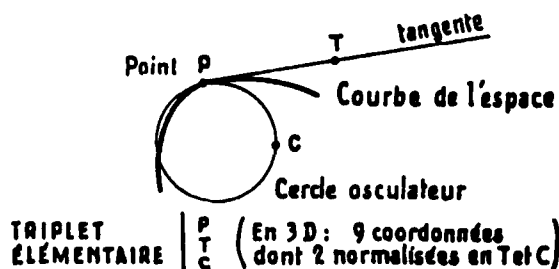
3.3 - La géométrie d'optimisation et conception rapide

Il est nécessaire de pouvoir disposer d'une géométrie de description de l'avion qui puisse satisfaire aux critères suivants :

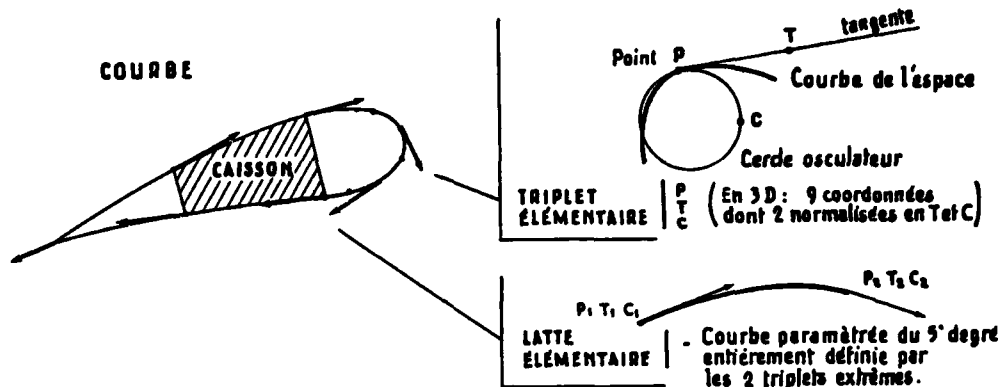
- accepter des formes complexes quelconques
- prendre en compte les contraintes imposées
- être utilisable en sous-programme dans une boucle d'optimisation
- être compatible avec les définitions requises en amont par les programmes aérodynamiques, en aval par les programmes de tracés
- être le plus léger possible en nombre de paramètres

La définition retenue est une définition par carreaux limités par des lattes élémentaires du 5ème degré. Ces lattes sont donc totalement définies par les données aux extrémités des points, pentes et courbures et les carreaux par les données sur les bords.

L'unité de définition de l'avion est un groupe de 3 points dans l'espace appelé triplet. Le point de base P définit le point extrémité de latte, le point T sur la tangente définit celle-ci par rapport au point de base avec une surabondance d'un paramètre, de même le cercle osculateur à la courbe est défini par un point C sur celui-ci.

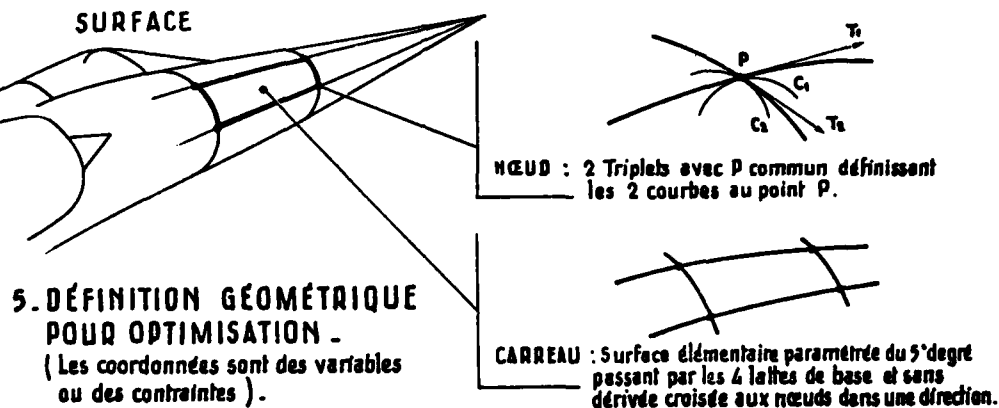


Le croquis ci-dessous rappelle ce choix. On notera que le choix d'un triplet de points réels permet de traiter globalement celui-ci lors de transformations géométriques simples telles que translation, rotation, homothétie. Pour des transformations plus complexes le point C ou le point T sera modifié.



La latte du 5ème degré attachée à deux triplets permet de reproduire toute courbe gauche avec une précision liée à la discrétisation.

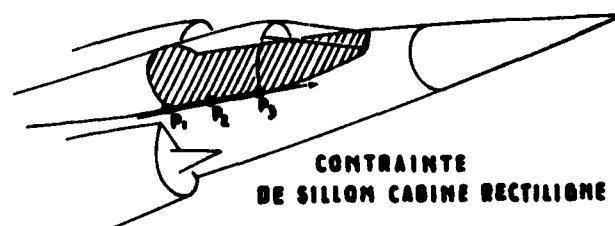
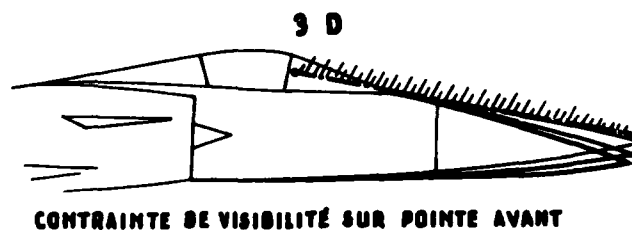
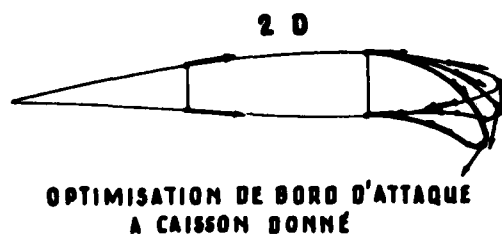
On définira de même le noeud assemblage de deux triplets sur des courbes concourantes et le carreau limité par les quatre lattes de base.



5. DÉFINITION GÉOMÉTRIQUE POUR OPTIMISATION - (Les coordonnées sont des variables ou des contraintes).

Les différentes coordonnées seront alors des variables ou des contraintes.

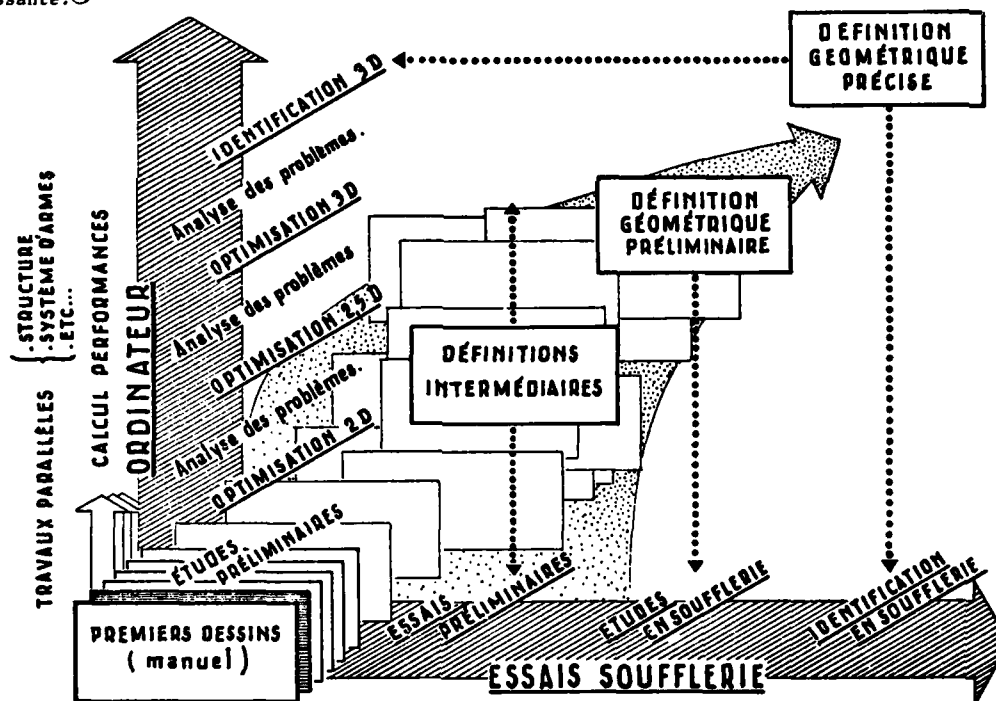
On donne ci-dessous un exemple de possibilités de contraintes dans le programme d'optimisation imposées soit a priori par le choix des degrés de liberté soit sous forme de contraintes équivalant à des relations entre ces degrés de liberté, la pénalisation correspondante a l'inconvénient de ne pas limiter le nombre de paramètres au minimum mais l'avantage de ne pas nécessiter l'explicitation des relations imposées par des contraintes complexes telle une contrainte de visibilité dans une pointe avant.



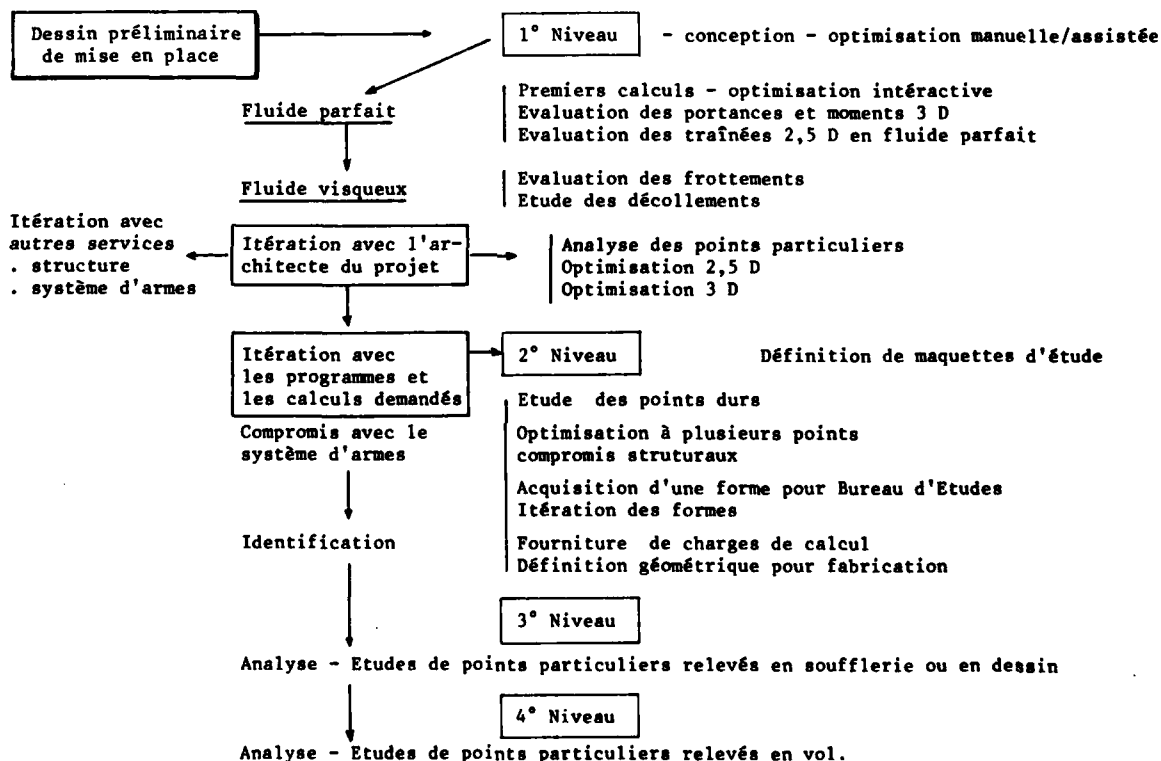
- EXEMPLES DE POSSIBILITÉ DE CONTRAINTES DANS L'OPTIMISATION

3.4 - Le processus de conception

On distinguera le processus général de conception du véhicule aérien du processus de conception des formes aérodynamiques qui n'en est qu'une petite partie. Cependant comme les formes aérodynamiques ont une importance essentielle dans la phase initiale de conception on peut considérer que les premières définitions générales des formes sont surtout un reflet du travail d'optimisation aérodynamique. Nous appellerons définition géométrique préliminaire celle qui résulte de ce travail préalable et qui s'appuie sur les calculs et les essais de soufflerie préliminaires. Les calculs iront du simple au complexe c'est-à-dire des dérivées de développement continu initial au calcul d'identification le plus complet en passant par les calculs 2 D, les optimisations 2 D puis 2,5 D, enfin 3 D, les essais en soufflerie occupant une place croissante. (2)



Outre la planche ci-dessus, on peut résumer les étapes clés des études aérodynamiques sur le schéma ci-dessous :



Une étude plus systématique des 1^{er} et 2^{er} niveau est donnée sous forme d'organigramme en annexe.

On notera un transfert progressif des travaux de l'ordinateur à la soufflerie, puis au vol à mesure que le projet se développe et se précise - l'ordinateur étant un outil d'analyse remarquable mais un médiocre outil d'identification complète pour l'aérodynamique. Par contre, la conception détaillée de la structure et la fabrication correspondront à une charge croissante de l'ordinateur grâce à des systèmes intégrés d'aide au dessin et à la fabrication.

4. CONCLUSION

On a vu que le niveau actuel des calculs d'aérodynamique que l'on peut effectuer sur ordinateur a permis de développer aux AMD-BA une chaîne de conception fortement assistée par l'ordinateur. L'expérience de l'optimisation assistée par ordinateur systématique que nous effectuons depuis nos derniers prototypes, particulièrement le FALCON 50 et le MIRAGE 2000, permet d'espérer des gains importants dans le dessin des formes aérodynamiques des avions en cours d'étude.

Elle conduit à l'emploi continu de techniques d'optimisation réservant à l'ingénieur un travail de réflexion beaucoup plus difficile et complexe que par le passé, par suite de la finesse des études faites, des implications enfin correctement évaluées des contraintes et des objectifs initiaux et de la nécessité continue de préciser les choix et les compromis qui étaient souvent faits autrefois de façon vague et floue.

C'est la difficile rigueur intellectuelle ainsi développée qui permettra cette amélioration - à condition que soient conservés le bon sens ... et l'humour nécessaire pour atténuer la sècheresse des résultats renvoyés en écho par l'ordinateur.

REFERENCES

- 1 - LELAND M. NICOLAI - Changing requirements in Aircraft Design - Astronautics & Aeronautics - June 79 Vol 17 N° 6 -
- 2 - P. BOHN - Aérodynamique de la nouvelle génération d'avions de combat à aile delta AGARD CP - 241 Octobre 77 -
- 3 - A.B. HAINES - Computers and wind tunnels : complementary aids to aircraft design - The aeronautical Journal July 77 -
- 4 - A.B. HAINES - Computer aided Design : Aerodynamics - The Aeronautical Journal - March 79 -
- 5 - LORES M. - Projected role of advanced computational aerodynamic methods at the Lockheed Georgia Company - N 78 19787 -
- 6 - P. PERRIER et W. VITTE - Eléments de calcul d'aérodynamique tridimensionnelle en fluide parfait - Colloque aérodynamique appliquée AFITAE - Nov. 70 -
- 7 - J. PERIAUX et P. PERRIER - Utilisation de la méthode des E.F. en aérodynamique non linéaire VKI computational fluid dynamic 1976 -
- 8 - P. PERRIER - Problèmes de calculs en transsonique - Symposium Transsonic Configurations DGFLR - June 78 -
- 9 - E. TEUPOOTAHITI - Programme 2,5 D interactif de calcul de pression et couches limites compressibles Note DEA 5259 Juin 73 -
- 10 - Philippe PERRIER - Optimisation de formes d'avions - Note DEA 6079 B - Mai 1976
- 11 - J.J. DEVIERS et P. PERRIER - Calculs tridimensionnels d'hypersustentation - Colloque Aérodynamique appliquée A.A.A.F. - Nov. 72 -
- 12 - M. LAVENANT et P. PERRIER - Progrès récents en hypersustentation mécanique - Colloque AGARD C.P. Avril 74 -
- 13 - D. CAUPENNE - Progrès récents des méthodes d'étude des écoulements turbulents - A.A.A.F. 1976
- 14 - J.C. COURTY - Problèmes de sillage - couche limite à l'aide d'un modèle élaboré de turbulence - Colloque aérodynamique appliquée A.A.A.F. - Nov. 76 -
- 15 - G. HECKMANN - Ecoulement à potentiel tridimensionnel portant - Colloque aérodynamique appliquée AFITAE - Nov. 71 -
- 16 - A. JAMESON - Transonic flow calculations - VKI lecture series 87 - Computational fluid dynamics 1976
- 17 - Philippe PERRIER - Calculs de configurations aile fuselage en transsonique - Rapport DEA int. 1977
- 18 - J. PERIAUX - Calcul tridimensionnel de fluide compressible par la méthode des éléments finis - Colloque aérodynamique appliquée Nov. 73 -
- 19 - J. PERIAUX - Three-dimensional analysis of compressible potential flows with the finite element method - International Journal for Num. meth. in eng. - Vol. 9 - 1975 -
- 20 - J. NAVES - Calcul d'ensembles aile-fuselage en régime transsonique - Problèmes posés par la mise en exploitation des méthodes d'éléments finis - Colloque aérodynamique appliquée A.A.A.F. - Nov. 75 -
- 21 - J. PERIAUX et ...^{*} - Use of optimal control theory for the numerical solution of transonic flows - International Symposium on F.E.M. - SWANSEA 1974 - S.M. LIGURE 1976 -
- 22 - P. SCHEIN - Calcul d'écoulement tridimensionnel en supersonique linéarisé - Colloque aérodynamique appliquée AFITAE - Nov. 73 -
- 23 - P. PERRIER et J. PERIAUX - Visualisations and calculations for air intakes at high angle of attack and low Reynolds number AGARD CP 247 - 1978 -
- 24 - J. PERIAUX et...^{*} - On the numerical solution of non linear problems in fluid dynamics by least square and FEM - FENOMECH 78 -
- 25 - P. PERRIER - Calcul de turbulence dans l'industrie aérospatiale - Colloque de la Société hydro-technique de France - Mai 1979 -
- 26 - J. PERIAUX et...^{*} - Approximation of Navier-Stokes Equations - Iterative methods IUTAM - 1979 -
- 27 - BERNARD F. - Un système de conception et de fabrication assisté par ordinateur - AGARD - CP 250 - 1979
- 28 - CHAPMAN D. - Computers versus wind tunnels for aerodynamics flow simulations - Aeronautics & Astronautics - April 1975 -

* M.O. BRISTEAU , R. GLOWINSKI , B. MANTEL , P. PERRIER , G. POIRIER, O. PIRONNEAU

TABLEAU DES OUTILS

EQUATION

CONDITION AUX LIMITES

ALGORITHMIQUE

subcritique parfait	a) Laplacien linéarisé (Effet de squelette) $U = \nabla \psi$, $\nabla \cdot U = 0 \Rightarrow \Delta \psi = 0$	2D	1) Profil isolé (transformation conforme) (Joukowski)	I - Analytique
	b) Laplacien complet			
	c) $\nabla \cdot \nabla U = 0$, $U = \nabla \psi$ - $-\nabla^2 \frac{\partial \psi}{\partial S}$ (Equation de Poisson subcritique)			
super-critique parfait	d) Equation linéarisée transsonique $-\nabla^2 \frac{\partial \psi}{\partial S} = -\nabla^2 \psi_{xx}$	+ modélisation de la viscosité par couches limites et couplages	2) Profils multiples (singularités) (Smith)	II - Développement asymptotiques
	e) Equation complète non conservative			
	f) Equation complète conservative			
fluide visqueux	g) Equation instationnaire (variables U, t)	Minimum requis pour l'optimisation sur ordinateur des profils et ailes en supercritique	3) Profil isolé transsonique D.F. (Garabedian)	III - Transformation conforme
	h) Equation d'Euler non isentropique (variables U, p, t)			
	i) Equation de Navier Stokes isenthalpique (variables U, p)			
fluide visqueux	j) N.S. avec modèle de turbulence	Maximum limité par la capacité des ordinateurs	4) Profils multiples E.F. (IRIA-AMD)	IV - Méthode intégrale Galerkin
	k) Equation de N.S. complète (variables U, p, T)			
	l) Equations de N.S. instationnaire (variable U, p, T, t)			
fluide visqueux	m) Equation de N.S.I. avec modèle de turbulence	+ modélisation de la viscosité par couches limites et couplages	5) Aile singularité (Bosing, Douglas...) sub-critique	V - Evolution en hyperbolique explicite - implicite
fluide visqueux		Minimum requis pour l'optimisation sur ordinateur des profils et ailes en supercritique	6) Avion complet singularités (Douglas, AMD ...)	VI - Méthode de relaxation
fluide visqueux		Minimum requis pour l'optimisation sur ordinateur des profils et ailes en supercritique	7) Aile D.F. avec transformation (Jameson)	VII - Contrôle optimal
fluide visqueux		Maximum limité par la capacité des ordinateurs	8) Aile simple + fuselage simplifié D.F. (Jameson, Gruman, AMD ...)	VIII - Solveur de Stokes
fluide visqueux		Maximum limité par la capacité des ordinateurs	9) Aile complexe + fuselage Volume fini (Jameson)	IX - Solveur de Stokes
fluide visqueux		Maximum limité par la capacité des ordinateurs	10) Avion complexe quelconque E.F. (IRIA-AMD)	X - Solveur de Stokes

PLACE DE L'AÉRODYNAMIQUE DANS LA CONCEPTION DE L'AVION

SPECIALISTES NON AÉRODYNAMIQUES

Calculs de performances
Calculs de structure préliminaires
Estimation de système d'armes
etc...

Etudes opérationnelles
Sélection des matériaux et structure
Evaluation des masses
etc...

Identification des performances
des problèmes structureaux
des problèmes opérationnels
etc...

Calculs structureaux
Etudes préliminaires des systèmes
Etudes opérationnelles
etc...

DIRECTION DU PROJET

Définition des objectifs généraux

Recalage des objectifs généraux

Dessin préliminaire

Sélection des problèmes d'architecture
des contraintes d'architecture
des contraintes non aérodynamiques

Choix des zones de développement continu et
nouvelles

Evaluation des masses

Identification des performances

Sélection des points durs
Sélection des contraintes
Choix des critères et qualités

Itération 1

Etude d'architecture
remise en cause des objectifs
et qualités requises

Synthèse globale

Itération 2

AÉRODYNAMIQUE

Définition des objectifs aérodynamiques
Etudes paramétriques préliminaires
Etudes de développement
Estimation calcul sur plan des caract. aérod.

Sélection de configurations aérodynamiques
Analyse des points durs aérodynamiques
Recherche des problèmes nouveaux

Etudes et recherches
fondamentales

Optimisation 2D
Identification 2D

Optimisation 2,5 D
Identification 2,5 D

Evaluation 3D

Evaluation des caract. aérod. globales

Essais en soufflerie préliminaires

Etude en ordinateur

- analyse 2,5 D
- optimisation 2,5 D
- analyse 3 D
- optimisation 3 D

Etude en soufflerie

- identification
- améliorations
- synthèse expérimentale

Synthèse aérodynamique

WING DESIGN PROCESS BY INVERSE POTENTIAL FLOW COMPUTER PROGRAMS

Luciano Fornasier

Combat Aircraft Group, Aeritalia Società Aerospaziale Italiana p.'A.'
Torino, C. so Marche 41 - 10146 - ITALIA

SUMMARY

Application of advances in the computational fluid dynamics now available can provide an useful basis for design studies of wings.

The present paper is intended primarily to illustrate the approach to wing design by inverse technique. A brief review of the numerical tools employed in the design process is given and the involved technology is discussed in some detail.

Finally an application to a design study aimed to demonstrate potential improvements of supercritical wing technology is described.

LIST OF SYMBOLS

A	Aspect ratio of wing
b	Span of wing
c	Chord of wing section
C_D	Drag coefficient
C_L	Lift coefficient
C_M	Pitching moment coefficient
C_P	Pressure coefficient
$\text{ETA} = \frac{2y}{b}$	Spanwise dimensionless distance
M	Mach number
R	Radius of curvature
Re	Reynolds number
t	Maximum thickness of wing section
x	Distance along chord line from leading edge of wing section
y	Distance along span from centreline of wing
z	Ordinate of wing section surface
α	Angle of attack
ϵ	Angle of twist
ϕ	Trailing edge angle of wing section
λ	Taper ratio of wing
Λ	Angle of sweep

Subscripts :

LE	Refers to leading edge
TE	Refers to trailing edge
2D	Two-dimensional value
3D	Three-dimensional value
25	Value at quarter chord
∞	Freestream conditions
*	Critical (M = 1.0) conditions

1. INTRODUCTION

In the last years both the developments of the computational fluid dynamics and the availability of large storage-high speed computers has strongly affected the aerodynamic design of aircrafts. Starting from potential theory numerical methods have been developed which give good predictions for the aerodynamic characteristics of a new configuration even at an early design phase, i. e. before wind tunnel tests allowing considerable savings of time and money.

Numerical solutions already available cover an increasingly wide range of types of flow, but this paper is limited to attached steady flows only. Calculation of subsonic and supersonic flows around 2-D and 3-D bodies as airfoil sections, wings and wing-body combinations are today routine jobs not only in research centers but in industry too. For the transonic flow, which is by far the most complicated one due to the strong non-linearity and the mixed elliptical and hyperbolic type of the governing equations, only 2-D solutions have been brought to an effective standard, whilst current solutions for the 3-D case are not yet satisfactory from a cost-effectiveness standpoint, due to the inaccuracies of the linearized solutions (Transonic Small Perturbation Methods) or to the high computer time required to solve the full potential equations (Finite Difference and Finite Volume Method).

A very attractive fallout of the numerical approach to the aerodynamic design is the supercritical wing technology which is one of the most promising answer to the demands for aircrafts to fly efficiently near the speed of sound. The problem of the aerodynamicist is to shape a wing of a given planform in such a way that at the design condition the recompression from supersonic to subsonic velocities on the upper surface of the wing occurs without or at least with weak shocks.

Within the computational tools suitable to overcome this difficult task, a basic subdivision may be done into analysis and design codes: the former solve the so-called direct problem which is the determination of the flow around a body flying at fixed speed; the latter deal with the inverse problem which consists in calculating the body, subject to certain geometrical restrictions, which produces a prescribed flow.

Inverse design computer programs for subsonic airfoils have successfully proven their capability to aid the design process allowing the aerodynamic designers to deal with pressure distributions rather than with airfoil geometry. Lift, pitching moment and boundary layer development are thus specified directly by input data and the inverse code output defines the shape of the airfoil which satisfies the requirements, if any. During last years new methods for the design of shock-free airfoils have been published: though their use is more complicated as they depend on numerical solution of the hodograph equations, they are a very helpful approach to design advanced airfoils for transonic speeds.

Both subsonic and transonic 2-D design codes have been implemented at Aeritalia through methods available in the open literature or contributed by partner firms. An original 3-D design computer program has been recently developed at Aeritalia and it is presented in this paper.

2. METHODOLOGY

Before discussing the wing design procedure, it seems necessary to remark here that while physical considerations ensure that there is always a solution to the direct problem (because it is the body which determines the flow) it is impossible to state that for any arbitrary flow field a solution can exist, or that the solution is physically meaningful. From an engineering standpoint this only means that the input conditions supplied to the inverse code must be carefully analysed in order to allow for a realistic solution of the problem.

For example, in the 2-D case the Morawetz's theorem [1] states that the problem of computing shock-free transonic flow around a given airfoil is not well-posed because smooth transonic solutions do not exist for any airfoil shape. In the 3-D case the inverse problem may be not well-posed even for subsonic flow because as shown in Sloof and Woogt paper [2] near the root of wings different geometries produce almost the same pressure distributions. Nevertheless convergence to a solution will be considered here in an engineering sense.

A reasonable way to use inverse technique for wing design is illustrated in Fig. 1. Usually at the beginning of the design loop wing planform, maximum thickness distribution along the span (or, at least, its mean value) and wing loading are given from parametric studies. Firm's past experience and state of the art of experimental and theoretical methods affect the choice of the basic aerodynamic philosophy which in turn makes possible the definition of the goals for the design. The following task to be performed is the choice of a proper design condition: for a transport aircraft the cruise condition must be selected but the variety of mission for combat aircraft requires that the choice of the design point makes compatible all the off-design conditions: hence for a combat aircraft wing the design point is strongly related to the chosen aerodynamic philosophy.

From the 3-D case the design point is derived for the basic airfoil section: for swept wings the sweep relationships are generally used (Fig. 2). If the inverse design code solves potential equations viscous effects can be taken into account by some empiricism modifying the lift coefficient and the Mach Number of the design point (see [2]). Now a target pressure distribution is selected and given as input to the numerical program which automatically produces the section geometry: generally many pressure distributions must be tested before obtaining a satisfactory airfoil shape so that both geometrical constraints and off design performance are satisfied.

Sweep relationships are used again to get the basic streamwise airfoil. The inverse code modifies the input geometry and automatically determines the twist and camber distributions along the span in order to match the prescribed pressure distribution over a set of spanwise stations. As in the 2-D design loop a trial-and-error procedure allows to get a compromise between geometry constraints and off-design performance.

At the end of the whole process geometrical details are available for the lofting of a wind tunnel model: however it is highly desirable to perform an extensive experimental verification of the basic airfoil section at the end of the 2-D design loop.

3. COMPUTATIONAL TOOLS

A brief survey of the numerical codes available in Aeritalia for aerodynamic design purposes is given. As emphasis is put on inverse procedure, only a list of the direct codes involved in the analysis of the off design conditions is given whilst the design codes are discussed in some detail.

3.1 Direct Codes

The following codes are available at present (1979):

- Bauer-Garabedian-Korn-Jameson (BGK) [3], [4], [5]

Finite Difference Methods for computation of flows with shocks past given airfoils. The latest version contributed by Jameson has allowance for viscous effects by calculation of boundary layer displacement.

- Subsonic Panel Method (MBB version) [6]

For computation of subcritical flows around any arbitrary 3-D configuration.

- Eberle Finite Element Method [7]

For computation of flows with shocks around given isolated wings.

- Walz Method [8]

For calculation of boundary layer characteristics.

3.2 Inverse Codes

- Weber Design Method [9]

The numerical code performs the calculation of the airfoil shape required for a given pressure distribution. The Weber Method deals with airfoils or sheared wings in incompressible flow. According to linear potential theory the perturbation velocities are split down in two terms due to thickness distribution and to camber and angle of attack: the former is represented by a source distribution over the chord line and the latter by a vortex distribution. From a basic thickness distribution the vortex distribution required to produce given velocities on the upper side may be solved and the airfoil shape determined. As linear theory is used the present method is limited to airfoils which are not too thick or too cambered to violate small perturbations assumption. Compressibility effects may be taken into account by use of similarity laws. A straight-forward application of this method is the so called "subcritical roof-top" airfoils.

- Multielements Airfoil Design Method [10], [11]

This design program is basically that illustrated in ref. [10] by Beatty and Narramore who have joined together the surface singularity method and the Wilkinson design method. Starting from an initial airfoil section, an iterative-direct scheme is used to define the geometry of the airfoil which gives the required velocity distribution on its upper side. As surface singularity method is used for the analysis of the converging solution, the present method overcomes the limitations inherent in the Weber inverse method. Furthermore it is possible to compute multielement sections too, which allow the initial design of high lift systems.

- Eberle Hodograph Method [12]

By this method, based on the reograph analogy of Sobieczky it becomes possible to design transonic airfoils which exhibits at least in the design condition a shock-free recompression from supersonic velocities. Some experience is required to use this numerical method mainly because for generating solutions one must prescribe the speed at infinity and a set of values for the local angle of flow and the local Mach number M at the airfoil contour: the dependence of maximum thickness and lift coefficient from these parameters is not too easy to establish a priori.

- Sobieczky Optimization Method [13]

A version of this method was recently implemented in Aeritalia by modifying the BGKJ code.¹ It enables to adjust the supersonic contour of an existing airfoil in order to get a shock free flow at the design condition. In spite of its attractiveness due to the very simple way of prescribing the input data (only the shape of the original airfoil, and the angle of attack and the Mach number which define the design condition, must be provided), it seems that the off-design conditions exhibited by the generated airfoils are not always satisfactory.

- Inverse Panel Method

This method is an extension to the 3-D case of the Multielement Airfoil Design Method presented hereinbefore which was recently developed in Aeritalia by the author.¹ The flow-chart of the iterative direct scheme is given in Fig. 3.¹ The flow of the program begins by definition of the pressure-specified bodies (wing) and the geometry specified ones (fuselage and/or external bodies such as engine nacelles or weapons): for the former a set of upper surface pressure distributions and the initial shape of their respective streamwise sections along the span must be given.¹ At the first step of the iterative loop the given configuration is analysed by the panel method program; then the computed pressure distributions are compared with the required ones and an array is built up, each element of which fits the difference between the streamwise component of the actual velocity and the value satisfying the given pressures. Now a distribution of vortices aligned to the x/c constant lines are put over the wing mean surface: these singularities induce the required tangential velocities on the external surface and normal velocities on the mean surface which may be interpreted like a change in the streamwise local slope because, according to linear theory, at each station the mean line must be a streamline.¹ A new mean surface thus results and the initial thickness distributions are wrapped around it (κ) to get a new wing shape, which in turn has to be analysed by the direct method.¹ The loop is automatically iterated until a satisfactory solution is approached.

Key features of the present method are:

- use of a panel type method for the solution of the direct problem by which the presence of the real fuselage and/or external stores may be taken into account;
- use of the Romberg algorithm [14] , for the integration of the velocities due to the vortices distribution.

4. COMPUTATIONAL CONSIDERATIONS

All numerical programs presented here are written in FORTRAN IV language and require at most a storage of 400K bytes.¹ The amount of computing time required by each program depends on the following items:

a) size of the computational grid; b) number of iterations performed; c) choice of the basic algorithms. In particular 3-D codes are more expensive than 2-D ones and panel type solutions of subcritical flows are faster than both Finite Difference Method and Finite Element Method used to calculate transonic flows with shocks.¹

From typical applications run at Aeritalia on an IBM 370/158 computer running times are spread from about 20-30 seconds needed for computation of subcritical flow past a given airfoil to about 60 minutes needed to solve transonic flow around a given wing.

5. APPLICATIONS

In order to assess the feasibility of improving transonic performance of a swept wing by use of "ad hoc" designed supercritical sections, a design exercise based on numerical methods has been performed and the geometry of an advanced wing defined. The new wing, called B, has the same plan form and maximum thickness distribution of the basic wing A, used as reference for theoretical comparison (Fig. 4).

(κ) Another option is available which allows to maintain the lower surface unchanged and to modify the upper surface only.

The basic philosophy involved in the present wing design is shown in figure 5. In designing the new airfoil section a compromise between the optimal target pressure distribution and good off-design characteristics was to be reached, which implies that, starting from the design point, the rate of increase of shock strength when increasing lift coefficient or Mach number would be as low as possible. The 3-D design was aimed at reproducing on the wing the pressure distributions given by the airfoil: furthermore as this is nothing more than a demonstrative exercise a straight isobar pattern for the upper surface and a constant thickness distribution across the span were chosen.

The design point for wing B was: $C_L = .50$ $M_\infty = .80$

which is well above the critical Mach number experienced by the more conventionally designed wing A. Beginning from these conditions the design loop of figure 6 was performed.

5.1 Design of the supercritical section A2

The development of the new section A2 was accomplished by Hodograph Method for the design point of $C_L = .70$ and Mach = .70 corresponding to a real viscous flow condition of about $C_L = .635$ and Mach = .71 obtained by cosine law from 3-D design point. Starting from the calculation of the flow characteristics around the section called A1, which is the normal to the quarter chord section of the wing A, a new boundary in the hodograph plane was defined in order to:

- attain the minimum pressure (corresponding to a local Mach number of about 1.25) close to the leading edge of the airfoil;
- get a smooth, isentropic recompression from the peak pressure to the subcritical pressures;
- realize a pressure recovery to the trailing edge velocity with adequate margins to rear separation;
- develop more lift in the aft region of the lower surface (rearloading).

Fig. 7 shows the input data in the hodograph plane and the resulting airfoil shape together with the output pressure distribution. In the next figure (Fig. 8) this pressure distribution is compared with those calculated by BGKJ code at the potential and viscous flow design conditions: although the comparison indicates a loss of rear loading for the viscous calculation and the appearance of a weak shock in the inviscid analysis, there is confidence that a shock-free flow near the design condition will be supported by wind tunnel tests.

The comparison with the airfoil A1 (Fig. 9) shows that the new section has a larger radius of curvature at the nose and is more cambered near the trailing edge; the thickness distribution aft of the location of the maximum thickness is quite the same, allowing the same arrangement of the basic airfoil for the trailing edge high lift devices.

Figures 10 and 11 compare the way in which the calculated viscous pressure distributions develop over airfoils A1 and A2 when increasing lift at the design Mach number (Fig. 10) or increasing Mach near the design lift coefficient (Fig. 11): the shock on the airfoil A2 develops later and grows weaker than that exhibited by A1.

This results in a delay of both drag rise and buffet: in Fig. 12 theoretically calculated drag polars predict a more favourable trend for drag characteristics of airfoil A2 above the design condition, in spite of the larger friction drag associated to the rearloading of this section.

Finally, theoretical calculations predict that a substantial improvement in buffet boundaries would be achieved, Figure 13. Buffet onset limits were calculated by Thomas Criterion [15], [16] which takes Reynolds effects into account; evaluation of moderate buffet were obtained using an empirical correlation between the strength and the chordwise position of the shock which induces a significant rear separation (see [17]).

A good comparison between theoretical and experimental data for drag rise and buffet limits of airfoil A1 has been found and it is reported in figures 12 and 13. Experimental data are not yet available for airfoil A2 although model manufacturing has been already performed: wind tunnel testing are scheduled for the end of this year (1979) at DFVLR-Braunschweig (FRG).

5.2 Design of wing B

In order to extend over the whole wing the design pressure distribution of the airfoil A2 by use of the Inverse Panel Method the following procedure was carried on:

- a basic streamwise section was defined by applying locally the sweep relationships to the coordinates of the airfoil A2 and it was put at seven control stations across the span;
- at each control station a uniform target pressure distribution was required.

Since Inverse Panel Method deals with elliptical equations and therefore supercritical flows cannot be exactly calculated, it was impossible to derive the target pressure distribution in a straight forward manner from the 2-D one: to overcome this, an expedience similar to that of ref. [2] was employed, that is a certain "equivalent" pressure distribution has to be fixed.

As it is well-known (see for example [18]) at subsonic speeds the pressure distribution near mid semispan of a swept-back wing of moderate aspect ratio and sweep with constant airfoil section is very similar to that on the infinite sheared wing, with iso bars parallel to the local geometric sweep line. Therefore the required "equivalent" pressure distribution was found by a direct Panel Method computation on a triangular wing derived from the basic one by tip extension (in order to increase the aspect ratio) with the streamwise section constant across the span.¹ These concepts are elucidated in Fig. 14 where pressure distributions computed by BGKJ code on airfoil A2 are compared with the 3-D ones scaled by sweep law

For both the subcritical flow computed by Panel Method (Fig. 14 a) and transonic flow computed by Finite Element Method (Fig. 14 b) a good agreement with the 2-D values may be seen; the discrepancies shown in case c) are due to the elliptic feature of the Panel Method and therefore this pressure distribution was selected as the target one for inverse computations.¹ Furthermore as the same mathematical model is used to define the target pressure distribution and to control it during the iterative process, this procedure enables to minimize the errors due to the discretization of singularity distributions.

After three iterations the geometry shown in Fig. 15 was produced by the inverse code.¹ In order to counteract the well-known centre and tip effects on pressure distributions of swept wings the distribution across the span of both twist and camber were determined by the inverse code.¹ The root section is nearly symmetric whilst the tip section is highly aft-cambered (κ); twist varies from 2.2° at the root to -2.35° at the tip.

A theoretical verification of the supercritical wing B was performed by the analysis codes for the conditions arranged in Fig. 16. In order to get theoretical comparison, calculations were carried out also for the reference wing A which is of constant section across the span, derived from the 2-D section A1 applied normal to the wing quarter-chord line. Figure 17 shows the pressure distributions at stations $\eta = .22, .49$ and $.86$ of wing B computed by Finite Element Method at the design condition: clearly, these pressure distributions are consistent with the 2-D computations on the airfoil A2 and the expected uniform flow conditions are achieved across a fair part of the span. The supercritical recompressions from peak suction near the leading edge and the amount of rear loading give a large contribution to the total lift of the wing. For the more conventional wing A calculations predict that the same lift is associated with a relatively large shock at mid chord (Fig. 18).

The development of the supercritical flow over wing B near the design condition is very smooth (Fig. 19): when increasing the lift from $C_L = .43$ to $C_L = .60$ at $M_\infty = .80$ the leading edge pressure peak rises quickly delaying the appearance of the shock up to the highest incidence.¹ Theoretical predictions for shock and pressure peak positions and for the extension of the supersonic and separated (σ) flow are presented in figure 20: there is evidence that substantial gains in separation margins have been achieved by wing B.¹ The low speed characteristics of this wing seems to be comparable with these of the reference wing, as results from Panel Method computations at $M_\infty = .40$ and lift $C_L = .22, .52$ and $.82$; both the local lift distributions across the span (Fig. 21) and the pressure peak distributions (Fig. 22) show that the flow is more uniform over wing B, in spite of the relatively sensitive feature of the supercritical sections to 3-D effects.

6. CONCLUSIONS

This paper describes the design of a supercritical airfoil and the application of this section to a swept wing. A numerical procedure by inverse potential flow programs has been employed to design a supercritical airfoil and the correspondent swept wing. The theoretical verification of airfoil and wing are presented.¹ Both 2-D and 3-D comparisons with a reference airfoil and the correspondent wing shows how computational approach to wing design can aid the designers to improve aircraft performance by incorporation of advanced aerodynamic technology.

Inverse technique enables to perform good initial wing design studies which can be evaluated by analysis computers programs so that extensive and expensive wind tunnel tests may be delayed to the optimization phase allowing appreciable savings of both time and costs.

(κ) Since in designing the wing B the thickness distribution was held constant across the span, the sections on the outer part of the wing result highly aft cambered: therefore the rear loading of the lower surface increases towards the tip and this could result in premature separation of the flow in that region and/or in too large negative pitching moment. To overcome these pitfalls it could be sufficient to reshape the lower surface of the wing but this is beyond the scope of the present exercise.

(¹) Calculated by application of the 2-D Walz Method to the 3-D inviscid pressure distributions.

Future advances in theoretical methods and availability of more powerful computers are expected to improve current state of the art in wing design by numerical methods.

REFERENCE

1. Morawetz, C. S. : "ON THE NON-EXISTENCE OF CONTINUOUS TRANSONIC FLOWS PAST PROFILES, I, II and III", *Comm. Pure Appl. Math.*, Vol. 9, pp. 45-68 (1956), Vol. 10, pp. 107-131 (1957), Vol. 11, pp. 129-144 (1958)
2. Sloof, J. W. and Voogt, N. : "AERODYNAMIC DESIGN OF THICK, SUPERCRITICAL WINGS THROUGH THE CONCEPT OF EQUIVALENT SUBSONIC PRESSURE DISTRIBUTION", DGLR/GARTEur Symposium on "Transonic Configurations", June 13-15, 1978, Bad Harzburg, Germany
3. Bauer, F., Garabedian, P. and Korn, D. : "SUPERCRITICAL WING SECTIONS", Berlin, Springer Verlag, 1972, Lecture Notes in Economics and Mathematical Systems, Vol. 166
4. Bauer, F., Garabedian, P., Korn, D. and Jameson, A. : "SUPERCRITICAL WING SECTIONS II", Berlin, Springer Verlag, 1975, Lecture Notes in Economics and Mathematical Systems, Vol. 108
5. Bauer, F., Garabedian, P. and Korn, D. : "SUPERCRITICAL WING SECTIONS III", Berlin, Springer Verlag, 1977, Lecture Notes in Economics and Mathematical Systems, Vol. 150
6. Kraus, W. : "PANEL METHODS IN AERODYNAMICS", VKI Lecture Series 87 on "Computational Fluid Dynamics", 15-19 March 1976, Rhode - Saint-Genese, Belgium
7. Eberle, A. : "TRANSONIC POTENTIAL FLOW COMPUTATIONS BY FINITE ELEMENTS : AIRFOIL AND WING ANALYSIS, AIRFOIL OPTIMIZATION", DGLR/GARTEur Symposium on "Transonic Configurations", June 13-15, 1978, Bad Harzburg, Germany
8. Walz, A. : "BOUNDARY LAYER OF FLOW AND TEMPERATURE", London, M.I.T. Press, 1969
9. Weber, J. : "THE CALCULATION OF THE PRESSURE DISTRIBUTION ON THE SURFACE OF THICK CAMBERED WINGS AND THE DESIGN OF WINGS WITH GIVEN PRESSURE DISTRIBUTION", ARC R&M No. 3026
10. Narramore, J. C. and Beatty, T. D. : "AN INVERSE METHOD FOR THE DESIGN OF MULTIELEMENT HIGH-LIFT SYSTEMS", AIAA Paper No. 75-879, 1975
11. Wilkinson, D. H. : "A NUMERICAL SOLUTION OF THE ANALYSIS AND DESIGN PROBLEMS FOR THE FLOW PAST ONE OR MORE AEROFOILS OR CASCADES", ARC R&M No. 3545, 1967
12. Eberle, A. : "AN EXACT HODOGRAPH METHOD FOR THE DESIGN OF SUPERCRITICAL WING SECTIONS", *Proceedings of Symposium Transsonicum II*, Springer Verlag, 1976, pp. 314-321
13. Sobieczky, H. : "TRANSONIC DESIGN IN 2 AND 3 DIMENSIONS", DGLR/GARTEur Symposium on "Transonic Configurations", June 13-15, 1978, Bad Harzburg, Germany
14. Wilf, H. S. : "ADVANCES IN NUMERICAL QUADRATURE", *Mathematical Methods for Digital Computers*, John Wiley & Sons, 1965, Vol. 2, pp. 133-144
15. Thomas, F. and Redeker, G. : "A METHOD FOR CALCULATING THE TRANSONIC BUFFET BOUNDARY INCLUDING THE INFLUENCE OF REYNOLDS NUMBER", *Agard Conf. Proc.* 83, 1971
16. Redeker, G. : "CALCULATION OF BUFFET ONSET FOR SUPERCRITICAL AIRFOILS" *Proceedings of Symposium Transsonicum II*, Springer Verlag, 1976, pp. 66-74
17. Haines, A. B. : "COMPUTER-AIDED DESIGN: AERODYNAMICS", *Aeronautical Journal*, March 1979, pp. 81-91
18. Bagley, J. A. : "SOME AERODYNAMIC PRINCIPLES FOR THE DESIGN OF SWEEPED WINGS", *Progress in Aeronautical Sciences*, 3, New York, Pergamon Press, 1962

ACKNOWLEDGEMENTS

The author wishes to acknowledge Aeritalia's permission to present this paper. The views expressed in this paper are those of the author personally and not necessarily those of Aeritalia.

In preparing this paper, the author is grateful to Mr. P. Sacher and A. Eberle, of MBB-Ottobrunn, for their helpful suggestions in using MBB's numerical codes and to Mrs. L. Marietti and G. Autino and Mr. P. Piana for their contribution in typewriting and drawing.

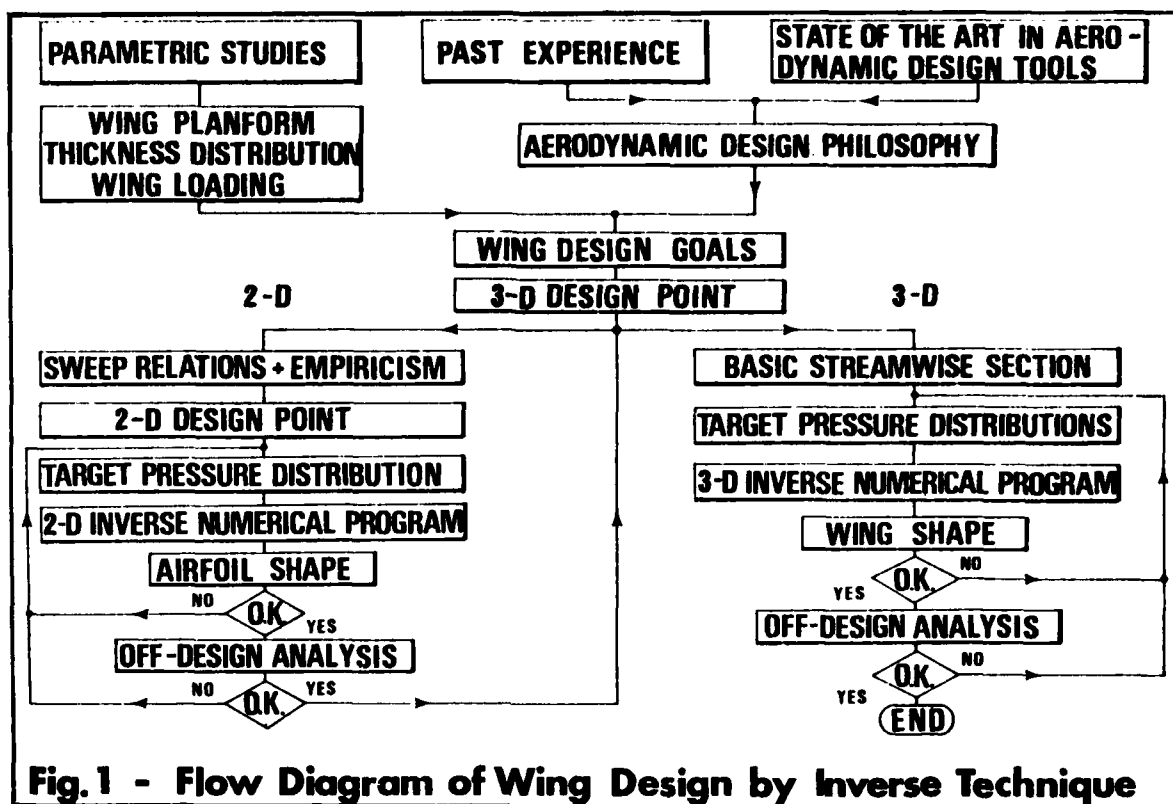


Fig. 1 - Flow Diagram of Wing Design by Inverse Technique

$$M_{2D} = M_{3D} \cdot \cos \Lambda_{25}$$

$$C_{p2D} = C_{p3D} / \cos^2 \Lambda$$

$$(z/c)_{2D} = (z/c)_{3D} / \cos \Lambda$$

$$C_{L2D} = C_{L3D} / \cos^2 \Lambda_{25}$$

$$d_{2D} = d_{3D} / \cos \Lambda_{25}$$

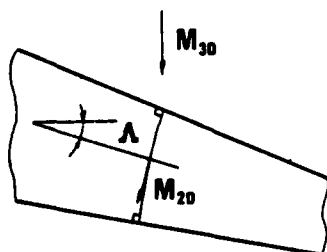
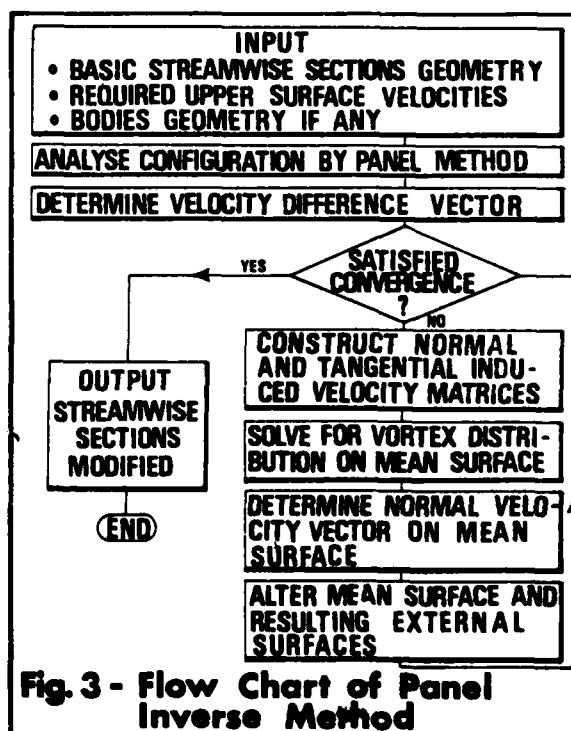


Fig. 2 - Sweep Relationships



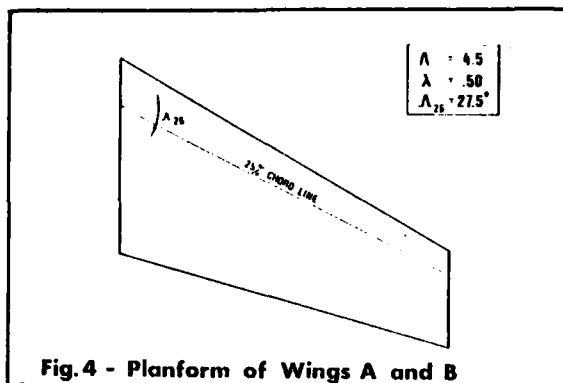


Fig. 4 - Planform of Wings A and B

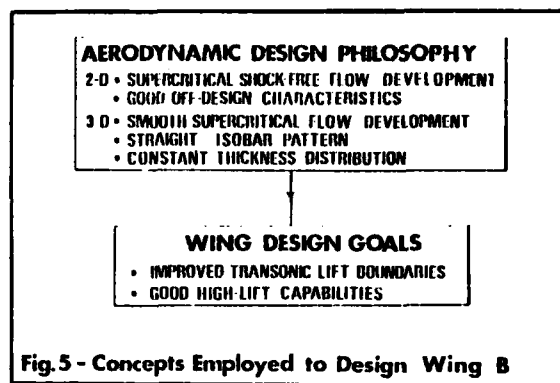


Fig. 5 - Concepts Employed to Design Wing B

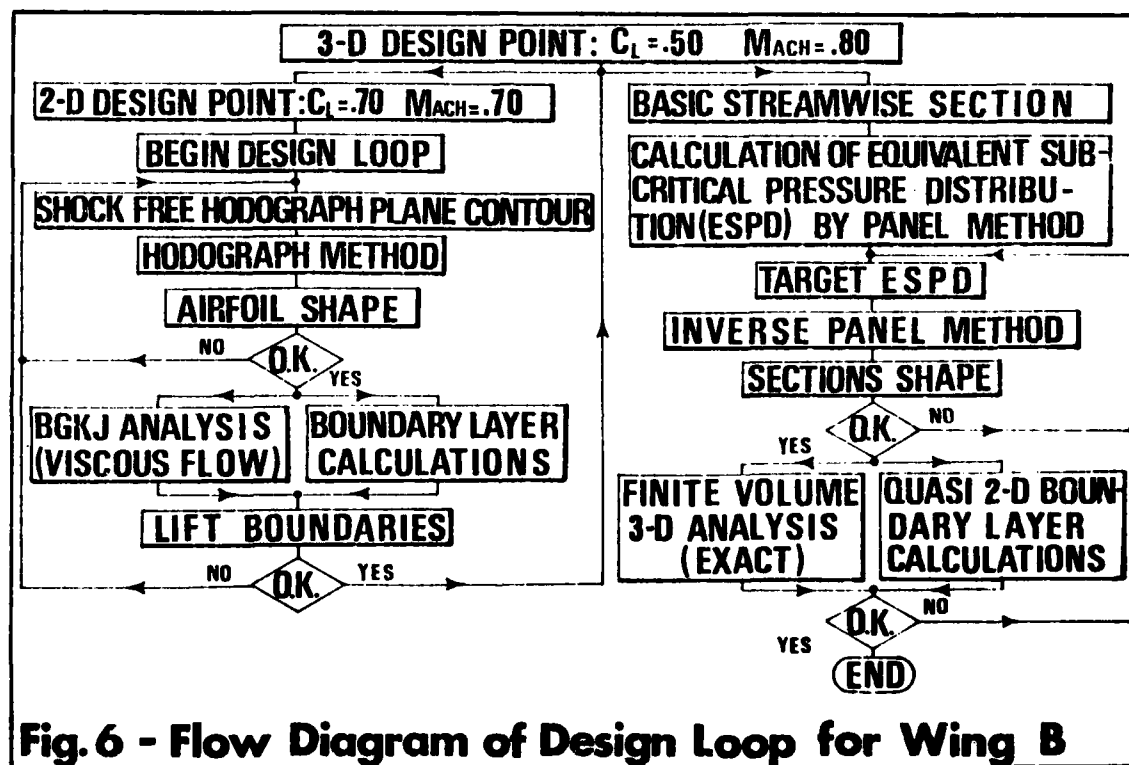


Fig. 6 - Flow Diagram of Design Loop for Wing B

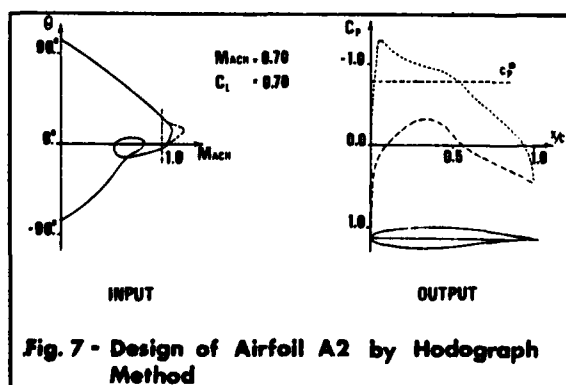


Fig. 7 - Design of Airfoil A2 by Hodograph Method

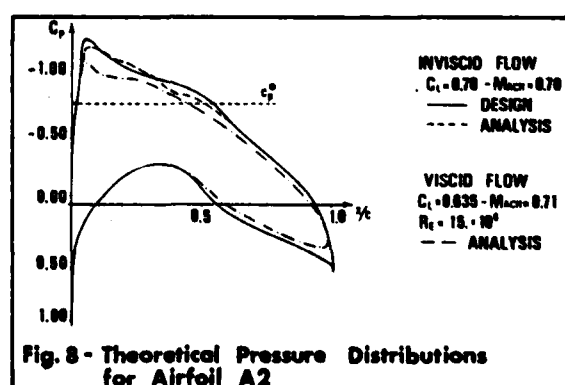
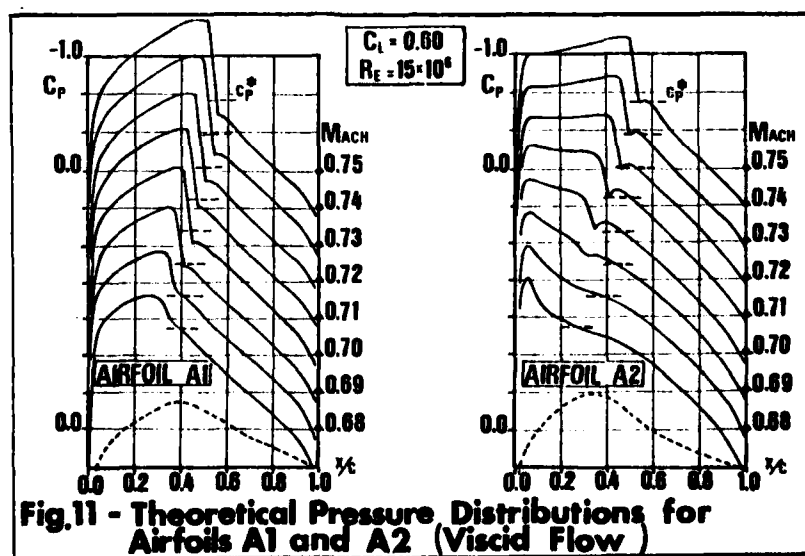
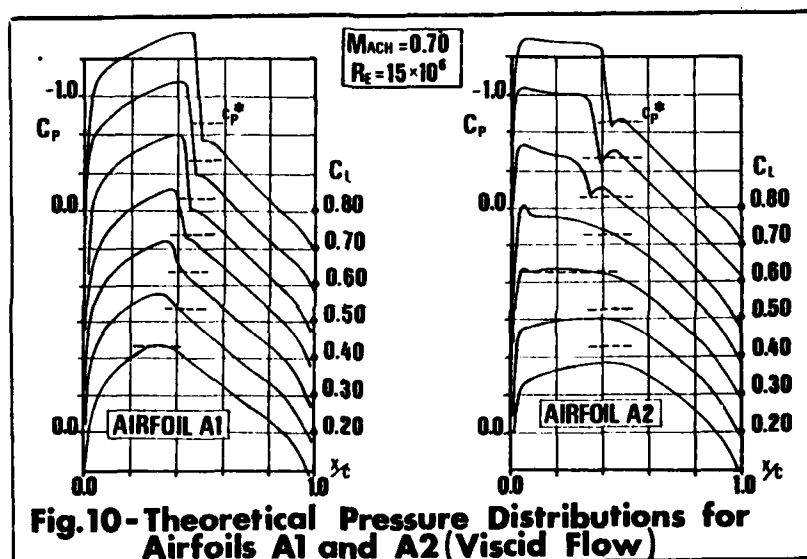
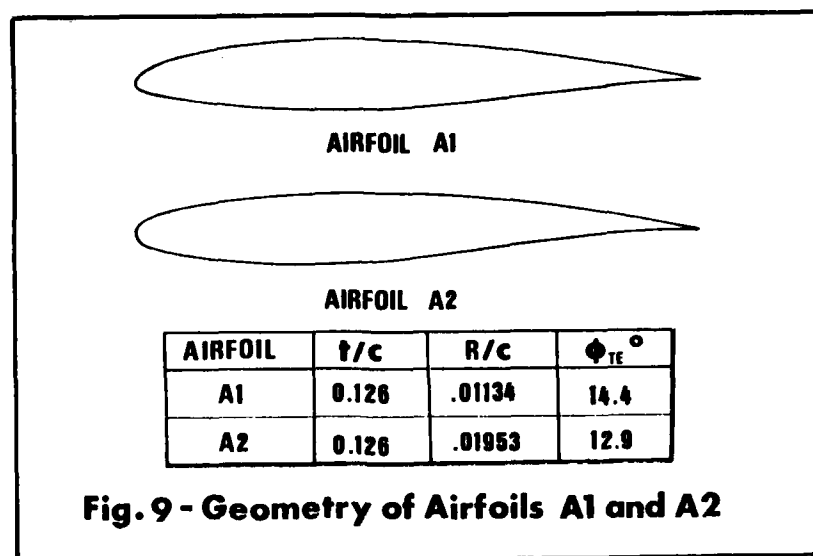
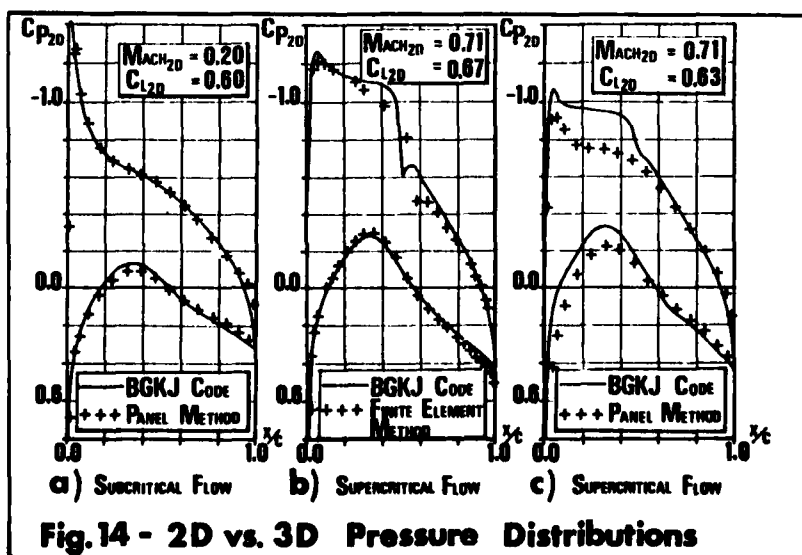
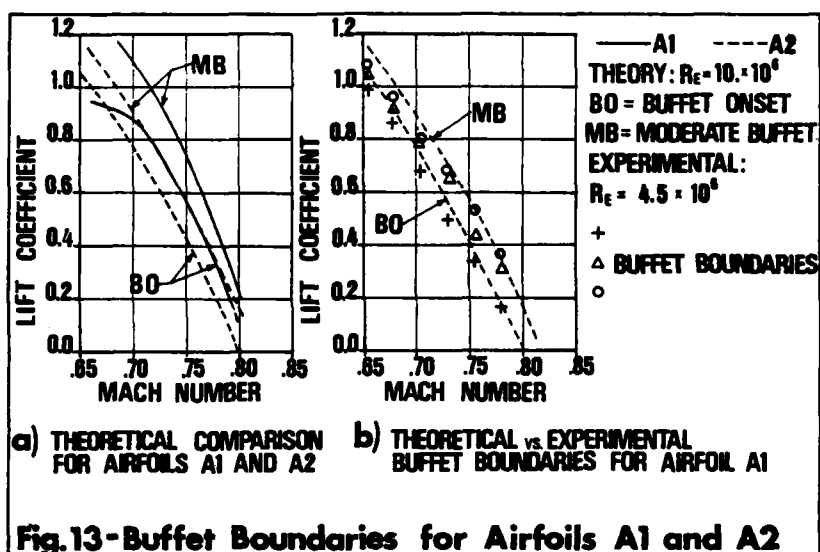
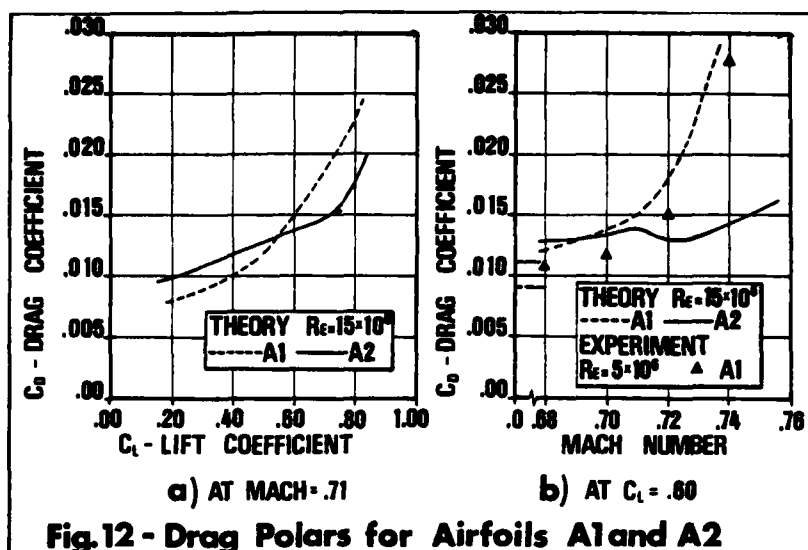
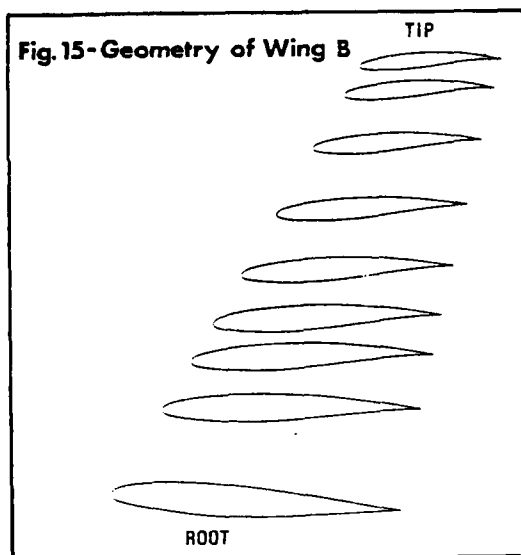


Fig. 8 - Theoretical Pressure Distributions for Airfoil A2

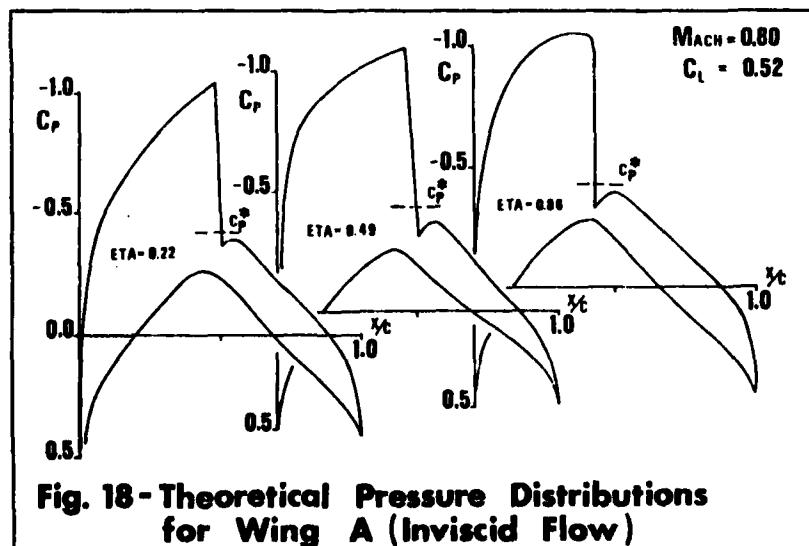
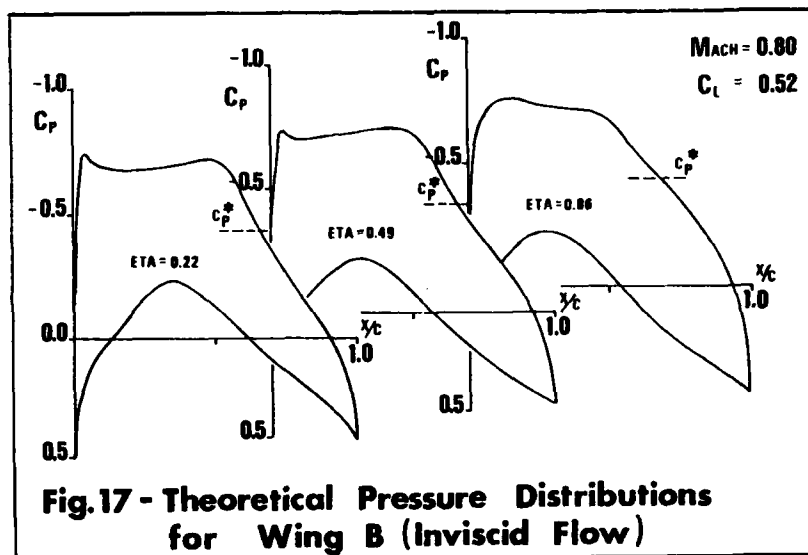


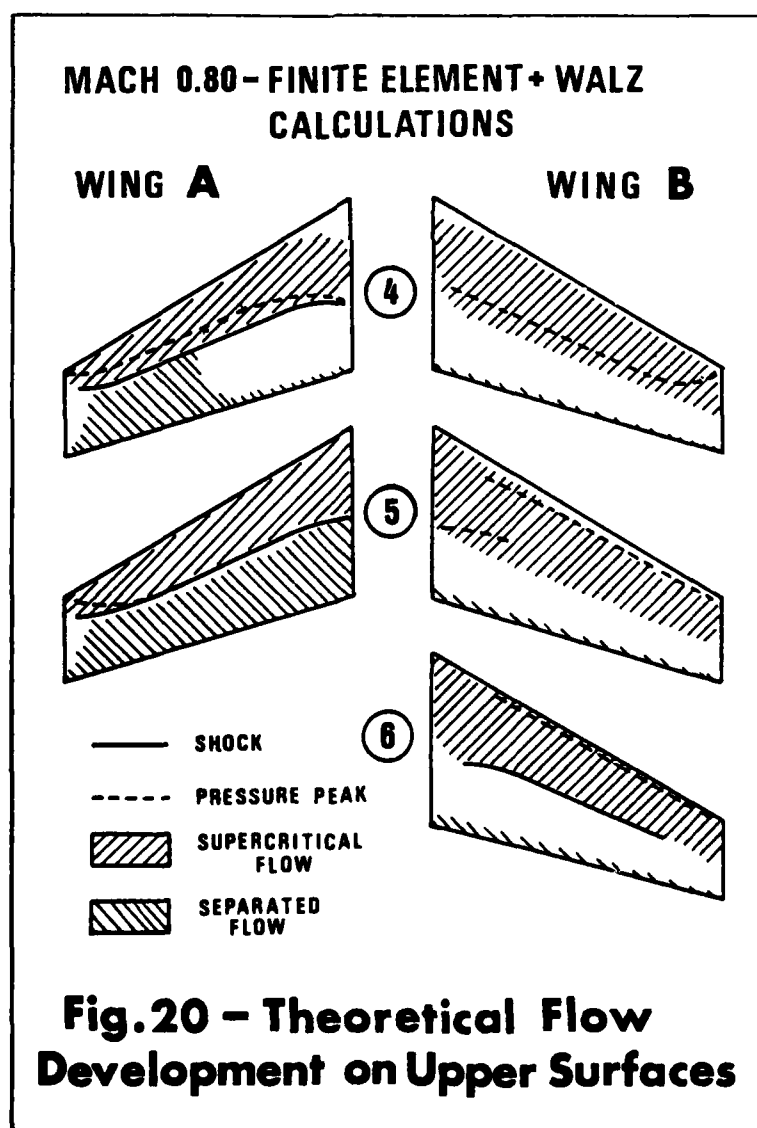
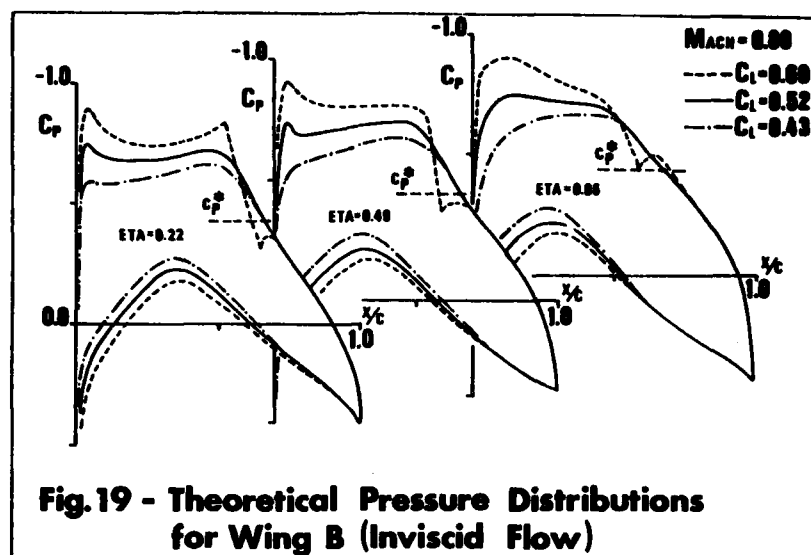




WING	CASE	MACH	ALPHA	C_L	C_{M25}
A	1	.40	8.0	.22	-.046
	2	.40	5.0	.52	-.038
	3	.40	10.0	.82	-.030
	4	.80	1.75	.41	-.030
	5	.80	3.25	.52	-.030
	6	—	—	—	—
B	1	.40	1.0	.22	-.061
	2	.40	4.0	.52	-.061
	3	.40	11.0	.82	-.061
	4	.80	3.2	.43	-.103
	5	.80	4.1	.52	-.102
	6	.80	5.0	.60	-.100

Fig. 16 - Test Cases for Theoretical Analysis of Wings A & B





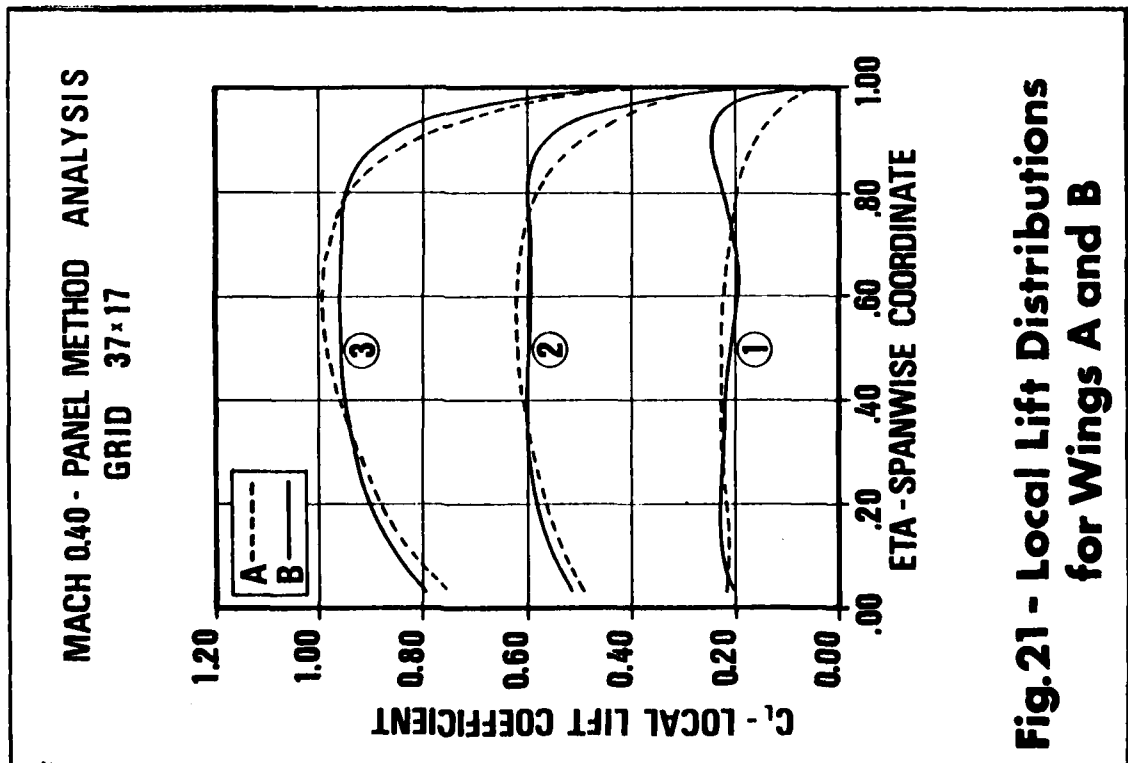


**Fig.21 - Local Lift Distributions
for Wings A and B**

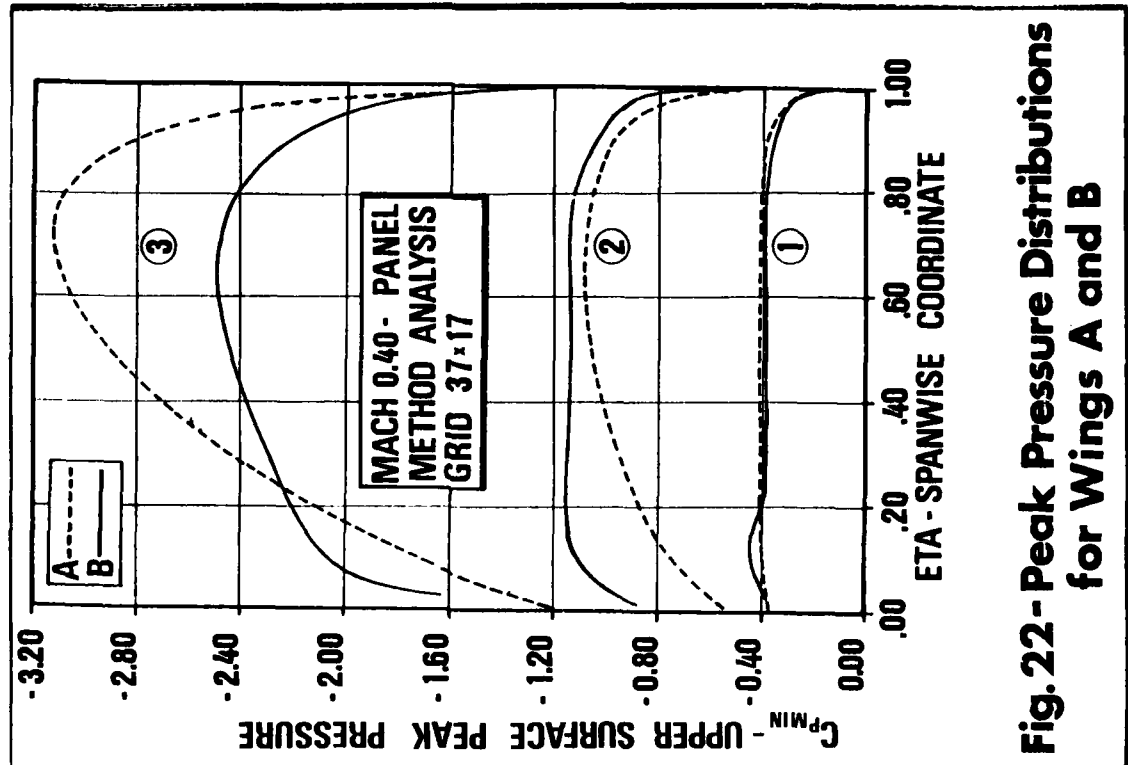


**Fig.22 - Peak Pressure Distributions
for Wings A and B**

THE ROLE OF COMPUTATIONAL AERODYNAMICS IN AIRPLANE CONFIGURATION DEVELOPMENT

by

Bertil Dillner and Chester A. Koper, Jr.
Boeing Commercial Airplane Company
P.O. Box 3707
Seattle, Washington 98124
U.S.A.

SUMMARY

The role of computational aerodynamics in the design of aircraft configurations in steady flow conditions is explored through several examples. These include subsonic high-lift and wing strake designs, and transonic and supersonic cruise wing designs. Use of these computer methods can substantially increase airplane performance capabilities, while reducing risk, flow time, and testing requirements. An assessment is made concerning the factors that have contributed to advancing computational aerodynamics. Deficiencies of existing programs are also noted.

A shortcoming of several advanced computer methods is that their application by design engineers is hampered by the long lead time required to learn to use these methods effectively, and by the inefficient user interfaces these methods generally possess. As a result, most of the advanced methods now available are only used by the few engineers who specialize in these methods. For computational aerodynamics to assume the larger role in aircraft design that the proponents of advanced computer hardware and software envision, much more attention will have to be given toward improving the engineering interface with these methods. A criterion that can identify a method as a design tool is for the total flow time required to conduct an analysis/design cycle to be less than one day.

NOMENCLATURE

b	= wing span	C_p	= pressure coefficient	x	= longitudinal coordinate
c	= wing chord	D	= drag	y	= lateral coordinate
c'	= wing chord including leading edge device	D_f	= skin friction drag	α	= angle of attack
c_{base}	= reference chord of baseline wing	D_p	= profile drag	β_{sw}	= cross flow angle
C_d	= section drag coefficient	D_w	= wave drag	Λ	= wing sweep angle
C_D	= drag coefficient	H_{sss}	= boundary layer shape factor using streamwise velocities	δ	= fin twist angle
C_{fd}	= skin friction coefficient in drag direction	L	= lift	δ^*	= displacement thickness
C_l	= section lift coefficient	M	= Mach number	Δ	= increment
C_L	= lift coefficient	Re	= Reynolds number	η	= $y/(b/2)$
C_{m_0}	= pitching moment coefficient	s	= intrinsic coordinate along a streamline	$()_0$	= baseline value
				$()_{TE}$	= trailing edge value

PREFACE

A tremendous development in computational aerodynamic methods has occurred in the last few years regarding the detail shaping of aircraft configurations. These advances are attributed to several factors: improved computer mainframes (faster, larger) and more offline data processing capability (minicomputers); more sophisticated codes; better engineer-computer interfaces (conversational terminals, remote job entry sites); and improved program usability (i.e., improved user interface). Over the years, hardware and software technologies have received considerable attention, e.g., see References 1 through 4. On the other hand, the design of computer programs so that engineers can use them easily has not received much consideration by their developers. This is unfortunate, since none of the four areas mentioned above is less important than the other. It has therefore required substantial time and effort by the users to develop these codes into usable tools. For computational aerodynamics to play a more extensive role in configuration development, it is necessary for this engineer-software interface to be more completely addressed.

Confidence in several of the computational aerodynamic methods has been generated due to their successful application in a wide range of design problems. As a result, computational aerodynamic tools are now having a large impact on current design of aircraft configurations. These methods guide the engineer in achieving efficient integrated designs, in gaining insight into complex flow fields, in understanding test data, and in exploring innovative configuration concepts. Even though aerodynamic design/analysis techniques have progressed considerably, most of the existing methods either contain areas of empiricism, cannot model the complete configuration, or are unable to account for all aspects of the physics of the flow. Consequently, present aerodynamic design still requires extensive configuration refinement through repeated wind tunnel testing.

The application of computational aerodynamics has led to valuable results, notwithstanding some of the complexities related to using these methods. The salient features of several examples relating to configuration design will be presented herein. Other examples can be found in References 5 through 11, to name a few.

1. HIGH-LIFT SYSTEM DESIGN

As transport aircraft design has matured, increasingly stringent requirements have been imposed upon the design of the high-lift system. Traditional airplane performance and cost trades have been supplemented with requirements to reduce noise and wake turbulence during terminal operations. The performance of high-lift systems is limited by viscous flow phenomena, such as confluent boundary-layer regions and small areas of separation at normal operating conditions. These phenomena are often compounded by complex spanwise flows. A three-dimensional viscous flow computation capability for high-lift wings is presently unavailable. Consequently, it is necessary to utilize two-dimensional airfoil methods in designing these systems (ref. 12, 13).

Computational methods have been developed that can provide flexible and efficient two-dimensional multielement airfoil analyses and design (ref. 14, 15). In addition, when combined with appropriate boundary and initial conditions, the methods can calculate the shape, position, and effects of separated wakes (ref. 14). These methods differ from existing techniques in that desirable boundary layer properties are specified and the pressure distribution required to produce these properties is calculated. The shape required to achieve this pressure distribution is then computed (ref. 15).

Example 1:

One application of high-lift system design was to study the possible improvements in take-off L/D of a given cruise airplane configuration operating out of high altitude airports. Takeoff from these airports is typically limited by the second segment climb L/D characteristics. The approach taken was to investigate the relative performance gains from extending the leading edge slat chord and from recontouring the slat. First, the baseline configuration planform was analyzed using a three-dimensional potential flow method (similar to ref. 16) to obtain sectional and total aerodynamic characteristics of the wing. Configuration paneling and section lift coefficients are shown in Figure 1.

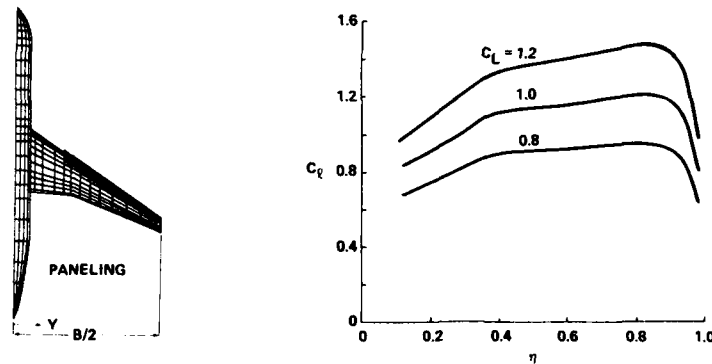


Figure 1. Configuration Paneling and Computed Sectional Lift Coefficient

Next, two-dimensional section coordinates were extracted from the wing as indicated in Figure 2. These sections were used as starting airfoils for design. They consisted of the basic wing airfoil geometry in the region of interest provided with a form of leading edge device representative of the desired extension. Design continued by conducting a potential flow analysis of these sections. The pressure distribution in the design region, i.e., ahead of the high-lift device trailing edge, was optimized using the interactive, inverse boundary layer program referred to above. Based on the optimized pressure distribution, the airfoil was reshaped in the design region to match the desired pressures. The results of the design effort are also shown in Figure 2. Recontouring the leading edge slat proved to be the most important contribution toward improving performance. Extending the leading edge device also provided L/D gains, but at a rapidly decreasing rate.

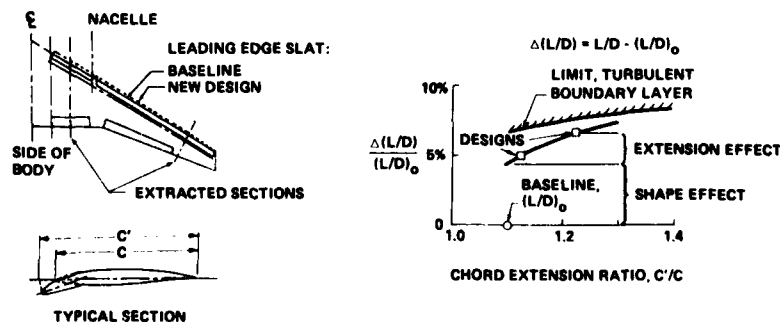


Figure 2. Results of Improved Leading Edge Design Effort

AD-A083 203

ADVISORY GROUP FOR AEROSPACE RESEARCH AND DEVELOPMENT--ETC F/8 9/2
THE USE OF COMPUTERS AS A DESIGN TOOL.(U)

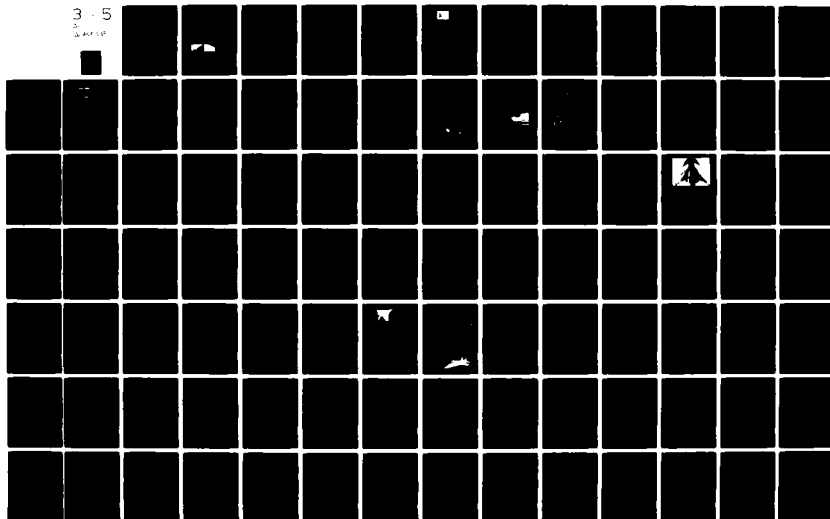
JAN 80

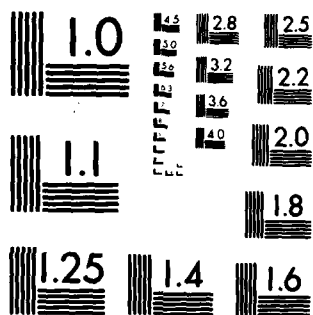
UNCLASSIFIED AGARD-CP-280

NL

3 - 5

3 - 5





MICROCOPY RESOLUTION TEST CHART
NATIONAL BUREAU OF STANDARDS 1963-A

A medium extension configuration was subsequently selected for wind tunnel testing. The comparison between wind tunnel test results and computed L/D 's at takeoff conditions is shown in Figure 3. Note that the analysis did not include nacelles, whereas the wind tunnel model had nacelles installed. At lower lift coefficients, the test verified the analysis of the baseline. However, at higher C_L 's the analysis predicted some separation that was alleviated in the test due to favorable nacelle interference. Predicted performance of the new slat was verified by the test. Specifically, the new slat resulted in a takeoff lift-drag ratio increase from 5% (sea level, standard conditions) to 7% (high altitudes, 33°C). Additionally, maximum lift coefficient at the various takeoff flap settings increased by increments of 0.12 to 0.16.

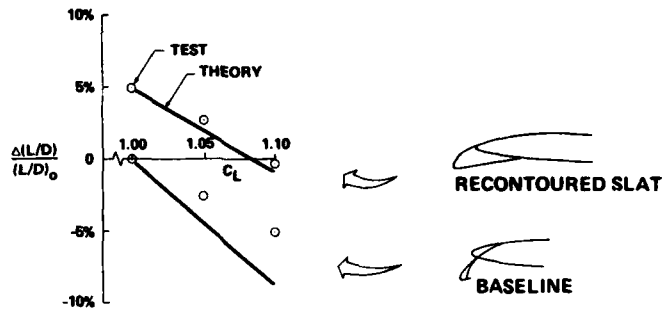


Figure 3. Test-Theory Comparison of Takeoff L/D

2. CONFIGURATION DETAIL DESIGN

A computational method has been developed at The Boeing Company that can analyze arbitrary three-dimensional configurations in potential flow (ref. 8). The configuration surfaces are divided into panels, and hence, this approach has come to be known as a panel method. Essentially, this is a general three-dimensional boundary value problem solver that is capable of being applied to most problems that can be modeled within the limitations of potential flow. Compressibility effects are approximated by the Gothert rule, but analysis of transonic flows is not possible, since the method is a solution of the linearized flow equation. Viscous displacement effects can be represented by either surface displacement or flow through the surface. This method is ideally suited for analyzing complex aircraft configurations in subsonic flow.

This method and similar methods (e.g., ref. 6) were introduced in the late 1960's and have been the mainstay of computational aerodynamics, insofar as complete configurations are concerned. Today, the newer transonic methods are used whenever wing design/analysis is concerned. However, panel methods are presently the only methods for analyzing complex configurations. Numerous examples have been cited in the past showing panel methods' analyses of complex aircraft configurations (e.g., see References 5, 6, 8, and 17). The present discussion will focus on a detail design application of this method.

Example 2:

A wing strake fairing was analytically designed through iterative analysis using the three-dimensional potential flow computer program mentioned above. Drag reduction was achieved by eliminating separated flow around the wing-root junction. In this region, the fuselage surface flow which approaches a wing root attachment (or stagnation) region experiences a strong adverse pressure gradient, and the boundary layer flow eventually separates. The separated flow merges with the corner flow at the wing-body junction producing increased drag. A wing strake is designed to prevent the flow separation by relaxing the adverse pressure gradient.

The wing-fuselage model utilized in this design is depicted in Figure 4a. A dense panel system was generated near the wing root to provide good resolution of the pressure variations in that region. Streamlines which approach the wing root stagnation point were first calculated in absence of a wing strake. A wing strake was then designed over the streamline by aligning the hi-lite of the strake with the streamline. A sample strake and calculated streamlines are shown in Figure 4b. Note that one streamline aligns well with the hi-lite of the wing strake.

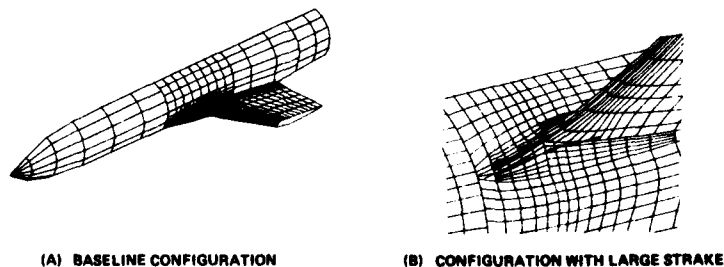


Figure 4. Computational Model Used in Strake Study

Three different sized wing strakes were designed and analyzed in this manner. Relative sizes of the strakes are depicted in Figure 5. The calculated pressure distributions along the streamlines which approach the attachment line are also shown in this figure. These pressure distributions are compared with the pressure distribution of the baseline configuration without a wing strake. The pressure coefficient for the baseline rapidly increases toward the wing leading edge. On the other hand, the pressure gradients are diminished when strakes were added. The results show that the largest strake analyzed resulted in the smallest pressure gradient. This would then provide the least risk of flow separation.

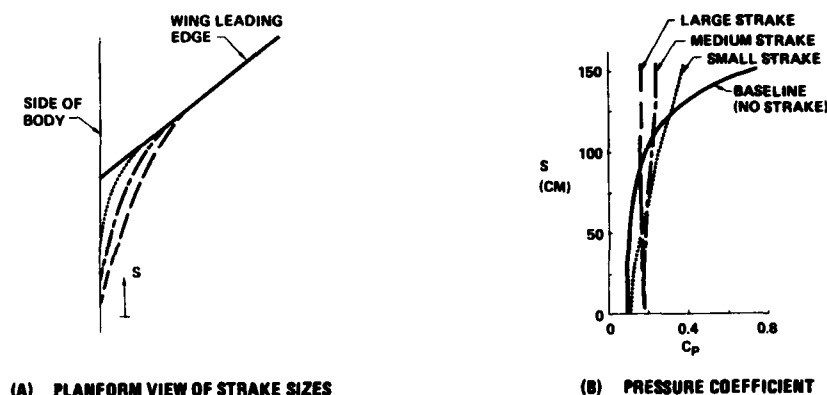


Figure 5. Several Strake Designs and Computed Pressure Distributions on Dividing Streamline

The three designed strakes were subsequently wind-tunnel tested to assess drag performance, since the computational method does not have the capability to predict drag levels resulting from these minor configuration differences. During the test, oil flow visualization was conducted. Oil flow patterns at the wing root area for the baseline and large strake configurations are shown in Figure 6a. The flow which approaches the baseline wing root does not penetrate into the wing-body junction because of the presence of separation. Note that the large strake completely eliminates the separated flow region ahead of the wing root, and attached flow is achieved at the wing-body junction. It was found that oil flow patterns were affected very little by off-design conditions. Similar flow patterns were observed for the medium and small sized strakes. Drag performance of the three straked configurations relative to the baseline configuration is shown in Figure 6b. The data represent averaged wind tunnel runs, and the corresponding data scatter is shown. The large wing strake achieves about 1% reduction of total airplane drag in the cruise lift range. Somewhat less drag reduction is obtained from the medium sized strake. The average data for the small strake shows a slight increase in drag, but it is observed that this increase is within the scatter of the data.

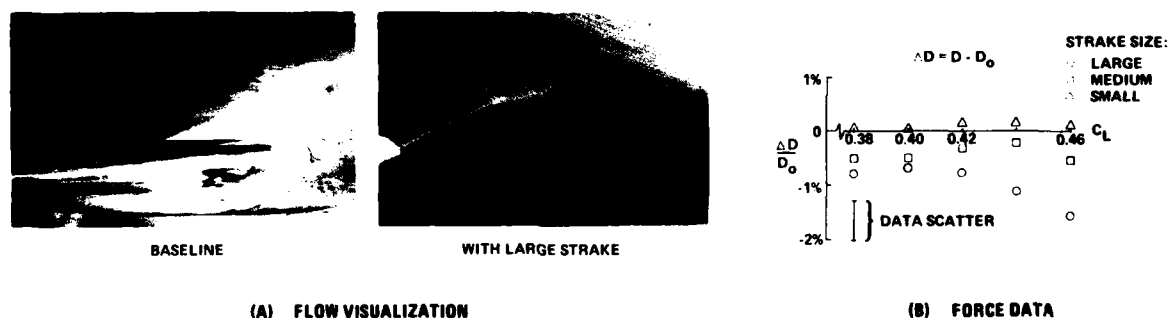


Figure 6. Wind Tunnel Results for Strake Design Study

3. TRANSONIC TRANSPORT CRUISE WING DESIGN

Engineers designing transport wings have begun to take advantage of recently developed methods for analyzing three-dimensional configurations in transonic viscous flow. Various organizations have developed three-dimensional transonic potential flow methods that are able to analyze either isolated wings or wing-fuselage combinations (see refs. 18 through 22). Evaluation of these methods indicates that the approach of solving the full transonic potential flow equation (ref. 19) that is coupled with a boundary layer method (ref. 23) demonstrates the best agreement between calculated and experimental results. A shortcoming of the program is that it is unable to treat arbitrary fuselages.

The three-dimensional viscous transonic wing analysis technique utilizes Jameson's wing analysis program (ref. 19) for calculating pressure distributions and surface velocity components on wings for freestream Mach numbers up to unity. The program uses finite volume methods to solve the exact transonic potential flow equation on a three-dimensional mesh constructed from small volume elements (or cells). The current version of the program does not adequately treat body effects, and thus, it is used only for wing alone analysis. It is assumed that any shock waves contained in the flow are weak enough so that the entropy and vorticity generated by the shock waves can be neglected. The potential flow equation is treated in conservation form, i.e., mass is conserved in each element.

The three-dimensional boundary layer program developed by McLean (ref. 23) uses finite difference methods to solve the compressible three-dimensional boundary layer equations for either laminar or turbulent attached flow. In the turbulent case, an eddy viscosity model is used for the turbulent shear stresses. Separation at a given wing span station is indicated by the program when the finite difference solution is no longer able to proceed in a normal manner (because it is not able to account for the reverse flow present in separated regions).

These methods are coupled through an interface program that constructs the boundary layer grid used for the analysis and interpolates the velocity components from the potential flow program onto the boundary layer grid. A second interface program obtains the three-dimensional boundary layer displacement thickness from the boundary layer solution. This is then added to the bare wing surface for another potential flow run. It is therefore possible to automatically cycle several times between viscous and inviscid programs. The number of cycles required to achieve convergence varies depending upon Mach number and lift coefficient. This method and a comparison of computed and experimental results are discussed in Reference 5.

Example 3:

The method described above was used to evaluate the possible drag penalty (due to increased wetted area) for extending a wing's trailing edge behind the rear spar. A possible reason for such a design effort would be to provide increased space for the stowed landing gear. The change in planform and the principal change in airfoil section are shown in Figure 7. Wing A in this figure is the original geometry, while Wing B is the stretched configuration. The airfoil was extended behind the rear spar fairing smoothly into the base airfoil. This led to a slight decambering of the wing.

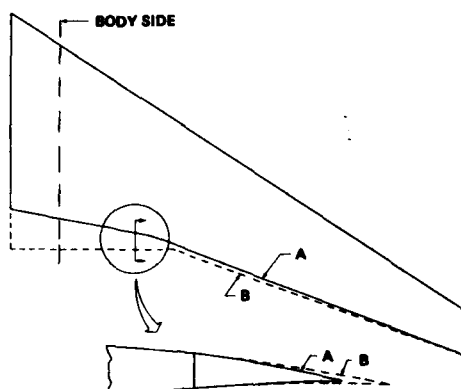


Figure 7. Wing Planforms and Sections Analyzed in Trailing Edge Extension Design Study

Typical results that are obtained from the coupled transonic potential flow and boundary layer programs are depicted in Figure 8. In addition to pressure coefficients, results include details about the boundary layer that are valuable in understanding the behaviour of a wing. As an example, the local chordwise variations of the drag component of skin friction for the two wings at an inboard span station are shown in Figure 9. Relative to Wing A, the stretching of the airfoil reduced the gradients in the pressure recovery region. Note that the reduced pressure gradient near the trailing edge led to an increase in skin friction. The spanwise distribution of profile drag, which was calculated using the Squire and Young formula (ref. 24), is shown in Figure 10a. Included in this figure is the integrated drag component of skin friction. The results show that the integrated skin friction is higher for the larger wing as expected. The form drag is less for the stretched wing, which arises from the less steep pressure recovery. When the wave drag is included, the total drag (at the same total lift) for the two wings was very close, as portrayed in Figure 10b.

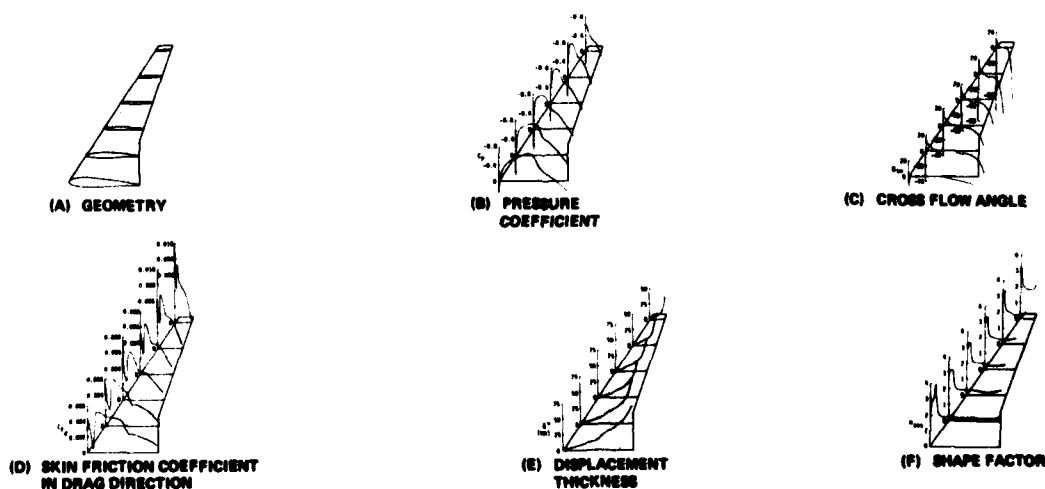


Figure 8. Computed Results From Viscous Transonic Analysis Method

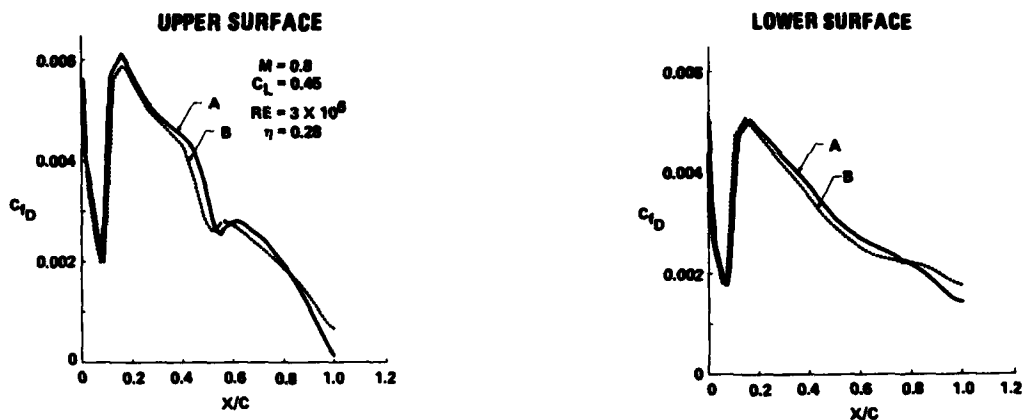


Figure 9. Drag Component of Local Skin Friction for Upper and Lower Surfaces

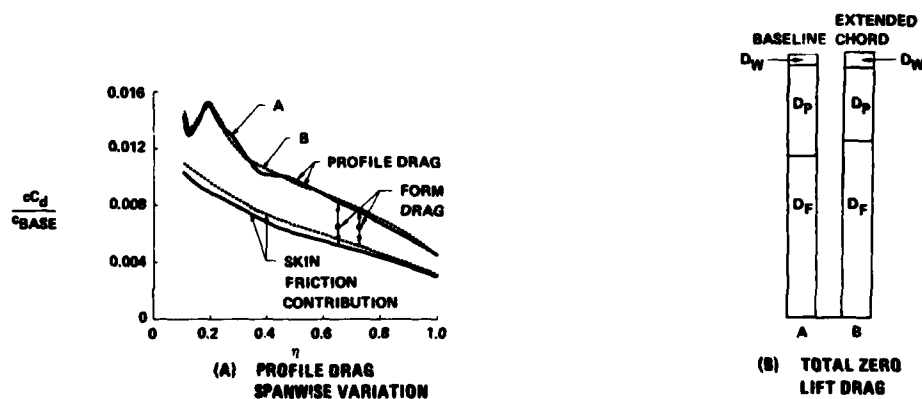


Figure 10. Comparison of Drag Components

4. SUPERSONIC CRUISE WING DESIGN

The design of wings for supersonic flight is complicated by real flow phenomena that presently cannot be accurately modeled, but have substantial effects on the performance of these configurations (ref. 25). Specifically, the linear inviscid methods cannot predict separation (either leading-edge, trailing-edge, or shock-induced types), they can provide unrealistically high negative pressures, and in design mode they may yield optimized solutions that have unfavorable, strong spanwise flow. A supersonic design and analysis method has been developed that is able to overcome these limitations to some extent by constraining the inviscid pressures to reflect favorable and realistic supersonic designs (ref. 26, 27). The method includes comprehensive wing design and optimization procedures that allow physical realism and practical considerations to be imposed as constraints on the optimum (least drag) solution. In addition to the usual constraints on lift and pitching moment, constraints can also be imposed on wing surface pressure level and gradients, and on camber surface shape. The program provides the capability of including directly in the optimization process, the effects of other aircraft components such as a fuselage, canards, and nacelles. The program also includes nonlinear methods that provide realistic determination of shock waves produced by general bodies, and also the intersection of the shock waves and pressure fields with adjacent bodies and wings. Application of this method is limited to supersonic Mach numbers, planar configurations, and bodies that can be represented by equivalent bodies of revolution. Typical loadings used for optimizing the wing shape as well as constraints that can be applied during a design are pictorially shown in Figure 11 (ref. 28). Examples of separation criteria are shown in Figure 12.

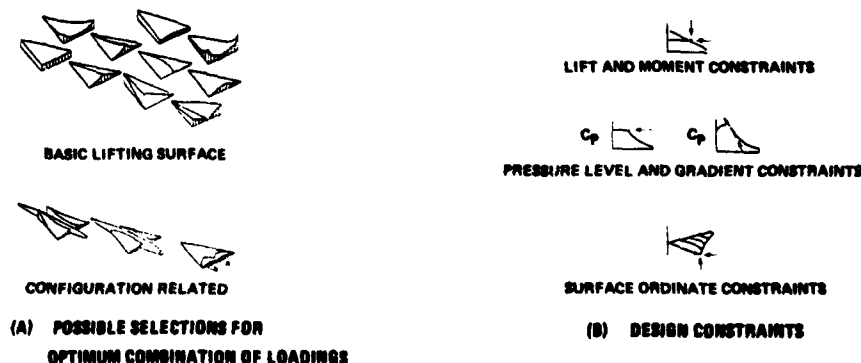


Figure 11. Program Capabilities for Optimization of Supersonic Configurations

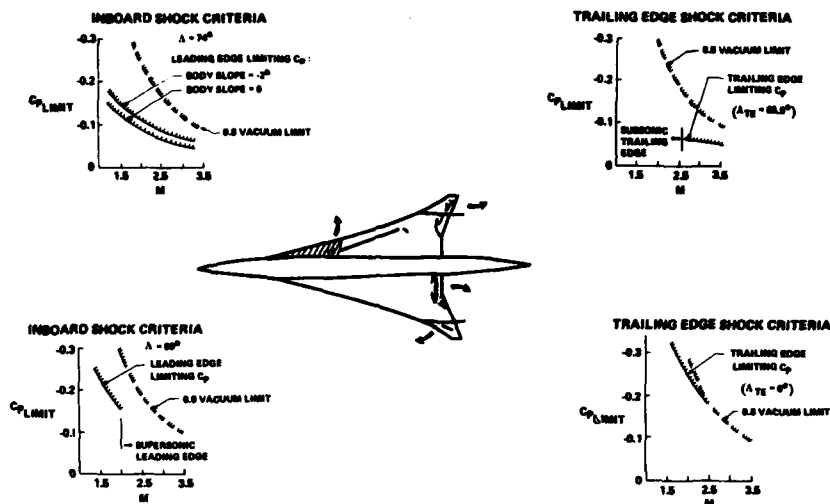


Figure 12. Example of Separation Criteria Application

Example 4:

Typical supersonic design begins with an aircraft layout that includes wing planform, spanwise and chordwise thicknesses, and critical fuselage cross-sectional areas. For example, the paneling layout for an SST configuration is shown in Figure 13. These data are then used in the supersonic area rule portion of the program to design an optimum (minimum zero lift wave drag) wing-body at the cruise Mach number that meets the specified geometric input constraints. The resulting fuselage area distribution, shown in Figure 13 (ref. 29), is then used to develop the body cross-sections in conjunction with an approximate inboard wing camberline. This is done to develop the body shape used in the wing design process.

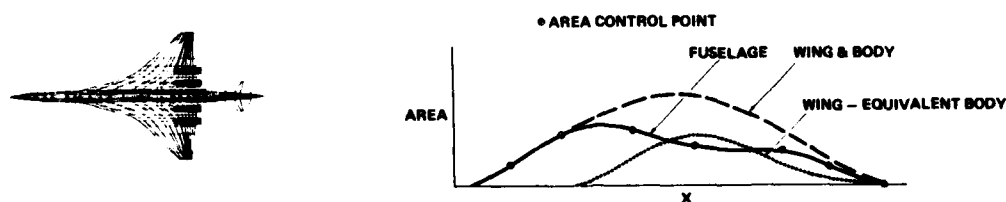
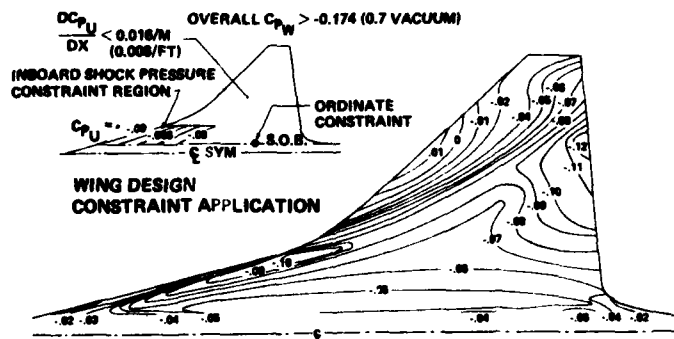


Figure 13. Fuselage Optimization for Minimum Wave Drag

The wing design portion of the program is then used to optimize the lifting pressure distribution acting on the wing subject to imposed constraint conditions. The constraints include fuselage side-of-body ordinates, upper surface shock criteria, upper surface minimum pressure coefficient, and upper surface pressure gradient. These constraints are depicted in Figure 14. The design solution can be readily checked by examining the resulting wing isobar pattern to obtain a global view of the effects of the applied constraints. Such an isobar pattern is also shown in Figure 14.

Figure 14. Applied Constraints and Resulting Theoretical Upper Surface Isobar Pattern at $M = 2.4$, $C_L = 0.12$

But this design, a model was constructed and wind tunnel tested. A drag polar comparison of experimental and theoretical results are shown in Figure 15. The drag at cruise conditions is reasonably well predicted. Moreover, at the design conditions there was no evidence of flow separation as shown by the oil flow picture in Figure 15.

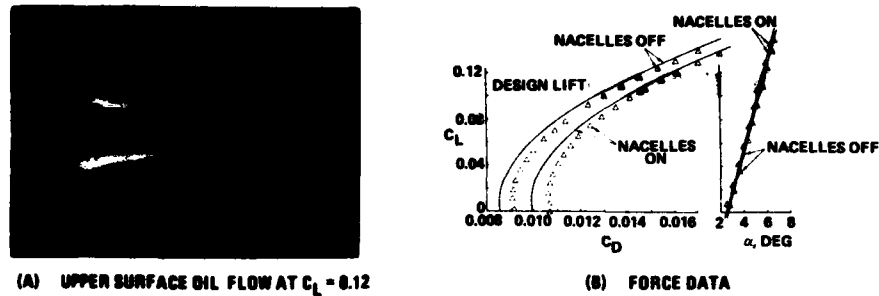


Figure 15. Test - Theory Comparison of Supersonic Configuration

Example 5:

A second example involving supersonic design, but for a nonplanar configuration, involved the Lightweight Experimental Supercruise aircraft (LES-216), whose paneling is shown in Figure 16a. This configuration was optimized for a Mach number of 1.8. The baseline wing was designed similar to the previous example. Stability for this configuration was achieved by drooping the wing tip 60° down and by adding a vertical fin. Fin alignment and wing twist were optimized by using a design/analysis program for nonplanar configurations (ref. 30). The method is based on linearized potential flow theory, which is valid at both supersonic and subsonic Mach numbers. The numerical solution is based on the constant pressure panel aerodynamic influence coefficient method of Woodward.

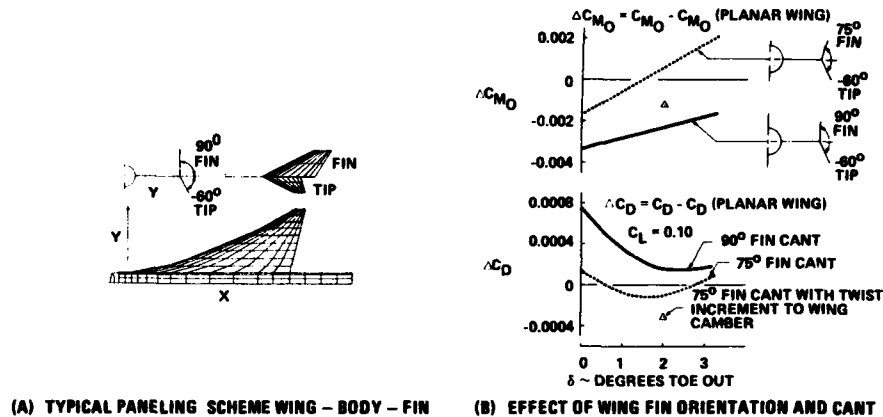


Figure 16. Computational Model for the Lightweight Experimental Supercruiser and Representative Theoretical Results

The configuration was optimized for two fin cant angles: 90° (or vertical) and 75° . These are depicted in Figure 16b. Theoretical drag increments for the resulting optimized configurations are also shown in this figure. Minimum drag occurs when the fins are aligned with 1.5° to 2.5° toe-out for the 75° cant case. Comparison between theoretical and experimental data (ref. 31) are shown in Figure 17. At the design lift coefficient the drag increment is in close agreement. However, the increments differ substantially at higher lift coefficients. Upper surface pressures shown in Figure 17 are in close agreement. Additional analysis of this configuration using a higher order panel method presently being developed can be found in Ref. 32.

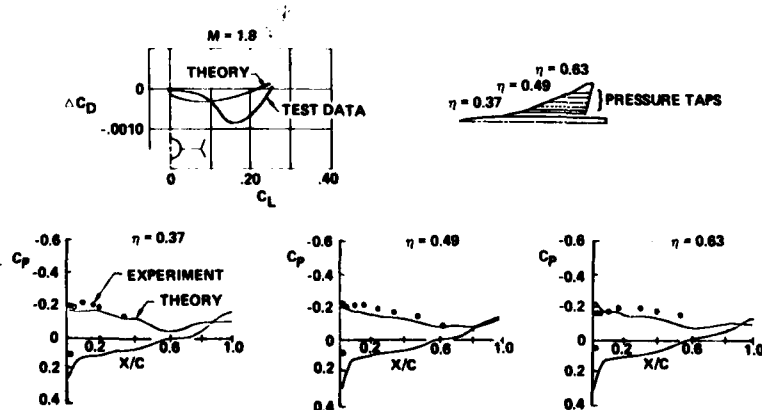


Figure 17. Comparison of Wind Tunnel and Computational Results

5. STATUS ASSESSMENT

The significant advances that have been made in computational aerodynamics are having considerable impact on the airplane design process as evident from the foregoing examples. As mentioned in the Preface, the factors that have contributed to these advances have been improved hardware technology, sophisticated software technology, better engineer-computer interfaces, and improved engineer-software interfaces. All of these factors affect the design cycle flow time required to obtain a solution. For the configuration design engineer, this time is the most important variable that determines whether a computational method is usable in the design environment.

Hardware Technology

Advances in computers have unquestionably had a significant impact on the use of computational aerodynamics and the capability to model more of the entire configuration while accounting for more of the actual physics of the flow. The progress in computer technology and its future outlook has been summarized in numerous reports and books (ref. 1 through 4). A gross measure of computing performance, which is useful for comparing CPU processing speeds for different computers, is the MIPS rating - the number of instructions (in millions) executed per second. It is an average of the number of typical operations required for data processing that can be carried out in a unit of time. In scientific processing, the set of typical operations might include a matrix multiplication, a square root evaluation, or a finite difference solution to a differential equation. The improvement in computer performance since 1950 based on the MIPS rating is shown in Figure 18 for several computers developed in the U.S.A. Data for this figure were obtained from Reference 2. These ratings indicate a better than three order of magnitude improvement over a 25 year period.

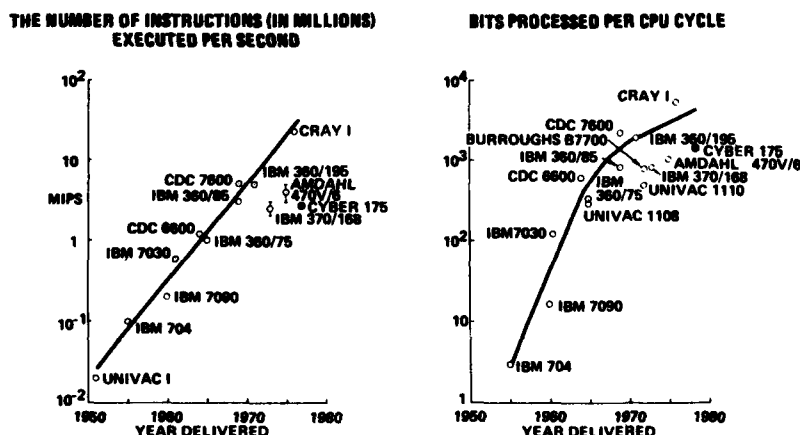


Figure 18. Improvements in Computer Performance

Another measure of hardware performance and complexity is the number of bits processed per CPU cycle time. The variation of this parameter with year delivered for several machines is also shown in Figure 18 (ref. 2). These data show a similar three order of magnitude improvement over roughly the same period as the previous rating.

Machines to be built in the near future will continue these trends. The proposed NASA Numerical Aerodynamic Simulation Facility (NASF, ref. 3) offers to solve Reynolds averaged Navier Stokes equations for practical three-dimensional wing-body configurations. An interesting feature of the NASF is that its design is accounting for the nature of the software it is to handle. The most advanced computers are not, however, the machines used by aircraft configuration designers. The NASF will probably not be used in the daily design process, but only for special problems in the manner that NASA's high Reynolds number test facilities are used. At The Boeing Company, the machines used for configuration design/analysis are currently CDC CYBER 175's, which are shown in Figure 18. Although other computers outside the company are available (such as the STAR and CDC 7600), they are generally used for methods research and development. Unfortunately, some new codes are written specifically for advanced machines, and they cannot be converted easily (or in some cases, not at all) to more generally available machines.

Software Technology

The rapid development in computational aerodynamics capability that has occurred in recent years is depicted in Figure 19. Most programs contain elements of empiricism where certain factors are chosen that give good agreement with test data. This is satisfactory for analysis/design of configurations similar to those for which the programs have been validated. Departure from that domain often leads to erroneous results. Some examples of specific areas of software development that requires timely attention are listed below.

STAGE	COMPUTED RESULTS	READINESS TIME PERIOD		
		3D AIRFOILS & SIMPLE BODIES	SIMPLE 3D BODIES & WINGS	PRACTICAL 3D WING BODY COMBINATIONS
I LINEARIZED INVISCID	<ul style="list-style-type: none"> PRESSURE DISTRIBUTION VORTEX DRAG SUPERSONIC WAVE DRAG 	1950	1960'S	1960
II NONLINEAR INVISCID	ABOVE PLUS: <ul style="list-style-type: none"> TRANSONIC FLOW HYPERSONIC FLOW 	1971	1973	1976
III NAVIER STOKES RE-AVERAGED MODEL TURBULENCE	ABOVE PLUS: <ul style="list-style-type: none"> SEPARATED FLOW TOTAL DRAG PERFORMANCE SUFFETING 	1975	1978	EARLY 1980'S
IV LARGE EDDY SIMULATION MODEL SUBGRID SCALE TURBULENCE	ABOVE PLUS: <ul style="list-style-type: none"> AERODYNAMIC NOISE 	EARLY 1980'S	MID 1980'S	CIRCA 1980?

Figure 19. Development of Computational Aerodynamics (From Ref. 4)

Geometry and Grid Generation: In order to perform an analysis or design, the definition of the geometry is usually one of the most time consuming tasks. The system in which the geometry is defined must be easy to input, provide smooth surfaces (preferably continuous curvature), provide adequate control of the surface characteristics, provide adequate accuracy, and permit local changes. No ideal geometry system exists today, although new systems are being developed (ref. 33). For certain types of analysis and design, typical of transonic finite difference computations, a spatial grid system must be defined. In order to give sufficient resolution around leading edges, the grid system should be surface fitted. Such grid generation systems exist today only for simple configurations. To conduct transonic analysis for complete configurations, a practical, automatic grid generation system needs to be developed.

Drag: Although many components of airplane drag can be computed (e.g., skin friction, wave drag, and induced drag), the determination of the total configuration drag relies heavily on empirical techniques, since no capability exists for accounting for complex component interactions, such as corner flows, vortex formation, and local separated flows. For example, no method of calculating the expected difference in drag was available for the simple case of the wing strake mentioned in Section 2. This is a major deficiency of present aerodynamic computer programs.

Three-Dimensional High Lift Configurations: Two-dimensional multielement high lift systems can today be adequately analyzed and designed with available methods. For high aspect ratio wings, three-dimensional high lift systems can be handled in the attached flow regime with panel methods. For cases involving partially separated flow, three-dimensional lifting surface methods are supplemented with two-dimensional strip analysis. It is important that methods accounting for three-dimensional viscous effects including separated flow be developed. For low aspect ratio wings where the high lift condition is dominated by the existence of free vortices, the new panel technology (ref. 34) promises to become an important analysis/design tool.

Three-Dimensional Transonic Flow: Analysis of three-dimensional configurations are limited to wing alone or wing-fuselage cases. Three-dimensional viscous effects can only be handled for wings with attached flow and weak shocks. There is an emerging technology for complete configurations (ref. 35), but it is not available today to the engineering community. Shock-boundary layer interactions and separated flows also need to be addressed.

Supersonic Analysis of Nonslender Configurations: Present technology is applicable to supersonic cruise vehicles at moderate angles of attack. A new panel technology (ref. 32, 36) promises to fill the void for complex and less slender configurations. Future requirements include the capability to handle nonlinear flow phenomena such as strong shocks and coalescing shock waves.

Engineer-Computer Interfaces

Good engineer-computer interfaces for aircraft design is contingent upon providing sufficient computing capacity and access. This problem has been well addressed at The Boeing Company. Improved computing capacity will lead to increased usage, and recent trends within The Boeing Company are depicted in Figure 20. As shown in this figure, the usage rate has increased dramatically in recent years. Several things are worth noting. The upper diagram shows the usage and the lower the available computing capacity. During 1977 to 1978, Boeing made a major upgrade of its scientific computing capability, replacing four CDC 6600's with five CDC Cyber 175's. Before this upgrade, turn-around was slow and sophisticated programs could only be run on weekends due to their long residency times. This made the use of these sophisticated tools impractical in the day to day design effort. Today, a few hours turn-around time is achieved for the more sophisticated programs. This increased capability is reflected in the dramatic increase of usage by the design aerodynamics groups. In contrast, the computer usage for method development and maintenance has increased relatively slowly. The point to be made here is that for method development adequate turn-around time is very beneficial, but for actual engineering use it is crucial. In addition to these large mainframes, the company supports sixteen PDP-11/70 minicomputer facilities to handle pre- and post-processing graphics and analysis. These machines are used directly by the engineers in evaluating and plotting results generated by programs executing on the large computers. It is also possible to transfer data directly between the minicomputers and the mainframes.

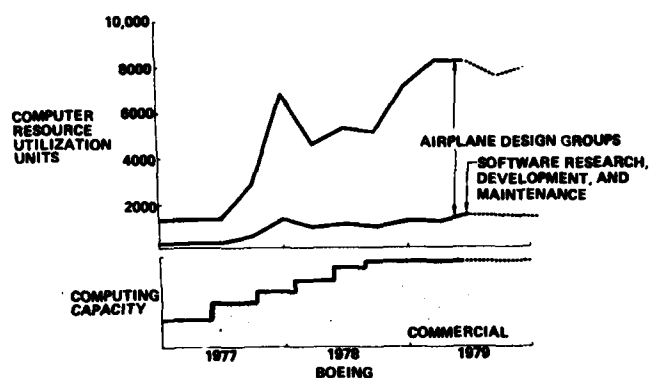


Figure 20. Computer Utilization by Aerodynamicists

Computer accessibility is also achieved by providing 240 conversational terminals throughout the company. In addition, 25 remote job entry stations provide rapid access to input and output. The computing facilities available for scientific computing within The Boeing Company are portrayed in Figure 21. Note that these facilities do not include machines dedicated to experimental facilities, manufacturing, business activities, and outside computing customers.

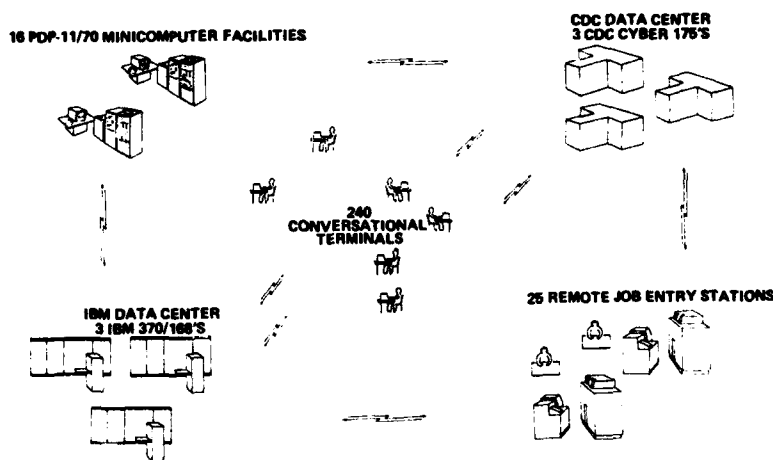


Figure 21. Improved Interface Between Engineers and Computers (at Boeing)

Engineer-Software Interfaces

The most serious barrier to making aerodynamic computer programs useful is in the area of engineer-software interface (ref. 37). In general, the engineering user has had to work with computer code written by the researcher, and apparently, for the researcher. Some researchers may disagree with this statement, but all one has to do is look at most of the computer code now available and review the program documentation. Most of the programs are very poorly documented internally and there is very little external documentation to tie the computer code to the theoretical development. All too often, very little thought has been given to the user and to the programmer who must work with, modify, and adapt the researcher's code. The end result has been tremendous hidden costs and greatly compromised effectiveness of the tool. These adaptation and maintenance costs can often be higher than the cost of the development of the original code.

From the engineering user's viewpoint, the development of program interfaces and pre- and post-processing capability for new computational methods is just as important as the primary algorithms and machine architecture. As new methods are developed that compute more details of the flow field, the visibility of output data becomes a major problem. The problem is then doubled when design capability is added to a method. It is very important that the user be able to see, understand, and interpret the results calculated by new and more powerful methods. Today, the engineering manhour costs expended because of the need to work with programs having only primitive user interfaces are enormous. The research/development community is beginning to recognize this fact and to improve the situation. As an example, Figure 22 depicts the automated three-dimensional viscous transonic analysis method discussed in Section 3. Once a wing geometry is defined, it is quite simple to set up an analysis run. The plots shown in this figure and in Figure 8 were machine generated using an interactive graphics terminal. Ease of data input, transfer of data between various programs, interactive computing and interactive graphics are all important elements that can ease the use for the design engineer.

Three-Dimensional Viscous Transonic Wing Analysis Procedure

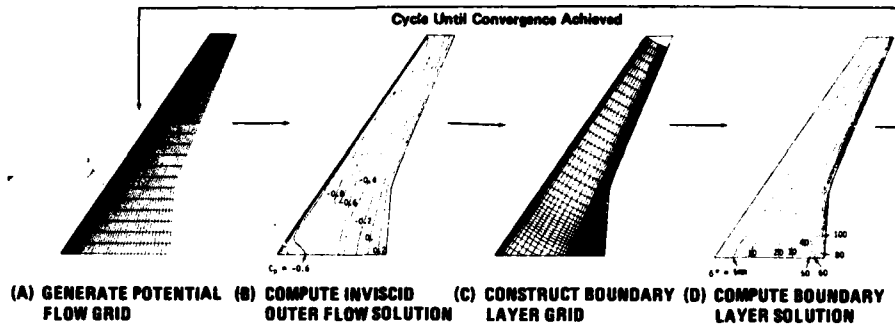


Figure 22. — Automated Analysis/Design Procedures to Improve Engineer-Software Interface

Design Cycle Flow Time

The dominating factor that determines whether a computer system and computational method can be considered an effective engineering design tool is the total flow time required for one cycle (a single analysis/design point). Cycle time includes total time including input preparation and output of essential results but assumes that the geometry definition is already available. An historical view of the development of computational methods and their cycle flow times are shown in Figure 23. Data for this figure were derived from studies conducted at Boeing. The symbols indicate when the method became generally available.

The data shown in Figure 23 indicate that cycle flow time has diminished with each enhancement of capability for both two- and three-dimensional methods. Thus, for two-dimensional methods, the initial subsonic inviscid methods required about three days flow time; when transonic methods became available, their flow times were down to about one hour; and cases can now be run using coupled viscous transonic methods in about one-half hour. This reduction in flow time has occurred primarily from incorporating improved user features, and to a lesser extent from quicker algorithms, and increased machine capacity. Note that although cycle times for subsonic inviscid methods has reduced, it has not become less than the transonic methods. The reason is that paneling for the panel methods requires substantial user experience to set up, whereas it is automatic for the transonic methods. Subsonic methods generally possess greater capabilities for analyzing more complete configurations, and consequently, there is a continued need for their existence and development. For example, some two-dimensional subsonic methods can handle multi-element airfoils, and some three-dimensional subsonic methods can handle complex wing-body configurations, including nacelles, pylons, winglets, and almost any aircraft component that can be simulated by appropriate paneling. Subsonic methods also offer some cost advantages compared to transonic methods for similar subcritical conditions. Another reason that flow times for subsonic methods has remained relatively long is that less emphasis is placed on improving existing methods compared to creating new methods. Cycle times for transonic methods appear to be stationary. Apparently, once these methods become sufficiently developed for production usage, little additional effort is placed upon improving them except for reducing computing costs, which has little bearing on usage flow time.

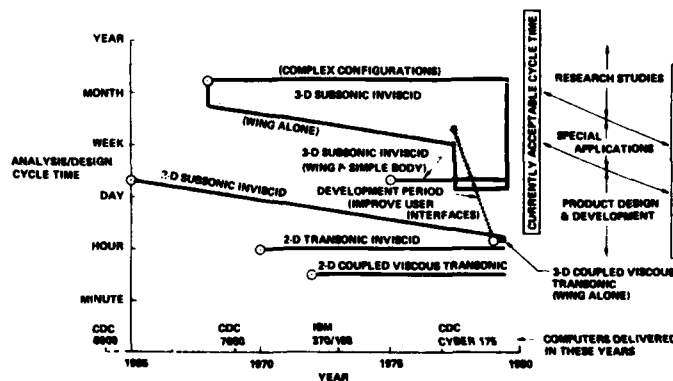


Figure 23. — Time Required to Conduct an Analysis or Design Using a Computational Method

Cycle time for any computational method could consist of the machine run time plus less than one hour of set up time. If a method does not possess this capability, it indicates that little consideration was given to providing proper user interface. An example of the importance of user interfaces is demonstrated by the recent development of the three-dimensional viscous transonic method used at Boeing. Preliminary studies in 1977 showing the feasibility of combining transonic potential flow and boundary layer methods required about two weeks to complete a single analysis cycle. In preparing a production version of this method, considerable effort was made to provide an easily usable method. As a result, analysis condition set up time is now less than one hour.

Experience at Boeing suggests that presently the available aerodynamic computational tools can be characterized in three usage categories:

1. Cycle time more than one month: Research code.
2. Cycle time more than a week and less than a month: Intermediate - used occasionally to support critical designs.
3. Cycle time less than a week: Engineering tool.

These are indicated on Figure 23. Cycle times acceptable by today's standards are longer than those needed for computational methods to become truly effective as engineering design tools. Essentially, a single day flow time is required. This permits rapid assessment of many configuration modifications, and the ability to analyze a configuration prior to wind tunnel testing. When the flow time is a month or longer, evaluation of different configurations is severely limited. Future requirements for cycle times are also shown on Figure 23.

6. CONCLUSIONS

Recent developments in computational aerodynamics have had a major impact on the aircraft configuration design process. It provides:

1. Better (higher technology) designs.
2. Less risk.
3. Better understanding of the design and test results.
4. Reduced requirements for testing or a better product for a given number of test cycles.

The major voids in our technology for steady state flows are from the airplane designers standpoint:

1. Better geometry systems and automatic grid generation for complete configurations.
2. Drag computation.
3. 3-D High-lift methods including viscous effects and separation.
4. 3-D Transonic methods for complete configurations including the effects of shock induced separation.
5. Supersonic analysis of nonslender configurations.

The major stumbling block in making computational aerodynamics an everyday engineering tool is in the user interface area. What is needed is:

1. True interactive computing with online graphic displays for input checkout and result analysis.
2. Automated interfaces between related programs used in the design process.
3. Faster turnaround (design cycle) times.

7. REFERENCES

1. Chapman, D.R., Mark, H., and Pirtle, M.W., "Computers vs. Wind Tunnels for Aerodynamic Flow Simulations," Aeronautics and Astronautics, Vol. 13, No. 4, April 1975, pp. 22-30, 35.
2. Matick, R. E., Computer Storage Systems and Technology, New York, Wiley-Interscience, 1977, pp. 1-70.
3. National Aeronautics and Space Administration, Future Computer Requirements for Computational Aerodynamics, 1978, NASA CP-2032, pp. 1-515.
4. Chapman, D. R., "Computational Aerodynamics Development and Outlook," 1979, AIAA Paper No. 79-0129.
5. da Costa, A. L. V., "Application of Computational Aerodynamic Methods to the Design and Analysis of Transport Aircraft," ICAS Proceedings 1978, Paper No. B2-01, pp. 261-269.
6. Haines, A. B., "Computer-Aided Design Aerodynamics," Aeronautical J., Vol. 83, No. 819, March 1979, pp. 81-91.
7. Krenz, G., "Transonic Wing Design for Transport Aircraft," 1979, AIAA Paper No. 79-0692.
8. Rubbert, P. E., and Saaris, G. R., "Review and Evaluation of a Three-Dimensional Lifting Potential Flow Analysis Method for Arbitrary Configurations," 1972, AIAA Paper No. 72-188.
9. Gillette, W. B., "Nacelle Installation Analysis for Subsonic Transport Aircraft," 1977, AIAA Paper No. 77-102.
10. Ishimitsu, K. K., "Aerodynamic Design and Analysis of Winglets," 1976, AIAA Paper No. 76-940.
11. Chen, A., Tinoco, E., and Yoshihara, H., "Transonic Computational Design Modifications of the F-111 TACT," 1978, AIAA Paper No. 78-106.
12. McMasters, J. H., and Henderson, M. L., "Low-Speed Single Element Airfoil Synthesis," The Science and Technology of Low Speed and Motorless Flight, 1979, NASA CP-2085, Pt. 1, pp. 1-31.
13. Lock, R. C., Aeronautical Research Committee, Equivalence Law Relating Three- and Two-Dimensional Pressure Distributions, 1962, Reports and Memoranda No. 3346.
14. Henderson, M. L., "Inverse Boundary-Layer Technique for Airfoil Design," Advanced Technology Airfoil Research, Vol. 1, 1979, NASA CP-2045, Pt. 1, pp. 383-397.
15. Henderson, M. L., "A Solution to the 2-D Separated Wake Modeling Problem and Its Use to Predict $C_{L_{max}}$ of Arbitrary Airfoil Sections," 1978, AIAA Paper No. 78-156.
16. Goldhammer, M. I., "A Lifting Surface Theory for the Analysis of Non Planar Lifting Systems," 1976, AIAA Paper No. 76-16.
17. Rubbert, P. E., and Saaris, G. R., "A General Three-Dimensional Potential-Flow Method Applied to V/STOL Aerodynamics," SAE J., Vol. 77, Sept. 1969, pp. 44-51.
18. Caughey, D. A., and Jameson, A., "Numerical Calculation of Transonic Potential Flow about Wing-Fuselage Combinations," 1977, AIAA Paper No. 77-677.
19. Jameson, A., and Caughey, D.A., "A Finite Volume Method for Transonic Potential Flow Calculations," 1977, AIAA Paper No. 77-635.
20. Bailey, F. R., and Ballhaus, W. F., "Comparisons of Computed and Experimental Pressures for Transonic Flows About Isolated Wings and Wing-Fuselage Combinations," Aerodynamic Analyses Requiring Advanced Computers, Pt. II, 1975, NASA SP-347, pp. 1213-1231.

21. Boppe, C. W., "Computational Transonic Flow about Realistic Aircraft Configurations," 1979, AIAA Paper No. 78-104.
22. Schmidt, W., and Vanino, R., "The Analysis of Arbitrary Wing-Body Combinations in Transonic Flow Using a Relaxation Method," Symposium Transonicum II, Berlin, Springer-Verlag, 1976, pp. 523-532.
23. McLean, J. D., "Three-Dimensional Turbulent Boundary Layer Calculations for Swept Wings," 1977, AIAA Paper No. 77-3.
24. Squire, H. B., and Young, A. D., Aeronautical Research Committee, The Calculation of the Profile Drag of Aerofoils, 1938, Reports and Memoranda No. 1838.
25. Kulfan, R. M., and Sigalla, A., "Real Flow Limitations in Supersonic Airplane Design," 1978, AIAA Paper No. 78-147.
26. Carlson, H. W., and Harris, R. V., Jr., A Unified System of Supersonic Aerodynamic Analysis, 1969, NASA SP-228, No. 27, pp. 639-658.
27. Middleton, W. D., and Lundry, J. L., A Computational System for Aerodynamic Design and Analysis of Supersonic Aircraft, 1976, NASA CR-2715.
28. Miller, D. S., Carlson, H. W., and Middleton, W. D., "A Linearized Theory Method of Constrained Optimization for Supersonic Cruise Wing Design," Proceeding of SCAR Conference, 1976, NASA CP-001, Paper No. 1.
29. Boeing Commercial Airplane Company, Advanced Concept Studies for Supersonic Vehicles, 1979, NASA CR-159023.
30. Woodward, F. A., Tinoco, E. N., and Larsen, J. W., Analysis and Design of Supersonic Wing-Body Combinations, Including Flow Properties in the Near Field, Part I - Theory and Application, 1967, NASA CR-73106.
31. Spurlin, C. J., Documentation of Wind Tunnel Test Data from the AFFDL Advanced Supersonic Configuration Test, 1976, AEDC-DR-76-96.
32. Tinoco, E. N., Johnson, F. T., and Freeman, L. M., "The Application of a Higher Order Panel Method to Realistic Supersonic Configurations," 1979, AIAA Paper No. 79-0274.
33. National Aeronautics and Space Administration, Workshop on Aircraft Surface Representation for Aerodynamic Computations, March 1-2, 1978, Ames Research Center.
34. Johnson, F. T., Tinoco, E. N., Lu, P., Epton, M. A., "Recent Advances in the Solution of Three-Dimensional Flows over Wings with Leading Edge Vortex Separation," 1979, AIAA Paper No. 79-0282.
35. Boppe, C. W., Toward Complete Configurations Using an Embedded Grid Approach, 1978, NASA CR-3030.
36. Moran, J., Tinoco, E. N., and Johnson, F. T., User's Manual Subsonic, Supersonic Advanced Panel Pilot Code, 1978, NASA CR-152047.
37. Mueller, G. E., "The Future of Data Processing in Aerospace," Aeronautical J., Vol. 83, No. 820, April 1979, pp. 149-158.

8. ACKNOWLEDGEMENTS

The authors wish to acknowledge the contributions of many individuals within The Boeing Company who conducted the analyses reviewed in this paper.

COMPUTATIONAL AERODYNAMIC DESIGN TOOLS AND TECHNIQUES USED AT FIGHTER DEVELOPMENT

by

P. SACHER/W. KRAUS/R. KUNZ
Messerschmitt-Bölkow-Blohm GmbH
AIRCRAFT DIVISION
P.O.B. 80 11 60
D-8000 München 80

SUMMARY

During fighter configuration development an optimization-cycle of techniques is necessary to cover the low speed range (high angle of attack), transonic speed (maneuvering capability) and the high speed supersonic region (maximum SEP). Various different numerical procedures are available to perform this trade-off in a short time, resulting in an optimized configuration.

Second stage optimization of components like direct design of wing, tail/canard or maneuver devices gives further improvements of performance and leads finally to the definition of wind tunnel models. Experimental data compare well with predictions and emphasize the reliability of applied numerical methods.

1. INTRODUCTION

Figure 1 shows in summary the main objects of the following paper. Configuration optimization, component design and experimental proof are main steps in each predevelopment fighter project.

Requirements for supersonic performance overrule at first all other aspects of the new aircraft. Maximum SEP's at high Mach numbers can at present time only be achieved by drag minimization. Wave drag is therefore the most important drag-component of the configuration. Recent publications on this subject [1], [2] and [3] agree very well with this first approach.

Next main component of the drag breakdown is sub- and supersonic induced drag due to lift and therefore wing and canard/tail design follows to give the desired efficiency L/D.

A little bit more in detail Figure 2 summarizes the main aerodynamic principles which are well known and in common use throughout many aircraft companies.

In the supersonic flow region the supersonic area rule [4] with some sophisticated extensions (as later shown) and the area transfer rule [5] is dominating, panel methods for sub- and supersonic flow and vortex lattice methods for subsonic flow, both solving the linearized potential flow equation, are applied for direct design. For analysis of complex configurations in design and off-design panel methods are available for sub- and supersonic flow [6], [7], [8], [9], [10] and for transonic flight it is necessary to solve the complete nonlinear potential flow equation [11] by finite element techniques.

(A) CONFIGURATION OPTIMIZATION

- SUPERSONIC AREA RULE
- NON AXISYMMETRIC EXTENSION
- AFTER BODY OPTIMIZATION

(B) CANARD/ WING DESIGN

- DESIGN FOR SUPERSONIC PERFORMANCE
- DESIGN FOR TRANSONIC MANEUVRABILITY
- TRADE OFF
- TRANSONIC "SUPERCRITICAL" OPTIMIZATION

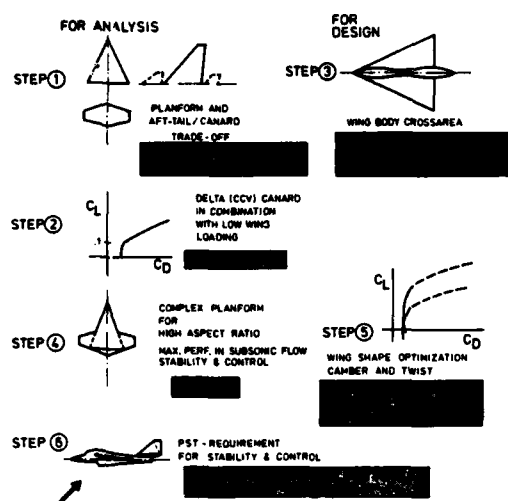
(C) EXPERIMENTAL VERIFICATION

- HIGH SPEED WIND TUNNEL TESTS
- COMPARISON WITH PREDICTED DATA

Figure 1 Predevelopment of new fighter projects

- 1 wing-body-tail area optimization procedure
 - area transfer rule
 - supersonic area rule
- 2 wing-design for transonic/supersonic flight
 - vortex lattice / panel methods
 - finite element techniques
- 3 analysis of complete configuration (including stores)
 - panel methods (sub- supersonic)
 - finite elements (transonic flight)
- 4 wind tunnel program
 - comparison with analysis

Figure 2 Aerodynamic design and analysis of 3D fighter configuration



But as Figure 3 demonstrates some additional procedures are very important which are based on empirical or at least semiempirical data to cover the nonlinear "off-design" region which extends to high angles of attack. Last not least a boundary layer concept is necessary to complete potential flow analysis and for AIC-methods the so-called "surface transpiration technique" [12] is superior to the surface displacement iteration.

Figure 3 The use of different computer codes in development of fighter aircraft

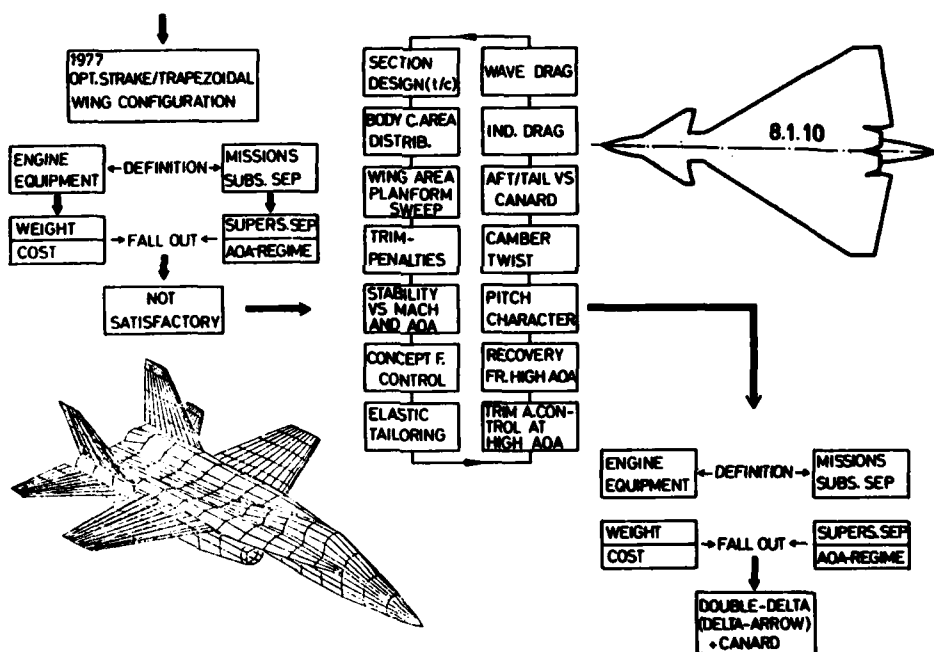


Figure 4 Development from "strake-trapezoidal" to "canard delta" concept

Starting 1977 with an optimized strake-trapezoidal wing concept the "fall out" for supersonic performance was not satisfactory. Due to the statement

"A new aircraft development can be justified if the performance of that new aircraft exceeds that of an old aircraft by at least 15% to 20%" [13].

an extensive configuration loop was initiated to come out with superior supersonic SEP's. Figure 4 gives only a weak impression of various trade-offs between geometry-weight-stress-control and cost which are of great influence in resulting performance.

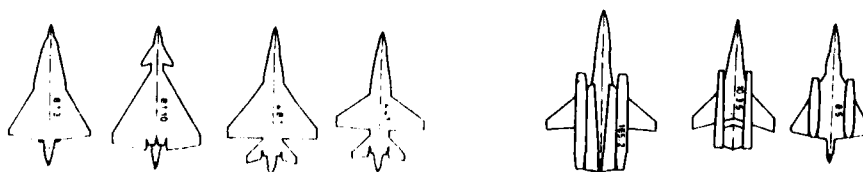


Figure 5 Configuration loop (1977 - 1979)

Figure 5 represents the main "mile-stone-configurations". For each the full optimization procedure has to be performed, or in other words in an average period of 3 to 4 months each configuration must be completed, including all aerodynamic numerical data. This is the main reason for the growing strong impact of numerical aerodynamics in aircraft development. But in contrary to [3], MBB does not apply "closed computation trade-off-loop". We prefer the use of component program-systems (e.g. for wave-drag, L/D-design, transonic flow) which allow the critical interpretation of intermediate results and give the opportunity of direct reaction. Close cooperation between aerodynamic, design and performance is absolutely necessary.

Now: How did we come from "strake-trapezoidal-wing" to the "canard-delta" concept?

2. CONFIGURATION OPTIMIZATION

As previously mentioned, the supersonic area-rule is the semiempirical law for the computation of wave drag [14]. Figure 6 shows in simple form the well known procedure on the lift side in vertical direction. Not so in common use is the variation of computing first an average area and afterwards only one value for the adequate wave drag. This helps the designer in smoothing the Mach-dependent slopes of cross areas.

Figure 7 sketches out the dialog between designer and aerodynamicist in order to obtain the desired "low drag" and "Mach-resistant" cross area distribution. It shows also clearly starting conditions ("constraints") which will accompany the development in every stage of optimization.

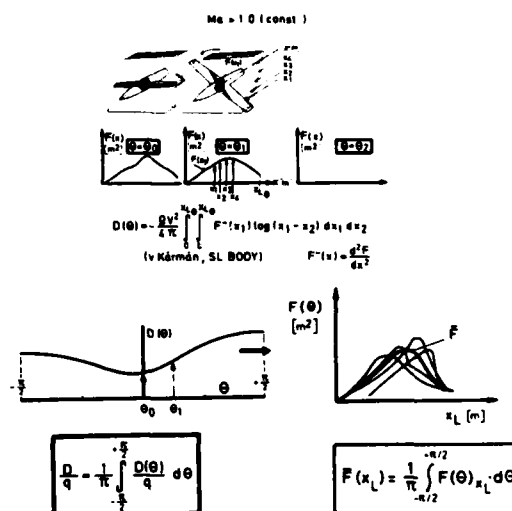


Figure 6 Supersonic "area rule"

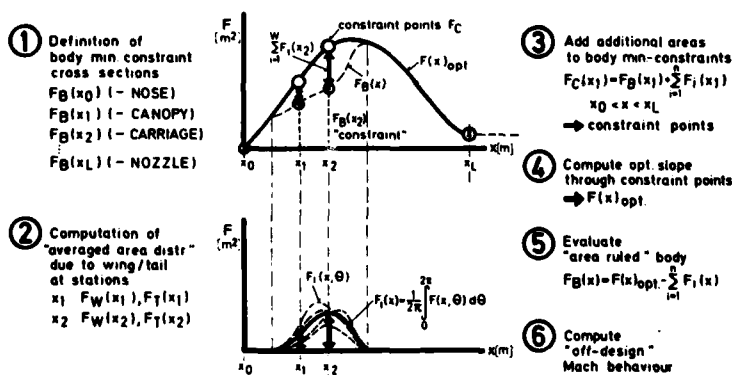


Figure 7 Computer aided design of smooth "optimized" area distributions

Figure 8 demonstrates the large differences in wave-drag-results. Please note that all configurations are optimized in the same level of accuracy for the same Machnumber and constant T/W.

Typically the effect of displaced engines and the susceptibility of arrow-type wings in off-design conditions.

The low level of drag in combination with the smooth off-design behaviour favors the delta planforms.

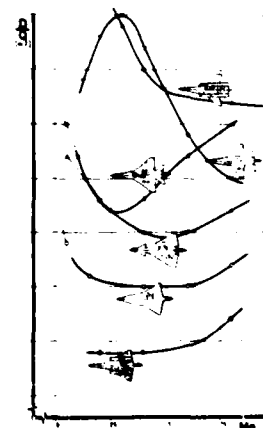


Figure 8 Wave drag of different optimized configurations

To investigate the influence of different wingplanforms on the supersonic drag the analysis in Figure 9 was performed. Applying consequently "area rule" there is no reason for the different slope of drag in fig. 8. But geometric constraints and Machnumber effects are clearly worked out.

Therefore: "For supersonic maximum SEP performance there is a choice between trapezoidal wing with about 32 degrees sweep (and a relativ high design Machnumber) or the wing with more than 50 deg. sweep (that means the delta-concept) independent from Mach".

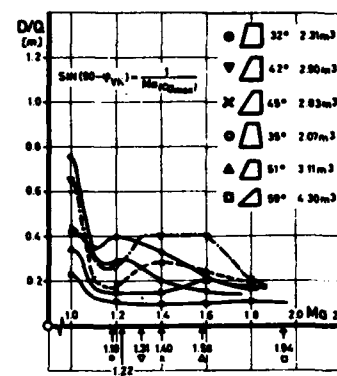


Figure 9 Wave drag for different wing planforms

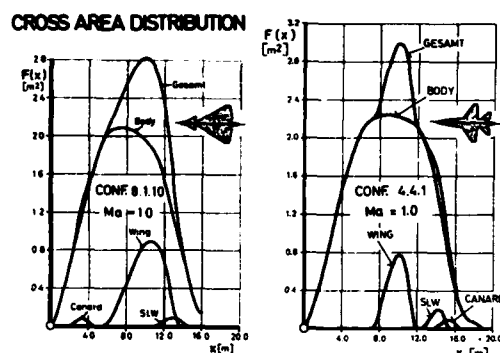


Figure 10 Comparison of optimized configurations at $M = 1.0$

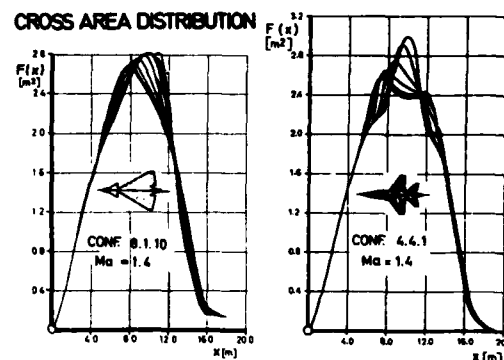


Figure 11 Comparison of optimized configurations at $M = 1.4$

The reason for the complete different behaviour at Machnumbers > 1.0 is shown in Figure 10 and Figure 11. Geometric optimization for $Ma = 1.4$ can never result in a constant slope of cross-areas for different Machplanes β at constant Mach. But for delta planforms the Machplane dependent area-slopes are nearly similar. In contrary, for strake/trapezoidal wing concept, the different slopes vary, resulting in very Machplane-sensitive drag values for different angles of Machplane inclination β° (Figure 12). This behaviour is even amplified at deviations from design Machnumber.

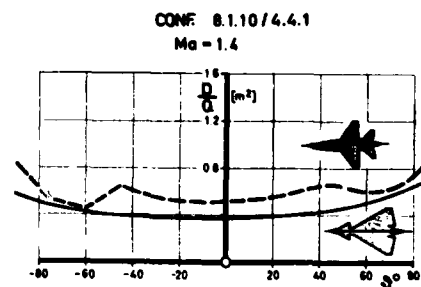


Figure 12 Drag for different Machplanes

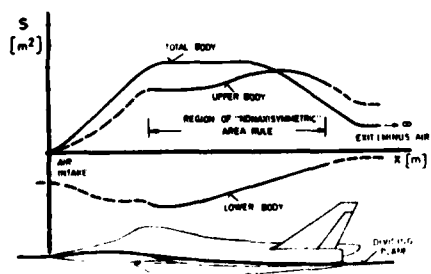


Figure 13 "Nonaxisymmetric area-ruling" concept

Second stage optimization was done by extending the supersonic area rule to "nonaxisymmetric area ruling". Choosing the delta wing concept you can define an upper and a lower region of your aircraft. Due to Figure 13 a dividing plane through your root-camberline of the wing can be defined and consequently there is at least a limited region along x-axis where no influence from upper to lower (and vice versa) area can be possible. That means you have to optimize "upper" and "lower" area distribution separately, the latter including all effects of inlet flow and

the first one covering the nozzle exit problem (max A/B). This leads automatically to problems of afterbody optimization (Figure 14).

Analysing the wavedrag formula in fig. 6 (v. Karman) you see easily that the AB slope of cross area is of dominating influence for the wave drag. Filling up irregularities by smoothing additional areas (displacement bodies, "Bürzel") reduces the gradient of area versus length. Stretching the body and opening the nozzle (max A/B) gives further important improvements of drag.

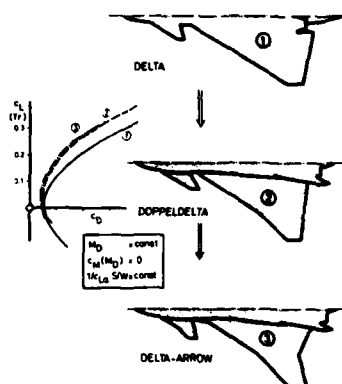


Figure 15 Delta planform refinements

As Figure 16 demonstrates, the penalty (due to wing volume) is nearly negligible, off design behaviour is the same.

After having found an optimum planform, the problem is to find out the final shape of the wing, that means to design twist and camber for best wing efficiency within given constraints (body shape, trim- and control concept).

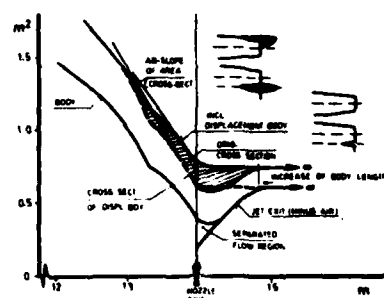


Figure 14 Afterbody area optimization

Aerodynamic wing design leads in most cases to variation of planform (extended span, hybrid planform). The question arises how strong is the influence of planform refinements due to L/D efficiency optimization on wave drag. Figure 15 shows two possible improvements for canard-delta-configurations in order to obtain better L/D at constant design conditions.

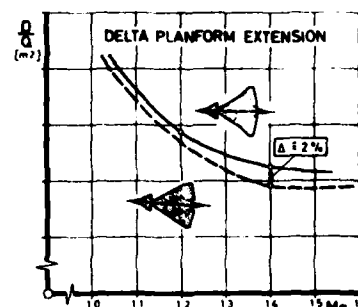


Figure 16 Wavedrag for improved delta planforms

3. CANARD / WING DESIGN

The final design of aerodynamic planforms means the evaluation of twist, camber, flap- and slat settings. The choice of the desired "design strategy", or the definition of basic constraints dominates in actual project work and gives strong limitations to the numerical aerodynamics. The desired minimum drag can only be achieved within realistic weight, stress and structure. Figure 17 shows design philosophy and a collection of computer options, which are available in our design code. Let us first consider the supersonic design case for $M = 1.4$ by our advanced panel method, which is based on "LAGRANGE operators" and additional geometric constraints. For practical purpose this means fuselage is frozen and the design must be performed for zero pitching moment, for both areas (wing + canard) together in one loop, (Figure 18).

• DESIGN-PHILOSOPHY

min ind drag
min wave drag
min trim drag
min wing root bend mom
min shock-extension

⇒ performance
⇒ stress/structure/weight
⇒ efficiency (long range/height)

• HOW TO PROCEED

DEFINITION OF
- pressure (u/l)
- pressure (u)-thickness
- ΔC_p - thickness
RESULT:
⇒ camber/thickness/twist
⇒ camber/twist/pressure (u)
⇒ camber/twist
MINIMUM PROCEDURE FOR DRAG
(or /and pitching moment)
- C_L -spline (x,y)
- thickness
- Cm
⇒ camber/twist/pressure (u)
[F = D = $\lambda_1 (L - \bar{L}) + \lambda_2 (M - \bar{M})$]
"LAGRANGE operator"

Figure 17 Aerodynamic design strategies

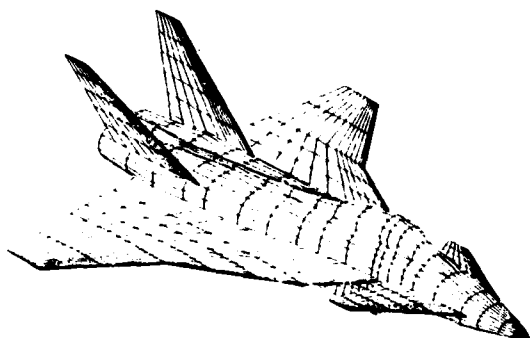


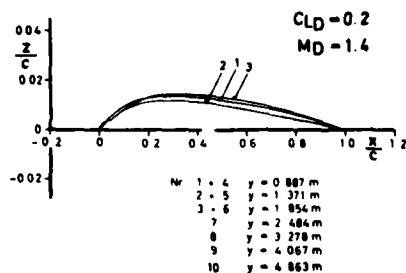
Figure 18 Panel-discretization of canard/delta concept

In contrary to all "conventional" designs of existing aircrafts there is no restriction for the wing shape in spanwise direction. Wings in advanced technology must not be generated by straight lines. Therefore you can accept so-called "potato chip" planforms like Figure 19 shows. This wing results not from superpositions of regular planform modes [15], it is more comparable with results published recently [16].

The design for $CL_D = 0.2$ shows relative high camber ($\approx 2\%$ chord) and up to 10 degrees twist. Although advantages at CL higher than 0.1 are about 20% the inevitable penalties in 1g-cases (lower CL) are too high in comparison with the plane configuration.

SUPERSONIC DESIGN

Camber Distribution CANARD



Camber Distribution WING

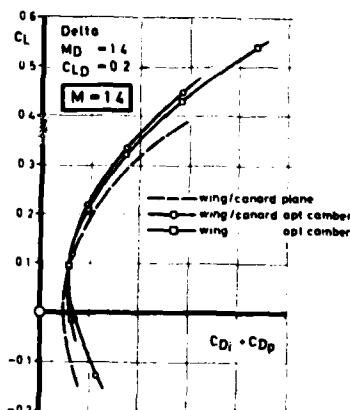
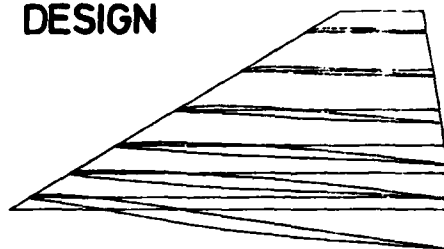
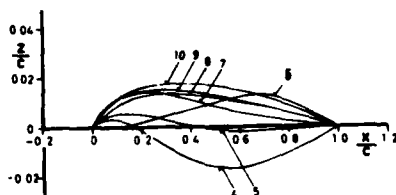


Figure 19 Design at Mach = 1.4 and $CL_D = 0.2$ by supersonic potential method

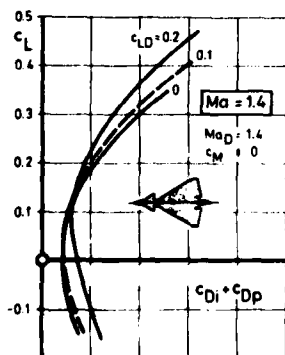


Figure 20 Drag polar for different CL_D

As Figure 20 presents, this drag "design" penalty can be drastically reduced by $CL_D = 0.1$. But consequently the advantages are also going down to about 10% for higher lift coefficients.

But this gain can be realized with only 6 degrees twist and 1% maximum camber (Figure 21).

Therefore the final decision for design CL must be made due to Figure 22. High maneuver CL in different height at lower drag can be achieved with nearly no penalties in 1g-level flight for a design CL of about 0.1 or less at trimmed condition.

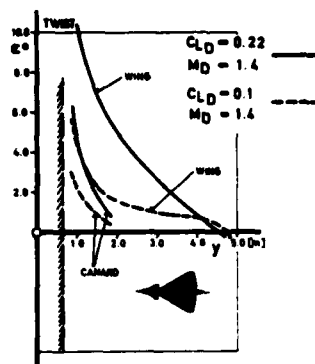


Figure 21 Twist due to supersonic C_{LD}

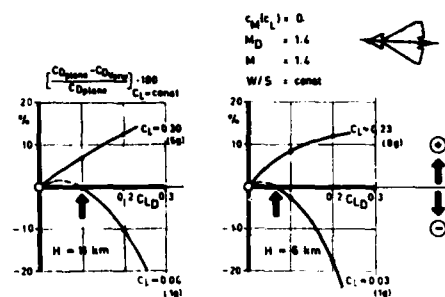


Figure 22 Trade off: Advantage at C_{LD} / Penalty at C_L (1g)

Unfortunately there is at least one additional design condition which is of great influence on wing definition. Transonic maneuvering with high wing efficiency needs (induced-) drag minimization procedures at high subsonic speeds. Linearized potential flow according to vortex lattice or panel methods are restricted to subcritical flow fields. But they may give the same tendencies like Figure 23 demonstrates. Later on it will be explained how local deficiencies of this geometric result will be optimized by an exact nonlinearized potential flow solution.

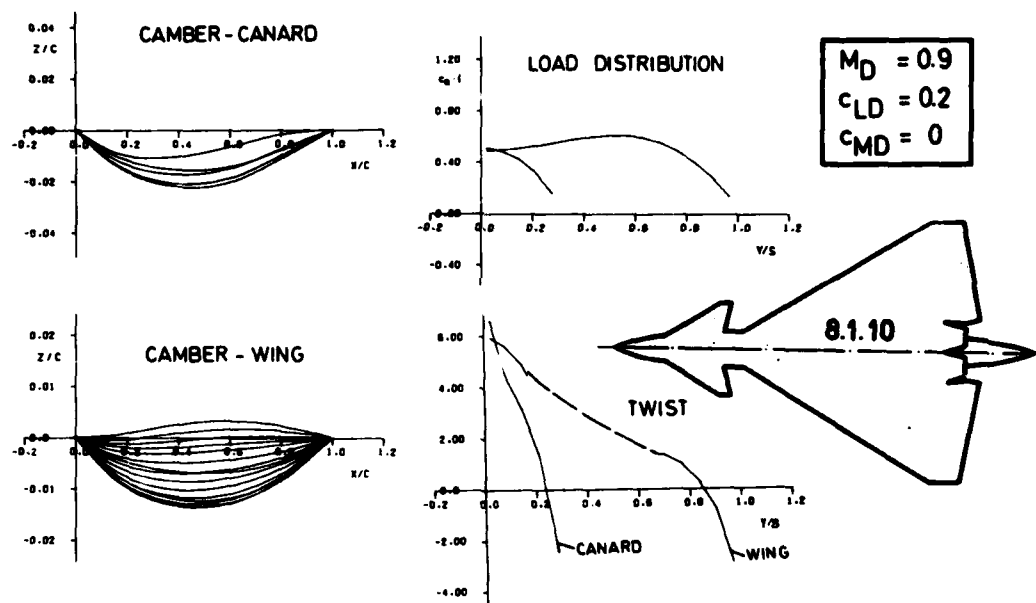


Figure 23 Subsonic canard/wing design by vortex lattice

The most important work is displayed in Figure 24. Supersonic/subsonic design trade-off gives the shape of wing/canard twist and ends with the well known statement that each benefit will have its price. But it seems, that the supersonic design for $M = 1.4$ produces less penalties in off-design for sub- and supersonic speeds and nearly comparable design benefits than the subsonic designed configuration.

Therefore the previous mentioned higher level transonic optimization follows, to give requirements

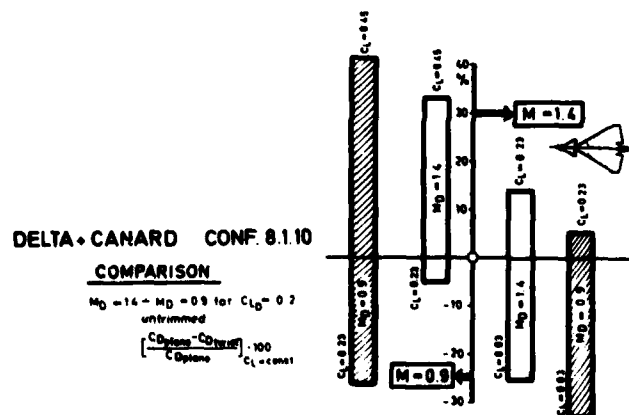


Figure 24 Trade-off: Subsonic/supersonic design

for the final wing shape. In order to obtain nearly shockless recompression in design-condition the "transonic shockless surface" optimization technique [17] is applied.

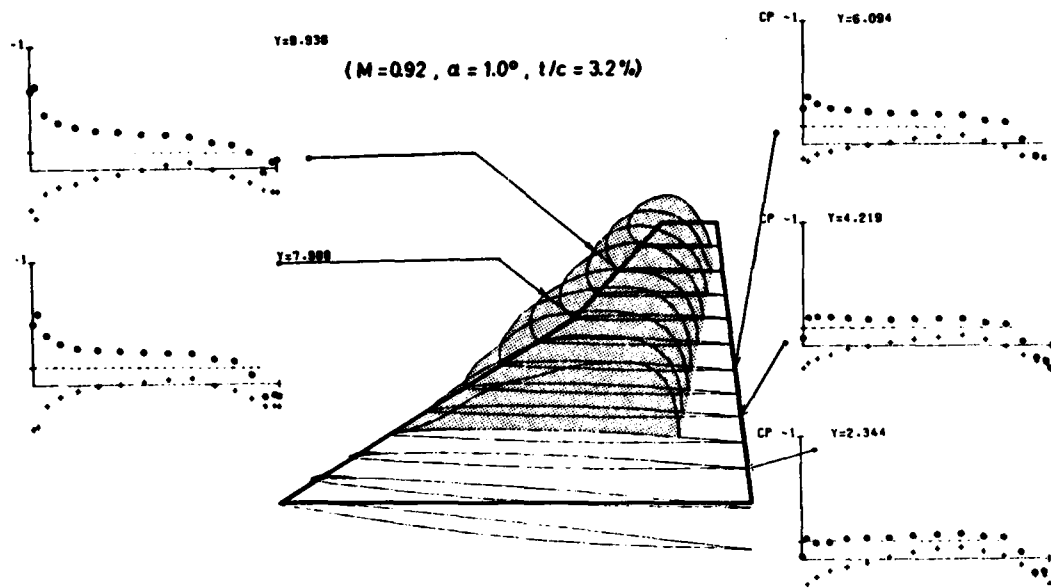


Figure 25 Transonic shockless surface optimization by finite element technique

As Figure 25 proves, shockless recompression is obtained at nearly all sections with about 50% lift from local supersonic flow at a relative high Machnumber (0.92).

One remark to the 2D section design. If somebody is missing this step - there is no reason for doing it. Wings with high sweep-hybrid planforms are of completely 3-dimensional character and no "sheared part" analysis is applicable. The same is true for "quasi-2-dimensional" boundary layer concepts.

Because of the lack of fully 3D boundary layer computer codes quasi 2D (integral-) approaches are combined iteratively with potential flow. In this case we prefer the so-called "surface transpiration" technique, which gives some advantages in computer cost in combination with AIC methods [12].

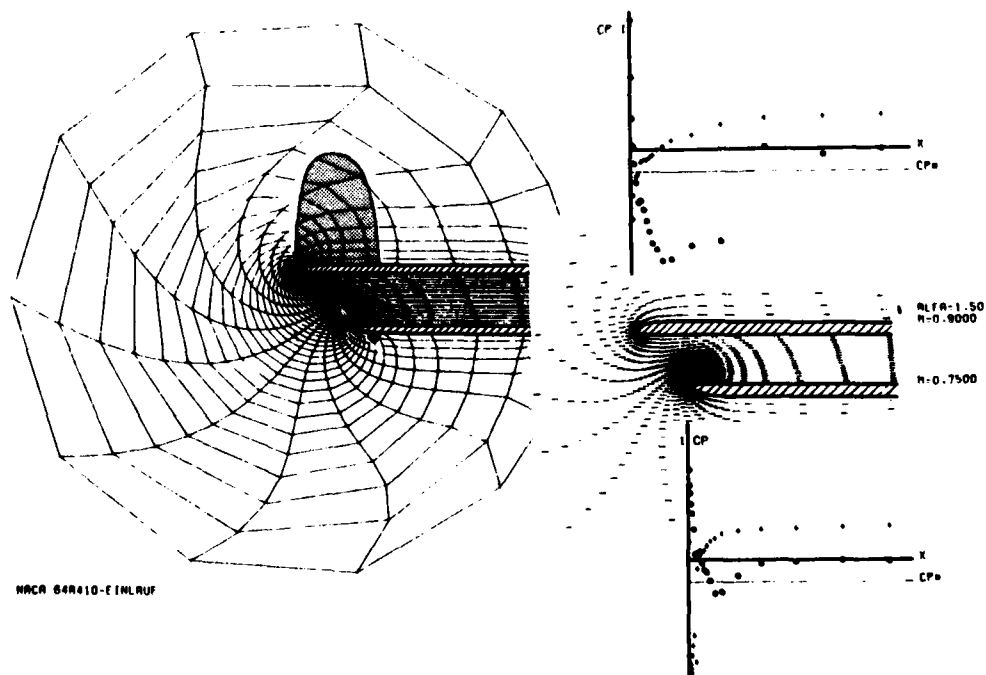


Figure 26 Analysis of air-intake by finite element technique (FPE)

The same FPE-finite element solution technique is applied to the development of intake lip geometry for transonic speed. Figure 26 shows some test results on a NACA 64A410 intake. Please note the very large extension of local supersonic flow and the sophisticated mesh grid which is the result of a great deal of work. Mass flow ratio is an additional parameter which has to be prescribed.

For subsonic analysis the modified MBB-panel code [18] is used to give cheaper results.

Last not least maneuvering devices for variable camber have to be designed.

To evaluate optimum slat/flap-settings the vortex lattice code is used to define flap- and slat-deflections due to Figure 27. It is clearly understood, that this will give only some compromise, but as measurement later on shows, this approximation works well [21].

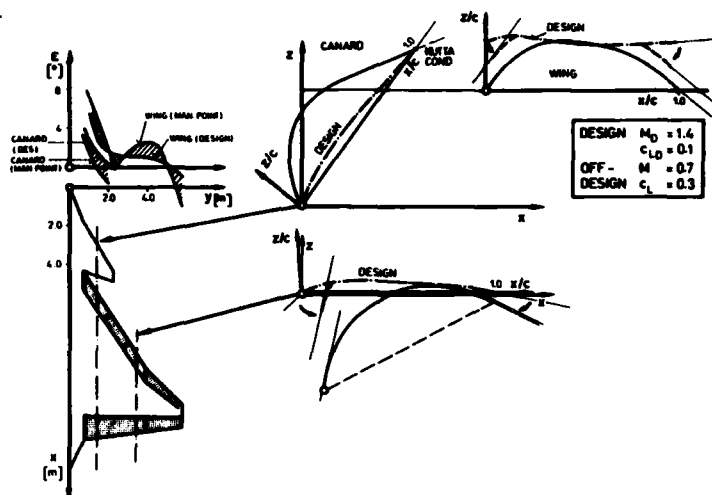


Figure 27 Variable camber design for maneuvering flight by vortex lattice

4. EXPERIMENTAL VERIFICATION

As experience shows, theoretical developments are only accepted by project management, if main features are supported by additional experiments.

Therefore a wind tunnel programme (Figure 28) was initiated to give more confidence on theoretical results and to complete answers for nonlinear flow regions and control.



Figure 28 1:25 Wind tunnel high speed model

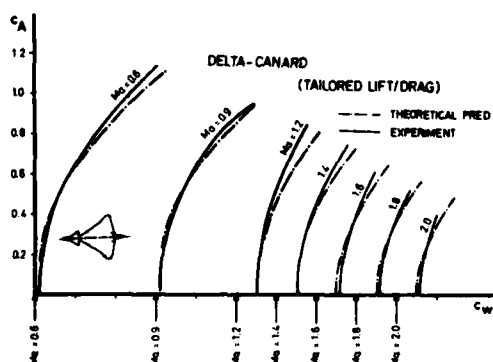


Figure 29 Comparison of theory and experiment

From Figure 29 you can pick out good agreement for low Machnumbers and moderate lift coefficients. For higher C_L 's, theory overestimates induced drag. The principle of "tailoring" is explained in Figure 30.

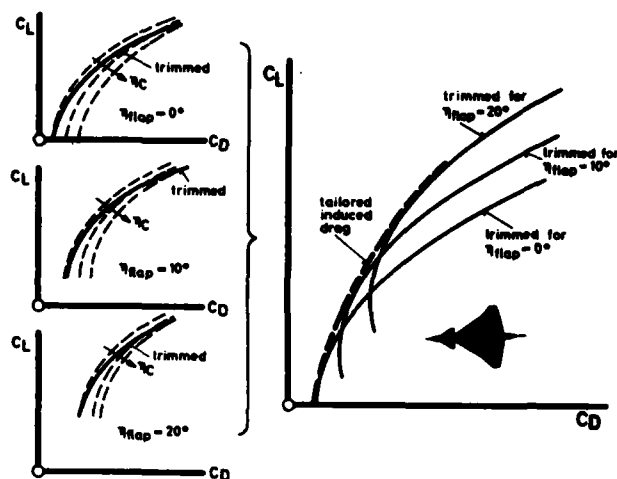


Figure 30 Tailored lift over drag

Special care is necessary for the extrapolation to real flight Reynolds numbers.

As Figure 31 demonstrates, predicted data agree well with experiment in two different wind tunnels. But it's still a long way to full scale!

For constant flap deflections the trim procedure is performed by canard deflection. This canard characteristic in presence of wing interference is input for an automatic high angle trim program [19]. Automatic optimum condition on the right side is represented by the dashed line envelope.

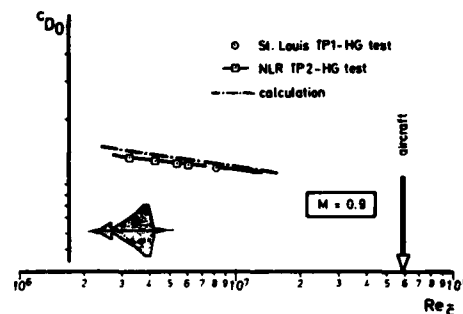


Figure 31 Effect of Reynolds number on zero lift drag

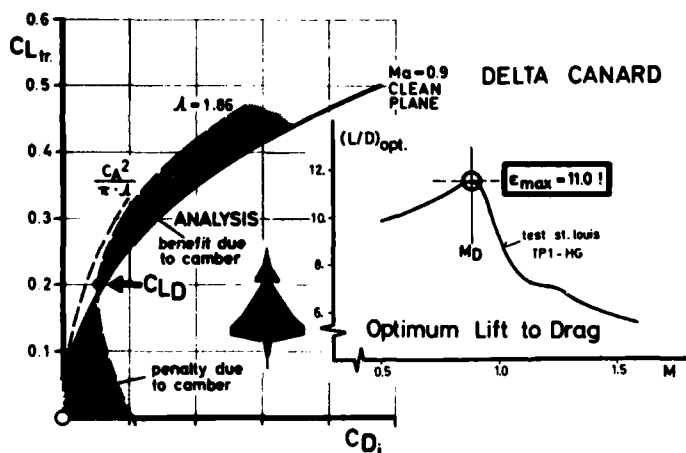


Figure 32 Theoretical design and experimental verification

As previously pointed out, the main requirement at the beginning was low drag level in supersonic and high wing efficiency $\epsilon = L/D$ in subsonic flow. The second requirement is demonstrated in Figure 32. The optimum lift to drag-ratio of about 11.0 for $M = 0.9$, obtained in wind tunnel tests proves the reliability of applied numerical methods.

5. CONCLUDING REMARKS

Rapid advances in numerical methods during the last decade have resulted in a strong influence of theory on project work.

Starting in 1968 with the panel solution for linearized potential flow, the transonic FPE solution is at present time the highest level routine for project work within limits of realistic computer time [20]. Nevertheless semiempiric "Handbook" based codes are necessary to cover the nonlinear angle of attack range and to support theoretical concepts for control.

As shown in the present paper, the intensive use of theoretical methods has led to the definition of only one single model configuration for wind tunnel tests and so to considerable savings in cost and time for predevelopment. Configuration optimization was performed without experimental tests.

6. REFERENCES

- [1] MEYER R.C. / FIELDS W.D.
Configuration Development of a Supersonic Cruise Strike Fighter
AIAA 78-148 1978
- [2] HENDRICKSON R. / GROSSMAN R. / SCLAFANI A.S.
Design Evolution of a Supersonic Cruise Strike Fighter
AIAA 78-1452 1978
- [3] RAYMER D.P.
A Computer-Aided Aircraft Configuration Development System
AIAA 78-0064 1979
- [4] WHITCOMB R.T. / FISCHETTI Th.L.
Development of a Supersonic Area Rule and an Application to the Design
of a Wing-Body Combination Having High Lift-To-Drag Ratios
NACA RM L53H31A 1953
- [5] WARD G.N.
The Drag of Source Distributions in Linearized Supersonic Flow
Col. Aero. Cranf. Rpt. 88 1955
- [6] KRAUS W. / SACHER P.
Das MBB-Unterschallpanelverfahren
3-dimensionale Potentialtheorie bei beliebig vorgegebener Mehrkörperanordnung
MBB UFE 672-70 1970
- [7] WOODWARD F.A. / TINOCO E.N. / LARSEN J.W.
Analysis and Design of Supersonic Wing-Body Combinations, Including Flow
Properties in the Near Field
Part 1: Theory and Application.
Part 2: Digital Computer Program Description (LOVE / LAROME)
NASA CR 73106/BOEING D6-15044-1 1976
- [8] WOODWARD F.A.
An Improved Method for the Aerodynamic Analysis of Wing-Body-Tail Configurations in Subsonic and Supersonic Flow.
Part 1: Theory and Application
NASA-CR-2228, Pt. 1 1973
- [9] LAMAR J.E. / GLOSS B.B.
Subsonic Aerodynamic Characteristics of Interacting Lifting Surfaces with
Separated Flow Around Sharp Edges Predicted by a Vortex-Lattice Method
NASA-TN-D-7921 1975
- [10] LAMAR J.E.
A Vortex-Lattice Method for the Mean Camber Shapes of Trimmed Noncoplanar
Planforms with Minimum Vortex Drag
NASA-TN-D-8090 1976
- [11] EBERLE A. / SOBIECZKY H.
Erweiterung des transsonischen 2D Panelverfahrens auf die Berechnung gepfeilter Tragflügel
MBB UF 1451 1978
- [12] SONNAD V. / LEMMERMAN L.
Application of the Viscous Inviscid Iteration Technique Using Surface Transpiration to Calculate Subsonic Flow over Wing-Body Configurations
AIAA 78-1203 1978
- [13] HERBST W.
Advancements in Future Fighter Aircraft
AGARD CP-147, Vol. 1, Paper 25 1973
- [14] HARRIS R.V.
An Analysis and Correlation of Aircraft Wave Drag
NASA TM X-947 1964
- [15] WEDEKIND G.
Methoden der Tragflügeloptimierung für ein taktisches Kampfflugzeug
Do 78/50B 1978
- [16] CENKO A.
Advances in Supersonic Configuration Design Methods
AIAA 79-0233 1977
- [17] EBERLE A.
Transonic Potential Flow Computations by Finite Elements:
Airfoil and Wing Analysis, Airfoil Optimization
MBB UFE 1428(8) / DGLR 78-65 1978

- [18] ZIMMER H.
Ein Verfahren zur Berechnung von 3-dimensionalen Unterschalltriebwerks-
einläufen auf der Basis der Quell-Senken-Wirbel-Panelmethode
Do Bericht 72/358 1972
- [19] KRAUS W.
Längsbewegung getrimmt / Delta - E7 0-Ma-2.0
MBB-UFE122-AERO-MT-345 1978
- [20] SACHER P.
Umströmung 3-dimensionaler Konfigurationen
DGLR 78-221 (Bonn) 1978
- [21] SONNLEITNER W.
Theoretische Untersuchung zur optimalen Nasenklappenstellung bei hohen
Anstellwinkeln
MBB-UFE122-AERO-MT-428 1979

USE OF COMPUTERS IN THE AERODYNAMIC DESIGN OF THE HIMAT FIGHTER

by

R. D. Child*, G. Panageas†, and P. Gingrich†
 Rockwell International Corporation
 North American Aircraft Division

SUMMARY

The highly maneuverable aircraft technology remotely piloted research vehicle (HiMAT/RPRV) configuration was designed to achieve a high degree of transonic maneuverability. The performance goals proposed by NASA for the advanced-fighter concept were a sustained 8 g-turn at mach = 0.9, altitude of 9,144 meters, and a mission radius of 300 nautical miles. Additionally, supersonic acceleration capability would not be compromised. Preliminary trade studies established a 7,740 kilogram fighter baseline along with a 44 percent scale RPRV that would allow a low-risk demonstration of the advanced technologies. Tests of the baseline configuration indicated deficiencies in the technology integration and design techniques. After substantial reconfiguring of the vehicle, with improvements in the analytical methods, the subcritical and supersonic requirements were satisfied. A high level of efficiency for subsonic conditions was realized with the linear theory-optimization techniques and variable camber system. Drag-due-to-lift levels only 5 percent higher than $1/\pi AR$ were obtained for the wind tunnel model at a lift coefficient of 1.0 for mach numbers of up to 0.8. The transonic drag rise was progressively lowered with the application of nonlinear potential-flow analyses.

SYMBOLS

AR	Aspect ratio	L/D	Lift-to-drag ratio
C	Canard or chord	M	Mach number
CG	Center of gravity	N_Z	Normal load factor
\bar{c}	Mean aerodynamic chord	P_S	Specific excess power
C_D	Drag coefficient	R_{e_c}	Chord Reynolds number
C_{D_L}	Drag due to lift coefficient	S	Wing area
C_L	Lift coefficient	T/W	Thrust-to-weight ratio
C_{l_l}	Section lift coefficient	t	Thickness
C_M	Moment coefficient	W	Weight or wing
C_p	Pressure coefficient	X, Y, Z	Cartesian coordinates
C_p^*	Critical pressure coefficient	α	Angle of attack
C_p		δ^*	Displacement thickness
e	Span-load efficiency factor	η	Wing semispan fraction
h	Altitude	η_c	Canard semispan fraction
		A	Sweep

SUBSCRIPTS

avg	Average	w	Wave
cp	Center of pressure	α	Differentiation with respect to
max	Maximum	\perp	Perpendicular
u	Upper	∞	Free-stream conditions

INTRODUCTION

Examination of the technologies required for the next generation of fighter aircraft has been pursued in recent years with the objective of increasing maneuvering performance. Additionally, it was envisioned that an advanced fighter designed for superior transonic maneuverability would not compromise mission radius requirements or supersonic acceleration capability. With these objectives proposed, NASA initiated a comprehensive program to evaluate high-maneuverability technologies, define advanced concepts, and ultimately design and build a demonstration vehicle.

The HiMAT/RPRV development encompassed detailed refinements to the baseline, necessary to meet the transonic maneuver goal as well as provide acceptable low-speed, transonic cruise, and supersonic acceleration capabilities. This continued with the definition of the detailed RPRV structure, leading to the construction of the test vehicle. An objective of the design process was to use the available theoretical design and analysis methods to their fullest extent in order to provide guidelines for future configuration developments and to minimize the wind tunnel test period.

* Supervisor, Aerodynamics

† Member of Technical Staff, Aerodynamics

The primary design objective is to enhance the maneuverability of the advanced-fighter concept to the point where a sustained 8 g-turn at $M = 0.9$ and $h = 9,144$ meters may be achieved while maintaining a 300-nautical-mile mission radius capability. The relation of this steady-state maneuver goal to state-of-the-art fighter performance is illustrated in Fig. 1. To realistically achieve this goal requires high efficiency at high lift coefficients in order to decrease the slope of the P_S versus load-factor relationship. The alternative brute-force approach of increasing thrust-to-weight ratio or decreasing wing loading becomes untenable for this performance goal and is incompatible with the other design objectives, including, in particular, the range requirement.

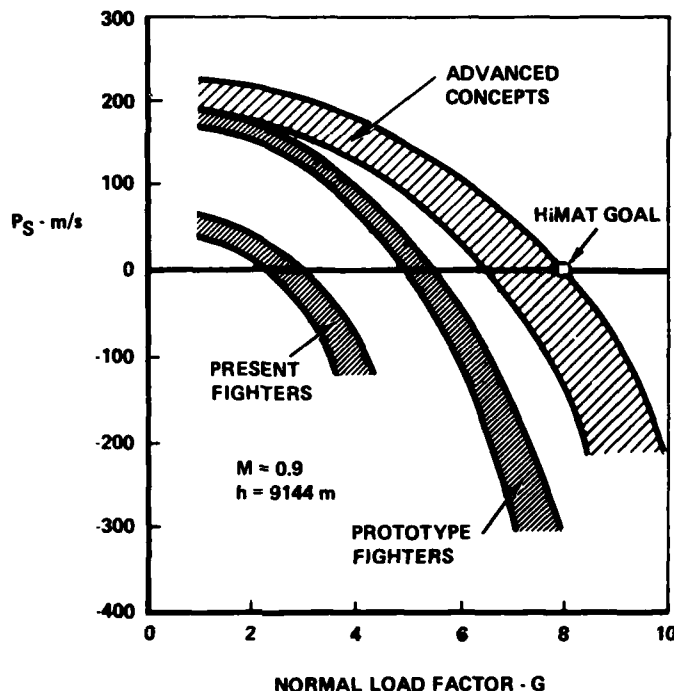


Figure 1. HiMAT Maneuvering Performance Objective

To achieve a practical design, all requirements must be properly balanced so that off-design performance is not severely degraded. In addition to the need for efficient subsonic cruise, there is also a supersonic dash requirement. The critical design considerations are:

1. Maneuver goal, 8 g, $P_S = 0$ at $M = 0.9$, $h = 9,144$ meters
2. Efficient subsonic cruise, 300-nautical mile range
3. Efficient supersonic cruise, wave drag $C_{D_W} = 0.02$ to 0.025
4. Low-speed $C_{L_{max}} = 1.6$ to 2.0
5. Stability and control with reduced static stability (adequate control must be provided, particularly near the flight envelope boundaries)
6. Maximum mach number $M = 1.6$
7. Maximum load factor $N_z = 12$
8. 1974 propulsion technology level

Balancing the first three considerations involved a compromise in wing loading between the maneuver requirement (low wing loading) and supersonic cruise requirement (high wing loading). The configuration sizing studies prescribed a wing loading of the order $W/S = 245$ to 270 kilograms per square meter. For the maneuver condition, the requirement for high efficiency (increased L/D) at high lift coefficients (C_L about 1.1) provides a selection criteria for assessing the various high-maneuverability technologies.

AERODYNAMIC DESIGN APPROACH

Optimization of the external contours is accomplished by a sequence of analytical design, test and redesign phases. The basic aerodynamic method is linear theory because of the extensive development which has occurred over the past few years. Linearized paneling methods are capable of analyzing or designing completely arbitrary nonplanar multiple-surface configurations. The use of present-day computers, with their interactive and graphics capability, allows numerous configuration modifications and optimizations to be evaluated in a short timespan at minimal cost. However, these methods have their limitations and must be supplemented with nonlinear theory and experimental data.

The HiMAT mission, which is a combination of subsonic cruise, a high degree of transonic maneuverability, and supersonic acceleration, requires the use of all these tools. The steps in the design process are:

1. Design efficient subcritical and supersonic configuration with linear theory
2. Modify the contours with the nonlinear analyses to meet the transonic requirements
3. Investigate the subsonic/supersonic consequences of the modifications
4. Test to determine the limitations and possible modifications of the theory to more closely achieve the goals

The analytical methods and optimization procedures are the technologies which transform the concept into the final configuration definition. The major aerodynamic analysis methods are summarized in Table I with their principal capabilities, limitations, and function in the design process. The use of these analytical tools is the design technology which ultimately satisfies the mission requirements. A brief description of the design technology is presented for subsonic, transonic, and supersonic operation.

TABLE I. - ANALYTICAL METHODOLOGY

Method	Capability and function	Limitations
Inviscid/linear theory Woodward distributed panel lifting surface theory	Multiple surface, nonplanar design and analysis with body for subsonic or supersonic flow	Chord plane singularities
Slender body theory	Arbitrary cross section slender body analysis - Fuselage shaping to modify pressure distribution	Slender body approximation
Total pressure drag (supersonic area rule)	Lift, volume, and interference far field pressure drag - volume optimization for minimum wave drag	Slender body theory approximation
Inverse thickness	Derive thickness for specified velocity distribution	Chord line singularities, two-dimensional
Inviscid/nonlinear theory Bailey-Ballhaus transonic wing analysis	Transonic analysis of wing-body or wing-winglet configurations	Small disturbance, moderate shock sweep, limited nonplanar, and multiple surface capability
Transonic airfoil analysis Bauer code	Full potential transonic analysis - hodograph design solution	Isentropic
Transonic scaling	Derive airfoils from known solutions	Small disturbance
Viscous analysis Bradshaw turbulent boundary layer code	Tapered, yawed wing turbulent boundary layer analysis - finite difference solution	Quasi-three-dimensional
Transonic airfoil analysis (Bauer)	Transonic viscous/inviscid interaction	Two-dimensional integral boundary layer analysis, no laminar solution
Yawed wing analysis	Yawed wing laminar/turbulent boundary layer and conformal mapping/sweep theory analysis	Subcritical, integral methods

SUBSONIC DESIGN

Within the framework of linear theory, high efficiency is sought by minimizing:

1. Vortex drag (optimum lateral loading for a set of constraints)
2. Separation (zero leading edge singularity at an appropriate lift)
3. Trim drag (moment constraint/self-trimming configuration)
4. Viscous-form drag and drag divergence (controlled subcritical flow by prescribing an upper surface pressure distribution)

TRANSONIC DESIGN

Controlled supercritical flow encompasses those techniques which minimize shock strengths and prevent shock-induced separation. Considerable progress has been made recently in the implementation of two-dimensional (2-D) shockless or weak-shock flows. For general 3-D flow, the design philosophy is still in the development stages.

SUPERSONIC DESIGN

The reduction of supersonic pressure drag is obtained with the following linearized-theory optimization techniques:

1. Inverse supersonic area rule (minimized wave drag through redistribution of volume)
2. Drag-due-to-lift optimization (lifting surface inverse solution minimizing 0 percent suction drag with moment constraint)

LINEAR THEORY DESIGN INITIALIZATION

The configuration design is initiated with a linearized lifting surface theory inverse solution using guidelines relative to drag-due-to-lift optimization and upper surface pressure distributions. The transonic characteristics are then examined to establish the strength, location, and sweep of shocks and their impact on boundary-layer separation. Modifications are then initiated through a trial-and-error process to reduce the shock strengths. A distinction must be made here between a subcritical design and a linear-theory initialization. For a subcritical design, the wing sections are designed with linear theory for a specific pressure distribution at a flight condition where subcritical flow is dominant. The HiMAT subsonic cruise point is an example. The use of linear theory for a transonic maneuver design is an intermediate step. The upper surface pressures are, of course, monitored to limit adverse gradients.

The drag-due-to-lift optimization proceeds by determining an optimum loading (constant downwash in the Trefftz plane) and then distributing the chord load such that there is no leading edge singularity and the configuration is trimmed. There are any number of chordwise loadings that satisfy these conditions which, in general, may be expressed by, for example, a sine series which produces no leading edge singularity and guarantees that the 0- and 100-percent suction drag polars are tangent at the design lift. For efficient operation at high lift coefficients, the design lift is usually selected at some intermediate value. It has been found that, through proper design, leading edge suction can be maintained well above $C_{L, \text{DESIGN}}$. Further, the resulting camber is structurally practical and results in efficient operation above and below the nominal design point. The sectional load may require constraints in order to limit the section lift at off-design conditions. In this case, the span load is prescribed and the vortex drag penalty monitored as the design cycle proceeds for the nonoptimum loading. The optimum and 100-percent suction drag polars are not coincident at the design point, but the 0- and 100-percent suction drag polars will be tangent at the design lift.

The thickness is derived by selecting a design point for which an upper surface pressure distribution is prescribed and calculating the contribution to the velocity due to lift (twist and camber) and, in some instances, wing-body interference. With an inverse solution, the thickness is obtained for the specified net velocity increment.

The linearized maneuver condition design establishes a practical starting point for later modifications. That is, many design possibilities can be rapidly investigated to assure a design which satisfies at least the subcritical design conditions. If deficiencies are present, the configuration is modified before substantial transonic design and analysis efforts are expended.

WING ALONE DESIGN

In the early phase of the configuration development, the design codes were separate entities so that a solution for a span and chord load for a trimmed condition could not be derived simultaneously. The approach was to derive first a cruise wing assuming a weakly coupled canard. That is, all the load would be carried on the wing at the design point. The maneuver wing was obtained by scaling the cruise camber to a design lift of $C_L = .5$. The wing with an uncambered canard resulted in a configuration which had a substantially lower design lift than desired.

A 0.147-scale model of the configuration designated -17A (Fig. 2) was tested in the LRC 8-foot transonic pressure tunnel. Drag due to lift was evaluated by removing the estimated skin friction drag based on flat plate turbulent skin friction and standard-form factor corrections. Drag due to lift is shown in Fig. 3 for the complete configuration and for the wing alone. Neglect of the canard interaction in the design process is illustrated by the increased drag due to lift relative to the wing alone at the design lift $C_L = 0.5$. The wing-alone performance was itself degraded at high-lift coefficients as a result of the lack of span-load constraints; i.e., constraints on the section lift at the wing tip.

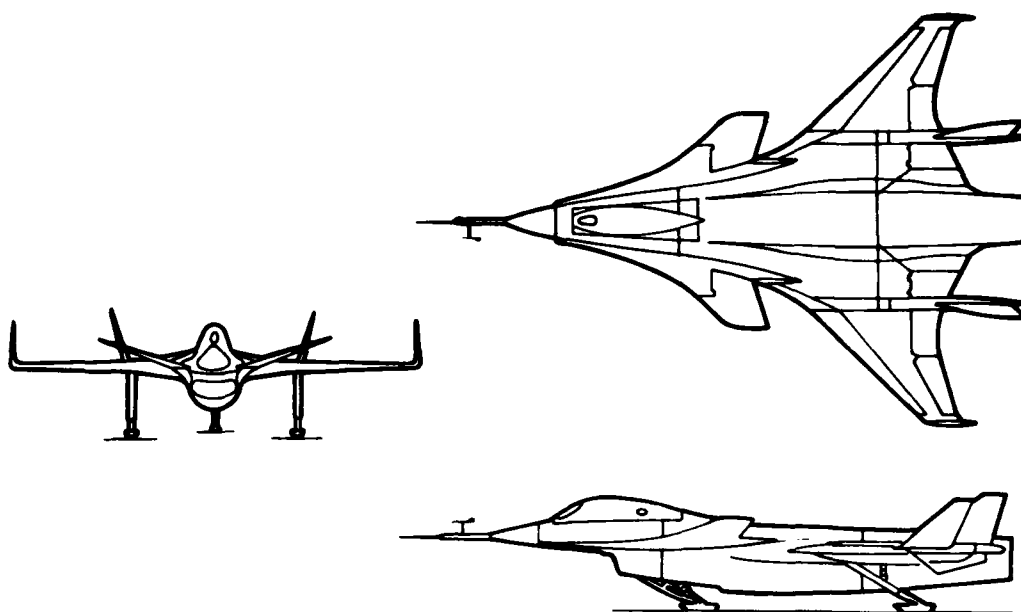


Figure 2. RPRV, -17A

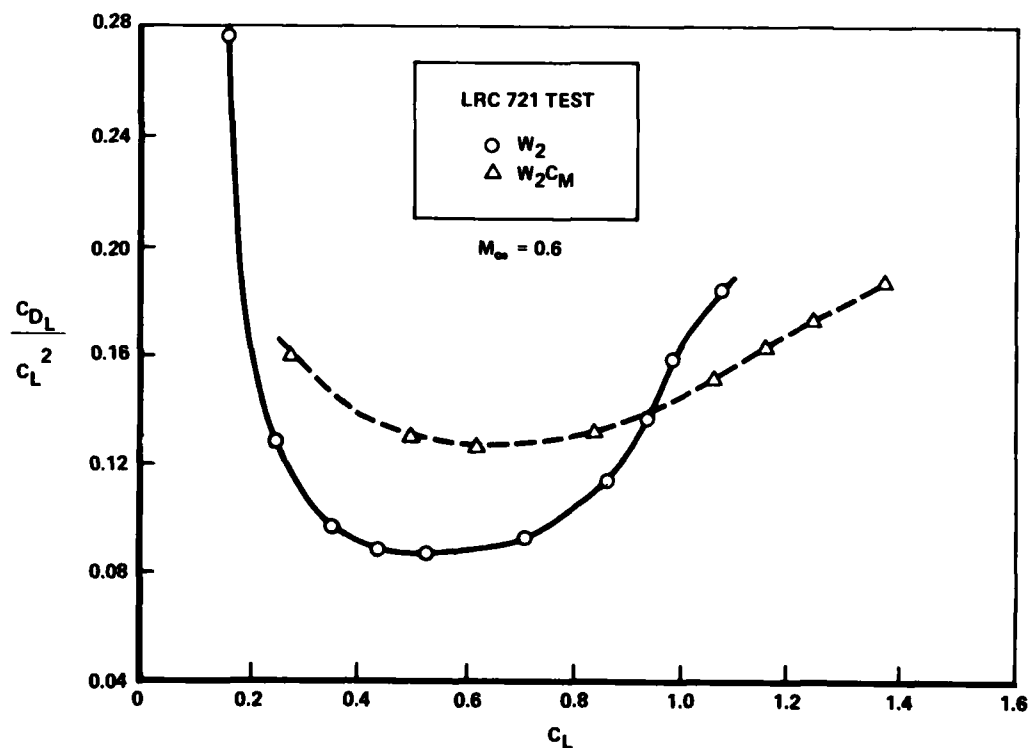


Figure 3. Effect of Canard on Maneuver Configuration (-17A) Drag Due to Lift

WING-CANARD DESIGN

The time involved in obtaining a subsonic optimization limited the number of design variables that could be surveyed. To increase the efficiency of the design process, existing separate computer programs and concepts were integrated into the distributed panel lifting-surface theory (1). The additions and extensions are summarized as follows:

1. An optimum loading solution with constraints by the method of LaGrange multipliers was incorporated. Provision was made for specifying an arbitrary loading in an interactive manner.
2. The capability to constrain the moment for multisurface configurations was added. Previously, this step was done manually.
3. The chord load calculation was incorporated with an interactive capability to modify the shape for a given section lift and moment.

These modifications allow the twist and camber to be derived in one step. Thus, the solution can be examined and parameters varied in an efficient manner. Typically, the calculation proceeded by specifying a design C_L and C_m and a spanwise center-of-pressure (X/C)_{cp} variation. The optimum span load was derived first. This could be overridden interactively. The program then shifted the center-of-pressure variation to satisfy the moment constraint. The chord load for each station is derived for the given lift and moment. This shape could then be modified interactively. The configuration is then analyzed at higher loadings to evaluate upper surface pressure distributions. (The thickness was derived for the cruise condition.)

The design points at $M_\infty = 0.7$ were $C_L = 0.5$ and 0.15 for the maneuver and cruise configurations, respectively. Additionally, the section lift would be limited to $C_{L1} < 0.75$ for $C_L = 1$.

Initial solutions obtained for an optimum span loading violated the wing and canard section lift constraints. The code was modified to allow specific regions of the configuration to be constrained to a given lift. An example is shown in Fig. 4. The twist required for this constrained solution is impractical. A sequence of solutions was obtained varying wing-tip planform and canard-wing load balance to achieve a smooth wing and canard twist distribution. The outboard wing area was increased and the percentage of the total load on the canard was increased from 15 to 30 percent. The wing twist derived is shown in Fig. 5. The wing twist distribution was then smoothed. At some span stations, the zero-singularity requirement will not be met at the design point. The net effect on drag due to lift was negligible. However, this compromise produced a leading edge peak on the outboard wing.

The maneuver sections were constructed and analyzed at $M_\infty = 0.7$ for a range-of-lift coefficient. For $C_L = 0.88$, the wing and canard upper surface pressure distributions are shown in Fig. 6. In general, the desired isobar sweep has been achieved, and the aft gradients are moderate. As noted previously, as a result of smoothing the twist, the outboard wing exhibits a leading edge pressure peak. An infinite yawed wing viscous calculation predicted transition due to cross flow instability near the leading edge but no separation of the turbulent boundary layer.

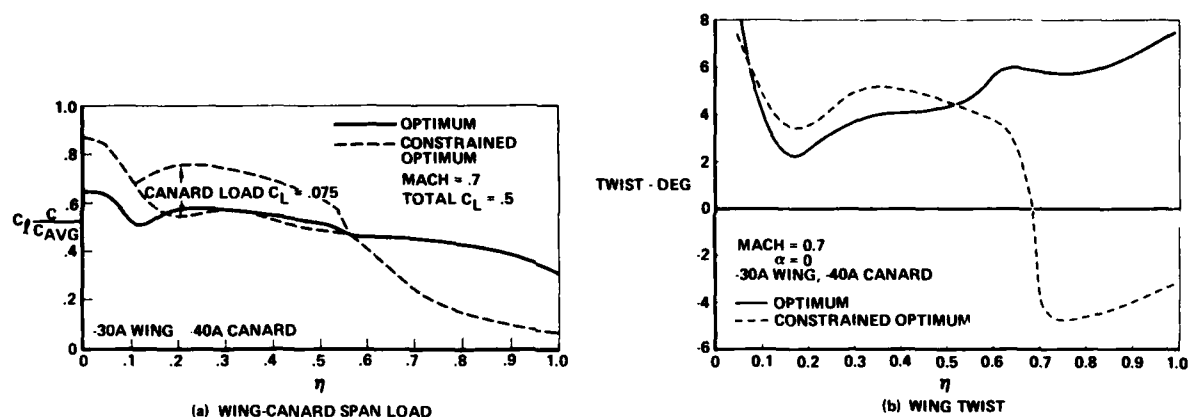


Figure 4. Wing-Canard Span Load Optimization

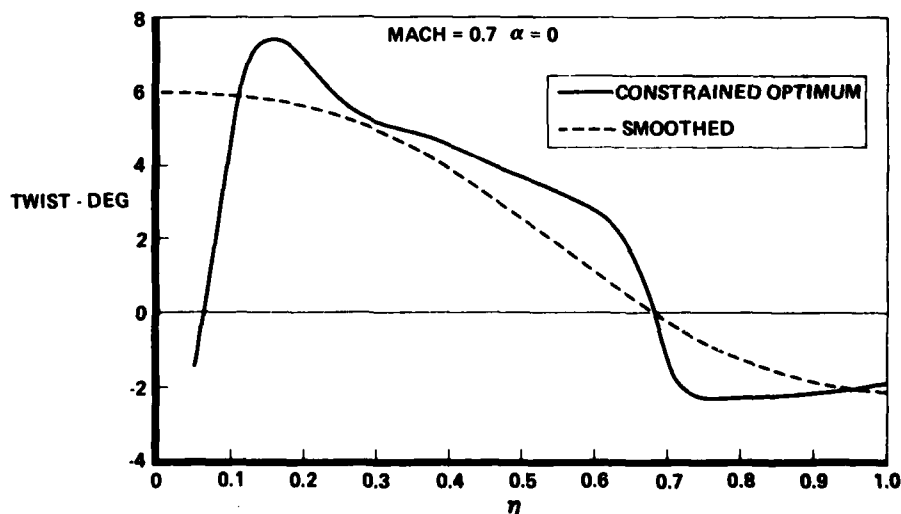


Figure 5. Wing Spanwise Twist Distribution

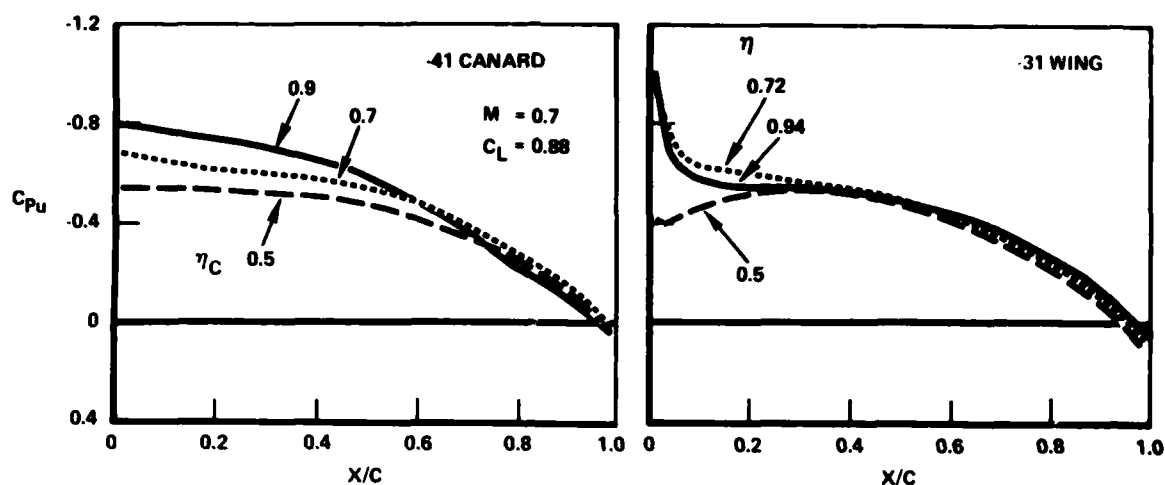


Figure 6. Maneuver Configuration (-18) Upper Surface Pressure Distributions - Linear Theory

REVISED SUBCRITICAL DESIGN

The objectives of the second subcritical wing-canard design cycle were to examine the various wing-canard loading combinations which would meet the section lift requirements and to derive a twist and camber that did not require modification. To accomplish both objectives, the constrained optimum solution was not used directly. Instead, the loading was prescribed at each span station so that all constraints would be met.

The 0.22-scale model of the -18 configuration was tested in the Ames 14-foot transonic wing tunnel. Longitudinal characteristics at subcritical conditions ($M = 0.6$) are shown in Fig 7 and 8. A linear theory lifting-surface analysis was made with the measured model coordinates. The agreement with the experimental lift and moment (Fig 7) is quite satisfactory. Drag due to lift is shown in Fig. 8. Increased efficiency at high lifts resulted from the improved upper surface pressure distribution on the outboard wing. The untrimmed drag rise characteristics of the first -18 configuration and the revised design are shown in Fig 9. The revised configuration meets the subcritical design goal but, as expected, both subcritical wing-canard designs are deficient at the transonic design point. The oil flow results for the transonic maneuver condition indicated shock-induced separation on the outboard wing and canard and an unswept shock near the trailing edge of the inboard wing.

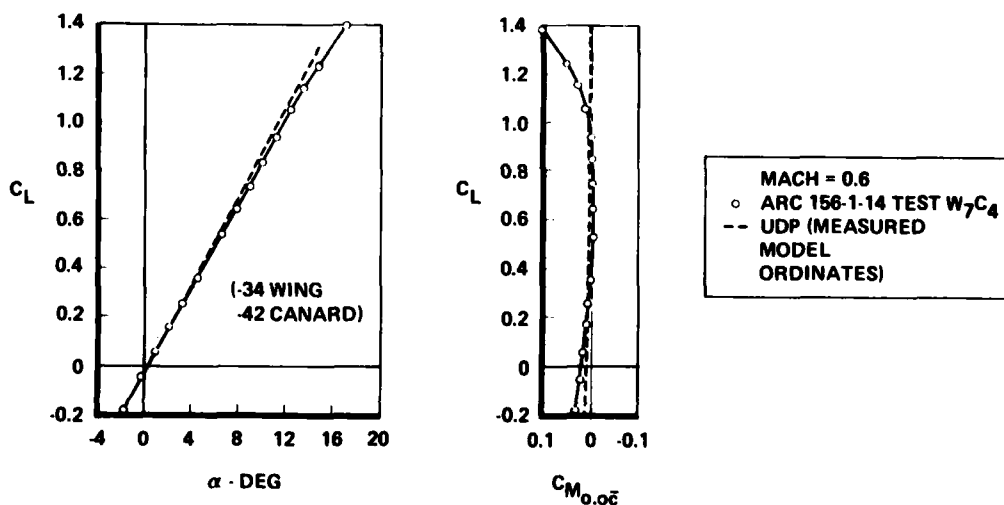


Figure 7. Longitudinal Characteristics of Linear Theory Revised Maneuver Design

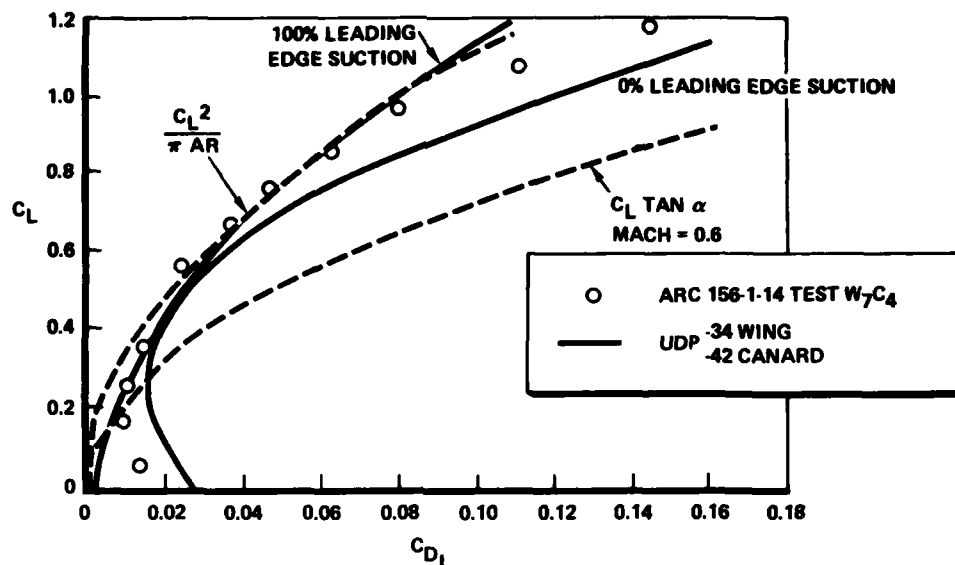


Figure 8. Drag Due to Lift of Linear Theory Revised Maneuver Design

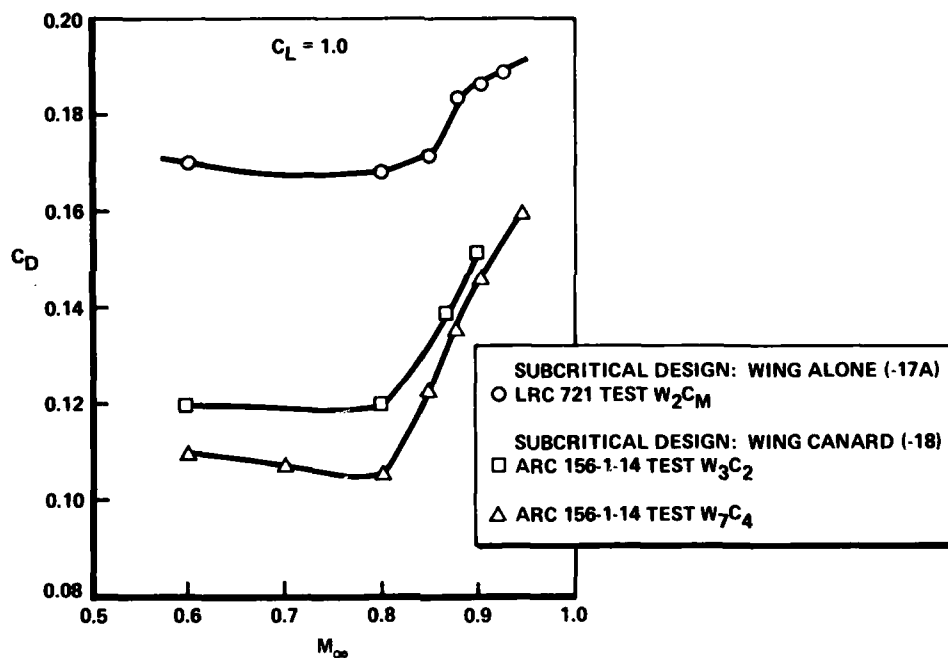


Figure 9. Maneuver Configuration Drag Rise - Subcritical Design

The test results confirm the validity of the design process for subcritical flow for high lift, high-efficiency operation. As a measure of the total efficiency achieved, reference is made to Fig. 8 where the flat plate drag-due-to-lift factors $1/\pi AR$ and $1/C_{L\alpha}$ are compared with the test data. Of course, for a nonplanar configuration, the optimum is $1/\pi AR_e$ where $e \sim 1.3$ for the HiMAT design. This optimum, though, can only be realized at high loadings to the extent separation can be eliminated. The subcritical design now provides a base point from which further modifications can be made for supercritical flow. The subcritical design process cannot be expected to yield satisfactory designs for low-aspect-ratio, highly loaded configurations operating in the transonic range. However, this process provides an effective means of initializing the design.

NONLINEAR DESIGN

The primary 3-D transonic analysis was the Bailey-Ballhaus classical small-disturbance code (2). This was applicable to a single planar surface. The presence of the canard and wing-tip fin on the HiMAT presented computational difficulties. As a first step, a vertical fin option was incorporated

into the code. The simulation was restricted to the X-Z plane but would allow an arbitrary spanwise position above and/or below the wing computational slit. Efforts were continued to simulate a wing-canard configuration. Calculations were made to determine the canard downwash on the wing plane. Nonlinear and linear theory calculations for the downwash were in good agreement. An application to account for the effect of the canard, which has been found useful a post facto, is to include the average chordwise downwash as a twist increment in the wing boundary conditions.

STATUS OF SUBCRITICAL DESIGN

When the first subcritical wing-canard design was completed, the intent was to use the Bailey-Ballhaus code to analyze and modify the maneuver wing for low-drag supercritical flow. The following considerations affected implementation of the transonic analysis. First, the simulation did not include the canard so that wing pressures would have to be treated in a qualitative manner. Second, the formulation was not well-suited to capture swept shocks. With these points in mind, there was initially some hesitation regarding the modification of the configuration until experimental pressure data were available. Nevertheless, some modifications were attempted, but they were minor in nature. The results of the transonic analysis of these designs are presented to illustrate the features of the transonic methodology and as a basepoint for later configuration modifications.

The conditions for which the small disturbance theory is applicable are not known a priori. At $M_\infty = 0.9$, the angle of attack corresponding to the subcritical intermediate design point was selected. The upper surface pressures for the wing are shown in Fig 10. The formation of an unswept shock extending outboard to $\eta = 0.7$ is indicated. With a relaxation solution, there is always the question of the required number of iterations for convergence. The previous fine-grid results were obtained with 450 iterations from a coarse-grid solution. Results after 2,000 additional iterations were qualitatively unchanged.

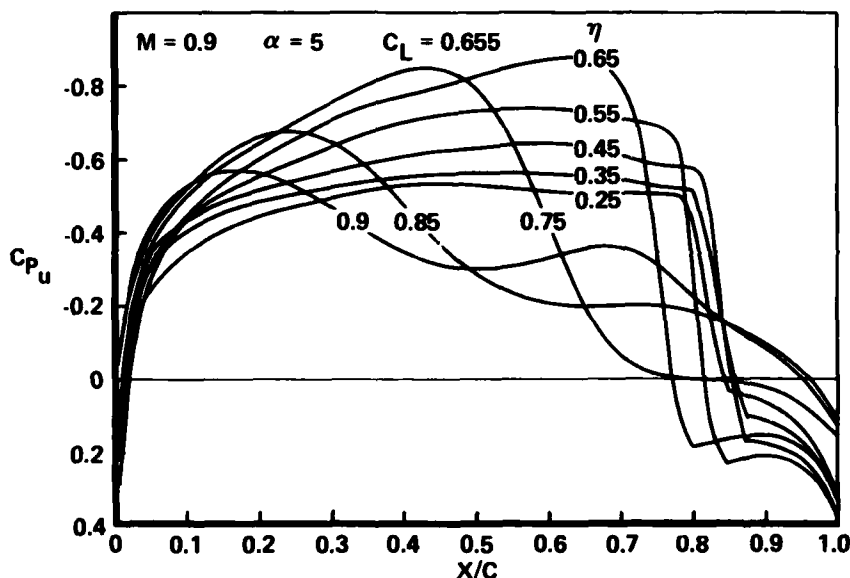


Figure 10. Fine Grid Theoretical Pressures for Maneuver Wing, Measured Model Coordinates

To resolve the configuration deficiencies at transonic conditions and provide some guidelines for implementation of the Bailey-Ballhaus analysis, a follow-up test was conducted (TWT 294) after the Ames series (ARC Test 156-1-14) to measure upper surface pressure distributions. For two spanwise stations the calculations were compared with canard-off measured pressures. At 55-percent span (Fig. 11a), the agreement (allowing for viscous effects) is satisfactory with regard to the shock locations. However, for the outboard wing (Fig. 11b), the shock is not captured. Oil-flow results indicated a swept shock and attached flow at $\alpha = 5^\circ$. The inability of the method to adequately capture swept shocks has been noted previously. The slower convergence of the solution for this region may account for some portion of the difference, but based on earlier results, it was concluded that no shock would be predicted with further iterations.

Some proposed modifications to the method similar to those of reference 3 were considered. These involved additional terms in the governing equation and revisions to the differencing scheme. However, at the time, no modification was available to impact the design effort. For the maneuver point, disparity in the experimental and calculated results for the highly loaded outboard wing will limit the analysis and design capability for the present small-disturbance formulation.

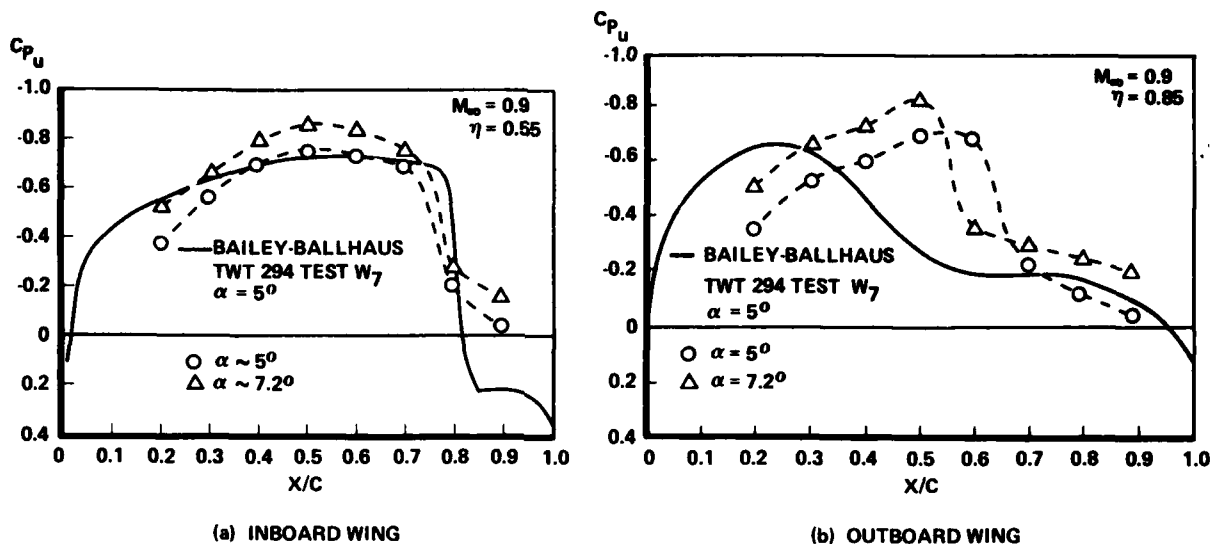


Figure 11. Calculated and Measured Canard-Off Wing Pressures

3-D TRANSONIC MANEUVER DESIGN

Based on the preceding transonic calculations and test analysis, redesign of the HiMat configuration was divided into two phases. The first was to improve characteristics of the maneuver wing through application of the nonlinear small-disturbance theory in an iterative manner. The second phase involved the design of those regions where the existing small-disturbance formulation was not adequate: the outboard wing and canard.

For the inboard and center regions of the wing ($\eta < 0.7$), the primary design objective was to reshape the sections to weaken the shock near the trailing edge. For this region, where the generator sweep is varying considerably, a triangular-type upper surface pressure distribution is used. The distribution must be such that at higher lifts ($C_L \sim 1$), at most, a series of weak shocks occur. To redesign the inboard and center wing sections, the camber was modified so that the load would be moved toward the leading edge. The wing was analyzed, and based on these results, the upper surface was varied in a trial and error process until an acceptable pressure distribution was obtained. The lower surface was then modified to produce a camber distribution which would retain the subcritical maneuver performance at high lifts.

The results of the first series of modifications are shown in Fig. 12 for 60-percent span. All calculations were made with the fine grid to properly resolve the shocks. Additional reshaping was not successful in further weakening the shock. The span load distribution prescribed in the subcritical design was generally maintained. To further weaken the shock in the center region, the trailing edge sweep was increased and the wing sections revised slightly to assure that the proper isobar sweep was maintained. The planform modification and the resulting change in the pressure distribution at 60-percent span are shown in Fig. 13.

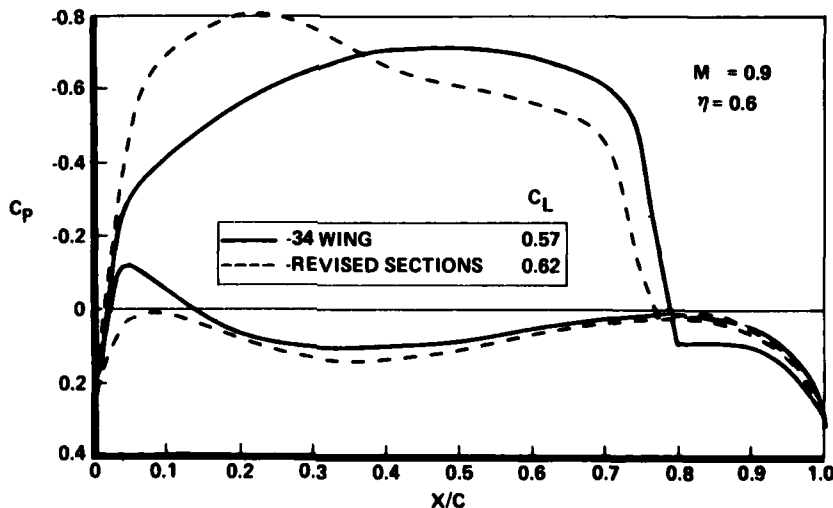


Figure 12. Three-dimensional Transonic Design - Effect of Section Modification

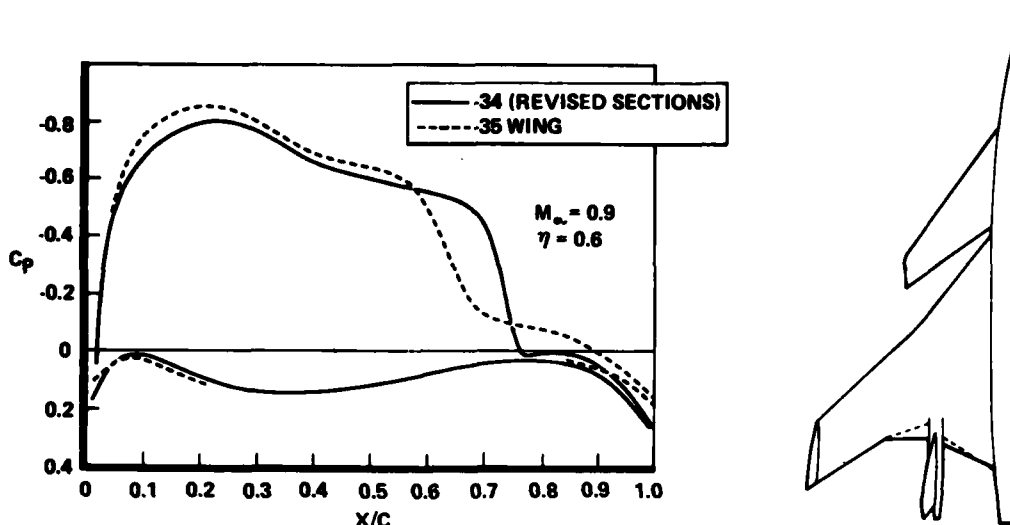


Figure 13. Transonic Wing Design - Effect of Planform Modification

The revised wing (-35) for the maneuver configuration was tested (TWT 296) to determine effectiveness of the supercritical modifications and provide additional pressure data for estimating the influence of the canard on the position and strength of the wing shocks. The modifications were successful in weakening the center wing shock and eliminating shock-induced separation at the design point. Pressure distributions at 55-percent span are shown in Fig. 14. For this design, there was a swept, weak shock at approximately 35-percent chord. Oil-flow results indicated that the shock at 85-percent chord did not separate the boundary.

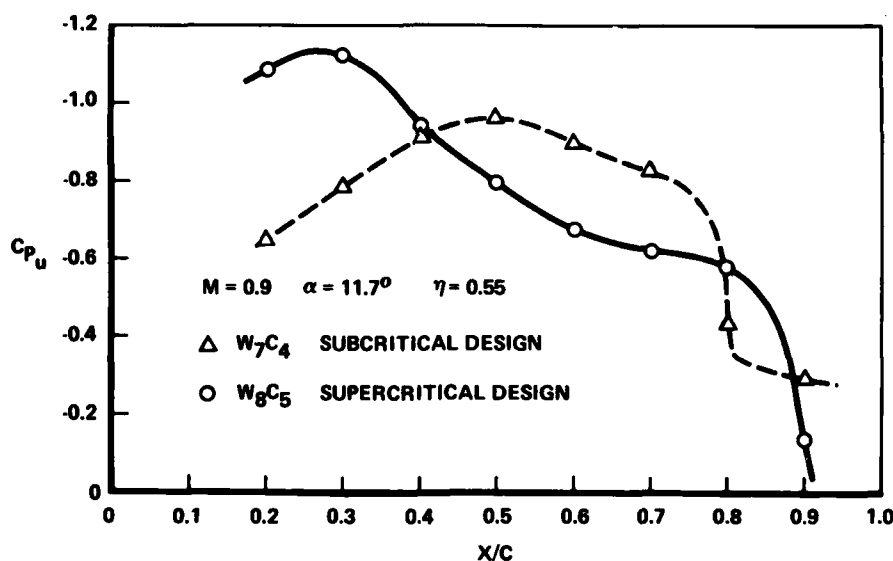


Figure 14. Experimental Verification of Weakened Shock by Transonic Design/Analysis Cycle

Use of the Bailey-Ballhaus nonlinear small-disturbance analysis was successful in satisfying design objectives for the wing alone. The unswept shock was essentially eliminated over the inboard 70 percent of the wing. This shock was replaced by a series of weak, swept shocks. Near the wing root the unswept shock remained, as expected. The experimental pressure data indicated that the shock strength at the wing root was moderate at the design condition, local mach (before the shock) of 1.2. The design objectives were generally maintained in the presence of the canard. The effect of the canard downwash over the center wing section did not change the weak, swept shock pattern.

2-D TRANSONIC DESIGN

The inapplicability of the small-disturbance analysis for the highly swept outboard wing required use of a 2-D/sweep theory design cycle. A higher order 3-D solution (4) would be preferable but could not be implemented in the time span required. The intent was to use 2-D section results and sweep theory to arrive at an appropriate upper surface pressure distribution for the relatively low-taper outboard wing. Then, if the wing can be shaped to reproduce the 2-D result, the 2-D design goals can be met.

The primary objective was to eliminate the shock-induced separation at the design point. At or near the design condition, a shockless or weak shock solution would be sought. Some trailing edge separation would be admitted.

First, the approximate 2-D section requirements were established. An estimate of the section lift on the outboard wing was made for the existing configuration. A nominal design total lift coefficient of $C_L = 1.0$ was selected. The section lift requirements are still quite high but attempts to further constrain the outboard wing load would result in impractical twist requirements. For this condition, using the midchord sweep ($\Lambda = 40$ degrees), the required 2-D section lift C_{L1} is of the order $C_{L1} = 1.2$ to 1.4 .

The normal mach number is $M_1 = 0.69$. Thus, if an airfoil section can be designed for efficient operation at these conditions, the corresponding pressure distribution ($C_p \cos^2 \Lambda$) can be prescribed as a design goal for the finite yawed wing. The second problem is to reshape the outboard wing sections to produce infinite yawed wing conditions.

The approach to the 2-D airfoil design was to start with (1) an existing airfoil or (2) scale a known solution with the transonic similarity rule and modify, if necessary, for the desired design condition. Of the available supercritical sections, an airfoil reported in reference 5 came closest to the design requirement. The section is designated 65-14-08 where the sets of digits refer to a nominal design mach number, lift coefficient, and thickness ratio. The Garabedian 65-14-08 airfoil was scaled to a nominal design mach number of $M = 0.7$, using the transonic similarity rule. The section was analyzed at the scaled design point with the transonic method of reference 5.

The actual section was obtained by removing the upper surface displacement thickness calculated for infinite yawed wing conditions. The displacement thickness for the model Reynolds number which was used and for a full-scale configuration are shown in Fig. 15. The lower surface displacement thickness correction could be similarly applied and a linear rotation would be used to adjust the trailing edge thickness.

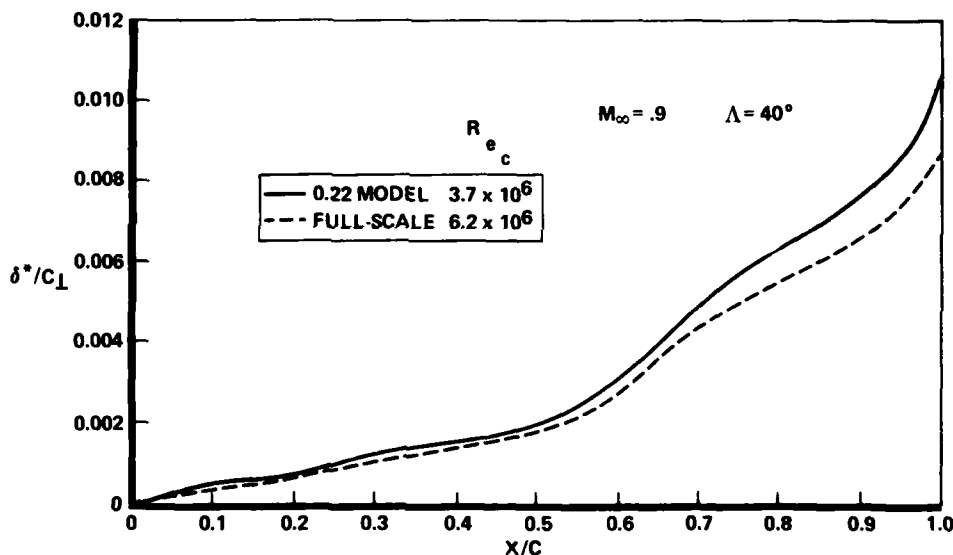


Figure 15. Scaled Garabedian Airfoil (70-11-06) Upper Surface Displacement Thickness

The section was then analyzed to assess the off-design performance with increasing lift. The Bauer analysis (5) did not include a yawed wing boundary-layer method; so the results must be viewed qualitatively. Pressure distributions at $C_L \sim 1.2$ and 1.4 are shown in Fig. 16. However, shock-induced separation is still predicted at the higher lift coefficient.

In a private communication from Richard T. Whitcomb of NASA/Langley Research Center, an alternate supercritical philosophy was suggested where the final recompression is not initiated until approximately 80-percent chord. There may be one or more smaller recompressions preceding this, and for supercritical flow, weak shocks are accepted. This philosophy is illustrated in Fig. 17 for the LRC/Whitcomb 74-10-06 airfoil. The initial supercritical region is terminated in a shock. Following this is an expansion to a slightly supercritical flow and a shockless recompression. Although at the design point there is some wave drag, the off-design performance has been found, experimentally, to be usually better than that of the shockless airfoils.

The 74-10-06 airfoil was analyzed at the design Reynolds number, displacement thickness was added, and the section was scaled to a design mach number of $M_1 = 0.69$. The inviscid pressure distribution was obtained at the scaled angle of attack and is shown in Fig. 17. The design lift ($C_l = 1.3$) was now much closer to the required value. The boundary-layer characteristics were calculated for infinite yawed wing conditions ($M_\infty = 0.9$ and $\Lambda = 40$ -degrees). Upper surface trailing edge separation occurred at approximately

95-percent chord. Several modifications to the contour were attempted, using the streamline curvature approach of reference 6, but the separation could not be eliminated. It was felt that some trailing edge separation could be tolerated if the existing shock-induced separation was delayed.

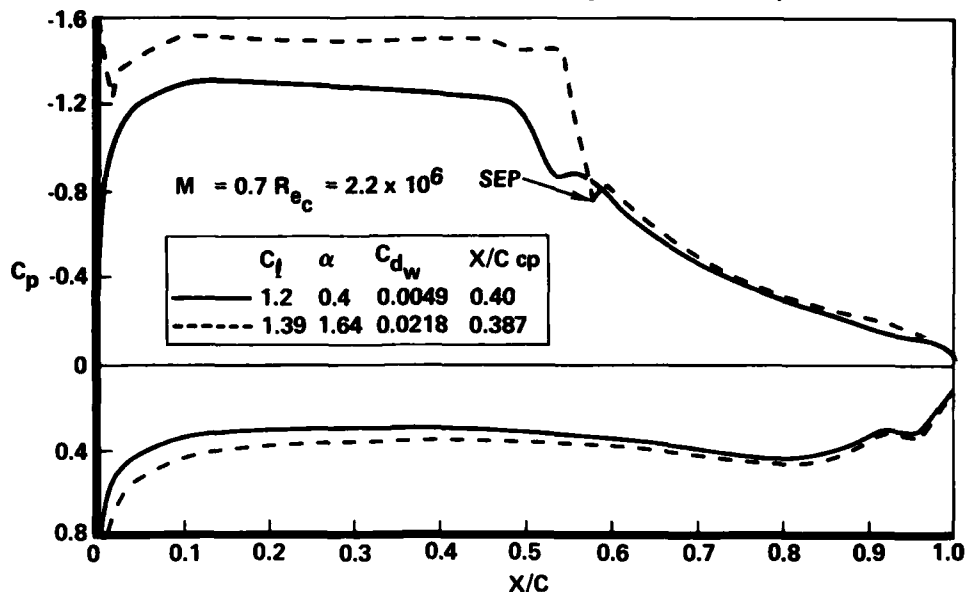


Figure 16. Two-dimensional Analysis of Modified, Scaled Garabedian Airfoil (70-11-06M)

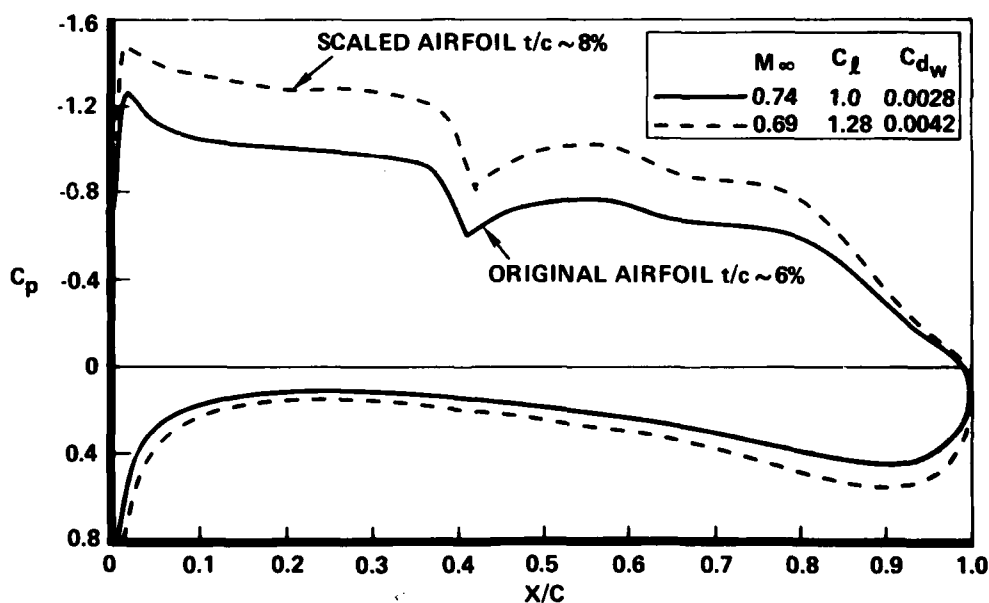


Figure 17. Pressure Distribution for Scaled LRC/Whitcomb Supercritical Airfoil

When the displacement thickness was removed from the inviscid shape, the contours crossed before the trailing edge. The lower surface was rotated to provide a suitable thickness in the trailing edge region, but the thickness ratio was now almost 9-percent (7-percent in the freestream direction). A supersonic pressure drag analysis indicated a substantial penalty. The lower surface was modified to reduce the thickness but not impact the upper surface flow quality.

The modified LRC/Whitcomb derivative was adapted to the outboard wing panel such that the isobar sweep would be maintained at the design condition. An oil flow for this wing (W_{17}) near the nominal design point is presented in Fig. 18. A weak swept shock on the outboard wing was achieved. Trailing edge separation is indicated, consistent with the analytical prediction.

The progressive reduction of transonic drag is summarized in Fig. 19. Major reduction resulted from the weakening of the inboard unswept shock. The drag was progressively lowered by improving the flow quality of the outboard wing and, to a lesser degree, the outboard canard.



Figure 18. Oil Flow of Maneuver Configuration With Scaled LRC/Whitcomb Airfoil,
 $W_{17}C_9$, $\alpha = 10$ Degrees, $M = 0.9$, $C_L = 0.93$

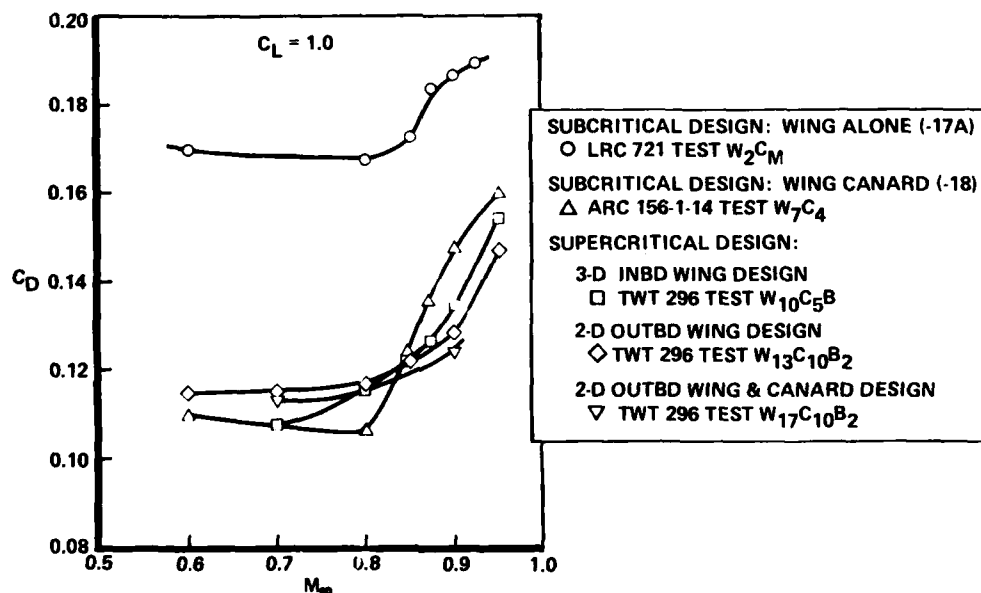


Figure 19. Reduction of Maneuver Configuration Drag Rise by Transonic Design Cycle

RECENT COMPUTATIONAL EXPERIENCE

Initial analysis used the Bailey-Balhaus classical small-disturbance (CSD) theory formulation (2). At the time, it was suggested that the CSD formulation would not adequately capture highly swept shocks. Some calibration would be necessary to determine those flow conditions or regions of the planform where the predictions could be used with confidence. Wind tunnel tests indicated that the computations adequately predicted the location and strength of the inboard shock. The existence of the outboard shock, however, was not produced numerically. This finding led to several approximate theoretical modifications (7) to enrich the Karman-Guderly transonic small-disturbance equation of motion by adding certain nonlinear cross

terms. The extended analysis was successful in predicting the entire upper surface wing flow. The before and after comparison is presented on Fig. 20. The modified small disturbance (MSD) theory derived in response to HiMAT tests has been adopted in more recent code developments (8,9) concerned with improving computational efficiency, including fuselage effects, etc.

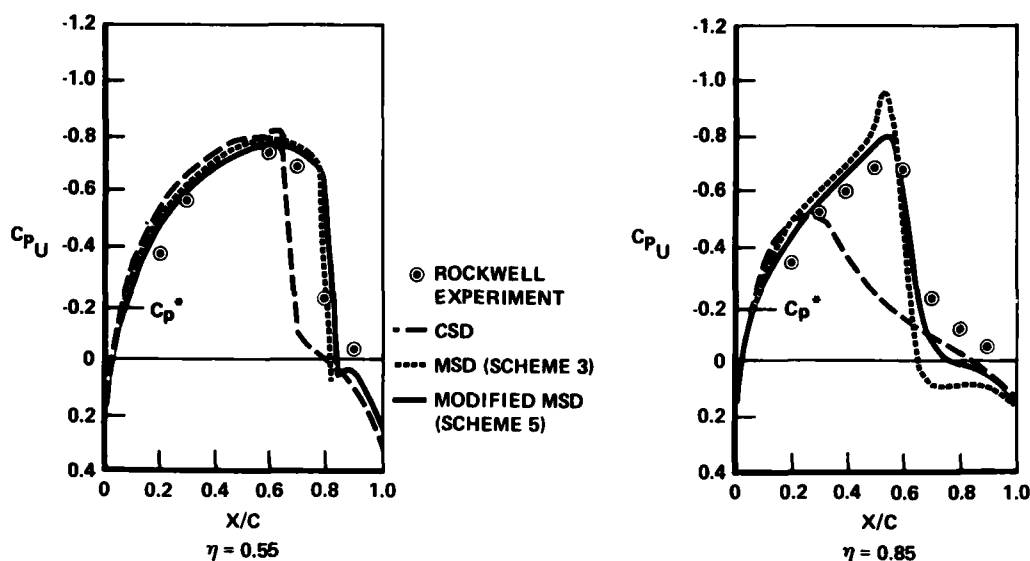


Figure 20. Comparison of Small-Disturbance Theory and Measured HiMAT Wing Upper Surface Pressure Distribution at $M_\infty = 0.9$, $\alpha = 5$ Degrees

A series of numerical experiments were subsequently performed on the maneuver wing to establish the consistency of various modified small-disturbance formulations (7,8) and the full-potential equation of motion solution (4,10) satisfying exact boundary conditions. Primary interest was in prediction of the existence, strength, and location of shock waves as a prelude to their weakening or elimination through design modifications. Representative results of the numerical computations are presented in Fig. 21 for the same nominal C_L . Examination of the chord load shapes indicates differences between the various predictions concerning the existence and strength of shock waves. The differences at 60-percent span are the most pronounced and indicate either a strong (supersonic to subsonic deceleration), weak, or no shock.

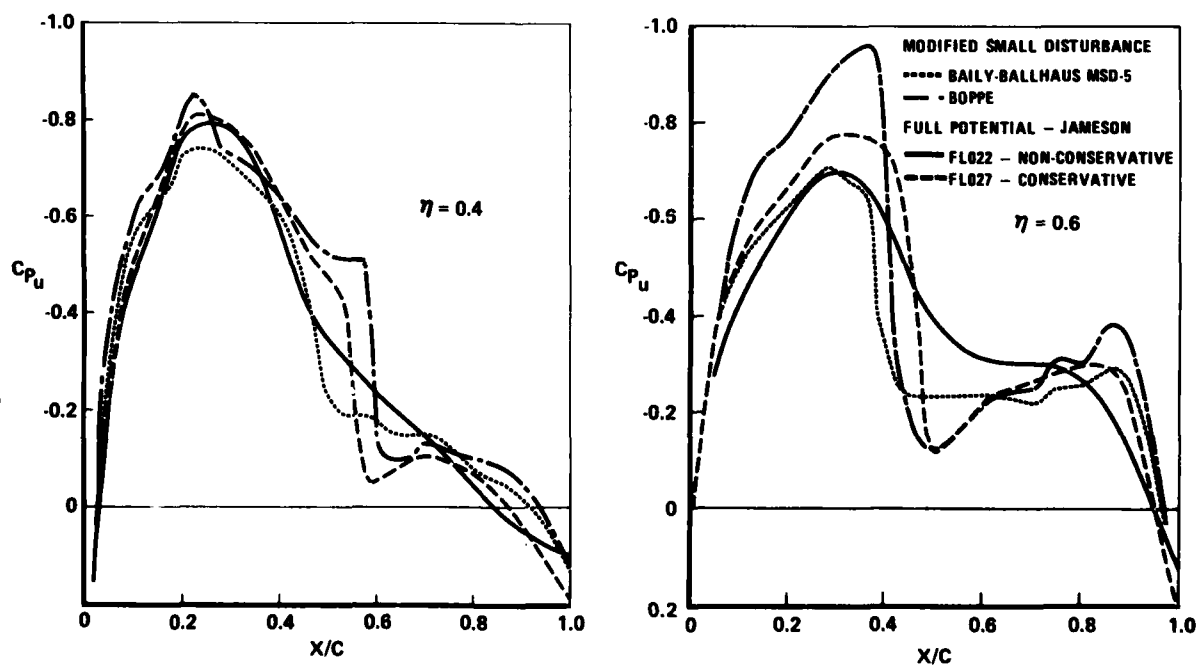


Figure 21. Comparison of Transonic Analysis Methods for HiMAT Wing-Alone Configuration, $M = 0.9$, $\alpha = 6$ Degrees

As noted previously, a possible approximation of the canard influence is the inclusion of its downwash in the wing boundary condition. To assess the premise, the downwash was calculated and applied as a twist increment to the wing geometry. It was found that the chordwise variation, at a particular spanwise location, was small. Calculations with the Jameson conservative code FL027 are compared with experiment in Fig. 22. The calculation did not include the fuselage or winglet.

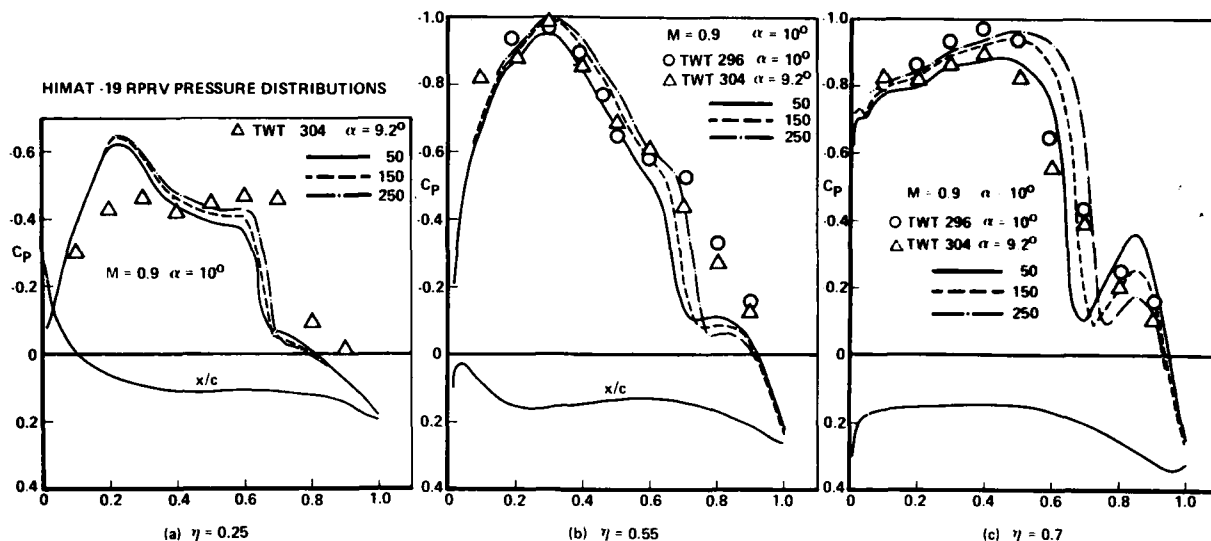


Figure 22. Comparison of Jameson Conservative Analysis (FL027) With Measured HiMAT (-19) Maneuver Wing Pressures

FLEXIBLE WING DESIGN

The cruise configuration is defined by deforming the maneuver shape so that satisfactory performance is obtained for transonic and supersonic cruise. The ideal situation would be a configuration that produced a nearly optimum loading with minimum viscous and wave drag as, for example, a pure subcritical cruise design. Designing primarily for maneuver performance will limit the freedom to design an optimum cruise configuration.

The variable camber system concept is based on obtaining optimum performance at two or more design conditions through a combined mechanical and aeroelastic deflection. Once the maneuver configuration is defined, the cruise shape is determined by iteration. Given a leading edge variable camber system and an unspecified twist increment due to structural bending, a linear or nonlinear analysis (or combination of both) is used to define the best cruise shape with the geometric constraints of the supercritical maneuver design. These constraints limit, obviously, the number of section shapes that can be defined, and a compromise between the span load shape and the upper surface pressure distribution may be required. The design is thus an iterative process, guided by the results of earlier optimum cruise designs.

The performance compromise which arose in the cruise configuration was due to the supercritical modifications associated with the maneuver design and the constraint imposed on the aeroelastic increment. The increment in spanwise twist was initialized with the first subcritical design and subsequently modified for the revised subcritical maneuver design. At this point, the aeroelastic twist increment goal was set so that the structural development could proceed in parallel with aerodynamic development.

A cruise configuration was defined for the design with the scaled Whitcomb section on the outboard wing. This section was characteristic of aft-cambered supercritical airfoils and presented difficulties in the derivation of the cruise wing. The trailing edge cusp would, if used in the maneuver position, result in a transonic and supersonic camber drag penalty. A subcritical analysis was performed to define the best compromise between trailing edge (aileron) deflection and twist distribution. The compromise is between average camber (twist) and local camber (trailing edge deflection). The design that resulted included a 4-degree aileron deflection to partially cancel the maneuver trailing edge camber. Additionally, only 70-percent of the aeroelastic twist increment originally expected was available.

The drag due to lift for the cruise configuration ($W_{19}C_{l1}$) is compared to an early subcritical design (W_1C_{l1}) and the goal in Fig. 23. The effective increase in design C_{l1} resulted in a substantial penalty at low-lift coefficients.

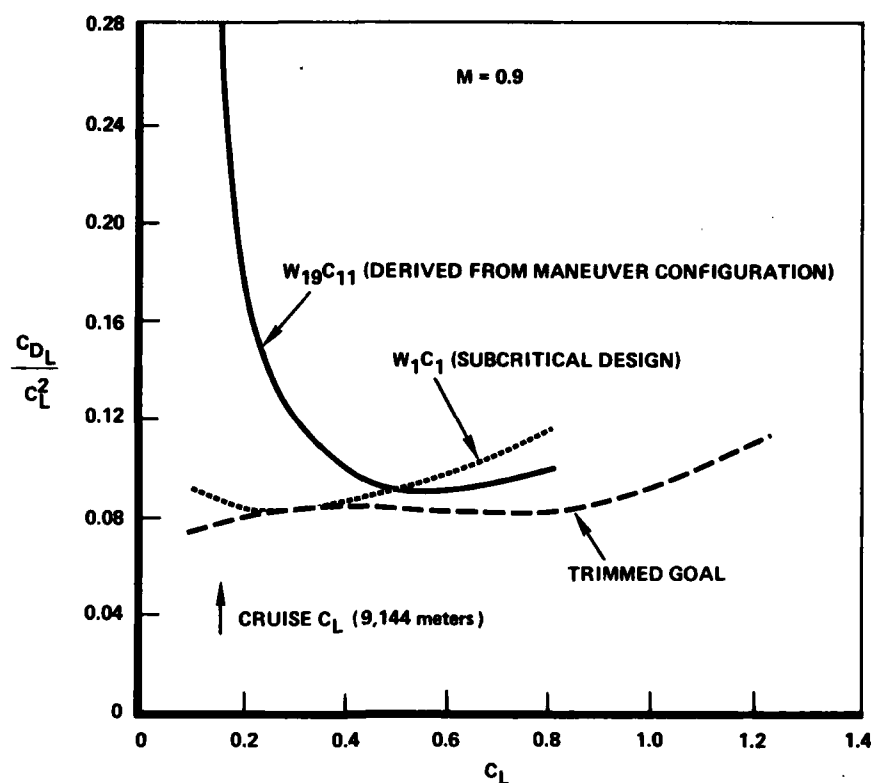


Figure 23. Cruise Configuration Trimmed Drag Due to Lift

EVOLVED CONFIGURATION AND PERFORMANCE

The final configuration presented at the preliminary design review (PDR) and performance status relative to the goals are presented in this section. Additional configuration modifications, progressing from the -18A to -19 designs, included: (1) an enlarged vertical tail and the addition of lower surface winglets for improved lateral-directional stability and (2) mass balances at the wingtips for flutter suppression. The PDR baseline configuration for the RPRV concept is shown in Fig. 24.

TOGW*	1528.6 kg
T/W LAUNCH	1.36
W/S LAUNCH	283.7 kg/m ²
STRUCTURE LIMIT	12 G
FUEL *	286 kg
CG, %C	8.13

* TARGET

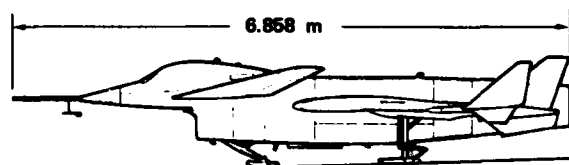
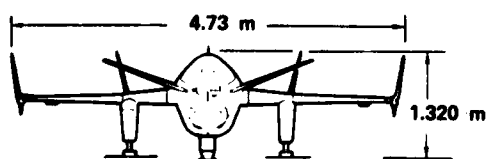
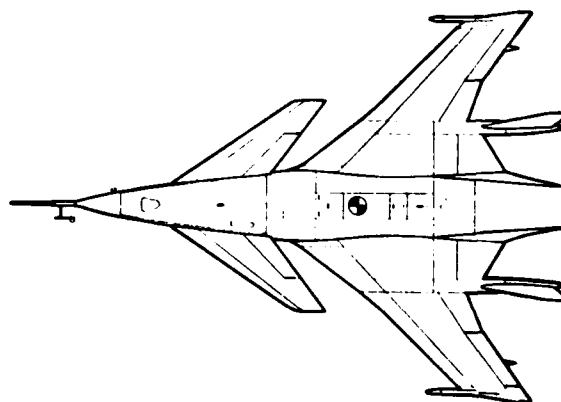


Figure 24. HiMAT RPRV Preliminary Design Review Baseline, (-19)

Test results are presented to indicate the extent to which the design objectives have been met. The primary goal is to minimize the transonic drag due to lift. In Fig. 25, trimmed and untrimmed drag due to lift are compared to the goal for mach 0.6 and 0.9. For subsonic conditions, the trimmed drag-due-to-lift objective was achieved or exceeded for lift coefficients up to $C_L = 1.2$. At a lift coefficient of 1, the efficiency factor (e) is approximately 0.95 for subsonic conditions. For transonic operation, the trimmed objective was not achieved. At the nominal design point ($M = 0.9$ and $C_L = 1$), the drag-due-to-lift factor (C_{DL}/C_L^2) was 0.014 above the trimmed objective. Still, considerable progress in reducing the transonic drag had been made since the drag-due-to-lift factor was 0.07 above the objective for the phase III baseline (-17A).

The HiMAT fighter maneuvering goal is a normal load of $N_z = 8.0$ for $P_S = 0$ at the design point of $M = 0.9$ and $h = 9,144$ meters. The -19 configuration maneuver performance status is $N_z = 7.3$ for $P_S = 0$.

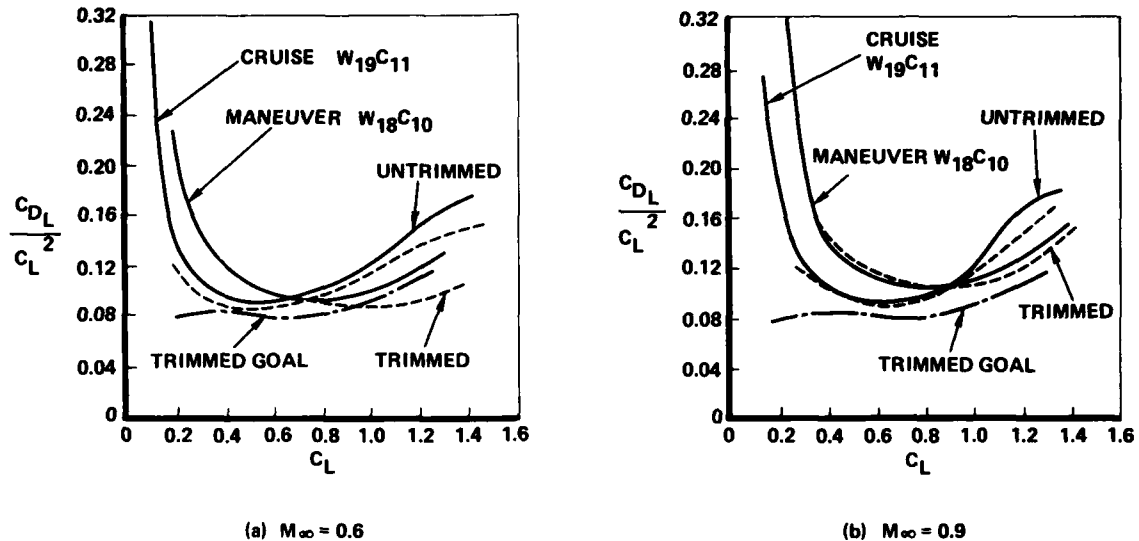


Figure 25. HiMAT RPRV (-19) Drag Due to Lift

CONCLUSIONS

The general conclusions of the HiMAT aerodynamic design experience are:

1. A substantial amount of the maneuver design effort involved linear theory. In the future, as more general transonic design and analysis techniques evolve, the extent of the linear theory design used should be diminished. At present though, linear theory provides a fast and efficient means of evaluating design requirements for preliminary and detailed design studies. The modifications to the computerized design procedure, necessitated by the HiMAT configuration and design objectives, produced a means of properly initializing the maneuver design so that lifting surface efficiency, structural requirements, and off-design performance could be examined and varied in an efficient manner.
2. The Bailey-Ballhaus transonic analysis, used in an iterative mode, was valuable in achieving the prescribed supercritical pressure distributions for regions of moderate shock sweep. Restrictions of the formulation were partially overcome by relying on a design/test cycle. This was necessary to account for the effects of the canard and evaluate conditions above the design point. Application of the transonic code was generally successful in weakening the shocks for the wing region inboard of 70-percent span. Further weakening of the root shock is desirable, but the possible decrease in wave drag cannot be quantified with the present small disturbance formulation in order to evaluate the overall impact.
3. Restrictions of the 3-D transonic analysis were most troublesome for the highly swept, highly loaded outer wing panel. Here, the recourse was a 2-D/sweep theory initialization, aided by a linear theory analysis to verify that constant sectional characteristics prevailed. The sweep theory design is a valid means of determining a pressure distribution that will produce attached flow for moderately tapered regions. Guidance for the transonic implementation of the sweep theory design was principally obtained through analysis of the test data. This was not the most effective design procedure. A more comprehensive set of methodology is required which would include a multiple-surface transonic design and analysis capability and a 3-D boundary layer.
4. For the cruise configuration, the consequences of using supercritical sections and variable camber was not fully resolved. This was due primarily to the imposed structural (twist) constraint and not a lack of inherent aerodynamic efficiency, although an arrangement without the structural constraints was not tested.

REFERENCES

1. Woodward, F. A., "Analysis and Design of Wing-Body Combinations at Subsonic Speeds," J. Aircraft, Vol 5, No. 6, 1968, pp 528-534
2. Ballhaus, W. F. and Bailey, F. R., "Numerical Calculation of Transonic Flow About Swept Wings," AIAA Paper 72-667, June 1972
3. Lomax, H., Bailey, F. R., and Ballhaus, W. F., "On the Numerical Simulation of Three-Dimensional Transonic Flow With Application to the C-141 Wing," NASA TN D-6933, 1973
4. Jameson, Antony, "Iterative Solution of Transonic Flows Over Airfoils and Wings, Including Flows at Mach 1," Commun Pure & Appl Math, Vol 27, 1974, pp 283-309
5. Bauer, F., Garabedian, P., Korn, D., and Jameson, A., "Supercritical Wing Sections II, Lecture Notes in Economics and Mathematical Systems," Springer-Verlag, New York, 1975
6. Barger, R. L., and Brooks, C. W., "A Streamline Curvature Method for Design of Supercritical and Subcritical Airfoils," NASA TN D-7770, 1974
7. Ballhaus, W. F., Bailey, F. R., and Frick, J., "Improved Computational Treatment of Transonic Flow About Swept Wings," Advances in Engineering Sciences, NASA CP-2001, 1976
8. Boppe, C. W., "Calculation of Transonic Wing Flows by Grid Embedding," AIAA Paper 77-207, January 1977
9. Mason, W. H., et al, "An Automated Procedure for Computing the Three-Dimensional Transonic Flow Over Wing-Body Combinations, Including Viscous Effects, AFFDL-TR-77-122, February 1977
10. Jameson, A., and Caughey, D. A., "A Finite Volume Method for Transonic Potential Flow Calculations," AIAA 3rd Computational Fluid Dynamics Conference Proc, pp 35-54, June 1977

NUMERICAL METHODS FOR DESIGN AND ANALYSIS AS AN AERODYNAMIC DESIGN TOOL FOR MODERN AIRCRAFT

Wolfgang Schmidt

Dornier GmbH, Theoretische Aerodynamik
D-7990 Friedrichshafen, Germany

SUMMARY

The application and validation of several computational aerodynamic methods in the design and analysis of transport and fighter aircraft is established. The main part of the paper is directed towards transonic flow problems. An assessment is made concerning more recently developed methods that solve transonic flow and boundary layers on maneuver-flaps, wings, inlets and bodies.

Capabilities of subsonic and supersonic aerodynamic methods are demonstrated by the inlet integration on the Alpha-Jet design, supersonic "Rautenflügel"-analysis, subsonic and supersonic wing optimization for a fighter and high lift device analysis.

The accuracy of transonic methods is demonstrated by comparison of computed results to experimental data for transport and fighter-type wing body combinations, axisymmetric inlet flowfields, two element airfoil systems and cascades. Special attention is given the capabilities of such methods to simulate wind tunnel effects.

INTRODUCTION

Aircraft development costs have escalated exceedingly within the last few years. Greater emphasis must be placed on exploring analytically and experimentally new configuration concepts aimed at substantially expanding airplane performance capabilities. The present state of the art in aerodynamic design requires extensive configuration iterations through repeated wind tunnel testing that is costly, time consuming and relies heavily on inhouse experiences and expertise. Significant advances have been achieved recently in aerodynamic computational methods which allow the numerical computation of flows around three dimensional configurations and provide valuable guides to those seeking understanding of specific problems or those pursuing innovative design concepts.

At Dornier a selection of numerical methods in fluid dynamics is available which has application to the analysis and design of transport as well as fighter type aircraft configurations in the transonic speed regime. A great amount of effort and emphasis has been placed on the validation of these methods and to establish limits of their applicability. Results to date have been encouraging and the use of those methods can provide a substantial reduction in time as well as cost required to achieve a good design. This paper addresses mainly to the validity and application of current three dimensional transonic programs including boundary layer effects. The accuracy, applicability, and limitations of threedimensional transonic TSP and full potential methods developed at Dornier were evaluated by comparison with experimental data obtained on advanced technology wing-body configurations. By combination with the Dornier three dimensional boundary layer code also the influence of viscous effects is shown. By inclusion of wind tunnel wall boundary conditions in the inviscid code finally a complete set of methods is described which can be semi-automatically used to evaluate the analysis as well as design problem of current transonic configurations in free flight as well as in windtunnels.

For completeness a summary of some of the currently available methods is presented for subsonic and supersonic flow and examples are shown of their application to a variety of aircraft design and analysis problems.

DESCRIPTION OF COMPUTATIONAL AERODYNAMIC METHODS

A large selection of computational methods are available that have broad application to the analysis and design of transport and fighter aircraft flying in the subsonic, transonic and supersonic speed regimes. A thorough review of these methods will not be given here since the background literature is easily accessible. On the other hand, their main features pertinent to the work presented herein are briefly discussed.

Three-Dimensional Subsonic Potential Flow Method for Arbitrary Configurations

A computational method has been developed that can treat arbitrary subsonic three-dimensional potential flows including inlet flow fields [1]. This is a linear method solving Laplace's equation satisfying exact boundary conditions based on [2], [3]. In this approach the velocity potential at any point in a flow field is expressed in terms of the induced effects of source and doublet (or vortex) sheets distributed on the boundary surfaces. The configuration surfaces are divided into panels, and hence, this

approach is known as a panel method. Essentially, this is a general three - dimensional boundary value problem solver that is capable of being applied to most problems that can be modeled within the limitations of potential flow. Compressibility effects are approximated by the Goethert rule, and thus analysis of transonic flow is not possible with this method. Viscous effects can be represented by the surface displacement concept. An improved higher order method [4] is available as a pilot code. These methods are ideally suited for analyzing complex aircraft configurations in subsonic flow.

Three-Dimensional Vortex Lattice Method for Arbitrary Configurations

A method based on vortex lattice theory has been developed at Dornier that can be applied to the combined analysis, induced drag optimization, nonlinear vortex lift (based on Polhamus Analogy) computation, and jet simulation of three-dimensional configurations of arbitrary shape [5],[6]. This is a linear method solving Laplace's equation satisfying thin wing boundary conditions on the camber surface and optionally curved wake influence. The optimization process utilizes the method of Lagrange multipliers. Compressibility effects are approximated by the mass flux rule. Its ease of use, high computational speed, and design capability make it particularly valuable in evaluating design variations, arriving at optimized configurations, and designing new wing camberline shapes.

Two-Dimensional Methods for Subsonic and Transonic Multielement Airfoil Analysis/Design

As a joint venture between Saab and Dornier a numerical method has been developed for the analysis and mixed analysis/design mode of two-dimensional transonic flow around twoelement airfoil systems [7], [8]. Arbitrarily shaped airfoil sections can be treated through the use of a series of conformal mappings. The physical domain outside the two sections is mapped into the ring domain between two concentric circles, the interior of the outer circle being the exterior of the main airfoil and the exterior of the inner circle being the exterior of the secondary airfoil. Within this ring domain the flow field is computed solving the nonconservative full potential equation by means of Jameson's rotated difference scheme and SLOR in combination with nonlinear extrapolation and multigrid technique. Viscous flow is simulated by coupling the inviscid code to a set of boundary layer methods [9].

For subsonic speed the codes are coupled to a two-dimensional panel method for multi-element airfoils correspondingly [10].

Two-Dimensional Methods for Transonic Airfoil and Cascade Analysis/Design

Several two-dimensional transonic methods have been developed, by various organizations, which are able to analyze airfoils or cascades [11], [12], [13], [14], [15], [16]. Some methods have been evaluated or developed by Dornier. The TSP-methods are highly improved by the mass-flux formulation [13] even for thick airfoils and have demonstrated its usefulness in as much as analysis and mixed analysis/design problems can be solved including viscous effects based on the displacement thickness as well as unsteady transonic flow for flutter prediction [14]. Flow time as well as computer costs are fairly small. The full potential methods are superior at high angle of attack and for analysis/design in the leading edge region. Jameson's FLO6 [15] has proven to be very accurate and fast due to his fast solver but is lacking flexibility due to the circle plane mapping involved. There is some indication that the finite volume techniques like the flux finite element method [16] for the full potential equation or the quasi-time dependent method [17] for the Euler eq. are the more interesting ones as far as the engineering environment to support and guide a design process is concerned. An advantage of the finite volume Euler method is the accuracy over the whole speed regime from subsonic to supersonic free stream Mach numbers even for flows with strong shocks.

A finite volume method for the solution of the two-dimensional time - averaged Navier Stokes equations is under development at Dornier [18] but more work has to be done to make it useful for practical design.

Two-Dimensional/Axisymmetric Methods for Transonic Inlet Flow Fields

Two different methods are being used at Dornier, one developed at Saab [19] to compute the transonic flow around axisymmetric inlets for a prescribed mass flow ratio. The inlet consists of an initial part of arbitrary geometry which is continued to downstream infinity as a straight circular tube. With a sequence of conformal mappings and a final coordinate stretching the whole exterior and interior flow field is mapped to a rectangular domain in which the full potential equation is solved using type-dependent line-relaxation. The second one is the Dornier-developed finite volume method for calculating axisymmetric and plane pitot-type inlet flow fields at supersonic free stream Mach numbers [20]. This second order accurate time dependent method solves the Euler equations in integral conservation-law form. The equations are written with respect to a cartesian coordinate system in which a body and bow shock fitted mesh adjusts in time to the motion of the bow shock that is automatically captured as part of the weak solution. At the compressor entrance plane inside the cowl static pressure is prescribed as subsonic boundary condition. The method can treat arbitrary lip shapes and is presently being extended to a three-dimensional version. The integration of the pressure distribution from the inlet throat to the crest will provide valuable data for the drag estimation as long as no large viscous effects are apparent.

Three-Dimensional Transonic Potential Flow Methods

Several three-dimensional transonic potential flow methods have been developed, by various organizations, which are able to analyze either isolated wing or wing-body combinations [21], [22], [23], [24], [25], [26]. Evaluation of the methods developed at Dornier [22], [24], [26], and a Dornier version of FLO22 indicate that the three-dimensional Dornier TSP-MF method based on the mass flux concept is a useful design tool, in as much as arbitrary fuselage shapes can be modeled, analysis as well as mixed analysis/design problems can be solved, shock strength as well as positions are well predicted, and the low computer cost in combination with the highly automated input provide the basis for a method to be used in the engineering environment. On the other hand the lack of dense mesh spacing in the nose region imply further improvements by use of grid embedding. FLO22 quite often is giving fairly good agreement with experimental results, but it should be kept in mind that this method is not conservative and neither does give correct drag data nor correct viscous results if a boundary layer method is coupled. The detailed two-dimensional studies indicated that the approach of using finite volume techniques to solve either the full potential equation or the Euler equations are the most promising ones for complex three-dimensional flow computations. Pilot codes on both approaches have been nearly completed [27], [28].

Three-Dimensional Supersonic Potential Flow Method for Arbitrary Configurations

The computational method of [29] has been modified and improved at Dornier [30] to treat very complex three-dimensional complete aircraft configurations at supersonic speed. This is a linear method solving the linear supersonic potential equation satisfying exact boundary conditions on bodies and linearized boundary conditions on wings. In this approach the velocity potential at any point in a flow field is expressed in terms of the induced effects of source and vortex sheets distributed on the boundary surfaces. The configuration surfaces are divided into panels. This method is ideally suited for analyzing complex aircraft configurations in supersonic flow as long as wing thickness effects can be treated in a linearized manner.

Three-Dimensional Supersonic Machbox Method for Arbitrary Wings

A method based on supersonic linear potential theory within a Mach-box scheme has been developed at Dornier that can be applied to the combined analysis, design, and drag optimization for thickness and/or camber distribution of three-dimensional wings of arbitrary planform [31]. This is a linear method satisfying thin wing boundary conditions on the wing surface for either camber or thickness, respectively given pressure distributions. The optimization process [32] utilize the method of Lagrange multipliers for given modes of camber/twist or thickness. Its ease of use, very high computational speed, and design capability make it particularly valuable in evaluating design variations, arriving at optimized configurations, and designing new wing camber surface shapes.

Aerodynamic Design and Analysis System for Supersonic Aircraft

An improved integrated system of computer programs has been installed at Dornier [33], [34] for the design and analysis of supersonic configurations. The system uses linearized theory methods for the calculation of surface pressures and supersonic area rule concepts in combination with linearized theory for calculation of aerodynamic force coefficients. To complete the supersonic area rule program a near-field (thickness pressure) wave drag program is included. To end up with realistic wing design, the fuselage is modeled in the lifting surface programs and the addition of configuration-dependent loadings in the design program allow for a wing design in the presence of fuselage and nacelle effects. Additional limiting pressure terms in the lifting pressure programs constrain the linear theory solution. The methods are characterized by their reliability in use and input simplicity, thus providing an integrated system for supersonic design and analysis of complete aircraft configurations, with recognition of the need for constraints on linear theory methods to provide physical realism, and with inclusion of interactive display for increased design control over optimization cycles.

Three-Dimensional Boundary Layer Method

A three-dimensional boundary layer method has been developed at Dornier that can analyse either laminar or turbulent compressible flows on finite swept wings and bodies [35], [36]. Three-dimensional laminar or turbulent, compressible, adiabatic boundary layers are computed in curvilinear orthogonal or nonorthogonal coordinates.

The laminar method is not restricted to small cross flows. For the evaluation of the integral thicknesses one parameter velocity profiles for the main stream direction and two parameter velocity profiles for the cross-flow direction are used. The one parameter profile family is based on the similar solutions of the boundary layer equations, the two parameter profile family results from a polynomial expression, where no boundary conditions of the Pohlhausen type (direct relation to gradients of flow properties at the outer edge of the boundary layer (compatibility condition)) are applied. The x - and y -momentum and the x - and y -moment of momentum integral equations are used for the solution. Only for the case of orthogonal coordinates 1st order moment of momentum equations are introduced. They result from the x - and y -momentum equations, which are multiplied by the velocity components u and v , respectively before the integration. For non-orthogonal coordinates 1st order moment of momentum equations do not produce solutions even when multiplying the momentum equations by linear combinations of the velocity components u and v . For curvilinear, non orthogonal coordinates 2nd order moment of momentum equations are developed, where the multiplication is done by the square of the resultant velocity U . Since these equations are much more complicated, the 1st order equations, which concern only the orthogonal case, are used for these problems.

The turbulent integral method has been developed at Dornier on the basis of [37]. The streamwise profiles are represented by power law profiles, the cross-flow profiles by Mager or Johnston profiles. The Ludwig-Tillmann relation is used for the skin friction description. The influence of compressibility is accounted for by applying Eckert's reference temperature concept. The equations finally solved are the x- and y-momentum equation and the entrainment equation (equilibrium entrainment). To provide for non-equilibrium entrainment lag entrainment has been included. Both methods have been tested extensively against finite difference methods, other integral methods and experimental results and have proven to be very reliable and fast tools.

To provide the inviscid outer flow field as output to the boundary layer program, interface programs are used to transfer the corresponding data from the inviscid method to the boundary layer program and vice versa. The inclusion of boundary layer technique into the analysis of transport and fighter aircraft design provides for a better representation of the real flow field for determining wing pressures, but also enables more accurate drag estimates to be made as well as estimates of maneuver-boundaries.

APPLICATION OF METHODS

Subsonic Panel Methods

Panel aerodynamic methods have been used at Dornier since 1971. During this time period, the panel method has been validated as a very reliable tool in predicting the aerodynamic characteristics of airplanes operating at subcritical Mach numbers. One interesting example of its use has been on the initial design phase of the Alpha Jet [1]. A typical example showing isobars is depicted in Fig. 1. In this example, main emphasis has been given to the design of the channel between the wing lower surface, the body side and the engine inlet.

The panel methods can also be used to study the mutual interference between different components including the engine inlet for different engine conditions. Panel arrangement and results in comparison with wind tunnel experiments are portrayed in Fig. 2.

Such results provide very accurate information for local design modifications, while only final selected ones are tested in the wind tunnel to verify predictions.

Vortex Lattice Methods

Vortex lattice methods are very easy to handle and fast tools for design studies not only for simple wing shapes, but also for winglets, high lift devices, wind tunnel wall interference, shrouded propellers, jet effects and wing-wing interference problems. They provide not only accurate lift and moment curves, but also very good induced drag results. This method has been used extensively at Dornier for linear flow problems, while the use in nonlinear aerodynamics is fairly new. As shown in Fig. 3 the vortex-lattice method in combination with Polhamus-Analogy is a very reliable tool to predict the nonlinear flow behaviour caused by leading edge separation [6]. The deviations in the moment curve for small, resp. negative lift is due to deficiencies in the body description. For modern fighter design with wings of large sweep this method plays an important role in wing as well as maneuver flap design.

Multi-Element Airfoil Analysis/Design

The performance of mechanical high-lift devices is of increasing importance for the overall economy and operational efficiency of all types of aircraft. The use of such devices for combat aircraft at transonic speed offers the chance of greatly enhancing maneuvering capabilities without affecting cruise performance. Climb and turn rates of existing modern fighters at transonic speed are remarkably improved by the use of slats and flaps, although these configurations have not been optimized as such devices.

At low speed such devices can be efficiently designed by means of numerical methods and a lot of available experimental data. At transonic speed, however we are lacking experimental data for airfoils with slats and flaps to establish a data base. Extensive wind tunnel testing on such airfoil systems is highly costly due to the large number of parameters and at transonic speed no simple interpolation in a data base is possible. Only since recently transonic viscous analysis/design methods are in use for configuration studies and improvements. In Fig. 4 results are depicted for an airfoil/slat configuration with upper slat surface and main airfoil shape plus lower surface slat pressure distribution as input. The results for this mixed analyses/design mode run agree very well with the experimental data and indicate clearly the large separated region on the lower slat surfaces. This mode can be used not only to understand the flow field characteristics of existing slats or flaps, but also to efficiently redesign configurations to avoid separation. Fig. 5 indicates a redesign process for the slat lower surface to a NACA 64A010 airfoil section.

For analysis problems viscous effects have to be included not only by means of laminar and turbulent boundary layers, but also short and long separation bubbles, confluent boundary layers and trailing edge separation. The present system of codes for viscous transonic two-element airfoil analysis has been successfully applied to simulate the flow field around the Do-A4 airfoil with a slat or flap. In Fig. 6 and 7 results are compared with the experimental data. The computed pressures agree fairly well with the experimental ones, even for cases with large separated regions where viscous effects completely dominate. Since such numerical simulations are rather fast and inexpensive, it is obvious that such computational methods are useful tools for designers looking for efficient high lift and maneuver devices. The design time as well as cost can be much reduced by using such numerical results.

Transonic Airfoil/Cascade Analysis/Design

The validation of two-dimensional transonic potential flow methods is almost established by numerous supercritical airfoil designs based on CFU methods. Fig. 8 shows computed versus measured pressure distributions for the Dornier A-1 12 % thick airfoil, viscous as well as wall effects in the computations included [11]. The result clearly indicates the importance of boundary layer effects even in the design region. Although design as well as analysis of this section have been done using TSP, we are aware of the limitations of TSP-methods. However, as depicted in Fig. 9, the type of numerical method, especially conservation of mass, can have stronger influence on the results than the TSP-assumptions. Therefore, more recent studies led to the development of a two-dimensional flux-finite element method for the full potential equation which at present only has been verified for the analysis/design of cascades [16], see Fig. 10, and to a finite volume method to solve the quasi time-dependent Euler equations around airfoils [17] as shown in Fig. 11. For comparison, also the results of Essers are included [43].

Both methods are very general in their application to arbitrary configuration shapes and nonorthogonal mesh systems. While the FFEM-method is very fast (0.15 ms per iteration and mesh point IBM 370/158), the finite volume method (0.8. ms) is best suited to produce datum solutions and accurate results for strong shocks which lie beyond the isentropic assumptions. Since transonic flow phenomena do not only play an important role in aerodynamic design, but also in flutter analysis, the Dornier-TSP method has been extended to treat harmonically oscillating airfoils [14]. The comparison in Fig. 12 indicates fair agreement with other transonic methods as well as experimental data. However, more work has to be done here to include viscous effects and nonlinear effects which imply the use of more complete unsteady equations.

Transonic Inlet Analysis

The efficiency of modern transonic and supersonic aircraft to quite a large extent depends on the recompression characteristics and the avoidance of separation causing distortion. Experience has proven pitot-type inlets to be well suited to design criterion at supersonic as well as subsonic and transonic speed. For the investigation of such types of flow fields with subsonic free stream Mach numbers Dornier has adapted Arlinger's method for axisymmetric inlets [19]. A typical result with good agreement is shown in Fig. 13. Although this method gives very accurate results, it lacks the generality for extensions to three-dimensional configurations. Since the study of pitot-inlets at supersonic free stream raises some questions about the disregard of total pressure losses due to shocks in methods using the potential equation, Dornier decided to develop its own method based on the numerical solution of the full Euler equations. First results of the plane and axisymmetric version of this finite volume method [20] are portrayed in Fig. 14. Fair agreement is reached for the fairly low supersonic Mach number with Arlinger's supersonic version as well as experimental data. Unfortunately we are lacking experimental data for a detailed evaluation at higher Mach numbers. For application in realistic aerodynamic design studies for fighters a three-dimensional version of the finite volume method is in development. For final flow simulations the corresponding viscous codes will be coupled.

Transonic Wing/Wing-Body Analysis

The validation of three-dimensional transonic potential flow methods has been reported recently in several papers, e.g. see References 24, 26, 38, 39 and 40, to name a few. During the application of the TSP-WF method for analysis as well as design case studies it was found, that the method is well suited to meet the requirements of engineering in as much as the code is fast (0.14 ms per iteration and grid point), designed for interactive treatment and very general in its use as depicted in Fig. 15.

For final results the full potential loop can be used to ensure no major errors due to TSP-assumptions. However, this code is suffering from its orthogonal grid system in as much as the leading edge representation for swept wings is poor as long as no extremely fine grid systems are used. The Figures 16-21 show some of the results for validation of the method for a wide range of configurations. Relatively thick large aspect ratio wings as well as moderate aspect ratio fighter wings with complex fuselage shape have been designed or analysed before the wind tunnel test became available.

For fighter configurations with complex bodies the deviations at higher Mach numbers don't seem to be to TSP assumptions rather than inadequate fuselage modelling. Full potential FLO22 computations for the wing alone did not improve the agreement.

For transport type configurations in analysis (Fig. 18) as well as mixed analysis/design (Fig. 17) mode the method proved to be very reliable, but is suffering from the poor leading edge description. However, the basic character of the pressure distribution and the shock position and strength is fairly well predicted. Fig. 19 clearly indicates the insensitivity of the pressure distribution against mesh spacing except in the nose region. The configuration is discussed in detail in [40].

Even for the very coarse 10 % grid (first mesh point on the wing at 10 % chord, five points at the wing tip section) the pressures indicate the correct distribution. The present development stage of this method is to include grid-embedding to improve its capabilities in the nose region.

The PT-7 configuration shown on Figure 20 has been a design case study [24] testing extensively the mixed mode capabilities of the TSP-method.

Since two-dimensional experience has indicated the large influence of the viscous effects, also in three-dimensional flows the viscous displacement thickness effect of the three-dimensional boundary layer over the wing has to be taken into account in order to produce accurate performance characteristics. The coupling of the three-dimensional boundary layer integral methods [35], [36] with inviscid potential flow programs provides the capability for better wing design, for diagnosis of specific wing design problems, and for evaluating the wing performance beyond the Reynolds number range of present wind tunnels. Since the boundary layer program allows for arbitrary, even nonorthogonal coordinate systems, no special interface programs are needed to convert grid systems. Only corresponding data handling in the inviscid method coordinate system is needed. Thereby it is possible to cycle several times between viscous and inviscid programs. In Fig. 20 the changes in pressure distribution corresponding to the number of iteration cycles is portrayed. It has been found that a number of cycles between the transonic potential flow program and the boundary layer code is necessary to achieve a satisfactory converged solution, i.e., until the pressure distribution and the boundary layer displacement thickness δ^* do not change significantly between cycles. The general trends of the measured pressure distributions are matched by the theory. However, a finer mesh would improve the agreement in the nose as well as shock region. In Fig. 21 the corresponding changes in displacement thickness for section 2 and the variation of the computed separation line are shown. It is clearly indicated that a boundary layer method within this cycle has to be able to treat separated regions since the fully inviscid initial solution might exhibit relatively large partial separation although the final converged viscous solution is almost free of separated regions. For completeness, the spanwise lift distribution and the computed dragrise curve are also included. Measured and calculated dragrise compare reasonably well. The capability of estimating the spanwise variation of wing drag components, lift distribution and separation, identifies the critical wing design regions and allows for proper wing modification with reasonable assurance of success.

Supersonic Panel Method

Supersonic panel methods based on Woodward's work have been used at Dornier since 1968 for quite different purposes. The possibly most complex configuration ever tested using a supersonic panel method has been the DORNIER fighter configuration "Rautenflügel" depicted in Figure 22. To evaluate the supersonic performance of such a configuration interference problems as well as lift, drag and moment behaviour have been studied extensively [41]. In Fig. 23 some typical results are shown in comparison with windtunnel test data. Measured and calculated data compare reasonably well in the linear angle of attack range. However, this panel method is suffering from the thin wing approximation since no separate studies of upper or lower surface effects are possible.

Supersonic Mach-Box Method

This linear supersonic wing method has been initially developed at Dornier in 1967 and has been validated through extensive computations for wings with and without twist and camber, different thickness distributions, and for wings with flaps. More recently it has been coupled to a numerical optimization procedure via Lagrange multipliers [32]. Providing a set of camber/twist distributions, each of which easy to manufacture, the program is looking for that combination of the different shape modes which provides minimum drag for given constraints on lift, moment. Fig. 24 depicts a typical result of such an optimization.

A similar procedure can be used for the optimum thickness distribution design with respect to wave drag of wings.

Supersonic Analysis/Design System

While in the preceding chapters only the verification of single computer codes has been described, this system is a set up of a lot of different programs. It provides not only single information on part of the configuration but also total configuration data. Fig. 25 shows the build-up of the system and the different approaches used. Presently this method is being used at Dornier for extensive supersonic performance studies, an example of which is portrayed in Fig. 26. This numerical tool is of great value for design engineers since it allows for modifications and optimizations within very short time cycles.

Three-Dimensional Boundary Layers

The three-dimensional boundary layer development greatly influences the performance of subsonic and transonic aircraft. While the use of boundary layer method to study wing characteristics has become quite popular, e.g. [35], [38], [39], only a few items are known for three-dimensional body analysis. Through its validation the Dornier method [36], [42] has been extensively tested for flows over ellipsoids at angle of attack. Fig. 27 portrays some of the results for an axis-ratio 8 ellipsoid.

Separation line pattern over the whole range of incidence agree well with those predicted by the finite difference method of Geissler and even the shear stress at the wall compares very well with that measured by DFVLR or computed by Cebeci's FD method.

However, more work has to be done to combine this method with inviscid programs in order to study separation and vortex shedding from bodies.

Numerical Wind Tunnel Simulation

Surprisingly only a few contributions are known of studying the implications of present or future wind tunnel concepts by means of numerical flow simulation, although panel methods and the existing transonic codes are well suited to such studies. Adaptive wall concepts, incomplete adaption, cryogenic concepts, and even wall corrections for existing tunnels can be simulated qualitatively with present methods fairly inexpensive. Fig. 28 and 29 portray two of the different applications being done at Dornier in the past. Fig. 28 is concerned with the complexity of three-dimensional adaptive wall concepts by showing the necessary wall deflection or porosity to simulate infinite wall conditions. Fig. 29 depicts the influence of cryogenic nitrogen on the shock wave-boundary layer interaction as test case for cryogenic wind tunnels. A lot of other applications can be thought of to improve the use of existing wind tunnels.

Concluding Remarks

The significant advances that have been made in computational fluid mechanics are having considerable impact on the aerodynamic design process. Subsonic and supersonic panel methods, when used within their limits of application, provide valuable insight into complex flow fields, guidance for achieving integrated designs, and ability to explore innovative configuration designs. The use of these methods can substantially increase airplane performance capabilities. The integrated computer program systems to analyse transonic, viscous flows over airfoils, two-element airfoil systems and wings and wing-body combinations for transport as well as fighter aircraft have emerged as a very important tool to support the wing design process, and to support diagnostic investigation of the aircraft performance.

Rewarding as the accomplishments in computational aerodynamic design have been, much work remains yet to be done. The three-dimensional transonic inviscid flow methods need to be generalized to include the complete configuration and to greatly simplify the user's input and output data manipulation and reduce computer as well as man costs. The three-dimensional boundary layer method needs to be enhanced to include the fuselage, to handle surface intersection problems, and to analyse separated flows. Most work has been towards better numerical methods at design conditions of modern aircraft. However, off design is limiting the capabilities of real configurations. A lot of work in CFD and experiments has to be done to understand those phenomena causing maneuver boundaries. This will imply more work on unsteady time-accurate flow simulations.

However, all integrated systems of computer programs are only operational as design tools within the project engineering area, if the easy preparation of input data, the visibility of output, the flow time required to get final results, and the computer costs of running these methods are highly improved. If these enhancements are not included, we may never experience the use of numerical simulation and reduced reliance on the wind tunnel in airplane design as many computer experts suggest and the basic capabilities of modern methods promise.

Acknowledgement

The author wishes to acknowledge the contributions of his colleagues at Dornier, FFA and SAAB who conducted many of the analyses reviewed in this paper. Appreciation is extended to Mr. Lynch at Douglas Aircraft Corporation, for his contribution to the Douglas-Wing comparisons, as well as to different agencies at the German BMVg and BMFT who supported method development and application.

REFERENCES

1. Zimmer, H.: Berechnung der Druckverteilung an dreidimensionalen Unterschall-Triebwerkseinläufen mit dem Panelverfahren. Paper given at the Meeting of the DGLR Fachausschuss für luftatmende Triebwerke, Dec. 1972, Friedrichshafen
2. Rubbert, P.E. et al: A General Method for Determining the Aerodynamic Characteristics of Fan-in-Wing Configurations. TR67-61A, USAAVLABS, 1967
3. Kraus, W. and Sacher, P.: Das Panelverfahren zur Berechnung der Druckverteilung von Flugkörpern im Unterschallbereich. ZfW, Heft 9, Sept. 1973, S. 301-311
4. Lucchi, C.W.: Ein Panelverfahren höherer Ordnung für kompressible Unterschallströmungen. Dornier FB 78/138, 1978
5. Lucchi, C.W. and Schmidt, W.: Vortex Lattice Approach for Computing Overall Forces on V/STOL Configurations. ACARD CP 204, p. 19-1-19-8, 1976
6. Wedekind, G.: Theoretische Berechnung der Polaren und der optimalen Manöverklappenausschläge im Unterschall für Konfigurationen mittlerer bis großer Vorderkantenpfeilung. Dornier Note BF10, 1979
7. Arlinger, B.: Analysis of Two-Element high Lift Systems in Transonic Flow. ICAS Paper 76-13, 1976
8. Arlinger, B. and Schmidt, W.: Design and Analysis of Slat Systems in Transonic Flow. 11th ICAS Congress, Lisbon, 1978
9. Leicher, S.: A Method for the Calculation of Viscous Flow over Airfoils with Slats or Flaps at Transonic Speed. US-German DEA-Meeting, April 1979, Meersburg

10. Leicher, S., and Torregiani,: Analysis of Multi-Element High Lift Systems in Subsonic Viscous Flow. Dornier Note BF30, 1979
11. Kühl, P., and Zimmer, H.: Die Entwicklung von Tragflügelprofilen für Verkehrsflugzeuge mit verbesserten Schnellflugeigenschaften. Dornier FB74/16, 1974
12. Sator, F.G.: Determination de Profils de Grilles d' Aubes Pour Compresseurs Axiaux Transsonique. These No 254 (1976), EPFL Lausanne
13. Schmidt, W.: A Self-Consistent Formulation of the Transonic Small-Disturbance Theory. In:Recent Developments in Theoretical and Experimental Fluid Mechanics, p. 48-57, Springer Verlag, 1979
14. Fritz, W.: Transsonische Strömung um harmonisch schwingende Profile. Dornier FB78/168, 1978
15. Jameson, A.: Accelerated Iteration Schemes for Transonic Flow Calculations Using Fast Poisson Solvers. New York Univ. ERDA Report C00-3077-82, 1975
16. Lucchi, C.W., and Schmidt W.: Nachrechnung transsonischer Gitter, Dornier FB79/258, 1979
17. Rizzi, A.W., and Schmidt, W.: Finite Volume Method for Rotational Transonic Flow Problems. Proc. 2nd GANN-Conf. on Num. Methods in Fluid Mech. Köln 1977, p. 152-161
18. Sator, F.G., and Schmidt, W.: Solution of the Navier-Stokes Equation for Turbulent Transonic Flow in Two-Dimensional Turbomachinery Cascades. 4th Int. Conf. on Num. Methods in Fluid Mech., 1978, Tiflis
19. Arlinger, B.: Calculation of Transonic Flow Around Axisymmetric Inlets. AIAA-Paper 75-80, 1975
20. Rizzi, A.W. and Schmidt, W.: Study of Pitot-Type Supersonic Inlet-Flowfields Using the Finite-Volume Approach. AIAA-Paper 78-1115, 1978
21. Lomax, H., Bailey, F.R., and Ballhaus, W.F.: On the Numerical Simulation of Three-Dimensional Transonic Flow with Application to the C141 Wing. NASA-TN-D 6933, 1973
22. Schmidt, W., Rohlf, S., and Vanino, R.: Some Results Using Relaxation Methods for Two- and Three-dimensional Transonic Flows. Proc. of the 4th Int. Conf. on Num. Methods in Fluid Dyn., Boulder 1974, Springer Verlag, New York, 1975, p. 364-372
23. Jameson, A., and Caughey, D.A.: Numerical Calculation of the Transonic Flow Past a Swept Wing. New York Univ. ERDA Report C00 3077-140, 1977
24. Schmidt, W., and Hedman, S.: Recent Explorations in Relaxation Methods for Three-Dimensional Transonic Potential Flow. ICAS-Paper 76-22, 1976
25. Jameson, A., and Caughey, D.A.: A Finite Volume Method for Transonic Potential Flow Calculations. AIAA Paper 77-635, 1977
26. Fritz, W., Leicher, S., Schmidt, W., and Stock, H.W.: Fortsetzung der Untersuchungen zur Auslegung überkritischer Tragflügel für Verkehrsflugzeuge. Teil II: Theoretische Arbeiten. BMFT-FB W79-07, 1979
27. Leicher, S.: Ein finites Volumen-Verfahren zur Lösung der vollen Potentialgleichung in dreidimensionaler transsonischer Strömung. Erscheint als Dornier FB, 1979
28. Schmidt, W., and Rizzi, A.W.: Finite Volumen-Verfahren zur Lösung der Euler-Gleichungen für dreidimensionale transsonische Strömungen. Dornier FB79/288, 1979
29. Woodward, F.A.: An Improved Method for the Aerodynamic Analysis of Wing-Body-Tail Configurations in Subsonic and Supersonic Flow. NASA CR-2228, 1974
30. Leicher, S.: PAN 79, ein Unterschall-Überschall-Panelverfahren, Dornier Note BF30-1419/79, 1979
31. Schmidt, W.: Die Umströmung von Flügeln beliebiger Grundrißform bei Überschall. Dornier FB 72/34, 1972
32. Wedekind, G.: Methoden der Tragflügeloptimierung für ein taktisches Kampfflugzeug. Dornier FB78/50 B, 1978
33. Middleton, W.D., and Lundry, J.L.: A Computational System for Aerodynamic Design and Analysis of Supersonic Aircraft. NASA-CR-2715, 1976
34. Fritz, W.: Bereitstellung eines Überschall-Entwurfs- und Nachrechnungs-Programmsystems. Dornier note BF30-1545/79, 1979
35. Stock, H.W.: Three-Dimensional Boundary Layers on Wings and Bodies of Revolution. US-German DEA-Meeting 1979, TR AFFDL-TR-78-111, p. 32-56, 1978
36. Stock, H.W., and Horton, H.P.: Ein Integralverfahren zur Berechnung dreidimensionaler, laminarer, kompressibler, adiabaler Grenzschichten. Dornier FB79-228, 1979

37. Smith, P.D.: An Integral Prediction Method for Three-Dimensional Compressible Turbulent Boundary Layers. ARC, R. & M. 3739, 1974
38. Lynch, F.T.: Recent Applications of Advanced Computational Methods in the Aerodynamic Design of Transport Aircraft Configurations. 11th ICAS Congress, 1978
39. Da Costa, A. Larry: Application of Computational Aerodynamics Methods to the Design and Analysis of Transport Aircraft. 11th ICAS Congress, 1978
40. Lynch, F.T., and Schmidt, W.: Viscid Three-Dimensional Flow Simulation on Transonic Wings. US-German DEA-Meeting, April 1979, Maersburg
41. Zimmer, H.: Theoretische Untersuchungen zum Rautenflügelkonzept in Überschallströmung. Dornier FB78/46B, 1978
42. Stock, H.W.: Laminar Boundary Layers on Inclined Ellipsoids. Dornier Note BF30-1511/79, 1979
43. Essers, J.A.: The Numerical Simulation of Steady Supercritical Flows over a Non Lifting Airfoil Using a Fast Artificial Time-Dependent Technique. Dornier FB 78/20 B, Oktober 1978

FIGURES

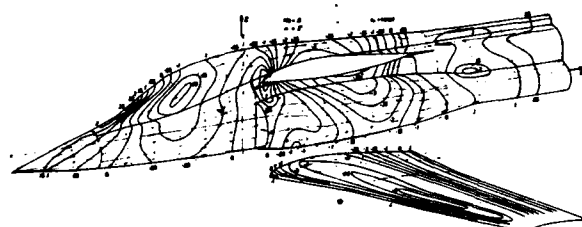
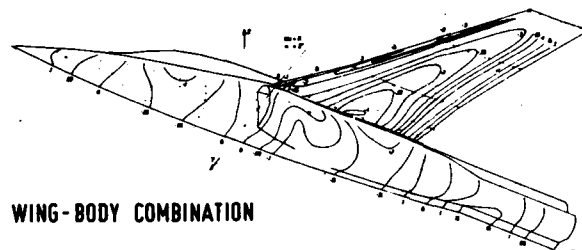


Figure 1: Computed Isobars on Alpha-Jet



ENGINE INLET

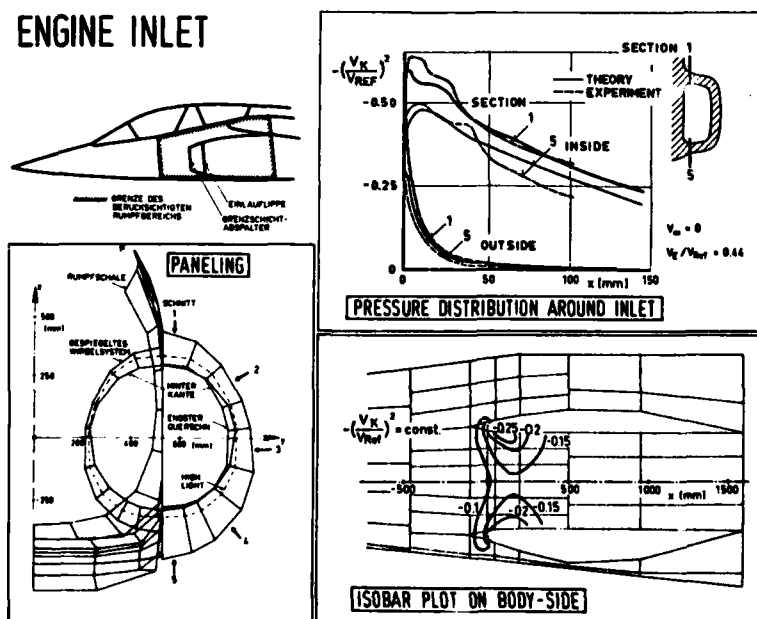


Figure 2: Subsonic Engine-Inlet Integration

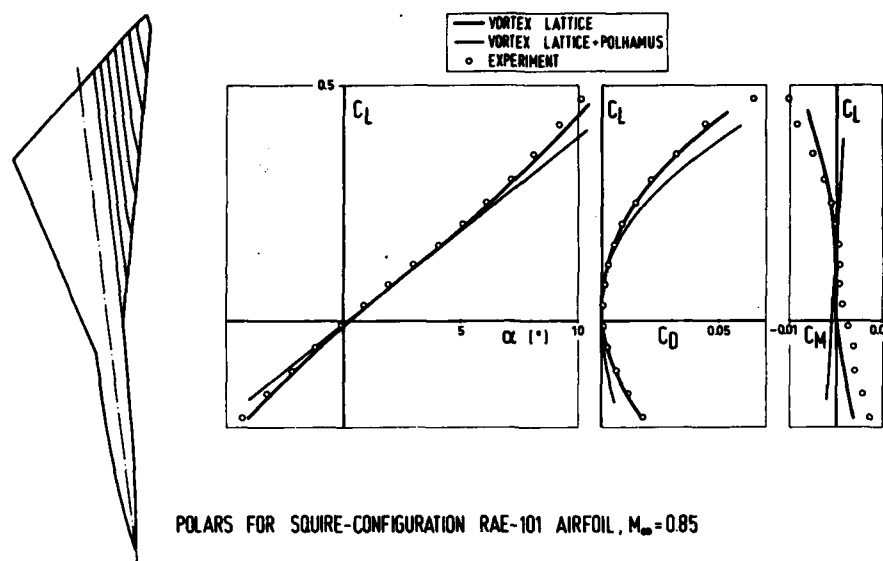


Figure 3: Analysis of Configuration with Leading Edge Separation

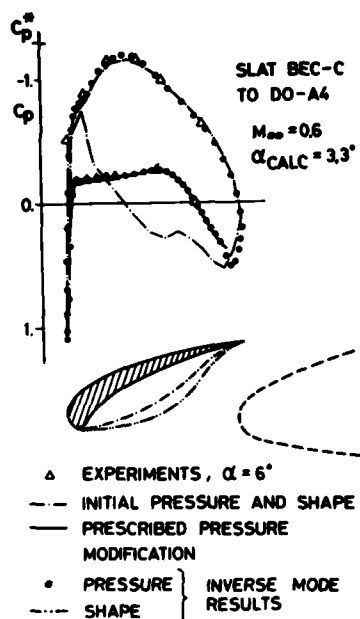


Figure 4: Slat Separation Determined by Mixed Analysis/Design Mode Runs

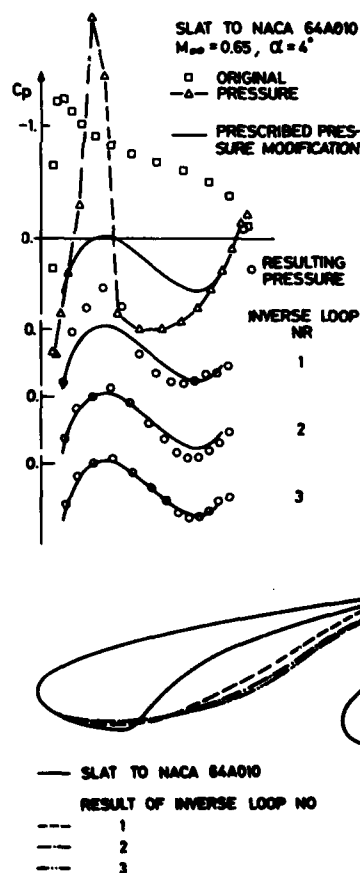
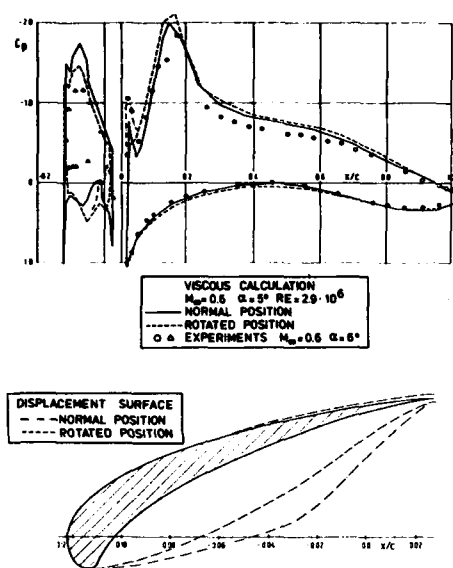
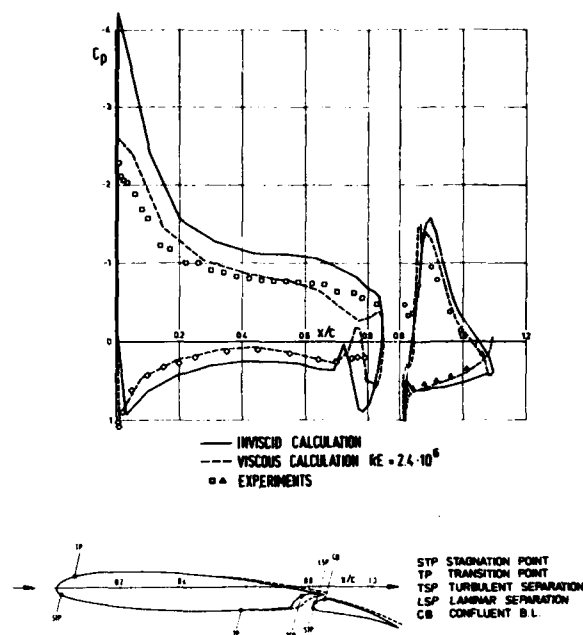


Figure 5: Redesign Process for Slat Lower Surface



DO-A4 WITH SLAT BEC-C
SLAT ROTATED FOR ONE DEGREE

Figure 6: Analysis of Separation on Slat/Airfoil Configuration by Viscous Mode Runs



DO-A4 WITH FLAP POS.1
 $M_\infty=0.5$, $\alpha=4^\circ$

Figure 7: Analysis of Flap/Airfoil Configuration

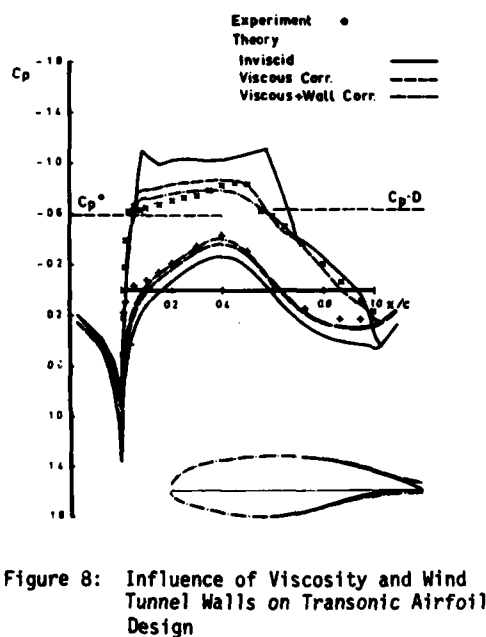


Figure 8: Influence of Viscosity and Wind Tunnel Walls on Transonic Airfoil Design

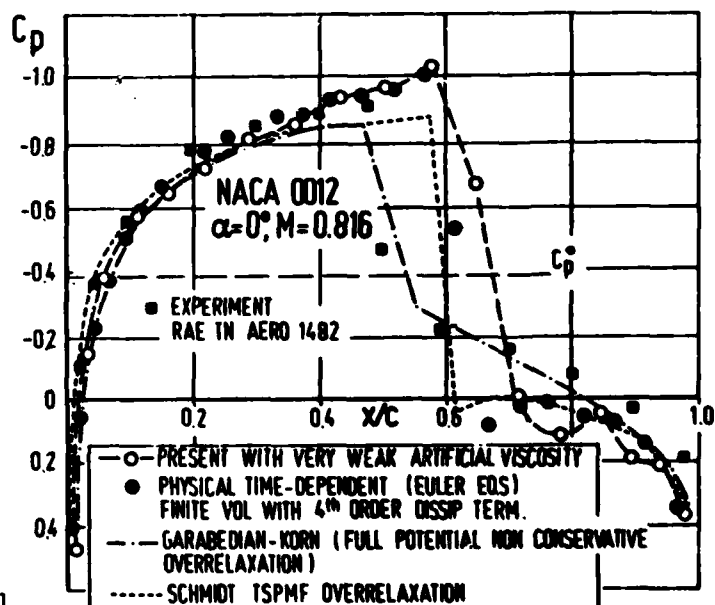


Figure 11: Transonic Flows with Strong Shocks

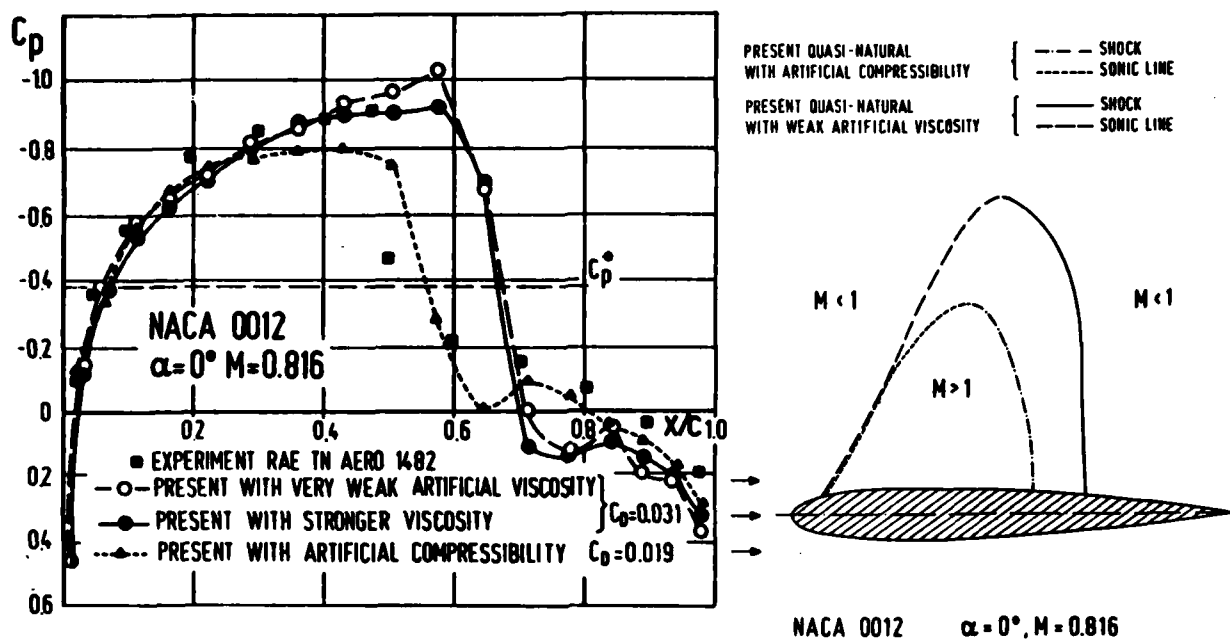


Figure 9: Inviscid Transonic Flow Simulation Errors

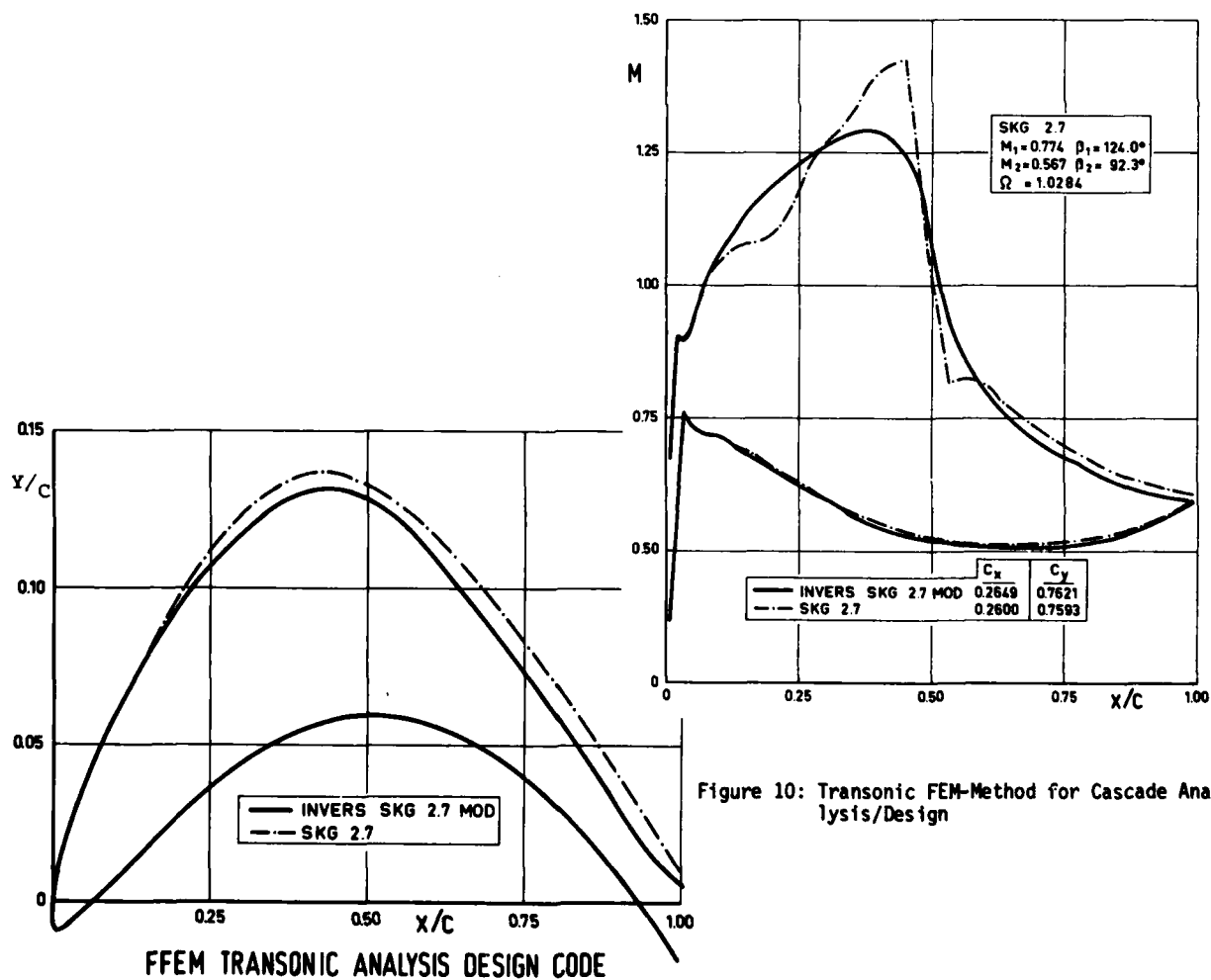


Figure 10: Transonic FEM-Method for Cascade Analysis/Design

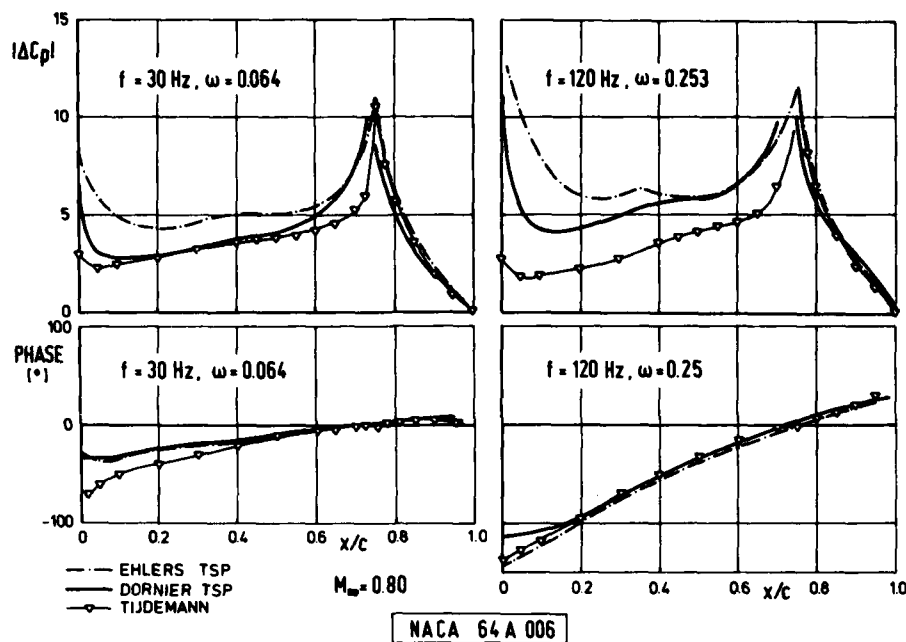
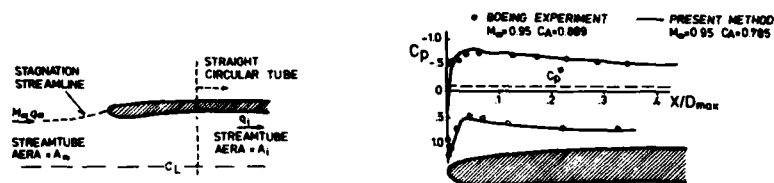


Figure 12: Harmonically Oscillating Flap Simulation



ARLINGER METHOD FOR TRANSONIC AXISYMMETRIC INLETS

Figure 13: Transonic Flow Around Axisymmetric Inlets

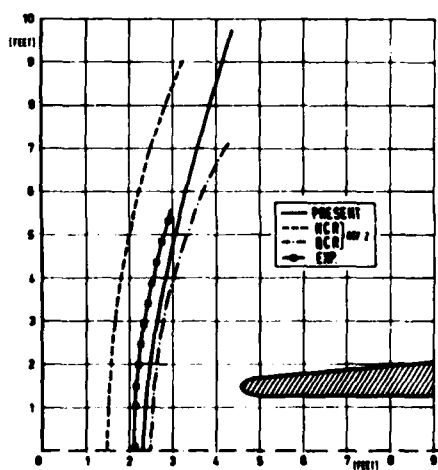
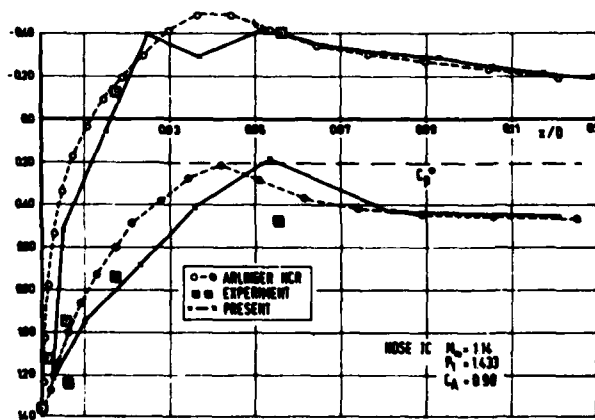
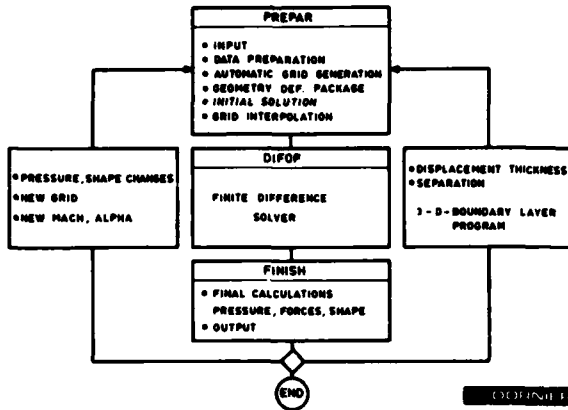
Comparison of bow shock standoff-distance and shape for inlet 1E. $M_\infty = 1.14$, $C_A = 0.91$ 

Figure 14: Supersonic Inlets with Detached Bow Shock

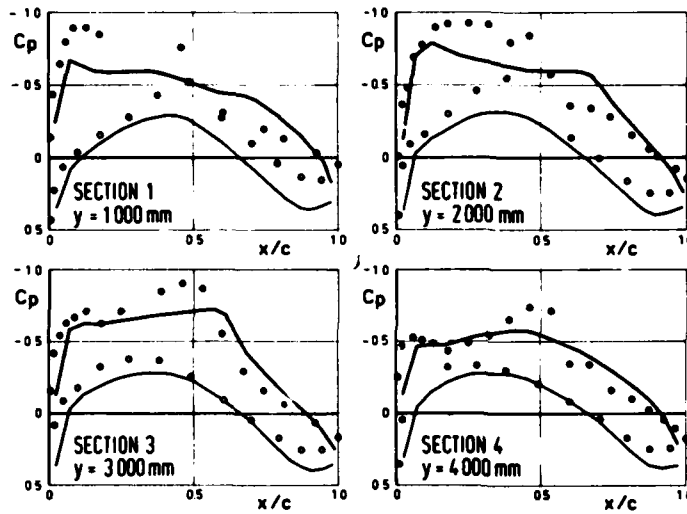
FLOW CHART OF ANALYSIS / DESIGN SYSTEM



ANALYSIS AND DESIGN OPTIONS

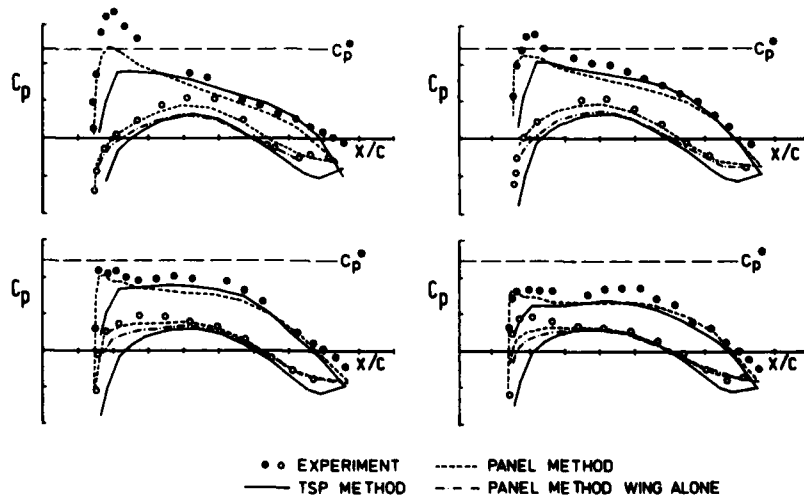
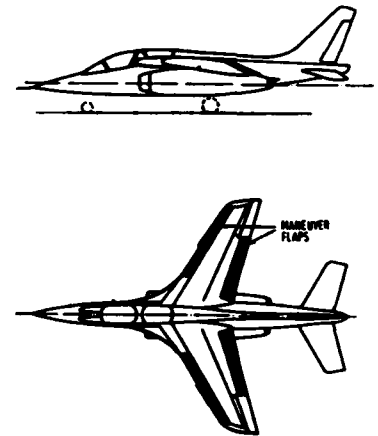
- 1 ANALYSIS NORMAL VELOCITY COMPONENT SPECIFIED, PRESSURE CALCULATED
- OPTIONALLY CAMBER OR THICKNESS CAN BE CHANGED ON PORTIONS
- 2 DESIGN TANGENTIAL VELOCITY COMPONENT SPECIFIED, NORMAL COMPONENT COMPUTED \rightarrow SHAPE
- ARBITRARY PORTIONS ON UPPER AND/OR LOWER SURFACE CAN BE CHANGED
- 3 MIXED PROBLEMS ON SOME PORTIONS TANGENTIAL, ON OTHERS NORMAL VELOCITY COMPONENTS SPECIFIED, FINAL SHAPE AND PRESSURE COMPUTED
- OVER SOME CHORDWISE PRESSURE IS PRESCRIBED ON UPPER AND/OR LOWER SURFACE SPAN-SECTIONS WHILE FOR THE REST SHAPE IS GIVEN
 - SHAPE ON SOME STATIONS IS CHANGED
 - PRESSURE ON UPPER OR LOWER SURFACE IS CHANGED WITH THICKNESS OR CAMBER CONSTRAINT

Figure 15: Transonic Viscous Analysis/Design System



THEORETICAL AND EXPERIMENTAL PRESSURE DISTRIBUTIONS
at $M=0.835$, $\alpha=2^\circ$, $Re=2.5 \cdot 10^6$

— calculation
•• test



SUBSONIC PRESSURE DISTRIBUTION FOR SKF, $M_\infty=0.716$, $\alpha=2^\circ$

Figure 16: Transonic Analysis for SKF Alpha-Jet

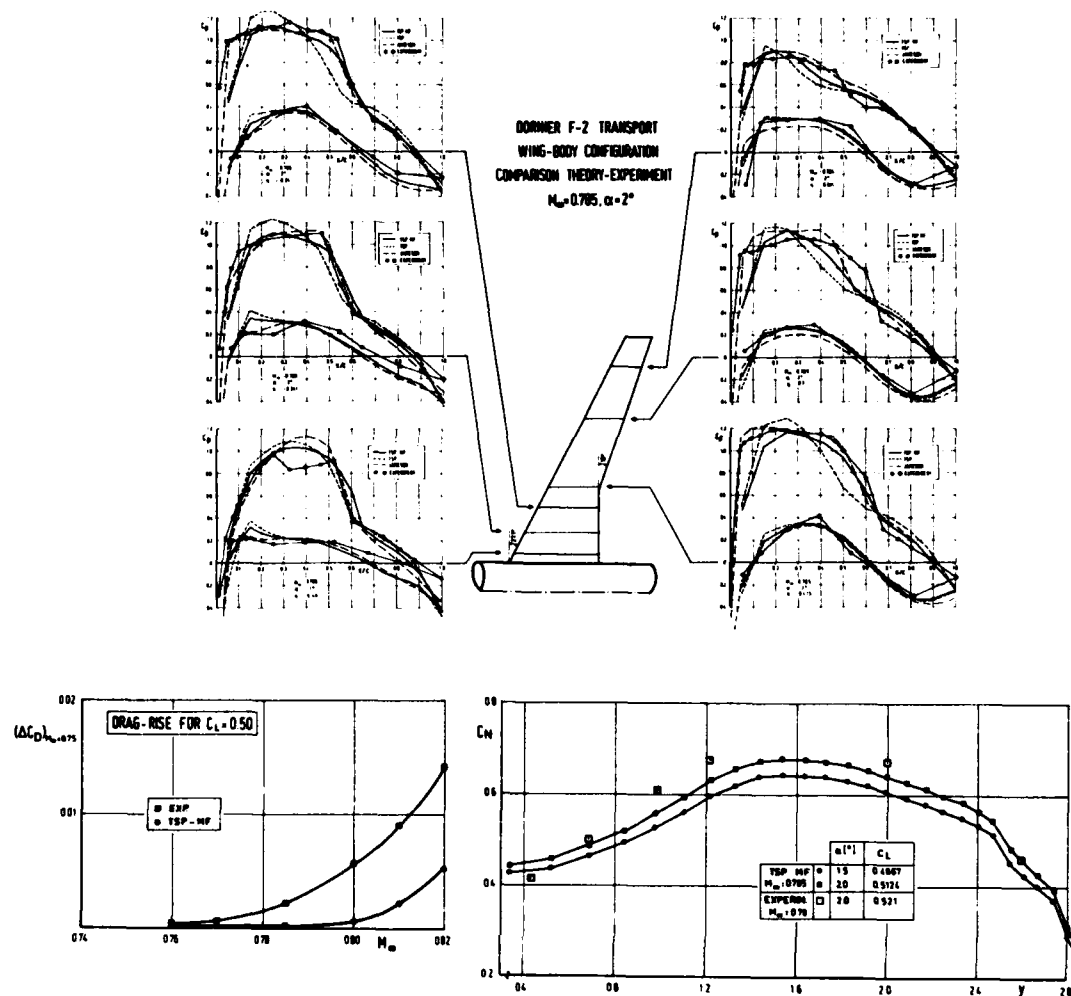


Figure 17: Transonic Analysis/Design for Transport Configuration DO-F2

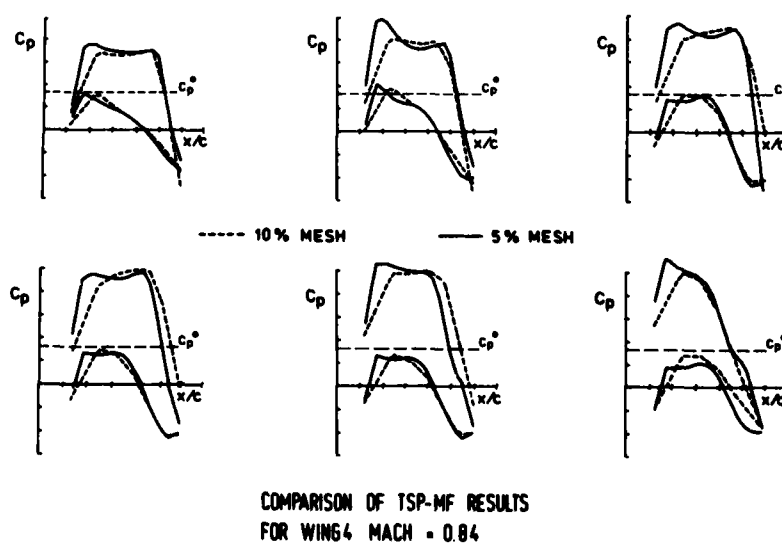


Figure 19: MESH-Influence in TSP-MF Method for Wing 4

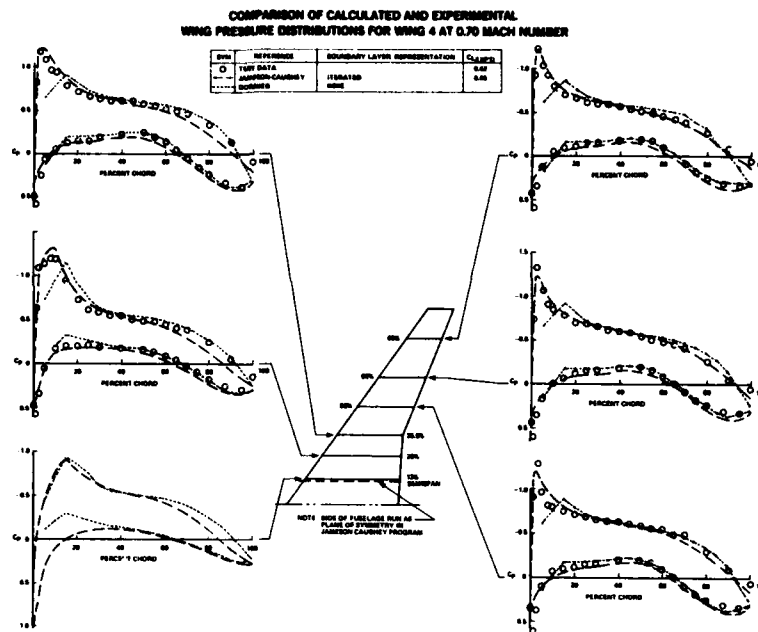
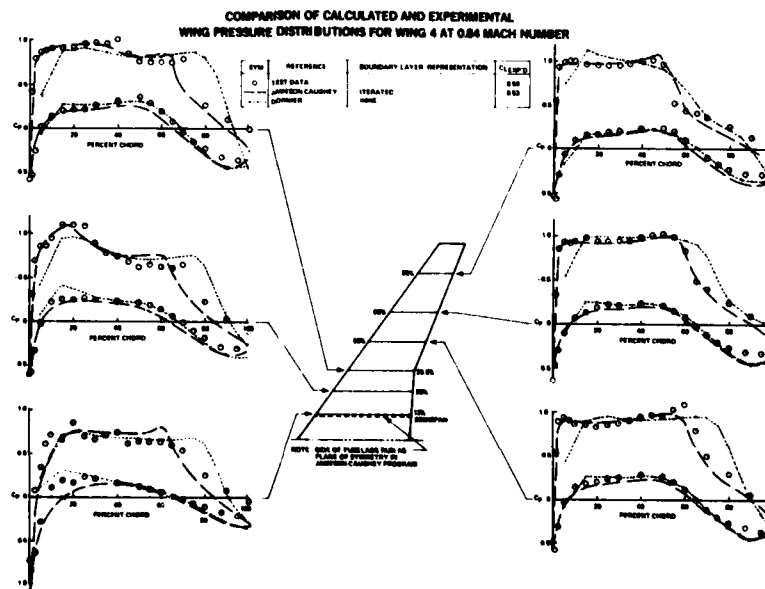


Figure 18: Transonic Analysis for Douglas Wing 4



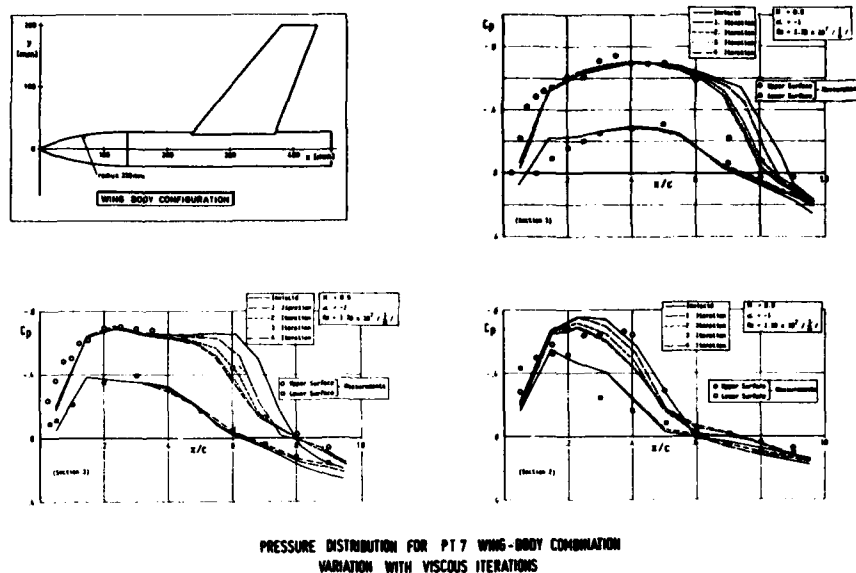


Figure 20: Design Case Study PT-7

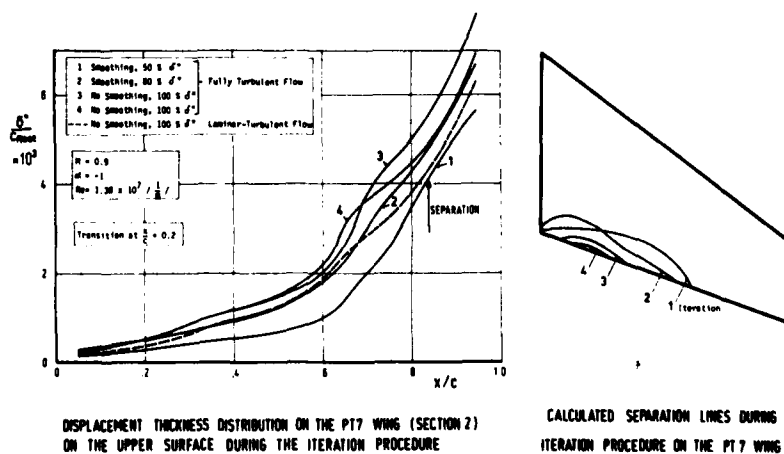
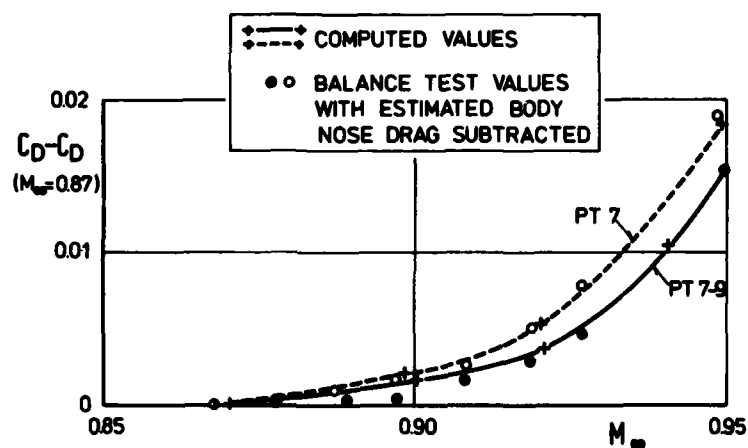


Figure 21: Boundary Layer on PT-7 Wing



Figure 22: Dornier Rautenflügel Configuration

POLARS FOR DORNIER RAUTENFLUEGEL CONFIGURATION

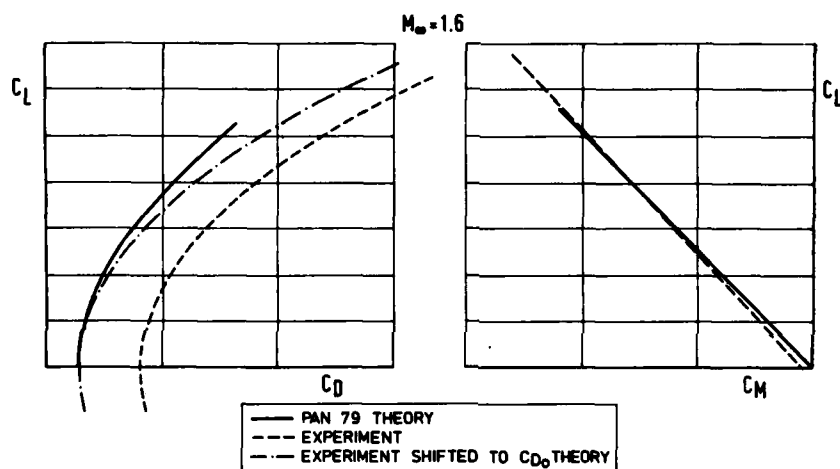
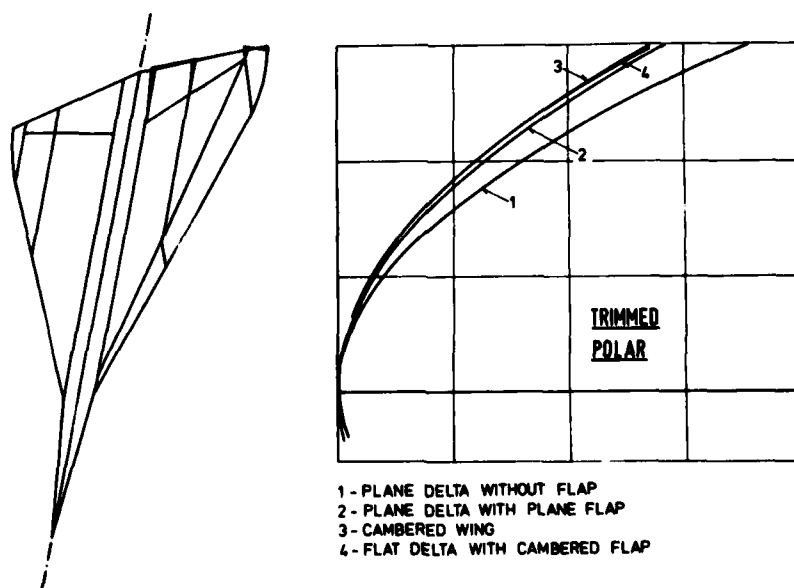
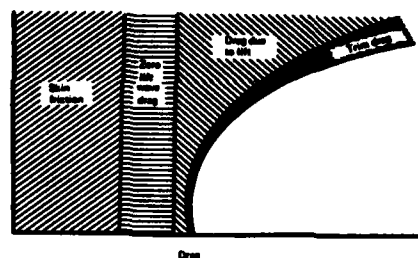
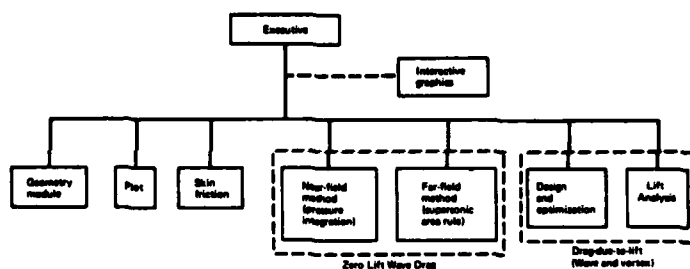


Figure 23: Supersonic Interfluence Analysis for "Rautenflügel"



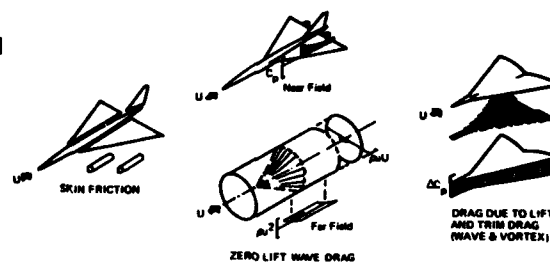
SUPERSONIC FLAP OPTIMIZATION

Figure 24: Supersonic Wing Optimization by Flap Design



INTEGRATED SUPERSONIC DESIGN AND ANALYSIS SYSTEM

Figure 25: Interactive Analysis/Design System for Supersonic Configurations



SUPERPOSITION METHOD OF DRAG ANALYSIS

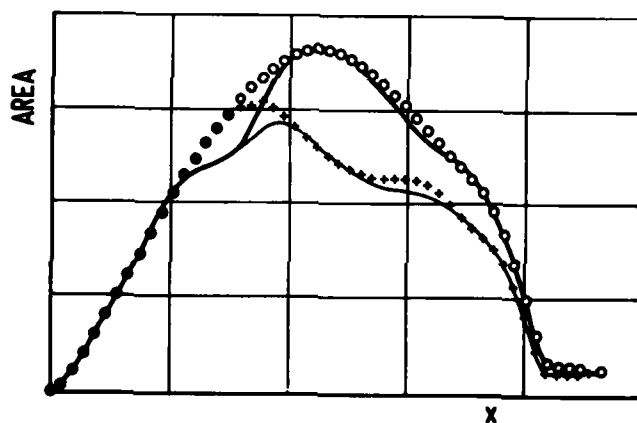
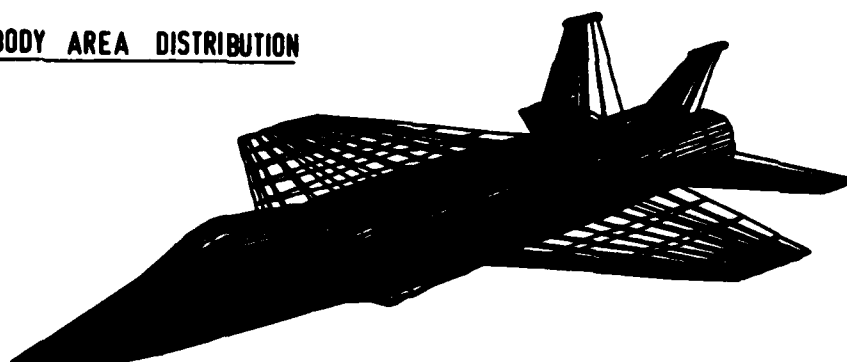


Figure 26: Supersonic Fighter Analysis/Design

— CONFIGURATION — FUSELAGE
 ooo OPTIMUM CONFIG. +++ OPTIMUM FUSELAGE

ADEQUATE BODY AREA DISTRIBUTION



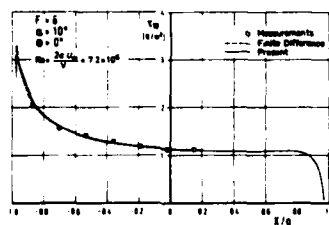
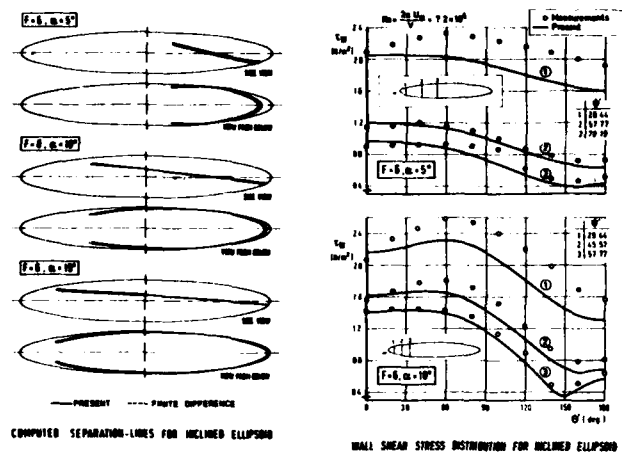


Figure 27: Laminar Boundary Layer on an Inclined Ellipsoid

TSP-STUDIES FOR ADAPTIVE
WALL CONCEPTS
PT-7 WING BODY

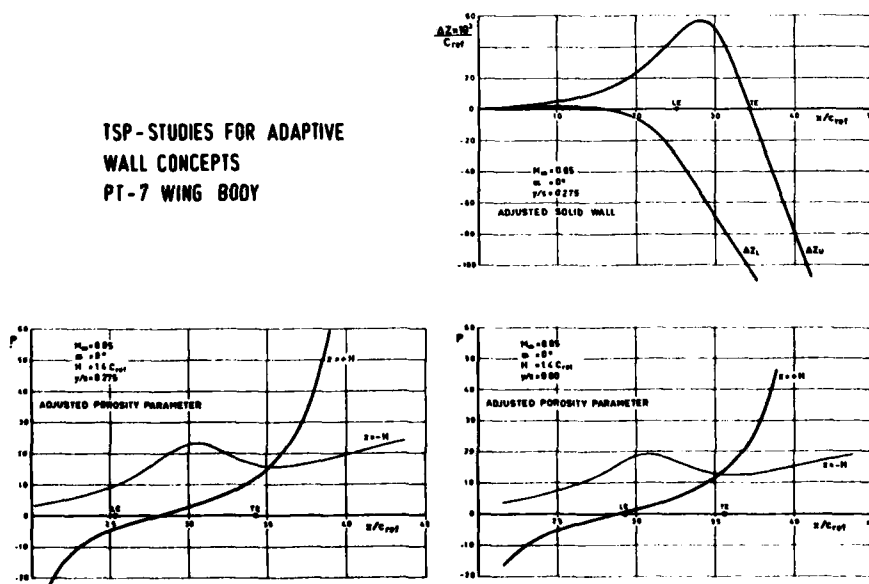
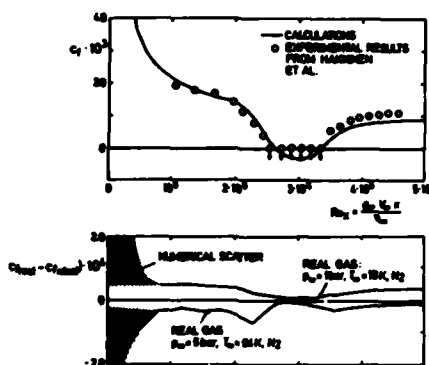


Figure 28: Numerical Simulation of Adaptive Walls

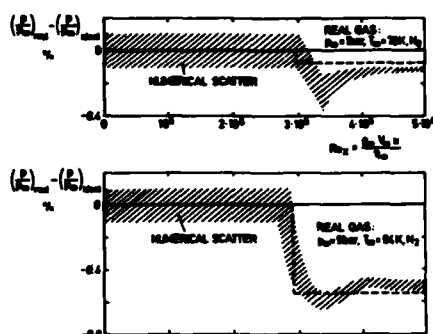
WALL SHEAR STRESS DISTRIBUTION FOR SHOCK WAVE-BOUNDARY LAYER INTERACTION

$Re = 2.96 \cdot 10^5$, $M_\infty = 2$, $\zeta = 32.585^\circ$



DIFFERENCES IN PRESSURE DISTRIBUTION FOR SHOCK WAVE-BOUNDARY LAYER INTERACTION

$Re = 2.96 \cdot 10^5$, $M_\infty = 2$, $\zeta = 32.585^\circ$



PRESSURE DISTRIBUTION FOR SHOCK-BOUNDARY LAYER INTERACTION

$Re = 2.96 \cdot 10^5$, $M_\infty = 2$, $\zeta = 32.585^\circ$

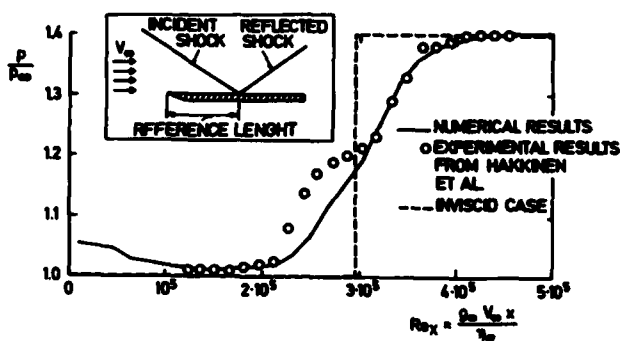
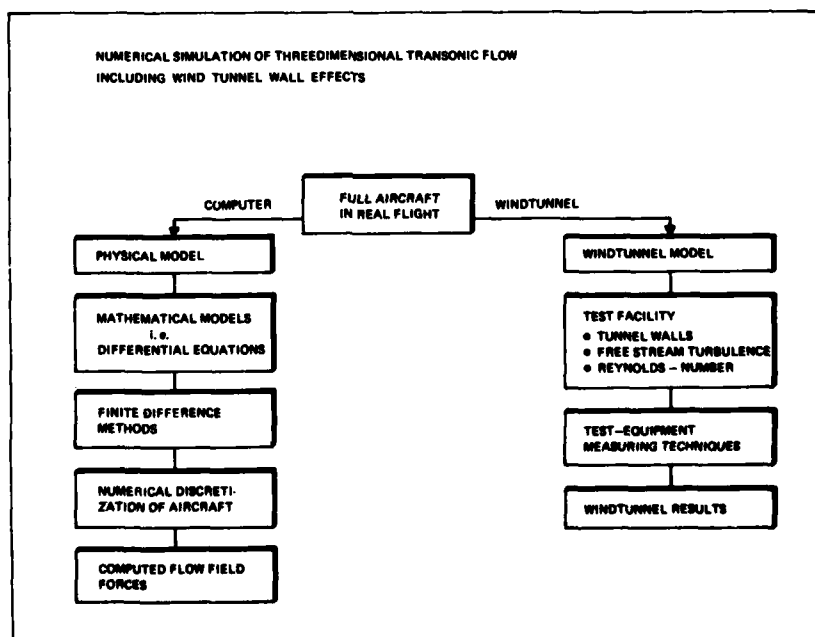


Figure 29: Simulation of the Influence of Cryogenic Nitrogen on Shockwave-Boundary Layer Interaction

NUMERICAL SIMULATION OF THREEDIMENSIONAL TRANSONIC FLOW INCLUDING WIND TUNNEL WALL EFFECTS



MAINTENANCE OF NASTRAN^R AS A STATE-OF-THE-ART COMPUTER PROGRAM

by

James L. Rogers, Jr.
Aero-Space Technologist
NASA Langley Research Center
Mail Stop 243
Hampton, VA 23665

SUMMARY

NASTRAN¹ (NASA STRuctural Analysis) is a large, general purpose, finite element computer program. Since Level 12, the first public release of the program in 1970, NASTRAN has been maintained as a state-of-the-art computer program by the NASTRAN Systems Management Office (NSMO) at NASA's Langley Research Center in Hampton, Virginia. NSMO is responsible for maintaining NASTRAN as state-of-the-art on three computer systems (IBM, CDC, and UNIVAC) with respect to both finite element and computer technology. There are four primary areas involved in a good maintenance effort: (1) error correction, (2) incorporation of advances in technology, (3) documentation, and (4) new level generation. The complexity of the maintenance effort is compounded by the sizes of the program (400,000 lines of code) and the documentation (7000 pages divided into seven manuals). This paper describes the areas of the maintenance effort in detail and offers some suggestions for reducing the complexity of maintaining a large computer program.

1. INTRODUCTION

NASTRAN¹ (NASA STRuctural Analysis) is a large, general purpose, finite element structural analysis computer program. It was developed under NASA sponsorship during the period 1965-1970, at a cost of about \$3.5 million and initially released to the public in 1970 in a form called Level 12. From 1970 through early 1979, NASTRAN was maintained as a state-of-the-art computer program by a contractor under the guidance of the NASTRAN Systems Management Office (NSMO) at NASA Langley Research Center, Hampton, Virginia. The purpose of this paper is to describe this activity and discuss features of the software maintenance work. The requirements of the maintenance activity were broad because of the size and generality of the computer program and its widespread acceptance and use in the U.S. and abroad. The primary aspects of this maintenance effort were error correction, addition of new capabilities, documentation, and quality assurance. New capabilities were added to keep the program up to the state-of-the-art with advances in structural technology and computer technology. A dominant factor in the total activity was that the program was maintained operational on three mainframe computers (CDC, IBM, UNIVAC). Each aspect is discussed in detail in this paper.

2. OVERVIEW

Growth in capabilities and size of the NASTRAN program are indicated in tables 1-6 (ref. 1). The term "Level" refers to a release of the program that is significantly different from previous releases and therefore deserves a separate identification number. From tables 1-6, it is seen that engineering capabilities grew from 13 to 23 analysis options between Levels 12 and 17.5 resulting in an increase in the size of the program from 150,000 to almost 400,000 source statements. Because of efficiency improvements, however, Level 17.5 shows approximately a 10 x 1 speed increase over Level 12. Documentation has grown with the software—from 3700 pages in four manuals (Level 12) to over 7000 pages in seven manuals (Level 17.5).

The use of NASTRAN has also grown. In 1970, Level 12 was released to approximately 50 organizations and there were less than 900 individual users. When Level 17.5 was released in early 1979, over 250 organizations and more than 2600 individuals were using NASTRAN. A map showing the sites where NASTRAN is in use in the U.S. is presented in figure 1. This increased usage made it imperative to be able to respond promptly when errors were found or new capabilities were required.

3. ERROR CORRECTION

The main thrusts of the error correction activity were to make the public aware of all known errors and to make corrections available as soon as possible. NSMO and its

¹NASTRAN: Registered trademark of the National Aeronautics and Space Administration (NASA), Washington, DC 20546.

maintenance contractor developed an efficient error reporting and correction process diagrammed in figure 2.

A problem was reported to NSMO in one of three ways: (1) from in-house users (NSMO or the maintenance contractor), (2) by mail, or (3) through the Error Correction Information System (ECIS). ECIS is discussed in detail later (also see ref. 2). NSMO determined (1) if the problem was really an error, (2) if the user had made a mistake, or (3) if the problem had been previously reported (Previously Reported Bug, PRB). If it was a user mistake or a PRB, a form letter (see form 1 in Appendix) or a message in ECIS was sent to the user describing what had been found. If the problem was an error in NASTRAN, a Software Problem Report (SPR) as shown in form 2 of the Appendix was filled out. The error was given a number and a priority, and was forwarded to the maintenance contractor. Priorities ranged from 0.0 to 5.0 in increments of 0.1. In general, priorities were assigned according to the following scheme:

- Priority 4-5 - Program gave answers that appeared to be correct, but were not.
- Priority 3-4 - A correction to the error was available, or program gave obviously wrong answers.
- Priority 2-3 - An often used capability was not working.
- Priority 1-2 - An avoidance procedure was available.
- Priority 1-0 - A seldom used capability was not working, or a desired new improvement was defined.

A priority of 5.0 received the earliest attention. The maintenance contractor first attempted to find a temporary fix; that is, a correction the user could apply without modifying the code. If one was available, it was included with the letter or message in ECIS to the user. Additional information such as dumps or listings might also have been requested from the user. All known information about the error was then entered into ECIS. An SPR log was also maintained containing a list of all active SPR's and available corrections. A new log was available from COSMIC every six months at a cost of \$15.

Once the maintenance contractor had the prioritized SPR, it was placed into a queue according to priority. Since 1969, there have been approximately 1500 errors reported. Of these, only 212 remained as of January 1979, with 17 having a priority greater than 4.0. When an error reached the top of the queue, the maintenance contractor defined the general steps, time, and money needed to effect a correction, and finally developed the subroutine changes needed for the correction. Simultaneously, all required documentation changes were initiated.

When an error was corrected and verified on all three computers, the maintenance contractor delivered an alter form (see form 4 in the Appendix) to NSMO along with verification listings. NSMO then verified that the reported error had been fixed by examining verification listings and code changes, and by making tests using known solutions. Although this effort duplicated some of that done by the maintenance contractor, it was deemed necessary to insure the fix was correct. After NSMO approved the correction, the code changes were placed into the next level of NASTRAN being readied for public release.

Since new levels of NASTRAN were released to the public on the average of once every 18 months, it was sometimes necessary to make a fix more readily available to the public or a particular user. This more rapid release was accomplished in several ways. If a user desired a particular correction, a copy of the alter form which contained the necessary code changes was sent to that user. Critical errors and their corrections were listed in the NASTRAN Newsletter which was published about once every six months.

The description of the error and its correction, when available, were also placed in ECIS. ECIS was a data base management system consisting of two data bases. The first data base was used for comments to and from users reporting SPR's. It was accessed (both read and write) by users as well as NSMO and the maintenance contractor on a daily basis. Response time to a user inquiry was usually 1-2 days. The second data base contained all error information and corrections pertinent to the existing public release level. It could also be accessed both by users (read only), and by NSMO and the maintenance contractor (read and write). The data base management system had extensive sorting capabilities. Thus, a user could query ECIS and receive information concerning only the SPR(s) of interest. Users could see all new errors and copy any fixes that were available. This data base was updated every 2-4 weeks, depending upon the level of the error reporting and correction activity.

The computer cost and manpower required to correct an error vary greatly depending on the error. Some errors involved merely changing one character on one line, while others required changing several subroutines. Manhours ranged from 1-150 and computer costs ranged from almost zero to over \$2000 for a single correction. It proved to be very difficult to predict costs and manhours required for a correction.

4. ADDITION OF NEW CAPABILITY

NASTRAN was kept state-of-the-art with respect to structural technology by adding new capabilities. Many times, new capabilities were added in response to users' needs. Examples of these additions include heat transfer for NASA Goddard, automated multistage substructuring for space shuttle contractors, and rigid elements for the helicopter industry. These new capabilities were developed in-house by NSMO or the maintenance

contractor, or by another contractor. No matter who the developer was, the maintenance contractor was responsible for incorporating the new code into the level of NASTRAN being readied for public release. The steps required for adding a new capability are shown in figure 3. To make the maintenance contractor's job of incorporation as smooth as possible, a NASTRAN general purpose interface requirements document was written (ref. 3). This document aided the new capability contractor in programming in the NASTRAN environment when developing new code or modifying existing code. It also defined the NASTRAN documentation format rules including detailed specifications for typists. The new capability development cycle was broken down into the following six phases:

1. Definition Phase
2. Design Phase
3. Programming Phase
4. System Test Phase
5. Installation Phase
6. Acceptance Phase

The IRD document described what was to be done in each phase and the items that were to be delivered at the conclusion of each phase. A new phase was generally not begun until the deliverable items of the preceding phase were accepted. A document of this type is a valuable cost- and time-saver when working in a multivendor software environment.

5. IMPACT OF ADVANCES IN COMPUTER TECHNOLOGY

NASTRAN was kept state-of-the-art on three types of computers: CDC, IBM, and UNIVAC. These computers were chosen initially because they were being used for scientific work at the NASA Centers at the time NASTRAN was originally initiated. When first released in 1970, NASTRAN ran on IBM 7094, CDC 6400 or 6600, and UNIVAC 1106. In 1978, NASTRAN ran on IBM 360/370 series, both CDC 6000 and CYBER series, and UNIVAC 1100 series. There were many advances in computer technology during this time period, and most of them had a direct effect on NASTRAN. The following paragraphs discuss the major problems encountered and the way these problems were addressed.

IBM periodically upgraded its disks (from 2314 to 3330 to 3330 Mod II to 3350). NASTRAN writes data blocks out to disk and then reads them back into memory as needed. Thus NASTRAN is dependent upon the type of disk available at each user's installation. When the disk would change, the code required to access the disk efficiently would also have to be modified. Since different users have different disks, it became necessary to generalize this area of code. As a result, NASTRAN now contains code to query the I/O supervisor of the operating system to determine characteristics of the particular disk device that is being used. The code then automatically accesses that disk efficiently. This process is transparent to the user and does not have to be changed each time an organization upgrades its disks.

The introduction of virtual storage (VS) operating systems on IBM computers also influenced NASTRAN execution. Until VS became available, NASTRAN executed under the OS/MFT and OS/MVT IBM operating systems. A study (ref. 4) indicated that VS1 was similar to OS/MFT and that VS2 Release 1 was essentially similar to OS/MVT. Thus only two changes had to be made to NASTRAN to make it operational under these two VS operating systems. However, the story was different for VS2 Release 2. NASTRAN uses an "open core" concept that makes certain assumptions about the way in which the GETMAIN/FREEMAIN operate. These assumptions broke down in VS2 Release 2 because all GETMAIN requests are satisfied from the beginning of the address space, which meant open core was fragmented. (More details can be found in reference 4). A joint effort by Bell Helicopter and Lockheed-California produced a deck of cards to allow Level 15.5 NASTRAN users to work under an IBM VS2 Release 2 operating system. This deck was generalized and incorporated into Level 16 by the maintenance contractor. Now NASTRAN executes under any of the OS IBM operating systems without having to make changes to the program.

Several problems were also encountered due to advances in CDC software. In 1976, Langley began conversion to the CDC NOS operating system from SCOPE. Because NSMO used Langley's computer system as its primary maintenance tool, NASTRAN also had to be converted to NOS. This conversion required almost a complete rewrite of the NASTRAN Linkage Editor. This Linkage Editor, which was designed and developed especially for NSMO, had been modeled after the IBM Linkage Editor to provide flexibility in the overlay structure. This Linkage Editor was maintained by the contractor as part of the CDC NASTRAN delivery package. A decision was made after Level 17 was delivered to drop the Linkage Editor and convert to the CDC Segment Loader, because the Segment Loader was standard CDC software and would be maintained by CDC. This decision required a complete rewrite of the overlay structure. Assembly language routines had to be modified because of the different way registers were passed. All of these modifications were made and released to the public in Level 17.5.

Throughout NSMO's maintenance period the UNIVAC system has been very stable. Most of the advances that were made were upward compatible and caused very little impact on NASTRAN maintenance.

6. DOCUMENTATION

Documentation for NASTRAN consisted of four major manuals containing about 6000 pages. These manuals were the Theoretical Manual, the User's Manual, the Programmer's manual, and the Demonstration Problem Manual (refs. 5-8). A User's Guide (ref. 9) was published primarily for beginning users of NASTRAN and periodically reissued to reflect new software additions. A guide to a Condensed Form of NASTRAN (ref. 10) was published for use by educational institutions or by organizations not requiring the full range of capabilities.

The four basic manuals were maintained and updated to keep abreast of software enhancements. Whenever a change was needed in a manual, a NASTRAN Documentation Change Report (DCR) was issued and given a DCR number (see Form 4 in Appendix). This DCR was associated with that particular change until the documentation review cycle (figure 4) was completed. A DCR ranged from a single sentence to over 100 new pages. Often, much original writing was needed. In the review cycle there were two editors for each manual: one in the maintenance contractor's office and one in NSMO. It was found that using two editors in this fashion produced the best documentation. Each editor got to see the documentation twice: first in an approval stage and finally after the changes had been typed. This final approval tended to be iterative. To insure that all manuals were consistent, there were specific rules for adding to or modifying the documentation. These rules are presented in the NASTRAN General Purpose Interface Requirements Document (ref. 3).

7. QUALITY ASSURANCE FOR NEW LEVELS

New levels of NASTRAN were released when major new capabilities were added and appropriate error corrections accumulated. When the decision was made to release a new level of NASTRAN, a deadline was set beyond which no new code (either error correction or new capability) would be added to the system, unless the code was of such a critical nature that the final NASTRAN level would not function within acceptable limits. On this date, the quality assurance (QA) cycle began for the total system. QA was an ongoing process for separate error corrections, new capabilities, and subsystems, but not on the system as a whole until a new level release decision was made. The majority of the maintenance effort was done on CDC computers because they are Langley's primary computers, and NSMO and the maintenance contractor were located at Langley. NSMO provided the maintenance contractor with both batch and interactive terminals so the IBM version (using a remote NASA IBM 360/95 computer) and the UNIVAC version (using a remote NASA UNIVAC 1110 computer) were maintained on an equal basis with the CDC version.

The cutoff date for new code was usually about one month prior to the scheduled delivery of the new CDC level to COSMIC. One month after the delivery of the CDC version, the IBM version was delivered, and in one more month the UNIVAC version.

QA was performed by using a set of standard NASTRAN demonstration problems with the known results. The set consisted of about 100 problems which test most of the capabilities and combinations of capabilities. Because of NASTRAN's size and generality, it was impossible to remove all errors. Thus the goal was to make sure that at least all of the demonstration problems ran to completion and produced correct results.

The demonstration problems were first executed on the CDC computer. When they ran correctly, a weekend trip was made to a NASA IBM facility to test the IBM version. It was found that on-site testing for a QA effort of this scale was much better than remote testing. After the IBM version was tested and corrected to allow demonstration problems to run correctly, corrections were fed back into both the CDC and UNIVAC versions. A week's trip was then taken to a NASA UNIVAC facility to test the UNIVAC version.¹ The corrections required for the UNIVAC were then fed back into the CDC and IBM versions. A subset of the demonstration problems was then run on the CDC version to insure that the corrections had no adverse effects. The CDC version was then released to the public through COSMIC. Wrap up work was done on the other two versions and they were subsequently released.

8. CONCLUDING REMARKS

NASTRAN cost about \$3.5 million to develop and was first released to the public in 1970. Since that time, approximately \$3.5 million more has been spent on improving and maintaining the system. The program has grown from 150,000 lines of code in 1970 to 400,000 lines of code in 1979. Many new finite element capabilities have been added as well as changes to remain state-of-the-art with respect to advances in computer technology. Efficiency improvements have resulted in 10 x 1 speed increase in NASTRAN. Because of the maintenance effort, of the approximately 1500 errors reported, only 212 remain active and just 17 of those have a high priority. The documentation kept pace with the expanding effort of

¹Because NSMO did not have batch terminal access to the UNIVAC facility, many of the QA chores done remotely prior to a trip to the IBM facility had to be done on-site for the UNIVAC, thus requiring a full week rather than a weekend.

the program and grew from 3700 pages in 1970 to 7000 pages in 1979. The usage of NASTRAN as a tool increased significantly. In 1970, there were 50 computer sites with about 900 employees using NASTRAN. By 1979, usage had increased to 265 computer sites with 2600 users. This increase was due primarily to general capabilities of the software and the continued maintenance as a state-of-the-art finite element computer program.

9. REFERENCES

1. Weidman, Deene J.: The NASA NASTRAN Structural Analysis Computer Program - New Content. Society of Automotive Engineers Technical Paper Series, 780074, March 1978.
2. Rosser, D. C., Jr.: The Design and Use of an Error Correction Information System for NASTRAN. NASA TM X-72651, November 1974.
3. Brown, W. K.; Douglas, F. J.; McDonough, J. R.; Ziobro, D. J.: NASTRAN General Purpose Interface Requirements Document. NASA CR-3038, August 1978.
4. McCormick, C. W.; and Redner, K. H.: Study of the Modifications Needed for Effective Operations of NASTRAN on IBM Virtual Storage Computers. NASA CR-2527, April 1975.
5. The NASTRAN Theoretical Manual. NASA SP-221 (04), 1978.
6. The NASTRAN User's Manual. NASA SP-222 (04), 1978.
7. The NASTRAN Programmer's Manual. NASA SP-223 (04), 1978.
8. The NASTRAN Demonstration Problem Manual. NASA SP-224 (04), 1978.
9. NASTRAN User's Guide (Level 15). NASA CR-2054, April 1975. (Universal Analytics Inc.).
10. Rogers, James L., Jr.: Guide to a Condensed Form of NASTRAN. NASA RP-1019, September 1978.

10. APPENDIX

This appendix shows the four primary forms used in maintaining NASTRAN. The four forms are:

1. A response letter to a user who had submitted a problem.
2. A NASTRAN software problem report (SPR).
3. A NASTRAN alter form.
4. A NASTRAN documentation change report (DCR).

Each form has been filled out showing a typical example.

NASTRAN SOFTWARE PROBLEM REPORT (SPR)

Date: 8-2-78
 Originator: Harry Jones
 Organization: Hercules, INC
 Address: Box 98
Thagima, UT 84044
 Phone No.: 801-250-5511 x2815

NSMD Use	
SPR No.	<u>1486</u>
Priority	<u>5.0</u>
Date Rec'd.	<u>8/5/78</u>
Date Assigned	<u>8/5/78</u>

Materials Submitted:

() Output: Runs

() Deck

() Plots

() Letter

() Dump

() Traceback

() Fix: _____

() Program Listing

() Link Map Listing

☒ Other: phoneLevel: 17Computer: IBM (all)
 Rigid Format: 7.0 ☒ Disp ☐ Heat ☐ Aero
 or ☐ DMAP ☐ Alters

Error Message: _____

Module: CEADSubroutine(s): CEAD

Avoidance (if known): _____

Estimate correction effort (if known): _____

* I, CEAD. 126

* G0 TO 40

* C, CEAD

Description:

E: Automatic switch from HESS to INV does not
happen after issuing message 2365.

NSMD Use	
Level Fixed	<u>17.1.0</u>
Test Problem	<u>See alter form</u>
Verified by NSMD	<u>11/3/78</u>

Rev 2/5/75

Form 2.- Typical NASTRAN software problem report.

DEFAULT APPROVAL DATE: 12/31/78		
SPR NO.: 1486	DATE: 11/1/78	PAGE: 1 OF 1
LEVEL REPORTED: 17.0.0	LEVEL OF FIX: 17.1.0	<input checked="" type="checkbox"/> CDC <input type="checkbox"/> IBM <input type="checkbox"/> UNIVAC
DESCRIPTION OF SPR: Inverse Power Method does not get used automatically when insufficient core exists for Upper Hessenberg.		
MAN HOURS: 5	CODING CPU COST: (Sysgen)	QA CPU COST: --
SUBROUTINE(s): CEAD		
<p>ALTER(s):</p> <p><u>Discussion of Problem:</u></p> <p>When there is insufficient core to complete computations using the Upper Hessenberg method, the original design concept included provision to automatically switch to the Inverse Power method after issuing a warning message to that effect. This switch will be successful if the EIGC card contains sufficient information to satisfy the requirements of the Inverse Power method since the Upper Hessenberg method does not need as much information. However, since the code did not support the actual switch in methods, the Upper Hessenberg method was attempted to be used after the core test, resulting in eventual failure.</p> <p><u>Correction of Problem:</u></p> <p>Following the issuance of the warning message, control should be transferred from the area of code in subroutine CEAD from Upper Hessenberg to Inverse Power. On CDC, this transfer is provided by the following change:</p> <pre>*I,CEAD,126 GO TO 40 *C,CEAD</pre> <p>The necessary correction is obvious. In view of the cost required to generate a test case which exceeds allowable core, no test is included. The correction is noted on the attached excerpt from subroutine CEAD.</p>		
<p style="text-align: right;">JLW 11/3/78</p> <p style="text-align: right;">NSM APPROVAL</p>		

DCR No. T-1010

(To be assigned by the NCM)

NASTRAN DOCUMENTATION CHANGE REPORT (DCR)

Organization: NSMO Date: 8/11/78Originator: DEENE WEIDMAN Phone No.: 827-2551

Manual ☒ Theoretical NEW
☐ User's _____
☐ Programmer's _____
☐ Demo. Problem _____

} Page Numbers

Reason for the Change: ADD DOCUMENTATION FOR
AUTOMATED MODAL SYNTHESIS PACKAGE.

Description of Change:
 (Attach a copy of the page(s) to be changed with corrections type. Use separate pages if necessary.)

SEE ATTACHED PAGES.

Comments:

Form 4.- Typical NASTRAN documentation change report (DCR).

Table 1 - NASTRAN Capabilities
Sept. 1970 (Level 12)

Engineering Capabilities

Static Stress
Buckling
Vibration
Large Deflection
Piecewise Linear
Transient Response (2 methods)
Random Response (2 methods)
Frequency Response (2 methods)
Complex Eigensolutions (2 methods)

Other Features

General Matrix Operations
Restart Provisions
Generalized Plotting

Size

150,000 Source Statements
519 Subroutines
99 Modules
3,690 Pages of Documentation
4 Manuals

Table 3 - NASTRAN Capabilities
Aug. 1973 (Level 15.5)

Engineering Capabilities

Level 15 Capabilities +
Complete Heat Transfer
(Conduction, Convection, Radiation)
(Steady State and Transient)

Other Features

Level 15 Features +
New Matrix Methods
Single/Double Precision Options
Random Access I/O
String Data Notation
New Elements
Error Information System

Size

230,000 Source Statements
994 Subroutines
111 Modules
4,525 Pages of Documentation
5 Manuals

Table 5 - NASTRAN Capabilities
Dec. 1977 (Level 17)

Engineering Capabilities

Level 16 Capabilities +
Subsonic Aeroelasticity Extension
Supersonic Aeroelasticity
(Including Gust Response)
New FEER Eigenmethods (Real and Complex)

Other Features

Level 16 Features +
Improved Rigid Rod, Membrane, Plate,
Shell Elements
Matrix Conditioning Checks
ECIS Expansion
Efficiency Improvements
Plotting Improvements

Size

320,000 Source Statements
1,500 Subroutines
170 Modules
7,000 Pages of Documentation
7 Manuals

Table 2 - NASTRAN Capabilities
July 1972 (Level 15)

Engineering Capabilities

Level 12 Capabilities +
Hydroelastic
Acoustic
Thermal Bending
Preliminary Heat Transfer
Preliminary Substructuring

Other Features

Level 12 Features +
General Machine I/O
Computer Efficiency Improvements
I/O Between Different Machines
Dummy Element
New Elements
Matrix Packing

Size

225,000 Source Statements
943 Subroutines
111 Modules
4,092 Pages of Documentation
4 Manuals

Table 4 - NASTRAN Capabilities
March 1976 (Level 16)

Engineering Capabilities

Level 15.5 Capabilities +
Fully Stressed Design
Subsonic Aeroelasticity
Vibration with Prestress
Automated Multi-Stage Substructuring
Cyclic Symmetry
Grid Point Forces
Element Strain Energy

Other Features

Level 15.5 Features +
Congruent Elements
New Matrix Routines
Complex Modal Plots
New Elements

Size

275,000 Source Statements
1,356 Subroutines
152 Modules
6,071 Pages of Documentation
5 Manuals

Table 6 - NASTRAN Capabilities
Jan. 1979 (Level 17.5)

Engineering Capabilities

Level 17 Capabilities +
Automated Modal Synthesis
Automated Substructuring Improvement

Other Features

Level 17 Features +
General Purpose Data Generator
Efficiency Improvements
Conversion to CDC Segmentation Loader

Size

400,000 Source Statements
1,675 Subroutines
175 Modules
7,200 Pages of Documentation
7 Manuals

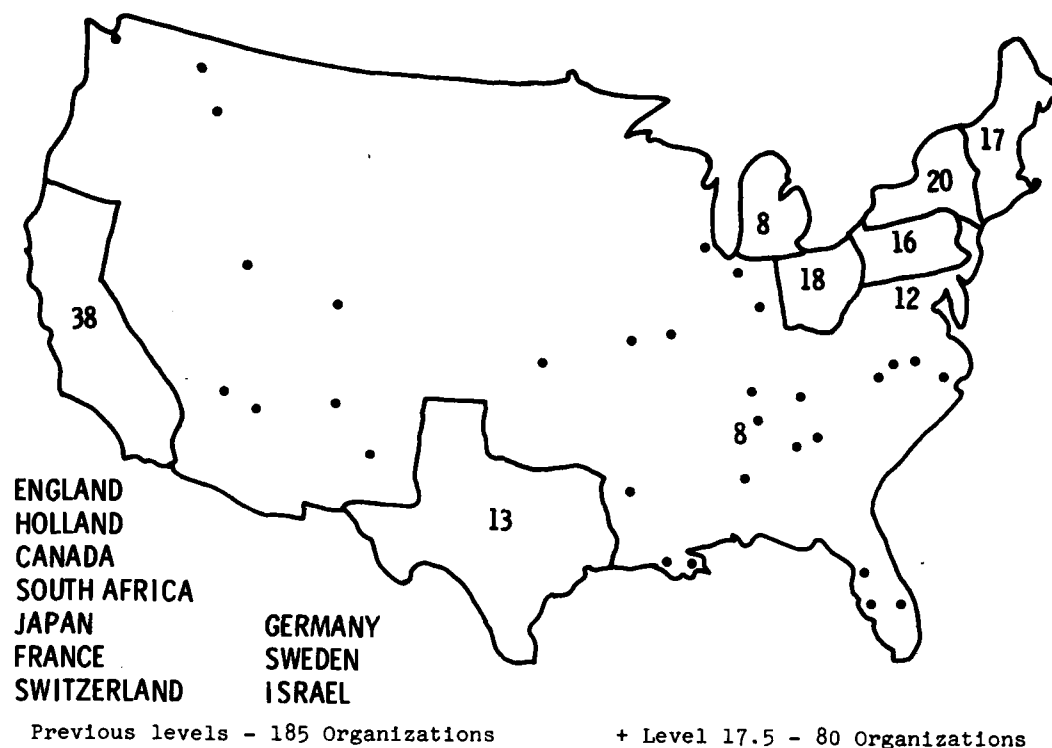


Fig. 1 Widespread usage of NASTRAN.

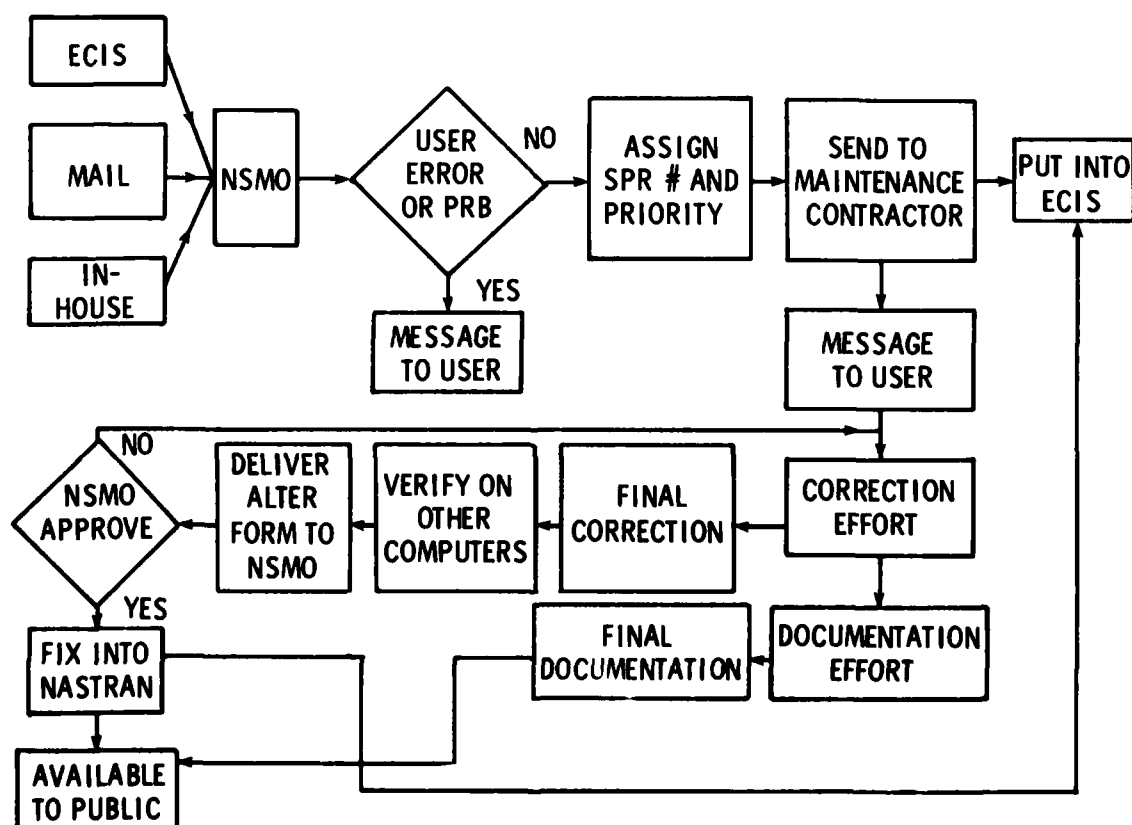


Fig. 2 Milestone program for NASTRAN error correction.

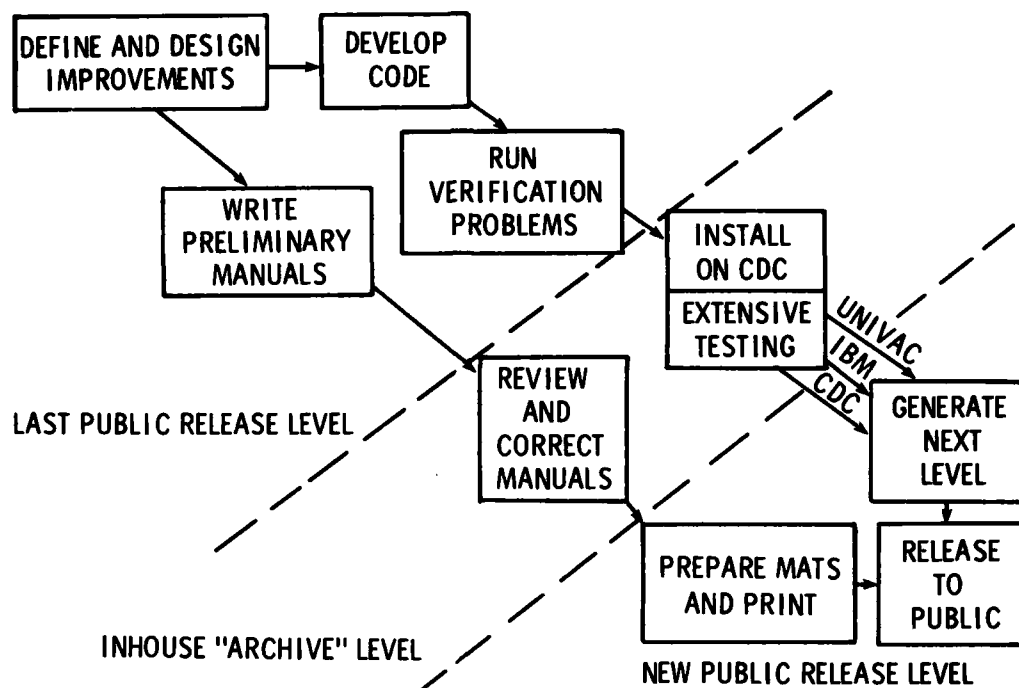


Fig. 3 Steps in adding a new capability.

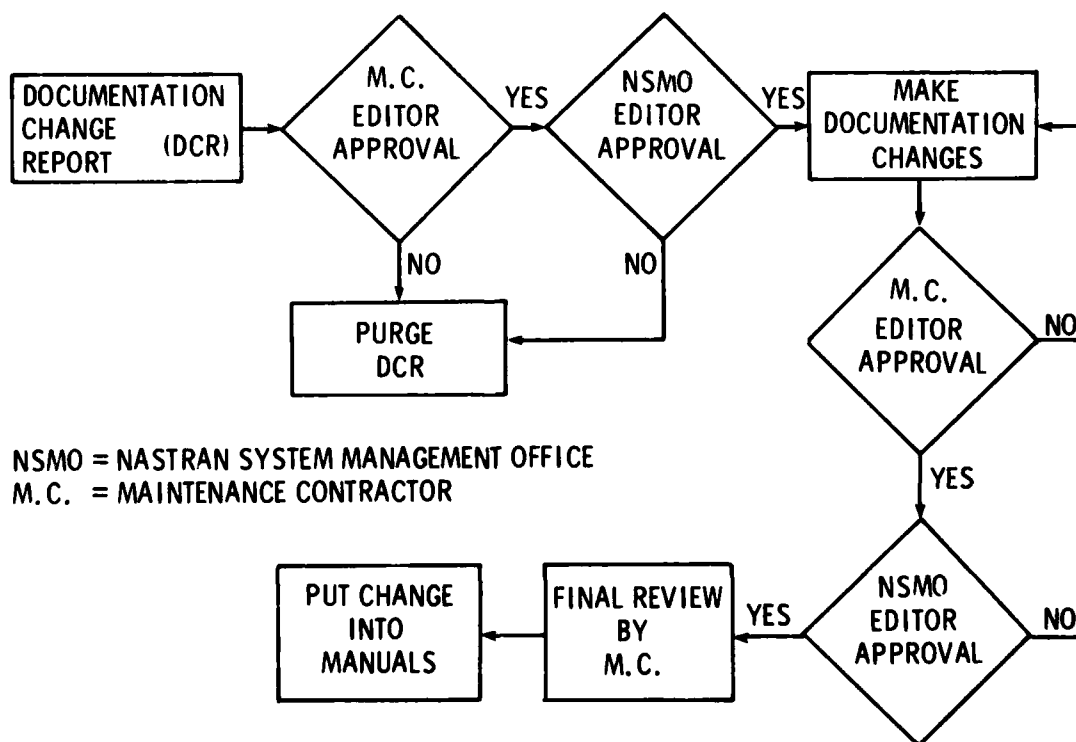


Fig. 4 NASTRAN documentation review cycle.

A COMPUTER BASED SYSTEM FOR STRUCTURAL DESIGN, ANALYSIS AND OPTIMISATION

by

A. J. Morris*
P. Bartholomew*
J. Dennis**

SUMMARY

The paper describes a new modular computer program developed by Structures Department, Royal Aircraft Establishment, for the automated design of optimum structures subject to a variety of constraints. The program employs several complex optimisation and duality techniques linked together by a control module which also provides a mechanism for interfacing the program with the commercially available structural analysis systems. Although this gives rise to a highly sophisticated program structure it is, nevertheless, made simple to operate by the aid of a convenient command language which provides the communication link with the design engineer. In addition, new modules and methods can be incorporated into the program as these become available thereby considerably easing the update problem.

1 INTRODUCTION

The theme of the Symposium is directed towards bridging the gap between the specialised research groups producing new computer based techniques and the design engineer who is familiar with the real problems but has little knowledge of computing. The present paper sets out to show how a computer program for automated structural design can be formulated to overcome many of the problems associated with handing over complex programs to the design community.

The need for an automated design or structural optimisation program has evolved from the developments which have taken place in computerised structural analysis where a range of computer programs are now available and routinely used in the design of major aircraft assemblies. Although the progress made in this area is satisfactory it does, in many ways, represent a rather limited application of the power of the computer - particularly with regard to the Class 6 or 'supercomputers'. A more effective use of this power which has great potential in rapidly creating efficient structures is to computerise the complete design cycle. This is essentially a looping operation where the analysis plays a central role supplying information which permits a redesign of the structure to meet the operational requirement. At the present time, for aircraft structures, the analysis would be performed by a large system of the NASTRAN type with the design engineer intervening to make what he believes are appropriate changes to the structure in order to achieve a satisfactory design. However, the task of selecting such changes is not easy and this is particularly true if an optimum design is to be sought. The solution lies in creating a computer program which combines analysis with some form of optimum seeking method which can make logical changes to the structure in a stepwise fashion and thereby achieve the design objective.

Theoretically, the creation of a structural optimisation or automated design program may appear relatively straightforward but practical considerations make the task complex. Over the past two decades a number of individual structural optimisation methods have been proposed and as we explain in section 2 each is effective for a different class of problem. A requirement of a comprehensive design program is that it is sufficiently flexible to accommodate a variety of these optimisation methods each of which can be easily accessed depending upon the class of problem under consideration. In a similar manner a general program should in principle also be able to interface with any of the available structural analysis packages, thereby allowing the user freedom of choice in selecting an analysis system appropriate to specific needs or computing power. The resulting algorithms achieved by blending optimisation and analysis programs together require some form of monitoring facility which is best obtained by an effective use of duality theory. This provides information for checking the performance of an optimisation method during a given computer run, indicates which constraints are active and also permits monitoring of the overall convergence of the algorithm. Clearly a computer program designed to provide all these features is being asked to control a group of interlocking individual programs which make up a flexible system able to respond to a range of problems. The architecture of such a program must be modular and, indeed, the RAE program described below has this type of structure. Modularity has the additional advantages that new techniques can be co-joined in the form of new modules when these are developed and the portability and reliability are also enhanced. In this latter context the RAE system is now available on ICL, IBM and CDC computers.

Although these concepts are important for an effective structural optimisation program perhaps the most essential feature from the practical design engineers viewpoint

* Structures Department, Royal Aircraft Establishment, Farnborough, Hampshire, UK.
** Scicon Consultancy International Ltd, Sanderson House, 49-57 Bemens Street, London W1P 4AQ, UK

is that such a powerful and flexible program should be easy to use. The procedures for loading and sequencing modules, together with the transmissions of information between modules, should be hidden from the user. Furthermore, the mathematical complexities associated with the optimisation and duality techniques must be controlled by the user without a requirement for more than a superficial understanding of the theory. For the program described herein this is achieved by the use of a control program which is manipulated by the user via a command language. This language is simple and easy to use yet provides the user with a sophisticated control of the entire modular program. It permits a selection to be made of the various optimisation and duality methods depending upon the specific design problem. The language also provides facilities for stopping and re-starting during an optimisation run and safeguards can be incorporated to recover from the computer going down before a solution has been achieved.

Having outlined the structure and nature of what is a rather complex computer program the question arises of how it might be used in practice. If the system is regarded as essentially an optimisation program then, for aeronautical structures, the designer will probably seek a minimum weight design subject to a range of behavioural constraints. The flexibility of the system permits a mixture of optimisation algorithms and the user may commence a solution run using the familiar stress-ratioing method if stress constraints are present and then ask the program to change to a more rigorous technique as the solution is approached or when non-stress constraints become important. Various convergence criteria may be applied or the program suspended en-route to a solution to allow the user to consider an interim design. An alternative approach is to regard the program more as an automated design system whose primary function is to provide the designer with a feasible solution. For example, in a specific design it may be more important to control vibrational response than to obtain a minimum weight. In such a case the program would be asked simply to create a design which satisfied the design constraints. However, by using the duality theory built into the program the designer would also be able to obtain an estimate of the optimum weight. A decision could then be made concerning the desirability of proceeding with the computer run to achieve this optimum. If further progress is necessary to re-start facilities allow for an easy resumption. Finally, if a new optimisation technique, for example employing an objective function other than weight, is required or if an alternative analysis is needed these can all be easily incorporated and the command language enlarged to accommodate such modifications.

A more detailed explanation of the RAE system is given in the remaining sections starting, in section 2, with an outline of the optimisation and duality modules currently available detailing their interface requirements. Section 3 describes the actual system or computer package and the relationship between the modules and indicates how the information flow is achieved through a common exchange file. This leads to section 4 and a description of the command language with some simple examples of its operation. More complex examples are reserved for section 5 where emphasis is placed on the packages' flexibility. The Appendices list the modules and directive cards and supplements the information given in the body of the paper.

2 BASIC OPTIMISATION MODULES

2.1 Introduction

Although certain structural design problems give rise to relatively simple optimisation problems most of the designs encountered with real structures generate highly complex optimisation problems. Here the real problem is usually too complicated for straightforward treatment and if an optimum design is required then some form of approximation, or simplification, is necessary. For example, approximate forms for the constraints may be sought or relationships between constraints can be assumed whereby they may be considered in some cases as acting independently, or on other occasions, all active together. An alternative or, indeed, additional simplification involves taking approximate forms for the objective function reducing it to linear or quadratic forms. When an optimum design is therefore sought for a specific structure then the mathematical form of the design problem dictates the level of approximation required thus selecting a specific optimisation method. However, there is no guarantee that a selected optimising procedure, appropriate at the beginning of an iteration history, will remain appropriate at the end and at some transition point it may be convenient to supplant the initially selected method by an alternative. Such a transition cannot be made on an arbitrary basis and it is our experience that an effective strategy may be developed based on information from the associated dual problem. The dual has also a part to play in some more sophisticated algorithms where the dual variables can be used for selecting, from the design constraints, those which are active at each stage of the iteration history. In addition, the dual problem has an important role in the termination of optimising algorithms by providing convergence criteria and bounds on the optimum.

We are, therefore, attempting to set up a general computer program incorporating several methods for solving the problem:

$$\begin{array}{ll} \text{minimise the structural weight} & W(x) \\ \text{subject to the constraints} & g_j(x) \leq b_j \quad j = 1, \dots, m \end{array}$$

together with monitoring routines.

The variables x_i ($i = 1, \dots, n$) are usually taken as simple design variables represented by a structural dimension such as the thickness or width of individual members

in which case $W(x) = \sum_{i=1}^n w_i x_i$ where w_i is a specific weight for a unit of the design

variable x_i . Although, in principle, no restriction need be placed on the form for $W(x)$ and several of the techniques described below can accommodate complex forms for the objective function a simple weight function is commonly used and is adopted here as the vehicle for developing the main optimisation arguments. However, based upon arguments derived from statically determinate structures, the inverse of these variables are usually employed as design variables so that the structural optimisation problem becomes

$$\left. \begin{aligned} \text{minimise} \quad W(z) &= \sum_{i=1}^n \frac{w_i}{z_i} \\ \text{subject to} \quad g_j(z) &\leq b_j \quad j = 1, \dots, m \end{aligned} \right\} \quad (2-1)$$

Our task is now to provide an effective computer based system which can solve this design problem employing the range of techniques and procedures outlined above. Since each technique has different requirements the system must be sophisticated enough to accommodate these without undue dislocation. The method used in the system described here employs a modular approach where each technique is programmed as a single module which communicates with the rest of the system through an interface. The remaining part of this section describes the optimisation and duality methods which make up these modules and outlines the information which must be supplied to each module through the interface with the rest of the system.

2.2 Optimality and simple algorithms

In order to establish the optimality conditions for the problem defined by (2-1) we need the associated Lagrangian which is given by the expression

$$L(z, \lambda) = \sum_{i=1}^n \frac{w_i}{z_i} - \sum_{j=1}^m \lambda_j (b_j - g_j(z)) \quad (2-2)$$

The Kuhn-Tucker optimality conditions are now obtained, in part, by differentiating the Lagrangian and the complete set is given by

$$\left. \begin{aligned} -\frac{w_i}{z_i^2} + \sum_{j=1}^m \lambda_j^* \frac{\partial g_j}{\partial z_i}(z^*) &= 0 \quad (i) \quad (i = 1, 2, \dots, n) \\ \lambda_j^* (b_j - g_j(z^*)) &= 0 \quad (ii) \quad (j = 1, 2, \dots, m) \\ g_j(z^*) &\leq b_j; \quad \lambda_j^* > 0 \quad (iii) \end{aligned} \right\} \quad (2-3)$$

If the problem is assumed to be convex then these conditions are necessary and sufficient for the solution vector z^* , λ^* to represent a global optimising point, otherwise they define a local optimum.

Since we can now describe the conditions which apply at the optimum it is natural to proceed and ask how these may be exploited to construct optimum seeking algorithms. We can begin by making some fairly severe assumptions about the nature of the problem which allow us to exploit parts of the Kuhn-Tucker conditions. For example, it can be assumed that each design variable z_i is associated with a specific constraint $g_j(z)$. Thus the number of constraints must equal the number of design variables, a situation which can occur when the constraints represent limits on the stress levels in the individual members of the structure being optimised. If the further assumption is imposed that all the constraints are active then (2-3(iii)) becomes

$$g_j(z^*) = b_j, \quad \lambda_j^* > 0 \quad (j = 1, 2, \dots, n)$$

and we can now look for an algorithm which ignores (2-3(i)) and simply seeks an optimum on the basis of constraint satisfaction. This leads naturally to the 'stress ratioing' method where estimates of the optimising values of the design variables z_i^* are obtained from initial values z_i by ratioing with respect to constraint limit, viz,

$$\left. \begin{aligned} z_i^* &= z_i \frac{b_i}{g_i(z)} & (i=1,2,\dots,n) \\ \text{or} \\ z_i^{(k+1)} &= z_i^{(k)} \frac{b_i}{g_i(z^{(k)})} & (i=1,2,\dots,n) \end{aligned} \right\} \quad (2-4)$$

for an iterative process. If such an algorithm forms a module within a large optimisation computer program then the basic information it requires can be obtained from the results of an analysis. Thus the main program supplying information to such an algorithm must contain an analysis capability.

Assuming that (2-3(ii)&(iii)) apply, has lead to a 'stress-ratioing' type of algorithm which has traditionally been used in the design of strength critical structures. If, however, we are interested in stiffness critical designs the number of constraints is likely to be few in number and it then becomes more appropriate to concentrate solely on the conditions (2-3(i)). At this point it is profitable to add the further assumption that only one constraint is active so that equation (2-3(i)) becomes

$$-\frac{\omega_i}{z_i^*{}^2} + \lambda^* \frac{\partial g(z^*)}{\partial z_i} = 0 \quad (i=1,2,\dots,n) \quad (2-5)$$

Taking the constraints to scale linearly in z then

$$\sum_{i=1}^n \frac{\partial g(z)}{\partial z_i} z_i = b$$

and estimated values z_i^* , λ^* which provide the solution to the optimisation problem are given by

$$z_i^* = \sqrt{\frac{b\omega_i}{\frac{\partial g(z^*)}{\partial z_i} \sum_{p=1}^n \sqrt{\omega_p \frac{\partial g(z^*)}{\partial z_p}}}}, \quad \lambda^* = \frac{1}{b} \sum_{p=1}^n \sqrt{\omega_p \frac{\partial g(z^*)}{\partial z_p}}$$

Normally the values of the constraint derivatives at the optimum are not known and thus the solution to the optimum design problem is sought through the iteration formulae:

$$z_i^{(k+1)} = \sqrt{\frac{b\omega_i}{\frac{\partial g(z^{(k)})}{\partial z_i} \sum_{p=1}^n \sqrt{\omega_p \frac{\partial g(z^{(k)})}{\partial z_p}}}}, \quad \lambda^{(k+1)} = \frac{1}{b} \sum_{p=1}^n \sqrt{\omega_p \frac{\partial g(z^{(k)})}{\partial z_p}} \quad (2-6)$$

algorithms based upon (2-6) are normally referred to as 'optimality criterion'. If more than one constraint is active then equation (2-5) does not yield the up-date formulae (2-6) and it is customary to employ some artifice such as the 'envelope method' if the simplicity of the optimality criterion approach is to be preserved. This general class of method requires that the derivatives of the constraints $\partial g/\partial z_i$ are supplied by the main program for each member of the constraint set. In order to describe how these derivatives are obtained we begin by considering a structure modelled by displacement finite elements where the stiffness matrix $\{K\}$ relates the vector of applied loads $\{P\}$ by the stiffness matrix $\{u\}$ to the vector of nodal displacements $\{K\}$, hence

$$\{P\} = \{K\}\{u\}$$

If the derivative of a specified nodal displacement u_j is required with respect to the design variable z_i , associated with the thickness of the i th element, this is given by the expression

$$\frac{\partial u_j}{\partial z_i} = \{\bar{u}_j^i\}^t \left\{ \frac{k_i}{z_i} \right\} \{u_i\} \quad (2-7)$$

The matrix $\{k_i\}$ is the stiffness matrix of the i th finite element, $\{u_i\}$ is the nodal displacements vector of this element under the application of the structural loads $\{P\}$, and $\{\bar{u}_j^i\}$ represents element nodal displacements occurring in i when a unit load acts at the point of application of and along the designated displacement u_j . Because we are dealing with displacement finite elements any other derivatives which may be required, ie stress derivatives, can be obtained from (2-7) by additional matrix algebra.

The requirement that derivatives are obtained resolves into a need for the optimisation module to supply the results of a structural analysis under the action of the applied loads and, in addition, the results of analysis under the action of unit loads applied in accordance with the type and number of active constraint. The question of how active constraints are selected is left until later.

2.3 Complex algorithms

2.3.1 A Newton-type method

Although the simple algorithms outlined above are extremely effective in certain design situations and must be included in any comprehensive structural optimisation program they are, nevertheless, limited in the type of problem they can efficiently handle and need supplementing by more sophisticated methods. An obvious procedure would be to construct an algorithm based upon satisfying all the equations (2-3) simultaneously without recourse to the rather special type of assumptions that lead to the 'envelope method' or other similar algorithms. Because the first and second derivatives of the objective function are readily available, in the case of the optimisation problem (2-1), a solution procedure based upon Newton's method can be constructed. We begin with the assumption that the objective function can be approximated by a quadratic function and the constraints by linear forms. Taking a feasible point z then the problem can be defined in terms of finding a steplength h which

$$\begin{aligned} \text{minimises} \quad & W(z+h) = W(z) + \{vW(z)\}^t \{h\} + \frac{1}{2} \{h\}^t \{H(z)\} \{h\} \\ \text{subject to the constraints} \quad & \{g(z+h)\} = \{g(z)\} + \{G\} \{h\} \leq \{b\} . \end{aligned} \quad (2-8)$$

The vector $\{vW(z)\}$ represents the first derivative of the objective function and $\{H(z)\}$ is the Hessian matrix thus

$$vW(z) = \begin{Bmatrix} -\frac{w_1}{z_1^2} \\ -\frac{w_2}{z_2^2} \\ \vdots \\ -\frac{w_n}{z_n^2} \end{Bmatrix} ; \quad H(z) = \begin{Bmatrix} \frac{2w_1}{z_1^3} & & 0 \\ & \frac{2w_2}{z_2^3} & \\ 0 & & \ddots \\ & & & \frac{2w_n}{z_n^3} \end{Bmatrix}$$

and the matrix $\{G\}$ contains the derivatives of the constraints $\partial g_j / \partial z_i$. The solution of this new sub-problem (2-8) is defined by the vectors $h^* = (h_1^*, h_2^*, \dots, h_n^*)^t$, $\lambda^* = (\lambda_1^*, \lambda_2^*, \dots, \lambda_m^*)^t$ such that,

$$\left. \begin{aligned} \{vW(z)\} + \{H(z)\} \{h^*\} - \{G(z)\}^t \{\lambda^*\} &= \{0\} , \\ \lambda_j^* \left(g_j(z) + \sum_{i=1}^n \frac{\partial g_j}{\partial z_i}(z) h_i^* - b_j \right) &= 0 , \\ \lambda_j &\geq 0 , \\ \{g(z)\} + \{G(z)\} \{h^*\} &\leq \{b\} , \end{aligned} \right\} \quad (2-9)$$

which represent the Kuhn-Tucker optimality conditions. In order to obtain a solution we can exploit the fact that the constraints can be divided into active and inactive sets. At the optimum the set of Lagrangian multipliers λ^* associated with inactive constraints are zero and can be ignored. If we exploit this fact and solve the equations (2-9) by using a Newton philosophy then

$$\begin{aligned} \{\tilde{\lambda}^*\} &= \{\{\tilde{G}(z)\} \{H(z)\}^{-1} \{G(z)\}^t\}^{-1} \{\{\tilde{b}\} - \{\tilde{G}(z)\} \{H(z)\}^{-1} \{vW(z)\}\} \\ \{h^*\} &= \{H(z)\}^{-1} \{\{\tilde{G}(z)\}^t \{\tilde{\lambda}^*\} - \{vW(z)\}\} , \end{aligned}$$

where the tilde denotes vectors and matrices associated with the active constraint set. These can now be used as the basis of an update formula and, providing that some form of active set strategy is employed, this leads to the forms

$$\left. \begin{aligned} \{\lambda^{(k+1)}\} &= \left\{ \{\tilde{G}(z^{(k)})\} \{H(z^{(k)})\}^{-1} \{\tilde{G}(z^{(k)})\}^t \right\}^{-1} \left\{ \{\tilde{b}\} - \{\tilde{g}(z^{(k)})\} \right. \\ &\quad \left. + \{\tilde{G}(z^{(k)})\} \{H(z^{(k)})\}^{-1} \{vW(z^{(k)})\} \right\} \\ \{z^{(k+1)} - z^{(k)}\} &= \{H(z^{(k)})\}^{-1} \left\{ \{\tilde{G}(z^{(k)})\}^t \{\lambda^{(k+1)}\} - \{vW(z^{(k)})\} \right\} \end{aligned} \right\} \quad (2-10)$$

It is normal in the case of the allied subject of mathematical programming to consider the estimate $\{z^{(k+1)} - z^{(k)}\}$ as a direction along which a search is made for a minimising point. However, in the case of structural optimisation this procedure would require a sequence of expensive re-analyses and is not normally performed. A module using this type of update formula would need to transmit active set information to an analysis system and would require an analysis of a structure with design variable $z^{(k)} = \{z_1^{(k)}, z_2^{(k)}, \dots, z_n^{(k)}\}$ under the action of both the actual applied loads and the unit loads necessary to generate the constraint derivative matrix $\{\tilde{G}(z^{(k)})\}$.

2.3.2 Beale's method

Linearisation is the main concept exploited in the above methods which lead to immense simplifications and results in the creation of very efficient algorithms. If, however, the objective function and/or the constraints are non-linear then some alternative philosophy must be considered. Whilst it would be possible to incorporate the approach of Miele, et al [Ref 1] into the method of (2.3.1) the package described uses the method of E.M. Beale [Ref 2]. Beale follows the Griffith and Stewart method and defines the objective function and constraints in terms of linear and non-linear design variables

$x = (x_1, x_2, \dots, x_n)^t$, $y = (y_1, y_2, \dots, y_p)^t$ such that the design problem becomes find values x^* , y^* which minimise

$$W(x, y) = \sum_{i=1}^n a_{ij} x_i + g_1(y_1, y_2, \dots, y_p)$$

subject to the constraints

$$\sum_{i=1}^n a_{ij} x_i + g_j(y_1, y_2, \dots, y_p) = b_j \quad (j = 1, \dots, m)$$

$$L_r \leq y_r \leq u_r \quad (r = 1, \dots, k)$$

$$x_i \geq 0 \quad (i = 1, \dots, n)$$

where the coefficients of x and the bounds are constant. If a generalised linear programming problem is sought by allowing new coefficients a_{ij} and b_j to be either constant or functions of the non-linear variables. Thus we seek x_0 which is minimised subject to the constraints

$$\left. \begin{aligned} x_0 + \sum_{i=1}^n a_{0i} x_i &= b_0 \\ \sum_{i=1}^n a_{ij} x_i &= b_i \end{aligned} \right\} \quad (j = 1, 2, \dots, m)$$

$$0 \leq x_i \leq B_i \quad (i = 1, \dots, n)$$

$$L_r \leq y_r \leq u_r \quad (r = 1, \dots, p)$$

A local solution to this optimisation problem can then be found by taking a local linear approximation about the current point in terms of the non-linear variables. Thus

$$a_{ij} = a_{ij}^0 + \sum_{r=1}^p \frac{\partial a_{ij}}{\partial y_r} (y_r - y_r^0) + O(\theta)$$

$$b_i = b_i^0 + \sum_{r=1}^p \frac{\partial b_i}{\partial y_r} (y_r - y_r^0) + O(\theta)$$

for the range.

$$\max(L_r, y_r^0 - \theta_r) < y_r < \min(u_r, y_r^0 + \theta_r) ,$$

where θ_r represents the tolerances on the variables y_r . Beale's method solves the resulting linear problem in terms of the variables x, y subject to the selected tolerances and bounds. This solution identifies a set of independent non-linear variables and the use of derivatives in the construction of the linearised problem are now further exploited to employ a conjugate gradient method to improve the values of the non-linear variables.

The full details of the technique are given by Beale but it is clear from the above outline that structural design problems exhibiting a large measure of linearity are well suited to this approach. The method is capable of selecting its own active constraints but does require that the main program supplies analysis and derivative information.

2.4 Duality

Associated with each minimum weight design problem there is another problem known as the dual which requires the maximisation of a dual objective function subject to dual constraints. For a large and complex optimisation/automated design system of the type described here the dual has an important role to play in monitoring the progress of the various algorithms within the package. In particular the dual can be used both to provide bounds on the optimum and to detect the failure of a specific algorithm to iterate towards the solution. The importance of the dual lies, therefore, in its capacity to provide information on the convergence of an algorithm whilst iterating to an optimum.

We begin by considering the Lagrangian form for the basic problem (2-2) and the dual problem is defined by looking for a set of Lagrangian multipliers λ^* and primal values z^* which maximise (2-2) subject to the constraints

$$\frac{w_i}{z_i^2} = \sum_{j=1}^m \lambda_j \frac{\partial g_j}{\partial z_i}(z) \quad (2-11)$$

$$\lambda_j > 0 .$$

If the problem is assumed to be convex then the optimum values for the dual objective function and the structural weight are the same. This information of itself is of limited value since the dual problem is a complex non-linear problem and is equally as difficult to solve as the original primal problem. However, we can take advantage of the fact that for convex problems the dual values obtained from any combination for λ, z which satisfies (2-11) represents a lower bound estimate of the optimum structural weight. This is done here by fixing the values of the design variables $z = (z_1, z_2, \dots, z_n)^T$ which render both the dual objective function and the dual constraints (2-11) linear. The resulting problem can then be solved by the application of a standard linear programming algorithm and the solution will provide a lower bound on the optimum value. If a bound is required at the end of iteration k (say) for one of the algorithms outlined above then, following Bartholomew [Ref 3], the linear program requiring a solution is that of finding a vector λ^* which maximises

$$V(\lambda) = \sum_{j=1}^m \lambda_j g_j(z^{(k)})$$

subject to

$$\sum_{j=1}^m \lambda_j \frac{\partial g_j(z^{(k)})}{\partial z_i} > \frac{w_i}{z_i^{(k)2}} \quad (2-12)$$

$$\lambda_j > 0 .$$

Equation (2-12) reveals that the actual value of the lower bound on the optimum structural weight is $V(\lambda^*)$ and thus for feasible values of the design variables

$$V(\lambda^*) < W(z^{(k)})$$

The optimisation package for the implementation of the above analysis in order to supply constraints and requires a robust linear

2.5 Active set strategy and algorithm selection

As we have already indicated several of the algorithms described above need some form of active set strategy whereby those constraints which at each point in the iteration history form equalities, can be identified. There are, however, two distinct phases an initial active set strategy required by the algorithm on entering the first iteration and an alternative main strategy which is employed for subsequent iterations.

The initial active set strategy uses the duality routine and solves the dual problem (2-12) with the design variables set to their initial values. The linear programming solution provides a set of Lagrangian multipliers and constraints associated with non-zero multipliers are designated as being members of the active set. The information flow for this part of the strategy is clearly the same as that of the duality module described in section 2.4.

The main active set strategy is more complex and to a limited extent the exact procedure followed is a question of taste. At the end of each iteration the violated constraints may be added to the active set whilst those associated with zero or negative Lagrangian multipliers may be deleted. However, in order to avoid zig-zagging, it is customary to use a more conservative constraint deletion policy. For example, in the case of algorithms which develop their own Lagrangian multipliers, such as the Newton method, one may delete a specific constraint at each iteration identified by the most negative multiplier. An alternative philosophy used in the RAE system performs a sensitivity analysis on the set of negative multipliers and identifies the constraint to be deleted through changes in the Lagrangian function. In both cases the information flow between the module responsible for constraint manipulation and the main system is identical to that required in the initial active set strategy. This information, in turn, is then passed onto the optimisation and analysis modules as the automated design program progresses.

The use of duality theory within the system and, particularly, the availability of the linear programming duality module provides a technique for logically changing algorithms during the course of iterating towards an optimum solution. If we consider the stress-ratioing method of (2-2) it is well known that this method converges on a non-optimal solution for those problems with free design variables at the optimum. Nevertheless, the method is very effective for strength critical designs and makes rapid, stable progress in the early phases of a computer run. The point where a transition to a more secure algorithm should be made, can be detected by examining the Lagrangian multipliers generated by the dual module. Zero multipliers can be trapped and the system instructed to employ an alternative method or to suspend and allow user intervention.

3 AUTOMATED DESIGN PACKAGE

As we indicated in section 2 the various types of algorithm, both simple and complex, have an information flow pattern associated with each of them. All require an analysis capability and most also require the availability of derivatives and several demand some form of active set strategy. When we come to assemble these in a unified system to create an effective computer package the type of program layout which results is outlined in block diagram Fig 1. Here the initial set strategy and part of the Newton algorithms of section 2.3 are illustrated and it is immediately clear that these procedures have a large measure of repeated operations. Not only is the information flow between the optimisation methods and the rest of the system similar, as indicated in section 2, but the sequence in which operations are required is similar. The optimisation or automated design process can be broken down into distinct stages which are implemented in a particular order and in these circumstances it is natural to think in terms of a modular program where each module corresponds to one of these stages. The complete automated design process is then recovered by scheduling together the modules to form the actual optimisation system.

In order to illustrate the precise manner in which the automated design package operates we consider the simple stress-ratioing algorithm shown in Fig 2 where the up-date formula and the underlying assumptions are given in section 2.2. The resulting stress-ratio algorithm has five distinct operations which form separate modules as shown in Fig 2:

- STIN - the STructural INput module reads the data defining the structure and includes the initial values of the design variables;
- CONS - the CONStraint module reads the data defining the stress constraints on the structure;
- ANAL - the ANALysis module generates the finite element model corresponding to a given set of design variables and solves it to give nodal displacements and element stresses;
- CONV - the CONVerge module which tests for convergence of the trial solution to the optimal solution. In a simple stress ratioing algorithm it performs this operation by comparing changes in the structural weight and the design variables between two iterations. These changes are compared with pre-set tolerances;
- FULL - the FULLy-stressing module changes the design variables according to the formula (2-3).

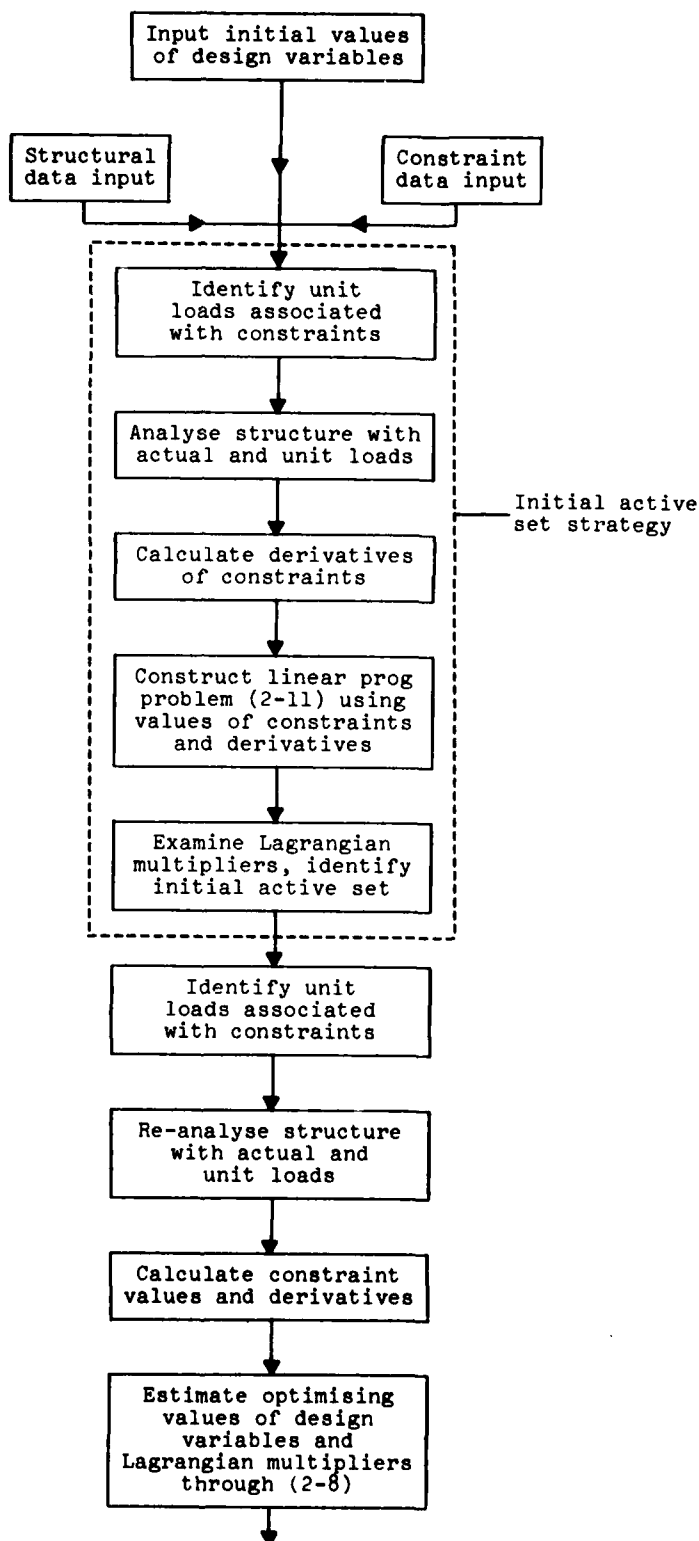


Fig 1 List of tasks

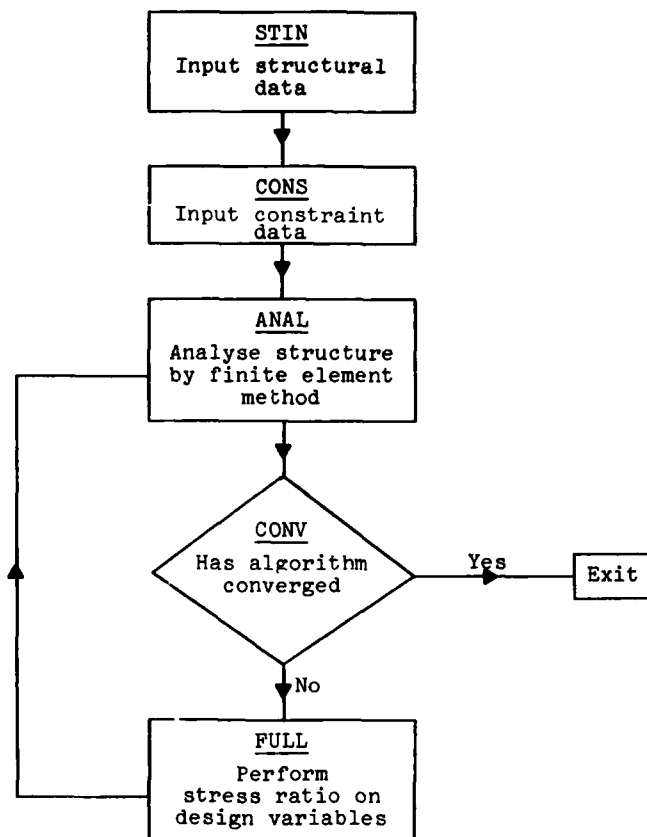


Fig 2 Stress ratioing algorithm

The last three modules are repeated until design variables changes lie within the pre-set tolerances and convergence is assumed. This cycling operation requires an interchange of information between the modules as the values of the desired variables are changed. In addition the analysis module requires repeated access to fixed information related to the configuration of the structure as originally supplied by the structural input module.

In the RAE package the modules communicate with each other by retrieving data from preceding modules and storing data for succeeding modules on a direct access data file called the *CX file*, the common exchange file. Information is stored on this file in the form of arrays and each array is referenced by using its particular eight-character key-name, an integer sub-key and, in addition, the core location and the number of data words to be transferred is specified. The actual set of arrays on the CX file will depend on the particular run and the stage that the run has reached. As each module is called in transfers are made from the CX file and an opposite flow of information takes place as the module is deleted. The scheduling of the individual modules is performed by a control program which interprets instructions given via a command language described later.

The stress-ratioing algorithm is particularly simple but the principles of the system with regard to the use of the CX file and the control program apply to the most elaborate configurations of modules. Clearly for the more complex optimisation modules the information flow between the modules and the CX file is similarly more complex. For example, the Newton based optimisation requires derivatives and an active set strategy. In this case the active set strategy identifies the active constraints and a corresponding set of unit loads are formed and stored on the CX file. These are subsequently processed by the analysis program to generate displacements needed to estimate local derivatives. In this situation the analysis module is being employed in two modes, a normal and a derivative mode. In the former mode the module creates the global stiffness matrix of the structure using a current set of design variables and computes the displacements, etc, for the set of actual specified design loads originally placed on the CX file by the structural input module. In the latter, derivative mode, the analysis module uses the established global stiffness matrix to compute the displacements for the unit loads corresponding to the active constraints. In order to distinguish between these two modes some form of switching operation is required and this is achieved through the use of control variables. These variables are also used to perform a variety of other switching activities to provide a highly flexible program structure.

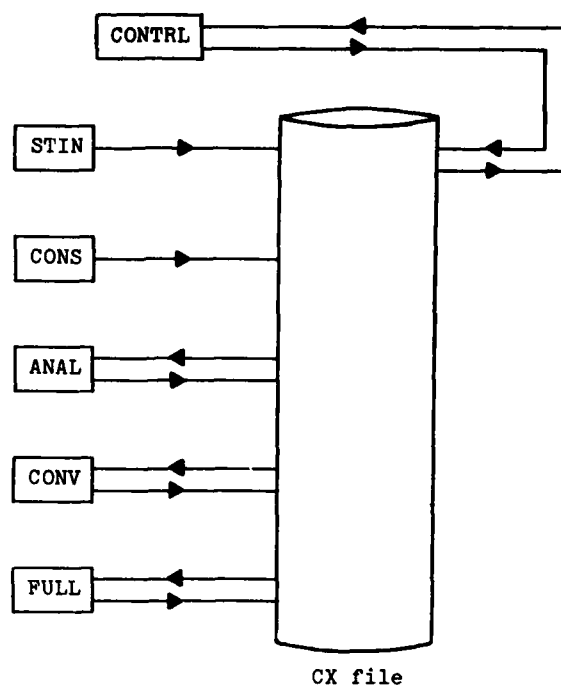


Fig 3 Schematic of modules and CX file for stress-ratioing

A large number of modules can now operate independently, communicating with each other through the CX file. Clearly an extensive range of modules can be linked through this system and the full list for the RAE package is given in Appendix A with a summary in Fig 4. These fall into several distinct categories; input/output, analysis, derivative calculation, optimisation, optimisation control, convergence and active set strategy. Because the optimisation and duality methods can be programmed as independent modules several of the methods can be used in the solution of a design problem. It might be advantageous for a problem containing both stress and displacement constraints to begin the solution process by using the stress-ratioing algorithm and changing to a more complex method at some stage during the iteration history. Such a blend incorporates the stability and robustness of the stress-ratioing method with the ability of an algorithm such as the Newton technique to actually locate the solution. The transition from one optimisation method to another can be made automatically through the intervention of one of the optimisation control and convergence modules or can be done by operator intervention.

Category of module	Input/output	Analysis	Derivative	Optimisation	Active set strategy	Optimisation control and convergence
Module name		In-house RAE	PSEU	QNEW	PNAD	CONV
	STIN	In-house BAe (FIESTA, GENDISP, GASP)	DERV	FULL	REMO	FEAS
	CONS			NLOP	SETA	ITER
	INSP			NASTRAN	OPCR	
				DRSR		SCAL
						OPCN

Fig 4 Summary of package modules

A further advantage of the inherent flexibility of the automated design package lies in the ability to change the analysis program forming the analysis module. In its original form the package uses a simple in-house analysis program developed at RAE for the solution of small-scale structural analysis problems. Subsequent development has produced interface programs to allow other analysis systems to communicate with the CX file. In particular a variety of analysis programs devised and used in the British Aerospace Industry have been interfaced with the package. A further recent development allows the use of NASTRAN as the analysis module though not all the facilities of this analysis system can, at this stage, be exploited by the optimisation modules.

4 COMMAND LANGUAGE

As we indicated in the previous section the scheduling of the modules for a particular problem is specified by the user at run time via the *command language*. The rules of the command language have been kept as straightforward as possible so that it is quick and easy to learn. The input cards specifying the optimisation scheme in terms of the command language are known as *command data cards*.

The user may reference a number of control variables within the command language which were referred to in the last section. These control variables are set by the package during a run and each variable has been given an appropriate four-character name. For example, the package sets the control variable called ENDT= YES when the changes in the trial solutions between two iterations do not exceed a suitable tolerance. A suitable command data set, therefore, for the stress-ratioing algorithm of Figs 2 and 3 is given by:

```
START
COMMAND DATA
    DO STIN;
    DO CONS;
LOO1:  DO ANAL;
        DO CONV;
        IF (ENDT.EQ.YES) GO TO LOO2;
        DO FULL;
        GO TO LOO1;
LOO2:  STOP;
        END;
```

This example clearly indicates the simplicity of the command language and ease with which it can be read, interpreted and understood. In order to enact these commands the command language first calls the *compilation module* to read and interpret the command data cards.

Although the example given above is particularly simple it does contain many of the main elements available in the command language and indicates the broad divisions into which the language falls. First of all the input consists of a directive card in this case START which indicates that a completely new problem is being initiated. However, other alternatives allow a previously saved CX file to be restarted either with the original command data set or with a new command data set of cards. This is achieved through the use of RESTORE and RESUME commands either with or without additional commands as indicated in Appendix B. With the aid of such directive cards the user can guard against the loss of expensively created information should the computer fail during a run and in this way the optimisation package mimics the procedures used in commercial finite element systems. However, it has the more important use of permitting a user the privilege of stopping the program so that intermediate results can be examined and then allowing a re-start with a new optimisation module.

The directive cards are followed by the remaining statements which constitute the complete command data set. Within the language being described a statement has the general form:

label: condition_prefix verb qualifier(s) : comment

where the dotted line denotes that the entry is optional. Thus the statements, forming the stress-ratioing example, constitute satisfactory statements as described by the above definition. In that example LOO1 is a label, DO and GOTO represent verbs, and IF (ENDT.EQ.YES) is a conditional prefix where ENDT is a control variable being tested. In addition to making the condition prefix test a logical expression containing a control variable it is also possible to use an internal flag and several of these are provided under user control. A variety of verbs such as DO, SET, SAVE, STOP, etc, are available, SAVE being especially important. Through SAVE a user can preserve the current information on the CX file together with all status data necessary for a re-start. Also there exists a procedure declaration PROC which allows a collection of statements within a command data set to be defined as a single entity. Thus a sequence of commands which are frequently

repeated in a given data set are collected together under a procedure name and then called from the main command sequence as appropriate, viz

```
START .
      .
      DO NAME;
      .
      DO NAME;
      .
      DO NAME;
      .
      PROC NAME;
      statements
      .
      END NAME;
```

The command data set is then read in, checked and compiled in the form of a table for interpretive execution. Once the program has been initiated the following information is held on the CX file:

- the compiled command data set,
- the current status of the command data set under execution,
- the current status of the control variables and flags.

The subsequent movement of information is then controlled by the user through the command data set.

Once a particular scheme has been developed, which may employ several of the optimisation modules and convergence techniques, the compiled command data may be stored as a *method* on a library file. Such a method must be given an eight-character alphanumeric name which is used to reference the method in future runs. The difference between this and the standard approach is that the control program now copies the compiled command data and the control variable variables from the library file to the CX file before starting to execute the method. In many ways, therefore, a 'method' is similar in philosophy and use to the 'rigid format' scheme used in several of the generally employed finite element analysis systems.

5 EXAMPLES

In order to illustrate how the operation of this structural optimisation package might be applied in a design situation we turn to the minimum weight of a structure subject to stress and other constraints. For large scale problems the designer would now be confronted with a large number of stress constraints and possibly a much smaller number of (say) displacement constraints. It would be clearly very time-consuming and thus expensive to immediately employ a complex optimisation method taking account of all these constraints starting from an arbitrary feasible initial design. Intuitively the design engineer would want to employ a simple method for initial sorting and traditionally one uses the stress-ratioing method on the stress constraints until either a fully-stressed design is reached or the technique becomes inappropriate due to the effect of the remaining constraints. As we indicated earlier at this point in the iteration history the designer must change to one of the more comprehensive optimisation methods in order to converge on the required optimum design.

The optimisation system described has the capability to perform this type of automated design process and can be commanded to perform this task by a suitable command data set. In essence such a set augments the rather simple example given earlier and may be conveniently described as a series of steps:

STEP 1: Input the initial design variables, structural geometry, constraints etc, and because the problem is large this should be saved,

```
DO CONS;
DO STIN;
SAVE;
```

STEP 2: A maximum number of iterations must now be set, the initial structure analysed and the print option APRT arranged to output the results,

```
SET MXIT = 10;
SET APRT = YES;
DO ANAL;
```

STEP 3: The stress ratioing part of the algorithm is now entered and the iteration counter is updated by ITER. After the stress-ratioing has been performed by the module FULL and the results examined, two completion tests are performed by the convergence module to

decide if the stress-ratioing algorithm should be abandoned. These check that the number of iterations have exceeded a set limit of five or that the rate of change of the structural weight from one iteration to the next has fallen below a pre-set limit. If the answer to either of these questions is yes the stress-ratioing algorithm is abandoned. Otherwise the answers so far are output through INSP and we continue stress-ratioing

```
L101: DO ITER;
      DO FULL, ANAL;
      DO CONV;
      IF (NOIT .GE .5) GO TO L102;
      IF (ENDT .EQ .YES) GO TO L102;
      DO INSP;
      GO TO L101
```

STEP 4: Simplicity is the reason for selecting stress-ratioing as the starting algorithm and it is clearly inappropriate to add to this the complexity of duality calculations which require expensive derivatives. However, when the simple algorithm is abandoned the argument no longer applies and we may now turn to the dual before advancing further along the solution path. This is done by recourse to the procedure OPTX, which is described later, and because the dual provides information which may cause us to abandon the run it is convenient to pause at this juncture giving time for thought - this is achieved through the SUSPEND directive. A flag FLO1 is also set to avoid an unwanted analysis:

```
L102: ON FLO1;
      DO OPTX;
      OFF FLO1;
      SUSPEND;
      SAVE;
```

STEP 5: If, after having examined the information generated, it is decided that further progress towards the optimum is required we turn to the quasi-Newton technique described in section 2. The duality information and analysis data are supplied again through OPTX and termination occurs if the duality gap is sufficiently small through ENDC or, if the number of iterations exceed 10, through ENDI.

```
LO01: DO ITER;
      DO QNEW;
      DO OPTX;
      DO INSP;
      IF (ENDC .EQ .YES) GO TO LO02;
      IF (ENDI .EQ .YES) GO TO LO03;
      SAVE;
      GO TO LO01;

LO02: DISPLAY 'CONVERGENCE SATISFIED';
      STOP;

LO03: DISPLAY 'MAXIMUM ITERATIONS EXCEEDED';
      STOP;
      END;
```

STEP 6: In the above the procedure OPTX is used on several occasions and this performs several operations:

- (i) If the flag is set a standard analysis is performed and the results printed.
- (ii) The active constraints are selected and hence the appropriate derivatives which are to be calculated indicated. The corresponding pseudo or unit loads are set up by PSEU.
- (iii) The module ANAL is used to re-analyse the pseudo-load cases by setting

$$A \log = D \text{ERV} ;$$
- (iv) The derivatives are then calculated and the module CONV used to check for convergence of the solution.

The command data cards to define this procedure are:

```

PROC OPTX;
IF (FLO1) GO TO LO10;
SET ALOG = NORM;
SET APRT = YES;
DO ANAL;

LO10: DO PNAD;
      DO PSEU;
      SET ALOG = DERV;
      SET APRT = NO;
      DO ANAL;
      DO DERV;
      DO CONV;
      END OPTX;

```

The input data cards for the control program for this optimisation scheme are given in Table 1.

Now that we have set up a suitable command set for a mixed optimisation scheme we can consider specific examples. We begin by looking at the minimum weight design of the well known 25 bar tower subject, in this case, to two load cases and constrained by stress and displacement limits and shown in Fig 5. The loads and constraints are given in Table 2. The results are shown in Fig 6 which indicates the variation of normalised structural weight W/W^* (where W^* represents the optimum weight) with iteration history. Where appropriate both primal and dual estimates to the optimum weight are given. The optimum design process starts by employing the stress-ratioing algorithm until the normalised structural weight attains 0.922 units. At this point the displacement constraints are incorporated and the associated feasible design generated in the procedure OPTX gives a primal weight estimate of $W/W^* = 1.055$. Following the instructions of the command data set the program calculates a value for the dual objective function which gives a lower bound estimate $W/W^* = 0.993$ and constitutes a sufficiently large duality gap for the SUSPEND command to be overridden by the user issuing a RESUME directive. The quasi-Newton method then comes into play and progress towards the optimum design resumes with the associated dual bound being calculated at each iteration.

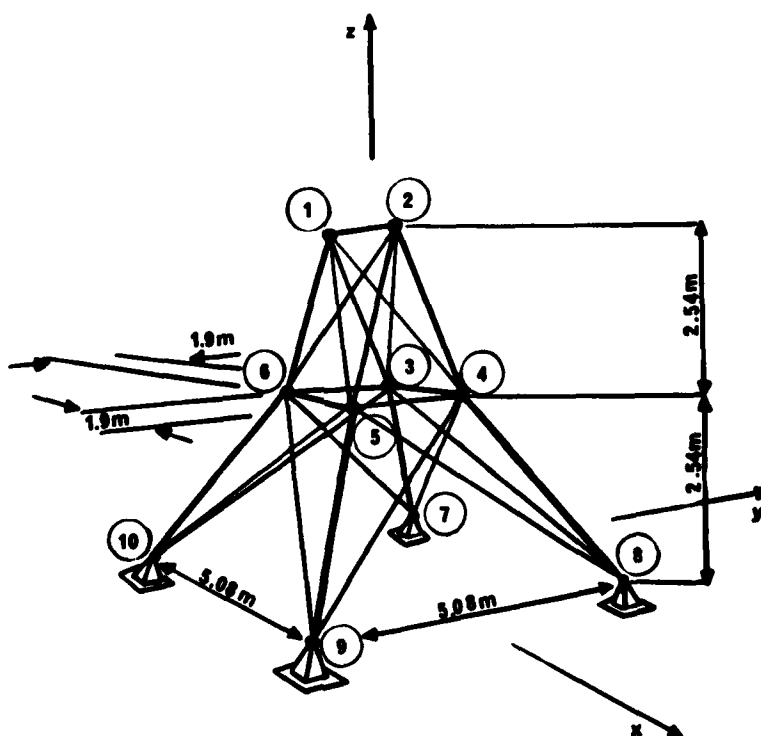


Fig 5 The 25-bar tower configuration

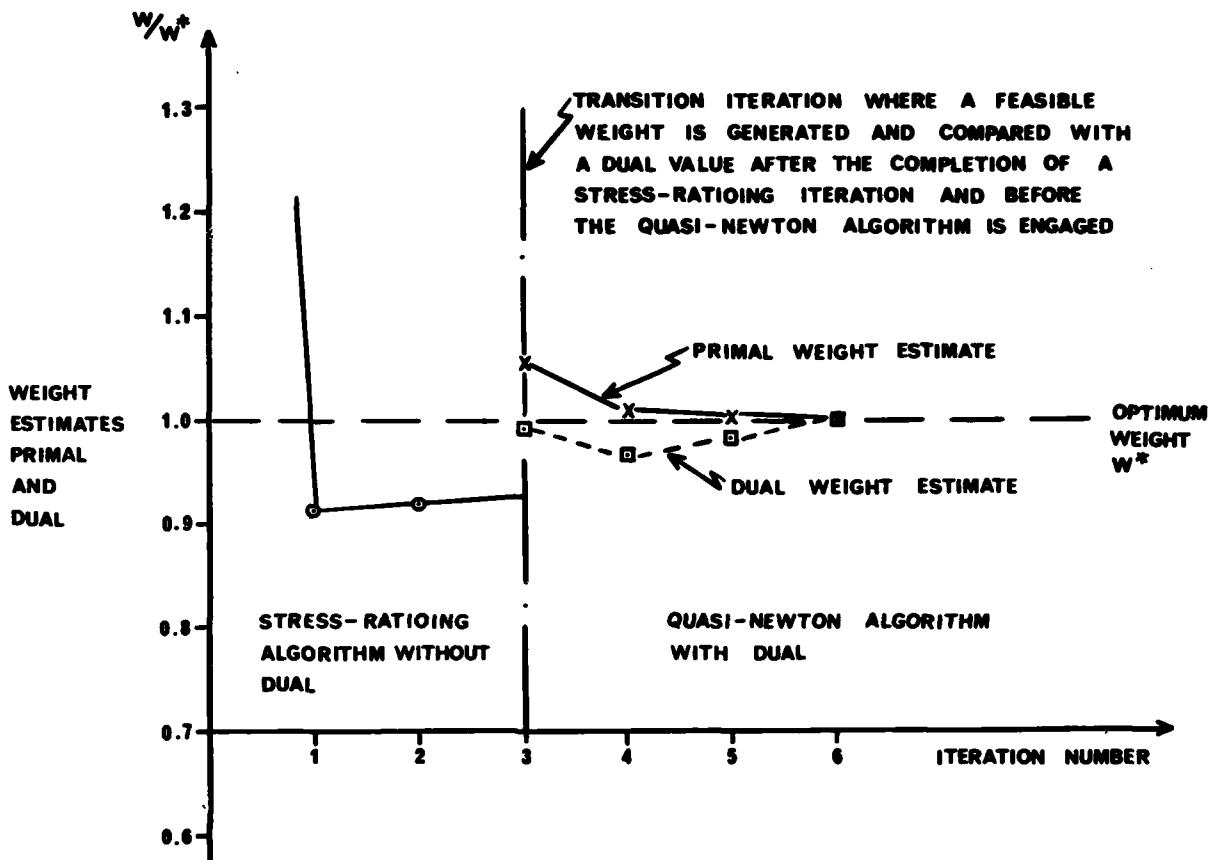


Fig 6 Iteration history for 25-bar tower using both stress-ratioing and quasi-Newton algorithms to generate an optimum design

A second example which can be used with this command data set is concerned with the design of structures subject to both stress and displacements constraint under static and dynamic loads. The structure is shown in Fig 7 and initially the bars are sized to carry the static loads of 5P horizontally and, as a separate load case, 3P vertically. After the initial sizing using the stress-ratioing method has been completed a vibrational load is applied horizontally at node 26 as shown in the figure with a forcing frequency ω chosen to lie between the second and third modes of the structures. In order to preserve the static strength achieved by the stress-ratioing method appropriate gauge constraints are involved and the complete solution to our problem achieved by using the quasi-Newton method. The forcing frequency is just less than the torsional mode and gives the largest deflections at the top of the tail which is controlled by the computer program by increasing the torsional rigidity of the structure. This is achieved by increasing both the thickness of the cross-bracing on the underside near the support and the cross-section of the outer longerons along the entire length of the tail. The primal-dual values associated with the quasi-Newton iterations are shown in Fig 8. The variation of natural frequencies before and after the optimisation process are shown in Fig 9. Other examples of this type of problem involving vibrational responses have been presented previously by Bartholomew [Ref 5].

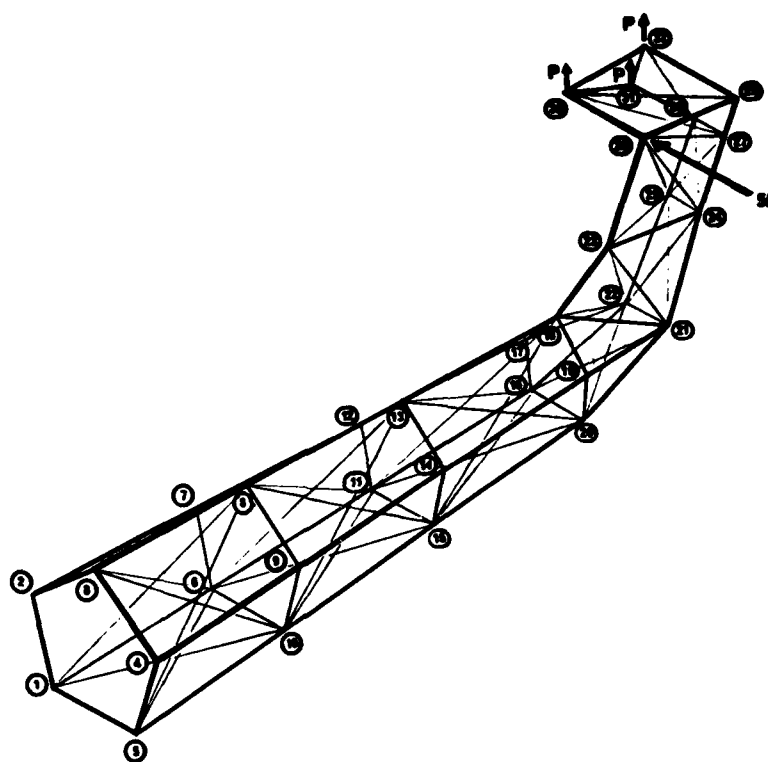


Fig 7 Tail boom (static loading)

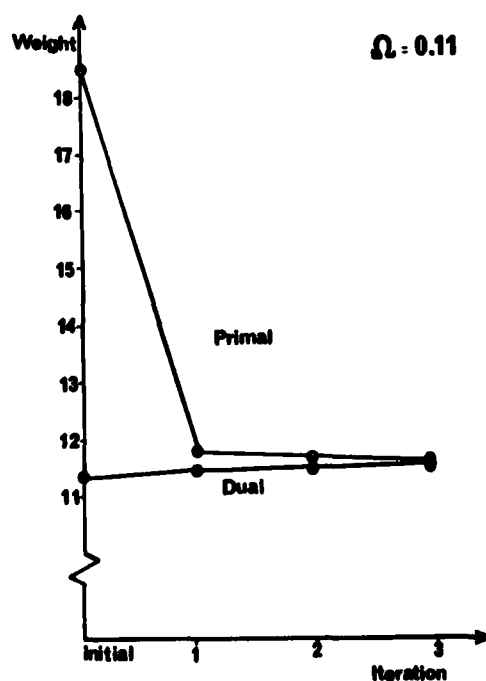


Fig 8 Iteration history for tail boom

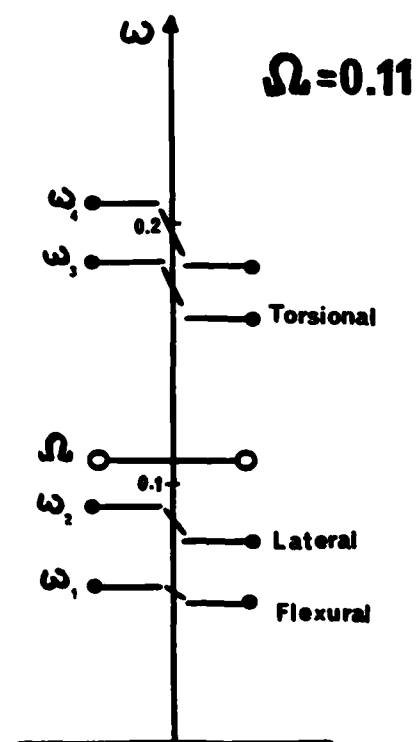


Fig 9 Normal modes of tail boom

6 CONCLUSION

The design engineer wishing to exploit the computer for automated structural design yet not wanting to become a sophisticated user can achieve this objective by using the optimisation package outlined in section 2 through 5. A flexible command language allows the exploitation of a variety of optimisation methods which can be initiated and changed at the beginning or during a specific solution. Not only are optimum designs sought by the program but a wide range of monitoring or bounding techniques are available to the user. The flexibility of the system is further advanced by the interfacing of the basic program with a selection of important structural analysis computer programs. The complete system thereby providing an extensive facility which can be regarded as a device for obtaining optimum structural designs or a convenient technique for creating satisfactory designs with complex or apparently conflicting requirements.

Acknowledgment

The authors take pleasure in acknowledging the untiring assistance of Mrs D. Bartholomew in the preparation of the computer program described here.

REFERENCES

- 1 A. Miele, H.Y. Huang, J.C. Heidemann: Sequential gradient-restoration algorithm for the minimisation of constrained functions - ordinary and conjugate gradient versions. *J. Optim. Theory Applics.*, 4, No.4, 213-243 (1969)
- 2 E.M.L. Beale, N.A. Wheble: Non-linear optimisation program. Internal RAE publication.
- 3 P. Bartholomew: A dual bound used for monitoring structural optimisation programs. *Engineering Optimisation*, Vol.4, pp.45-50 (1979)
- 4 A.J. Morris: Generalisation of dual structural optimisation problems in terms of fractional programming. *Quart of Applied Maths*, Vol.26, No.2, pp.115-119 (1978)
- 5 P. Bartholomew: Optimisation of structures subject to forced vibrations. Presented at Euromech 107, Edinburgh, September 1978

Appendix A

PACKAGE MODULES

A.1 Input modules

A.1.1 CONS - constraint input

This module reads in, prints and stores on the CX file all data on the constraints of the problem. The constraints consist of:

- (i) Lower and upper bounds on the displacements at specified nodes.
- (ii) Lower and upper bounds on the stresses in specified elements.
- (iii) Lower and upper bounds on the values of the design variables.

The program allows a sub-set of the constraints to be specified as belonging to the initial active set.

This module also reads in, prints and stores initial values for all of the design variables.

The details of the required card input formats are described in Appendix B.

The nodes must be numbered in an unbroken sequence from 1 to number of nodes. Similarly, the elements must be numbered from 1 to number of elements.

Once the user has specified a constraint on a particular node or element a statement of the form:

LIKE node/element IS/ARE $n_1 - n_2, n_3 - n_4, \dots$

may be used to specify nodes/elements which are similarly constrained.

A.1.2 STIN - structural input

This module reads in, checks, prints and stores on the CX file all the data required to define a loaded structure of bars in order to perform a structural analysis.

The input data consists of:

- (i) node co-ordinates
- (ii) element specifications
- (iii) material properties
- (iv) fixed nodes
- (v) loadings for several load cases.

An element may be associated with a material code which in turn has an associated value of cross-section, elasticity and design variable. Alternatively values of these may be specified for each element.

This module also computes and stores on the CX file element lengths and direction cosines. A warning is printed for:

- (i) any node which does not appear in an element specification;
- (ii) any node which appears in only one element, as a check on isolated elements.

Alternative input modules are employed in the case of the other analysis systems which can be used by the automated design package.

A.2 Structural analysis modules

A.2.1 ANAL - structural analysis

This analysis module may be used in either of two modes, depending on the value of the control variable ALOG:

- (i) If ALOG = NORM, the module forms the global stiffness matrix of the current structure and computes the displacements and stresses for the set of load cases specified as part of the structural input.
- (ii) If ALOG = DERV, the module uses the established global stiffness matrix and computes the displacements for a specified set of load cases. This mode is used to calculate pseudo-displacements from pseudo-loads during the calculation of derivatives.

The global stiffness matrix is symmetric large and sparse. However, by a suitable numbering of the nodes, the non-zero elements can be made to cluster around the main

diagonal. The matrix can then be stored in a compact form called symmetric banded. Since the matrix is positive definite, it can be factorised in the form:

$$K = LL^T$$

and it is, in fact, L which is stored on the CX file for use in the solution for subsequent load cases.

The calculated displacements and stresses are stored on the CX file, and are printed if control variable APRT = YES.

A.3 Optimisation control modules

A.3.1 CONV - convergence test

This module tests for convergence of the trial solution to the optimal solution as follows:

- (i) Module FEAS is called to calculate the scale factor, s, which, when applied to each design variable gives a structure that is just feasible.
- (ii) Module LPBO is called to solve the linear programming problem defined in section 2.4.
- (iii) The results from (i) and (ii) are used to estimate the primal weight, W_s , and the dual weight, W^2/F . If the difference between these estimates is less than the tolerance defined by control variable TGAP, the module sets control variable ENDC = YES.
- (iv) If the change in the primal weight is less than the tolerance specified by control variable TPWT, then the module sets control variable ENDP = YES. The change in the primal weight is defined as:

$$\frac{W_s - W'_s}{W_s}$$

where W_s is the current primal weight and W'_s is the previous primal weight.

- (v) If the change in the trial solution is less than the tolerance specified by control variable TTRI, then the module sets control variable ENDT = YES. The change in the trial solution for a particular design variable is defined as:

$$\frac{Z_a - Z'_a}{Z_a}$$

where Z_a is the current value, and Z'_a the previous value. The change in the trial solution must be less than the tolerance for all design variables, for the module to set ENDT = YES.

A.3.2 DERV - compute derivatives

This module calculates the derivatives of the constrained values with respect to changes in the design variables, eg. $\partial g_j / \partial z_i$, using the results of an analysis with the pseudo-loads set up by module PSEU.

A.3.3 DRSR - directed search optimisation

This module executes a non-linear optimisation algorithm due to Beale. The method is an approximation programming method and uses series of conjugate gradient search directions, where possible, for moving towards an optimum point.

Line searches are achieved by analysing the solutions of a series of sub-problems which approximate the true problem. Linear approximations are made to the true constraints and limits are imposed on the extent to which variables may depart from their trial values. Each sub-problem produces an optimum value of the true objective function, but with only local validity.

Variables having non-zero reduced costs in a sub-problem are defined as 'independent variables'. The objective function may be regarded as a function of these independent variables and their reduced costs are the negative components of the objective function gradient at the current trial solution. Any gradient based standard technique for unconstrained optimisation can now be used to select a suitable new trial point for the next local optimisation. The particular technique used in this implementation is the conjugate gradient method which has good theoretical convergence properties without requiring the storage of any square matrices.

Sub-problems are solved using module NLOP which must be provided with linear approximations to all constraints. Since it is expensive to calculate these coefficients before each sub-problem is solved, a trial solution is used to calculate

AD-A083 203

ADVISORY GROUP FOR AEROSPACE RESEARCH AND DEVELOPMENT--ETC F/G 9/2
THE USE OF COMPUTERS AS A DESIGN TOOL.(U)
JAN 80

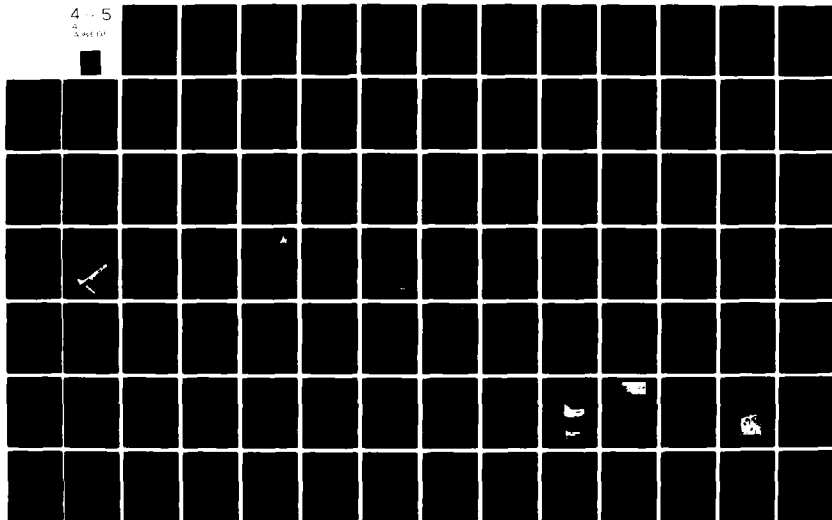
UNCLASSIFIED

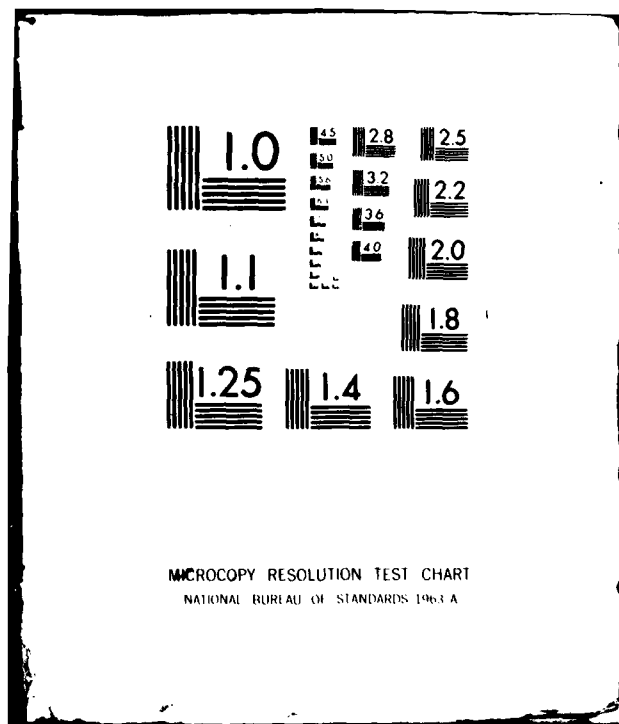
AGARD-CP-280

NL

4 - 5

2 - 10





All constraints are approximated initially, using modules PSEU, ANAL, DERV (scheduled automatically). Subsequently constraints are re-computed, either (a) when they were active in the last sub-problem or (b) when they were shown to be active after re-analysis of the structure at a new trial point.

It is necessary to set control variables initially as follows:

IDSR = YES Flag directed search method.
 IFEZ = 2 Initialise the indicator of the feasibility of the previous
 local optimisation as 'feasible'.
 ISCG = 3 Use unscaled gradients as basis for conjugate directions.

A.3.4 FEAS - compute feasible scale factor

This module calculates the scale factor which when applied to each design variable gives a structure that is just feasible. The scale factor is defined as:

$$\text{maximum} \left\{ \frac{\text{displacement value}}{\text{displacement limit}}, \frac{\text{stress value}}{\text{stress limit}} \right\}$$

for all constraints in the active set.

A.3.5 FULL - fully stressing

This module scales all the design variables to give a fully stressed structure, and writes the new design variables to the CX file.

The scale factor for design variable Z_a is:

$$\text{maximum} \left\{ \frac{\text{stress value}}{\text{stress limit}} \right\}$$

for all stress constraints on elements with associated design variable Z_a .

If the scaled value of a design variable is less than the lower limit on that design variable, the new value will be set equal to the lower limit. Similarly, if the scaled value is greater than the upper limit, the new value will be set equal to the upper limit.

A.3.6 INSP - optimisation report

This module prints an optimisation report giving the following information:

- (i) values of the design variables, Z_a ;
- (ii) actual weight;
- (iii) feasible weight (primal weight);
- (iv) dual weight;
- (v) values of the dual variables;
- (vi) details of the constraints in the active set including lower and upper bounds, current value, etc.

A.3.7 ITER - iteration count

This module increases the number of iterations by one and tests whether the number of iterations now equals the maximum number of iterations.

The number of iterations is stored in control variable NOIT and, if the maximum number of iterations has been reached, the module sets control variable ENDI = YES.

This module also prints the iteration number so that the iterations may be identified.

A.3.8 LPBO - lower bound on dual weight

This module solves the linear programming problem defined in section 2.4. The new values for the Lagrange multipliers and the value of the objective function, F , are stored on the CX file.

A.3.9 OPCN - optimisation control

This module co-ordinates several modules which together control the optimisation according to the user's specification as follows:

- (i) If the number of iterations is not equal to zero, module INSP is called to print an optimisation report.
- (ii) Module ITER is called to update the iteration count.

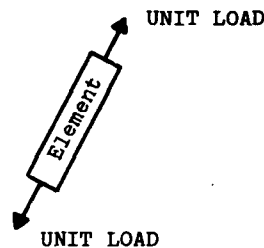
- (iii) If control variable IFSC = YES, module SCAL is called to scale the current design.
- (iv) If control variable DECI = SETA, module SETA is called to set details of the initial active set. Otherwise, if control variable DECI = PNAD, module PNAD is called to add constraints that have recently been violated to the active set.
- (v) Module PSEU is called to calculate the pseudo-loads.
- (vi) Module ANAL is called to calculate the pseudo-displacements.
- (vii) Module DERV is called to calculate the derivatives of the constrained values with respect to changes in the design variables.
- (viii) Module CONV is called to test for convergence of the trial solution to the optimal solution.

A.3.10 PSEU - computer pseudo-loads

This module sets up the pseudo-loads to be applied to the structure in order to calculate the derivatives of constrained values with respect to changes of the design variables.

For displacement constraints, a unit load is applied at the node in the X, Y or Z direction as appropriate.

For bar elements with stress constraints, a unit load is applied at each end node, in the direction away from the element, as shown below.



More complicated elements are handled in an analogous manner. However, for any fixed nodes, the components of the unit loads in the fixed directions will be reset to zero.

A.3.11 SCAL

This module uses the dual variables to compute a scale factor and then scales the current design accordingly.

The scale factor is defined as s_1/s_2 where

$$s_1 = \sum \text{dual variable} * \text{displacement or stress value}$$

$$s_2 = \sum \text{dual variable} * \text{displacement or stress limit}$$

and the summation is over all constraints in the active set.

A.4 Active set strategy modules

A.4.1 PNAD - add to active set

This module adds constraints that have recently been violated to the active set.

A.4.2 REMO - remove from active set

This module removes constraints from the active set for which the dual variable, λ_j , is less than or equal to zero.

A.4.3 SETA - initial active set

This module sets the sense of activity of the constraints in the initial active set, and so should be called after the normal analysis of the initial structure.

A.5 Local optimisation modules

A.5.1 FULL - fully stressing

This module was described as an optimisation control module in section 2.2, and it may also be used as a local optimisation module.

A.5.2 NLOP - non-linear optimisation

This module uses the non-linear optimisation algorithm due to Beale and writes the new values for the design variables and the dual variables to the CX file.

A.5.3 OPCR - optimality criterion step

This module carried out an optimality criterion step, as defined in section 2.2. The new values for the design variables are stored on the CX file. If control variable IFEV = YES, this module uses Berke's envelope method to accelerate convergence to the optimum solution. The exponential factor is set by the user in control variable ENVF.

A.5.4 QNEW - Newton step

This module carries out a Newton step as defined in section 2.3, and writes the new values for the design variables and the dual variables to the CX file. Module REMO is then called to remove constraints from the active set for which the dual variable, λ_j , is now less than or equal to zero.

Appendix B DIRECTIVE CARDS

The directive cards define the type of run, as described in the table below.

	Directive cards	Type of run
1	START COMMAND DATA	Start a problem from scratch, using the command data given on the cards that follow.
2	RESTORE	Restore the CX file, <i>ie</i> copy the CX save file to the CX file, and continue from the save point, using the existing command data.
3	RESUME	Run with the current CX file and continue from the suspend point, using the existing command data.
4	RESTORE COMMAND DATA	Restore the CX file and run using the new command data given on the cards that follow.
5	RESUME COMMAND DATA	Run with the current CX file using the new command data given on the cards that follow.
6	START METHOD xxxxxxxx	Start a problem from scratch using the method called xxxxxxxx.
7	RESTORE METHOD xxxxxxxx	Restore the CX file and run using the method called xxxxxxxx.
8	RESUME METHOD xxxxxxxx	Run with the current CX file using the method called xxxxxxxx.
9	INSERT METHOD xxxxxxxx	Insert the method called xxxxxxxx, as defined by the command data cards that follow, on the library file.
10	REPLACE METHOD	Replace the method called xxxxxxxx on the library file. The new version of this method is defined by the command data cards that follow.

Table 1
COMMAND DATA FOR STRESS-RATIOING AND QUASI-NEWTON METHODS

```

START
COMMAND DATA SET
      SET PRGX = YES;
      DO STIN;
      DO CONS;
      SAVE;
      SET MXIT = 10;
      SET APRT = YES;

L101:  DO ITER;
      DO FULL, ANAL;
      DO CONV;
      IF (ENDT. EQ. YES) GO TO L102;
      IF (NOIT. GE. 3) GO TO L102;
      DO INSP;
      GO TO L101;

L102:  ON FLO1;
      DO OPTX;
      DO INSP;
      OFF FLO1;
      SUSPEND;
      SAVE;

L001:  DO ITER;
      DO QNEW;
      DO OPTX;
      DO INSP;
      IF (ENDC. EQ. YES) GO TO L002;
      IF (ENDI. EQ. YES) GO TO L003;
      SAVE;
      GO TO L001;

L002:  DISPLAY ENDC;
      STOP;

L003:  DISPLAY ENDI;
      STOP;
      END;
      PROC OPTX;
      IF (FLO1) GO TO L010;
      SET ALOG = NORM;
      SET APRT = YES;
      DO ANAL;

L010:  DO PNAD;
      DO PSEU;
      SET ALOG = DERV;
      SET APRT = NO;
      DO ANAL;
      DO DERV;
      DO CONV;
      END OPTX;

```

Table 2
DESIGN DATA FOR 25-BAR TOWER

Load case	Node	X-load Newtons	Y-load Newtons	Z-load Newtons
1	1	4448.00	44480.00	-22240.00
	2	0.00	44480.00	-22240.00
	3	2224.00	0.00	0.00
	6	2224.00	0.00	0.00
2	1	0.00	888960.00	-22240.00
	2	0.00	888960.00	-22240.00

Young's modulus: 99.64 GN/m²
Yield stress: 275.76 MN/m²
Displacement limits: ± 5.08 cm at all nodes in all directions

STRUCTURAL OPTIMIZATION WITH STATIC AND AEROELASTIC CONSTRAINTS

D. Mathias, Structural Engineer (Analysis)
H. Röhrlé, Head of Structural Dynamics Department
J. Artmann, Head of Aeroelastics Department
Dornier GmbH
Postfach 1420
D-7990 Friedrichshafen 1
Germany

SUMMARY

This publication presents an optimization method according to which wing structures can be designed with the minimum weight. The constraints which have to be satisfied in these minimization processes require that the permissible stresses in the wing components are not exceeded. Furthermore the flutter speed must be higher than a given speed. The design variables of the structure are the cross-sectional areas or the thicknesses of the skin panels. The geometry of the calculation model remains unchanged.

This task is solved by iteration. Starting from estimated values for the cross-sections the structural design is improved from iteration step to iteration step until the optimum is obtained with the desired accuracy.

Here the DYNOPT optimization program is presented. It is based on the Finite-Element-Method and, within the actual optimization step, works according to the gradient method. The program sequence is automatic and does not require any intervention by the user.

The DYNOPT computer program was applied to a clamped straight wing. The wing is statically loaded and has eccentric masses and rotational inertias representing rudders and actuators. These eccentricities ensure the coupling between the bending and torsional deformations. The minimum weight of the structure is obtained after 15 iteration steps while all boundary conditions are observed.

1. INTRODUCTION

Regarding the selection of an optimization method for a certain task it has to be taken into account that there are two kinds of optimization methods in principle:

- a) Methods, based on optimality criteria
- b) Mathematical methods

The selection of a method from the two mentioned groups depends among others on the following aspects:

- a) Is the finally designed structure the real optimum?
- b) Rapidity and safety of the convergence
- c) Amount of the calculation costs
- d) Possibilities to extend the method to additional boundary conditions and design variables

If those methods which are based on optimality criteria are considered it can be said that it is possible that they lead not necessarily to the real optimum. In most cases, however, the result will be satisfactory. The best known optimality criterion is the fully stressed design which is applied especially for the stress design of statically and dynamically loaded structures. It is presupposed that the structural weight reaches its minimum when the stresses in the components are as close as possible to the permissible values (1).

For the fulfilment of a flutter speed restriction with respect to the weight minimum a further criterion has to be found. This means, however, that the adherence to different boundary conditions requires a sequence of different iteration processes. This may adversely affect the quality of the convergence.

The gradient method is a mathematical procedure working with a system of real boundary conditions. Furthermore, the function which shall become the minimum is directly included in the calculation. This means that the optimization problem is described in a mathematically exact way and that, in this form, the solution in each iteration step is done. The system of the boundary conditions may be composed of the most different requirements and is not restricted to one type as is the case with the optimality criteria. In this case the restriction system consists of the constraints for the stresses in the components and of the boundary condition for the flutter speed. Further boundary conditions may be added, if required, as far as they can be represented as functions of the design variables (3).

Using the gradient method the number of calculations is higher than for the determination according to an optimality criterion. The convergence is good, even if the system approaches the real optimum (4).

For the task to design a wing structure with the optimum weight while the static and aeroelastic boundary conditions are fulfilled the gradient method is suited best. It is described in detail in the following paragraphs.

2. SYSTEM OF BOUNDARY CONDITIONS AND MINIMAL FUNCTION

Boundary conditions are required for the static stresses in the finite elements and for the flutter speed. The structures to be optimized are statically loaded by forces and moments. This load is applied to the knots of the calculation model. The optimization problem which, in general, is nonlinear is partially linearized if the gradient method is used. For each improved structural design, i.e. for each iteration step, the system of the boundary conditions has to be established anew (2).

For this purpose the limited quantities are represented as a function of the design variables x . In this case these quantities are the cross-sectional areas or the thicknesses of the flanges and webs for the beam elements and the skin thicknesses for the membranes.

$$\begin{aligned}\sigma &= \sigma(x_1, x_2, \dots, x_m) \\ \tau &= \tau(x_1, x_2, \dots, x_m) \\ v_F &= v_F(x_1, x_2, \dots, x_m)\end{aligned}\quad (1)$$

whereby σ and τ are the maximum normal stresses and shear stresses in the elements and v_F is the flutter speed of the wing.

For the formulation of the minimum condition the structure weight W is expressed as a function of the design variables x .

$$W = W(x_1, x_2, \dots, x_m) \quad (2)$$

The application of the ∇ -operator to the limited quantities leads to the gradients.

$$\nabla = \begin{Bmatrix} \frac{\partial}{\partial x_1} \\ \frac{\partial}{\partial x_2} \\ \vdots \\ \frac{\partial}{\partial x_m} \end{Bmatrix} \quad (3)$$

The boundary conditions for the normal stresses, the shear stresses and the flutter speed can be represented as follows in the form of matrices:

$$\begin{aligned}\underline{\sigma}^{(v)} + ((\nabla \underline{\sigma})^{(v+1)})^t \Delta \underline{x}^{(v+1)} &\leq \underline{\sigma}_{all.} \\ \underline{\tau}^{(v)} + ((\nabla \underline{\tau})^{(v+1)})^t \Delta \underline{x}^{(v+1)} &\leq \underline{\tau}_{all.} \\ v_F^{(v)} + ((\nabla v_F)^{(v+1)})^t \Delta \underline{x}^{(v+1)} &\geq v_{Fall.}\end{aligned}\quad (4)$$

The same applies to the weight function

$$W^{(v+1)} = W^{(v)} + \Delta W^{(v+1)} = W^{(v)} + (\nabla W)^t \Delta \underline{x}^{(v+1)} \stackrel{!}{=} \text{Min.} \quad (5)$$

The index (v) stands for the respective iteration step. The quantity ΔW is the modification of the structural weight, and $\Delta \underline{x}$ is the vector with the modifications of the design variables.

The stress gradient $\nabla \underline{\sigma}$ establishes a relation between the modifications of the limited quantities and the modifications of the design variables. It is determined via the equation system of statically loaded structures and the deformation gradient. Starting from the definition equation system for statically loaded structures (according to the Deformation-Element-Method)

$$\underline{K} \underline{q} = \underline{R} \quad (6)$$

the deformation gradient is obtained by derivation of the Eq. (6) with respect to the design variables. The stiffness matrix \underline{K} and the deformation vector \underline{q} depend on the design variables, the load vector \underline{R} is constant. The deformation gradient in the form of a matrix thus reads as follows:

$$\nabla \underline{q} = - \underline{K}^{-1} \nabla \underline{K} \underline{q} \quad (7)$$

The stresses σ in the element coordinates and the deformations q in the global coordinates are connected with each other via the relation

$$\underline{\sigma} = \underline{D} \underline{T} \underline{q} \quad (8)$$

The matrix \underline{D} is obtained from the mathematical statement for the strains in the element. The conversion of the deformations q from the basic coordinate system into the element coordinate system is done by using the matrix \underline{T} . For the spring elements and the membrane elements both matrices \underline{D} and \underline{T} are independent of the design variables x . The stress gradient for these elements thus is given by:

$$\underline{\nabla \sigma} = \underline{D} \underline{T} \underline{\nabla q} \quad (9)$$

For the membrane element the reference stress is restricted according to an energy hypothesis. For the bending/torsion bars the matrix \underline{D} depends on the design variables in those lines, which contain the terms for the calculation of the shear stresses τ .

The stress gradient for these elements can thus be represented as follows:

$$\underline{\nabla \sigma} = \underline{D} \underline{T} \underline{\nabla q} + \underline{\nabla D} \underline{T} \underline{q} \quad (10)$$

The flutter speed v_F is computed according to the modified k-method. It is a reference value for the calculation of gradients. The flutter speed gradient can be found by approximation by determining the differential quotients or, in the case of additional restrictive assumptions, in a closed form.

3. THE RIGHT-HAND SIDES OF THE RESTRICTION SYSTEM

The determination of the gradient matrix is described in the paragraph 2. This matrix gives some information on the progress direction and the progress speed with which the limited quantities change between two consecutive iterations. To complete the boundary conditions it is necessary to introduce the limit values for the stresses and the flutter speed.

The limited stresses may result from compression as well as from tensional loads. Their absolute maximum values are thus to be considered as the upper and lower limits.

$$-\sigma_{all} \leq \sigma \leq \sigma_{all} \quad (11)$$

For the further computation it is necessary to consider the progress direction of the restricted quantities towards the positive or negative limit.

As shown by Eq. (4) the restrictions are inequality relations. They have to be converted into an equation system by adding further variables $\Delta \underline{x}$.

With the definition

$$\text{sign } \sigma = \begin{cases} -1 & \text{für } \sigma < 0 \\ 0 & \text{für } \sigma = 0 \\ 1 & \text{für } \sigma > 0 \end{cases} \quad (12)$$

the right-hand sides of the stress restrictions can be written as follows:

$$\Delta \underline{\sigma} = \text{sign } \underline{\sigma} \text{ abs } \underline{\sigma}_{all} - \underline{\sigma} \quad (13)$$

For the conversion of the boundary conditions into equations two cases have to be distinguished:

- a) The considered stresses are lower than the permissible stresses

In this case the considered boundary conditions with Eq. (12) and Eq. (13) can be written as follows:

$$[(\underline{\nabla \sigma})^t \mid \text{sign } (\Delta \underline{\sigma})] \begin{Bmatrix} \Delta \underline{x} \\ \Delta \underline{x} \end{Bmatrix} = \Delta \underline{\sigma} \quad (14)$$

- b) The considered stresses exceed the permissible stresses

For the respective boundary conditions with Eq. (12) and Eq. (13) the following applies:

$$[(\underline{\nabla \sigma})^t \mid \text{sign } \underline{\sigma}] \begin{Bmatrix} \Delta \underline{x} \\ \Delta \underline{x} \end{Bmatrix} = \Delta \underline{\sigma} \quad (15)$$

For the flutter speed boundary condition the following equation is valid at any case:

$$[(\underline{\nabla v_F})^t \mid 0, 0, \dots, 0, -1] \begin{Bmatrix} \Delta \underline{x} \\ \Delta \underline{x} \end{Bmatrix} = \Delta v_F \quad (16)$$

$$\text{with } \Delta v_F = v_{F_{all}} - v_F \quad (17)$$

4. THE LINEAR PROGRAMMING PROBLEM

The restriction system according to Eq. (14), Eq. (15) and Eq. (16) and the minimal function according to Eq. (5) represent a linear programming problem which has to be solved in each iteration step by means of the Simplex algorithm. In the following text the restriction system is written in the form

$$(G)^t \Delta x = r \quad (18)$$

whereby G is the gradient matrix and r is the right-hand side vector.

The modifications of the design variables shall be able to become positive as well as negative values.

$$\Delta x_{ll} \leq \Delta x \leq \Delta x_{ul} \quad (19)$$

The indices ll and ul stand for "lower limit" and "upper limit".

The conditions for the solvability of the linear programming problem are as follows:

- The number of the design variables must be higher than that of the definitive equations.
- The elements of the solution vector Δx in Eq. (18) must be greater or equal to 0.

Condition a) is always fulfilled for the present problem. It is already given by the fact that additional variables $\Delta \bar{x}$ are introduced due to the inequalities. Condition b) has to be fulfilled by a transformation since the values of the vector Δx_{ll} are generally negative.

$$0 \leq \Delta \bar{x} \leq \Delta x_{ul} - \Delta x_{ll} \quad (20)$$

The solution vector of the linear programming problem then is

$$\Delta \bar{x} = \Delta x - \Delta x_{ll} \quad (21)$$

With the converted design variables $\Delta \bar{x}$ the system of the boundary conditions can be written as follows:

$$(G)^t \Delta \bar{x} = \bar{r} \quad (22)$$

with

$$\bar{r} = r - (G)^t \Delta x_{ll} \quad (23)$$

For the minimal function this conversion is practically without importance as only one constant value of the quantity $(\nabla W)^t \Delta x_{ll}$ is added. The gradients and the sign-dependent progress direction which are decisive for the performance of the Simplex calculation are not changed by the conversion.

The boundary conditions in the transformed design variables $\Delta \bar{x}$ represent limitations for the space of the admissible solutions (see fig. 1).

This space of the solutions must be closed and convex. The objective function is an area which is shifted towards the space of the admissible solutions. The progress direction is determined by the demand for a minimum or maximum for the objective function. The solution of the linear programming problem is achieved when the objective function touches the space of the admissible solutions in one corner.

The simplex algorithm is run through once per iteration step. The results are correction values $\Delta \bar{x}$ for the design variables. According to Eq. (21) the solution vector has to be retransformed.

$$\Delta x = \Delta \bar{x} + \Delta x_{ll} \quad (24)$$

The improved design variables in the $(v+1)$ th iteration step then result in

$$x^{(v+1)} = x^{(v)} + \Delta x^{(v+1)} \quad (25)$$

The modified structural weight is obtained from Eq. (5)

$$W^{(v+1)} = W^{(v)} + \nabla W^t \Delta x^{(v+1)} \quad (26)$$

The structural design has reached its optimum when the weight curve over the iterations is horizontal and when the modifications of the design variables have become small.

In practice the calculation is stopped when the modifications of the structural weight and the design variables do not exceed a given percentage.

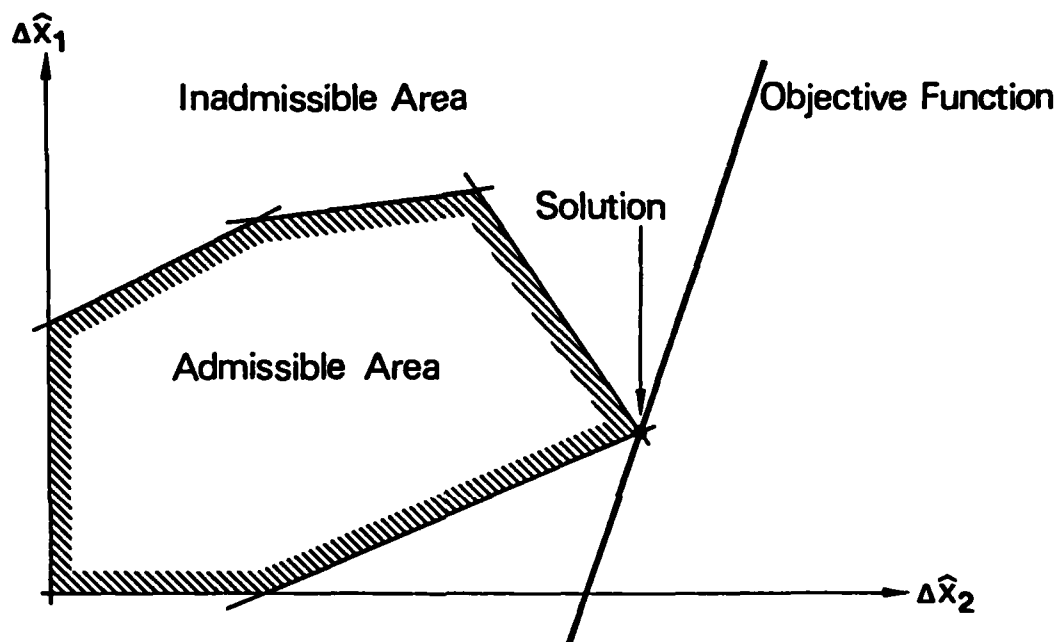


Fig. 1: Geometric Description of the Simplex Algorithm

$$\frac{\Delta x^{(v+1)}}{x^{(v)}} \leq \epsilon_x$$

is fixed as the convergence criterion for the design variables and

$$\frac{\Delta W^{(v+1)}}{W^{(v)}} \leq \epsilon_W$$

for the structural weight.

In general the structural weight heads monotonously for its minimum. The course of the design variables can be a little more unsteady. In practice a convergence limit ratio $\frac{\epsilon_x}{\epsilon_W}$ of 10 has proved to be suitable.

5. THE CALCULATION PROCESS IN THE DYNOPT PROGRAM SYSTEM

The DYNOPT computer program uses the iteration principle. Fig. 2 shows a flow diagram of the calculation process in the DYNOPT program. It is composed of two main program parts. The first part encompasses the organization, the allocation of the initial values, the data input and processing as well as the program control. The second part represents the actual optimization loop which is run through once for each new structural design. Here, the system matrices are established, the stress and flutter calculations are executed, the stress and flutter speed gradients are determined and the linear programming problem is solved. At the end of each optimization loop the convergence is checked. Should the linear programming problem turn out to be unsolvable during an iteration the restriction system is revised in an intermediate step. When the calculation is terminated a final routine prints the development of the stresses, the weight, and the flutter speed in the form of a print plot diagram.

6. APPLICATION OF THE DYNOPT PROGRAM TO A MODEL WING

The DYNOPT program system is applied to a firmly clamped wing model. The calculation model is composed of six beams with two design variables each. The number of the degrees of freedom is 18. By the application of eccentric masses the coupling of bending and torsional deformations is guaranteed. To establish the system of restriction the limits with respect to normal stresses and the shear stresses are fixed. Furthermore the flutter speed shall be greater than 300 m/sec. The calculation model of the wing is laid down in fig. 3.

The bending/torsion beams have a rectangular cross-section with thin walls, a wall thickness t , and additional stiffening elements t_s in the belts. The two wall thicknesses t and t_s are varied independently in the course of the calculation run. They are the design variables of the structure.

Fig. 4 displays the wall thicknesses t plotted against the iterations. The optimization process is terminated in the main after eight iterations. The wall thicknesses of the elements 2 and 3 approach their minimum in six and four iterations respectively, falling monotonously, while the development of the wall thickness of element 1 shows slight oscillations. All design variables are reduced within the first eight iterations to about one third of their original values.

In fig. 5 three of the limited normal stresses σ are plotted against the iteration steps. The stresses in the elements 2 and 3 reach the limit of 20 000 N/cm² after the seventh and the fourth iteration step respectively.

The stress in element 1 does not reach the limit and approaches its maximum much more slowly, too. However, the gain in weight after 15 iterations as compared with the weight obtained after the first eight iterations is insignificant.

Fig. 6 shows the shear stresses of the three elements under consideration, plotted against the iterations. All stresses are far below the given limit of 10 000 N/cm². An additional reduction of the cross-section values with the shear stresses being increased simultaneously is no longer admissible since the structure would then become too soft with respect to torsion in view of the flutter speed limit.

The lower limit of the flutter speed is 300 m/sec. As the structure was initially laid out too rigid the model wing is constantly in the flutter-safe range. There is a close connection between the torsional rigidity and the flutter safety of a structure. In the present example, the minimum flutter speed is the decisive restriction. It is reached within the first eight iterations and is then maintained (see fig. 7). Since this point is, at the same time, the lower limit for the torsional rigidity, the shear stresses, displayed in fig. 6, do no longer change.

The weight curve above the iterations is falling monotonously towards the minimum. The weight reduction within the first eight iteration steps amounts to about 45 % referred to the initial weight of the structure. The further reduction of the structural weight is unimportant as shown in fig. 8.

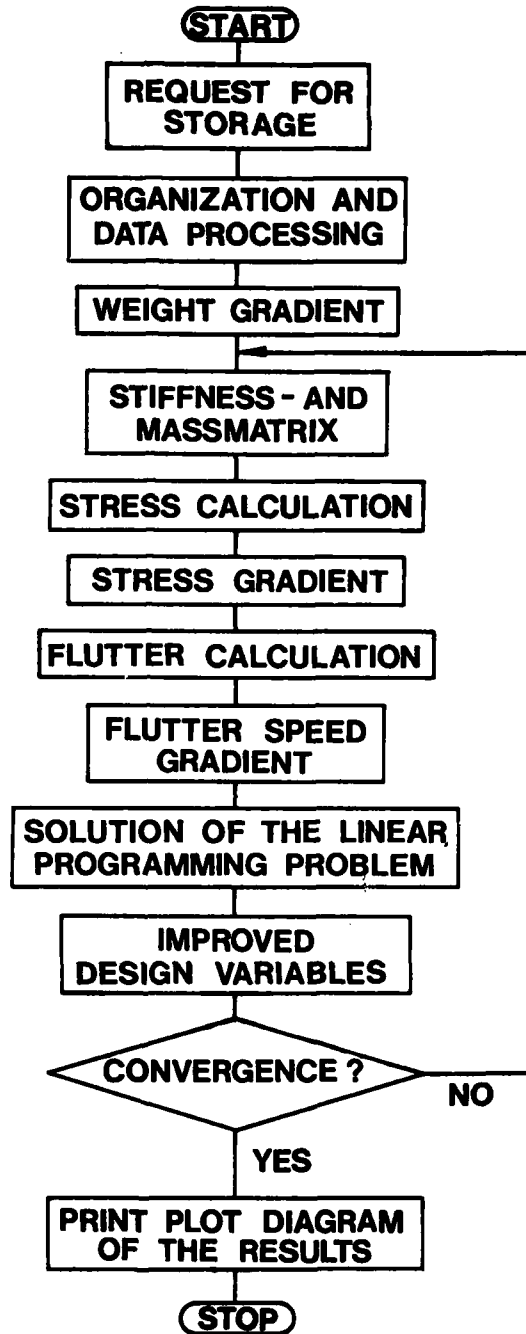
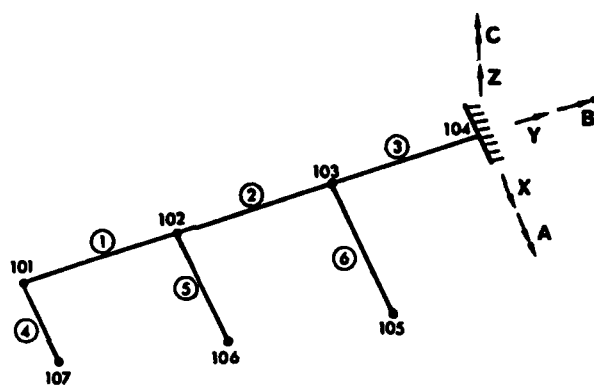


Fig. 2 : Flow Diagram of DYNOPT Calculation



Degrees of Freedom

Regular System:	101	Z	A	B
	102	Z	A	B
	103	Z	A	B
	105	Z	A	B
	106	Z	A	B
	107	Z	A	B

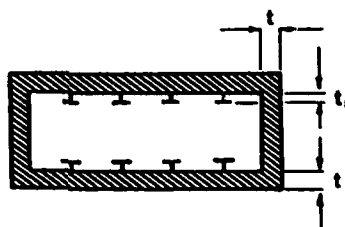


Fig. 3: 18 DOF Model of a Clamped Wing

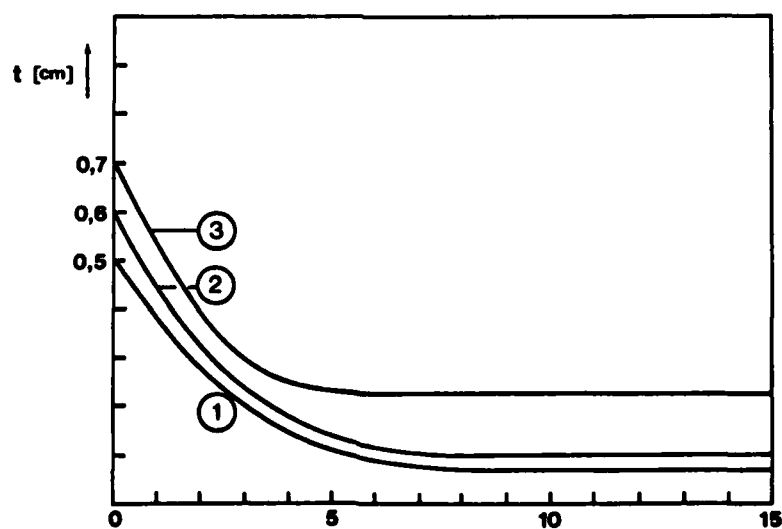


Fig. 4: Cross Sectional Areas against Iterations

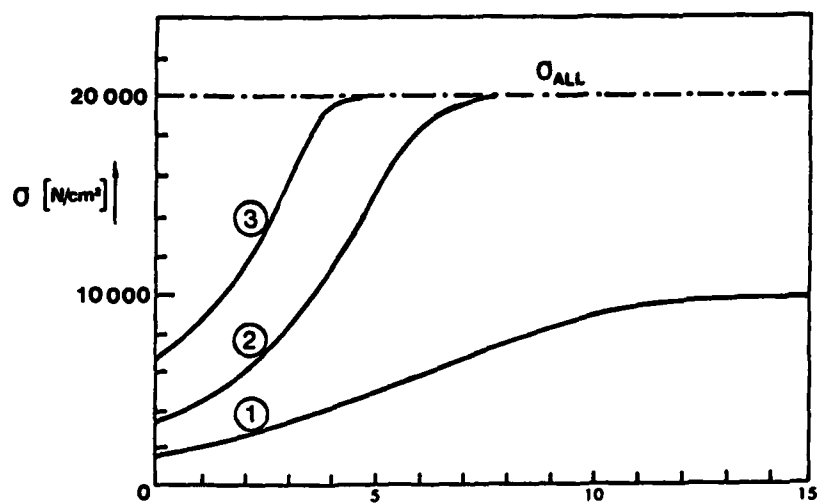


Fig.5: Normal Stresses against Iterations

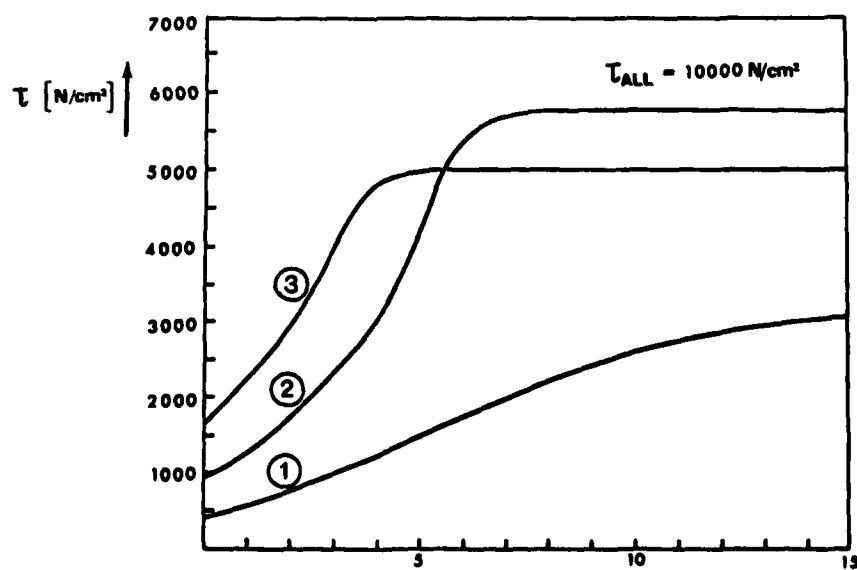


Fig.6: Shear Stresses against Iterations

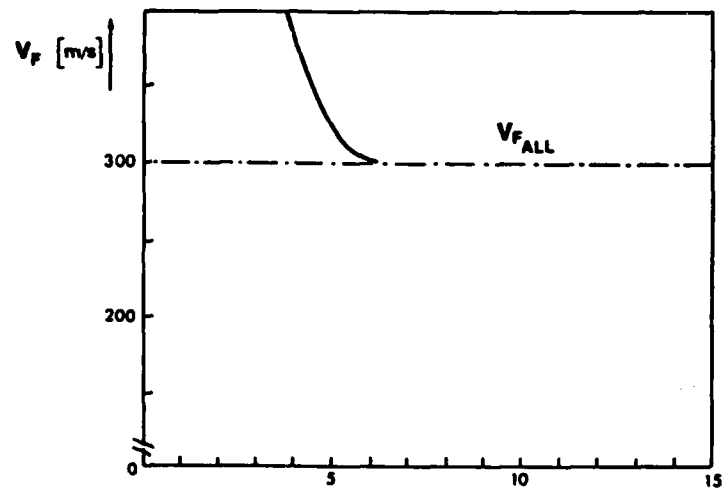


Fig.7: Flutter Speed against Iterations

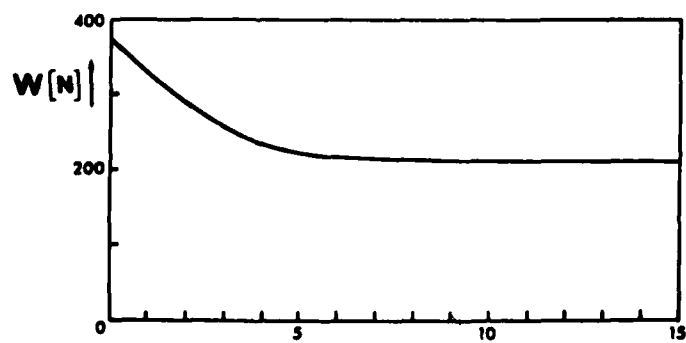


Fig.8: Structural Weight against Iterations

7. FINAL CONSIDERATIONS

A general optimization program was presented by means of which statically loaded structures can be designed optimally with respect to weight. The boundary conditions to be fulfilled are the upper limits for normal and shear stresses in the elements and for the minimum flutter speed.

The DYNOPT program system, presented here, is based on the finite-element-method. For the actual optimization part the gradient method is used. The program contains springs, beams, and membrane elements. It can, however, be extended to any other type of element. Also further restrictions can be taken into consideration. The convergence of the described method is good. Numerical difficulties will not occur.

REFERENCES

- 1 R.A. Gellatly, L. Berke
Optimal Structural Design Technical Report AFFDL-TR-70-165, February 1971
- 2 H.-P. Mlejnek, J. Bühlmeier, M.M. Mai
Untersuchung und Weiterentwicklung einiger Verfahren zur optimalen Dimensionierung von Tragwerken, ISD-Bericht Nr. 159, Stuttgart, Juli 1974
- 3 D. Mathias, K.H. Burkhardt, G. Hornung, H. Rührle
Entwicklung, Erprobung und Anwendung eines allgemeinen Rechenprogrammes zur gewichts- optimalen Auslegung von Satelliten- und Raketenstrukturen, Dornier Report 77-9-B, April 1977
- 4 D. Mathias, J. Artmann, K.H. Burkhardt, H. Rührle
Rationalisierung der Strukturdynamik: Modifikationsrechnungen und Optimierung
ZTL 1978, FAG 2, Do 2.23-3; Dornier Report 78/35 B
- 5 D. Mathias, H. Rührle
Optimal structural design of dynamically excited systems using the finite-element- method
International Council of the Aeronautical Sciences Congress, 11th, Lisbon, Portugal, September 10-16, 1978; Proceedings Volume I, pp. 582-589

APPLICATIONS OF MIXED AND DUAL METHODS IN STRUCTURAL OPTIMIZATION

by G. SANDER⁽¹⁾, C. FLEURY⁽²⁾ and M. GERADIN⁽³⁾

Aerospace Laboratory, University of Liège, Belgium
Rue du Val Benoît, 75

B - 4000 Liège

ABSTRACT

It is shown that a powerful approach to structural optimization has now emerged, which consists in replacing the initial problem with a sequence of simple explicit problems. In the optimality criteria and mathematical programming approaches, the behavior constraints are approximated using virtual load considerations and linearization with respect to the reciprocal design variables, respectively. An attractive strategy is to solve partially each explicit problem, using a primal solution scheme, before reanalyzing the structure and updating the approximate problem statement. This process facilitates generation of a sequence of steadily improved feasible designs. This approach can be interpreted as a mixed primal-linearization method and it introduces an interesting possibility of controlling the convergence of the optimization process. An alternative approach is to recognize that the explicit but approximate problem statement is of such high quality that it can be solved exactly, using a dual solution scheme. This dual method approach can be viewed as a rigorous generalization of the conventional optimality criteria techniques. Examples of applications of the mixed and dual methods to various structures include cases with stress, displacement or flexibility constraints, as well as frequency constraints.

INTRODUCTION

The optimum design of any significant structure is the result of a delicate compromise between many complex factors. Some are rational and can be quantified, such as the strength of the structure; some are just as rational but are difficult to quantify, such as the experience in a given technology; some others are much less rational, like styling, but are just as important for the final goal of the process, which is the marketing. Naturally a good designer considers structural optimization as a technique that should take into account all possible aspects of the design. Consequently the designers are often reluctant to the concepts of structural optimization developed in connection with finite element programs.

However a more detailed examination of the design process allows to isolate a phase that appears frequently, during which the shape of the structure is more or less frozen and the problem is limited to giving adequate dimensions to the various members. Such a situation is often the case in the aerospace, naval or automobile industries, where the external shapes are, to a large extent, dictated by aero-or hydrodynamic considerations, or by styling, while internal forms are often determined by various other non structural considerations. If the ultimate goal of the designer can be identified as corresponding to the minimization of an explicit function of the member sizes, and if the limitations in the design can be defined as, eventually implicit, functions of the member sizes too, such as displacements, stresses, eigenfrequencies, etc..., then the problem is tractable by automatic algorithms. They allow the engineer to speed up significantly this part of the design process and to explore more systematically the various feasible designs.

The optimization problems, which in fact should be called automatic sizing problems, are especially crucial when composite materials such as reinforced resins are employed, and when complex structural forms are involved. In both cases it becomes difficult, if not impossible, for the designer to have an intuitive understanding of the structural mechanics that is sufficient to lead to optimum sizing of the various members. Furthermore the designer is most of the time unable to take into account global constraints in the structure, like global flexibility, restriction on displacements, frequencies of vibration, global buckling modes, etc... It is only possible to verify a posteriori that such constraints are satisfied. Again these global constraints become more important in the context of highly complex, indeterminate structures made of composite materials. In the aerospace industry, the rapid extension of the use of composite materials has motivated significant research efforts to derive algorithms permitting a rapid and systematic exploration of the design space to determine the optimum material utilization.

It is worth pointing out that optimization methods should be considered as especially useful in the preliminary design phase. Using them when the design is practically frozen, with the hope of an ultimate improvement, is often disappointing. This is due to the fact that the optimization of a detailed design implies the formulation of a large number of constraints, some of which are not easily quantified. At the preliminary design stage however the constraints are usually more global and therefore more easily handled by the available formulations.

The structural optimization problem considered in this paper consists of the weight minimization of a finite element model with fixed geometry and material properties. The transverse sizes of the structural members (i.e. cross-sectional areas of bar elements; thicknesses of shear panel and membrane elements) are the design variables. For presenting

(1) Professor ; (2) Aspirant FNRS ; (3) Chercheur Qualifié FNRS

the fundamental concepts used in the formulation, we restrict the optimization problem to the mathematical form :

$$\text{minimize } W(a) = \sum_{i=1}^n l_i a_i \quad (1)$$

$$\text{subject to } h_j(a) > 0 \quad j = 1, m \quad (2)$$

$$\bar{a}_i > a_i > \underline{a}_i \quad i = 1, n \quad (3)$$

where a_i denotes the n design variables which correspond to member sizes of either a given finite element or, more often, of a given group of finite elements. In this latter case the number of design variables, n , is smaller than the number of finite elements (design variables linking). The objective function to be minimized is the structural weight. It is a linear function of the design variables a_i . In Eq.(1) l_i denotes the weight of the i th member when $a_i=1$ (i.e. specific weight times length of a bar truss member ; specific weight times area of a membrane element).

The inequalities expressed in Eq.(2) represent behavior constraints, which impose limitations on quantities describing the structural response, for example : the stresses and the displacements under multiple static loading cases, the natural frequencies, the buckling loads, etc... The design variables are also subjected to the side constraints (3), where \underline{a}_i and \bar{a}_i are lower and upper limits that reflect fabrication and analysis validity considerations.

The structural optimization problem embodied in Eqs(1) through (3) is a nonlinear mathematical programming problem to which standard minimization techniques can be applied. However this problem exhibits some characteristics that make it complicated when practical structural design applications are considered. The main difficulty arises from the fact that the behavior constraints (2) are in general implicit functions of the design variables and their precise numerical evaluation for a particular design requires a complete finite element analysis. Since the solution scheme is essentially iterative, it involves a large number of structural reanalyses. Therefore the computational cost often becomes prohibitive when large structural systems are dealt with.

The well known necessary KUHN-TUCKER conditions characterize any local minimum of the nonlinear programming problem (1-3) [1]. They are written as follows for each design variable :

$$\frac{\partial W}{\partial a_i} - \sum_{j=1}^m r_j \frac{\partial h_j}{\partial a_i} - v_i + t_i = 0 \quad i = 1, n \quad (4)$$

with the complementarity conditions :

$$r_j h_j = 0 \quad r_j > 0 \quad j = 1, m \quad (5)$$

$$v_i (a_i - \underline{a}_i) = 0 \quad v_i > 0 \quad i = 1, n \quad (6)$$

$$t_i (\bar{a}_i - a_i) = 0 \quad t_i > 0 \quad i = 1, n \quad (7)$$

The quantities $(r_j, j = 1, m)$, associated with the behavioral constraints (2), and $(v_i, t_i, i = 1, n)$, associated with the side constraints (3), are called dual variables as opposed to the primal variables, which are the a_i . They have the meaning of lagrangian multipliers conjugated to the constraints. Depending upon whether a given constraint becomes an equality or not at the optimum (i.e. is active or inactive), the corresponding dual variable is positive or equal to zero (see Eqs. 5-7). The KUHN-TUCKER conditions are in general only necessary. In the special case of a convex problem, they become also sufficient and characterize a global optimum. They can then be used to relate the primal variables - i.e. design variables a_i - to the dual variables - i.e. lagrangian multipliers r_j -.

In the last decade essentially two main approaches have been used to solve the problem (1-3). One is based on the many rigorous numerical methods of non linear mathematical programming. The other uses the more intuitive concepts of optimality criteria. These approaches have often been opposed in the past and two corresponding schools developed. The advantages claimed for the mathematical programming methods are their sound foundations, their convergence properties which can most often be guaranteed and their generality which permits consideration of any type of constraints. Their essential disadvantage lies in the computing time which increases rapidly with the size of the problem, leading to unacceptable cost even for relatively simple problems.

The optimality criteria are based on explicit approximations of the behavior constraints which are exact in special cases, most of the time in statically determinate cases. These approximations are supposed, on intuitive basis, to hold in the general case. Then the statement of the problem (1-3) often disappears since redesign formulas can be derived by various means, like, for instance, the KUHN-TUCKER conditions (4-7) in which the explicit approximations are introduced. The advantages of using the optimality criteria are the computing cost which is low and the intuitive basis, which is often appealing to the engineer. In fact the number of reanalysis cycles does not increase with the complexity of the structure, nor with the number of design variables. As a consequence of this property, until recently, large scale examples of structural optimization have only been solved by optimality criteria. The essential disadvantages of the optimality criteria approach are its lack generality and of sound mathematical foundations, which explains the often unpredictable convergence properties and even the convergence to non

optimal solutions.

It has been shown in a recent work [2,3,4] that these two approaches are in fact related to each other and that the optimality criteria can be viewed as special mathematical programming methods using approximations for the constraint surfaces.

THE LINEARIZED PROBLEM

Most of the optimality criteria approaches deal with problems involving constraints on static stresses and displacements, in which case the behavior constraints (2) can be written

$$h_j(a) \equiv \bar{u}_j - u_j(a) > 0 \quad (8)$$

where \bar{u}_j denotes an upper bound to a response quantity $u_j(a)$ (stress, nodal displacement, relative displacement, etc...). Using virtual load consideration, explicit approximations of the behavior constraints (2) can be generated:

$$\tilde{h}_j(a) \equiv \bar{u}_j - \sum_{i=1}^n \frac{c_{ij}}{a_i} > 0 \quad (9)$$

where the coefficients c_{ij} are related to virtual energy densities in the structural members [5,6]. At each stage in the optimization process, the c_{ij} 's are assumed to be constant coefficients, which leads to using simple redesign formulas. After new values have been obtained for the design variables, a structural reanalysis is performed and the c_{ij} 's are updated. The whole process is repeated until convergence is achieved.

It is essential to note that in the case of a statically determinate structure, the c_{ij} 's are really constant quantities and Eq.(9) represents the exact explicit form of the behavior constraints (8). Therefore, in this case only one structural analysis is sufficient for generating the optimal design. In the case of a statically indeterminate structure the c_{ij} 's depend implicitly on the design variables, since structural redundancy leads to redistribution of the internal forces when the member sizes are modified.

On the other hand the mathematical programming approach, after a period of inefficiency, has finally evolved into a powerful and now well established design procedure based on explicit approximations of the constraints. This approach was developed independently by SCHMIT [7,8,9,10] as the "approximation concepts approach" and by FLEURY [11, 12,13] as the "mixed method". Both methods proceed by constructing a high quality explicit approximation of the initial problem and solving it partially, using a primal mathematical programming algorithm, before reanalyzing the structure and updating the approximate problem statement. This process facilitates generation of a sequence of steadily improved feasible designs, which is an attractive feature for practical design purposes.

The key idea in both the approximation concepts approach [7-10] and mixed method [11-13] is to linearize the behavior constraints with respect to the reciprocal design variables

$$x_i = \frac{1}{a_i} \quad (10)$$

In the reciprocal design space, the constraint surfaces are very shallow and close to planes in a moderately hyperstatic case. It is then possible, in a method of projected gradient, to progress with much larger steps along tangent planes without seriously violating the constraints. Moreover the shallowness of the constraint surfaces implies that their linearized forms are usually very good approximations and therefore the structure does not need to be reanalyzed after each iteration in a mathematical programming algorithm. The linearized behavior constraints are obtained using a first order Taylor series expansion in terms of the reciprocal variables x_i :

$$\tilde{h}_j(x) \equiv \bar{u}_j - [u_j^0 + \sum_{i=1}^n \left(\frac{\partial u_j}{\partial x_i}\right)^0 (x_i - x_i^0)] > 0 \quad (11)$$

where the superscript 0 denotes quantities evaluated at the actual design point x^0 , where the structural reanalysis is performed. Note that the finite element analysis must include auxiliary sensitivity analyses, which evaluate first partial derivatives of the response quantities. Most often the well known pseudo-loads technique is employed [14]. This procedure requires that a certain number of additional loading cases be treated in the structural analysis phase.

Now it can be shown (see Refs. [3,4]) that the explicit approximations of the behavior constraints used in both the optimality criteria and mathematical programming approaches (Eqs 9 and 11, respectively) are identical. Indeed the virtual energy densities c_{ij} , employed in the optimality criteria approaches are nothing else than the gradients of the response quantities with respect to the reciprocal variables:

$$c_{ij} \equiv \frac{\partial u_j}{\partial x_i} \quad (12)$$

Furthermore the definition of the c_{ij} 's following from the virtual load technique clearly indicates that

$$u_j^0 \equiv \sum_{i=1}^n c_{ij}^0 x_i^0 \quad (13)$$

Therefore Eq.(11) can be written

$$\tilde{h}_j(x) \equiv \bar{u}_j - \sum_{i=1}^n c_{ij}^0 x_i > 0 \quad (14)$$

which is equivalent to Eq(9).

In conclusion a unified structural optimization approach has emerged, which consists in replacing the initial problem (1-3) with a sequence of explicit approximate - or linearized - problems. Each linearized problem exhibits the following form when written in terms of the reciprocal variables :

$$\text{minimize } W = \sum_{i=1}^n \frac{L_i}{x_i} \quad (15)$$

$$\text{subject to } \bar{u}_j - \sum_{i=1}^n c_{ij} x_i > 0 \quad j = 1, m \quad (16)$$

$$\underline{x}_i < x_i < \bar{x}_i \quad i = 1, n \quad (17)$$

where $\underline{x}_i = 1/\bar{a}_i$ and $\bar{x}_i = 1/a_i$ are the new side constraints. Various solution schemes are available to treat the explicit problem embodied in Eqs(15-17). Depending upon their primal or dual character the convergence properties of the whole optimization process will be different.

PRIMAL SOLUTION SCHEME (MIXED METHOD)

The linearized problem (15-17) is still a non-linear programming problem (because the objective function keeps its nonlinear character), however it is now explicit and easily treated by standard minimization techniques. In order to maintain a primal philosophy (sequence of steadily improved feasible designs), the approximation concepts approach, as initially proposed in Ref [9], employed either a feasible direction method or an interior penalty function method to solve partially the linearized problem. In this way it is possible to preserve, at each stage of the process, the feasibility of the design point with respect to the primary problem (1-3). Later the interior penalty function method (called NEWSUMT) only was retained [10,15]. So the NEWSUMT optimizer of the ACCESS 3 program [15,16] tends to generate a sequence of design points that "funnels down the middle" of the feasible region. This represents an attractive feature from an engineering point of view since it provides the designer with acceptable non critical designs at each stage of the process. Furthermore the convergence properties of the method can be controlled by modifying the number of response surfaces (typically 1 or 2) and the response factor decrease ratio (typically 0.5 through 0.1).

On the other hand, starting from an optimality criteria approach, a method similar to the approximation concepts approach was independently developed in Refs.[11,13]. This mixed method uses virtual load considerations to generate a first order approximate problem which is identical to the linearized problem posed by Eq.(15-17). This problem is also solved partially using a primal solution scheme, with the aim of preserving the design feasibility as in the approximation concepts approach. Each iteration in the mixed method is made up of a restitution phase and a minimization phase.

The restitution phase consists in bringing the design point back to the boundary of the feasible region. It is based upon the concept of scaling, which is classical in the optimality criteria approaches. Scaling does not introduce any redistribution of the internal forces in the structure and therefore it permits generation of a feasible boundary point without any additional structural analysis. In the design space scaling corresponds to a move along a straight line joining the origin to the current design point, where the structural analysis is made (see Fig. 1).

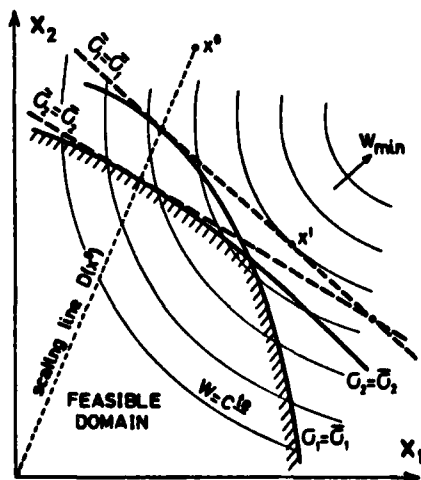


Fig. 1 LINEARIZED PROBLEM

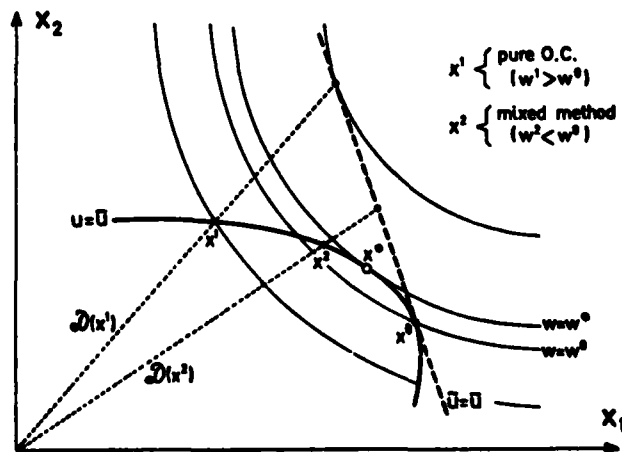


Fig. 2 MIXED METHOD

Along the scaling line the coefficients c_{ij} (see Eq.9) remain constant and the explicit approximations lead to the exact values of the constraints and their gradients [13]. As a result the linearized problem statement is not affected by scaling. Geometrically each real restraint surface is approximated, in the space of the reciprocal variables, by its tangent plane at its point of intersection with the scaling line (see Fig.1).

Starting from a feasible boundary point, the minimization phase in the mixed method consists in reducing the objective function in the subspace defined by the tangent planes to the constraint surfaces. This is achieved by solving the linearized problem (15-17) using a projection algorithm, but stopping the minimization after a limited number of steps, denoted k , before reaching the minimum of the linearized problem. After k one dimensional minimizations have been accomplished, the structure is reanalyzed, scaling is performed, the linearized problem is reformed and again solved partially.

That optimization process is illustrated on Fig.2 in a hypothetical 2-dimensional space. When k is limited to one step, the method is a strict application of a gradient projection type of algorithm to the original problem (1-3). The method then exhibits all the properties of the primal mathematical programming approaches, that is high cost but guaranteed convergence. When k is not limited, the linearized problem is solved completely before reanalyzing the structure and updating the linearized problem statement. The method then becomes an optimality criteria approach (see next section). The corresponding properties of fast but uncertain convergence are to be expected. Finally, when k is limited to a given finite number, the method is mixed. This leads to considering the number of steps k as a convergence control parameter that should be assigned high values for economy and reduced when divergence occurs. As implemented in the SAMCEF program [19,20], the minimization algorithms used in the mixed method are based either on the conjugate gradient method with an orthogonal projection operator or on the generalized Newton's method with a weighed projection operator. This latter method has also been introduced in the ACCESS 3 program [15,16].

From a mathematical programming point of view, the approximation concepts approach and the mixed method can be classified as mixed primal-linearization methods. The initial problem is transformed into a sequence of linearized problems, which is classical in the linearization methods of mathematical programming. However each subproblem is solved only partially using a primal solution scheme that insures feasibility of the intermediate designs at each stage.

DUAL SOLUTION SCHEME (GENERALIZED OPTIMALITY CRITERION)

In the previous section a primal philosophy has been adopted that leads to partial solution of the linearized problem (15-17) using an interior penalty function formulation with a small number of response surfaces or a projection algorithm with a small number of one dimensional minimizations. This primal solution scheme produces a sequence of feasible designs with decreasing values of the objective function. An alternative viewpoint is to recognize that the approximation made by linearizing the constraints with respect to the reciprocal design variables is of such high quality that the current explicit problem (15-17) can be solved exactly, rather than partially, after each structural reanalysis. This idea leads to abandoning the primal philosophy in favor of a pure linearization approach in mathematical programming, but it can also be viewed as adopting an optimality criteria strategy.

Since only the final exact solution of each linearized problem needs to be known at each redesign stage, any minimization algorithm can be chosen to solve it. In order to improve the computational efficiency, it is advisable to select a specialized nonlinear programming algorithm, well suited to the particular mathematical structure of the explicit problem (15-17). The objective function is strictly convex and the constraints are linear, so that the problem (15-17) is a convex programming problem. Moreover all the functions defining this problem are explicit and separable. In such a case at least two kinds of methods seem to be efficient: the second order primal projection methods and the dual methods (see next section).

The dual method formulation is especially attractive, because the dual problem presents a much simpler form than the primal problem. Indeed, for a convex problem, the lagrangian multipliers associated with the constraints have the meaning of dual variables in terms of which an auxiliary and equivalent problem can be stated. Under some unrestrictive conditions, this dual problem can be reduced to the maximization of the lagrangian functional with simple nonnegativity requirements on the dual variables. Since, in addition, the explicit problem (15-17) is of separable form, the dual formulation leads to a very efficient solution scheme because each primal variable can be analytically expressed in terms of the dual variables. Furthermore the dimensionality of the dual problem is equal to the number of linearized behavior constraints (16), which is most often small when compared to the number of design variables. Therefore the dual problem exhibits a simpler form and a lower dimensionality than the primal problem.

The dual methods are thus likely to provide the most efficient solution scheme to the linearized problem (15-17), provided this problem can be solved exactly at each stage, rather than partially using a primal method. This demands that the original behavior constraints exhibit a moderate nonlinearity with respect to the reciprocal variables, which is actually true for most problems involving stress, displacement, frequency and buckling constraints [2]. Another significant advantage of the dual methods is that they can take into consideration discrete design variables without weakening the efficiency of the optimization process [15,18]. Discrete variables are useful for representing commercially available gage sizes of sheet metal, the numbers of plies in a laminated com-

posite skin, etc...

Turning now to an optimality criteria strategy, the simple form of the linearized problem (15-17) suggests to make use of its explicit character in order to derive redesign formulas for the design variables. In fact, as shown in Ref. [6], the whole process of combining the linearization of the behavior constraints with respect to the reciprocal design variables and a dual solution scheme can be viewed as a generalization of the optimality criteria approaches. This process consists in solving exactly, after each structural reanalysis, the linearized problem (15-17), which can be recast as follows in terms of the direct design variables :

$$\text{minimize } W = \sum_{i=1}^n l_i a_i \quad (18)$$

$$\text{subject to } \bar{u}_j - \sum_{i=1}^n \frac{c_{ij}}{a_i} > 0 \quad j = 1, n \quad (19)$$

$$\bar{a}_i > a_i > \underline{a}_i \quad i = 1, n \quad (20)$$

Instead of employing primal or dual mathematical programming methods, an alternative approach, which is typical of the optimality criteria philosophy, is to use the explicit character of the approximate problem (18-20) in order to express analytically the optimal design variables. This can be achieved using the KUHN-TUCKER conditions (4-7) which, in view of the convexity of the problem, are sufficient for global optimality. These conditions lead to a generalized optimality criterion yielding explicitly the design variables :

active design variables :

$$a_i = \left(\frac{1}{l_i} \sum_j c_{ij} r_j \right)^{1/2} \quad \text{if} \quad l_i \underline{a}_i^2 < \sum_j c_{ij} r_j < l_i \bar{a}_i^2 \quad (21)$$

passive design variables :

$$a_i = \underline{a}_i \quad \text{if} \quad \sum_j c_{ij} r_j < l_i \underline{a}_i^2 \quad (22)$$

$$a_i = \bar{a}_i \quad \text{if} \quad \sum_j c_{ij} r_j > l_i \bar{a}_i^2 \quad (23)$$

In these expressions, the lagrangian multipliers r_j are associated with the linearized behavior constraints (19). They must satisfy the complementary conditions (5), namely :

active constraint :

$$r_j > 0 \quad \text{if} \quad \sum_i \frac{c_{ij}}{a_i} = \bar{u}_j \quad (24)$$

inactive constraint :

$$r_j = 0 \quad \text{if} \quad \sum_i \frac{c_{ij}}{a_i} < \bar{u}_j \quad (25)$$

The equations (21-23) relating the design variables a_i to the lagrangian multipliers r_j provide a basis for separating the design variables in two groups. The passive variables are those that are fixed to a lower or an upper limit (see Eqs 22 and 23 respectively) while the active variables are explicitly given in terms of the lagrangian multipliers using Eq.(21). This subdivision of the design variables into active and passive groups is classical in the optimality criteria approaches [5,21-27].

When the lagrangian multipliers satisfying (24,25) are known, the optimal design variables can be easily computed using the explicit optimality criterion (21-23). Therefore the problem has been replaced with a new one, which is defined in terms of the lagrangian multipliers only. To solve this new problem, the conventional optimality criteria techniques usually make the assumption that the set of active constraints is known in advance, avoiding thus the inequality constraints on the lagrangian multipliers appearing in Eqs (24,25). An update procedure for the retained lagrangian multipliers is then employed, so that the optimal design variables can be sought iteratively by coupling the update procedure and the explicit optimality criterion (21-23). The essential difficulties involved in applying these optimality criteria methods are those associated with identifying the correct set of active constraints and the proper corresponding set of passive members [5,25]. These difficulties were recognized and addressed with varying degrees of success in studies such as those reported in Refs. [26,27]. However it was only with the dual formulation set forth in Refs [3,28] that these obstacles were conclusively overcome.

The dual method approach consists in maximizing the lagrangian function subject to nonnegativity constraints on the lagrangian multipliers. This approach can therefore be viewed as using an update procedure for the lagrangian multipliers, exactly like the conventional optimality criteria techniques. After the update procedure is completed, the design variables can be evaluated using the optimality criteria equations (21-23). Since the dual maximization problem exhibits a remarkably simple form, its exact solution can be generated at a low computational cost, which is comparable to that required by the recursive techniques of conventional optimality criteria approaches. The dual algorithms can handle a large number of inequality constraints and they intrinsically contain a rational scheme for identifying the active constraints through the non-negativity constraints

on the lagrangian multipliers (or dual variables). They also automatically sort out the active and passive design variable groups using the explicit relationships between primal and dual variables.

Two maximization algorithms are available in the SAMCEF program to solve the dual problem : a first order conjugate gradient type of algorithm and a second order Newton type of algorithm [3,20]. Recently these dual algorithms were implemented in the ACCESS 3 program, which is based on the approximation concepts approach [15-18]. The second order algorithm was improved by employing a simple but efficient one dimensional maximization scheme. The first order algorithm was deeply modified and it is now capable of treating problems involving discrete design variables. Indeed it can be shown (see Refs [15] and [18]) that the optimality criteria equations (21-23) must read as follows for a discrete variable :

$$a_i = a_i^k \quad \text{if} \quad l_i^k a_i^{k-1} < \sum_j c_{ij} r_j < l_i^{k+1} a_i^{k+1} \quad (26)$$

where it is understood that $\{a_i^k, k=1,2,\dots\}$ denotes the set of available discrete values for the i th design variable.

In summary a generalized optimality criteria approach can be defined in the mathematical programming terminology as a special form of the linearization methods. It amounts to replacing the original problem with a sequence of linearized problems and applying a dual solution scheme to each subproblem. It should be noted however that only the behavior constraints are linearized with respect to the reciprocal design variables, while in classical linearization methods, the objective function is also linearized. This is not the case in the present approach because the structural weight is an exact explicit function of the reciprocal variables.

OPTIMIZATION ALGORITHMS

The explicit problem to be solved in each redesign stage (see Eqs. 15-17) is strictly convex and separable. Because of its special simple structure, this problem can be solved efficiently in either its primal or dual form by employing second order algorithms (derived from the well known Newton's method). It should be again emphasized that the primal algorithm can be used to solve only partially the approximate problem (15-17), while the dual algorithm cannot, because intermediate points in the dual space usually correspond to highly infeasible points in the primal space. Therefore the possibility of controlling the convergence of the overall optimization process is available in the SAMCEF [19,20] and ACCESS 3 [15,16] programs only when a primal optimizer is selected. On the other hand, it is important to remember that using a dual algorithm yields results and convergence equivalent to that obtained using optimality criteria. The same is true for the primal algorithms if the approximate problems are solved completely.

Second order primal algorithm (PRIMAL 2)

When the Newton's method is extended to take linear constraints into account, the following weighed projection operator must be used [29] :

$$P = I - F^{-1} N (N^T F^{-1} N)^{-1} N^T \quad (27)$$

where N is a rectangular matrix made up of the gradients of the currently active constraints (16) and F is the hessian matrix of the objective function (15). Since the objective function is separable it follows that the matrix F is diagonal, which makes the second order algorithm no more complicated than the well known (first order) gradient projection method [30].

At each iteration the Newton search direction, projected on the intersection of the active constraints, is computed as follows :

$$z = -P F^{-1} g = -F^{-1} (g - Nr) \quad (28)$$

where g is the gradient of the objective function and r denotes the vector of the second order estimates for the lagrangian multipliers (or dual variables) :

$$r = (N^T F^{-1} N)^{-1} N^T F^{-1} g \quad (29)$$

They can be used to decide whether the current active constraints must remain active or not in the subsequent iterations. At the optimum, each active constraint must be associated to a positive dual variable.

They next design point is given by

$$x^+ = x + \tau z \quad (30)$$

where τ is the step length determined so that the objective function attains its minimum along the direction z (one dimensional minimization). At x^+ a new search direction can be computed using (28) and this minimization process is repeated until the optimum is reached.

In view of Eqs (27) and (29) this second order primal algorithm requires inversion of a matrix at each iteration. This matrix is explicitly given by

$$(N^T F^{-1} N)_{jk} = \frac{1}{2} \sum_{i=1}^n \frac{c_{ij} c_{ik} x_i^3}{z_i} \quad (31)$$

It is worth mentioning that the algorithm can easily be modified so that only the main linear constraints (16) have to be introduced via the projection relations. The side constraints (17) can indeed be treated separately (see Ref [2] for more details).

Second order dual algorithm (DUAL 2)

The minimization problem (15-17) [or the equivalent problem (18-20) recast in the direct variables] can also be solved efficiently as an auxiliary maximization problem in the m lagrangian multipliers r_j associated with the linearized behavior constraints (19). This dual problem reads as follows [3,17,28] :

$$\text{maximize } \gamma(r) = \sum_{i=1}^n z_i a_i(r) + \sum_{j=1}^m r_j g_j(r) \quad (32)$$

$$\text{subject to } r_j > 0 \quad j = 1, m \quad (33)$$

where $g_j(r)$ denotes the components of the dual function gradient, which are equal to the values of the primal constraints :

$$g_j(r) = \frac{\partial \gamma}{\partial r_j}(r) = \sum_i \frac{c_{ij}}{a_i(r)} - \bar{u}_j \quad (34)$$

The primal variables $a_i(r)$ are explicitly given in terms of the dual variables by the relations (21-23), previously interpreted as defining a generalized optimality criterion. Therefore the dual function (32) is formulated in terms of the dual variables only.

The dual problem (32,33) exhibits an attractive feature, namely it is a quasi-unconstrained problem [taking care of the nonnegativity requirements (33) is straightforward]. Given some positive dual variables the corresponding primal variables are computed from (21-23) and the primal constraints are then evaluated using (34). The dual function (32) and its gradient (34) are directly known and a feasible direction can therefore be determined.

In a second order algorithm the hessian matrix of the dual function has to be evaluated :

$$H_{jk} = \frac{\partial^2 \gamma}{\partial r_j \partial r_k} = \frac{\partial g_k}{\partial r_j} = -\frac{1}{2} \sum_i \frac{c_{ij} c_{ik}}{z_i a_i^3} \quad (35)$$

Knowing the gradient (34) and the hessian matrix (35) furnishes the Newton search direction :

$$z = -H^{-1}g \quad (36)$$

The next dual point is then given by

$$r^+ = r + \tau z \quad (37)$$

where τ is the step length determined so that the dual function attains its maximum along the direction z [3]. In a more recent version of the algorithm the one dimensional maximization scheme is considerably simplified and most often a regular Newton unit step is taken [15,17].

The DUAL 2 optimizer implemented in SAMCEF [19] and ACCESS 3 [16] has been especially devised so that it seeks the maximum of the dual function by operating in a sequence of dual subspaces with gradually increasing dimension, such that the effective dimensionality of the maximization problem never exceeds the number of active behavior constraints. This number has been found to be relatively small in practice, which explains the remarkable efficiency of the dual method approach.

To conclude this section, it is interesting to notice that in both primal and dual second order algorithms, precisely the same matrix must be inverted at each iteration [see Eqs.(31) and (35)]. This matrix seems to play an important role in structural optimization, since it is also involved in many conventional optimality criteria techniques [31].

NUMERICAL EXAMPLES

In this section numerical results for several structural optimization problems are presented in brief summary form. Attention is focused on the comparison of various primal and dual optimizers available in the SAMCEF [19,20] and ACCESS 3 [15,16] computer programs, including the second order algorithms previously described (PRIMAL 2 and DUAL 2). Detailed tabular input data and results can be found for all examples in Refs. [2,3,15].

72-bar truss

The first example is the widely used 72-bar four level tower represented in Fig.3. In addition to stress and minimum size constraints, displacement limits are imposed on the four uppermost nodes in the X and Y directions. By symmetry the problem involves 16

independent design variables after linking. In an interesting computational experience reported in Ref. [15], this problem was solved using the NEWSUMT option of ACCESS 3, with three different couples of values for the response factor decrease ratio and the number of response surfaces: (0.5×1) , (0.3×2) and (0.1×3) . Thus increasingly exact solutions are generated for each linearized problem (see Eqs. 15-17) and the approximation concepts approach gradually changes from a pure primal method (with partial solution of each explicit problem) to a pure linearization technique (with complete solution of each explicit problem). The convergence curves of the weight with respect to the number of structural reanalyses are represented in Fig.3. They clearly demonstrate that the more precise solutions of the linearized problems lead to faster convergence. In the limiting case where the explicit problems are solved exactly at each stage, the NEWSUMT optimizer would of course generate the same sequence of design points as the DUAL 2 optimizer.

In fact the iteration history data produced by SAMCEF (generalized optimality criterion), by ACCESS 3 (approximation concepts) and by the conventional optimality criteria techniques of Refs [5,24,27] are identical (see Fig.3). These results numerically confirm that a unified approach to structural optimization has now emerged, which can be interpreted as a linearization method in mathematical programming or as a generalized optimality criteria approach.

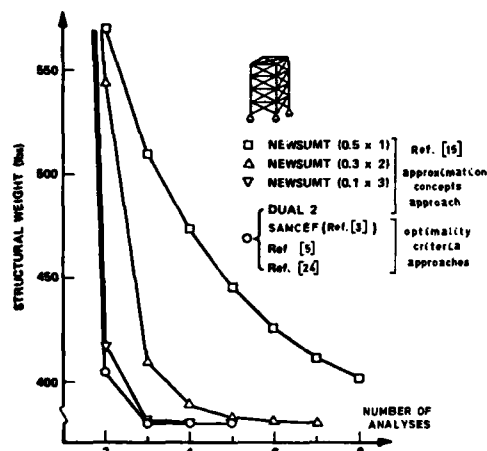


Fig. 3 ITERATION HISTORY FOR 72-BAR TRUSS
63-bar truss

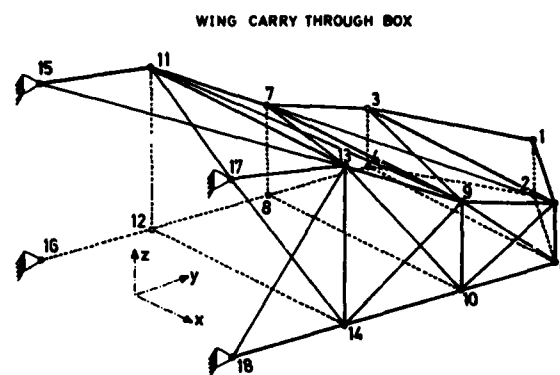


Fig. 4 63-BAR TRUSS

The second example involves a 63-bar truss idealization of the wing carry through box for a large swing wing aircraft. Minimum weight design is sought considering stress and minimum size constraints, as well as a torsional rotation limit on the relative displacement of the tip nodes in the X direction (see Fig.4). The iteration history data reported in Refs. [3,5,15] are compared in Table 1.

	weight (lbs)					
	ACCESS 3 [15]				SAMCEF	Conventional
			DUAL 2		[3]	optimality
Analysis	NEWSUMT	NEWSUMT			PRIMAL 2	criterion
number	(0.5 x 1)	(0.5 x 2)	unscaled	scaled		[5]
1	66628	66628	66628	30214	30214	30214
2	16914	12543	6706	7573	7680	7577
3	11137	8667	6316	6546	6591	6884
4	9338	7293	6195	6733	6398	6928
5	8305	6697	6157	6292	6270	6801
6	7620	6402	6138	6243	6246	6609
7	7154	6259	6129	6201	6199	6473
8	6836	6189	6124	6161	6159	6388
9	6620	6154	6121	6132	6126	6333
10	6467	6137	6120	6123	6123	6293
11	6362	6128	6119	6121	6121	6263
12	6289	6123	6118	6120	6120	6241
13	6238	6121	<u>6118</u>	<u>6119</u>	6119	6231
14	6203	6120			6118	6216
15	6178	<u>6119</u>			<u>6118</u>	6220
...
50						<u>6159</u>
CPU time (sec)						
total	108	163	60			
analysis	44	46	41			
optimization	59	113	14			

Table 1 Iteration history data for 63-bar truss

The NEWSUMT option of ACCESS 3 [15] leads to a sequence of non critical feasible designs with monotonically decreasing weight, which corresponds well to the primal philosophy of this solution scheme. Once again, when the linearized problem is solved with more accuracy, the convergence of the weight becomes faster, but the computational cost increases substantially. Solving exactly each linearized problem using the DUAL 2 optimizer yields a sequence of infeasible designs (unscaled weights in Table 1). Consequently scaling produces feasible critical designs with an occasional increase in the feasible weight from one iteration to the next (scaled weights in Table 1). It can be seen that DUAL 2 furnishes an optimal design after a smaller number of structural reanalyses than NEWSUMT, and at a much lower computational cost (60 sec for DUAL 2 and 163 sec for NEWSUMT on IBM 360-91 at CCN, UCLA). It is worthwhile noticing that the computer time expended in the optimizer portion of the program remains small when DUAL 2 is employed, despite the relatively large dimensionality of the dual problem (15 active behavior constraints at the optimum design).

The PRIMAL 2 option of SAMCEF [3] yields also excellent results for this problem. This is not surprising, since the optimality criteria method used in SAMCEF consists in solving exactly each linearized problem generated in sequence, just as ACCESS 3 does when the DUAL 2 optimizer is selected. As a result, the iteration histories produced by both computer programs are about the same. The small differences are due to the fact that the SAMCEF results were obtained by using zero order approximations for some of the stress constraints, instead of first order ones (hybrid optimality criterion; see Refs [3,6]).

Finally the conventional optimality criteria technique of Ref. [5] does not lead to very good results for this example, mainly because it employs zero order approximations for all the stress constraints (fully stressed design criterion). Consequently 50 structural reanalyses do not suffice to achieve convergence, while methods based on first order approximation of the stress constraints generate an optimum design after less than 15 stages.

I-beam

Attention is now directed to the I-beam structure depicted in Fig.5. The purpose of this example is to show that the generalized optimality criterion set forth in Ref.[2] remains valid when natural frequency constraints are considered. The problem consists in minimizing the weight of the I-beam while controlling the frequencies of its three first eigenmodes: flange flexion, torsion, and web flexion. The analysis model involves 35 second degree displacement elements, among which the 10 diaphragms are fictitious (without mass). These dummy members are introduced to obtain a good representation of the torsional mode.

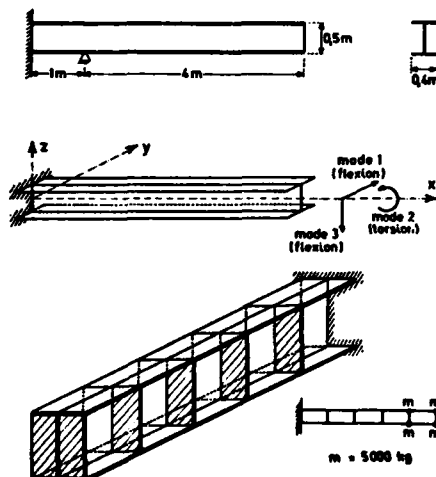


Fig. 5 I-BEAM MODEL

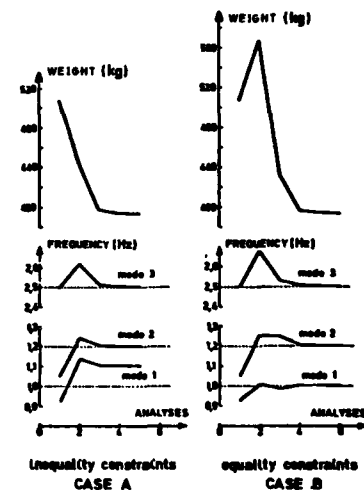


Fig. 6 ITERATION HISTORY FOR I-BEAM

In a first optimization exercise lower and upper bounds were imposed on each three eigenfrequencies. The curves represented in Fig.6 reproduce the variation of the weight and frequencies with the number of structural reanalyses. Only 5 analyses are sufficient to generate an optimum design. The fundamental frequency does not reach the prescribed lower bound, nor the upper bound. The two next frequencies are equal to their respective minimal allowable value.

Next, equality constraints were assigned to each three frequencies, in order to reduce the fundamental frequency to 1 Hz, while keeping the two other frequencies at 1.2 Hz and 2.5 Hz, respectively. The iteration history presented in Fig.6.B again demonstrates the remarkable efficiency of the generalized optimality criterion. The increase in the weight after the first redesign stage is due to the equality constraint which is now imposed on the first frequency. Note that only six structural reanalyses are required to achieve convergence.

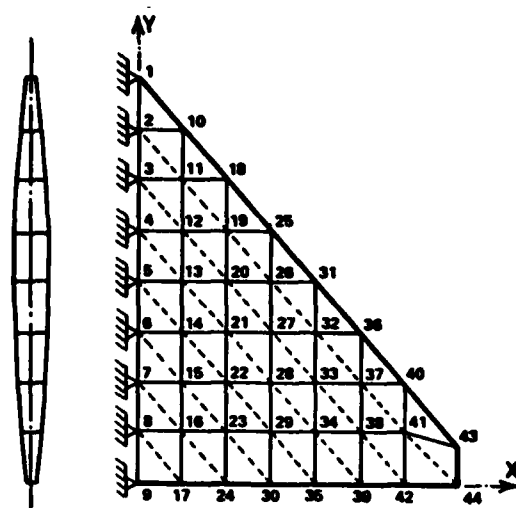


Fig. 7 DELTA WING MODEL

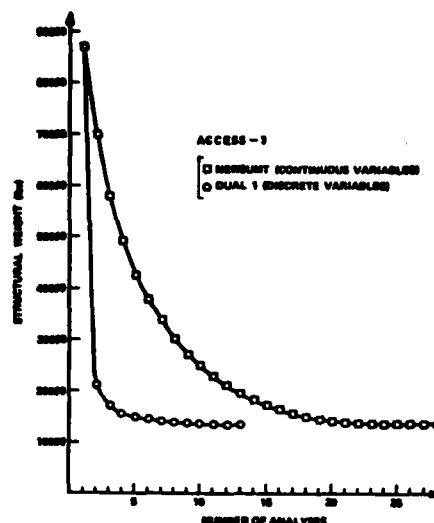


Fig. 8 ITERATION HISTORY FOR DELTA WING

Delta wing

Consideration is now given to a thin delta wing structure with fiber composite skins and metallic webs (see Fig.7). Several more and more realistic versions of the problem were studied in Refs. [8,9,10,15] using the ACCESS code. In the final version the skins are assumed to be made up of 0° , $\pm 45^\circ$ and 90° high strength graphite epoxy laminates. The laminates are required to be balanced and symmetric and they are represented by stacking four constant strain orthotropic elements in each triangular region shown in Fig.7. Therefore the upper half of the delta wing is modeled using 252 orthotropic membrane elements to represent the skin and 70 symmetric shear panel elements for the vertical webs. However, after design variable linking the number of independent variables is reduced to 60. The wing is subject to a single static loading acting in combination with a temperature change condition. Static deflection constraints are imposed at the wing tip nodes and the strength requirements are based on the maximum strain failure criterion. In addition, a lower bound is assigned to the fundamental natural frequency while fixed masses simulate fuel in the wing. Minimum gage sizes are also specified.

analysis number	NEWSUMT (continuous)		DUAL 2 (continuous)		DUAL 1 (mixed)	
	weight ($\times 10^3$ lbs)	frequency (cps)	weight ($\times 10^3$ lbs)	frequency (cps)	weight ($\times 10^3$ lbs)	frequency (cps)
1	86.82	2.829	86.82	2.829	86.82	2.829
2	70.26	2.650	21.39	2.016	20.83	2.009
3	58.11	2.516	16.75	1.961	17.17	2.000
4	49.16	2.196	14.34	1.937	15.40	1.974
5	42.64	2.293	14.85	2.007	14.99	2.000
6	38.04	2.209	13.98	1.987	14.40	1.994
7	33.93	2.127	13.81	2.003	14.08	1.996
8	29.86	2.042	13.62	2.007	13.92	2.003
9	26.78	2.010	13.41	2.005	13.52	1.998
10	24.56	2.009	13.24	2.004	13.41	2.003
11	22.64	2.010	13.10	2.002	13.37	2.009
12	20.95	2.010	12.99	2.001	13.29	2.003
13	19.48	2.010	12.91	2.001	13.29	2.000
14	18.21	2.010	12.85	2.000		
15	17.12	2.009	12.81	2.000		
...				
20	14.06	2.003				
25	13.56	2.002				
29	13.47	2.002				
CPU time (sec)						
total	719		261		253	
analysis	564		252		234	
optimization	145		2		12	

Table 2 Iteration history data for delta wing

Iteration history data presented in Table 2 were obtained using the NEWSUMT, DUAL 2 and DUAL 1 optimizers available in ACCESS 3 [15]. Since the fundamental natural frequency constraint is the main design driver in this example, its value as well as the weight for each design in the sequence is given. Initially the problem was treated using a continuous representation for all the design variables, although the fiber composite skins must in fact be described by discrete variables (number of plies). The aim was simply to compare the efficiency of the NEWSUMT and DUAL 2 optimizers. It can be seen

that the advantages of using the dual method approach are significant for the delta wing example (see Table 2). Not only is the computational effort expended in the optimizer portion of the program reduced dramatically (from 145 sec for NEWSUMT to 2 sec for DUAL 2), but the number of structural reanalyses required for convergence is also considerably decreased (29 and 15 stages for NEWSUMT and DUAL 2, respectively). Note that the NEWSUMT optimizer again produces feasible improved designs (primal solution scheme), while some of the designs in the DUAL 2 sequence are slightly infeasible with respect to the frequency constraint.

Attention is now focused on the results obtained in the mixed continuous-discrete variable case, where the metallic web thicknesses are still taken as continuous design variables while the variables describing the laminated fiber composite skin are discrete (more precisely, integer variables representing the number of plies). The DUAL 1 option of ACCESS 3 must therefore be employed (see Ref. [15]). Iteration history data are given in Table 2 and illustrated in Fig. 8. It should be emphasized that DUAL 1 obtains a solution to the mixed variable problem in fewer stages (and less time) than DUAL 2 requires to obtain the pure continuous variable solution.

Aircraft spoiler

The spoiler represented in Fig. 9 has been analyzed in detail in an optimization exercise using the mixed method available in SAMCEF [3]. The structure is classically designed in light aluminum alloy sheet. The front spar and the secondary spar are joined by twelve ribs and covered by two skins reinforced by stringers. The spoiler is hinged at three points and activated at one, in the midspan. The loads consist in pressure distribution on both faces, corresponding to two flight configurations. In one of them a flexibility constraint is imposed, which stipulates that the trailing edge has to remain straight within a tolerance $\epsilon = 0.5$ mm, in order to eliminate contact with the flap. In the initial design this requirement was achieved by precambering the spoiler (see Fig. 9). This costly procedure had to be avoided in the final optimized design. So differential flexibility constraints are introduced which assign an upper limit $\epsilon = 0.5$ mm to the absolute value of the difference between any two deflections along the trailing edge (see Fig. 11). In addition maximum allowable stresses and minimum thicknesses are imposed, which differ from places to places depending on the material used and manufacturing considerations.

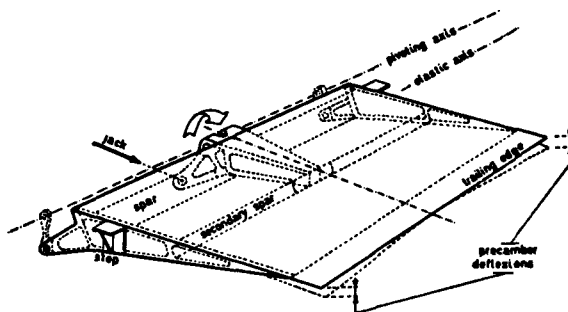


Fig. 9 AIRCRAFT SPOILER

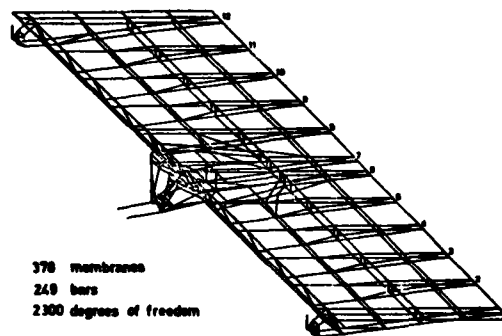


Fig. 10 FINITE ELEMENT MODEL OF THE SPOILER

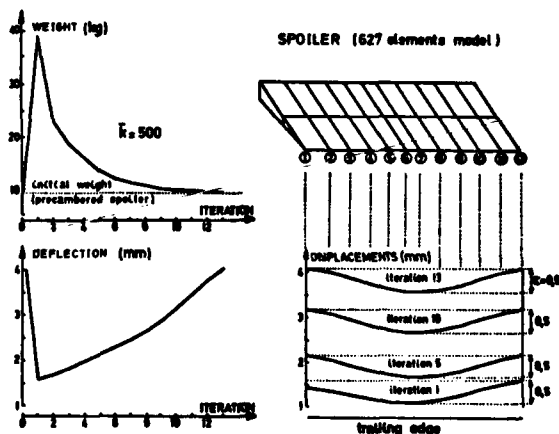


Fig. 11 ITERATION HISTORY FOR AIRCRAFT SPOILER

of design variables. Note that the initial scale up of the weight is due to the fact that the original design of the spoiler did not satisfy the differential flexibility constraints when precambering was suppressed. Hence after scaling up the member sizes to

Several final element models of the structure were investigated, made up of 27,64,125 and 627 elements (see Ref. [2]). The final model is illustrated in Fig. 10. It involves 627 second degree displacement elements and 2300 degrees of freedom. Based upon experience accumulated from the study of the simpler models, it was concluded that the mixed method had to be used for solving the spoiler problem. So a first order projection algorithm was employed and it was necessary to limit the number of minimization steps k to avoid divergence of the process (note that the second order primal algorithm previously described was not available at the time of the investigation). This means that any method based on optimality criteria, (including dual algorithms) would not succeed in solving this problem.

Results are presented in Fig. 11. As expected from the experience gained with the simplified problems, a good convergence was obtained with the mixed method by setting $K = 500$, that is, slightly below the number

obtain a feasible design the weight jumps from 10 to 40 kg. After 13 structural reanalyses, the original weight of 10 kg is recovered, but it corresponds of course to a very different design (see Ref. [2]).

CONCLUSIONS

A powerful and rather general approach to structural optimization is achieved by replacing the original problem with a sequence of explicit approximate problems and solving them using either primal or dual algorithms. A primal solution scheme yields a mixed method, with properties lying between those of the optimality criteria techniques and those of pure mathematical programming methods. A dual solution scheme leads to generalization of the optimality criteria approaches, with a rational procedure for identifying the strictly critical constraints (including the classical subdivision of the design variables into passive and active groups).

The advantages and drawback of both mixed and dual methods can be outlined as follows :

- . dual methods are usually efficient and computationally economical but they are subject to instability in the convergence of the structural weight ; on the other hand mixed (primal) methods facilitate better control over convergence of the entire optimization process, at the price of a higher computational cost ;
- . mixed methods can be applied to objective functions that are more complex than the structural weight, or to problems requiring non separable approximation of the behavior constraints, while dual methods cannot ; on the other hand dual methods are readily extendable to problems involving discrete design variables (see Refs.[15,18], while known primal methods appear to be cumbersome and computationally expensive for such problems ;
- . finally, because the dual problem exhibits a much simpler form than the primal problem, the computer implementation of the structural optimization method seems to be more reliable with dual algorithms than with primal ones.

ACKNOWLEDGEMENT

The research from which the SAMCEF optimization capability is developed has been sponsored by the Air Force Office of Scientific Research under Grant AFOSR-77-3118.

REFERENCES

- [1] FIACCO, A.V. and Mc CORMICK, G.P., Non linear programming : sequential unconstrained minimization techniques, John Wiley, New York, 1968
- [2] FLEURY, C., "Le dimensionnement automatique des structures élastiques", Doctoral thesis, LTAS Report SF-72, University of Liège, 1978
- [3] FLEURY, C. and SANDER, G., "Structural optimization by finite elements", AFOSR Final Scientific Report, Grant 77-3118, LTAS Report SA-58, University of Liège, 1978
- [4] FLEURY, C., "A unified approach to structural weight minimization", to appear in Comp. Meth. Appl. Mech. Eng., LTAS Report SA-62, University of Liège, 1978
- [5] BERKE, L. and KHOT, N.S., "Use of optimality criteria for large scale systems", AGARD-LS-70, 1974, pp. 1-29
- [6] FLEURY, C., "An efficient optimality criteria approach to the minimum weight design of elastic structures", to appear in Computers and Structures, LTAS Report SA-61, University of Liège, 1978
- [7] SCHMIT, L.A. and FARSHI, B., "Some approximation concepts for structural synthesis", AIAA Journal, Vol 12, n° 5, 1974, pp. 692-699
- [8] SCHMIT, L.A. and MIURA, H., "Approximation concepts for efficient structural synthesis", NASA CR-2552, 1976
- [9] SCHMIT, L.A. and MIURA, H., "A new structural/synthesis capability - ACCESS 1", AIAA Journal, Vol 14, n° 5, 1976, pp. 661-671
- [10] SCHMIT, L.A. and MIURA, H., "An advanced structural analysis/synthesis capability- ACCESS 2", Int. J. Num. Meth. Engng., Vol 12, n° 2, 1978, pp. 353-377
- [11] FLEURY, C. and FRAEIJIS de VEUBEKE, B., "Structural optimization", Lecture Notes in Computer Sciences, n° 27, Springer Verlag, 1975, pp. 314-326
- [12] FLEURY, C. and GERADIN, M., "Optimality criteria and mathematical programming in structural optimization", Computers and Structures, Vol 8, n° 1, 1978, pp. 7-17
- [13] SANDER, G. and FLEURY, C., "A mixed method in structural optimization", Int. J. Num. Meth. Engng., Vol 13, n° 2, 1978, pp. 385-404
- [14] FOX, R.L., Optimization methods for engineering design, Addison - Wesley, 1971, pp. 242-250

- [15] FLEURY, C. and SCHMIT, L.A., "Dual methods and approximation concepts in Structural synthesis", NASA CR in preparation
- [16] FLEURY, C. and SCHMIT, L.A., "ACCESS 3 - Approximation Concepts Code for Efficient Structural Synthesis - User's Guide", NASA CR in preparation
- [17] SCHMIT, L.A. and FLEURY, C., "Structural synthesis by combining approximation concepts and dual methods", submitted to the AIAA Journal, 1979
- [18] SCHMIT, L.A. and FLEURY, C., "Discrete-continuous variable structural synthesis using dual methods", submitted to the AIAA Journal, 1979
- [19] SAMCEF, Système d'analyse des milieux continus par éléments finis, LTAS, University of Liège
- [20] SANDER, G., "Optimization in the SAMCEF program", paper presented at the UUA/E 7th Structural Analysis S.I.G., Nice, France, 1978
- [21] PRAGER, W. and MARCAL, P.V., "Optimality criteria in structural design", AFFDL-TR-70-166, 1971
- [22] GELLATLY, R.A. and BERKE, L., "Optimal structural design", AFFDL-TR-70-165, 1971
- [23] VENKAYYA, V.B., "Design of optimum structures", Computers and Structures, Vol 1, n° 1-2, 1971, pp. 265-309
- [24] TAIG, I.C. and KERR, R.I., "Optimization of aircraft structures with multiple stiffness requirements", AGARD Conf. Proc. n° 123, 2nd Symp. Structural Optimization, Milan, Italy, 1973
- [25] KIUSALAAS, J., "Minimum weight design of structures via optimality criteria", NASA-TN-D-7115, 1972
- [26] DOBBS, M.W. and NELSON, R.B., "Application of optimality criteria to automated structural design", AIAA Journal, Vol 14, n° 10, 1976, pp. 1436-1443
- [27] RIZZI, D., "Optimization of multi-constrained structures based on optimality criteria", Proc. AIAA/ASME/SAE 17th Structures, Structural Dynamics and Materials Conference, King of Prussia, Pennsylvania, 1976, pp. 448-462
- [28] FLEURY, C., "Structural optimization by dual methods of convex programming", to appear in Int. J. Num. Meth. Engng., LTAS Report SA-60, University of Liège, 1978
- [29] GILL, P.E. and MURRAY, W. (ed.), Numerical methods for linearly constrained optimization, Academic Press, 1974
- [30] ROSEN, J.B., "The gradient projection method for nonlinear programming - Part I : linear constraints", SIAM Journal, Vol 8, n° 1, 1960, pp. 181-217
- [31] KHOT, N.S., BERKE, L. and VENKAYYA, V.B., "Comparison of optimality criteria algorithms for minimum weight design of structures", Proc. AIAA/ASME 19th Structures, Structural Dynamics and Materials Conf., Bethesda, Maryland, 1978, pp. 37-46

ELEMENTS FINIS ET OPTIMISATION

DES STRUCTURES AERONAUTIQUES

PAR

C. PETIAU et G. LECINA

Avions Marcel Dassault - Bréguet Aviation
78 Quai Carnot
92214 SAINT-CLOUD
France

SOMMAIRE

Nous présentons la méthode d'optimisation sur modèle d'éléments finis utilisée couramment aux AMD-BA pour minimiser la masse structurale, développée avec le support de la DRET

Les paramètres de l'optimisation sont des facteurs multiplicatifs de l'échantillonnage de groupes d'éléments finis.

Les contraintes d'optimisation sont de diverses natures :

- Minimum technologique, loi d'usinage simple.
- Limitation des déformations, des contraintes élastiques, d'efforts généraux, par critères de rupture complexes.
- Limitation des coefficients aéroélastiques, des efficacités de gouverne.
- Limitation dynamique ; fréquence propre, vitesse de Flutter, réponse transitoire et forcée.

Le processus d'optimisation est itératif. Chaque itération comprend trois étapes :

- Analyse : statique, dynamique et aéroélastique.
- Calcul des dérivées partielles des contraintes par rapport aux paramètres.
- Optimisation non linéaire avec une formulation explicite approchée des contraintes.

La convergence est obtenue pratiquement en 3 à 4 itérations. Le coût de l'optimisation est de 6 à 10 fois celui d'une simple analyse.

Nous présentons 2 exemples d'applications pratiques :

- Optimisation d'une voilure Δ
- Optimisation d'un empennage en matériaux composites.

SUMMARY

The optimization method used at AMD-BA for minimising weight by a finite element model is described.

Now, this method is a routine process in our new designs.

The optimization parameters are multiplicative factors of the stiffness of linked finite elements.

The optimization constraints can be of different types :

- Technological minimum thicknesses, simple tooling rules, etc...
- Limited displacements, stresses and strains, miscellaneous failing under tensile stress and local buckling
- Static aeroelastic limitations on aeroelastic coefficients and control efficiencies.
- Limitations on flutter speed and dynamic responses.

The optimization process is iterative, each iteration including three steps :

- Analysis : static, dynamic and aeroelastic
- Computation of partial derivatives of the constraints relative to the parameters
- Explicit non-linear optimization

Convergence is obtained after 3 to 4 iterations, the global cost of an optimization reach from 8 to 12 times the cost of a simple analysis.

Two practical examples are presented :

- optimization of a Δ wing
- optimization of a carbon epoxy empennage.

1 - EVOLUTION DE NOTRE METHODE

Traditionnellement, le dessinateur optimise une structure vis-à-vis des contraintes élastiques par la méthode du "fully stress design" (F.S.D.) ; on pose que le "cheminement des efforts" est peu sensible aux variations d'échantillonnage, ce qui conduit pour alléger, à multiplier les sections, les épaisseurs ou les inerties, par le rapport de la contrainte calculée (ou mesurée) à la contrainte admissible. Ce processus converge plus ou moins bien, il a des défauts majeurs :

- Subjectivité des hypothèses sur le "chemin des efforts" dans les structures hyperstatiques.
- Le point de convergence n'est pas forcément optimum et, de plus, il amène à faire travailler partout la structure à sa contrainte maximale admissible, ce qui n'est pas le cas à l'optimum réel trouvé par notre méthode.
- On ne tient pas compte de façon rationnelle des contraintes de rigidité, aéroélasticité, flutter...

La nécessité d'utiliser un processus plus efficace s'est accentuée avec nos derniers projets d'avion militaire à structure très hyperstatique, sensible à l'aérodistorsion et comportant de nombreux sous-ensembles en matériaux composites.

La mise au point de l'outil d'optimisation s'est faite par phases successives.

a) Mise au point d'un outil d'analyse performant

L'optimisation n'est envisageable qu'après la mise au point d'un outil d'analyse suffisamment efficace pour pouvoir itérer sans coût prohibitif. Le module d'optimisation est construit autour de notre code ELFINI qui regroupe autour d'un noyau éléments finis les grandes branches de l'analyse des structures aéronautiques (planche 1).

- Calcul des contraintes statiques linéaires et non linéaires.
- Aéroélasticité statique, calcul et gestion des charges.
- Réduction dynamique, flutter, réponse transitoire et forcée.
- Transfert de chaleur, calcul des cartes de température.
- Propagation de fissures.

Cet outil est utilisé pour le calcul de tous nos avions depuis 1970, citons parmi ses caractéristiques les plus importantes pour l'optimisation :

- Résolution des équations d'équilibre par une variante très performante de la méthode de Gauss Frontale qui fournit la matrice de rigidité factorisée, à partir de laquelle les résolutions avec de nombreux chargements sont faites en différé, à bon compte ; ces séquences de résolution font l'essentiel du temps de calcul des grandes branches du programme, en particulier de l'optimisation pour le calcul des "dérivées partielles" des contraintes.
- Elaboration et maniement des maillages en mode interactif ou en batch par la "méthode topologique" (réf. 5) qui permet de décrire les noeuds et les éléments par "pavé" de propriété constante dans un espace d'indices.
- Gestion automatique et quasi-transparente par l'utilisateur de la banque des données générées par chaque module sur un fichier unique.
- Un moniteur gère l'appel des modules en allouant dynamiquement la mémoire, permettant d'introduire très aisément les itérations sur les modules et les branches du programme.

b) Dérivées partielles

La première phase de l'optimisation a été le calcul direct des dérivées partielles des contraintes d'optimisation par rapport aux paramètres λ_i qui sont des facteurs multiplicatifs de l'échantillonnage de groupes d'éléments finis.

Nous disposons de la dérivation :

- des déformations,
- des contraintes élastiques, contraintes principales, contraintes équivalentes et critères de flambage locaux,
- des efforts locaux, des réactions entre sous-ensembles,
- des coefficients aéroélastiques, des vitesses de divergence et d'inversion de gouverne,
- des fréquences propres,
- des vitesses de Flutter,
- des réponses dynamiques transitoires.

c) Introduction d'algorithmes d'optimisationc1 - Optimisation linéaire

A partir des dérivées partielles des contraintes, il est tentant de calculer automatiquement le rééchantillonnage optimal minimisant la masse et satisfaisant aux contraintes d'optimisation, en utilisant une méthode d'optimisation linéaire et d'itérer. Nous avons posé que les contraintes sont des formes linéaires des paramètres, la masse de la structure étant elle aussi une fonction linéaire des paramètres. Nous avons résolu ce problème de programmation linéaire par la méthode du simplex. Malheureusement, ce processus ne converge pas directement, il n'est praticable qu'en rajoutant à chaque itération des contraintes sur l'amplitude de la variation des paramètres qui en rendent le coût prohibitif.

c2 - Optimisation non linéaire

Pour palier à cet inconvénient, nous avons fait l'hypothèse (exacte pour les structures isostatiques) que les contraintes étaient des fonctions linéaires de l'inverse des paramètres. La masse devenant homographique, le problème à traiter devient non linéaire. Nous avons utilisé des méthodes de linéarisation pas à pas combinées à un gradient projeté, puis de gradient conjugué projeté. Ces algorithmes qui traitent le cas des contraintes admissibles fonctions des paramètres (flambage local), convergent en 3 à 4 rééchantillonnages.

Nous perfectionnons cet algorithme en programmant diverses lois approchées d'évolution des contraintes en fonction des paramètres, lois définies à partir de valeur de la contrainte et de ses dérivées au point d'analyse ; l'utilisateur fait son choix en fonction de la contrainte d'optimisation sélectionnée.

c3 - Maximisation des marges de sécurité

Dans le problème habituel d'optimisation de structure, la fonction minimisée est la masse ; dans un certain nombre de cas, nous sommes amenés à minimiser le rapport "contrainte/contrainte admissible" le plus défavorable, tout en ne dépassant pas une masse donnée. Le caractère non linéaire de ce problème est plus accentué que celui de la minimisation de la masse.

2 - DESCRIPTION DE LA METHODE2.1 - Organigramme général (Pl. 2)2.2 - Calcul des dérivées partielles des contraintes d'optimisation

C'est la phase du calcul la plus importante en temps ordinateur, la façon de calculer différant notablement entre les problèmes statique et dynamique.

2.21 - Contrainte fonction linéaire des déplacements statiques (déplacement, contrainte élastique, effort local, réaction, etc...)

Les déplacements X sont obtenus par la résolution du système :

F = forces extérieures

$$\textcircled{1} \quad F = [K] X$$

$[K]$ = matrice de rigidité

La matrice de rigidité $[K]$ est inversée, implicitement par la méthode de Gauss Frontale dans l'analyse E.F.; sa forme en fonction des paramètres λ est :

$$\textcircled{2} \quad [K] = K_0 + \sum \lambda_i [\partial K / \partial \lambda_i]$$

Les matrices $[\partial K / \partial \lambda_i]$ sont la somme des matrices de rigidité des éléments constituant le paramètre λ_i

En différenciant 1, il vient la relation fondamentale :

$$\textcircled{3} \quad \Delta X = -[K]^{-1} [\Delta K] X$$

sachant que :

$$\sigma = [\partial \sigma / \partial X] X$$

il vient :

$$\textcircled{4} \quad [\partial \sigma / \partial \lambda] = -[\partial \sigma / \partial X][K]^{-1} [\partial K / \partial \lambda] X + \left[\frac{\partial}{\partial \lambda} (\partial \sigma / \partial X) \right] X$$

$[K]$ étant symétrique, 4 peut se transformer en

$$\textcircled{5} \quad [\partial \sigma / \partial \lambda] = -\left([K]^{-1} [\partial \sigma / \partial X]_t \right)_t [\partial K / \partial \lambda] X + \left[\frac{\partial}{\partial \lambda} (\partial \sigma / \partial X) \right] X$$

Dans les relations 4 et 5, les seuls calculs coûteux en ordinateur sont les résolutions :

$$[K]^{-1} [\partial K / \partial \lambda] X$$

pour la formule 4

$$[K]^{-1} [\partial \sigma / \partial X]_t$$

pour la formule 5.

La formule 4 coûte le prix de Nbre paramètres X Nbre de chargements seconds membres au système 1.

La formule 5 coûte le prix de Nbre contraintes examinées seconds membres au système 1.

La pratique guide le choix entre ces 2 formules à partir des considérations suivantes :

- le nombre de contraintes élastiques examinées est en général de 2 à 3 fois celui des paramètres,
- si il y a plusieurs cas de charges, les contraintes sensibles ne sont pas nécessairement aux mêmes points, ce qui entraîne que la méthode 5 n'est rentable que si nous avons plus de 3 ou 4 chargements dimensionnants.

2.22 - Contrainte fonction non linéaire des déplacements statiques (contrainte principale, contrainte équivalente, critère de rupture, etc...)

On se ramène aux formules 4 et 5 précédentes, l'opérateur $[\partial \sigma / \partial X]$ étant linéarisé au voisinage de $X(\lambda)$

2.23 - Dérivées des contraintes aéroélastiques statiques

L'exposé de leur calcul et de leur dérivation est assez complexe. Il est détaillé dans la référence 1 et brièvement résumé dans l'annexe 1. Il faut retenir qu'elles sont calculées exactement par un processus issu de la formule 5 et que leur coût est celui de 1 second membre au système 1 par contrainte.

2.3 - Contraintes dynamiques

Comparées au calcul statique où les formules de dérivation sont exactes, les dérivations des contraintes dynamiques ne sont qu'approchées ; ce phénomène vient du fait que les calculs dynamiques s'effectuent sur une base réduite par rapport aux éléments finis (en général, une base de modes propres), et il est nécessaire que les chargements intervenant dans le calcul des dérivées puissent se décomposer dans la base réduite.

Cette condition étant remplie, les calculs de dérivation sont moins chers qu'en statique car les manipulations ont lieu dans la base réduite.

2.31 - Dérivées d'une fréquence propre

Ces dérivées sont d'un coût insignifiant, en effet, si V est mode propre et ω^2 valeur propre du système :

$$[M] X'' + [K] X = 0$$

le quotient de Rayleigh

$$z(X) = X_t [K] X / X_t [M] X$$

est stationnaire et égal à ω^2 pour

$$X = V$$

entraînant la nullité des dérivées par rapport à X soit :

$$\Delta \omega^2 = V_t [\Delta K] V / V_t [M] V - \omega^2 V_t [\Delta M] V / V_t [M] V$$

2.32 - Dérivées d'un extremum d'une réponse transitoire

Nous avons dans la base E.F. l'équation de la mécanique linéarisée

$$(6) \quad [M] X'' + [K] X = F(t)$$

supposée résolue dans la base réduite $X = [V] x$

$$\text{par intégration de } [m] x'' + [k] x = f(t) \quad (7)$$

$$\text{avec } [m] = V_t [M] V \quad [k] = V_t [K] V \quad f(t) = V_t F(t)$$

Une contrainte dynamique \mathcal{G} s'écrivant :

$$\mathcal{G} = [\partial \mathcal{G} / \partial X] X = [\partial \mathcal{G} / \partial x] [V] x = [\partial \mathcal{G} / \partial x] x$$

La réponse dérivée de l'équation 6 s'écrit :

$$(8) \quad [M] \Delta X'' + [K] \Delta X = -[\Delta M] X'' - [\Delta K] X$$

qui ne diffère de 6 que par le second membre, si on pose que ce dernier se décompose dans $[V]$, il vient :

$$(9) \quad [m] \Delta x'' + [k] \Delta x = -[\Delta m] x'' - [\Delta k] x$$

$$\text{avec } [\Delta m] = V_t [\Delta M] V \quad [\Delta k] = V_t [\Delta K] V$$

l'intégration de 9 conduit aux réponses dérivées :

$$(10) \quad \Delta \mathcal{G}(t) = [\partial \mathcal{G} / \partial x] \Delta x_t$$

Formule valable pour la variation des extremum de \mathcal{G}_t

car

$$d \mathcal{G}(\lambda, t) = [\Delta \mathcal{G} / \Delta \lambda] d\lambda + (\partial \mathcal{G} / \partial t) dt$$

2.33 - Dérivées d'une fonction de transfert d'une réponse forcée, d'une réponse à une excitation aléatoire

Elle s'effectue par dérivation exacte dans la base réduite (calcul détaillé réf. 1).

2.34 - Contrainte de vitesse de flutter

Son calcul est complexe, il s'apparente à celui de la variation d'une fréquence propre. On trouvera le détail dans la référence 1, nous le résumons dans l'annexe 2.

3 - MODULE D'OPTIMISATION EXPLICITE

L'idée directrice est de remplacer le comportement exact des contraintes qui n'est connu qu'implicitement au travers de l'analyse E.F. par une formulation explicite $\mathcal{G}^*(\lambda)$ approchée permettant toutes les tabulations nécessaires à bas prix.

$\mathcal{G}^*(\lambda)$ est choisie telle que pour $\lambda = \lambda_{\text{analyse}}$

$$\mathcal{G}^*(\lambda) = \mathcal{G}_{\text{E.F.}} \quad \partial \mathcal{G}^*(\lambda) / \partial \lambda = \partial \mathcal{G}_{\text{E.F.}} / \partial \lambda$$

$\mathcal{G}^*(\lambda)$ doit être exacte pour les structures isostatiques

$\mathcal{G}^*(\lambda)$ doit avoir un bon comportement quand $\lambda \rightarrow \infty$ et $\lambda \rightarrow 0$

Nous avons essayé plusieurs types de comportement $\sigma^*(\lambda)$ (Réf. 1). Celui qui semble le plus efficace, jusqu'à nouvel ordre, est de poser que les contraintes sont linéaires par rapport à l'inverse des paramètres (exact en isostatique).

Soit avec $\alpha_i = 1/\lambda_i$

$$a_{ij} = -1/\alpha_i^2 \partial \sigma_j \text{ E.F.} / \partial \lambda_i$$

$$\sigma_j^*(\alpha) = a_{0j} + \sum_i a_{ij} \alpha_i$$

$$a_{0j} = \sigma_j \text{ E.F.} + \sum_i a_{ij} (\alpha_i - \alpha_{i0})$$

Le problème d'optimisation devient :

$$\sum m_i / \alpha_i \text{ minimal}$$

en satisfaisant aux inéquations

$$\left\{ \begin{array}{l} a_{0j} + \sum_i a_{ij} \alpha_i \leq \sigma_j \text{ ad}(\alpha) \\ \alpha \leq 1/\lambda_i \text{ mini} \end{array} \right.$$

La valeur admissible des contraintes $\sigma_j \text{ ad}(\lambda)$ n'est pas constante dans les cas de contraintes de flambage local ; nous la prenons alors comme fonction d'un seul des paramètres, obtenue par les critères de flambage local classiques.

Nous utilisons 2 types de méthodes pour résoudre ce problème d'optimisation explicite :

- cas général :

séquences de programmations linéaires avec introduction de contraintes supplémentaires de linéarité.

- cas où les contraintes admissibles sont constantes :

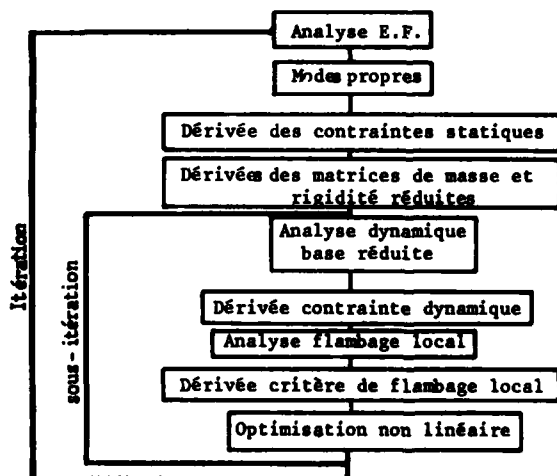
gradient conjugué projeté avec normalisation adéquate.

L'algorithme du gradient conjugué projeté, détaillé dans la réf. 1 minimise la fonction de coût par gradient conjugué non linéaire (réf. 3) et cela dans le sous-espace des contraintes touchées (gradient remplacé par sa projection dans le sous-espace des contraintes touchées). La condition d'abandon des contraintes est celle du simplex (composante positive de la projection du gradient sur les contraintes touchées). Le coût de cet algorithme est de l'ordre de grandeur de quelques fois l'inversion d'une matrice de rang N paramètres.

L'algorithme est accéléré en effectuant une mise à l'échelle rendant unitaire le Hessien tangent de la fonction de coût à certains pas du calcul.

4 - SOUS-ITERATION

Le coût du calcul d'optimisation sous certaines contraintes, contrainte dynamique, Flutter, critère de flambage, etc..., étant relativement peu élevé par rapport au coût de l'analyse, il est quelquefois avantageux pour améliorer la convergence de procéder à des sous-itérations selon le modèle ci-dessous :



5 - COUP DE POUCE FINAL

Cette option est très utile en pratique. Elle permet de voir immédiatement, en conversation à l'écran, l'effet de petites modifications des paramètres sur les contraintes sélectionnées, à partir du tableau des dérivées partielles. On prend ainsi en compte très facilement les petites différences inévitables entre le dessin réel et le résultat de l'optimisation.

6 - MAXIMISATION DES MARGES

Nous venons de mettre au point récemment cette option. Elle permet pour une masse limitée de minimiser le maximum des rapports contrainte/contrainte admissible.

Pour traiter ce cas, en s'inspirant de la référence 6, on introduit un paramètre supplémentaire μ représentant le rapport contrainte/contrainte admissible maximum. Le problème d'optimisation non linéaire s'écrit :

$$\begin{aligned} \mu & \text{ minimale} \\ \sigma_j^*(\lambda) & \leq \mu \sigma_j \text{ ad } (\lambda) \\ \sum m_i \lambda_i & \leq \text{Masse admissible} \end{aligned}$$

Ce problème est rapidement résolu par steps d'optimisation linéaire avec des contraintes supplémentaires de linéarité sur les λ (voir planche 6).

7 - EXEMPLES D'OPTIMISATIONS

Nous présentons 2 exemples caractéristiques parmi les calculs que nous avons effectués.

7.1 - Voilure Δ avec contrainte d'aéroélasticité

L'idéalisation de la structure à optimiser est représentée sur la Pl. 3 ; elle comporte 4269 degrés de liberté, sans compter ceux du fuselage dont l'influence est introduite par la méthode des super-éléments (réf. 4).

Nous avons 88 paramètres d'optimisation (épaisseur de maille et section de semelles de longeron, voir pl. 3).

Nous avons 198 contraintes d'optimisation :

- Contraintes élastiques sous 2 chargements (ressource et roulis)
 - . contrainte principale dans les parties de revêtement en traction.
 - . contrainte normale dans les semelles de longerons.
 - . critère de flambage plastique dans les parties de revêtement en compression.
- Réactions aux attaches fuselage limitées pour avoir des oeils identiques (contrainte technologique).
- Contraintes d'aéroélasticité.
 - . avancée de foyer limitée.
 - . pertes sur les efficacités de braquage limitées.

La convergence a été acquise en 3 itérations.

Nous présentons l'évolution de la masse sur la Pl. 3 , le gain de masse a été de 41 kg sur 254 kg de structure paramétrée par demi-voilure, à partir d'un échantillonnage initial raisonnable.

Nous présentons sur la Pl. 3 l'évolution des contraintes les plus significatives.

On trouve sur la Pl. 3 l'évolution des paramètres. On constate que le programme a tendance à transférer la masse vers l'implanture arrière, ce qui n'est pas la tendance qu'on aurait eu en échantillonnage classique ; ce fait est essentiellement dû aux contraintes aéroélastiques ; un relâchement de ces contraintes (Pl. 3') conduit à un allègement supplémentaire de 24 kg par demi-voilure.

7.2 - Empennage en fibres de carbone

Cet empennage à revêtement en fibres de carbone et nid d'abeilles traversant est idéalisé par un maillage à 5500 degrés de liberté (planche 4) comportant des éléments de membrane et de plaque anisotropes ainsi que des éléments tridimensionnels isoparamétriques anisotropes pour le nid d'abeilles.

Le dessin de l'empennage est conditionné par 2 aspects :

- Tenue statique, en particulier, éviter les surcontraintes résultant de l'effet d'entaille dans la zone de l'implanture (94 contraintes type critère de rupture fibre).
- Repousser en dehors du domaine de vol un flutter naturel à cette formule.

On a choisi 135 paramètres d'optimisation représentant l'épaisseur de fibre dans chacune des 4 directions 0°, 45°, 90° et - 45° sur la zone structurale représentée sur la planche 4

La solution optimale où seule la contrainte de flutter est en butée a été obtenue en 4 analyses, à partir de l'échantillonnage résultant de l'optimisation statique ; elle fait passer à Mach 0,9 la vitesse de flutter de 310 m/s à 360 m/s ; cette performance est obtenue par un renforcement important des couches à - 45° (voir pl. 4 et 5).

Remarque : le problème d'optimisation explicite de la première itération n'ayant pas de domaine faisable, il a été nécessaire de relaxer la contrainte de Flutter entre les itérations.

8 - TEMPS DE CALCUL ET TAILLES DE PROBLEME TRAITABLE

Dans les problèmes que nous avons traités jusqu'à présent, le coût est fait en gros de 30 % par les analyses, 60 % par les dérivations, la part de l'optimisation non linéaire étant de l'ordre de 10 % ; le coût global de l'optimisation est de 8 à 12 fois celui d'une simple analyse.

Du point de vue de la taille du problème éléments finis, la limitation est celle de l'analyse (au-delà de 15000 degrés de liberté en une sous-structure).

La limitation la plus sévère est le nombre des paramètres pour le module d'optimisation dont le coût croît entre la puissance 3ème et 4ème du nombre de paramètres, alors que celui de la dérivation est quasi linéaire. Les algorithmes que nous utilisons devront donc être sensiblement améliorés pour passer aux problèmes de la classe des 1000 paramètres.

9 - DEVELOPPEMENT

Nous développons notre outil d'optimisation sur les voies suivantes :

- facilité d'emploi : définition en conversationnel avec contrôle par visualisation sur écran des données de l'optimisation (paramétrage, contraintes et valeur admissible des contraintes).
- calcul approché des dérivées des contraintes élastiques à partir de la réduction modale qui aboutit à un coût intermédiaire entre celui du F.S.D. et de la dérivation exacte actuelle.
- intégration de l'optimisation du dessin local avec l'optimisation générale ; en particulier pour la définition des raidissages optimaux.
- amélioration de l'algorithme d'optimisation non linéaire, pour faire face à une augmentation du nombre de paramètres et de contraintes ainsi qu'à une plus grande non linéarité des contraintes ; pour faire face à ce problème nous utilisons la propriété de "creusité" du tableau des contraintes en fonction des paramètres (dû à la non dépendance de chaque contrainte de tous les paramètres).

Sur le plan théorique, nous essayons d'approfondir les règles de la convergence globale de l'algorithme sans limitation sur l'amplitude des variations de paramètres dans les itérations extérieures ; cette convergence est liée au choix de la formulation explicite approchée des contraintes.

10 - CONCLUSION

Notre approche de l'optimisation représente une évolution radicale par rapport aux méthodes préconisées jusqu'à ces dernières années, notamment sur les méthodes de critères d'optimalité (réf. 8) ; ce progrès se concrétise sur 3 points fondamentaux :

- possibilité d'introduire des contraintes de toutes natures et sans crainte de redondances.
- conditions d'optimalité vérifiées au point de convergence.
- temps de calcul acceptables industriellement.

Un autre avantage de notre processus est sa simplicité théorique apparente qui rend les grandes lignes de l'algorithme compréhensibles par des non spécialistes.

Dans notre approche, analyse et optimisation sont étroitement imbriquées ; pratiquement elles doivent être programmées par la même équipe ; ainsi, la dérivation exacte des contraintes, qui est le point principal de notre processus, a rebuté nombre de nos prédécesseurs, alors que si sa programmation est intégrée à celle de l'analyse, cette séquence devient praticable.

La méthode a rencontré immédiatement un vif succès auprès de notre bureau d'études ; elle est appliquée systématiquement pour tous nos projets après avoir été inaugurée sur le Mirage 2000 et le Mirage 4000.

Sans insister sur les avantages évidents de l'échantillonnage automatique, il faut souligner que la méthode renforce l'emprise du Chef de projet, bien loin de diluer sa responsabilité vers une informatique lointaine et mystérieuse, l'application de la méthode exigeant une vision synthétique préalable du problème traité :

- pour le choix des paramètres qui intègre en partie les contraintes de fabrication.
- pour le choix des contraintes contrôlées.
- pour les règles de contrainte admissible qui doivent être explicitées préalablement.

REFERENCE

- 1 - Optimisation des structures sur modèle d'éléments finis
Marché DRET N° 76.34039
- 2 - C.FLEURY
Le dimensionnement automatique des structures élastiques - Thèse Université de Liège 1977
- 3 - POLAK
Computational method in optimization - a unified approach
- 4 - C.PETIAU N.S. N° 1300 (AMD-BA)
Résolution des grands systèmes linéaires creux
- 5 - C.PETIAU - 14ème congrès International Aéronautique PARIS Juin 1979
Maillage par la méthode topologique conversationnelle et optimisation dans les calculs de structure.
- 6 - Rapport DRET 76/452
Optimisation d'une pièce plane élastique pour minimiser les contraintes (1978)
- 7 - AGARD - Lectures séries No70 on structural optimisation (1974)

ANNEXE 1

PRINCIPE DE LA DERIVATION DES COEFFICIENTS AEROELASTIQUES STATIQUES

1 - RAPPEL DES RELATIONS DE BASE DE L'AEROELASTICITE STATIQUE AVEC ELEMENTS FINIS

- Champ de pression discrétisé

$$K_p = [\partial K_p / \partial q_r] q_r + [\partial K_p / \partial q_s] q_s$$

q_r = effet aérodynamique rigide (incidence, braquage gouvernes, etc...)

q_s = déformation de la surface portante discrétisée dans une base de monome.

- Equation de vol

$$f_{C.D.G.} = 1/2 \rho V^2 ([C_r] q_r + [C_s] q_s)$$

$$[C_r], [C_s] \text{ torseur résultant de } [\partial K_p / \partial q_r], [\partial K_p / \partial q_s]$$

(coefficients
aérodynamiques)

- Charges sur E.F.

$$F = 1/2 \rho V^2 [R] K_p \rightarrow \begin{aligned} \partial F / \partial q_r &= [R] [\partial K_p / \partial q_r] \\ \partial F / \partial q_s &= [R] [\partial K_p / \partial q_s] \end{aligned}$$

- Déformée E.F.

$$X = [K]^{-1} F \Rightarrow \begin{aligned} \partial X / \partial q_r &= [K]^{-1} [\partial F / \partial q_r] \\ \partial X / \partial q_s &= [K]^{-1} [\partial F / \partial q_s] \end{aligned}$$

- Lissage passage E.F. $\rightarrow q_s = [L] X$

$$\textcircled{1} \quad q_s = 1/2 \rho V^2 ([A_1] q_r + [A_2] q_s) \quad \begin{aligned} [A_1] &= [L] [\partial X / \partial q_r] \\ [A_2] &= [L] [\partial X / \partial q_s] \end{aligned}$$

- Elimination effet souple

$$\textcircled{2} \quad q_s = 1/2 \rho V^2 [\mu] q_r, \quad [\mu] = [D]^{-1} [A_1], \quad [D] = [I - 1/2 \rho V^2 [A_2]]$$

- Coefficients aérodynamiques souples

$$\textcircled{3} \quad [C] = [C_r] + 1/2 \rho V^2 [C_s] [\mu]$$

2 - DERIVATION PAR RAPPORT AUX PARAMETRES STRUCTURAUX

- Différenciation de 1 sachant que $\Delta ([K]^{-1} F) = -[K]^{-1} [\Delta K] X$

$$\Delta q_s = -1/2 \rho V^2 [L] [K]^{-1} [\Delta K] ([\partial X / \partial q_r] q_r + [\partial X / \partial q_s] q_s) + 1/2 \rho V^2 [A_2] \Delta q_s$$

- en éliminant q_s par 2

$$\Delta q_s = -1/2 \rho V^2 [D]^{-1} [L] [K]^{-1} [\Delta K] ([\partial X / \partial q_r] + [\partial X / \partial q_s] [\mu]) q_r = [\Delta \mu] q_r$$

- Différenciation de 3 $[\Delta C] = 1/2 \rho V^2 [C_s] [\Delta \mu] \longrightarrow$

$$[\Delta C] = 1/2 \rho V^2 [C_s] [D]^{-1} [L] [K]^{-1} [\Delta K] \left[\left(\partial X / \partial q_r \right) + \left(\partial X / \partial q_s \right) [\mu] \right]$$

- Préférable sous les formes

$$\bullet [\Delta C] = 1/2 \rho V^2 \left([K]^{-1} ([C_s] [D]^{-1} [L]) \right)_t [\Delta K] \left[\left(\partial X / \partial q_r \right) + \left(\partial X / \partial q_s \right) [\mu] \right]$$

qui demande la résolution de l'équilibre sous un seul chargement par coefficient aérodynamique à 1 Mach et une pression dynamique donnée.

$$\bullet [\Delta C] = 1/2 \rho V^2 [C_s] [D]^{-1} \left([K]^{-1} [L] \right)_t [\Delta K] \left[\left(\partial X / \partial q_r \right) + \left(\partial X / \partial q_s \right) [\mu] \right]$$

qui demande le rang de q_s résolutions (quelques dizaines), qui s'amortissent pour tous les Mach et pressions dynamiques.

ANNEXE 2

Dérivation de la vitesse de Flutter (Méthode de J.P. BREVAN)

I - ANALYSE

- On pose résolu l'équation de Flutter à un Mach donné

$$\left[K(\lambda) - \omega^2 (1 + i g)^2 M(\lambda) - \rho V^2 A \left(\frac{\omega}{V} \right) \right] q = 0$$

- [K] matrice de rigidité réduite
- [M] matrice de masse réduite
- ω pulsation de la solution
- g amortissement ($g=0 \longrightarrow$ Flutter)
- V vitesse
- [A] matrice des forces aérodynamiques
- p solution droite
- q solution gauche

- Soit sous forme simplifiée

$$\textcircled{1} \quad [D(\lambda, \omega, g, V)] p = 0$$

$$\textcircled{2} \quad P_t [D(\lambda, \omega, g, V)] = 0$$

avec $g = 0$ (ou donné)

II - DIFFERENTIATION

$$\textcircled{1} \quad \longrightarrow \Delta ([D] q) = [\Delta D] q + [D] \Delta q$$

en multipliant par P_t

$$P_t [\Delta D] q + P_t [D] \Delta q$$

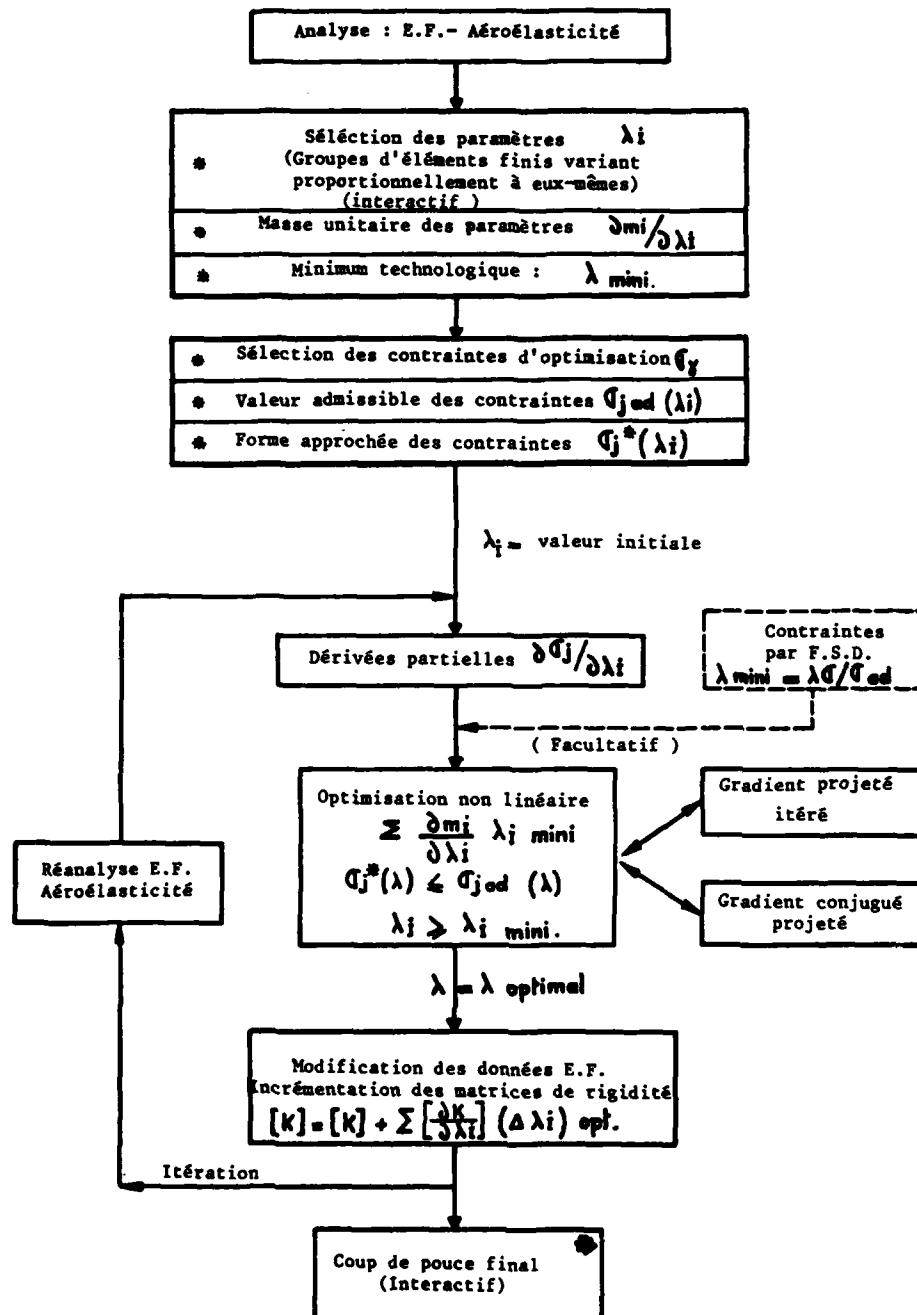
$$\text{par } \textcircled{2} \quad P_t [D] \Delta q = 0$$

Soit si on fixe l'amortissement g

$$\textcircled{3} \quad P_t \left[\partial D / \partial \lambda \right] q + P_t \left[\partial D / \partial \omega \right] q + P_t \left[\partial D / \partial V \right] q = 0$$

Equation complexe dont la résolution donne les dérivées de la pulsation de la solution et de la vitesse de Flutter.

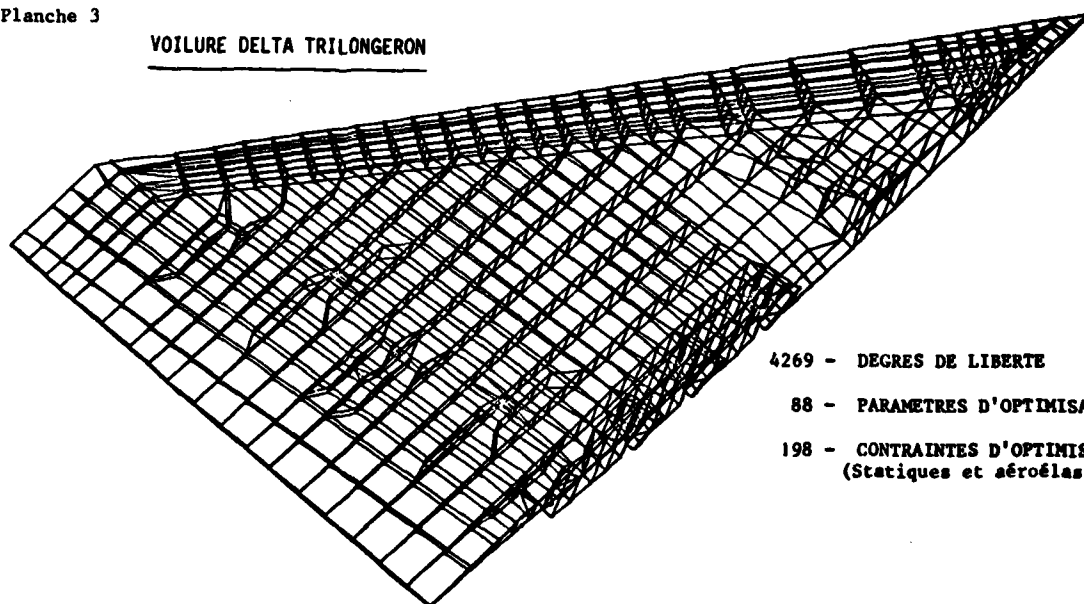
ORGANIGRAMME GENERAL DE L'OPTIMISATION



* Phase interactive

Planche 3

VOILURE DELTA TRILONGERON

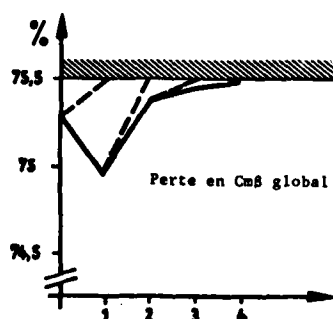
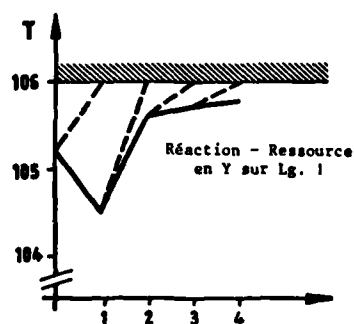
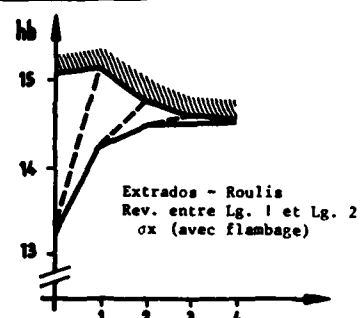
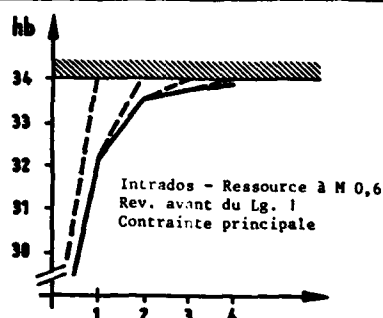
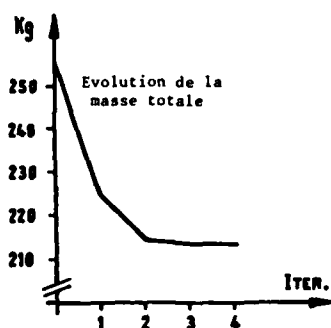


4269 - DEGRES DE LIBERTE

88 - PARAMETRES D'OPTIMISATION

198 - CONTRAINTES D'OPTIMISATION
(Statiques et aéroélastiques)

EVOLUTION DE LA MASSE TOTALE ET DE DIVERS TYPES DE CONTRAINTES



— contraintes calculées
- - - contraintes estimées

EXTRADOS

CARACTERISTIQUES COMPAREES DES PARAMETRES

- AVANT OPTIMISATION
- APRES OPTIMISATION AEROELASTICITE BLOQUEE
- ESTIMATION AEROELASTICITE LIBREE
- GAIN DE MASSE 25 Kg

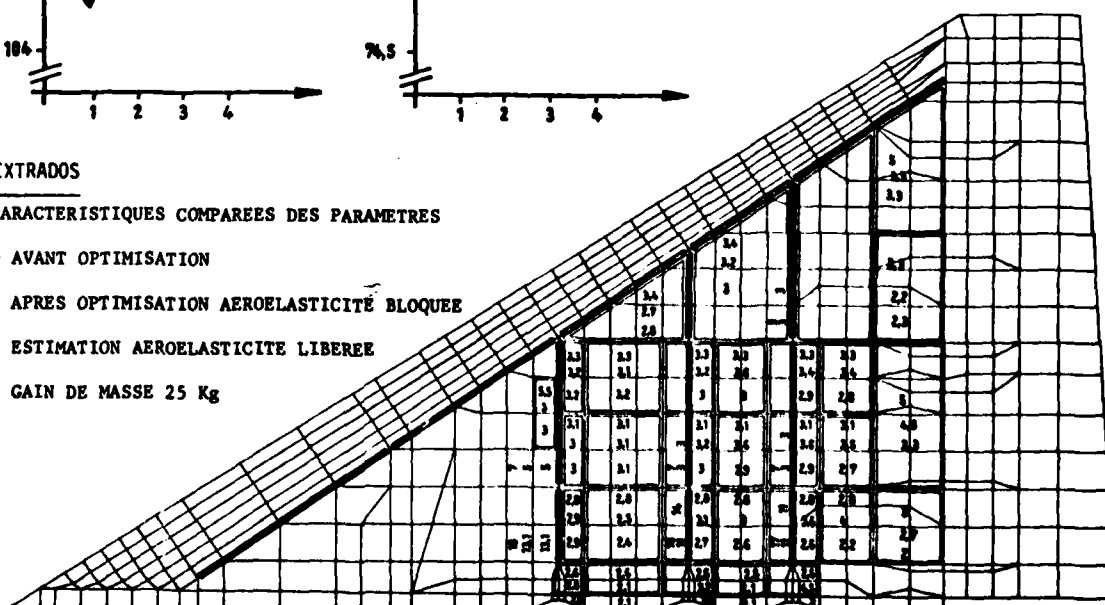
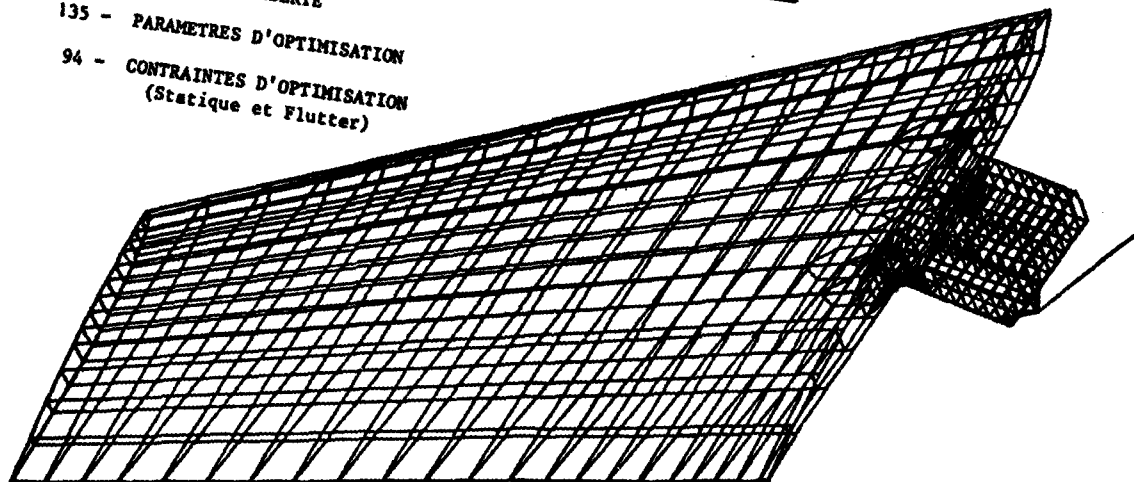


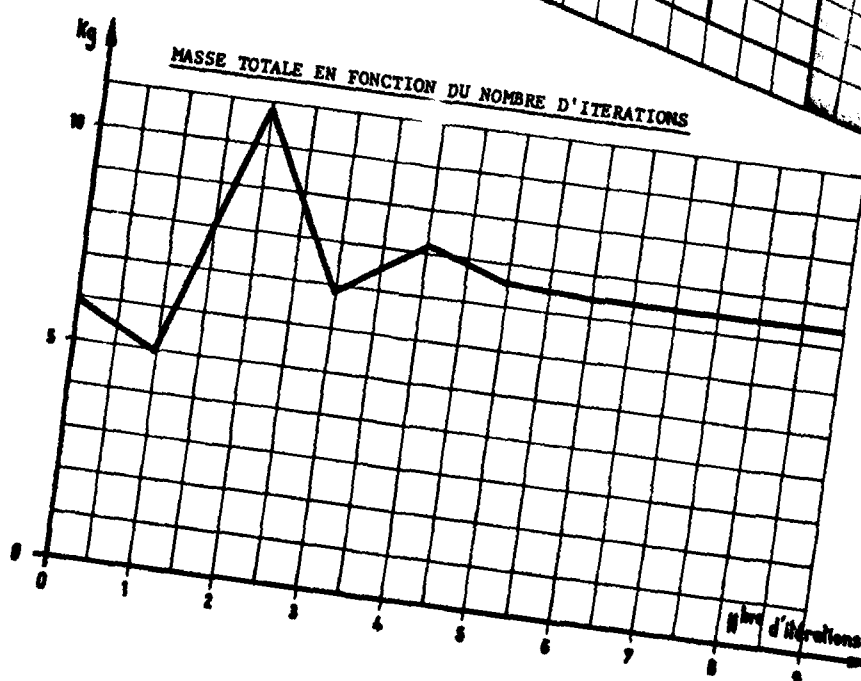
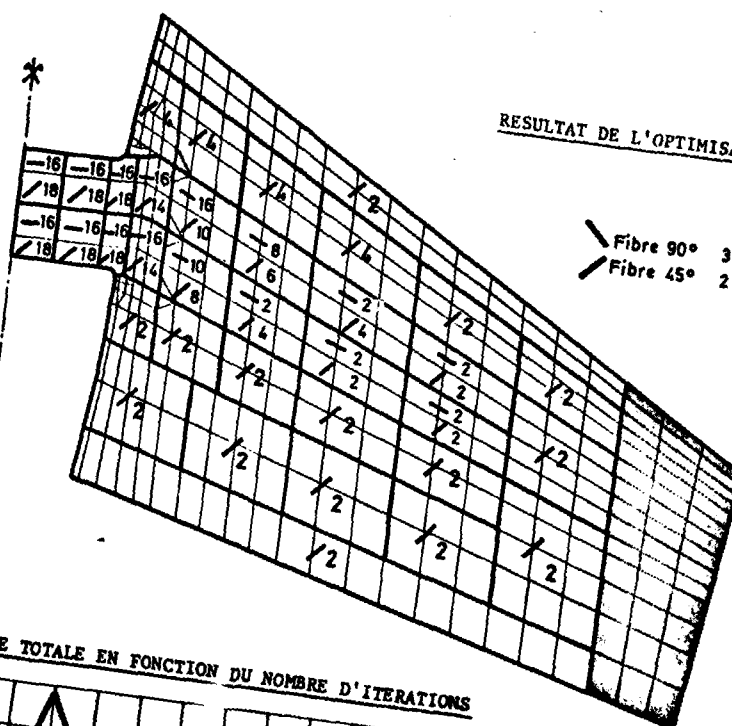
Planche 4

EMPENNAGE EN FIBRE DE CARBONE

- 5300 - DEGRES DE LIBERTE
 135 - PARAMETRES D'OPTIMISATION
 94 - CONTRAINTES D'OPTIMISATION
 (Statique et Flutter)



RESULTAT DE L'OPTIMISATION



EMPENNAGE EN FIBRE DE CARBONE
EVOLUTION DU FLUTTER

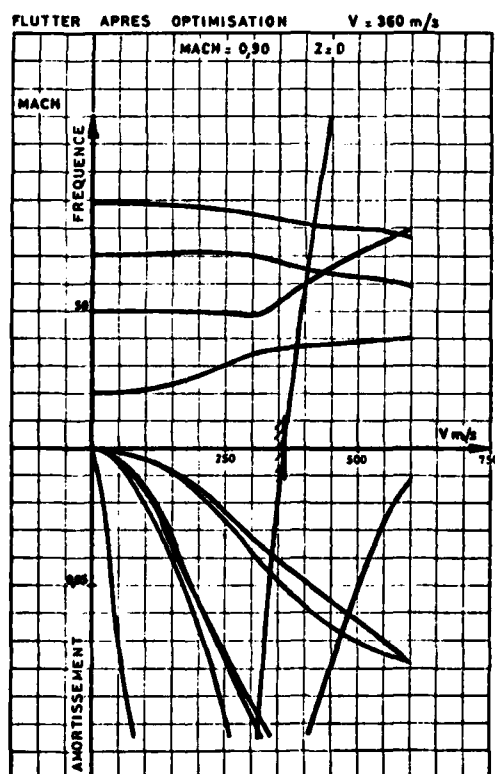
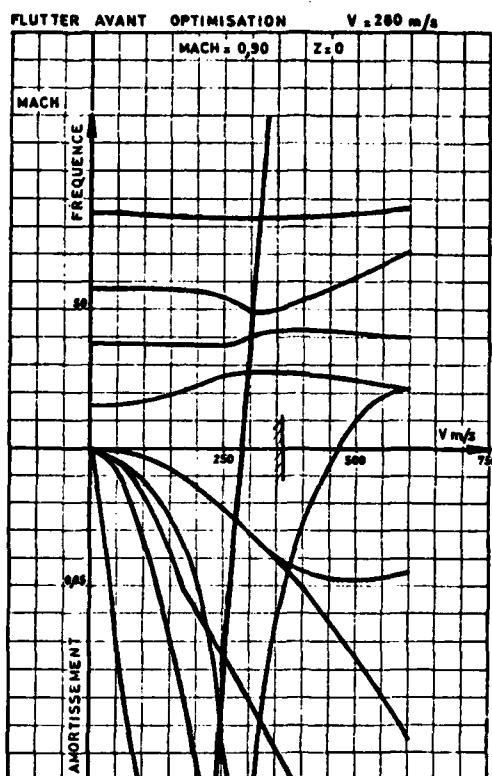
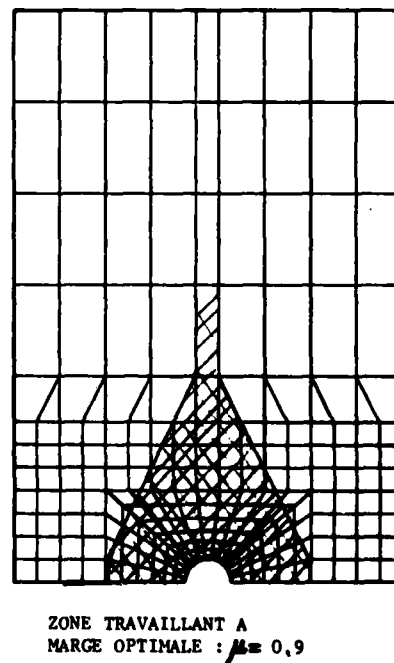
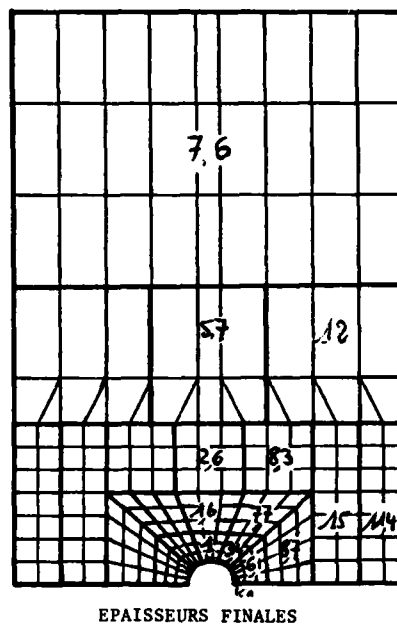
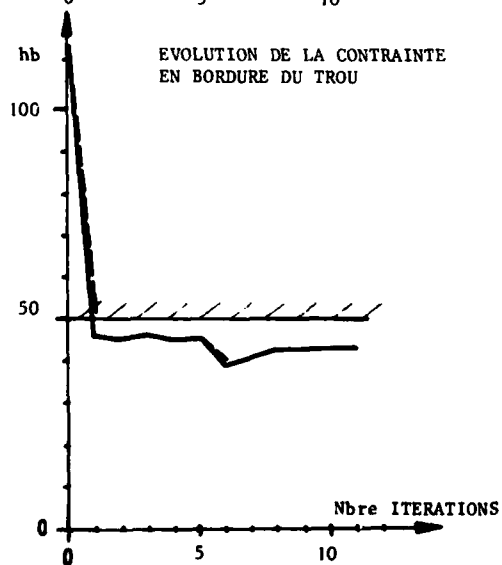
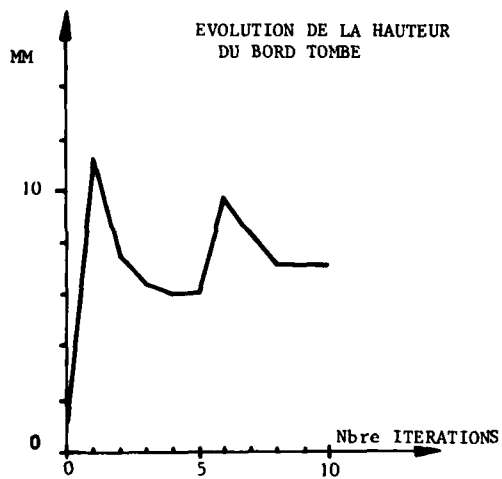
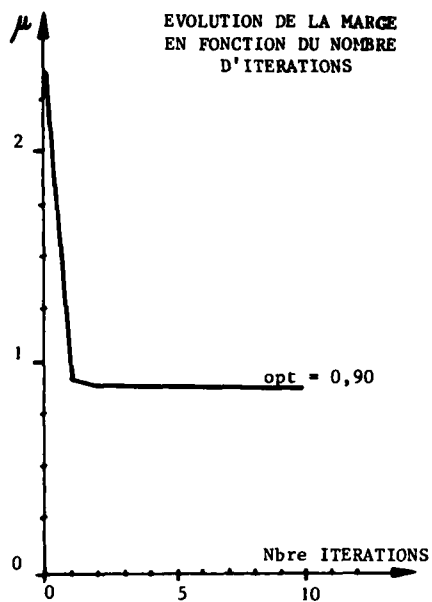


Planche 6

MAXIMISATION DE LA MARGE SUR UN TROU BORDE



NEW COMPUTER APPLICATIONS FOR SPECIAL STRUCTURAL PROBLEMS

by

Dipl.-Ing. Jürgen Maßmann

Industrieanlagen-Betriebsgesellschaft mbH
Einsteinstraße 20, 8012 Ottobrunn, Germany

Summary

Characteristic properties of both the Finite-Element and Finite Difference method are discussed concerning their efficient applicability for nonlinear dynamic structural analysis and design. Then a mixed Finite Element / Finite Difference method is pointed out which combines the advantageous parts of the respective approaches. Special features of the code are explained and their relevance is demonstrated in several examples concerning penetration and perforation problems, pressure distribution resulting from explosions in fluids, blast loading and shock wave propagation. Further research is indicated to complete the experimental data and to improve the codes, e.g. concerning the pre- and post processing capabilities.

Moreover the need for more efficient hardware configurations is confirmed.

1. Introduction

In many spheres of engineering solutions of stress distributions are required, taking into consideration elastic-plastic flow, large displacements and dynamic response. Special cases of such problems may range from two dimensional plane stress or strain distributions, axisymmetrical configurations, plate bending and shells to fully three dimensional high velocity impact calculations and fluid-structure interaction. In many cases parametric tests on structures or parts are unfeasible so that appropriate calculation methods have to be applied. The Finite-Element method (FE-method) as well as the Finite-Difference method (FD-method) rendered to be efficient tools in solving a wide range of structural problems.

The subject of this paper is first to give a short summary of the different methods and their efficient application and second to show a new approach which takes advantage of the benefits of both the FE- and the FD-method. Special characteristics of the approach are shown too. The relevance will be demonstrated in several applications. Finally the necessity for further development in this field is indicated.

2. Comparison of the Finite-Element and Finite-Difference method

Most of the present problems of the analysis and design of complex structures cannot be solved using traditional methods. However, the FE- and FD-method is appropriate to determine the structural behavior including nonlinear and dynamic response. To show the differences between both methods, a short description of the essential parts of the methods will be given first.

2.1 FE-method

The Finite-Element method is essentially based on the following concept: The continuum which should be analysed is separated into a number of "Finite Elements" of almost arbitrary shape.

Special functions define the state of strain within an element in terms of the nodal point displacements with high accuracy. These strains together with any initial strains and the constitutive properties of the material will define the state of stresses throughout the element and the nodal point forces. Equilibrium of these nodal point forces, of loading and - in case of a dynamic response - the forces of inertia and damping lead together with the compatibility criteria to the well known stiffness matrix approach.

This assembly process is fundamental for the Finite-Element method. Once the solution of the unknown displacements has been obtained the stresses and internal forces of each element can be computed. In case of nonlinear constitutive relationships a solution can be achieved using a tangential stiffness matrix with either the initial strain or the initial stress method.

Large deformations are taken into account by continuously updating the nodal point co-ordinates and thus by using actual stiffness-relationships; to involve large strains special procedures are applied. However, to perform any kind of nonlinear analysis the piecewise linear solution process shown above has to be done repeatedly.

2.2 FD-method

As distinguished from the FE-method the basic idea of the FD-method is to approximate the differential equations of the problem by the corresponding difference equations. For all points of the solution field the 'finite' equations can be defined in a system of uncoupled algebraic equations for the unknown parameters. Consequently the equations of motion can be solved by performing an explicit integration.

The quality of the results depends much on the size of the quadrilateral zones which represent the discretization scheme widely used in the FD-application. The finite time steps are achieved by a partition of the time axis whereby the single time step may not exceed the upper bound governed by some convergence criteria to ensure stability of the difference integration scheme.

Since the solution algorithm embraces the uncoupled equations of motion and the actual nodal point locations and forces the FD-method allows the adding of nonlinear effects during each time step without significant increase of computing time.

Both the FD- and FE-method offer the ability to handle the problem in a Lagrangian co-ordinate system in which the co-ordinates move with the material. In addition the FD-method contains also an Eulerian co-ordinate system where the material flows through a fixed grid. This formulation is extremely useful for fluid flow problems. A further feature is the coupling of the Lagrangian and the Eulerian co-ordinate system.

2.3 Valuation of the FE- and FD-formulation

The basic statements of both the FE- and FD-method show the FE-method to be the more flexible approach as to the discretization of complex structures. The FE-method does not require a sequential arrangement of nodes and elements compared to the FD-method. In addition the FE-method allows to use different types of elements which lead to high accuracy of the stress and strain fields in the structure depending on the complexity of the shape functions. As a consequence the accuracy of the FD-method in general will be exceeded by a Finite-Element approach using at least a quadratic polynomial formulation for the shape function.

Moreover the FE-method allows an unconstrained consideration of arbitrary structural configurations with any boundary conditions. In fact most of the FD-methods only use a constant approximation of the stress fields within the zones; however, related to the investigation of dynamic problems involving elastic plastic flow with large displacements and large strains the FD-method based on the direct integration of the equations of motion yields an acceptable solution at significant lower costs than the FE-formulation does. In addition to this the FD-method includes the ability to consider the effects of shockwave propagation and the use of Lagrangian and Eulerian co-ordinate systems and their coupling.

2.4 Application of the FE- and FD-method

As shown before, linear static and dynamic problems will be solved efficiently using the FE-method, especially for the three dimensional analysis of structures this approach proved to be the most appropriate method due to the accurate idealization of the structure's geometry and the boundary conditions. As a result of its general validity which for instance are appropriate to solve stability-, temperature- or fracture mechanics problems. Concerning nonlinear dynamic problems however, a more economic solution will be achieved by the use of the FD-method. In contrast to the FE-method which requires the permanent updating of the stiffness- and mass matrix and hence the recalculation of Eigenvalues and Eigenvectors, the FD-method with its straight forward integration scheme enables for instance the inclusion of nonlinear material behavior, crack formation, contact problems as well as hydro-mechanical problems at acceptable costs. Especially short term effects can be handled adequately with the FD-method.

2.5 Mixed Finite-Element / Finite-Difference formulation

Accounting for all the profits of both, the FE- and FD-method a mixed Finite Element/ Finite-Difference method has been established which not only makes use of the higher order Finite-Elements and of the ability to idealize even more complex structures but also takes advantage of the explicit integration procedure of the FD-method in order to deal with any nonlinearity. As the Lagrangian co-ordinate system is better suited to handle the plastic flow of materials and to perform large deformation analysis with large strains, here the Eulerian formulations are mainly used to investigate fluid flow problems. The coupling of both the Lagrangian and the Eulerian co-ordinate systems allows the efficient treating of fluid/structure interaction.

In this section a review is given concerning this mixed FE/FD-method and some of its special features. As to the idealization of the structure and the description of its boundary conditions the same procedure is used as it is known from the FE-method. Then the initial conditions of the problem are established in assigning starting values for

the displacements, velocities and the loading to corresponding element nodes. At these nodes also the distributed mass is proportionately concentrated (lumped masses). This information is sufficient to calculate in a first step the nodal point's displacements and velocities; these are used in a further step to obtain the corresponding strains and strain-rates within the elements. With the adopted model of the material's behavior the resulting stress and nodal point forces are computed within the element. The nodal point forces in conjunction with the corresponding masses are the information used to perform the integration scheme. As a result the nodal point displacements, velocities and accelerations of the actual integration cycle are achieved. These results are supplied by the actual boundary conditions and by possibly enforced displacements in order to get the actual element stresses and hence the element nodal forces. After adding an appropriate time-increment the whole integration- and updating process is repeated until the time of interest has elapsed. To prevent numerical instability during computation the time-increment is controlled. Depending on element's characteristic length d and on the material's sound speed c the time-increment Δt should be less than $x \cdot d/c$ whereby the safety factor x ranges between 0.5 and 0.7. The flow chart in Figure 1 shows the overview of the algorithm covering the Lagrangian part of the formulation.

This consideration of the motion of material points is essentially the Lagrangian formulation; hereby the conservation of mass is achieved automatically and the variation of an element's volume is adjusted by the respective variation of the material's density. In contrast to this in the Eulerian formulation, the material flows through a fixed co-ordinate system, and due to the fact that the conservation of mass is not obvious, the balance of momentum obtains an additional term concerning the mass transportation.

After the establishment of initial values of the problem, the loop on the cycles is opened starting the calculation of the strain rates, the pressures and the appropriate time-increment. The resulting deviator stresses are used to update the momenta and the energy of the cells. To update the cell-masses, momenta and energy due to the effects of transport, the volumes of material leaving the cells are computed. Finally if conservation of energy is ensured the whole procedure can be performed adding the corresponding increments of time until the projected period of time has elapsed. The flow chart of an Eulerian code is shown in Figure 2.

Coupling the Eulerian- and Lagrangian formulations, the pressure of the Eulerian cells at the interfaces is transferred to the Lagrangian part and the velocities of the Lagrangian elements at the interfaces are transmitted to the Eulerian part of the code respectively.

To make use of the described advantages a code has been developed to handle the dynamics of structures with multiple material behavior and arbitrary shapes (DYSMAS). This code includes one, two and three dimensional FE/FD-formulation in both a Lagrangian and Eulerian co-ordinate system.

2.6 Special features of the mixed FE/FD-method

Some special features are mentioned which effect this approach to be an efficient tool for the analysis of dynamic response of structures, fluid problems and fluid-structure interaction.

2.6.1 Material behavior

Preliminary to a plastic flow problem is the adoption of a reasonable yield criterion. Figure 3 shows the linear and parabolic Mohr-Coulomb yield criterion which for example can be used to model rock behavior. For structures made of steel and aluminium alloy the well-known von Mises yield criterion has proved to be a good approximation. Figure 4 contains a comparison between the test results and calculated values using the von Mises criterion. The flow rule defines the plastic strain increment in relation to the yield surface. For steel and aluminium alloy the flow rule according to Prandtl-Reuss (associated flow rule) gives best results as compared to the test data whereas the non-associated flow rule according to Hencky supplies an approximation of the plastic flow with significantly lower computing time. These rules are applied to ideal elastic-plastic materials. To realize arbitrary stress-strain relationships the so-called sublayer model or Mroz plasticity is used which results from a special superimposition of several ideal elastic-plastic stress-strain curves. Figure 5 shows schematically the principle of the Sublayer Model. To demonstrate the accuracy of the Sublayer Model Figure 6 shows the calculated stresses and strains for loading and unloading conditions.

This example illustrates the ability of the Sublayer Model to describe the hysteresis effects in the material (Bauschinger effect) and to perform a closed loop for cyclic loading. Furthermore experiments and calculation have been performed in parallel to check the accuracy of this model. In Figure 7 is shown a half of a notched specimen which is loaded with a bending moment and in Figure 8 the measured and calculated strains are compared. As a result, the Sublayer Model provides an accurate description of the elastic-plastic strain field.

2.6.2 Cracking

In most Lagrangian FE-codes failure within a cell is handled by modifying the stress tensor, e.g., if the pressure is negative all stress components are set to zero and for positive pressure only the deviatoric stress components are set to zero. The mesh will not be changed. Therefore the idealization of cracks in the structure is not taken into consideration properly. However, the modification of the mesh is essential for some calculations, e.g. for the penetration process.

This is the reason why a cracking procedure has been adopted to modify also the idealization of the structure. If a user-defined failure criterion is exceeded in an element this element will be separated from the surrounding elements by defining new nodal points and their physical properties, initial conditions etc. Figure 9 shows a flow chart of the principle process. It is possible with this procedure to start with one structure consisting of n -FE-elements and stop the calculation having n structures with one FE-element in an extreme case. To demonstrate this feature a test case is shown in Figure 10. The crack direction was found by the code itself.

To take into account closing of the crack properly the contact problem has to be solved by using masterplanes, -lines and slave points. Some details are described in the following (see also Figure 9).

2.6.3 Contact problem

The contact problem occurs, when two or more structures or parts of a structure come into contact at predefined surfaces, e.g. in the case of impact or crack closing. Following the contact of surfaces three main parts have to be performed after each time step. First, coordinates of overlapping parts of the structure have to be modified to fulfill the geometric conditions of contact. Second, the velocities of the points in contact must be corrected due to the conservation of momentum with respect to the direction of impact and third, the contact forces caused by impact and friction have to be generated. The definition of the contact surfaces has been done by the use of so-called masterplanes, -lines and slave points with the condition that slave points are not allowed to penetrate a masterplane or -line.

This procedure becomes complicated if there are more than two structures in contact which especially occurs when the cracking option is applied. Figure 11 shows an example of a structure with 4 opened cracks and in addition, the new position of the nodal points before the contact processor is used. The above described rule - which stops the movement of the slave points at the masterplane - does not define a definite solution. It is necessary to take into account some additional considerations to solve this problem, e.g. to stop the movement of a masterplane or -line if a slave point will be overrun. Figure 12 shows a precracked structure under compression after certain time steps. It is shown that the applied procedure is able to handle the multiple contact problem.

2.6.4 Automatic subcycling

In general fully three dimensional calculation as is required for instance to process striking and penetration problems is time consuming and hence expensive. This fact has induced the implementation of procedures checking special parameters for their exceedance of user-defined bounds. If there is not significant change in the resulting physical properties of an element, then this element will be skipped for further considerations within the respective cycle. This procedure results in a considerable reduction of computing-time.

2.6.5 Switch from simple to complex element types

The reduction of computing time requires the application of complex types of elements with higher order functions for the strains and stresses only in those structural regions where it is necessary. A practical solution for this problem is obtained by a procedure which automatically changes a simple element type into a more sophisticated one if a special criterion is satisfied, e.g. if the bending strain in a constant strain element exceeds a defined level.

2.6.6 Solution of static problems

If special damping coefficients are established the mixed FE/FD-method is also applicable for the solution of static problems. In this case the solution scheme is similar to the 'dynamic relaxation' approach. Optimal damping results in a fast convergence to the state of equilibrium. This procedure can be applied efficiently for highly nonlinear problems, e.g. large deformation, contact, friction and nearly incompressible material behavior.

3. Special applications of the FE/FD-codes

To show the relevance of the methods described above and to illustrate their applicability some special structural problems are discussed.

3.1 Penetration and perforation problems

The description of the penetration and perforation process of a projectile through a target is a relevant question in the field of the design of armour and projectiles. The needed result is the ballistic limit velocity for different impact angles which requires a fully three dimensional analysis. Figure 13 shows a cylindrical fragment striking a thin plate (only a quarter of the total structure is idealized). The deformation of the fragment can be seen. In this case the residual velocity is zero which agrees with test results very well. In Figure 14 a long rod projectile penetrates a plate. The presented view indicates the formation of a plug. Further applications of the FE/FD-method have been performed to investigate the structural behavior of warheads.

3.2 Pressure distribution resulting from an explosion in a fluid

The FE/FD-method (Eulerian formulation) allows the calculation of pressure distributions as a function of time caused by a detonation in a fluid. As an example some results of an underwater explosion are shown. In Figure 15 the idealization of the problem is demonstrated. Figure 16 reveals the size of the gas bubble and deformed shape of the water surface. Figure 17 presents contours of equal pressure.

As a further example calculated and measured results of an explosion in a test tube will be compared. Figure 18 contains the geometry of the test case. Figures 19 and 20 show the measured and calculated pressure as a function of time. Not only the maximum pressure (see Tab. 1) but also the subsequent peaks are in good agreement.

3.3 Blast loading

A critical loading of a structure can be the blast loading induced by a detonation of explosives. To analyse the response of the structure analytical solutions, FE-, FD- and FE/FD-methods can be applied. Figure 21 points out the results of these different methods. The comparison shows a good agreement of the results of the respective methods. The deformation of the structure as function of time is illustrated in Figure 22. The formation of different shapes of the deformed structure can be seen. This effect is demonstrated best by the FE- and FE/FD-methods. However, the calculation time differs significantly. In this case including large deformations, nonlinear material behavior and dynamic response the FE/FD-method requires by a factor of 50 less computing time than the FE-method does. This example shows the advantages of the explicit integration procedure of the FE/FD-method.

For another example of a blast loaded structure the boundary conditions and the loading are shown in Figures 23 and 24. For this shell structure special consideration is given to the following nonlinearities

- large displacements and strains
- nonlinear material behavior
- different boundary conditions along the edges
- instabilities like snap buckling of the dynamically loaded shell.

Figures 25, 26 and 27 show at different times the deformation which finally results in the buckling of the shell. This behavior is in good agreement with test results.

3.4 Shockwave propagation in a structure

The shock induced loading of some components can be the most critical strength concerning the functionality. Therefore field tests and calculations of the highly dynamic loaded structure have been performed to obtain the occurring accelerations as a function of time or shock spectra respectively to determine the most important design parameters. Figure 28 shows a comparison between measured and calculated results for different design parameters. Due to the good agreement the investigated structure has been optimized using the calculation method. Only a few field tests have been performed to check the recommended solution.

Conclusion

The discussion of the current FE- and FD-methods for structural analysis and design proved the mixed FE/FD-formulation to be highly qualified to perform nonlinear dynamic structural response. This is not only due to the comprehensive abilities concerning the handling of most different structural problems but also to the fact that it's solution algorithm yields the structural response consuming less computer time than the FE-method but keeping the accuracy of the solution. Concerning the idealization of complex structural configurations, the FE/FD-method turned out to be the more flexible approach compared to the FD-method. This valuation is confirmed with regard to the realization of advanced features and their implementation into the code. These improvements of the FE/FD-code should be referred to an extension and completion of the physical models. Moreover advanced cavitation models should be implemented to improve the description of the fluid structure interaction. Further refinement should be applied to the failure models in order to improve the prediction of crack occurrence and direction. To reduce the processing time an advanced subcycling as well as an appropriate coupling of one and two dimensional or two and three dimensional formulations may contribute. In addition the coupled application of analytical methods is supposed to reduce the computing time considerably.

Furthermore pre- and postprocessors should be refined in order to reduce the costs for the idealization of the structure and the interpretation of the results. Faster computers allow a more detailed investigation of these problems within a reasonable computing time. Also an enlarged memory should be applied to handle most of the problems in core. In addition parallel processing may reduce the computation time significantly. However, the compiler should support the program or the organization of the program itself has to be adjusted.

Condition to improve the calculation method and to verify the results data from parametric tests are necessary. These data can be used to find out more sophisticated physical formulations and validate the calculation results in detail.

TABLE 1

Comparison of Calculated and Measured Maximum Pressure

	TEST (BAR)	CALCULATION (BAR)
CASE 1	11	12
CASE 2	28	29.5

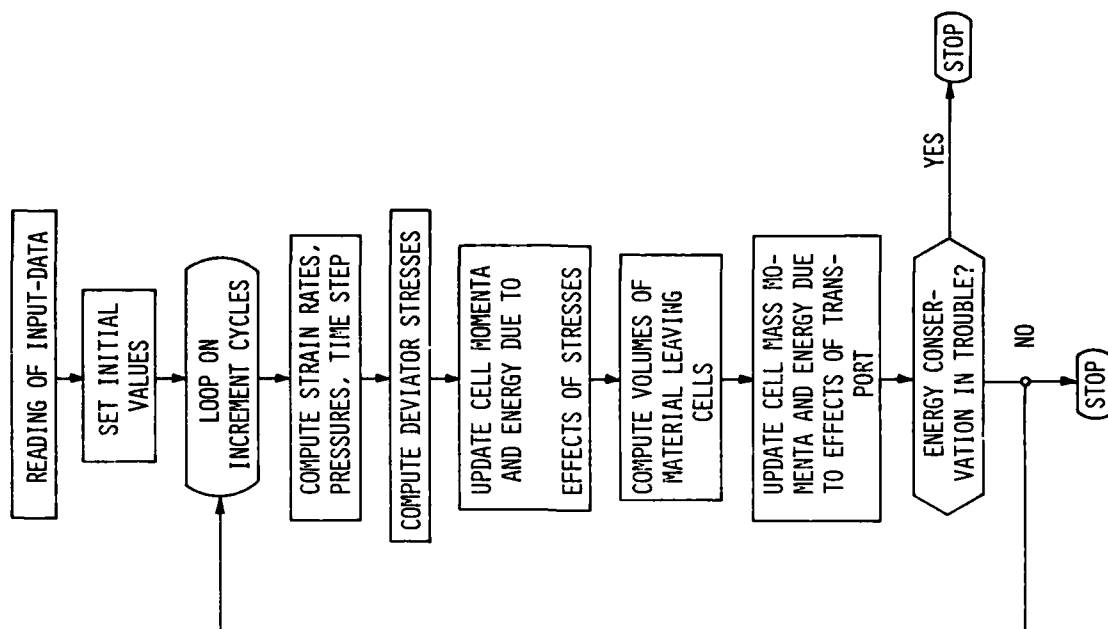


Fig. 2 Flow chart of the Euler-code

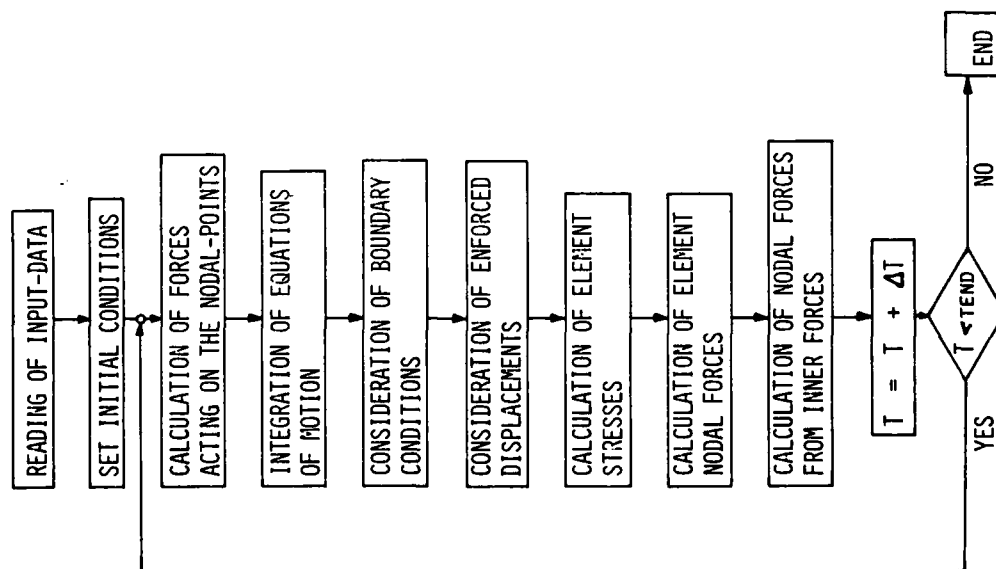
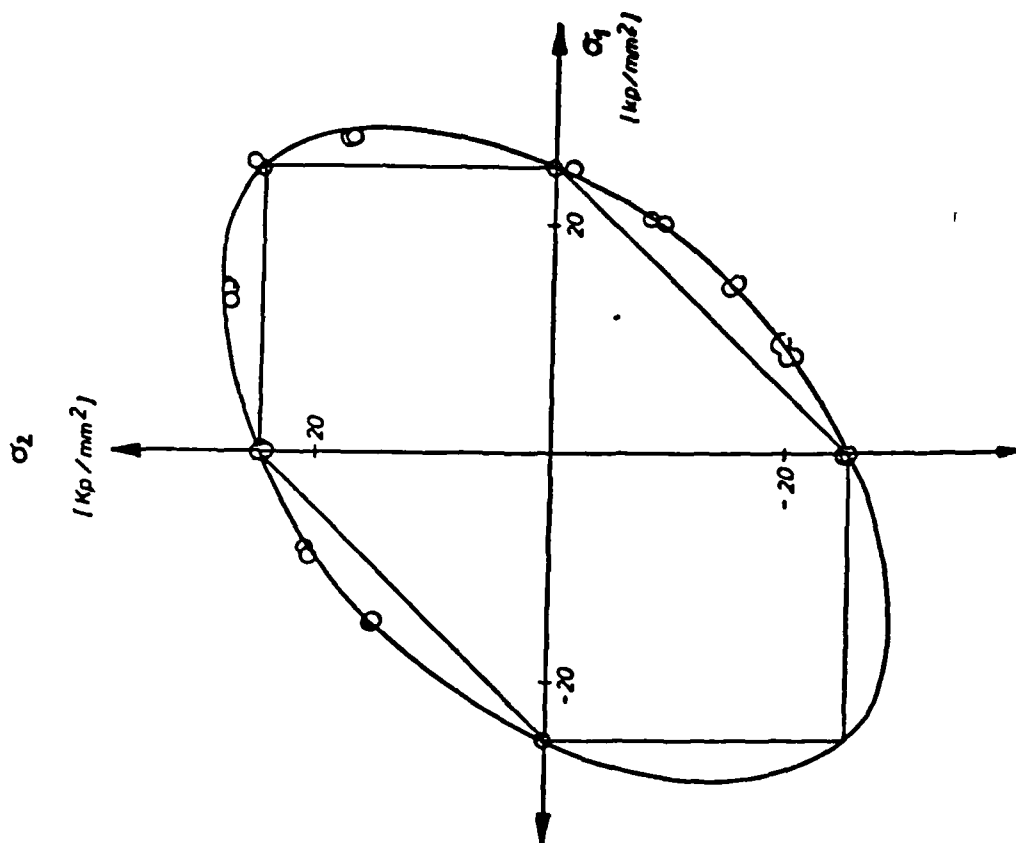
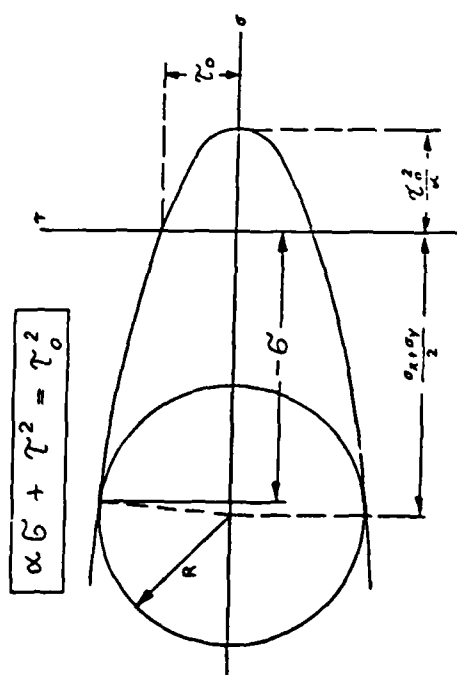
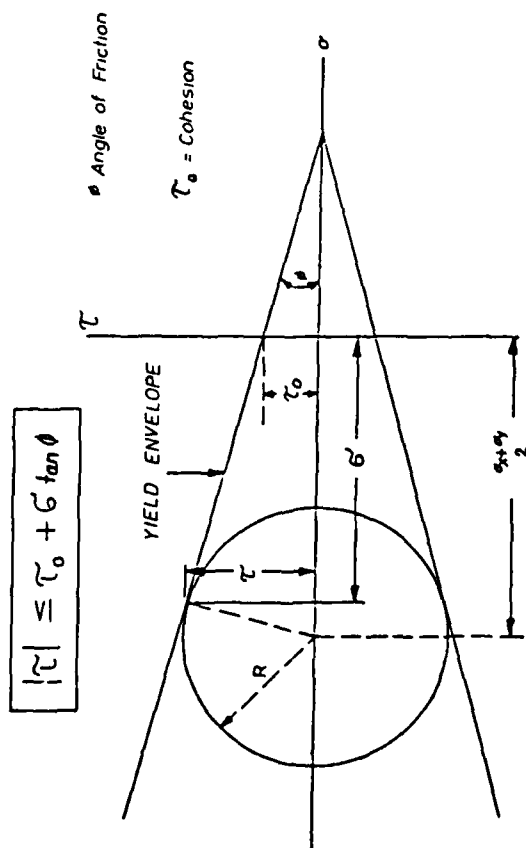
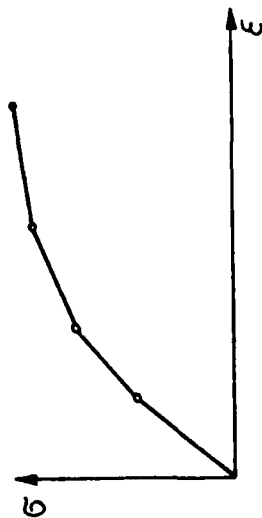
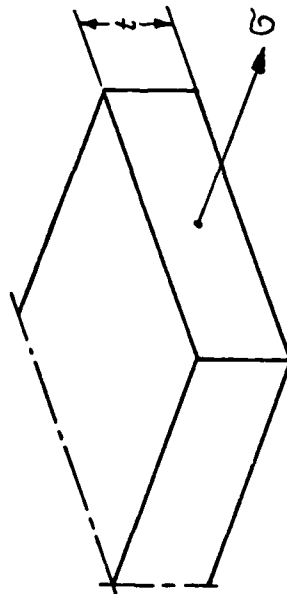


Fig. 1 Flow chart of the FE/FD-code (Lagrange)

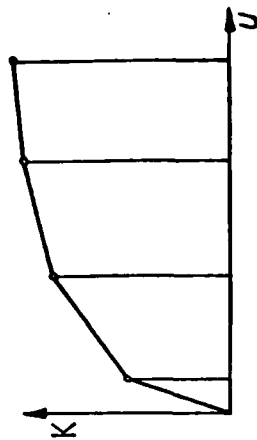




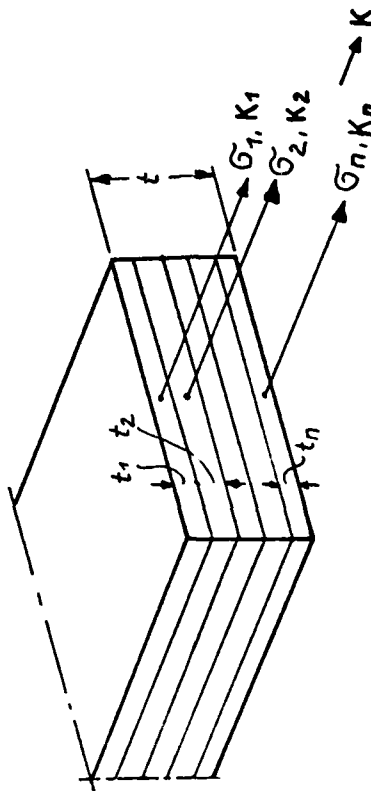
A1) STRESS-STRAIN-CURVE IDEALIZED WITH A PIECEWISE LINEAR FUNCTION



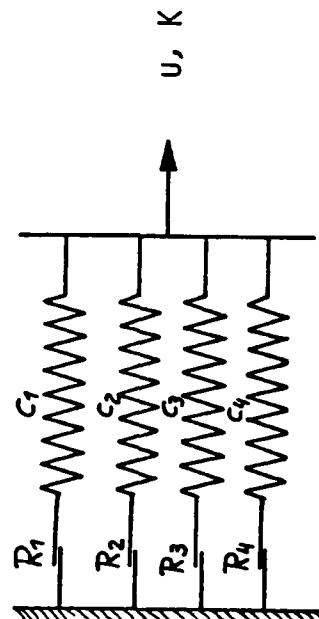
B1) CROSS-SECTION



A2) RESULTANT STRESS-STRAIN-CURVE OF THE SUBLAYER MODEL



B2) CROSS-SECTION WITH SUBLAYERS



C2) MODEL FOR SUPERIMPOSITION OF DIFFERENT SUBLAYERS WITH IDEAL ELASTIC-PLASTIC MATERIAL BEHAVIOR

Fig.5 A1-C2
Description of the sublayer model
(MROSZ-plasticity)

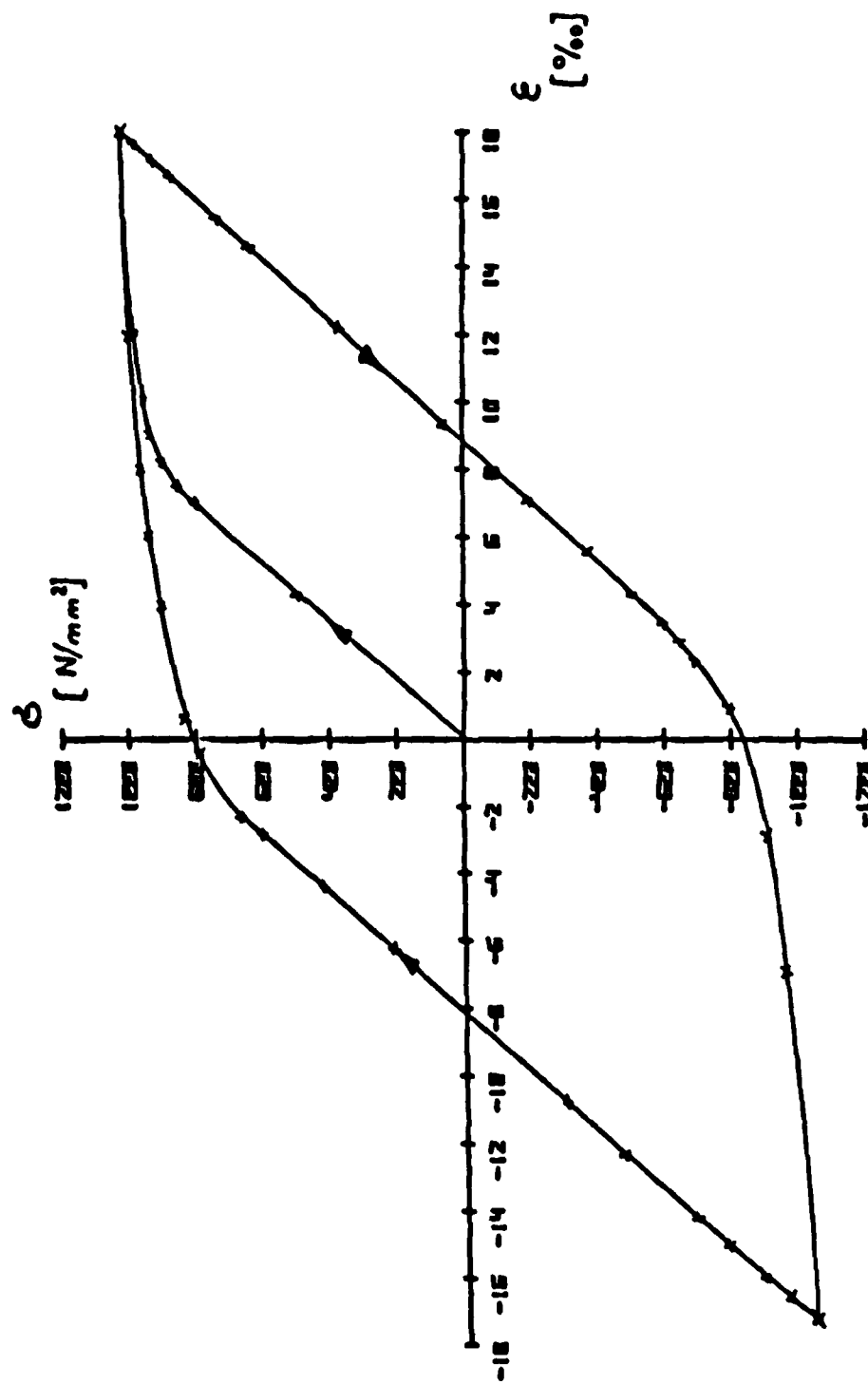


Fig.6 Stress as function of strain for an unnotched specimen with cyclic loading

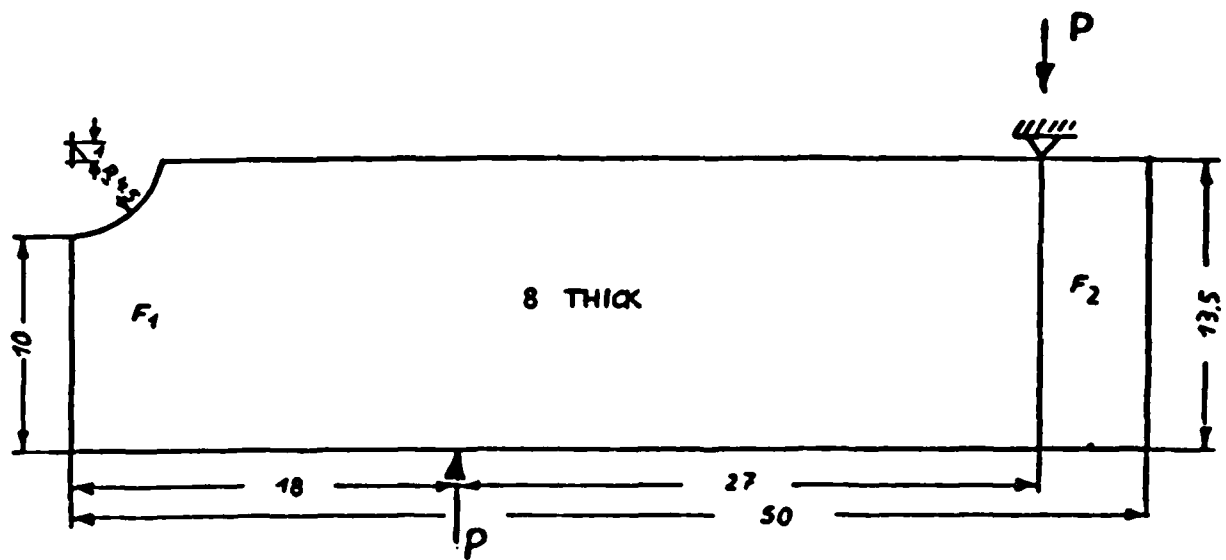


Fig.7 Notched specimen

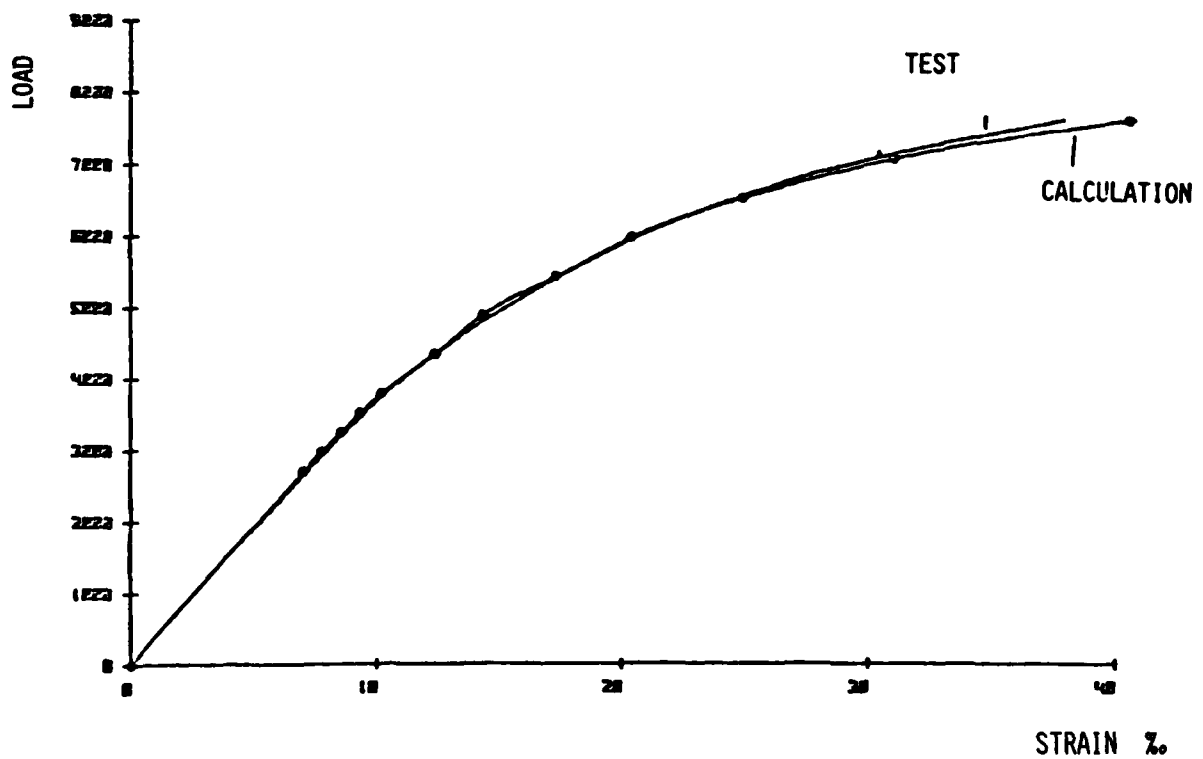


Fig.8 Comparison between measured and calculated strains of a notched specimen

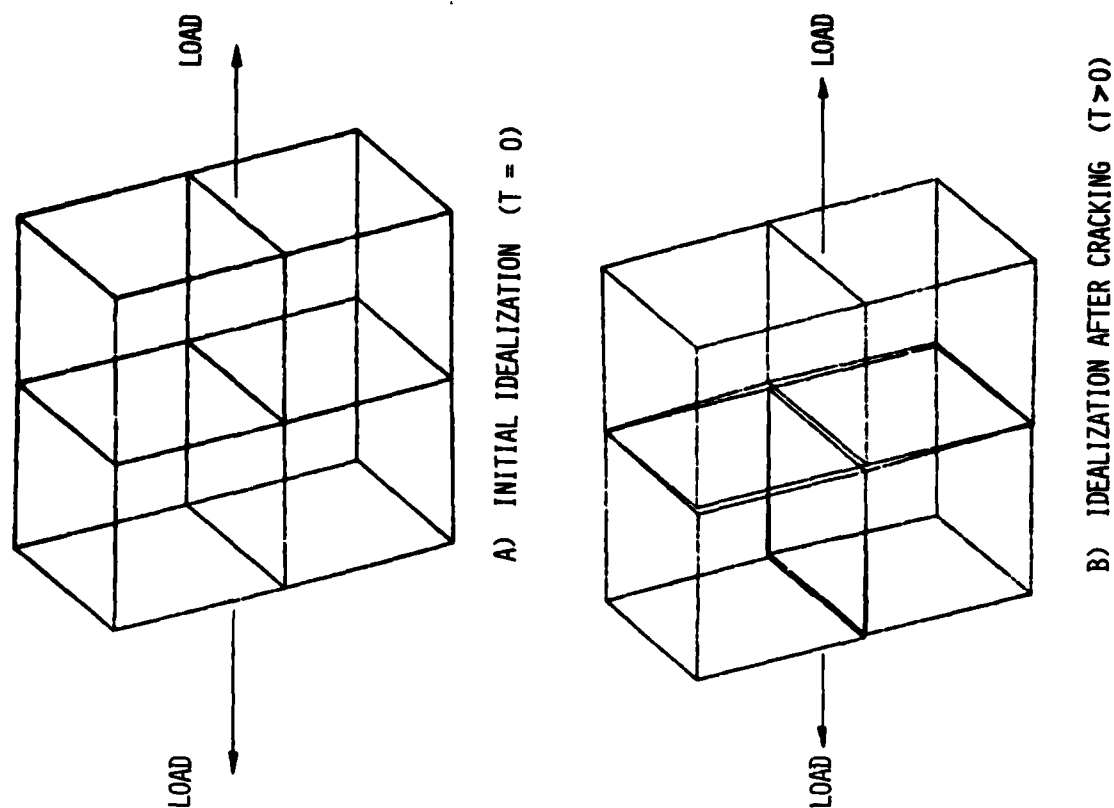


Fig.10 Test case of a cracked specimen

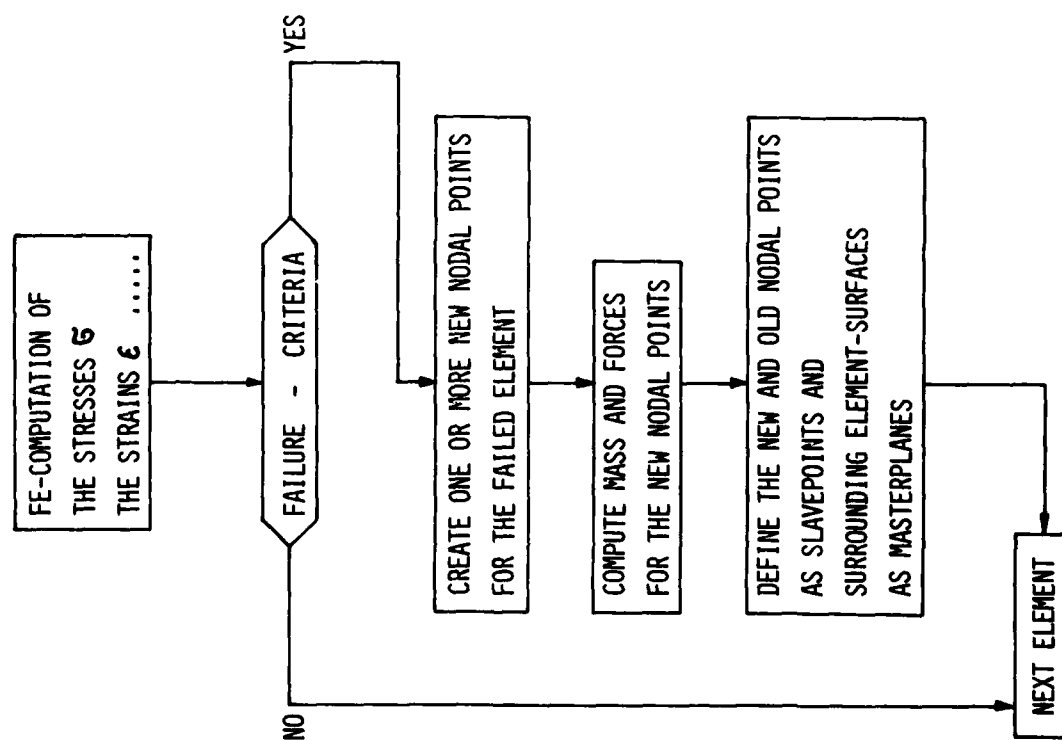
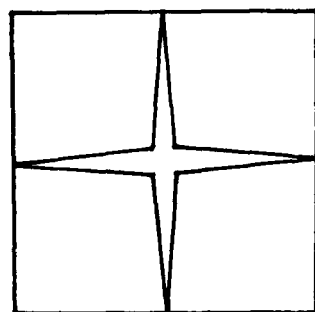
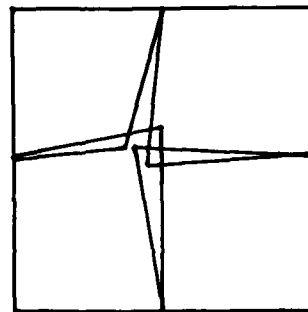


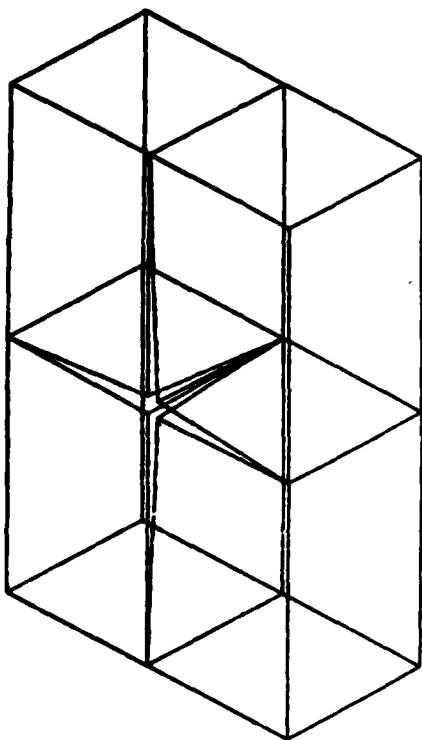
Fig.9 Cracking model flow chart



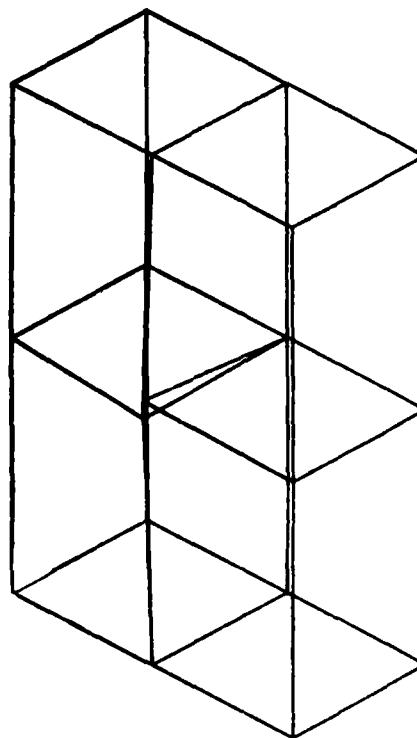
STRUCTURE WITH CRACKS OPENED



STRUCTURE BEFORE THE CONTACT PROCESSOR IS USED



STRUCTURE WITH CHACKS OPENED



STRUCTURE WITH CRACKS CLOSED

Fig.11 Example of a structure with 4 cracks

Fig.12 Crack closing of a precracked structure

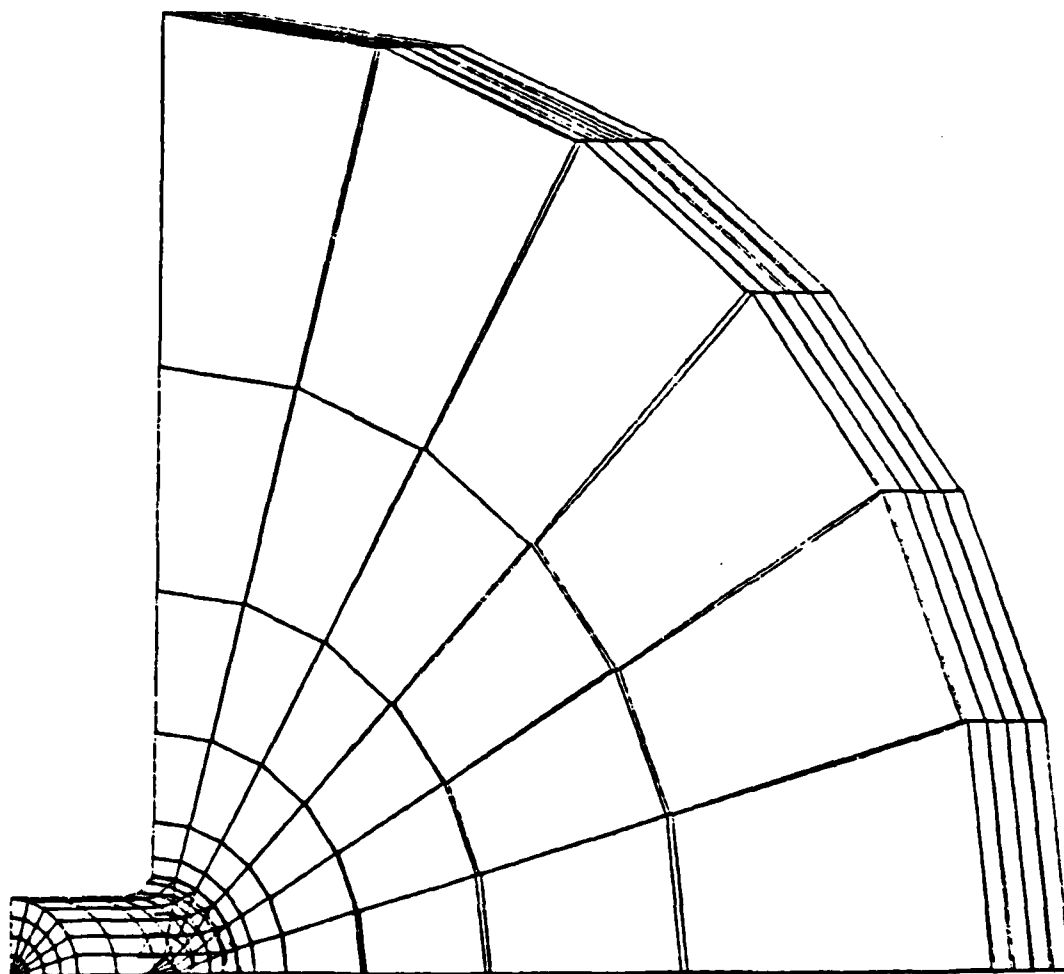


Fig.13 A cylindrical fragment striking a thin plate

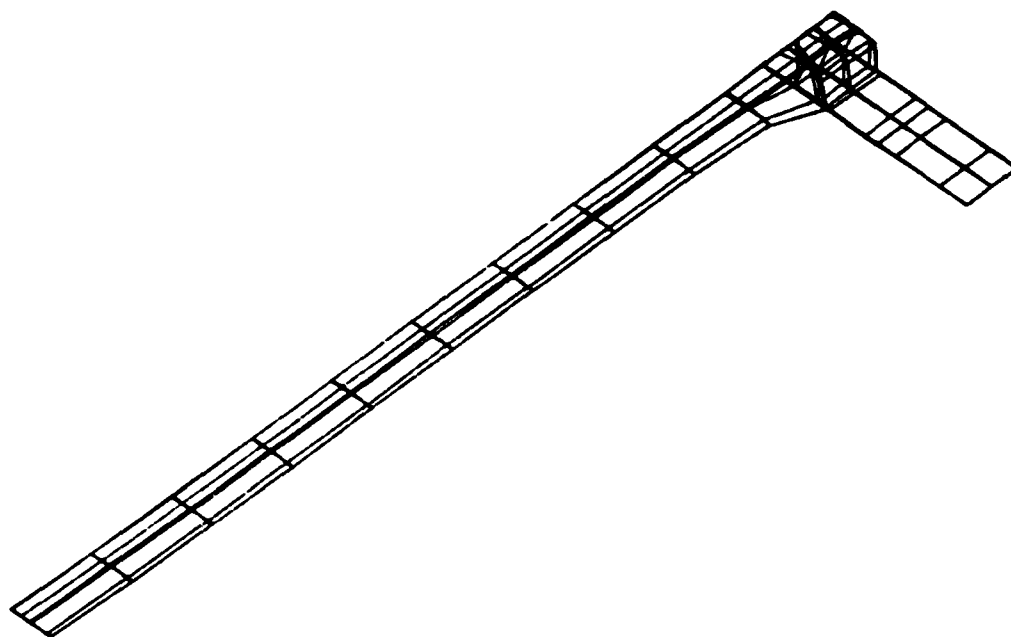


Fig.14 A long rod projectile penetrates a plate

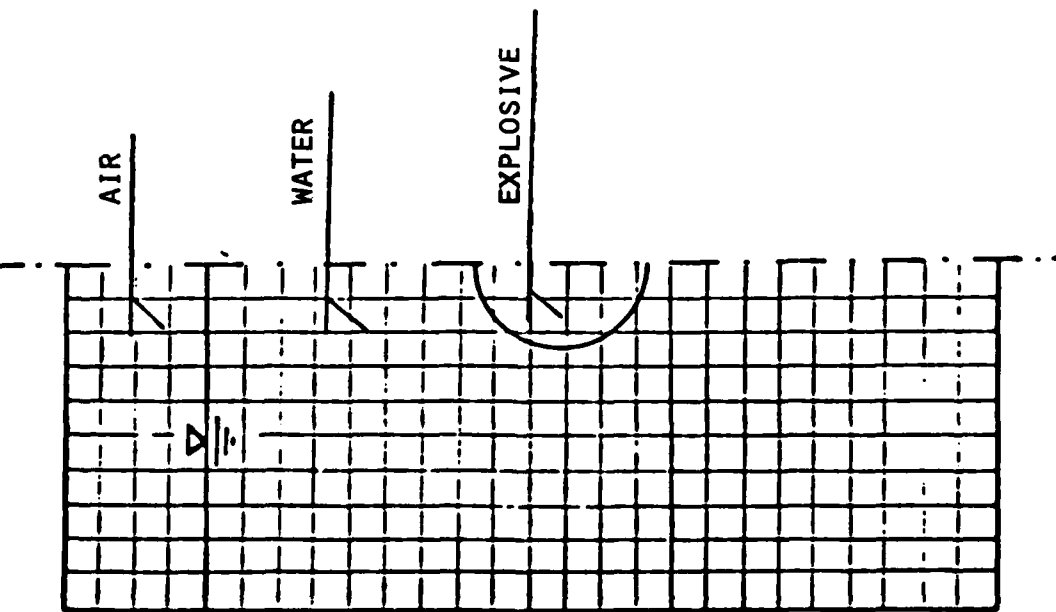


Fig.15 Idealization for an under-water explosion

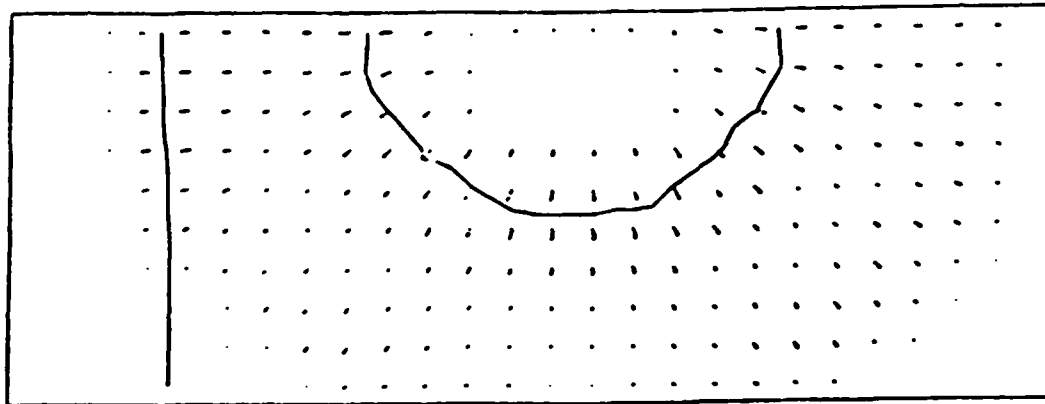


Fig.16 Under-water explosion
Velocity vectors and material flow

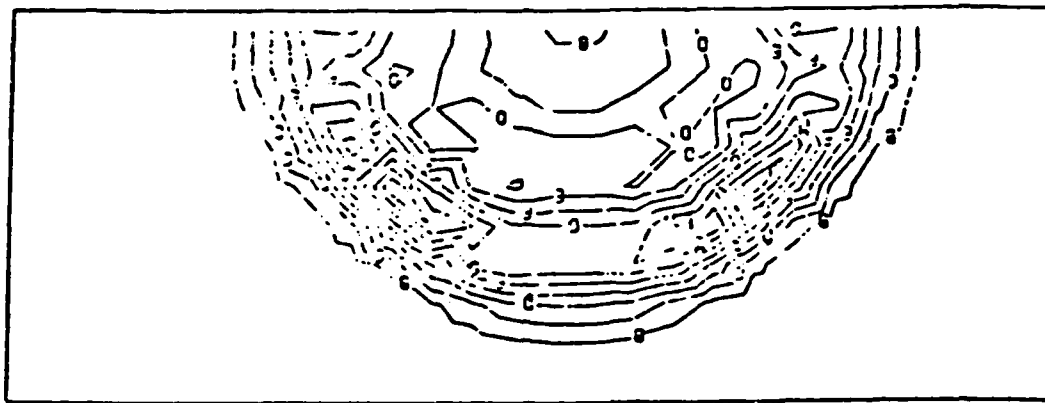


Fig.17 Under-water explosion
Pressure distribution

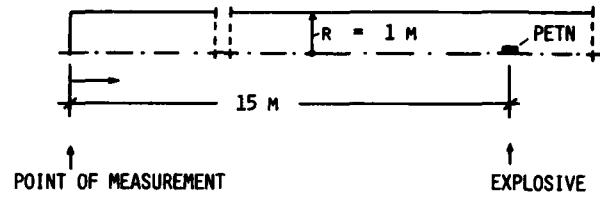


Fig.18 Geometry of the test case

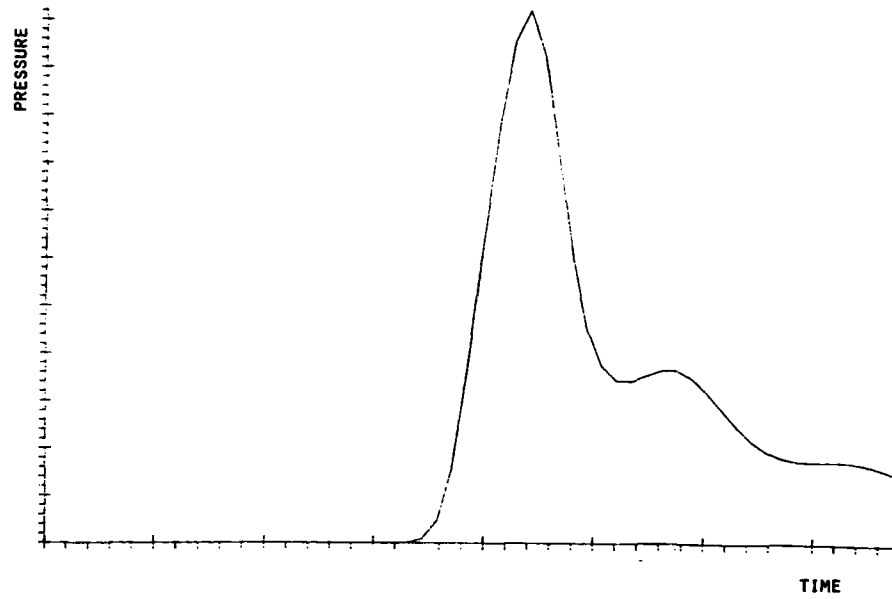


Fig.19 Calculated pressure as function of time

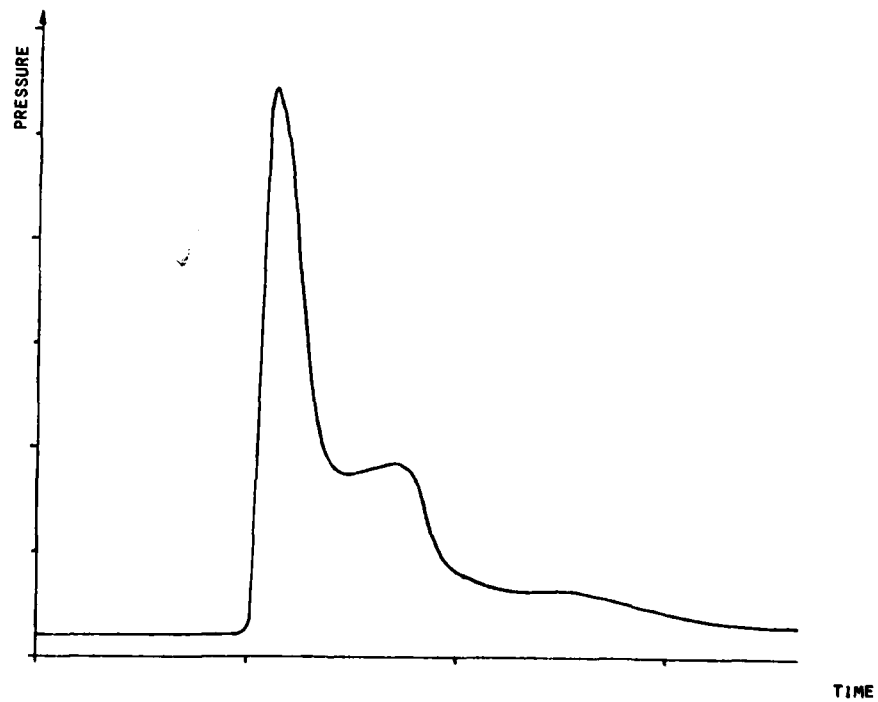


Fig.20 Measured pressure as a function of time

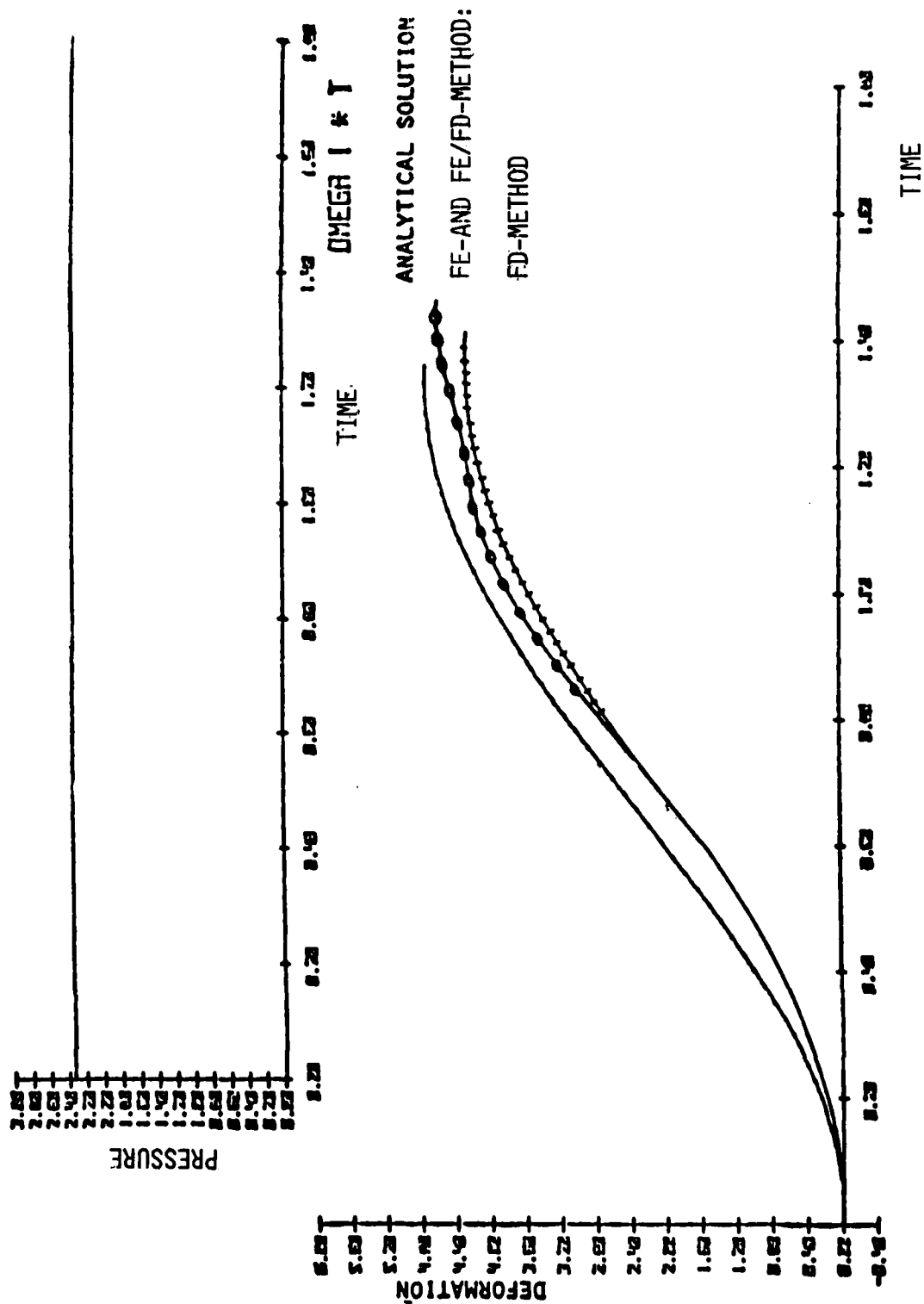
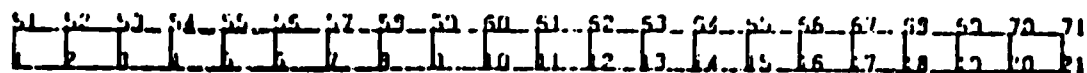
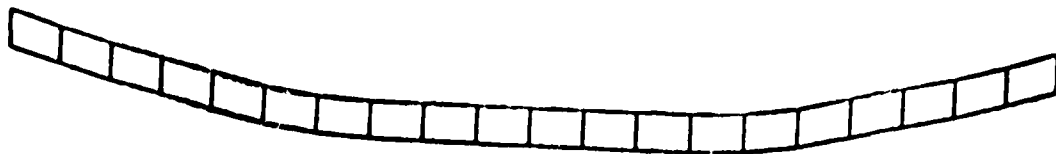


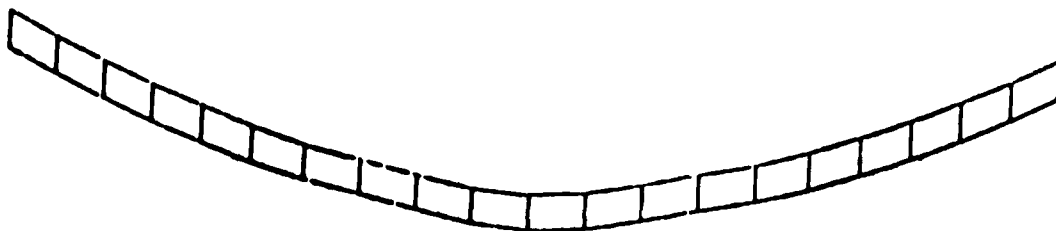
Fig.21 Deformation of a plate (midpoint) as a function of time



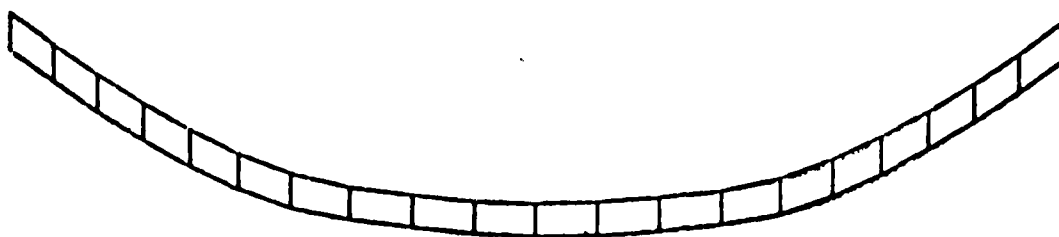
$t = 0$



$t = 1.0$ msec



$t = 1.5$ msec



$t = 2.0$ msec

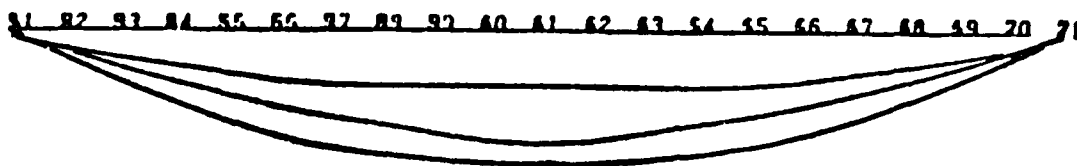


Fig.22 Deformation of a plate
Finite element finite difference method

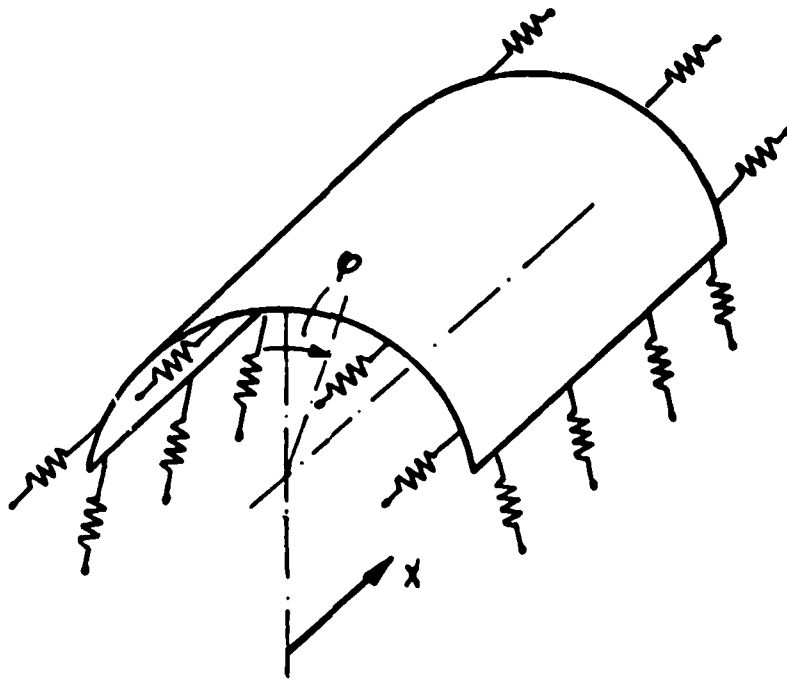


Fig.23 Elastic boundary conditions of the shell

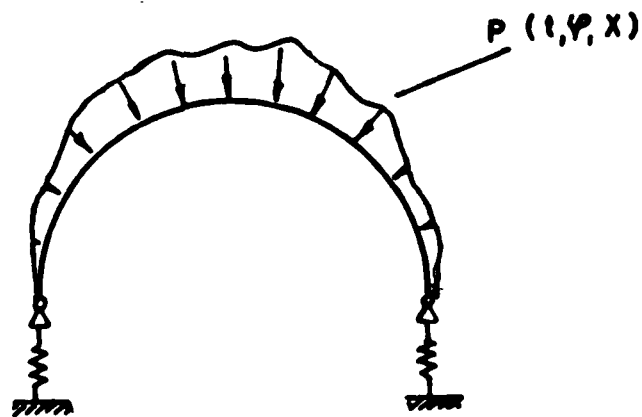


Fig.24 Loading of the shell

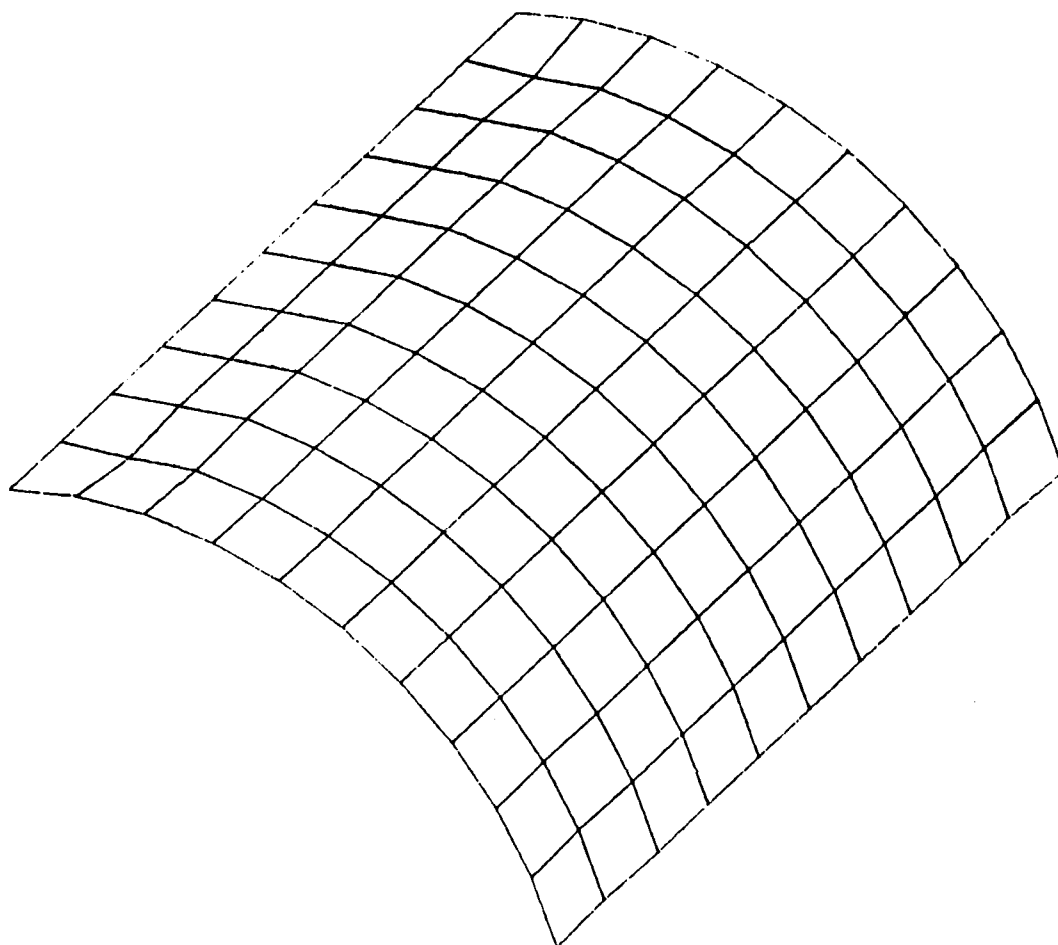


Fig.25 Buckling of a shell under outer pressure
Deformed structure after 400 cycles

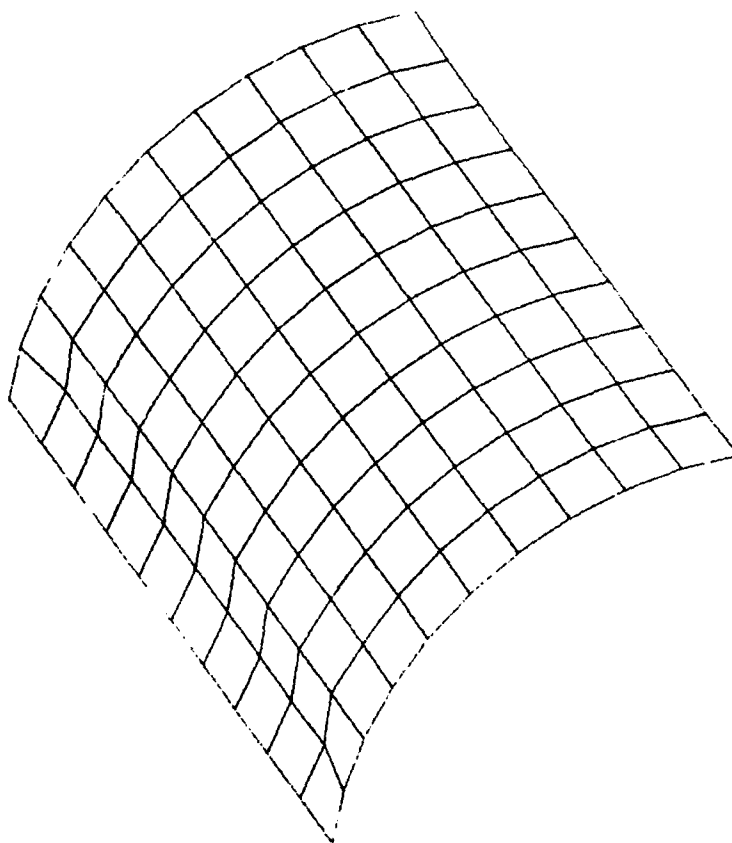


Fig.26 Buckling of a shell under outer pressure
Deformed structure after 600 cycles

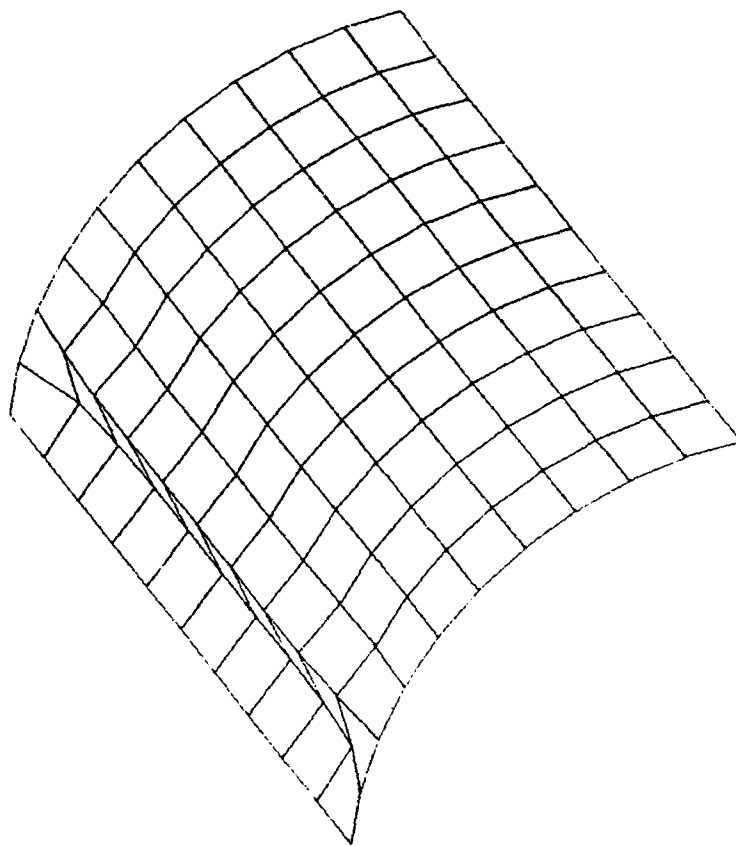


Fig.27 Buckling of a shell under outer pressure
Deformed structure after 800 cycles

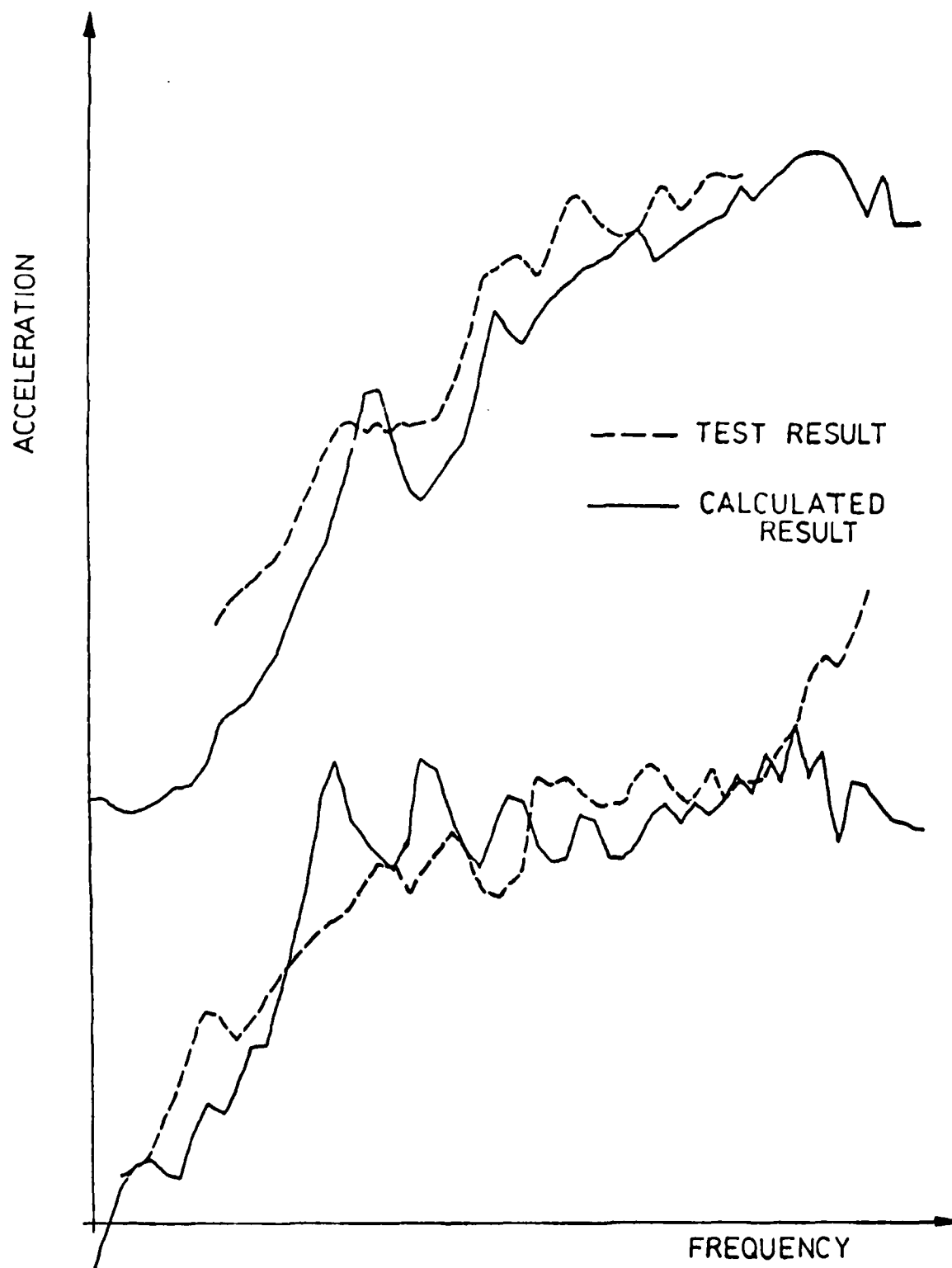


Fig.28 Shock spectra for two different designs

COMPUTER PROGRAMMES FOR THE DESIGN AND
PERFORMANCE EVALUATION OF NACELLES
FOR HIGH BYPASS-RATIO ENGINES

by
Richard Smyth
VFW-Fokker GmbH
Propulsion
D 2800 Bremen
Germany

SUMMARY

High bypass ratio engines offer a variety of significant design options towards achieving an optimum combination of engine and airframe for specific applications. These design options are mainly bypass-ratio, length of fan-cowl, use of mixing or non-mixing nozzles, accessory arrangement and noise suppression methods. All these features influence the size of the engine nacelle and therefore also weight and drag, which finally determine the economics of the aircraft under consideration. Computer-aided methods for the design and performance evaluation of such engine nacelles taking into account the different variations possible and also constraints provide a very useful tool in determining the best nacelle design for a given application. Effective use of such computerized methods require reliable prediction of nacelle drag and realistic bookkeeping techniques for the installed nacelle compatible with wind tunnel and engine manufacturers data.

LIST OF SYMBOLS

A	- area	L	- inlet length, afterbody length
A_c	- inlet capture area	LDN	- Long Duct Nacelle
A_{th}	- inlet throat area	M_∞	- freestream Mach number
A_∞	- area of inlet stream tube in freestream	M_∞^*	- critical Mach number for sonic velocity at inlet external contour
C_{Dp}	- pressure drag of afterbody	P_{t2}	- total temperature at engine/inlet connection plane
C_{Dpz}	- pressure drag of afterbody with nozzle pressure ratio 1 : 1	R	- radial coordinate
C_p	- pressure coefficient based on freestream condition	SDN	- Short Duct Nacelle
$C_{D_{Spill}}$	- spillage drag coefficient based on A_c and freestream conditions	T	- gross thrust
d	- afterbody exit diameter	T_{t2}	- total temperature at engine/inlet connection plane
D	- afterbody maximum diameter, drag	V_c	- mean velocity in inlet capture area
D_f	- friction drag	V_∞	- freestream velocity
D_{Nac}	- nacelle drag	W	- engine mass flow
D_p	- pressure drag	WAT	- $W\sqrt{T_{t2}/P_{t2}}$ engine flow parameter
F_N	- nett thrust	x	- axial coordinate
		α	- angle of attack
		β	- boattail angle
		η	- x/l_R (l_R = length of paraboloid)

1. INTRODUCTION

Fuel-efficient high bypass-ratio engines constitute the state of the art of today's powerplants for modern subsonic transport aircraft. Figs. 1 and 2 show typical powerplant variants for a twin-engined wide-body transport. The nacelles are characterized by the relatively large dimensions with different types of primary nozzle shapes. A comparison of dimensions between the previous generation of low bypass-ratio engines and present-day engines with bypass-ratios of 4 to 6 is shown in Fig. 3.

The purpose of this paper is to identify the main factors which determine the basic dimensions of the engines for today's and future transport aircraft and to demonstrate how the computer can be used in the design and evaluation of the nacelle. Trends in propulsion system development and methods of calculation suitable for computerized work with nacelles will be discussed.

Typical trends of specific fuel consumption and engine dimensions with increasing bypass-ratio is shown in Fig. 4. It can be seen that going from bypass-ratio 1 to 8 reduces cruise fuel consumption by the order of 30 % but also doubles the external dimensions of the engine, mainly due to the large fan.

Further improvements in turbofan engine technology, especially in the face of rapidly increasing fuel prices and more stringent emission requirements will be towards even higher bypass-ratios, e.g. NASA QCEE (Quiet Clean Efficient Engine) programme with bypass-ratio of 10 : 1. Fig. 5 shows a comparison of today's typical turbofan with bypass-ratio 5 : 1 and a future engine of the QCEE type. Thus even larger engine dimensions than today are to be expected.

Since the final form of installation of these engines is with a nacelle attached to the aircraft (mainly the wing) in a given position by means of a pylon, the installed performance of the propulsion system will be determined by the design of the nacelle and the

resulting interaction with the airframe. It is thus obvious that

- careful design of the isolated nacelle and
 - correct integration with the airframe
- are required to achieve maximum overall benefits with respect to
- performance
 - operating cost
 - life-cycle cost.

The modern digital computer is a very useful tool in different stages of nacelle development and performance evaluation, because it can handle the large number of parameters involved - even in the design of the isolated nacelle - very efficiently. A step-by-step method of nacelle synthesis starting from the bare engine and a method of optimization for overall performance evaluation in preliminary design work will be shown. The main object will be the isolated nacelle.

Integration with the airframe requires taking account of local flow fields induced by the presence of the airframe (e.g. wing in high-speed flight or at high angles of attack). There is no simple solution for this complex flow problem, except the use of generalized empirical data from wind-tunnel tests or the application of extensive advanced computational methods for detailed analysis of specific problems.

2. DEFINITION OF THE PROBLEM

The problem of nacelle design consists mainly of 2 tasks:

- 1) Design and performance evaluation of the isolated nacelle, either for a given engine or together with an engine cycle variation for an optimum combination of engine and nacelle.
- 2) Integration of the nacelle with the airframe (wing mounted, fuselage-mounted).

These different steps are explained in schematic form in Fig. 6.

Correct synthesis of the isolated nacelle is the initial step in nacelle development and has to take account of a larger number of requirements with respect to the internal and external flow. It defines the baseline for further work especially with respect to the integration with the airframe and for trade-offs concerning weight and cost.

The flow problem to be handled is shown in Fig. 7. This consists of high subsonic Mach number flow conditions and even supersonic flow in the nozzles at cruise Mach numbers of 0,78 to 0,82.

3. SYNTHESIS PROGRAMME FOR NACELLE DESIGN

3.1 Description of the Programme

The starting point of a Synthesis Programme is the bare engine in its basic dimensions as defined by the engine manufacturer during testbed development. For development of the engine, a simplified ideal inlet (normally a Bellmouth-Type for good flow measurement) and some sort of a calibrated exit nozzle system are used, which with exception of the primary nozzle in many cases do not correspond to the final geometry of nacelle in the aircraft. In Fig. 8 the position of engine mountings and the gear-box for the accessories (pumps, etc.) should also be noted. Positioning of the gear-box either on the fan-casing or directly to the core engine has a significant influence on the nacelle design.

The main elements of nacelle synthesis are shown in Fig. 9. This component breakdown forms the working structure in the application of computers for the design and performance evaluation of nacelles for high bypass-ratio engines.

A Computer Programme for Nacelle Synthesis has been developed [8] which consists of a Main Executive Programme using programme modules based on the component breakdown as shown in Fig. 9. The most important programme modules are:

- Geometrical Requirements
- Inlet Definition
- Nozzle and Afterbody Definition
- Flow Calculation.

The programme can be run on CDC 6600 and IBM 360 computers.

3.2 Geometrical Requirements

Apart from the fixed dimensions of the bare engine as already described the length of the fan duct relative to the overall nacelle length is a major parameter influencing the design of a high bypass-ratio engine nacelle.

Two extreme solutions are possible

- Long Duct Nacelle (LDN) and
- Short Duct Nacelle (SDN)

as shown in Fig. 10. It is evident that intermediate duct lengths may in some cases present an overall optimum solution.

Minimum length for the Short Duct Nacelle (SND) is determined by the following internal and external flow requirements:

- distribution of cross-sectional area in fan duct
- duct curvature
- engine front mounts and pylon
- volumetric requirements of gas-generator and its surrounding systems. This determines the inner diameter of the fan nozzle.
- blockages in fan exit
- required internal area for noise absorbing linings
- integration with the inlet geometry with respect to
 - a) Fan Cowl afterbody design
 - b) Transition length between inlet and fan-cowl afterbody. In the simplest case is a cylindrical piece.
 - c) Provision of potential increase in fan area for further development.

Design requirements taking into account the influence of cross-flow around the fan cowl at high angles of attack and the integration with the wing present a complex flow problem which is not handled in this synthesis programme. One exception here is the possibility of defining inlet droop based on local upflow conditions at the inlet.

3.3 Inlet Design

The inlet is defined as shown in Fig. 11 and determines the cross-sectional area of the nacelle to a large extent. Requirements for good inlet design are:

- low internal pressure loss at take-off, climb and cruise conditions.
- minimum spillage drag at cruise.

The synthesis programme thus divides the inlet design into an internal and external flow problem. The internal flow problem determines

- lip thickness and throat area
- diffuser design up to the engine/inlet connection flange.

Throat Mach number is an important parameter here and can be computed from the engine flow parameter WAT, where

$$WAT = \frac{W \sqrt{T_{t2}}}{P_{t2}} = f(\text{flight conditions, power setting})$$

W = mass flow

T_{t2} = total temperature at the engine entry plane

P_{t2} = total pressure at the engine entry plane.

The data base for the generalized experimental data consists of curves for total-pressure loss for different lip-thicknesses and throat Mach numbers M_{th} at a given freestream Mach number M_{∞} as shown in Fig. 12.

Data is available for

lip-thickness $A_c/A_{th} = 1,0 - 1,33$

$M_{th} = 0,3 - 1,0$

$M_{\infty} = 0 - 0,4$

where

A_c = inlet capture area

A_{th} = throat area

M_{th} = throat Mach number

M_{∞} = freestream Mach number

The result of the internal flow computation is to define the shape of the inlet from the capture area A_c up to the engine/inlet connection at the engine front flange.

Typical requirements are

- a) Total pressure loss at take-off $\leq 0,3 \%$
- b) Maximum Throat Mach number $\leq 0,75$

From the capture area A_c and the mass-flow parameter WAT the external flow problem can be solved for given flight conditions. The main requirement is to avoid spillage drag at specified points. Spillage drag arises due to flow separation on the external inlet contour and is a function of mass-flow ratio A_{∞}/A_c , freestream Mach number M_{∞} and inlet shape. Spillage drag normally occurs at $A_{\infty}/A_c < 1,0$ when the engine demands less mass flow than the inlet would ideally deliver. Fig. 13 shows an example of spillage drag.

The synthesis programme uses an empirical approach based on the NACA-1 family of high-speed inlet contours [4], [7]. The relationship between freestream Mach number for spillage-drag rise, inlet dimensions and mass-flow ratio is shown in Fig. 14. The drag-rise Mach number in this diagramme is defined by the occurrence of sonic velocity at the inlet surface. Inlets designed by this method generally show a reasonable margin up to actual drag rise. Drag rise can occur either by an increase in freestream Mach number or a reduction of inlet mass flow. Other classes of inlets can also be used.

The results of the external flow programme are

- external inlet length
- maximum inlet diameter, which is equal to the first estimation of maximum fan-cowl diameter
- external shape
- flow parameters (mass-flow ratio, pressure recovery).

For nacelles with gear-boxes on the fan-casing (see Fig. 10) an increase in external inlet contour with a resulting enlarging of the local maximum diameter in the section of the gear-box may be necessary. This leads to a "bump", which is normally in the lower section of the fan-cowl.

Inlet droop and inclination of inlet front plane can be accommodated in the computer programme.

3.4 Nozzle and Afterbody Definition

The definition of the nozzles and their surrounding afterbodies for the fan and gas generator are required for the final design of the complete nacelle.

The first step is to complete the fan cowl by integrating the fan nozzle into the inlet geometry. Here the requirements of good fan-cowl afterbody shaping must be taken into account. These are mainly

- boattail angle (max. 12°)
- even distribution of curvature along the cowl.

The fan nozzle can be either convergent or convergent/divergent.

The next step is to handle the gas generator problem by defining the primary nozzle, which is mainly a simple convergent-type of nozzle with or without a centre-body. The computer programme can take care of both cases. The gas generator afterbody or core cowl must be of a low drag design (boattail and friction drag) and can be designed to fulfil the following alternative requirements for a given contour (circular arc, parabola):

- boattail angle fixed
- core cowl length fixed.

Regarding the core cowl as a section of a rotational paraboloid the basic relationships for boattail angle, length and surface can be solved by a set of simple equations as shown in Fig. 15. Other forms of core cowl surface curvature, i.e. even straight line, are also possible. The shape of the centre-body is normally taken as a cone, with a given taper-radius.

3.5 Demonstration of Results

Results of the Synthesis Programme for the design of a short duct type of nacelle with a bare engine as defined in Fig. 16 and with the following variations are shown in Figs. 17 to 19:

- axisymmetrical nacelle
- nacelle with inlet droop of 4°
- nacelle with asymmetric core cowl.

3.6 Flow Calculation

Following the geometric definition of the nacelle by means of the synthesis programme defined above a check of flow conditions can be done by applying the Method of Streamtube Curvature (STC) for the calculation of internal and external pressures. This method assumes axisymmetric flow and is described in [3]. It has been developed to handle flow problems associated with engine nacelles. A typical result is shown in Fig. 20.

4. PERFORMANCE EVALUATION

4.1 Performance Requirements

The internal losses in the inlet and nozzles and the external drag of isolated nacelles can amount to about 7 - 10 % of equivalent thrust loss of the installed engine for a given fuel consumption. This alternatively leads to an increase in fuel consumption of the same order for a constant thrust of the engine. The above figure assumes no spillage drag, i.e. the inlet operating at optimum conditions. Changes in operating conditions can easily lead to a rise in spillage drag which due to the very large size of the inlets for the nacelle of high bypass-ratio engines can mean an appreciable increase in overall drag.

In addition to the drag of the isolated nacelle, drag of the pylon and interference drag due to the presence of the nacelle near the wing must be taken into account. Depending on the configuration of nacelle, wing and pylon the interference drag can even be favourable.

Performance evaluation of nacelles plays an important role in aircraft design work, both in the development of new configurations and in the case of nacelle comparisons when e.g. reengineering an existing aircraft. This requires a method of calculating all internal and external losses due to the nacelle using a suitable bookkeeping of individual items.

4.2 Nacelle Drag and Internal Losses

After definition of the nacelle geometry the performance loss due to the isolated nacelle (i.e. without influence of wing or pylon) for a given flight Mach number and given conditions of inlet and nozzle flow can be calculated. This is a first estimation of the performance penalty due to the engine installation.

Experience shows that careful bookkeeping of thrust and drag is necessary in order to take account of different definitions of inflight thrust by the leading engine manufacturers. The following cases are possible:

- 1) Ideal nozzles (thrust coefficient = 1,0) and no core cowl drag
- 2) Real nozzles and core cowl drag assuming
 - isolated nacelle
 - no freestream flow!
 - nozzle pressure ratios corresponding to a given flight condition.
 Result of a simple static force measurement with a blowing nozzle system.
- 3) Real installation with influence of the airframe, i.e. pylon (can be cambered) and wing.

Without a bookkeeping system for accounting all the possible internal and external losses due to the nacelle the drag estimation of a given engine/nacelle combination or the drag comparison of different engine installations can be misleading. The following definitions based on Thrust minus Drag of the nacelle/engine combination are recommended.

(Thrust-Drag) of the isolated nacelle is defined as

$$(T-D)_{is} = F_{N_{id}} - \Delta F_{N_{INTAKE}} - \Delta F_{N_{NOZZLES}} - \underbrace{D_{f_F} - D_{f_C} - D_{f_{Plug}}}_{\text{friction}} - \underbrace{D_{SPILL} - D_{P_{FR}} - D_{P_C}}_{\text{pressure}}$$

Individual terms are explained in Fig. 21 and below.

- $F_{N_{id}}$ = ideal nett-thrust of the engine
- $\Delta F_{N_{INTAKE}}$ = thrust loss due to inlet pressure loss
- $\Delta F_{N_{NOZZLE}}$ = thrust loss due to nozzle pressure loss
- D_{f_F} = friction drag of fan cowl
- D_{f_C} = friction drag of core cowl
- $D_{f_{Plug}}$ = friction drag of core nozzle centre body
- D_{SPILL} = spillage drag
- $D_{P_{FR}}$ = pressure drag of fan afterbody
- D_{P_C} = pressure drag of core cowl

$$\text{Isolated Nacelle Drag } D_{Nac is} = D_{f_F} + D_{f_C} + D_{f_{Plug}} + D_{Spill} + D_{P_{FR}} + D_{P_C}$$

$$\text{Installed Nacelle Drag } D_{Nac inst} = D_{Nac is} + \Delta D_{Nac inst}$$

$\Delta D_{Nac inst}$ to be determined from wind tunnel tests.

Pressure losses in the inlet and in the fan duct (duct length variation) can be estimated by standard methods. The corresponding thrust losses $\Delta F_{N_{INTAKE}}$ and $\Delta F_{N_{NOZZLES}}$

can be calculated from knowledge of the engine cycle and are mainly a function of the nozzle pressure ratios.

Calculation of individual drag terms have been developed in the form of programme modules which can either be used individually or as subprogrammes in a larger programme. The use of programme modules facilitates updating and refinement of each individual subprogramme.

For preliminary design purposes simplified assumptions for turbulent flow (e.g. flat plate friction) can be used for the individual friction drag coefficient.

In the case of the core cowl D_{fC} fan nozzle exit conditions are assumed in order to give a realistic estimate of the "Scrubbing Drag" on that surface.

There are several methods of calculating the drag of afterbodies with jets. Quite a number have been developed for the determination of rear-end drag of fighter-type aircraft. One method suitable for the Mach number range of 0,6 to 0,9 uses correlated experimental data and is based on the following equation:

$$C_{D_P} = C_{D_{Pz}} + \Delta C_{D_P}$$

C_{D_P} = pressure drag with jet

$C_{D_{Pz}}$ = pressure drag of body with zero jet defined as
nozzle pressure ratio 1 : 1

ΔC_{D_P} = correction term for nozzle pressure ratio 1,0.

Fig. 22 shows $C_{D_{Pz}}$, which was found to be a function mainly of boattail angle and diameter ratio d/D of the P_z afterbody in [5]

The correction term for jet interference ΔC_{D_P} is a function of

- nozzle pressure ratio
- temperature
- boattail angle and
- diameter ratio d/D .

Spillage drag $C_{D_{Spill}}$ can be calculated by empirical methods making use of constant-pressure inlet theory [4] or a method proposed by Mount [6]. A typical result is shown in Fig. 23. Alternatively experimental data can be used if the inlet under consideration has already been tested at a sufficient number of mass flow ratios A_{∞}/A_c and freestream Mach numbers M_{∞} to provide input data for a computer programme.

4.3 Power Unit Optimization

The Power Unit is the complete propulsion system consisting of nacelle and bare engine as attached to the pylon of the aircraft. Thrust minus drag of this unit is the nett force acting on the rest of the aircraft in flight direction.

Optimization of the Power Unit by variation of

- engine cycle parameters e.g. bypass-ratio, overall pressure ratio and turbine temperature
- nacelle design, i.e. either short duct nacelle (SDN) or long duct nacelle (LDN)

can lead to an indication of the best combination of engine cycle and nacelle design to fulfil a given mission with respect to

- maximum take-off weight and
- operating cost.

Fig. 24 shows the optimization process, which is best done by computer due to the large number of variable parameters. The computation of internal and external nacelle losses as already described is part of the computing process.

The result of this overall optimization of the Power Unit with respect to the best nacelle design for a twin-engined short-haul aircraft with

- bypass-ratio variation between 1 and 7
- turbine entry temperature of 1373°K and 1573°K
- total pressure ratio of 18 : 1

is shown in Fig. 25. This diagramme shows where SDN and LDN should be used depending on bypass-ratio. The use of more efficient mixing nozzles in the LDN-versions will extend the range of applicability to higher bypass-ratios. The final result for the optimum engine cycle based on minimum weight is shown in Fig. 26.

This example shows a typical application of modern computers for solving an overall aircraft design task with the nacelle performance as one of the key subprogrammes.

4.4 Interference of Nacelle on Wing

The effect of the nacelle on the wing can be calculated using panel methods based on the singularity method of Smith and Hess. The surface of the investigated configuration is panelled, allotting a constant source distribution to each panel. Suction and displacement effect of the jet can be simulated by solid-body panels with the exception that the source strength is obtained by prescribing non-vanishing normal velocities.

The panel model of an aircraft with an overwing nacelle is shown in Fig. 27. Comparison of test and calculation for the case of a faired inlet at low speed conditions are in good agreement.

5. FURTHER WORK

Further work is desirable in developing computerized methods for determining the impact of the nacelle integration on the overall aerodynamic, structural and stability characteristics of a given aircraft. Since the development of the first generation of wide-body jets (Lockheed C-5A, Boeing 747, DC-10, Airbus A 300 B) using high bypass-ratio engines a data base already exists, which can be used for first-order results and even well qualified predictions in the case of aircraft families. Efficient use of available data and automatic updating can be facilitated by a computerized "Nacelle Installation Data Bank". Fig. 28 shows a schematic proposal with respect to the different aspects of nacelle influence on the overall aircraft. Main inputs into the data bank will be from wind tunnel and actual flight tests results. Such a data bank also provides a means for making better use of the large amount of measured data available from modern wind tunnel test facilities and aircraft flight test programmes.

The need to efficiently install high bypass-ratio engines closer to the wing in order to achieve the same ground clearance as on previous aircraft requires the use of improved computational methods which take account of the effect of the non-axisymmetrical fan efflux on the local flow field and overall drag as it emerges on both sides of the pylon into the corner between pylon and wing.

5. CONCLUSIONS

The use of the computer as a design tool for the different stages of nacelle development and integration with the airframe has been demonstrated. Results were shown of practical applications, typical of work in a preliminary design phase. Further requirements of the individual solutions are possible using more detailed analytical methods. These will be characterized by longer computing times and higher costs. Future progress in computer technology and the use of appropriate higher-order languages will prove very useful for these purposes.

Although the work described here has centered mainly an aerodynamic shaping and performance similar computational approaches can be applied to other disciplines of nacelle design, e.g. weight bookkeeping, moments of inertia, structures and acoustics.

A computerized "Nacelle Installation Data Bank" will provide a useful tool in making efficient use of the increasing amount of data already being generated from wind tunnel and flight-test programmes, especially for aircraft families.

Further application to design and analysis should include the effect of three-dimensional jets on future wing, nacelle and pylon combinations.

Increased effectiveness of application and better acceptance of the computer as a design tool can be achieved by improving the man/machine relationship in the design process. This can be facilitated by using graphical displays, especially the new generation of colour graphics.

7. REFERENCES

1. Bergmann, D., "An Aerodynamic Drag Study of Jet Engine Nozzles", AGARD-CPP-91-71.
2. Hilbig, R., K.-D. Klevenhusen, G. Krenz and R. Smyth, "Application of Advanced Technology for Improving the Integration of Engine and Airframe for Future Transport Aircraft", 11th Congress of the International Council of the Aeronautical Sciences (ICAS), Lisboa, Portugal, September 10-16, 1978.
3. Keith, J.S., D.R. Ferguson, C.L. Merkle, P.H. Heck and D.J. Lahti, "Analytical Method for Predicting the Pressure Distribution about a Nacelle at Transonic Speeds", NASA CR-2217, July 1973.
4. Küchemann, D. and J. Weber, "Aerodynamics of Propulsion", McGraw-Hill Book Company, New York, Toronto, London, 1953.
5. McDonald, H. and P.F. Hughes, "A Correlation of High Subsonic Afterbody Drag in the Presence of a Propulsive Jet or Support Sting", Journal of Aircraft, May-June 1965.

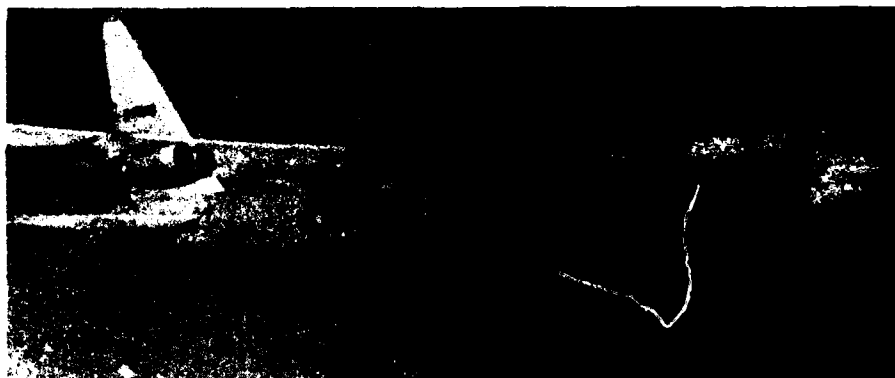
6. Mount, J.S., "Effect of Inlet Additive Drag on Aircraft Performance", Journal of Aircraft, Spet.-Oct. 1965.
7. Pakendorf, H. and R. Smyth, "Die Einlaufauslegung für Triebwerke mit hohem Bypass-Verhältnis", Technical Report TB Eft-2-68, VFW-Fokker, 1968.
8. Rudolph, K., "Syntheseprogramm Einlauf, Triebwerk, Heck", VFW-Fokker Report Ef 44 BR 8/76, 1976.
9. Sens, W.H., "Low Energy Consumption Engines", AGARD-LS-96, Aircraft Engine Future Fuels and Energy Conservation, Munich, 16-17 October 1978.
10. Swan, W.C. and A. Sigalla, "The Problem of Installing a Modern High Bypass Engine on a Twin Jet Transport Aircraft", AGARD-CP-124, Flight Dynamics Panel Specialists Meeting, Izmir, Turkey, 10-13 April, 1973.
11. Weichert, S., "Synthese des Einlaufwiderstandes bei der Triebwerk/Zellenintegration von Kampfflugzeugen", BMVg-Auftragsnr. T/RF 42/RF 420/51043.
12. Weichert, S., "Fehler bei der praktischen Anwendung von Widerstandssyntheseverfahren für Einlaufsysteme und die Vorbereitung einer Einlauf-Datenbank", BMVg-Auftragsnr. T/RF 42/60004/61035.



Fig.: 1 Nacelle with Plug-Type Primary Nozzle



Fig.: 2 Nacelle with Simple Short Primary Nozzle



Comparison of Dimensions

2 x J57-P43W	28.000 lb	thrust	bypass-ratio 1,0
1 x CF6	42.000 lb	thrust	bypass-ratio 6,0

Fig.: 3 Comparison of Engine Sizes

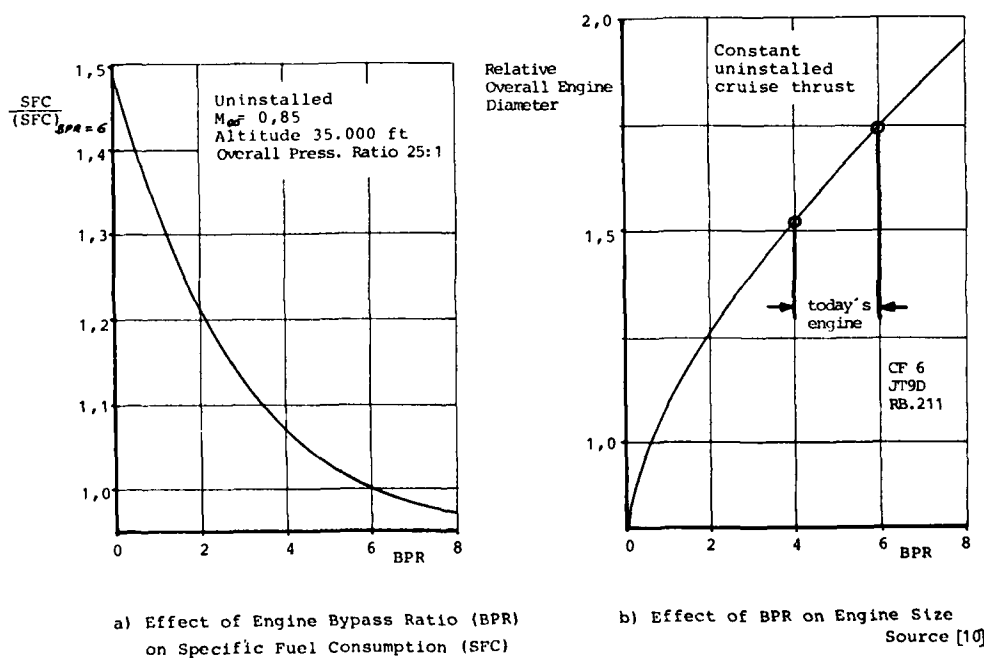
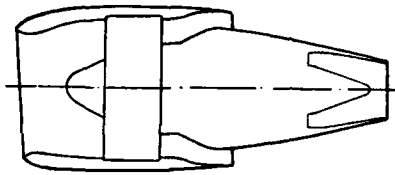


Fig.: 4 Engine Development Trends



	Second generation turbofan (1970 - 1985)	Advanced turbofan (1985 - 2000)
Bypass ratio	6	7-8
Fan pressure ratio	1,45	1,6-1,7
Cycle pressure ratio	25:1	35-45:1
Turbine inlet temperature	1530 °K	1675 °K

Fig.: 5 Present-Day and Future Engines

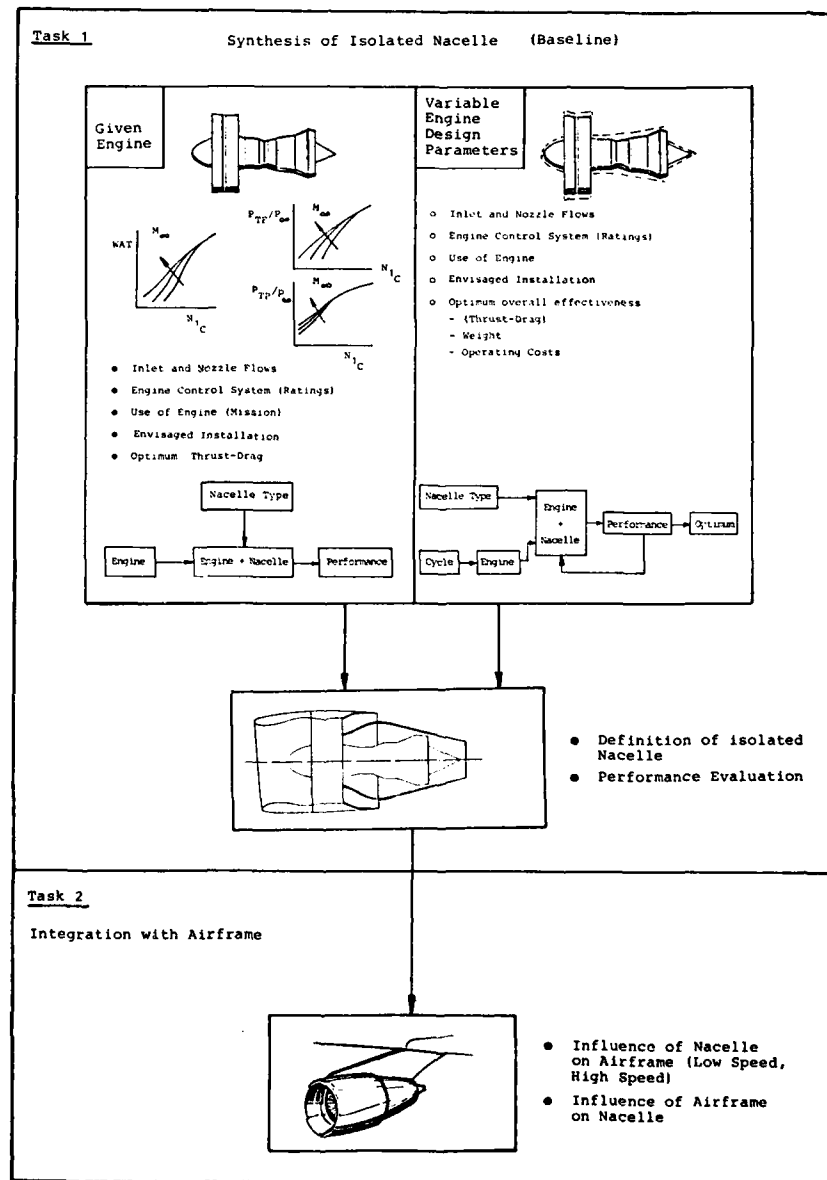
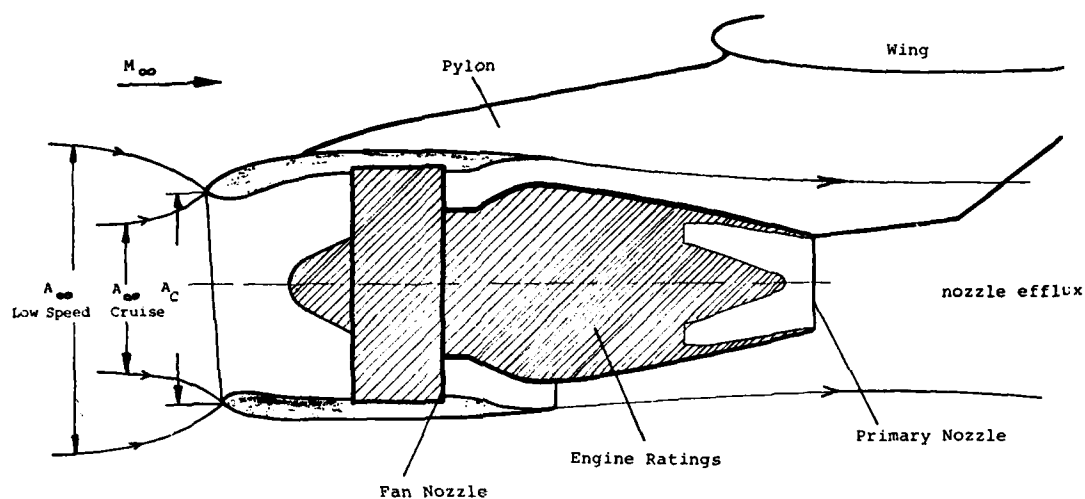


Fig. : 6 Steps in Nacelle Development



Typical Standard Day Conditions				
	Rotation at Take Off	Approach	31.000 ft Climb	31.000 ft Cruise
Inlet Mass Flow Ratio A_{∞}/A_C	≥ 1	$\approx 1,0$	0,75	0,7
Machnumber	0,2	0,3	0,8	0,8
Fan Nozzle Press. Ratio	1,6	1,085	2,8	2,6
Primary Nozzle Press. Ratio	1,45	1,05	2,2	2,1

Fig.: 7 Flow Conditions around Nacelle

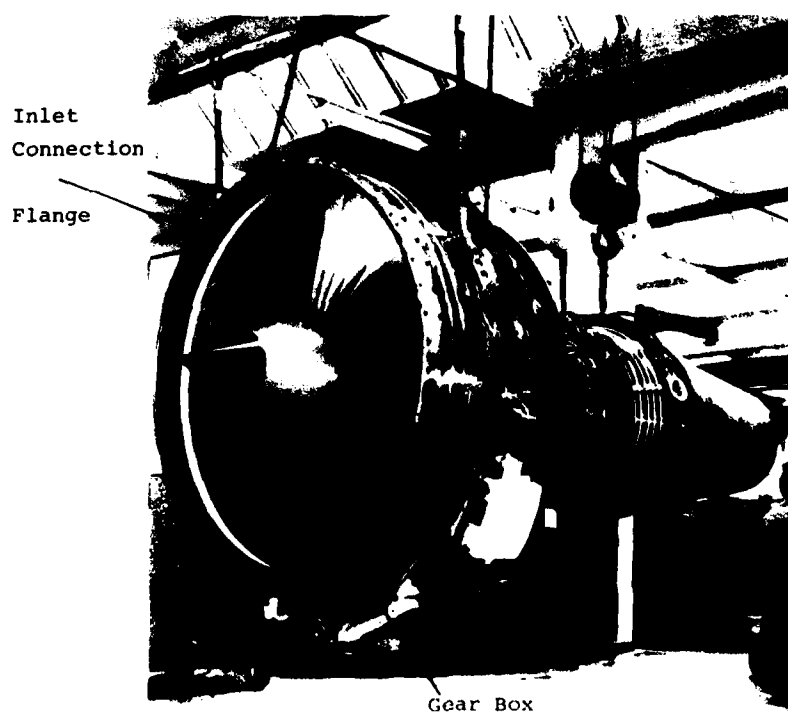


Fig.: 8 Typical Bare Engine

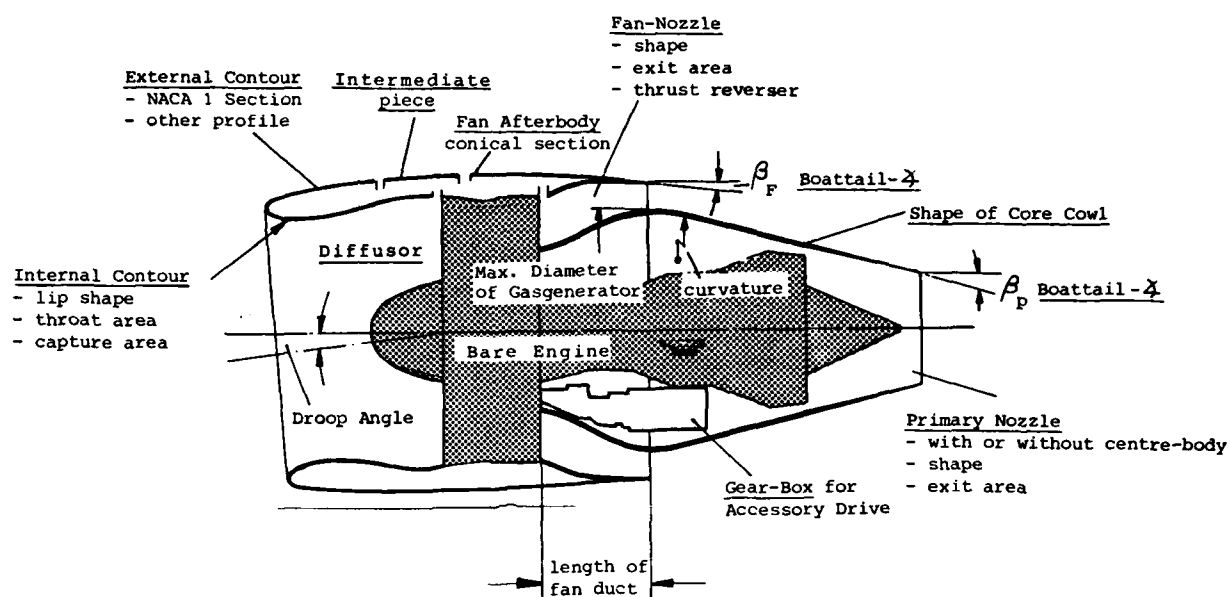
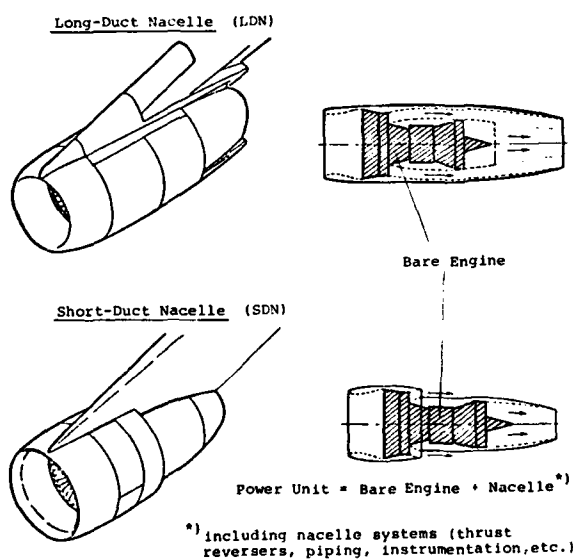


Fig.: 9 Main Elements of Nacelle Design



	Length of Fan Duct	Gearbox
	3/4	gas generator
	long (mixing nozzles)	fan casing
	long (mixing nozzles)	fan casing
	short	gas generator
	3/4	gas generator
	3/4	fan casing

Fig.: 10 Installation of Bypass-Engines in Long-Duct or Short-Duct-Nacelles

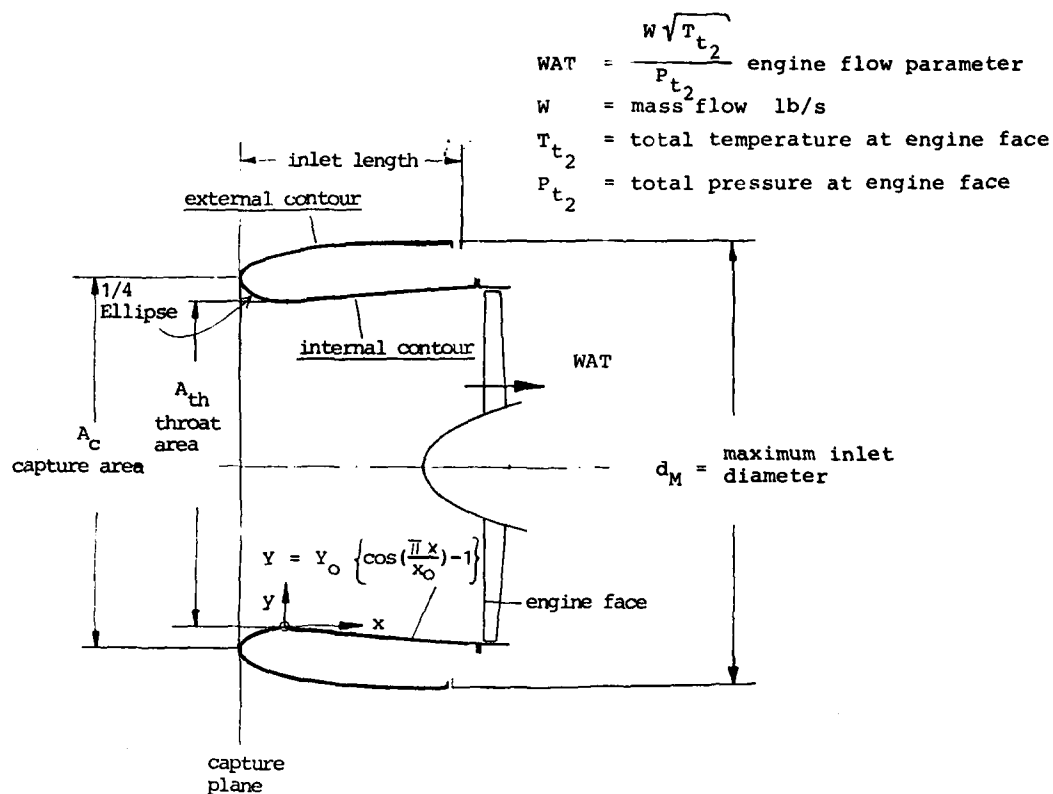


Fig.: 11 Definition of Inlet Geometry

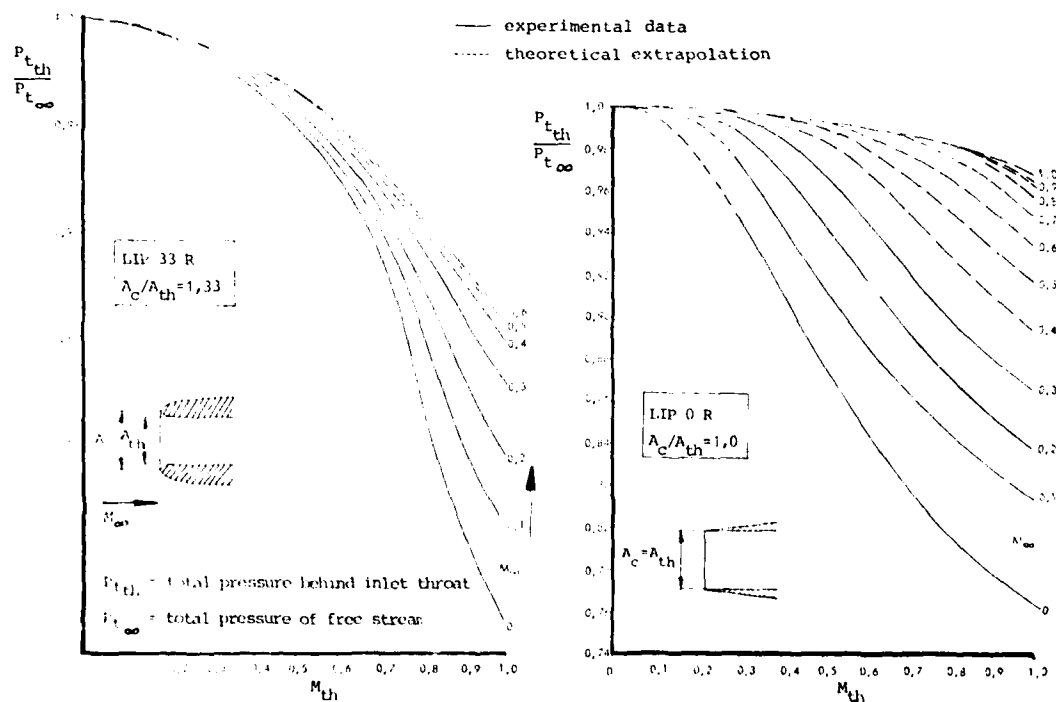


Fig.: 12 Pressure Loss in Inlets

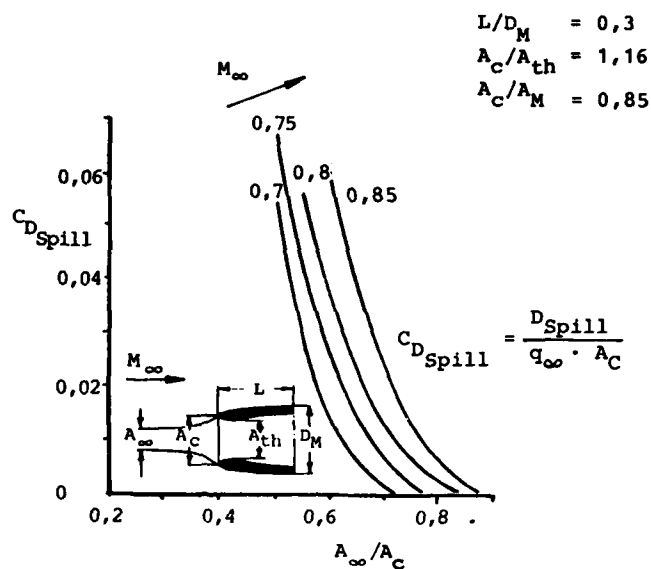


Fig.: 13 Spillage Drag

Angle of incidence $\alpha = 0^\circ$

Results of Inlet Programme

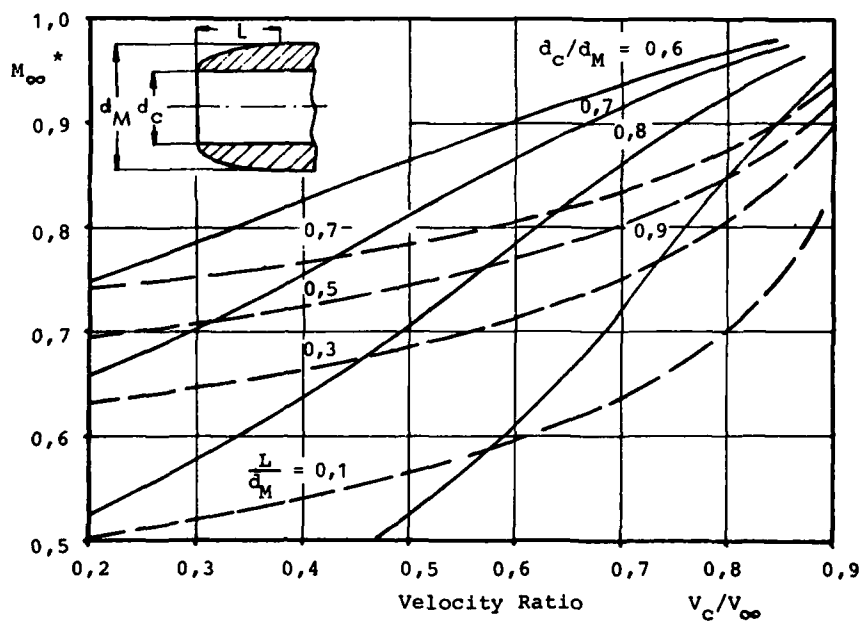
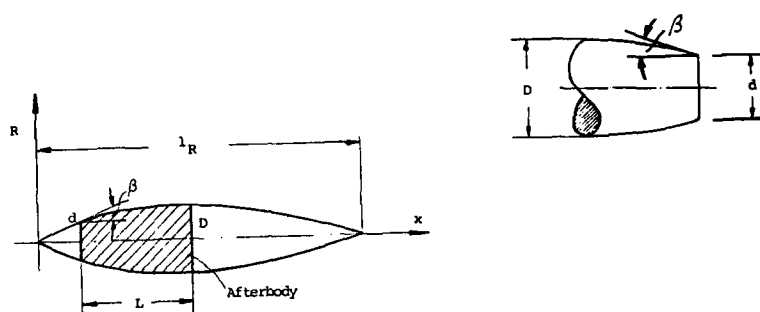


Fig.: 14 Design Parameters for NACA-1 Inlet Family



$$\begin{aligned}\delta_R &= D/l_R & R &= 2D\eta(1-\eta) \\ \eta &= x/l_R & \tan\beta &= 2\delta_R(1-2\eta) \\ d/D &= 4(\eta-\eta^2) \\ \text{Surface } S &= 12,565 \cdot D \cdot l_R \left[0,0833 - \left(\frac{\eta^2}{2} - \frac{\eta^3}{3} \right) \right]\end{aligned}$$

Fig.: 15 Rotational Paraboloid for Approximation of Afterbody Shaping

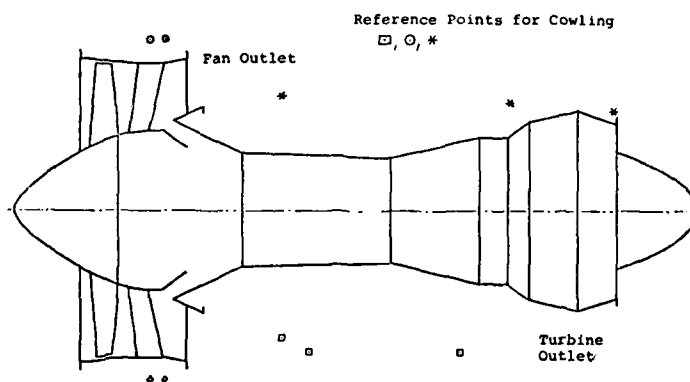


Fig.: 16 Bare Engine

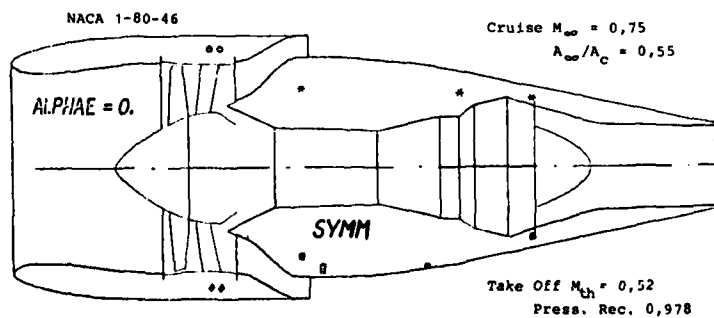


Fig.: 17 Synthesis of Symmetrical Nacelle with Straight Inlet

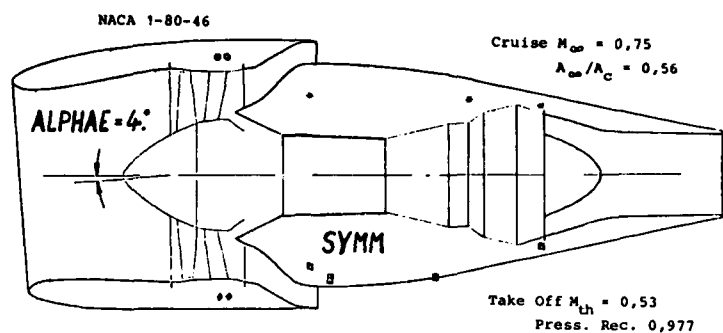


Fig.: 18 Synthesis of Symmetrical
Nacelle with Drooped Inlet

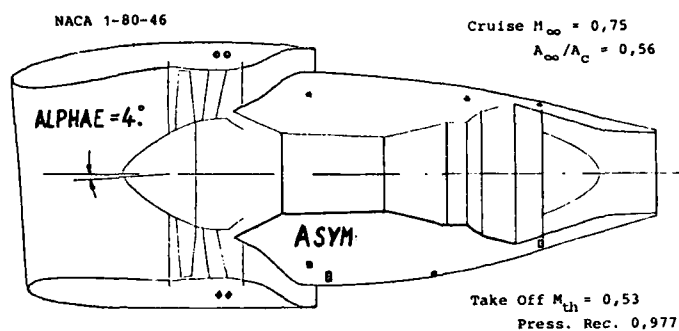


Fig.: 19 Synthesis of Asymmetrical
Nacelle with Drooped Inlet

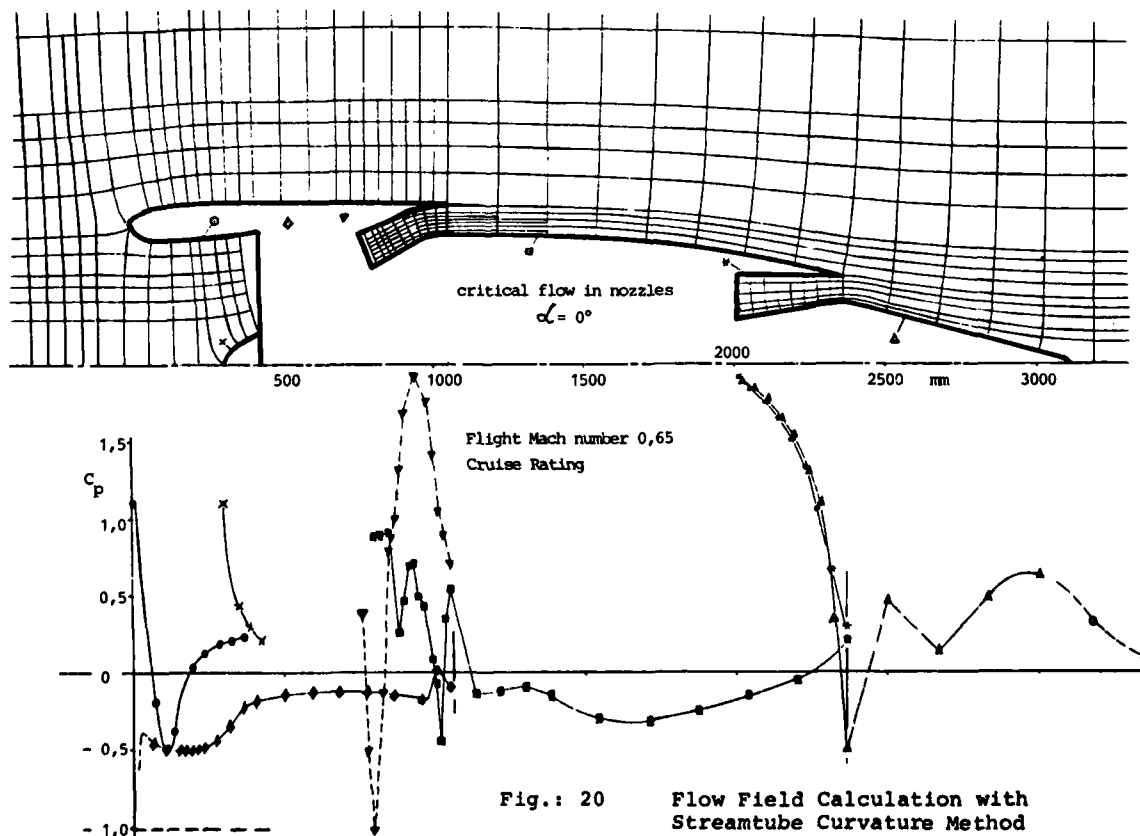


Fig.: 20 Flow Field Calculation with
Streamtube Curvature Method

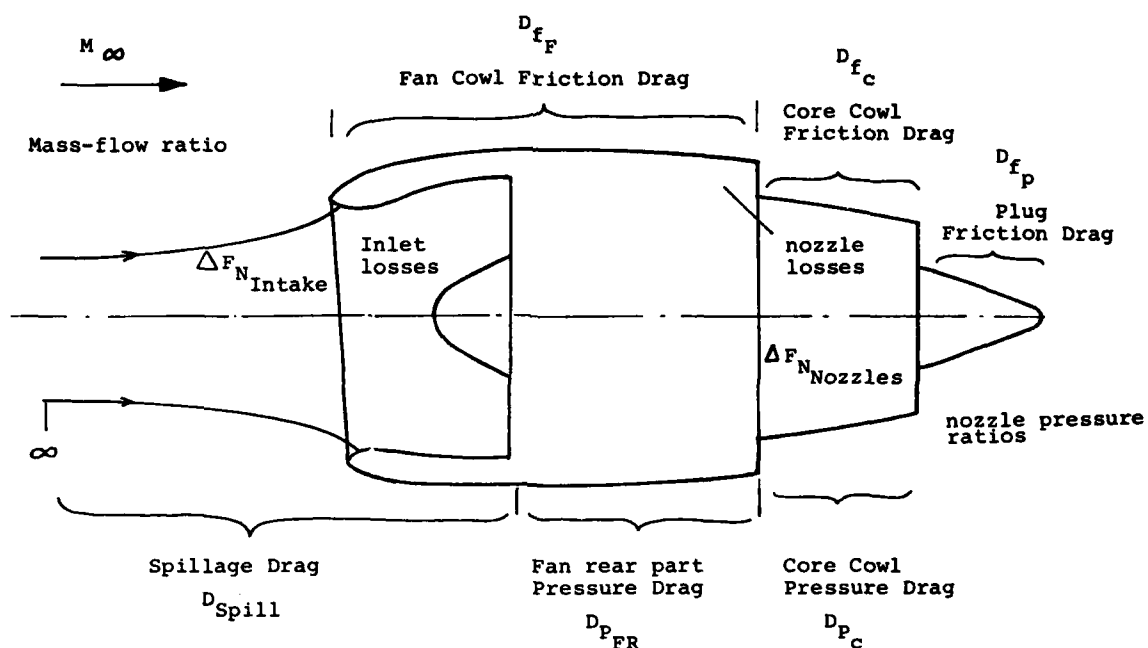


Fig.: 21 Nacelle Drag and Internal Losses
(isolated Nacelle)

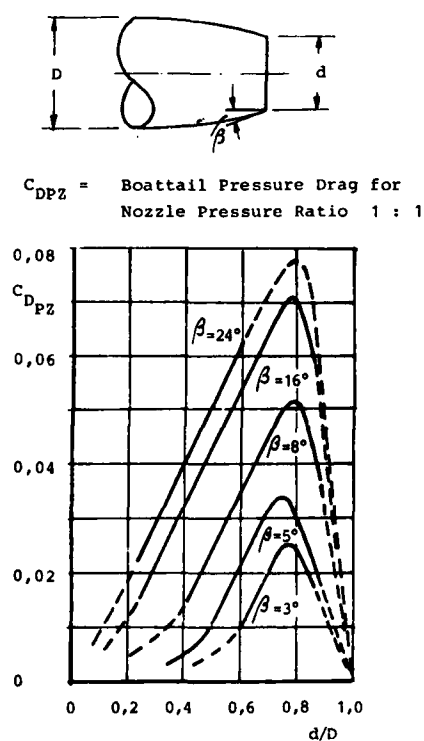


Fig.: 22 Boattail Pressure Drag for Nozzle Pressure Ratio 1 : 1

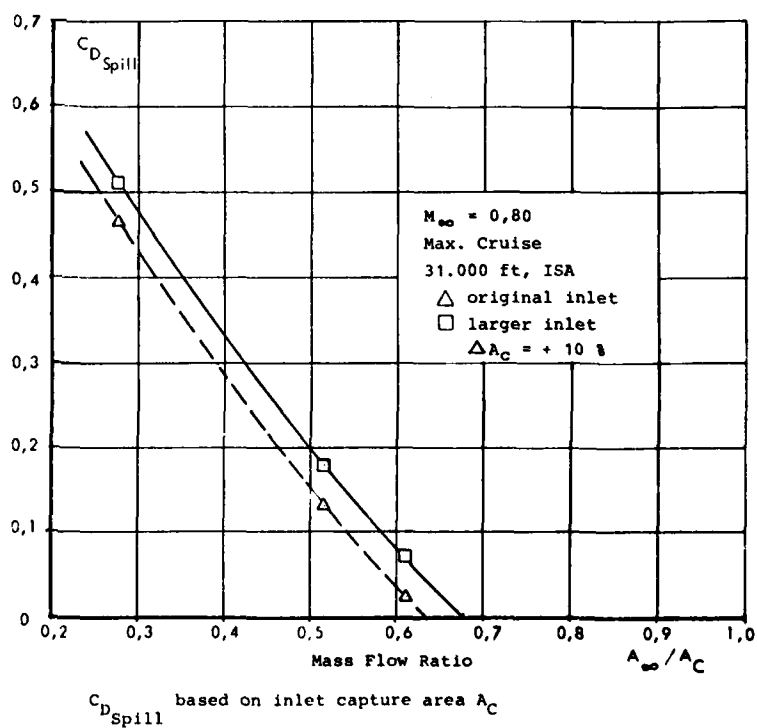


Fig.: 23 Results of Spillage-Drag Computation

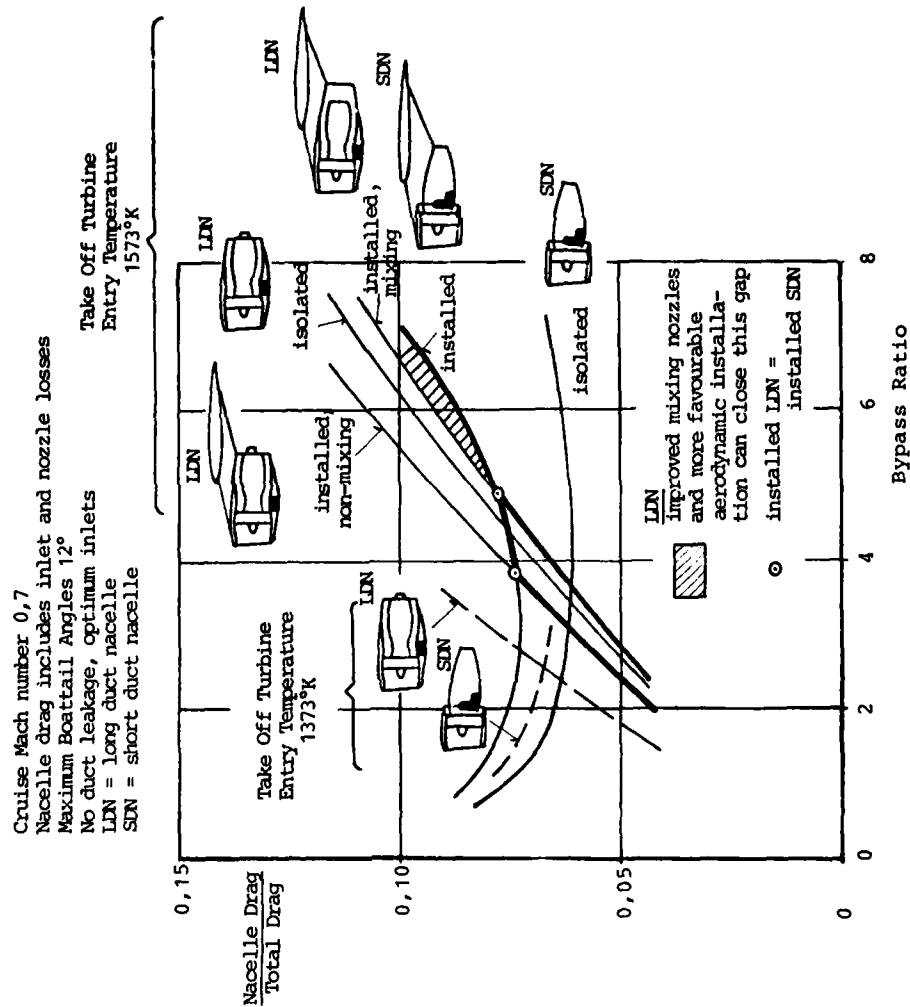


Fig.: 25 Influence of Nacelle Type on Nacelle Drag at Cruise Conditions

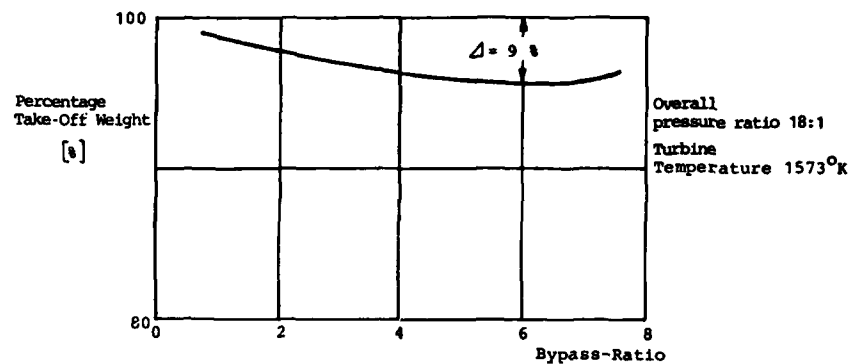
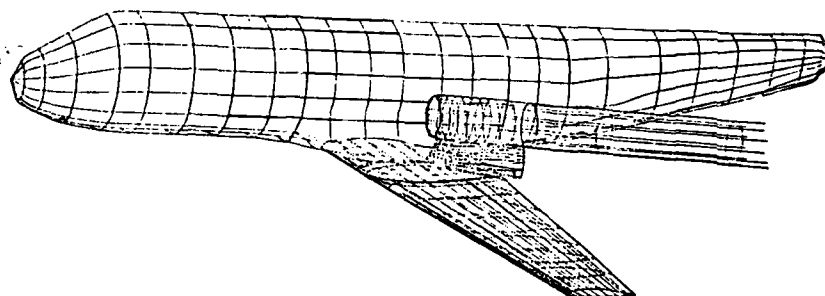
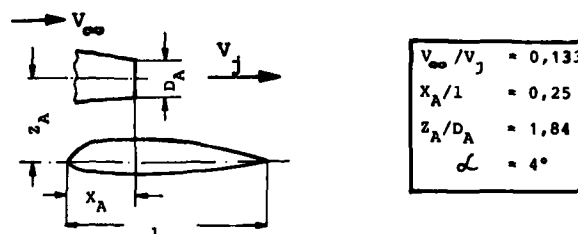
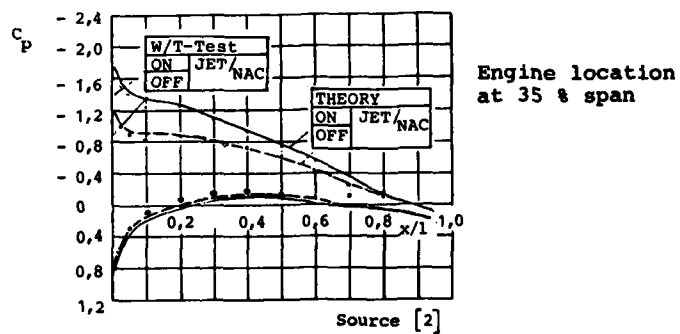


Fig.: 26 Optimization of Engine Cycle
(including nacelle design)



a) Panel Model of Transport Aircraft



b) Jet Influence on Wing

Fig.: 27 Panel Model of Transport Aircraft and
Comparison with Test Results

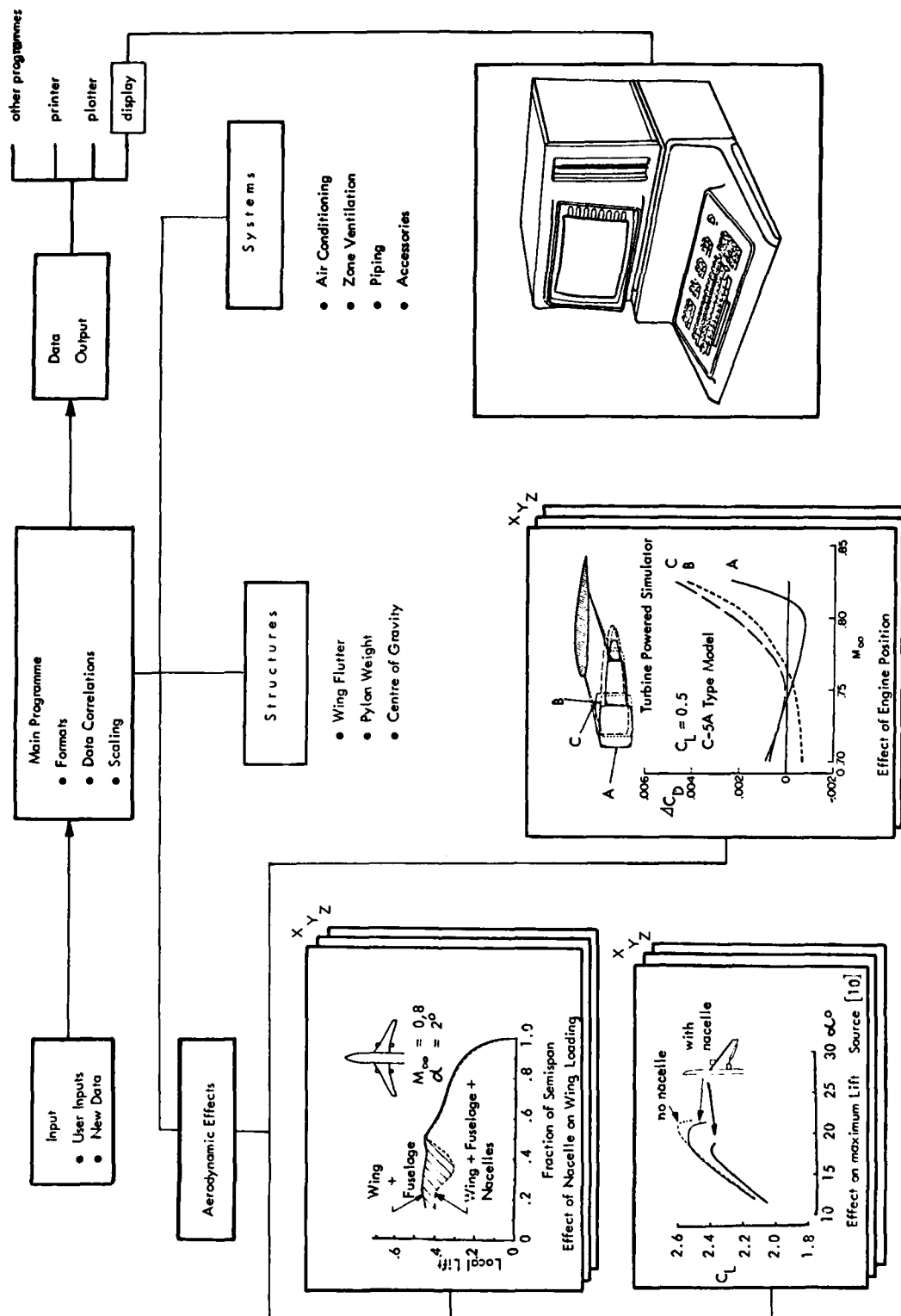


Fig.: 28 Nacelle Installation Data Bank

COMPUTERIZED SYSTEMS ANALYSIS AND OPTIMIZATION OF AIRCRAFT ENGINE PERFORMANCE, WEIGHT, AND LIFE CYCLE COSTS

by
Laurence H. Fishbach*
National Aeronautics and Space Administration
Lewis Research Center
Cleveland, Ohio
44135
USA

SUMMARY

Availability of a suitable propulsion system is generally acknowledged to be a key requirement for the successful development of a new airplane. This paper describes the computational techniques utilized at Lewis Research Center to determine the optimum propulsion systems for future aircraft applications and to identify system tradeoffs and technology requirements.

Over the last five years, the NASA Lewis Research Center has obtained a greatly increased capability of performing detailed studies of engine cycles on the computer. Many more parameters can now be accounted for in the engine selection process. We can calculate cycle performance, engine weight, predict costs and account for installation effects as opposed to fuel consumption alone. Almost any conceivable turbine engine cycle can be studied since we do not rely on preconfigured simulation codes but can input the engine cycle externally to the codes. Most of this capability has come through the joint efforts of the Naval Air Development Center, The Boeing Company and NASA Lewis.

These computer codes are:

NNEP - a very general cycle analysis code that can assemble and arbitrary matrix of fans, turbines, ducts, shafts, etc., into a complete gas turbine engine and compute on- and off-design thermodynamic performance

WATE - a preliminary design procedure for calculating engine weight using the component characteristics determined by NNEP

LIFCYC - a computer code presently being developed in conjunction with the Navy to calculate life cycle costs of engines based on the output from WATE

INSTAL - a computer code presently being developed under contract to calculate installation effects, inlet performance and inlet weight

POD DRG - a table look-up program to calculate wave and friction drag of nacelles

Examples will be given to illustrate how these computer techniques can be applied to analyze and optimize propulsion system fuel consumption, weight and cost for representative types of aircraft and missions.

INTRODUCTION

The airplanes, engines and missions of today are far more complicated than those of just a few years ago. The ability to determine the optimum combination of airplane and engine is of paramount importance. But what is the optimum combination. Is it the engine that burns the least fuel?; Costs the least to operate?; Can minimize installation penalties?; Minimizes fuel plus engine weight?; A combination of the above?

Each airplane/engine system probably has its own criteria of optimization. It is therefore necessary to develop the analytical tools capable of calculating all the factors which enter into the selection process. This paper discusses the computer techniques employed at the NASA Lewis Research Center to perform these calculations. The process by which almost any conceivable turbine engine can be evaluated as to fuel consumption, engine weight, cost and installation effects is described. Examples are shown as to the benefits of variable geometry and of the tradeoff of fuel burned versus engine weight. Future plans for further improvements in the analytical modeling of engine systems are also described.

HANDMATCHING

In order to determine engine operating characteristics at specified flight conditions, methods were developed in the 1940's for superimposing engine component matching maps for simple engines such as turbojets and turboprops. These methods involved laborious hand calculations and performance map transformations to determine at what operating conditions of the engine components continuity of mass and energy, and mechanical speed relationships were satisfied. Needless to say, especially when methods were developed for a two spool engine, hours and even days were required to determine an operating line for an engine. A thorough discussion of these methods can be found in reference 1. Figure 1 illustrates the time frame and capabilities that existed.

*Head, Flight Performance Section, Mission Analysis Branch, V/STOL and Noise Division.

EARLY COMPUTER BASED MATCHING CODES

With the advent of high speed computers, the task of matching of the engine components could not only be solved faster but more complex engines such as two-spool engines with a bypass flow (turbofan) could be simulated. Many companies, universities, and government installations developed computerized methods. One of the earliest of these matching computer codes was called SMOTE and was developed at Wright Patterson Air Force Base (ref. 2). SMOTE was capable of matching two spool turbofan engines. This capability was expanded by the development of GENENG and GENENG II at NASA's Lewis Research Center. The GENENG codes (refs. 3 and 4) were capable of matching one, two or three spool engines with as many as three nozzles. Turbofans with booster or supercharger stages on the compressors could be simulated as well as aft-fan engines. GENENG served as the main simulation code in NASA and was adopted for use by over 20 Government agencies, companies, and universities. A version of GENENG called DYNGEN was developed at Lewis to simulate transient behavior of turbofan engines (ref. 5) for use in control system studies.

THE NAVY/NASA ENGINE PROGRAM (NNEP)

Since 1973, the NASA Lewis Research Center has been conducting studies of advanced supersonic engines including Variable Cycle Engines or VCE's. These engines take advantage of the use of variable geometry components and in-flight flow switching capabilities such as from mixed flow to separate flow to attempt to deliver good engine performance at supersonic conditions as well as subsonic. By optimizing the exhaust profile during take-off significant decreases in jet noise can also be achieved. It became apparent that GENENG and similar codes could not simulate some of the concepts coming out of the studies. The new cycles did not fit into any of the engine concepts already built into the codes.

Two options were available. A new specific code could be developed for each new engine concept, or a general code capable of simulating any engine could be developed. The second alternative was chosen as being more time efficient in the long run and more responsive to any immediate need. We, therefore, decided to develop a new computer code in which an arbitrary engine configuration consisting of selected combinations of components could be described at input time. It was also necessary to allow changes in engine configuration while running the code to simulate the operation of various VCE concepts. Furthermore, because of the large number of variables, it was highly desirable to optimize the settings of variable components such as nozzle or turbine areas (e.g., to minimize SFC for a given thrust).

Contact with the Naval Air Development Center, Warminster, PA, revealed that they had a computer code, NEPCOMP (ref. 6), which already contained some of the features desired and whose structure was flexible enough to permit the addition of others. This code lacked optimization capability and the ability to operate with "stacked" maps which would represent variable component performance. However, it already had the capability for processing arbitrary engine configurations. NASA-Lewis therefore contracted with the Naval Air Development Center for the joint development of an improved computer code. The objective of the joint effort was to obtain a code capable of: simulating any turbine engine the user could conceive, simulating variable component performance, changing air-flow paths while running, and optimizing variable-geometry settings to minimize the specific fuel consumption or maximize the thrust.

An interim version of this new code given the acronym NNEP (Navy NASA Engine Program) became operational in May of 1974 and has been continuously refined since then to include all of the desired capabilities.

NNEP contains almost all of the subroutines and incorporates the philosophy of construction of NEPCOMP as described in reference 6. The major improvements incorporated in NNEP relative to NEPCOMP are the addition of: (1) a performance optimization capability, (2) processing of stacked component maps for VCE operation, (3) multiconfiguration (modes) to simulate flowpath switching, (4) a computer generated engine configuration schematic, (5) throttle dependent inlet and boattail drag calculations, and (6) a simpler input data format.

As previously mentioned, the engine is configured at input time in running NNEP. First, the user draws a schematic of the engine he wishes to study, for example, a simple turbofan as shown in figure 2. He assigns a flow station number 1 at the entrance to the inlet and labels the inlet as component number 1. After this he is free to assign any number at the other flow stations in the engine and to label each of the components with any component number. One problem that does arise is that is not possible at all times to label the flow stations in accordance with the Aerospace Recommended Practice ARP 753A.

The components that can be simulated in NNEP are as follows:

Flow components - falling under this classification are

- (1) Inlets
- (2) Ducts/burners
- (3) Compressors

- (4) Turbines
- (5) Mixers
- (6) Heat exchangers
- (7) Splitters
- (8) Nozzles
- (9) Water injectors

Mechanical components -

- (1) Shafts
- (2) Loads

Control and optimization components -

- (1) Controls
- (2) Optimization variables
- (3) Limit variables

There is a limit of a total of 60 components (including all of the flow, mechanical, control and optimization variables) allowed within the code. The maximum number of any one type of flow or mechanical components is 24 and the maximum number of controls + optimization variables is 20. A KONFIG input card is then generated by the user for each component as shown in figure 3. This figure is for the compressor in figure 2. The component is identified as component number 4, that it is a compressor and that its primary upstream flow station number is 4, there is no secondary upstream flow; that the primary downstream flow station is number 5; and the secondary downstream flow station is number 13 (bleed flow). After all the components have been "configured," NNEP generates its own flow path logic by joining components by the station numbers.

Each component has associated with it up to 15 required inputs describing the component. These inputs are usually design values such as pressure rise or map numbers corresponding to prestored performance maps for the component. An illustration of the specifications for the compressor in figure 3 is shown in figure 4.

Control information is also entered as input identifying both the independent and dependent variable as shown in figure 5. Optimization variables are entered similarly as shown in figure 6.

NNEP has proven to be a powerful analytical tool. Its primary purpose is to generate engine performance data for mission analysis studies. A typical use is shown in figure 7. This figure illustrates the specific fuel consumption of a supersonic turbofan engine as a function of engine thrust when the supersonic engine is operated at a subsonic cruise condition Mach 0.9 at 11 000 meters (36 089 ft). Shown on the figure are three curves. The bottom curve represents the engine performance on an uninstalled basis, that is, a pure thermodynamic cycle calculation. None of the variable-geometry features of the engine have been utilized.

An engine and inlet which are sized for supersonic cruise can suffer significant installation losses subsonically. At the reduced power settings the inlet will be capable of swallowing more air than the engine requires resulting in inlet spillage drag. The boattail aft of the engine will not be filled with engine air resulting in additional drag. Installed performance for the fixed-geometry engine is represented by the uppermost curve. As can be seen the difference between installed and uninstalled performance increases as engine thrust is reduced. The engine specific fuel consumption increases rapidly at the lower power settings.

The introduction of variable geometry features into the engine can greatly change the shape of the installed performance curve. The performance of the engine with a variable geometry nozzle and variable area low pressure turbine is shown on the remaining curve. The optimization capability of NNEP has been used to determine the optimum values of the two independent variables. As can be seen, the curve is essentially flat. The components have varied to maintain as high an airflow as possible through the engine to reduce the spillage and boattail drag. NNEP has proven to be a very versatile engine cycle computer code and is now in use at approximately 30 government installations, companies and universities.

WEIGHT ANALYSIS OF TURBINE ENGINES - WATE

With NNEP we are capable of simulating almost any turbine engine cycle the user can conceive of. Being able to calculate engine performance and hence the fuel consumed on a mission is an important part of calculating the vehicle performance. It is also necessary to be able to calculate the engine weight, length and diameter. The engine weight represents a significant part of the empty weight of an airplane. The length and diameter of the engine are important in calculating friction and boattail drags. In order to

develop the capability, NASA Lewis awarded a contract to the Boeing Military Airplane Development Division of the Boeing Company to develop an engine weight estimation code.

The first version of this code WATE-1 (ref. 8) was completed in 1977. It used a preliminary design approach where stress level, maximum temperature, material, geometry, stage loading, hub-tip ratio and shaft mechanical overspeed are used to determine individual component weights. The total engine weight was then calculated as the sum of the individual components. The contract required that the code predict both individual component and total engine weight within ± 10 percent accuracy.

A relatively high level of detail was found necessary in order to obtain the required accuracy. Component weight data for 29 different engines were used as a data base. This data base is shown in the figure 8. The list of engines includes military and commercial, turbofans and turbojets, augmented and dry, hardware engines and proposed engines, and supersonic and subsonic engines.

WATE 1 was constructed to operate as an adjunct to NNEP. After running a cycle point on NNEP the thermodynamic properties were fed to the WATE-1 set of subroutines along with inputs representing the design features of the components. The engine weight, length, and dimensions were then calculated. At the same time, parts counts are generated for the engine such as number of blades, size of discs, etc.

In 1978, NASA Lewis awarded a follow-on contract to the Boeing Company to extend the capabilities of WATE 1. This new version, WATE 2 (ref. 9) was completed in 1979 and has added many desirable features. Weight determination is done for each component at its critical operating point as follows: NNEP is now used to "fly" the engine throughout the flight envelope of the aircraft and the maximum values of the flow, temperature, pressure and engine speed stored for use in sizing the components. Based upon these critical conditions, the weight is determined. The capability to calculate the weight of radial flow components and of small engines was added in conjunction with a subcontract to the Garrett Division of AiResearch Manufacturing Company of Arizona. The engine center of gravity and moments of inertia are also now calculated.

The accuracy of the code is shown in figure 9. As can be seen, all of the engines fall within the ± 10 percent band and, in most cases, approach ± 5 percent or better especially in terms of engine weight.

WATE has built-in default values for most of the inputs. If the user does not enter values, these default values are automatically used. Many of these were used in the calculation of these weights. If more information was available to us, especially in terms of geometry inputs of the rotating components, these already small errors could probably be reduced even further.

The combination of WATE and NNEP is a very powerful analytical tool. As an example, a recent study considered the question of optimum cycle parameters for a duct burning turbofan for a supersonic cruise airplane (ref. 10). Some of the results of this study are duplicated here. The fuel mass and bare engine mass for 88 950 newton (20 000 lb) thrust engines flying 6440 kilometers (4000 mile) operating at Mach 2.4, 16460 meters (54 000 ft) initial altitude are shown in figure 10. These masses are shown as functions of Bypass Ratio and Overall Pressure Ratio (OPR) with and without duct burning. The cycle analyst looking only at the fuel mass in figure 10 would conclude that the optimum engine would operate dry and have an OPR of about 16 at a Bypass Ratio of 1.8 or more. However, when the mission analyst adds the fuel and engine masses as shown in figure 11, the optimum engine operates with the ductburner on, an OPR of 12 and a BPR of 0.8.

LIFE CYCLE COSTING - COST/LIFCYC

The question of cost is entering more and more into the selection process for optimum engines. The initial cost is not the only criteria for selection. Total life cycle cost including maintenance, spares, operating costs, etc. must be considered for many applications. In order to develop the capability of calculating Life Cycle Cost, NASA Lewis contracted with the Naval Air Development Center (NADC) in 1978 to receive their costing model. NADC in turn subcontracted with Boeing to supply them with the production cost of the engine. As previously mentioned the weight code WATE calculates parts counts and weights as well as total component and total engine weight. These weights are transferred to cost estimating routines which are based on correlations developed by NADC and Naval Air Systems Command. This procedure is flow diagramed in figure 12. The correlation parameter is based on a system of classifying materials by similarity of applications in engines (ref. 11). In this procedure, materials used in jet engines are placed in one of a total of six relative cost categories having to do with a combination of manufacturing cost and raw materials cost. Carbon steel and aluminum are assigned the lowest classification and used as a reference. High-strength high-temperature nickel cobalt alloys which are costly and difficult to machine are placed in the highest (fifth) classification. Because of peculiar differences in cost and machinability, titanium alloys are assigned a separate (sixth) classification. Two indices are developed for each material class, namely

- (1) Relative material cost
- (2) Relative machining cost

The product of these two indices is called the "relative weighing factor."

In the cost estimation procedure, the estimated weight of each engine component is first converted to raw material weight. A raw material weight to finished material weight scaling factor, referred to as "Buy/Fly" ratio, has been estimated for each component for state-of-the-art and for advanced production methods. Raw material weight is then multiplied by the relative weighing factor, and the sum of all such component products is formed. The summation for all engine components is called the "Maurer factor" in honor of its originator, R. J. Maurer. The production cost of the engine is estimated by the linear correlation (fig. 13) between engine manufacturing cost and the Maurer factor (ref. 11).

This code is just becoming operational at NASA Lewis and no results have as yet been generated except for isolated check cases in which predicted costs have been compared to the actual and appear reasonable. A final report should be published sometime during the summer of 1979.

Having determined the engine cost, it is now possible to determine the Life Cycle Cost based upon the NADC Life Cycle Costing Model. The interrelationship of COST with LIFCYC is shown in figure 14. NADC will supply the inputs and models to calculate all the parts of the pie other than manufacturing costs. It is anticipated that this work will be performed in the fall of 1979.

IMPROVED INSTALLATION EFFECTS MODEL - INSTAL

The previous example (fig. 7) of varying engine flow by the use of variable geometry to reduce installation effects showed the importance of inlet and nozzle component performance, external as well as internal. That figure was generated with a simplified model for inlet and boattail drag that is built into the NNEP program.

It was decided that NASA Lewis should obtain a more sophisticated method for these calculations. Consequently, a contract was awarded to Boeing in 1978 to provide a broad subsidiary program for determining power-dependent inlet and afterbody installation effects and also inlet/nacelle weights (presently not in the WATE code). Nozzle weights are already calculated within WATE. In addition to generating the component performance maps for NNEP, the code can be interactive with the cycle and hence a tradeoff of inlet, afterbody, and cycle can be utilized in the design process.

The types of performance maps to be generated are shown in figures 15 and 16 for inlets and nozzles respectively. The necessary maps are obtained from either a data base or theoretical calculations (ref. 13). The data base contains performance data (usually experimental) for a spectrum of inlet (axisymmetric, 2D, pitot, mixed compression) or nozzle (axisymmetric, 2D, twin, etc.) types. A derivative procedure (ref. 13) can be used to adjust the data base for changes in design Mach number, sideplate shape, subsonic diffuser loss, cowl lip bluntness, takeoff door area, external cowl initial angle, bleed system design, and bypass system exit design. Items not included in the data are determined analytically. Nozzle/afterbody data are treated in a similar manner. The data base, being primarily experimental, offers increased confidence in areas that are difficult to treat theoretically such as viscous effects.

After selecting the inlet size or sizing Mach number, the inlet and nozzle are matched to the NNEP cycle data and the installed performance calculated as well as the respective weights. Trade off studies can now be made of such effects as the best combination of bypass and spillage for minimum specific fuel consumption.

The final report for the work being performed under this study contract is scheduled to be published in the early fall of 1979.

WAVE AND FRICTION DRAG - PODDRG

Under contract to NASA Langley Research Center, Rockwell International developed a method of evaluating the effects of nacelle shape on drag and weight of a supersonic cruising aircraft (ref. 14). Under this contract, Rockwell determined wave and friction drag increments for a range of parametric shapes. As part of a follow-on contract with NASA Lewis Research Center, Rockwell developed a computer code (PODDRG) capable of interrogating the data points generated under the previous contract in order to determine drag increments for any nacelle shape of interest (ref. 15).

These nacelle incremental drags are only applicable to the NASA arrow-wing supersonic transport configuration (ref. 16). The program yields the incremental wave and friction drags of nacelles as functions of nacelle geometry variables and airplane Mach number. The drag increments are for the total vehicle relative to the vehicle with nacelles removed. That is, all interference effects with the airframe are accounted for. The nacelle shape parameters used as inputs to the program are:

- (1) A_c Inlet capture area
- (2) A_{MAX} Nacelle maximum cross-sectional area
- (3) A_n Nozzle exit area (supersonic cruise position)
- (4) X_{MAX} Distance from inlet cowl leading edge to maximum cross-sectional area

AD-A083 203

ADVISORY GROUP FOR AEROSPACE RESEARCH AND DEVELOPMENT--ETC F/6 9/2
THE USE OF COMPUTERS AS A DESIGN TOOL.(U)
JAN 80

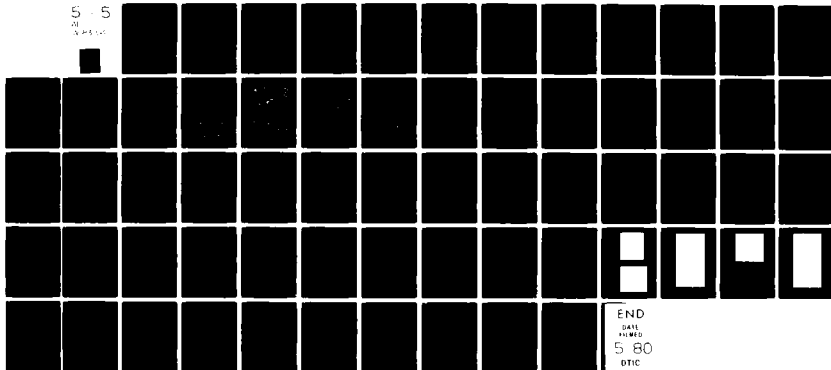
UNCLASSIFIED

AGARD-CP-280

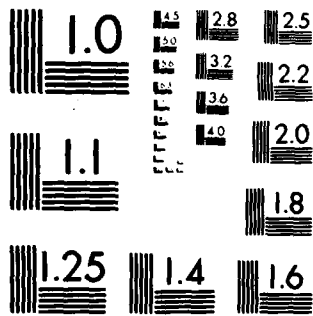
NL

5-5

20
3/8/80



END
DATE
FILMED
5-80
DTIC



MICROCOPY RESOLUTION TEST CHART
NATIONAL BUREAU OF STANDARDS 1963 A

- (5) l Nacelle total length
- (6) S_{REF} Reference wing area

The output of this program includes, for the nacelle of interest:

- (1) The aforementioned input data
- (2) Drag coefficients at Mach 1.2, Mach 2.32, and the input Mach number for friction (CDF), wave (CDW), and total (CDO) drags
- (3) The nondimensional parameters of position of maximum cross-sectional area (X_{AMAX}/l), nozzle-to-capture area ratio (A_n/A_c), maximum-to-capture area ratio (A_{MAX}/A_c), and fineness ratio (l/d_c)

In addition, incremental drag coefficients of the reference airplane nacelle (ref. 16) are printed.

Typical nacelle incremental wave drag variations are shown in figure 17. Note that a properly shaped nacelle can produce a lower total airplane drag than that of the airframe alone ($\Delta C_{DW} < 0$). The nacelle drags thus calculated are fed into mission flight computer codes in evaluating systems performance.

CONCLUDING REMARKS

NASA Lewis Research Center with a combination of in-house, joint, and contracted efforts has been and is continuing to develop the capability to determine the engines for optimum mission performance. In the selection process we can account for cycle performance, engine weight, life cycle costs, and installation effects. Future efforts will be directed towards improvement in the current capabilities, mainly in the areas of developing better optimization methods to reduce computer time and analytically determining performance maps for rotating machinery. For example, we are about to award a contract for turbine map generation, to be used for new cycles in which simple scaling of pre-existing maps is not sufficient. We believe that all of these methods will greatly reduce the effort expended in performing mission analysis by narrowing in more quickly on the engine cycles of greatest interest.

REFERENCES

1. Dugan, James F., Jr.: Compressor and Turbine Matching. in Aerodynamic Design of Axial-Flow Compressors, NASA SP-36, 1965, pp. 469-496.
2. McKinney, John S.: Simulation of Turbofan Engine. Part I. Description of Method and Balancing Technique. AFAPL-TR-67-125, pt. 1, Air Force Aero Propulsion Lab., Wright-Patterson AFB, Ohio, Nov. 1967. (Available from DDC as AD-825197.) Part II. User's Manual and Computer Program Listing. AFAPL-TR-67-125, pt. 2, Air Force Aero Propulsion Lab., Wright-Patterson AFB, Ohio, Nov. 1967. (Available from DDC as AD-825198.)
3. Koenig, Robert W.; and Fishbach, Laurence H.: GENENG: A Program for Calculating Design and Off-Design Performance for Turbojet and Turbofan Engines. NASA TN D-6552, 1972.
4. Fishbach, Laurence H.; and Koenig, Robert W.: GENENG 2: A Program for Calculating Design and Off-Design Performance of Two- and Three-Spool Turbofans with as Many as Three Nozzles. NASA TN D-6553, 1972.
5. Sellers, James F.; and Daniele, Carl J.: DYNGEN - A Program for Calculating Steady State and Transient Performance of Turbojet and Turbofan Engines. NASA TN D-7901, 1975.
6. Shapiro, S. R.; and Caddy, M. J.: NEPCOMP - The Navy Engine Performance Program. ASME Paper 74-GT-83, Mar. 1974.
7. Fishbach, Laurence H.; and Caddy, Michael J.: NNEP - The NAVY-NASA Engine Program. NASA TM X-71857, 1975.
8. Pera, R. J.; Onat, E.; Prewitt, N. L.; Klees, G. W.; and Tjonneland, E.: A Method to Estimate Weight and Dimensions of Aircraft Gas Turbine Engines. Volume I, Method of Analysis. Volume II, User's Manual. Volume III, Programmer's Manual. D6-44258-Vol. 1, Vol. 2, Vol. 3, Boeing Co., Seattle, Wash., May 1977. NASA CR-135170, Vol. I, NASA CR-135171, Vol. II, and NASA CR-135172, Vol. III, 1977.
9. Onat, E.; and Klees, G. W.: A Method to Estimate Weight and Dimensions of Large and Small Gas Turbine Engines. Boeing Military Airplane Development, Seattle, Wash., Jan. 1979.. NASA CR-159481, 1979.
10. Fishbach, Laurence H.: Preliminary Study of Optimum Ductburning Turbofan Engine Cycle Design Parameters for Supersonic Cruising. NASA TM-79047, 1978.

11. Brennan, T. J.; Taylor, R. N.; and Steinert, A. G.: Cost Estimating Techniques for Advanced Technology Engines. SAE Paper 700271, Apr. 1970.
12. Sharp, B. M.; and Howe, J. P.: Procedures for Estimating Inlet External and Internal Performance. McDonnell Aircraft Co., St. Louis, Mo., Apr. 1974, Naval Weapons Center, NWC-TP-5555, 1974.
13. Ball, W. H.; et al.: Rapid Evaluation of Propulsion System Effects, Vol. 1: Final Report; Vol. 2: PIPSI User's Manual; Vol. 3: Derivative Procedure (DERIVP) User's Manual; Vol. 4: Library of Configurations and Performance Maps. Boeing Aerospace Co., Seattle, Wash., July 1978. AFFDL-TR-78-91-Vol.1-4, Wright-Patterson AFB,, Ohio, 1978. (AD-B031629L, V.1; AD-B031766L, V.2; AD-B031768L, V.3; AD-B031555L, V.4.)
14. Bonner, E.; Mairs, R. Y.; and Tyson, R. M.: Effects of Nacelle Shape on Drag and Weight of a Supersonic Cruising Aircraft. Rockwell International Corp., Los Angeles, Calif., Oct. 1975. NASA CR-144893, 1975.
15. Tyson, Ray M.; Mairs, R. Y.; Halferty, F. D., Jr.; Moore, B. E.; and Chaloff, D.: Methods for Comparative Evaluation of Propulsion System Designs for Supersonic Aircraft. NA-76-470, Rockwell International Corp., Los Angeles, Calif., June 1976. NASA CR-135110, 1976.
16. Advanced Supersonic Technology Concept Study Reference Characteristics. LTV Aerospace Corp., Hampton, Va., Dec. 1973. NASA CR-132374, 1973.

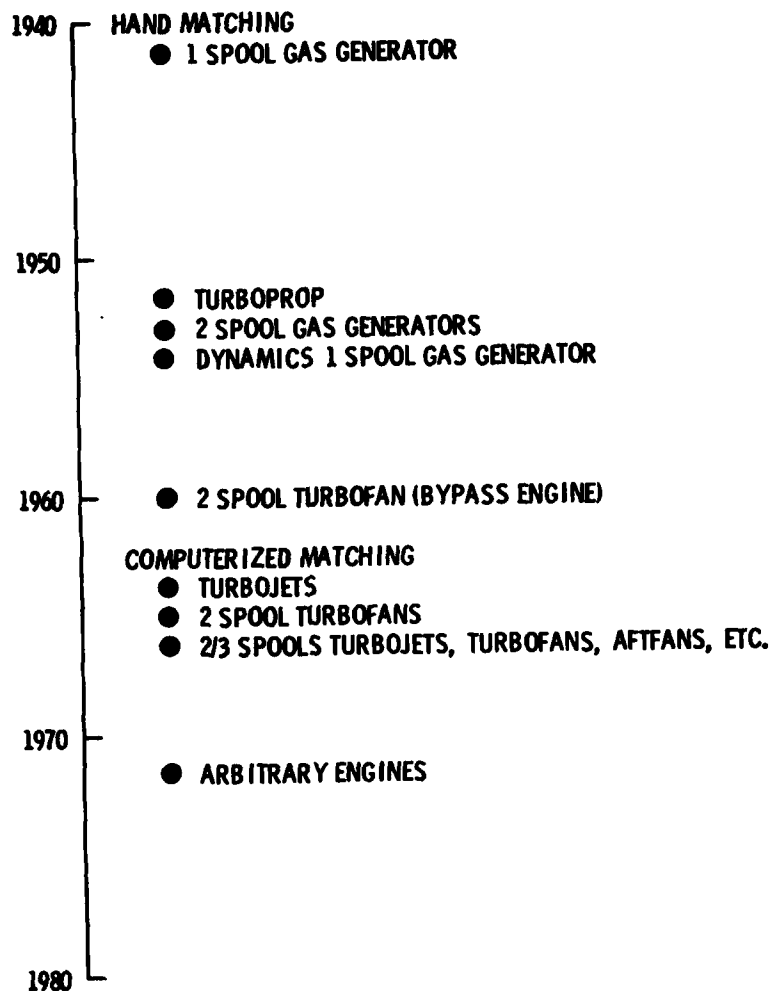


Fig.1 Approximate history of methods of matching turbine engines

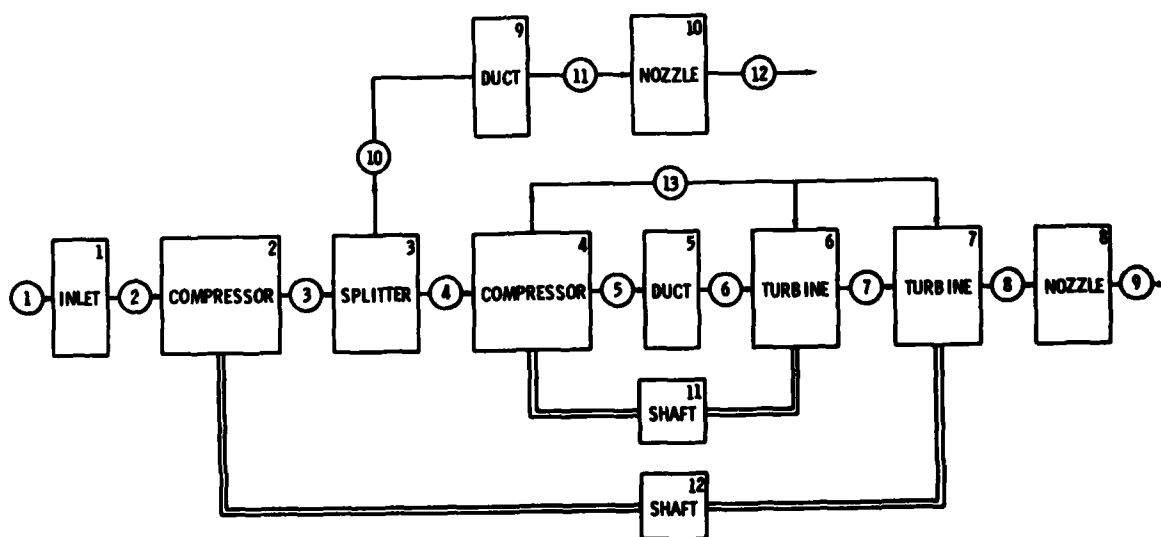
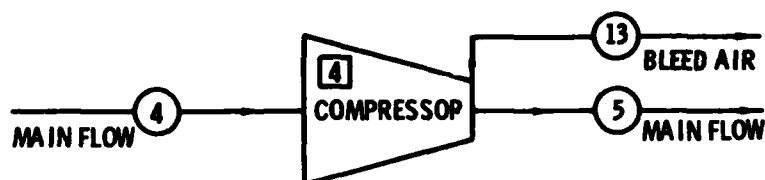


Fig.2 Simple 2 spool turbofan with cooled turbines



KONFIG (1, 4) = 'COMP', 4, 0, 5, 13

COMPONENT # TYPE
 PRIMARY UPSTREAM
 SECONDARY UP-STREAM
 PRIMARY DOWNSTREAM
 SECONDARY DOWNSTREAM
 FLOW STATION NUMBERS

Fig.3 Define component type and location in flowstream

SPEC (1, 4) = 1.1, 0.036, 1, 3707, 1, 3708, 1, 3709, 1, 0, 0, 0.88, 4.1, 1.0, 0,
 (1) (2) (3) (4) (5) (6) (7) (8) (9) (10) (11) (12) (13) (14) (15)

- (1) 'R' VALUE ON MAP = 1.1
- (2) BLEED FLOW/TOTAL FLOW = 0.036
- (3), (5), (7), AND (9) SCALE FACTORS ON $N/\sqrt{\theta}$, $W\sqrt{\theta}/\delta$, η , AND PR ON MAPS. THESE ARE INITIALLY SET = 1 AND ARE INTERNALLY COMPUTED
- (4) MAP REFERENCE NUMBER OF $W\sqrt{\theta}/\delta$ VERSUS 'R' = 3707
- (6) MAP REFERENCE NUMBER OF η VERSUS 'R' = 3708
- (8) MAP REFERENCE NUMBER OF PR VERSUS 'R' = 3709
- (10) 3rd DIMENSIONAL ARGUMENT ON "STACKED MAPS" - STATOR ANGLE = 0
- (11) FRACTIONAL HORSEPOWER LOSS DUE TO INTERSTAGE BLEED = 0
- (12) DESIRED ADIABATIC EFFICIENCY η AT DESIGN POINT ON MAP = 0.88
- (13) DESIRED PRESSURE RATIO PR AT DESIGN POINT ON MAP = 4.1
- (14) DESIGN POINT CORRECTED SPEED $N/\sqrt{\theta}$ = 1.0
- (15) NOT USED

Fig.4 Defining component characteristics (for a compressor)

KONFIG (1, 30) = 'CNTL'

SPCNTL (1, 30) = 1, 4, 'STAP', 8, 10, 0, 0.001, 1, 2.2,

VARY SPEC ()
 OF COMPONENT ()
 SO THAT STATION PROPERTY
 AT FLOW STATION ()
 HAS A VALUE OF ()
 AND A TOLERANCE OF ()
 THE MINIMUM ALLOWABLE
 VALUE OF THE VARIABLE IS ()
 AND MAXIMUM VALUE IS ()

Fig.5 Defining controls

KONFIG (1, 37) = 'OPTV', 0, 0, 12, 0,
 SPEC (1, 37) = 0, 248, 826, 1, 4* 0., 0.1,

THE COMPONENT NUMBER
WHICH HAS THE
FREE VARIABLE

NOT USED
 MIN. ALLOWABLE VALUE
 MAX. ALLOWABLE VALUE
 WHICH SPEC IS FREE VAR.
 4 SLOTS NOT USED
 ABSOLUTE TOLERANCE TO
 WHICH THIS VARIABLE IS
 TO BE OPTIMIZED

Fig.6 Defining optimization variables

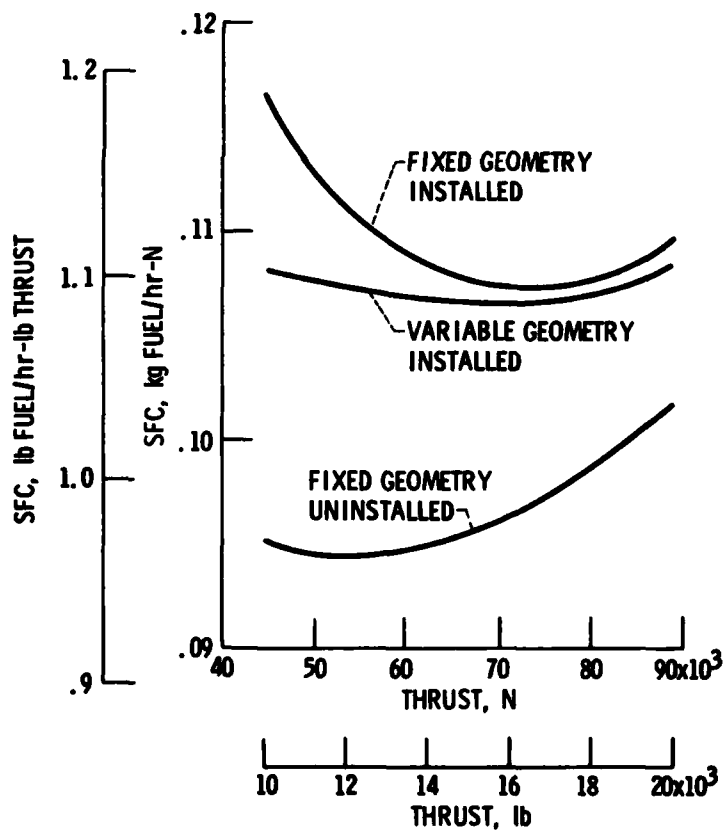


Fig.7 Engine specific fuel consumption as a function of engine thrust

ENGINE	MANUFACTURER	MANUFACTURING STATUS ¹	TYPE OF CYCLE ²	AUGMENTATION ³	PRIMARY USE ⁴
GE4/J4C	GE	P	TJ	AB	C
GE4/J5	GE	X	TJ	AB	C
GE9/F2B	GE	X	TF	AB	M
JT11F	P&WA	P	TJ	AB	M
TJ70	WE	S	TJ	AB	C
GE4/J6G	GE	S	TJ	AB	C
GE4/J5H2	GE	S	TJ	--	C
JT8D-15	P&WA	P	TF	--	C
JT9D	P&WA	P	TF	--	C
TF34	GE	P	TF	--	M
VSCE-502	P&WA	S	TF	DH	C
VCE-201A	P&WA	S	VCE	--	C
VCE-201B	P&WA	S	VCE	--	C
VCE302A	P&WA	S	VCE	--	C
VSCE-502B	P&WA	S	TF	DH	C
VCE-112B	P&WA	S	VCE	--	C
VSCE-501	P&WA	S	TF	DH	C
VCE-110B	P&WA	S	VCE	--	C
A/B TF-2	P&WA	S	TF	AB	C
D/H TF-2	P&WA	S	TF	DH	C
D/H TF-12	P&WA	S	TF	DH	C
JT10D	P&WA	X	TF	--	C
CFM56	GE/SNECMA	P	TF	--	C
CF6-50	GE	P	TF	--	C
CF6	GE	P	TF	--	C
JT8D	P&WA	P	TF	--	C
CJ805-23	GE	P	TF	--	C
YJ93	GE	P	TJ	AB	M
JT3D	P&WA	P	TF	--	C

¹MANUFACTURING STATUS P - PRODUCTION, S - STUDY PROPOSAL, X - EXPERIMENTAL

²TJ - TURBOJET, TF - TURBOFAN, VCE - VARIABLE CYCLE ENGINE

³AUGMENTATION TYPE AB - AFTERBURNER, DH - DUCTHEATER

⁴C - COMMERCIAL, M - MILITARY

Fig.8 Data base engines

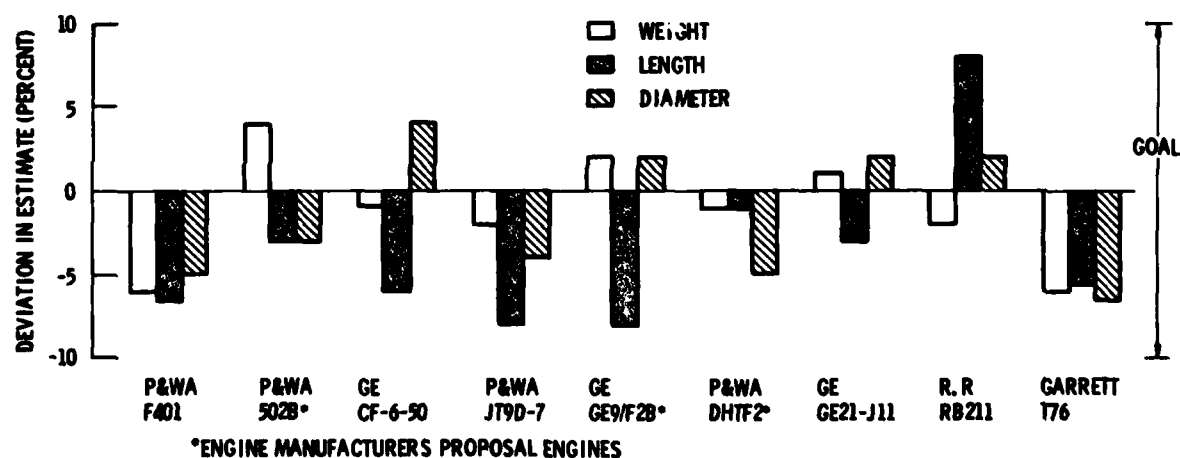


Fig.9 Program results compared to manufacturers quotations

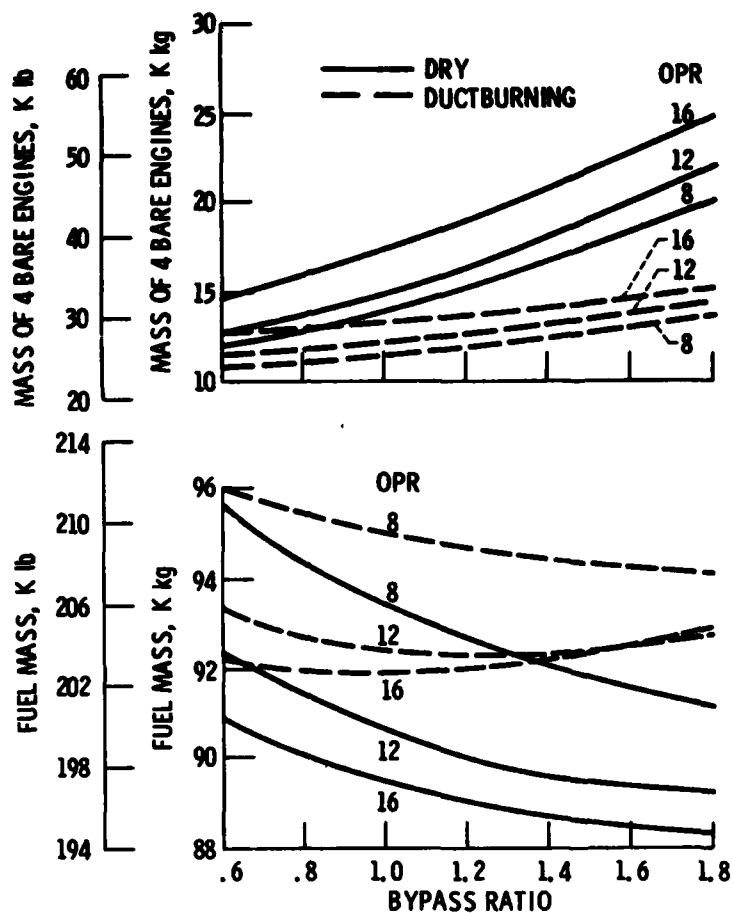


Fig.10 Fuel mass and bare engine mass, 88 950 N (20 000 lb) thrust engines

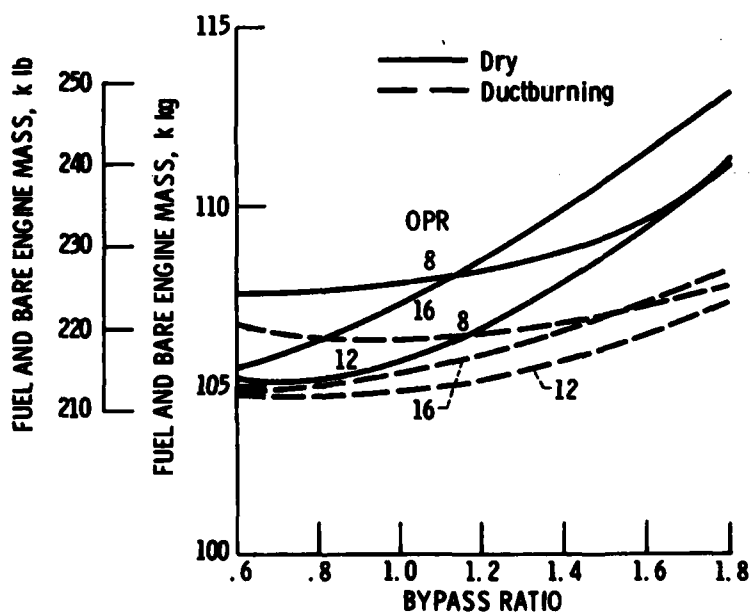


Fig.11 Sum of engine plus fuel mass, 88 950 N (20 000 lb) thrust engines

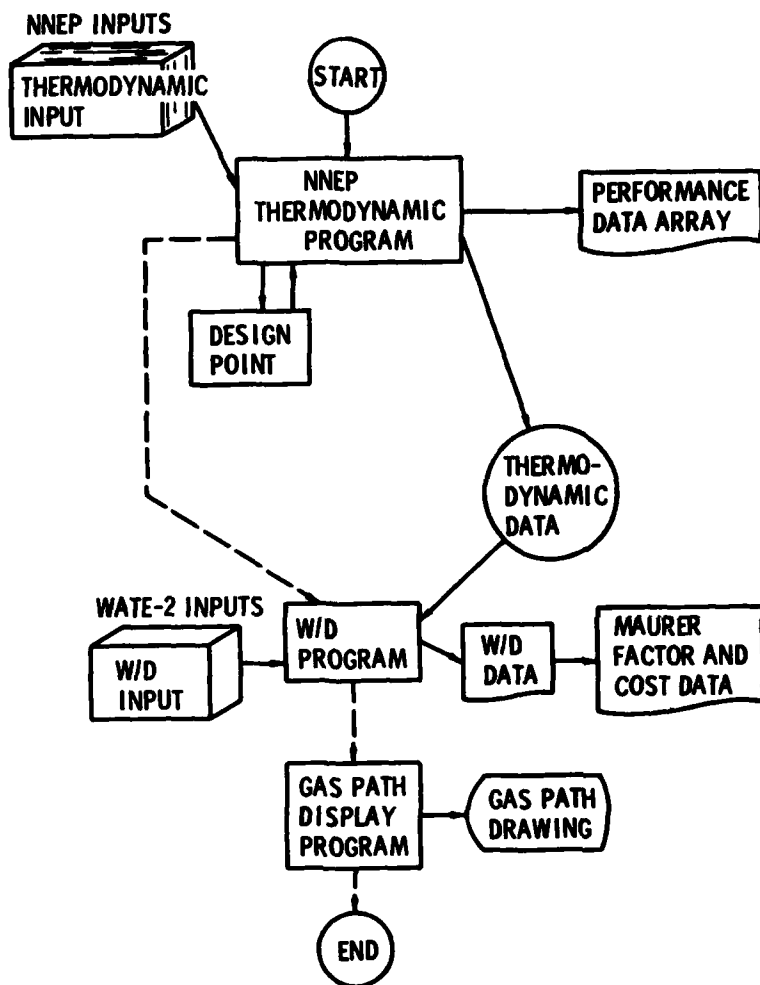


Fig.12 Overall program structure

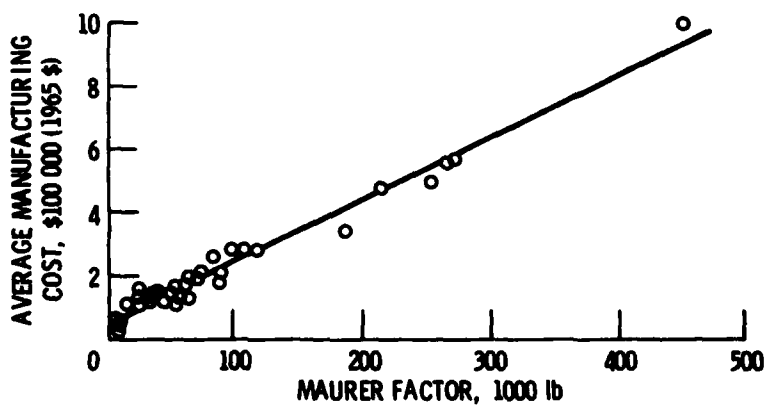


Fig.13 Maurer factor correlation with cost

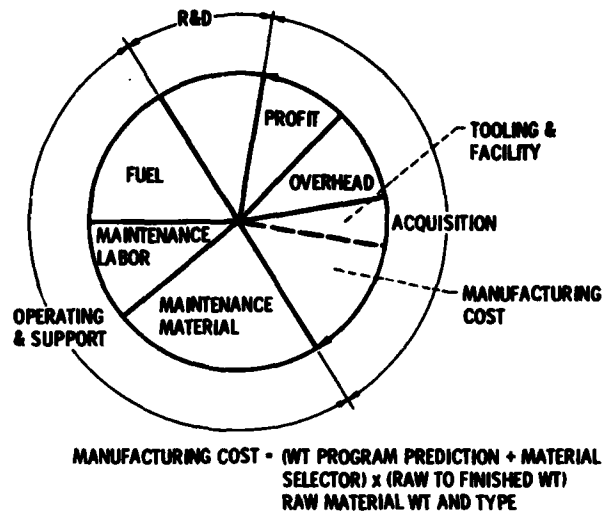


Fig.14 Engine life cycle cost

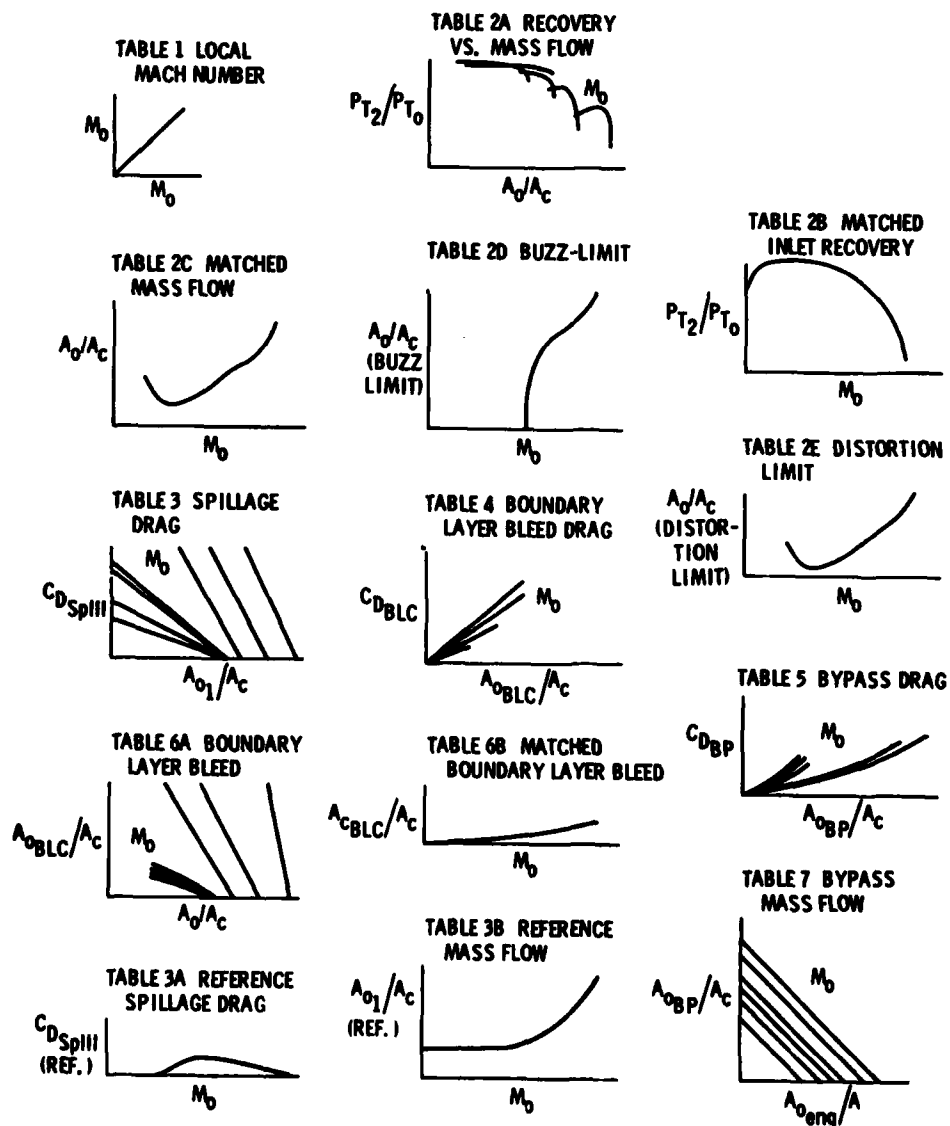
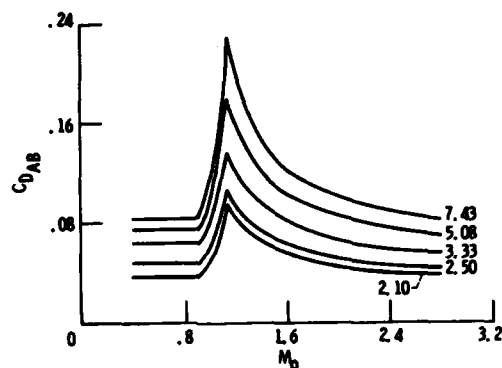
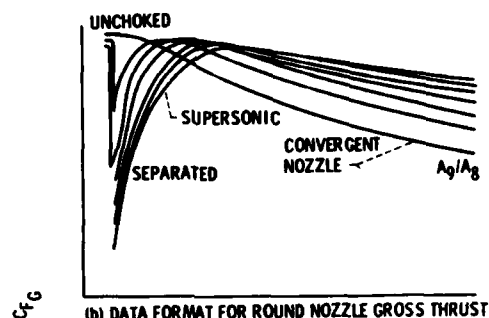


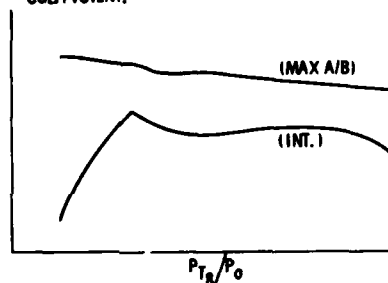
Fig.15 Format for inlet performance characteristics maps



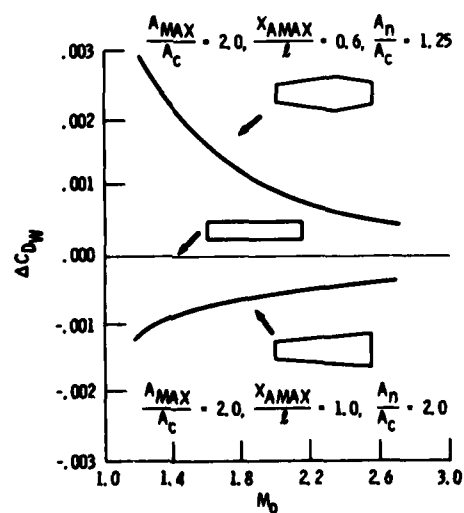
(a) DATA FORMAT FOR NOZZLE/AFTBODY DRAG.



(b) DATA FORMAT FOR ROUND NOZZLE GROSS THRUST COEFFICIENT.



(c) DATA FORMAT FOR NOZZLE GROSS THRUST COEFFICIENT FOR TWO-DIMENSIONAL NOZZLES.

Fig.16 Format for nozzle/afterbody drag and C_{FG} mapsFig.17 Typical nacelle incremental wave drag variations with Mach number $A_c = 2.79$ sq m (30 sq ft), $l/d_c = 5.5$

MATHEMATICAL MODELLING IN MILITARY AIRCRAFT WEAPON SYSTEM DESIGN

by

N. Mitchell
British Aerospace
Aircraft Group
Warton Division

Warton Aerodrome, Preston, Lancashire PR4 1AX

SUMMARY

Modern aircraft weapon systems are increasing in complexity and performance and require detailed assessment to define their capabilities and limitations. One of the main tools used in weapon system design and analysis is the mathematical model, ie a complete mathematical representation of the aircraft weapon system, programmed for running on a digital computer. The main elements of a model are described and the use of models is discussed in the chronological phases of weapon system design and development, including trials planning and analysis, with the associated model matching. Examples of the use of models to investigate and resolve design problems are given, including integrated modelling between several companies. There is a rapid growth in number and use of digital computers in aircraft weapon systems and some typical modelling input to the software of these airborne computers is discussed.

INTRODUCTION

The subject of this paper is Mathematical Modelling and its use in the design and analysis of aircraft weapon systems. It is particularly appropriate for presentation at this symposium on the use of computers in design, because modelling didn't really take off until the appearance of more powerful digital computers in the early sixties, and modelling activity has grown in parallel with computer developments since then. The purpose of the paper is to describe the main features and uses of models and then go on to describe some particular applications, as examples of the way they are used in the design process. Although the paper deals with mathematical modelling of aircraft weapon systems, similar modelling techniques are applicable over a very wide range of technical and commercial activities.

THE FUNCTION OF MILITARY AIRCRAFT

Much attention is rightly paid to particular key aspects of weapon system design, eg aerodynamics, structures, engines etc., but it should not be forgotten that the main function of military aircraft weapon systems is to kill and destroy. The need for national air forces and the NATO alliance is generally accepted and, therefore, they must be given the best equipment possible if they are to do the job well.

The aim of a weapon system design organisation is to produce weapon systems which will deliver the weapon warhead to the target as accurately, efficiently, reliably and cheaply as possible. Often in the past the aircraft was built as a sleek high speed flying machine and the weapons and aiming systems added on as an afterthought. The modern weapon system concept involves early integration of all elements of the weapon system, including aircraft, crew, avionics and weapons. This is more necessary nowadays, because of the increasing cost and complexity of weapon systems.

The two main offensive roles of military aircraft are air attack and ground attack, ie the engagement of airborne and ground (or maritime) targets respectively. A modern trend in military aircraft design is to have a capability in both areas (multi role), but most specialise in one. The British Aerospace Lightning was initially designed to intercept high altitude bombers threatening the UK, but later it was given a ground attack capability. The current versions of Jaguar and Tornado (IDS) are primarily ground attack aircraft but both have an air combat capability also. The air defence variant (ADV) of Tornado has switched the major role to air attack by the installation of new avionics and weapons.

WEAPON SYSTEMS ANALYSIS - MATHEMATICAL MODELLING

Modern weapon systems are continually increasing in complexity and performance and need detailed assessment to define their capabilities and limitations and to assess the benefits of any modifications. In the old days guns were the main armament in air combat, speeds were slow and the fighter was in close visual contact with the target throughout the attack. Modern supersonic interceptors using AI radars and air-to-air missiles can attack supersonic targets head-on. This involves closing speeds of 2000 mph and the target may be destroyed without the fighter pilot ever seeing it. The rapid advances in computer technology during the last two decades have provided the facility for detailed evaluation of such weapon systems.

One of the main tools used in weapon systems analysis is the mathematical model, ie a complete digital simulation of the aircraft weapon system for running on a digital computer. The advantages and potential of such modelling work have become increasingly apparent now that reliable and powerful computers are available. There are many different levels of modelling, from individual pieces of equipment in one aircraft through to a full model of the whole of a battle sequence containing many aircraft and other forces. Most of the modelling discussed in this paper concerns the operation of a particular aircraft attacking particular targets.

Several aircraft weapon system models have been developed by British Aerospace at Warton, including both air attack and ground attack models. These models simulate the aircraft and weapon dynamics and include the pilot and avionics representation. Using the models it is possible to "fly" many different types of attack and so assess the weapon system capability. A simplified block diagram of a model is shown in Figure 1, where it can be seen that aerodynamic data (lift, drag) and engine data (thrust, fuel flow) are used in the equations of motion to produce aircraft and weapon trajectories, ie time histories of position, velocity, acceleration and attitude. The pilot block controls the aircraft flight path by applying bank angle and g and throttle according to the particular requirements at the time. All of the relevant aerodynamic, structural and pilot limitations are respected. The targets are represented and the full

attack geometry is computed and used to simulate the displays seen by the crew. In the tracking phase of an attack the pilot will be applying control demands to reduce the errors on his weapon aiming display.

USE OF MODELS

Mathematical models enable the design engineer to examine the performance of a weapon system and so obtain a better understanding of its capability. The information provided by the models can be used for many purposes, depending on the type of weapon system and the stage in its design or development.

Some of the main areas of modelling activity are:-

- . Early project work to assess and refine design concepts.
- . Prediction of overall weapon system performance and limitations.
- . Development of optimum attack techniques to achieve maximum effectiveness.
- . Provision of detailed attack profiles for use in flight trials and ground tests.
- . Driving of ground rigs (dynamic testing) and flight simulators.
- . Analysis of test results.
- . Definition of software requirements for airborne computers.
- . Evaluation of new requirements and modifications (eg new weapons, sensors, aiming systems, attack manoeuvres).
- . Provision of tactical/operational data to the user.

The use of models is particularly attractive, because of the small cost of a 'flight' on the computer (£10) compared with an actual flight trial (£10,000). Many modern weapon systems are designed to be used in a wide variety of threat situations and can deal with the threat in many different ways. It is much cheaper and quicker to "fly" a large number of attacks on the computer in order to assess the optimum methods of attack, which can then be tested in flight trials.

One of the essential items in any modelling programme is model 'matching' or validation. This is done by comparing model predictions with what actually happens when the real system hardware is tested on the ground or in flight. If necessary, appropriate changes can be made to the model to 'match' it to the real system, ie make it represent the real system more accurately. If, however, a malfunction has occurred during the test, then the model can be made to 'malfunction' in the same way and this affords a very useful facility for investigation and correction of the real system; clearly such malfunction modifications to the model are not part of the 'matching' process, in that they are not retained.

AIR ATTACK

The air attack role is concerned with the destruction of enemy aircraft. These airborne targets have a number of characteristics which strongly influence the design of an air attack weapon system and hence the nature of the computer modelling work. Some of the main characteristics of airborne targets are discussed below, and their influence on air attack requirements is shown in Figure 2.

Target size

Compared with most ground targets, airborne targets are very small and one of the principal requirements in an air attack weapon system is the ability to detect targets. This places emphasis on good visibility from the cockpit and the need for airborne intercept (AI) radar.

Target speed and manoeuvrability

Most modern aircraft have transonic or supersonic speed capability and a good level of manoeuvrability. In order to destroy such targets it is essential for the aircraft and/or the weapon to have good speed and manoeuvre performance. With unguided air-to-air weapons, eg guns, the aircraft alone has to have sufficient speed to catch the target and sufficient turn capability to bring the guns to bear on it. With air-to-air guided missiles, some of these demands on the aircraft are taken over by the missile, but the attack aircraft must still have sufficient performance to get into a missile firing position or to evade the enemy when necessary.

Target vulnerability

In general airborne targets are relatively 'soft', such that small warheads when delivered with sufficient accuracy will inflict the necessary damage. A 30mm cannon shell typically weighs about $\frac{1}{2}$ lb and contains about $1\frac{1}{2}$ oz of high explosive. A direct hit is essential. An air-to-air missile warhead, usually fragmentation or continuous rod type, typically weighs about 50 lbs. In addition to contact fuses, the missile is usually proximity fused and with a lethal radius of about 30 feet it can take out any small miss distance as the missile passes the target.

The above three target characteristics are reflected in the weapon system modelling work which examines target detection and evaluation, target tracking, steering courses towards the target, weapon aiming, weapon firing, weapon performance, and hit probability or miss distance. Air attack may be subdivided into two main categories, interception and close combat.

Interception

Interception is primarily a defensive task, as the name suggests, the object being to detect enemy aircraft and to intercept and destroy them before they inflict any damage on friendly positions. It is essential that such interceptor defences are highly organised if they are to achieve the rapid response and accurate interception demanded in many cases.

A typical air defence scenario is shown in Figure 3. The defending aircraft will normally operate under close ground control, but under degraded circumstances may operate autonomously. They may operate from base, using quick reaction alert (QRA), or fly combat air patrol CAP to give a more rapid response to an incoming threat. They may be supported by air refuelling tankers and airborne early warning aircraft (AEW) as well as surface forces such as ships. They will be called upon to engage a wide variety of targets who can be expected to employ defensive manoeuvres and ECM, if not active aggressive retaliation.

The main battle scenario variables could include such parameters as:

- . number of targets single, multiple
- . type of target slow/fast, high/low
- . raid disposition width, depth, track
- . target behaviour fly straight, turn
- . number of defending aircraft single, multiple
- . defending bases single, multiple
- . warning range short, medium, long
- . environment clear, jamming

The attack features used by the defending aircraft might include:

- . level, climb, dive
- . front, rear
- . cruise, dash, energy manoeuvre
- . collision, pursuit
- . MRAAM, SRAAM, gun
- . radar CW, pulse, visual
- . track-while-scan, lock-on, kinematic ranging

Even with only a few different values of each variable one quickly reaches many thousands of attack situations. For each of these situations the attack can be carried out in many different ways. With such scope to its operations, careful consideration has to be given to the way in which the weapon system performance is to be predicted and demonstrated. It is here that mathematical modelling can be used, being fast and relatively cheap.

The best method of attacking any given threat is not obvious and in order to use the weapon system to maximum effect a detailed evaluation of its performance is necessary. In Figure 4 is shown a hypothetical multiple target attack. By running several attacks on the model, the optimum way of killing the four targets can be assessed. In addition, the model run affords full time histories of key parameters such as target range and closing rate, sightline angles and angle rates, aircraft acceleration, speed, height, attitude. It is, therefore, possible to examine in detail the performance of any element of the weapon system throughout this attack profile. By co-ordinating the modelling activity of the main contractor and the major subcontractors (eg radar, missile) a full suite of models can be applied to the task. Having agreed the most likely threat situations and assessed the optimum method of attack, the attack profiles can then form a co-ordinated basis for weapon system assessment, development and test.

In Figure 5 are illustrated some modelling results used in the optimisation of nose radome shape. Here the two primary considerations were aircraft aerodynamic performance and radar performance. As both are very important in achieving overall aircraft effectiveness, the best method of determining the optimum solution is to examine their effects on the attack profiles. The radar performance can be studied for the complete attack profile, which defines aircraft speed, height, attitude, sightline angles range, range rate etc., to see whether any adverse clutter or detection problems occur. The effect of radome shape on aircraft acceleration, maximum speed, manoeuvrability or fuel consumption can be assessed on an aircraft performance model. The final solution will maximise the combined aerodynamic and radar performance.

Another example of computer modelling, this time to optimise aircraft and missile performance, is illustrated in Figure 6. When attacking very high altitude targets the interceptor may have to zoom above its sustained flight domain. The optimum point to launch the missile to achieve maximum success can be determined by computer runs on the aircraft and missile models. Unlike aircraft, missiles cannot be used again and again, so that the prediction of missile performance is very strongly based on computer modelling, suitably validated by a limited number of firing trials. A set of runs on the missile mathematical model will define a particular launch success zone, examples of which are shown in Figure 7. These launch success zones show areas from which the missile may be successfully fired against the specified target.

The major boundary limitations and the effects of target manoeuvre can also be determined.

The results of the aircraft and missile modelling work may feed directly into the airborne software, ie into the programs used by the aircraft computers. Such things as missile launch indication, aircraft performance data, optimum steering direction, weapon aiming can be computed and displayed to the crew. These have usually taken the form of data or algorithms, but the increasing power of airborne computers is now making it possible to run 'models' in the airborne software.

Close combat

Unlike the highly organised interception discussed earlier, close combat very often results from chance encounter between aircraft of opposing forces. They may both be air superiority (fighter) aircraft or one a ground attack intruder or perhaps on occasions both ground attack aircraft. In general the fighter aircraft will be seeking to engage the enemy, whereas the ground attack aircraft will have a main mission to attack ground targets and would not normally seek to engage in air combat. As mentioned earlier, many modern aircraft have a multi-role capability, such that ground attack aircraft have significant performance and manoeuvre levels and are usually fitted with short range air combat weapons for self defence. Close combat differs from interception in that it is a close range, highly manoeuvring environment, usually subsonic, in which both aircraft may be using aggressive tactics. The three main factors which influence the outcome of a particular close combat are:

- . aircraft characteristics
- . weapon characteristics
- . tactics

A deficiency in any one of these three can seriously affect the combat performance of the total. The 'right' characteristics for a close combat aircraft are the subject of considerable debate and combat modelling is giving a deeper insight into the significance of such parameters as thrust/weight ratio, wing loading, maximum speed, maximum g etc. The combat model simulates on a computer the combat between two aircraft and is of particular use in the early project phase where there is a need to translate a particular aircraft parameter change into effectiveness terms. Combat models used to drive simulators and rigs are currently yielding much new information on weapon system design and optimisation. By having men in the loop, a more realistic assessment of tactics and weapon system performance is possible. A typical close combat engagement is shown in Figure 8, where after a couple of initial 'scissors' manoeuvres the two aircraft get locked into a series of head-on passes.

GROUND ATTACK

This second major role of military aircraft weapon systems is concerned with the attack and destruction of ground or maritime targets. These targets are usually stationary or move at very slow speed compared with aircraft speed. Target types vary over a wide spectrum from relatively 'soft' (eg troop concentrations, parked aircraft) to much harder targets (eg armoured vehicles, building, bridges, runways). Target size also varies from small point targets (eg a tank) to large targets (eg an airfield). Because of the variety of possible ground targets, several different types of weapon have been developed to destroy them and several attack manoeuvres are used to deliver these weapons. In general much bigger warheads are required to destroy ground targets and they must be accurately delivered in order to achieve their maximum effect. Many ground targets will be defended, some very well defended, so weapons have been developed which can be delivered onto the target without exposing the attacking aircraft to enemy retaliation. Computer modelling of the ground attack weapon systems is used to investigate the optimum delivery techniques for this variety of weapons and targets taking due account of accuracy and safety.

Dive Attacks

When anti aircraft defences were less effective, level attacks from medium altitude were widely used. However, the considerable improvement in ground and ship defences in more recent times have led to the adoption of low level penetration tactics by modern ground attack aircraft; at low level the ground attack aircraft has less chance of being detected and is more difficult to shoot down. However, low level attacks expose the attacking aircraft to new hazards, namely being damaged by its own weapons and colliding with the ground. These hazards are illustrated in Figure 9 where it can be seen that risk from bomb fragments is the limiting factor for lower dive angles and risk of ground collision is limiting at higher dive angles. In general the pilot will wish to get as close to the target as possible before releasing the weapon to achieve maximum accuracy. Computer modelling of the aircraft trajectory, bomb trajectory, and fragmentation pattern enables the minimum safe release condition to be determined. This will of course vary with speed, dive angle, pull out g etc. This minimum release condition can be programmed into the software and displayed to the crew as part of the aiming picture.

Dive attacks with guns place particular emphasis on getting as close to the target as possible in order to achieve the required number of hits. Explosive shells may be used, but they do not present a significant fragment risk, although ricochet may occur. The main limiting factor is ground avoidance, and by modelling the pullout behaviour of the aircraft and the shell ballistic trajectory, a plot of minimum firing range can be produced as shown in Figure 10. This shows that minimum firing range occurs at shallow dive angles.

Level Attacks

Similar studies can be carried out for retarded bomb delivery, which is usually done straight and level at extremely low altitude. The retarder on the bomb causes it to rapidly fall behind the delivery aircraft after release, so that a safe separation distance exists when the bomb explodes. Modelling studies enable the minimum safe release heights to be determined as shown in Figure 11.

Loft Attacks

A typical loft attack is shown in Figure 12. The aircraft pulls up from a high speed low level entry to release the bomb in the climb and then rapidly returns to low level so as to avoid enemy defences. The main use of the loft attack is to achieve stand off range from the target. By computer modelling of the aircraft and bomb trajectories, plots can be produced as shown in Figure 13, which is a typical plot of pullup range from bomb impact as a function of release angle. As expected maximum range occurs around 45° release angle, but it is not possible to design for release at 45° , because variations in aircraft weight and performance, pilot execution of the manoeuvre and the weather will vary the maximum forward throw of the bomb and could preclude release. Computer modelling analysis of these effects enable the optimum release angles to be defined which will accommodate the likely variations in attack parameters. Typically 30° and 60° are suitable low loft and high loft release angles and they still give 80% of the maximum forward throw.

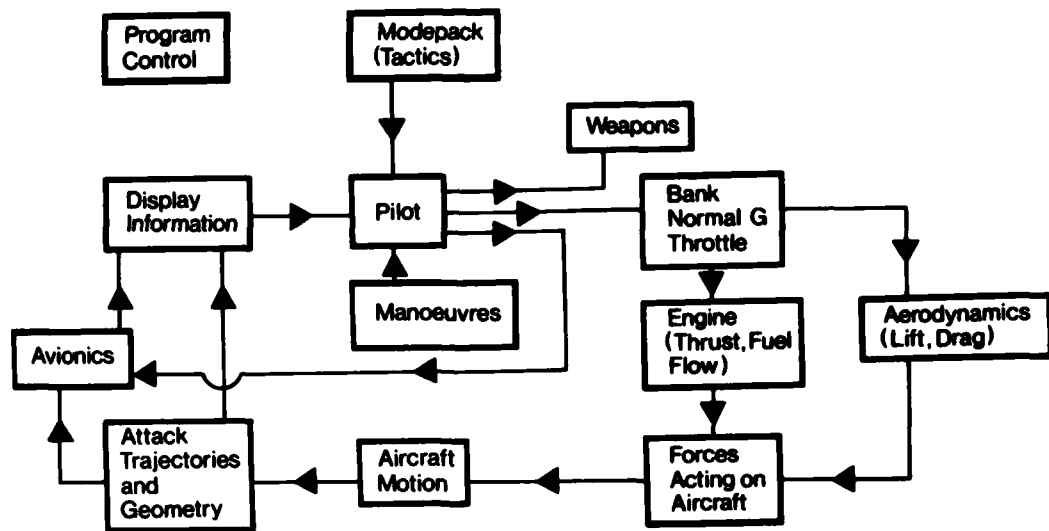
Guided Weapons

An increasing number of guided air-to-ground weapons are being developed and these, like the air-to-air missiles, require detailed modelling to predict their performance capability. They are clearly more complex, and, therefore, more expensive than bombs, and the justification for the expenditure is their ability to provide long stand-off range and high accuracy. Into this category of weapons come electro-optically guided bombs, air to surface missiles, anti ship missiles etc. Modelling can determine how tolerant the missiles are in their requirement for accurate target information at release, what their maximum and minimum firing ranges are, how they deal with target motion etc.

CONCLUDING REMARKS

In addition to the aircraft and weapon modelling discussed so far, there are other related areas of computer modelling to study system performance. One is the detailed modelling of weapon separation from the aircraft, which involves a definition of the airflow around and close to the aircraft. The effects of these local flows on the weapon behaviour as it leaves the aircraft can have a critical effect on the weapon's success. A full understanding of this phase of the weapon trajectory enables the system to be optimised to give maximum capability. Computer programs are also used to assess system accuracy, based on specified tolerances on equipment performance. This is done by modelling the effect of tolerances on performance. Another area is the assessment of gun lethality based on the main parameters: target size, firing range, muzzle velocity, rate of fire, shell lethality, shell ballistics, calibre, aiming accuracy. This is particularly useful in comparing different gun installations.

The use of computers in the design process is growing daily and will continue to do so in the foreseeable future. Computer models, particularly when linked to general purpose hardware facilities (controls, displays), will improve in their representation of real life and eventually enable a full definitive system to be designed and "proved" on the ground before deciding on the particular hardware solution to be implemented.



Simplified Aircraft Weapon System Model

FIGURE 1

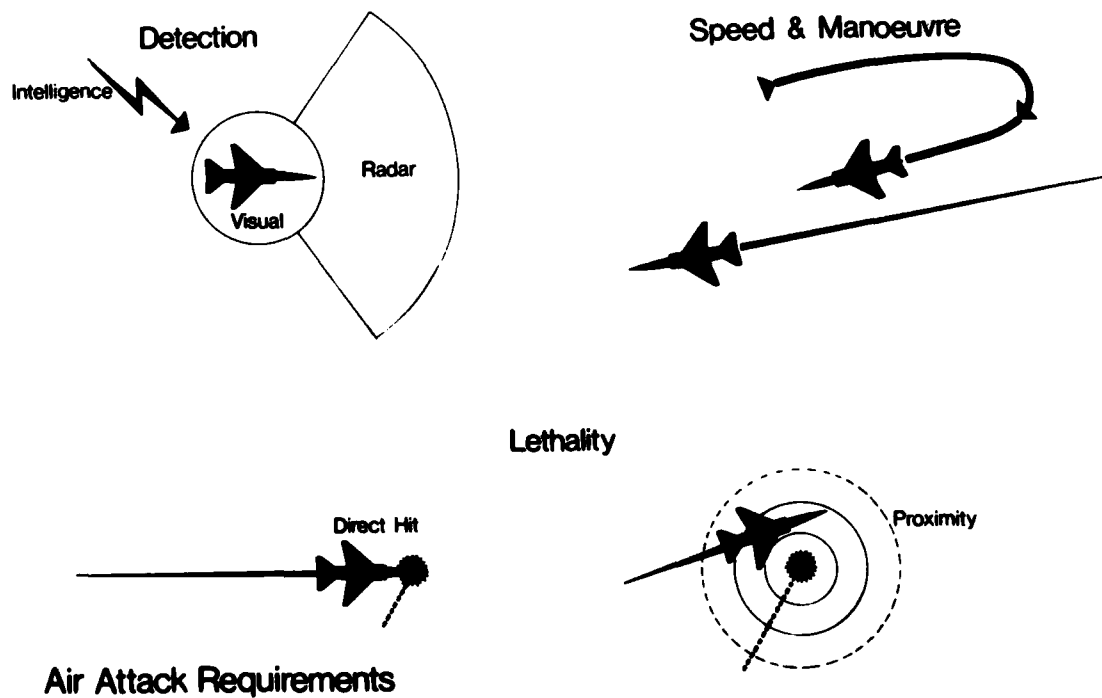


FIGURE 2

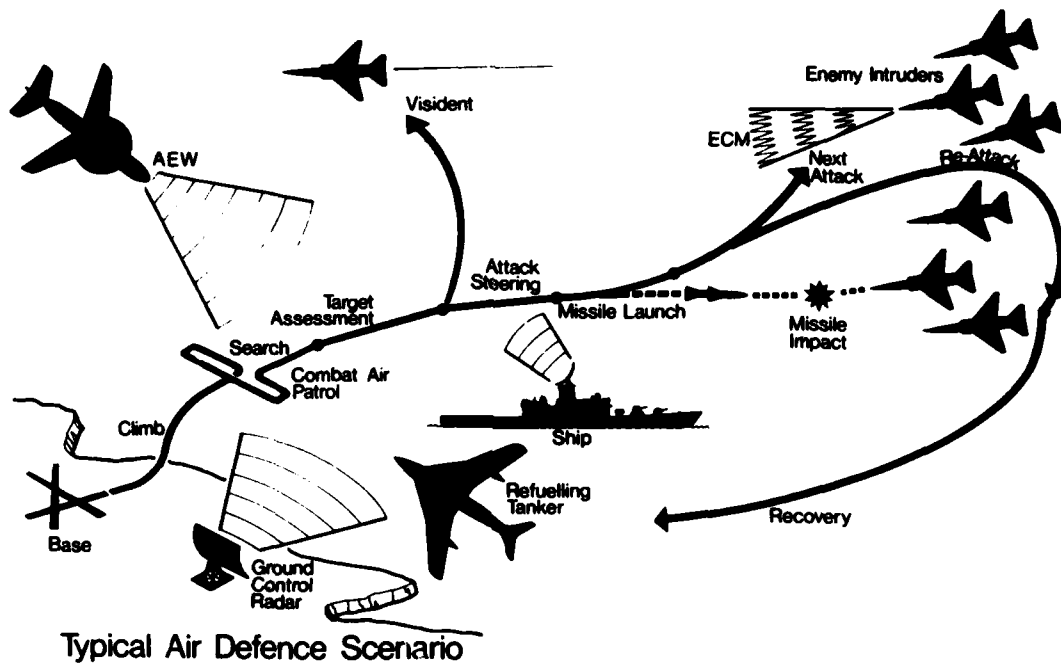
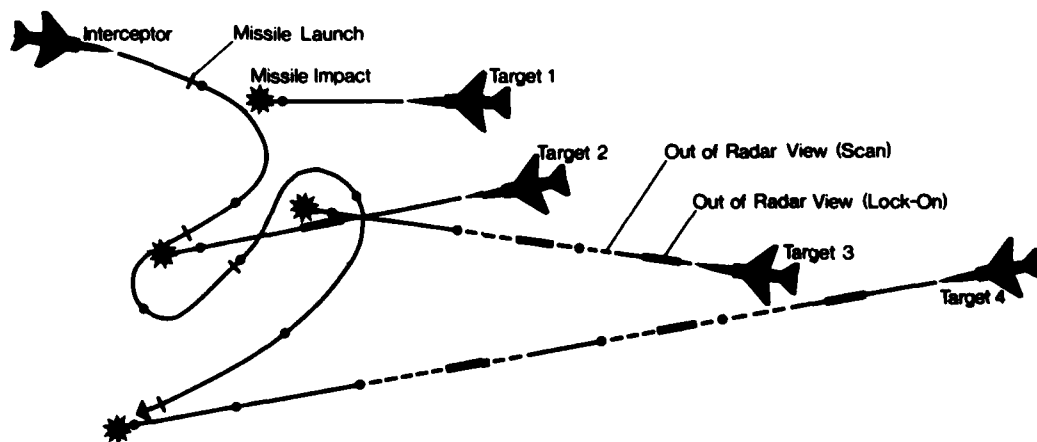


FIGURE 3



Multiple Target Attack

FIGURE 4

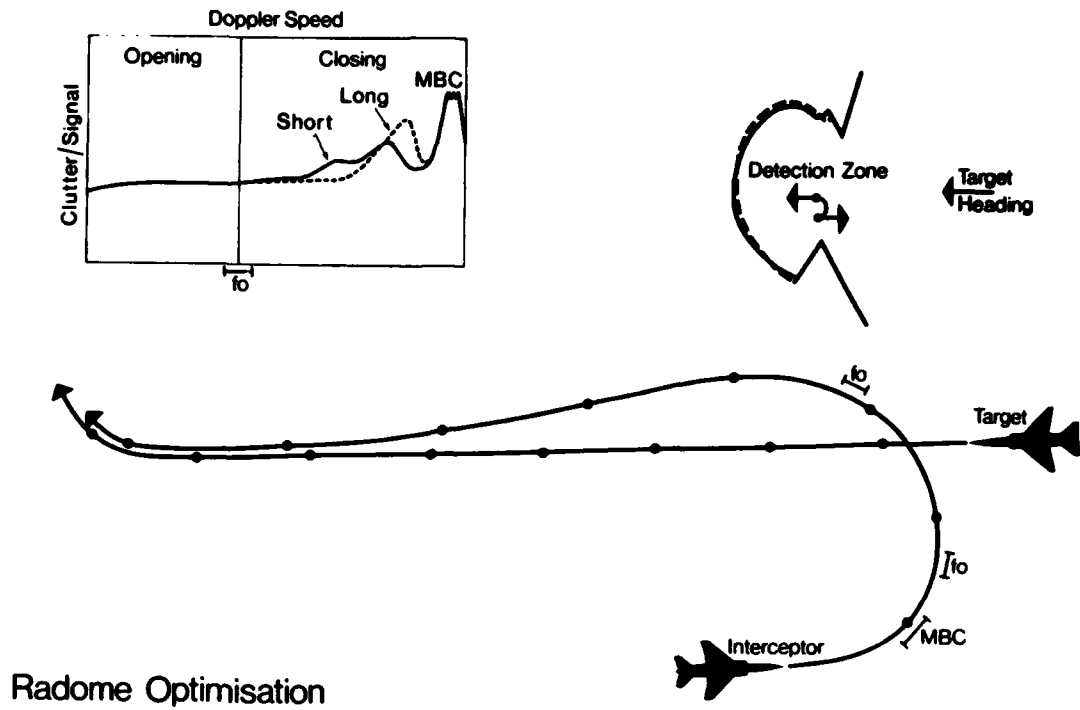


FIGURE 5

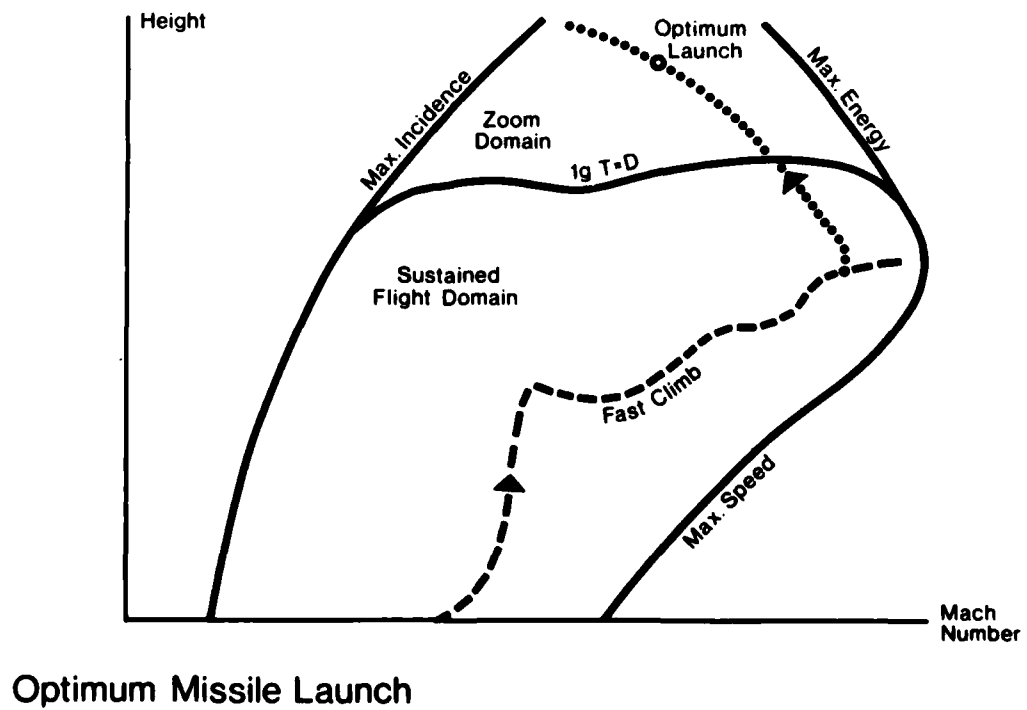
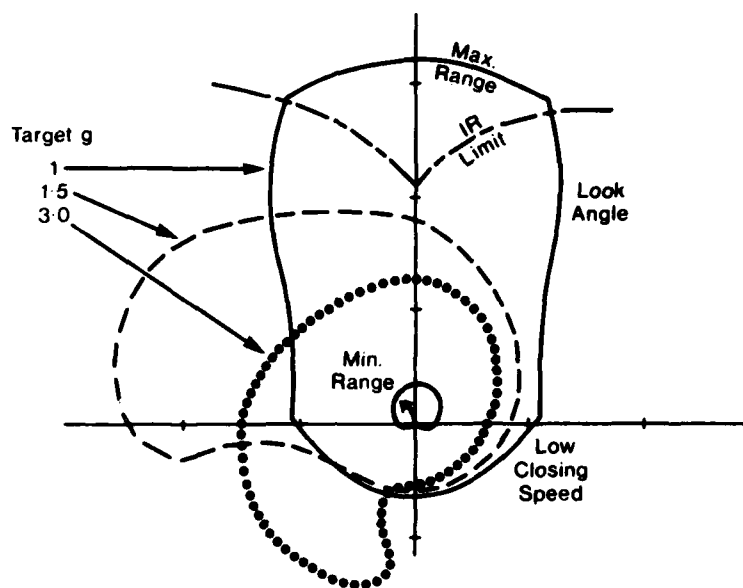
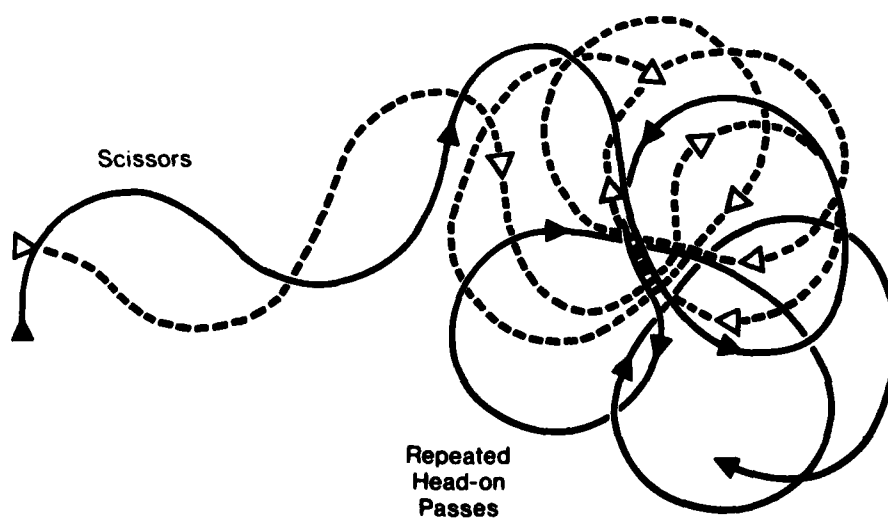


FIGURE 6



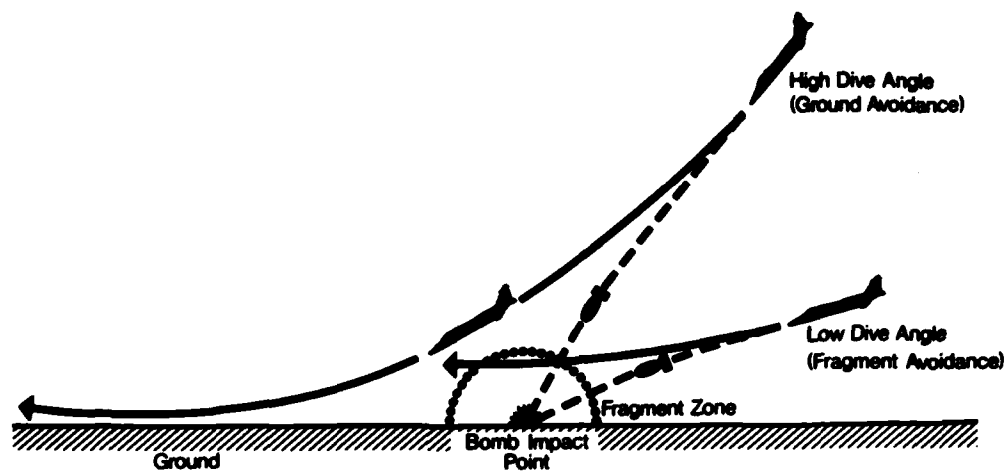
Missile Launch Success Zones

FIGURE 7



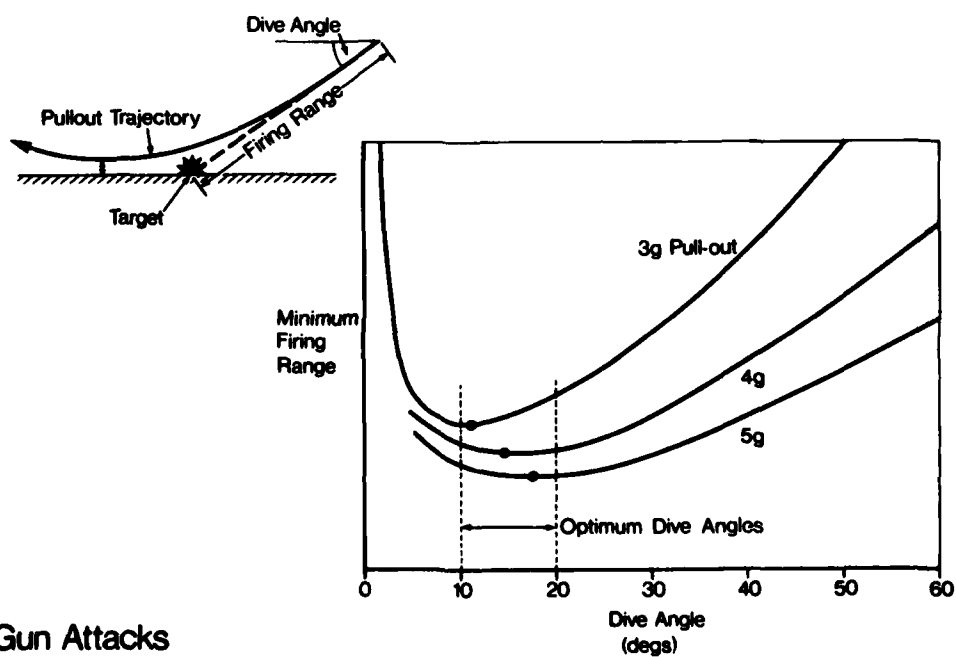
Close Combat Engagement

FIGURE 8



Ground Attack Hazards

FIGURE 9



Gun Attacks

FIGURE 10

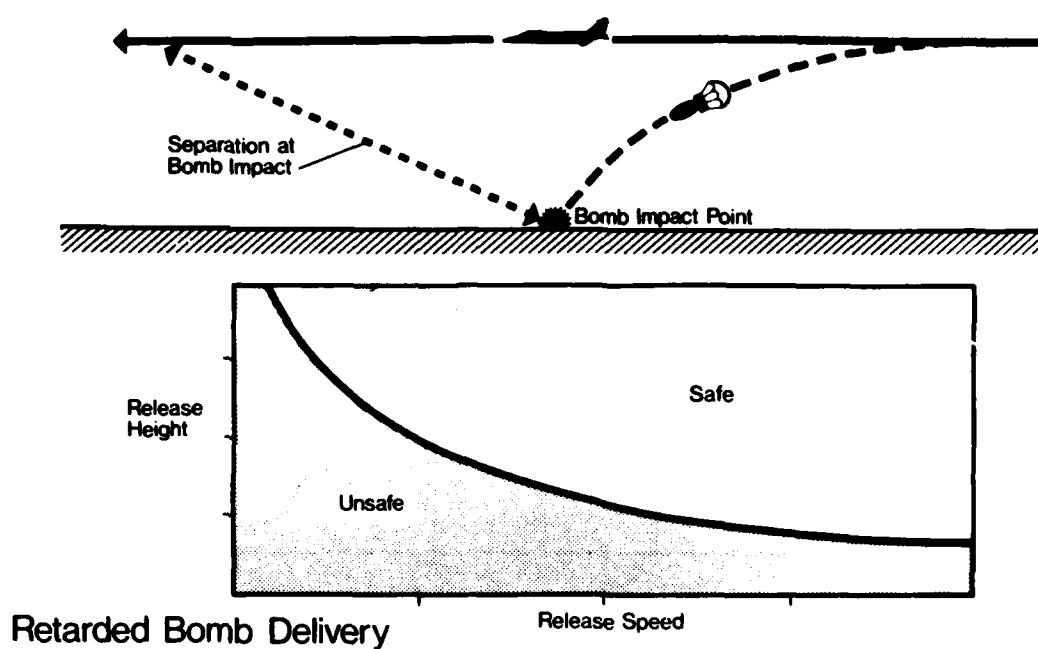


FIGURE 11

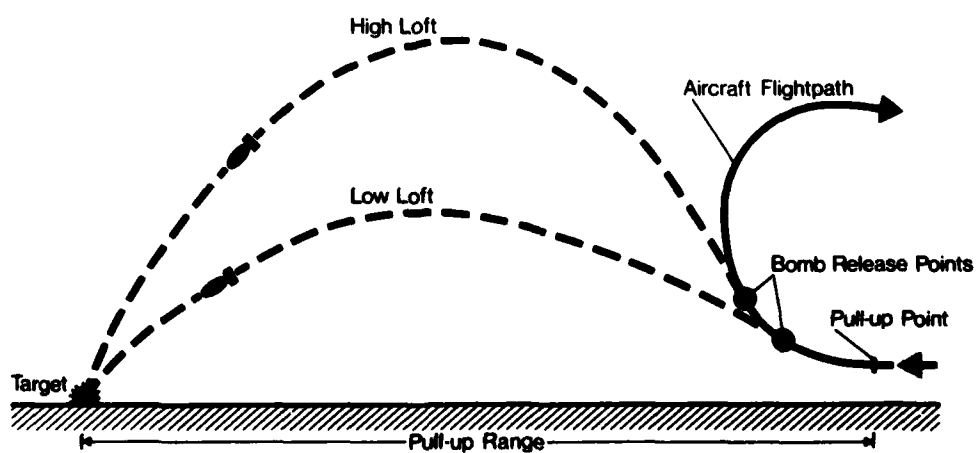
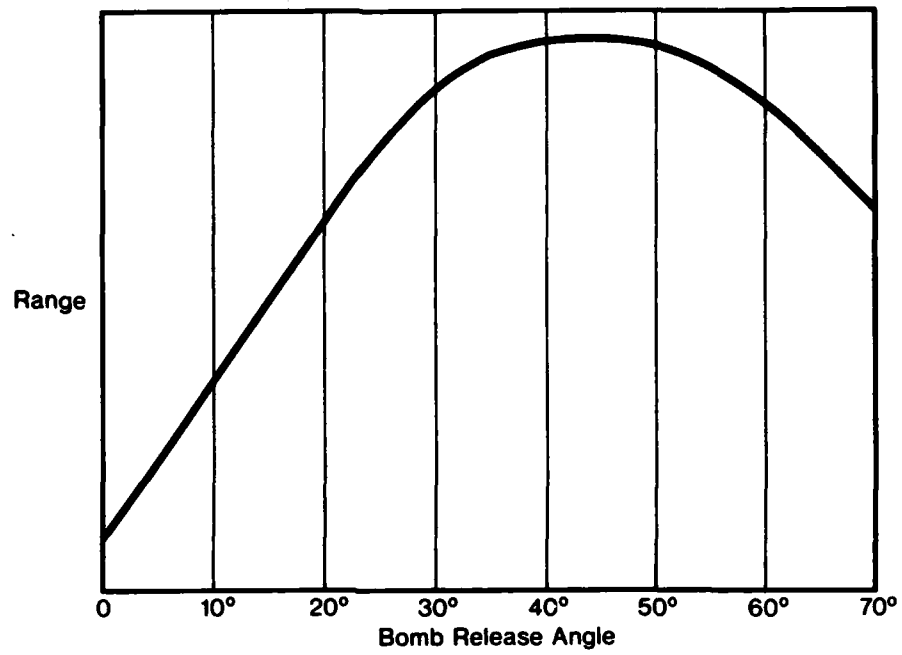


FIGURE 12



Loft Attack Range

FIGURE 13

BACTAC - A COMBAT-WORTHY COMPUTERISED OPPONENT

Ian Jones
Principal Aerodynamicist, Air Combat Studies,
British Aerospace, Aircraft Group
Warton Aerodrome,
Preston,
Lancashire, PR4 1AX.
United Kingdom.

SUMMARY

This paper describes the formulation and performance of a computerised opponent used at British Aerospace, Warton Division, for air combat simulation. Over a period of seven years BACTAC has progressed from its initial state as a digital computer model of close combat without the man in the loop, to a versatile and tenacious interactive opponent for use in a single-dome, piloted, air combat simulator.

The process of matching the mathematical model against fighter pilots in the simulator is described, together with an account of the learning which took place on both sides of the fight, and adjustment of tactics to the radically different performance of a new generation of aircraft and missiles.

It is only in the combat simulator that fighter pilots and designers can investigate future generations of fighter aircraft. In this environment BACTAC is proving its value to scientific research as a combat-worthy adversary, capable of exploiting the higher levels of performance and providing a known datum against which to rank pilots, competing aircraft and their weapon systems.

BACTAC

The BAC mathematical model of Tactical Air Combat (BACTAC) was written in 1970-71 to assist in the systematic examination of all stages of one-on-one combat (Figure 1):-

- . long range interception
- . 1st pass attack
- . penetration, pursuit and evasion
- . dog-fight
- . break-off and escape

The tactical rules have their origin in pilot training manuals and prolonged discussion (and argument) between fighter pilots.

The opportunity to include the pilot in the loop emerged several years later when the computer model was already considerably developed and in daily use to support operational analysis of aircraft and their weapon systems at Warton.

When the single-dome simulator was built in 1975 it was clear that considerable cost saving could be achieved by using one half of BACTAC as the combat opponent.

The task then was to adapt and develop the mathematical model to provide interactive, realistic and competitive combat against the pilot.

COMBAT SYSTEM

Let us examine in some detail the ingredients of a one-on-one combat system (Figures 2 & 3). It consists of the following basic elements:-

- (a) A line of sight linking the two aircraft in space which provides most of the information available to each pilot about his opponent, e.g. position, speed, orientation, manoeuvre and weapon state.
- (b) Tactical rules against which the pilot compares his view of the fight in order to decide his best manoeuvre.
- (c) Control inputs by which the pilot attempts to make the aircraft fly his chosen manoeuvre.
- (d) The performance of the aircraft is limited by aerodynamic lift and drag, the thrust of its engines and the structural 'g' limits to which it is designed. (Figure 4).
- (e) Manoeuvres must also be within the pilot's own physiological ability to withstand prolonged 'g'.
- (f) The aircraft then responds to these competing forces to produce its flight path through the gravitational field and air mass of the combat arena.
- (g) The weapon system is also an integral but intermittent part of the combat system, operating only when the pilot succeeds in manoeuvring his aircraft into a firing position.

The opponent aircraft constitutes a 'mirror image' of this system. As the two aircraft manoeuvre in space the line of sight continually changes, and so the system loop of tactical appraisal, decision, manoeuvre demand and aircraft response starts again.

TACTICAL DECISION PROCESS

The pilot's tactical decisions are governed by an overall philosophy which gives highest priority to survival. His objectives can be listed in the following order:-

- (i) stay alive
- (ii) prevent the opponent achieving a threat position
- (iii) achieve an offensive position behind the enemy
- (iv) kill him.

In line with this philosophy the pilot continuously re-assesses his view of the fight (Figure 5). This process has been mechanised within BACTAC by collecting together in an ordered fashion a set of vital questions, as shown in Figure 6. In effect these questions partition the state space surrounding the BACTAC aircraft by determining whether the enemy is:-

- . ahead or behind
- . pointing towards or away
- . at what range
- . closing or opening range

If the answers to these questions indicate that the enemy is behind, pointing at the BACTAC aircraft and within weapon range, then a highly dangerous situation exists. BACTAC must perform a last ditch manoeuvre, such as a max-rate break, in order to survive.

If, however, the roles are reversed and the BACTAC aircraft is behind the enemy then the priority is to attack and fire at him.

Between these two extremes a gradation of defensive, neutral and offensive positions exists in which less extreme manoeuvres of an energy-conserving nature can be performed. These include loops, barrel rolls, wing-overs and stall turns all of which involve the interchange of potential and kinetic energy.

A sample view of a combat between two agile aircraft flown by the computer model is shown in Figure 7. An attempted evasive penetration run is shown in Figure 8.

THE COMBAT SIMULATOR

Many combat simulators have been constructed in the present decade, both in the US and in Europe. They usually consist of two aircraft cockpits each surrounded by a large diameter sphere containing equipment for projecting an image of the opposing aircraft, the ground and the sky on the inner surface of the dome. At least one three-dome simulator exists (at McDonnell Douglas) for investigation of two-on-one combat. The Warton simulator is almost unique in having only one dome (Figure 9). The pilot, therefore, fights against an opponent whose logic is generated entirely within a computer using one half of the BACTAC model. The computer opponent is fed continuously with line of sight information about the manned aircraft and the correct image of the BACTAC aircraft is displayed to the pilot on the surface of the dome as they manoeuvre against each other in combat. Both aircraft are driven through similar control, performance and response calculations so that neither pilot nor BACTAC has any computational advantage.

DEVELOPMENT OF COMPUTER OPPONENT

From the outset it was clear that pilots regarded it as a point of honour not to be beaten by the computer opponent. BACTAC was recognised as a tenacious opponent which never gave up, and would exploit their slightest mistakes without mercy. But it was not infallible.

The first hole which pilots found in the computer logic was in its turn-reversal logic. They were able to force the BACTAC aircraft to change its direction of turn when defending, which gave them an easy shot. The second flaw was its limited use of vertical manoeuvres. By zooming upwards in the opening manoeuvres the pilot could eventually dominate the fight from above. Then diving down on top of BACTAC (Figure 10) the pilot could change his plane of manoeuvre very easily by rolling whilst in a vertical attitude to emerge in a firing position behind the BACTAC aircraft.

Both of these faults were soon rectified in the tactical logic, and with pilot and BACTAC both using vertical manoeuvres to a similar extent the fights reverted to stalemate.

The introduction of very high performance aircraft into the arena revealed a new and interesting phenomenon which has been nick-named the 'black-hole'. Pilots entering combat at high speeds could not tolerate the 'g' level which their aircraft were now able to deliver. To represent pilot black-out the illumination in the simulator is progressively reduced until eventually the pilot is left in darkness. If he chooses to pull continuously on the edge of black-out using full throttle, these aircraft have an excess of power over drag (Figure 11) and will accelerate, moving along the boundary BCD on the agility plot. The consequence of this increased speed however, is to reduce the angular rate of turn of the aircraft, whilst greatly increasing the turn radius. However, BACTAC had been programmed to seek a desired fighting speed (corner point speed A on the agility plot) and would throttle back briefly in order to decelerate to this speed. In so doing the angular turn rate of the BACTAC aircraft was maximised and pilots suffered many defeats until they learned to do likewise. The doctrine of using maximum power to increase energy, especially in the opening manoeuvres of combat, is firmly implanted in the minds of present day

fighter pilots and they are extremely reluctant to adopt a fundamentally different piloting technique. This is still the first traumatic lesson which visiting pilots to the Warton simulator have to learn.

However, those pilots who made the change and throttled back long enough to achieve the correct fighting speed eventually discovered they could tip the balance yet again by exploiting the 'wind-up turn' to gain an early shot (Figure 12). This consists of pulling 'g' right up to the attainable limit (A on the agility plot) in order to achieve a very high transient turn rate. The consequence of this manoeuvre is a rapid loss of speed as the aircraft tracks down the lift limited boundary AE of the agility plot. The only defence against such an attack is a similar wind-up turn.

And so the pendulum of success has swung from pilot to BACTAC and back to pilot several times as both sides learned new tactics and adjusted to the performance of the new generation of aircraft.

Perhaps the most frequent mistake of pilots who are unfamiliar with such aircraft is their belief that they can still fight 'fast-and-loose', or 'hit-and-run'. This is a technique much favoured by Phantom and Lightning pilots, of accelerating into combat at transonic speeds for a fast slashing attack (Figure 13), followed immediately by a dash out of the combat arena. With the new agility of opponent aircraft and their weapons, this has become a hazardous procedure. Firstly, the escaping attacker himself becomes the target for a snap shot, as the defender (or his wing-man) now has sufficient agility to turn and shoot before the hit-and-run aircraft can escape beyond missile range. Secondly, if the escaping pilot wishes to turn back into the fight it is unlikely he can open the range from his pursuers sufficiently to execute this turn safely without again being shot at.

We may, therefore, be approaching a time when 'hit-and-run' or 'slashing' attacks are no longer a safe and viable mode of attack.

PILOT FIGHTS COMPUTER

From time to time BACTAC is checked out in combat against the pilot by a validation experiment, to ensure as nearly as possible an equal fight with equal aircraft and weapons on both sides. In one such experiment seven highly skilled combat and test pilots participated, an account of which follows. It is believed there has been only one previous successful pilot-versus-computer experiment, that conducted in the NASA Dual Manoeuvring Simulator (Reference 1).

The Warton experiment was conducted in three phases, as follows:-

Phase	BACTAC Aircraft	Piloted Aircraft
1	A	A
2	A	B
3	B	A

The aircraft simulated were agile light-weight fighters such as might appear in the 1990's. Aircraft B was significantly more agile than Aircraft A. Each carried short range dog-fighting missiles. Engagements started from neutral head-on positions at 0.8M/14000' and lasted for three minutes. The seven pilots each flew at least three practice fights before each phase of the experiment, followed by between three and five scored engagements. The results are presented in Figure 15.

Phase 1

With both sides flying identical aircraft the average scores for and against individual pilots were mostly small. Two pilots defeated BACTAC, whilst BACTAC beat three others and drew with the remaining two. The overall average result for all pilots taken together was very close to a draw with BACTAC.

Phase 2

When the pilots flew the superior aircraft (B) they all defeated BACTAC flying Aircraft A. But again there was significant variation in their individual scores, with one pilot only achieving a draw and that with a very low score on both sides.

Phase 3

In the third part of the experiment aircraft A and B were interchanged, BACTAC now flying the superior Aircraft B against six of the pilots in Aircraft A (One pilot was unavailable to complete the experiment). In this phase BACTAC won decisively against four pilots, lost marginally to another, and lost more heavily to the remaining pilot. However, the overall average score for BACTAC in Aircraft B almost exactly balances the average pilot score from Phase 2.

It is concluded, therefore, that the combat capability of the developed BACTAC computer opponent lies well within the spectrum of pilot performance, and close to the median. BACTAC is one of the family of pilots.

APPLICATIONS

In practice the simulator application of BACTAC has been used to evaluate the combat performance of future aircraft and weapon system point designs. Pilots have been able to assess and experiment with several radical design innovations, including vectored thrust and post stall manoeuvring. The tactics which they employ are carefully monitored and where appropriate they are incorporated into the logic of

the computer model. This process exploits to advantage the pilot's natural flair for innovation, to seek out the best piloting techniques and tactics, a process which would be extremely protracted on the model alone.

In off-line form without the pilot in the loop, BACTAC versus BACTAC combats can be computed 10-20 times faster than real time, enabling many parametric variations of aircraft and weapon system designs to be studied quickly and cheaply, and ranked in order of effectiveness. Figures 16, 17 illustrate the results of one such experiment in which aircraft design parameters were varied about a datum design to assess their sensitivity. The results are found to correlate extremely well with a combination of familiar aircraft design variables such as $\frac{T}{W}$ ratio, span loading and wing loading, and in another form with a combination of aircraft performance criteria such as sustained and attained turn rates and specific excess power. These Combat Correlation Parameters enable preliminary rankings to be made of close combat capability of alternative configurations at an early conceptual stage of military aircraft design. Similar experiments in which missile aspect and acquisition limits have been varied have yielded useful results (Figure 18). Experiments such as this give the Project Office insight into the interaction of the major aircraft and weapon system design variables, and assist the process of configuration and weapon selection for future aircraft.

PROS AND CONS OF COMPUTER OPPONENT

In making an impartial appraisal of the computerised opponent the following points for and against can be listed:-

- FOR:
- . fearless, tireless, merciless
 - . adapts to aircraft and weapons on both sides
 - . never exceeds manoeuvre limits
 - . provides a datum pilot of known capability
 - . can be tuned up or down
 - . has great training potential
 - . takes only one pilot out of the flying programme
 - . cost effective simulation
- AGAINST:
- . has continuous, perfect information
 - . lacks flair for innovation
 - . deterministic, repeatable, predictable
 - . only as clever as the program
 - . requires modification for new tactics
 - . cannot learn

CONCLUSION

The achievements of the BACTAC computerised combat opponent have been considerable and have surprised many pilots.

- (a) It provides an evenly balanced fight against the human pilot when both sides fly similar aircraft.
- (b) If dissimilar aircraft are used, BACTAC and the human pilot achieve a similar scoring advantage with the superior aircraft.
- (c) BACTAC performs realistically and aggressively, ranking in ability close to the average fighter pilot.

It can, therefore, be fairly claimed that the computerised model BACTAC is a combat-worthy opponent.

This high level of validity and competitiveness has only been achieved after concerted and dedicated team effort lasting many months by a trio consisting of:-

- . a highly proficient combat pilot
- . a first class simulation engineer/programmer.
- . a weapon system analyst/aerodynamicist.

Without this combination of expertise and experience it is doubtful if such a result could have been achieved.

The side by side location on the same site of the piloted combat simulator and the computer model has enabled BACTAC to "learn" from the pilot's natural flair for tactical innovation in exploiting new performance features, and then to be applied off-line many times faster than real-time to parametric studies of future aircraft and their weapon systems. This combination of model and simulator represents a uniquely powerful operations research facility. They complement each other.

REFERENCES

- "Interactive Computerised Air Combat Opponent"
Walter W. Hankins III
AGARD FMP/GCP October 1975

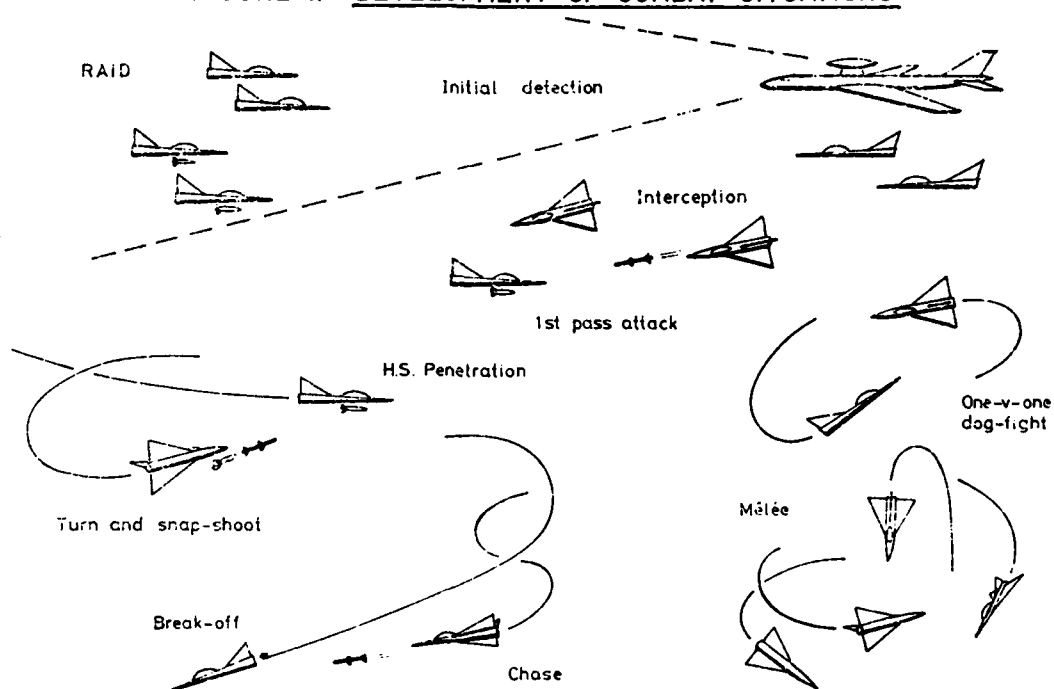
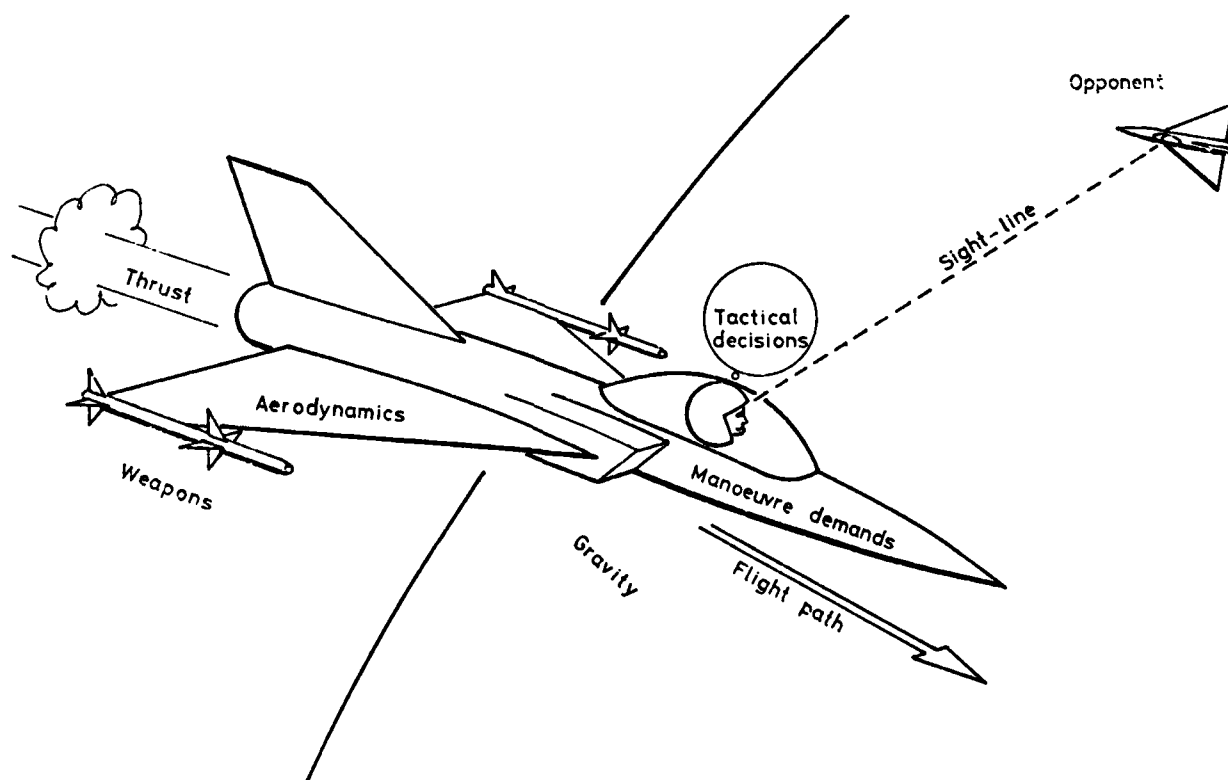
FIGURE 1. DEVELOPMENT OF COMBAT SITUATIONSFIGURE 2. COMPONENTS OF AN AIR COMBAT SYSTEM

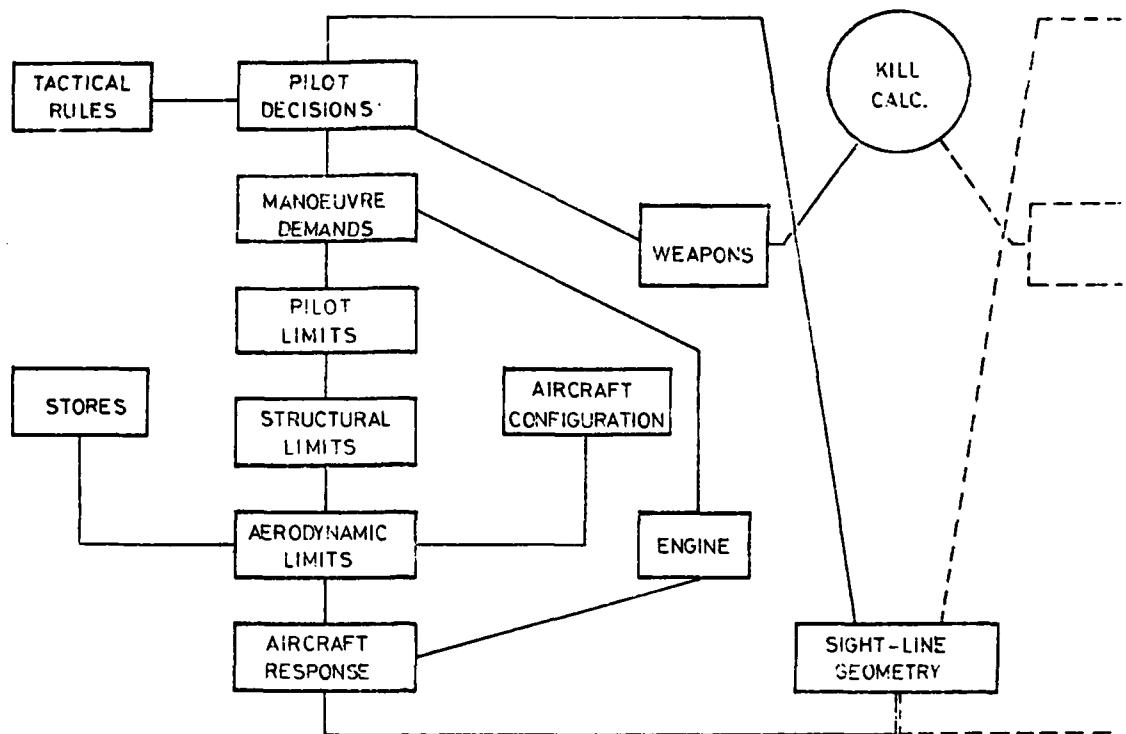
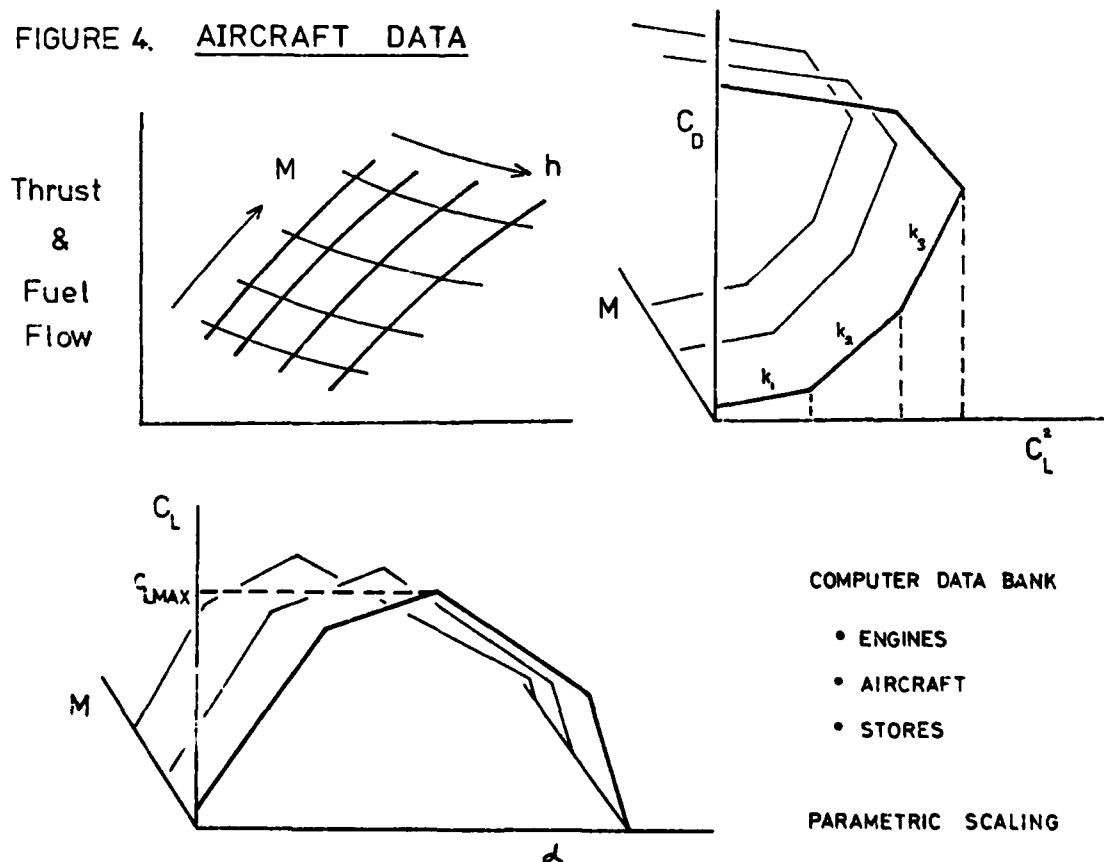
FIGURE 3. BACTAC FLOW DIAGRAMFIGURE 4. AIRCRAFT DATA

FIGURE 5. PILOT'S VIEW OF THE FIGHT

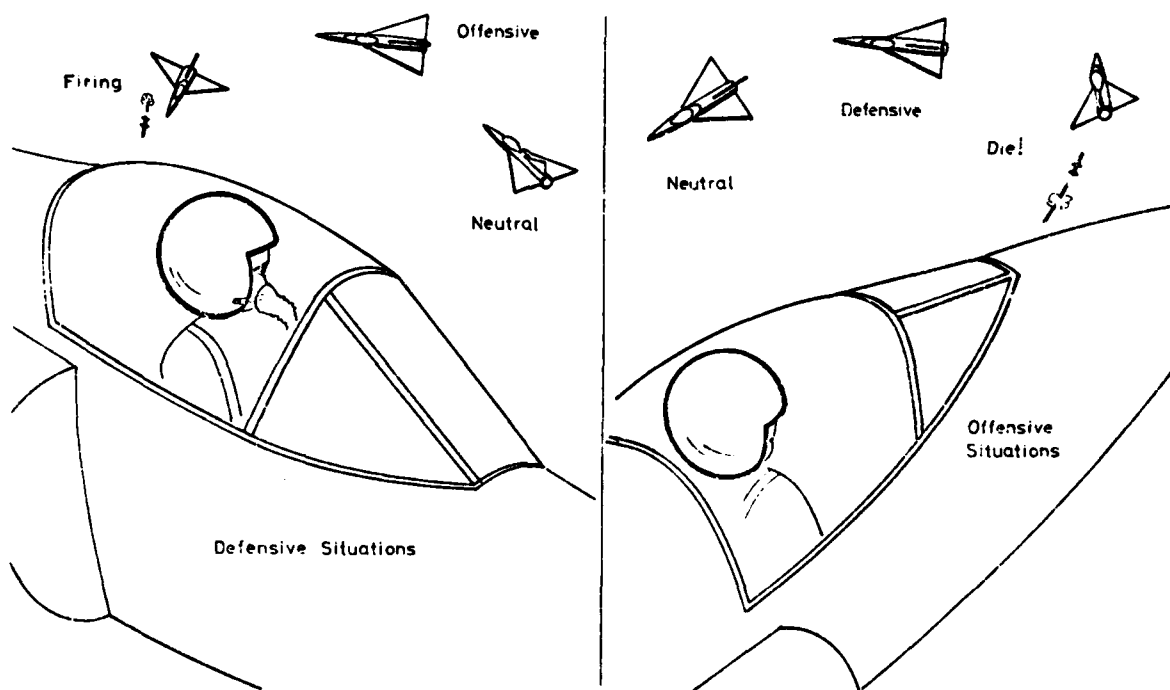
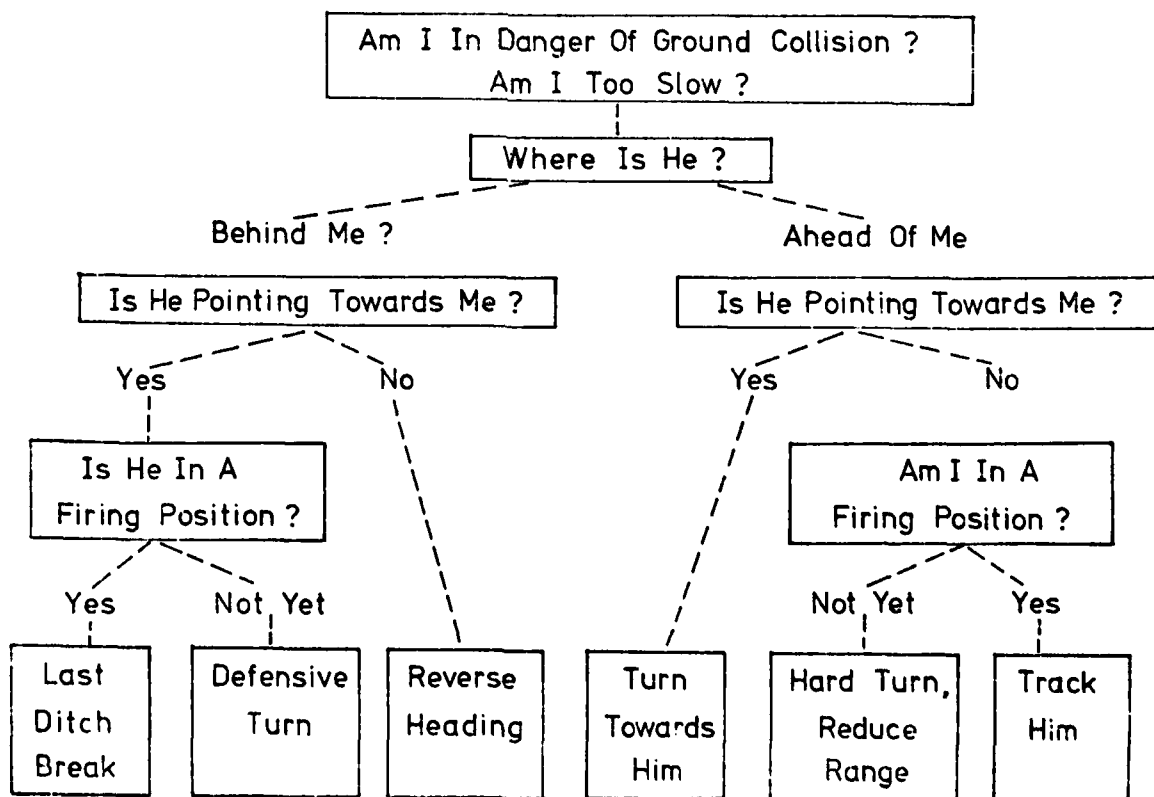
Figure 6. Tactical Decision Logic

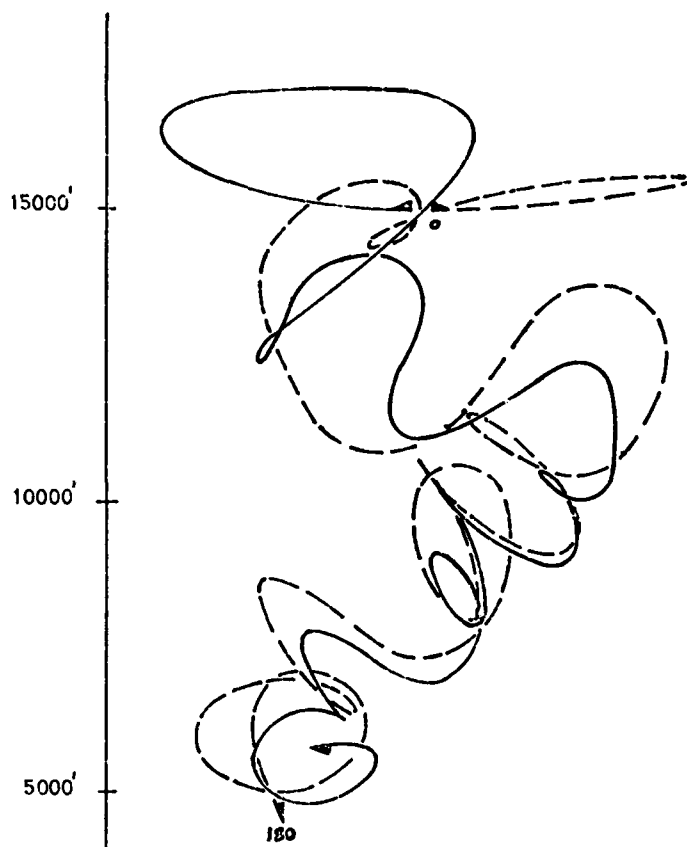
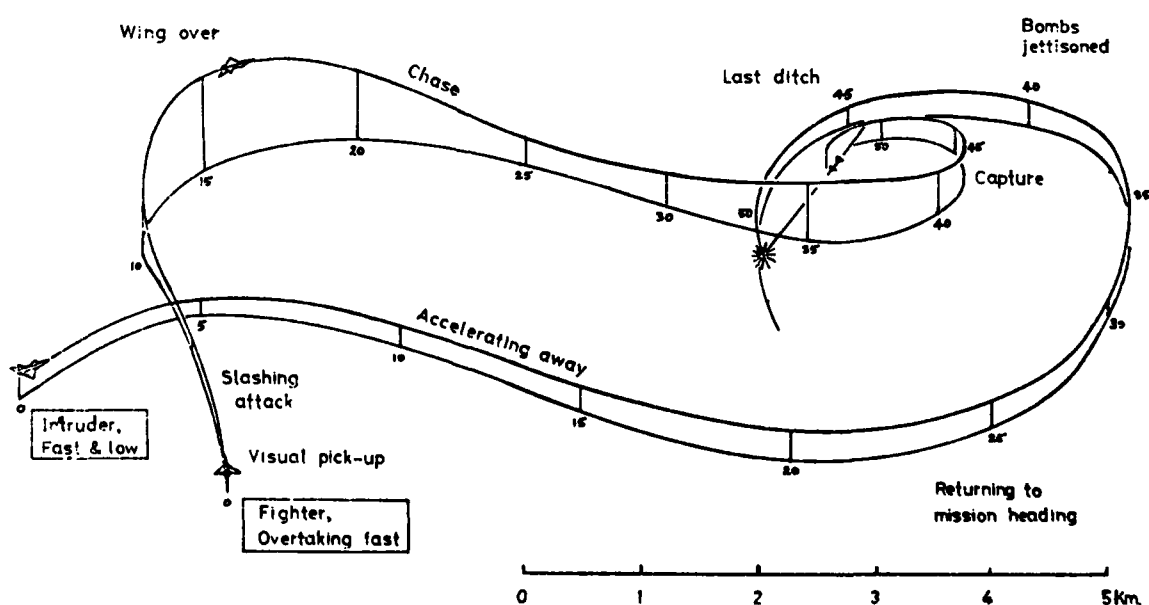
FIGURE 7. BACTAC DOG-FIGHTFIGURE 8. ATTEMPTED PENETRATION

FIGURE 9. COMBAT SIMULATOR INTERACTIVE
TARGET

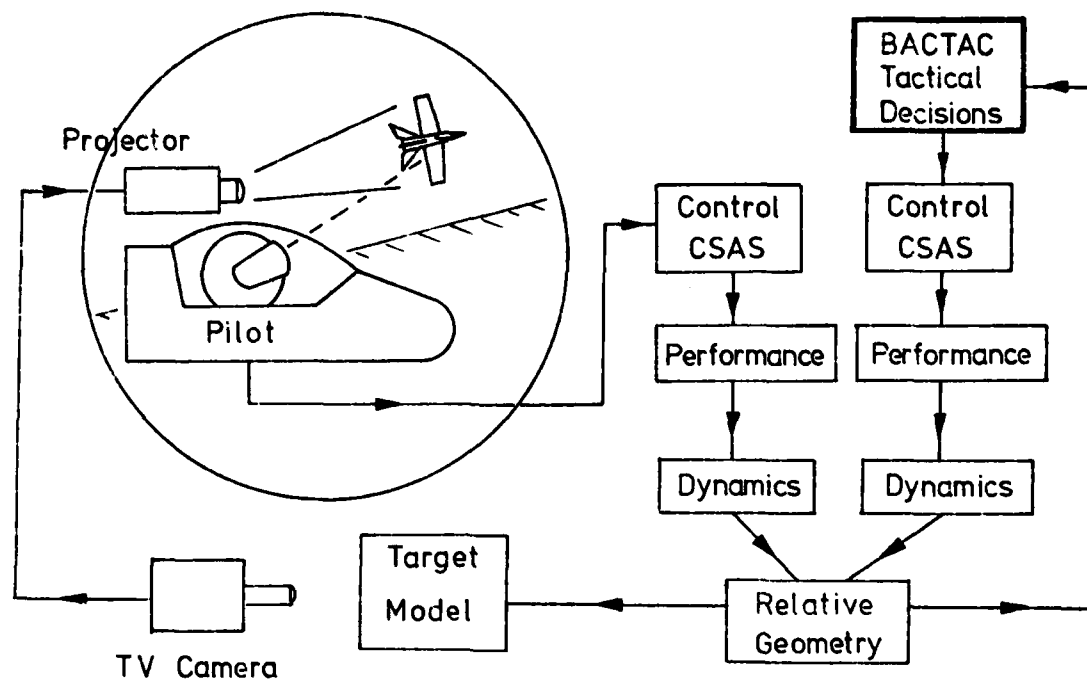


FIGURE 10. VERTICAL MANOEUVRE

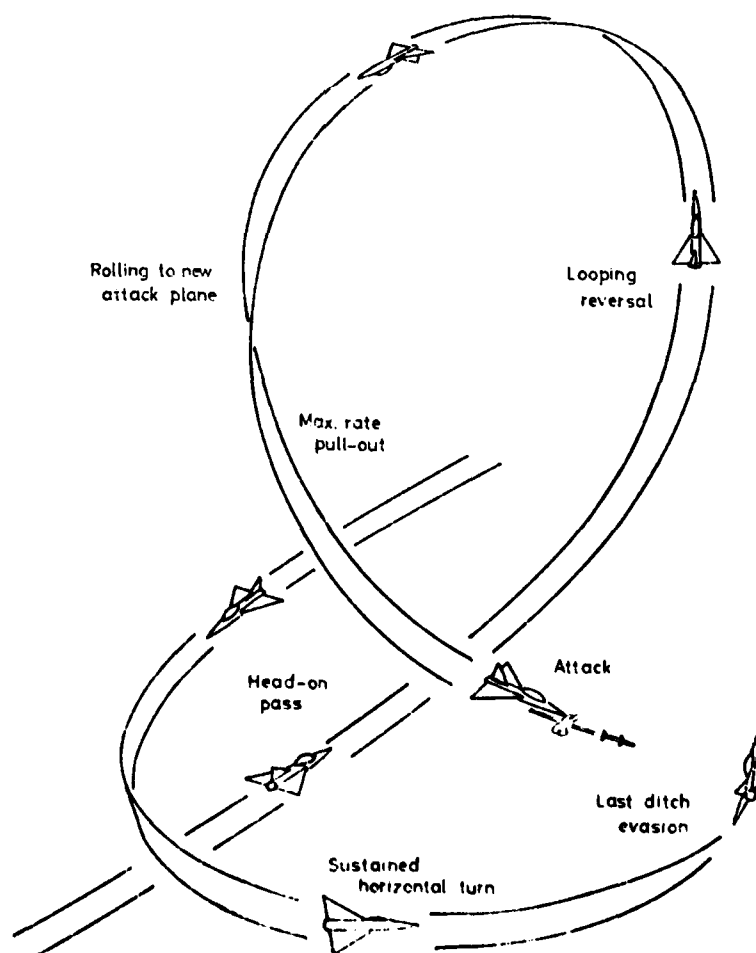


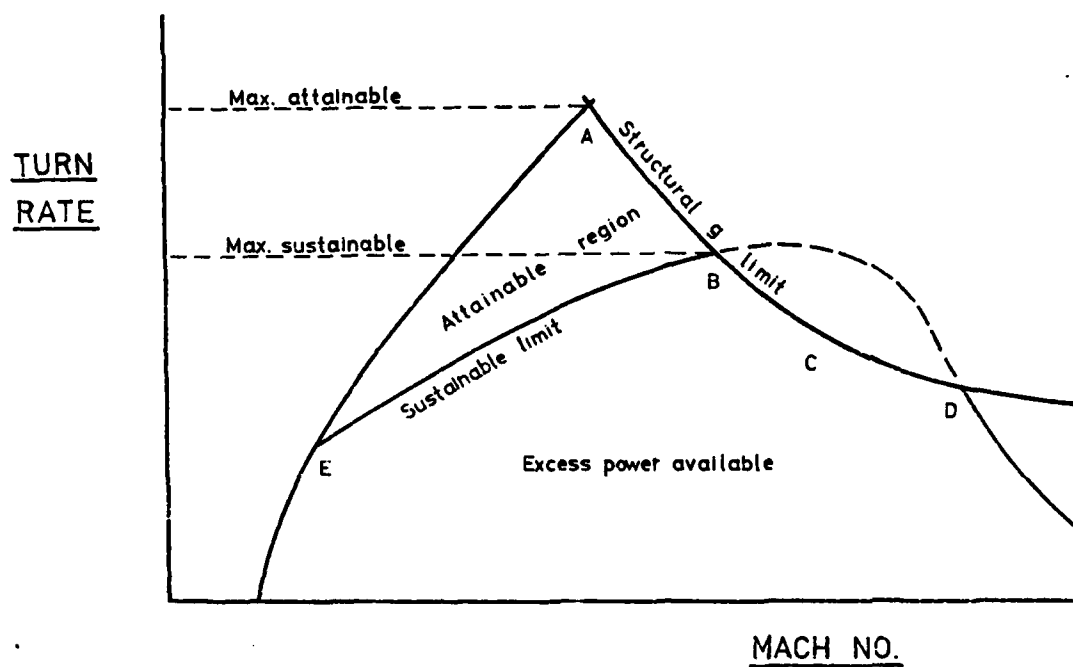
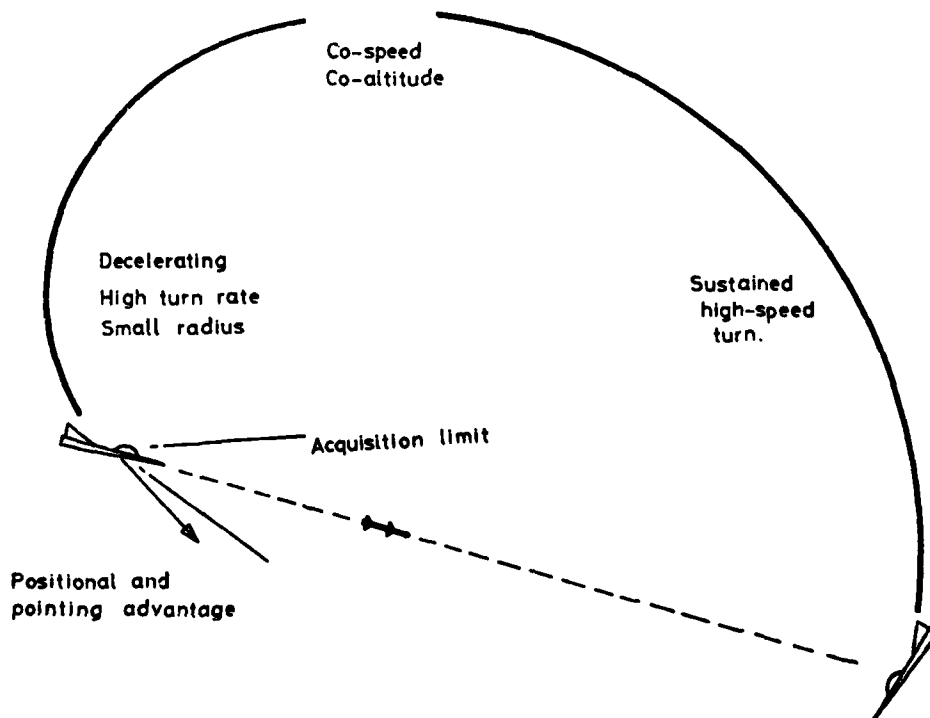
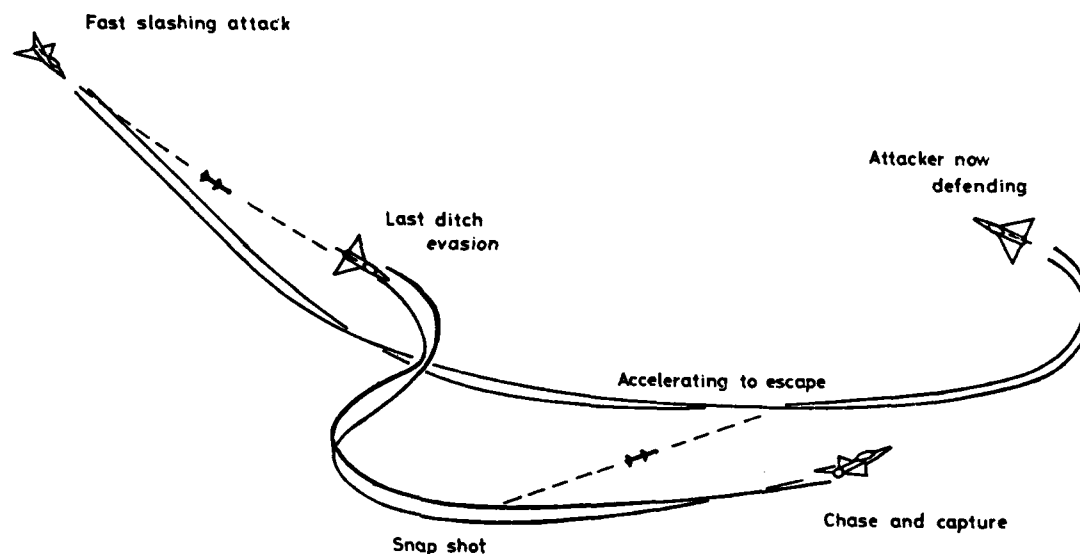
FIGURE 11. MANOEUVRE LIMITATIONSFIGURE 12. TACTICAL USE OF A WIND-UP TURN

FIGURE 13. HIT-AND-RUN ATTACK, ESCAPE DENIEDFIGURE 14. EXPERIMENTAL CONDITIONS

PILOT-VERSUS-BACTAC

- AGILE LIGHTWEIGHT FIGHTER AIRCRAFT
- SHORT RANGE DOG-FIGHTING MISSILES
- VISUAL RANGE, FULLY AWARE COMBAT
- NEUTRAL HEAD-ON START POSITION 0-8 M/14000'
- 3 MINUTE ENGAGEMENTS
- 3 PRACTICE FIGHTS IN EACH AIRCRAFT
- 3-5 FIGHTS SCORED IN EACH CONFIGURATION
- SEVEN PILOTS

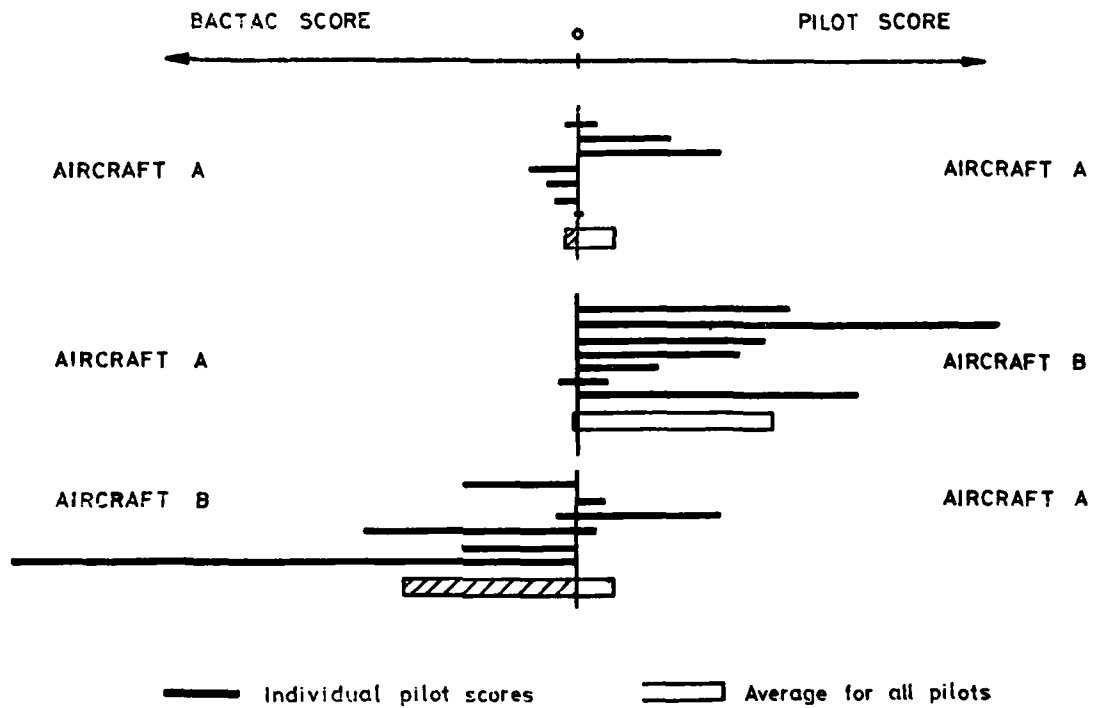
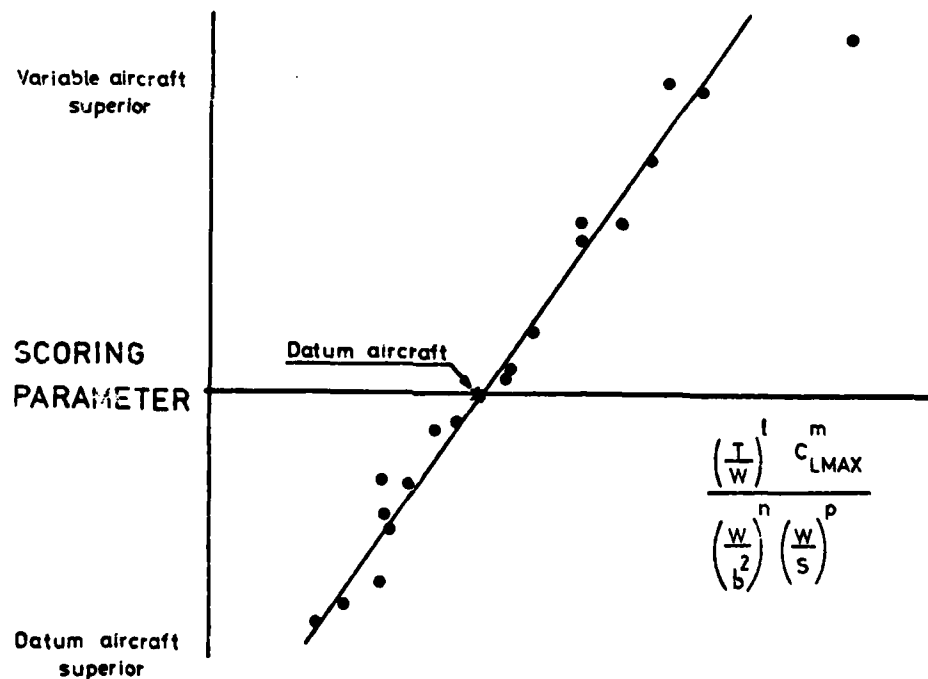
FIGURE 15. COMBAT SIMULATOR SCORESFIGURE 16. BACTAC 7 CORRELATION OF AIRFRAME VARIABLES

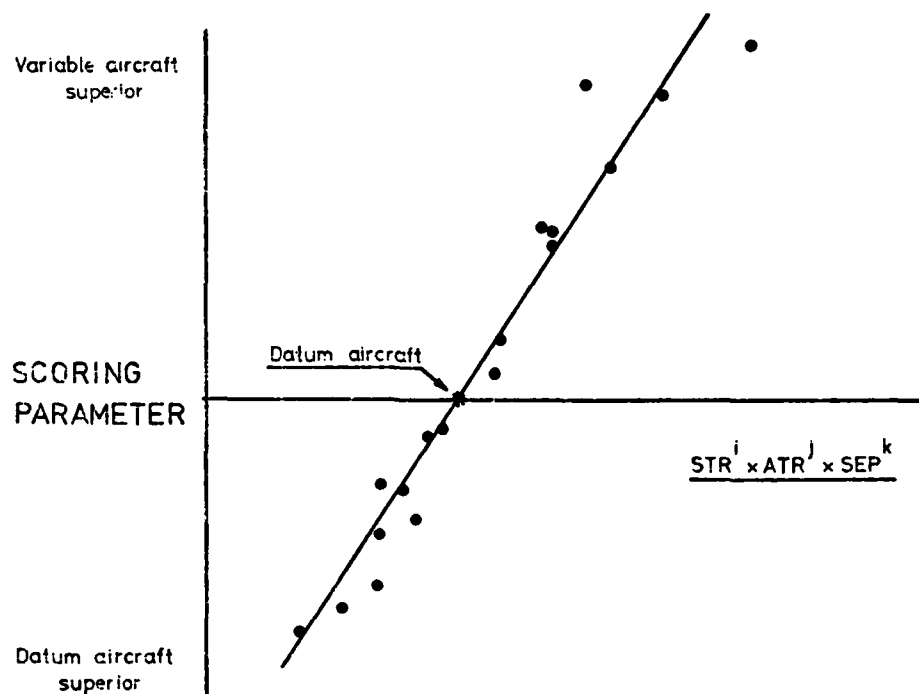
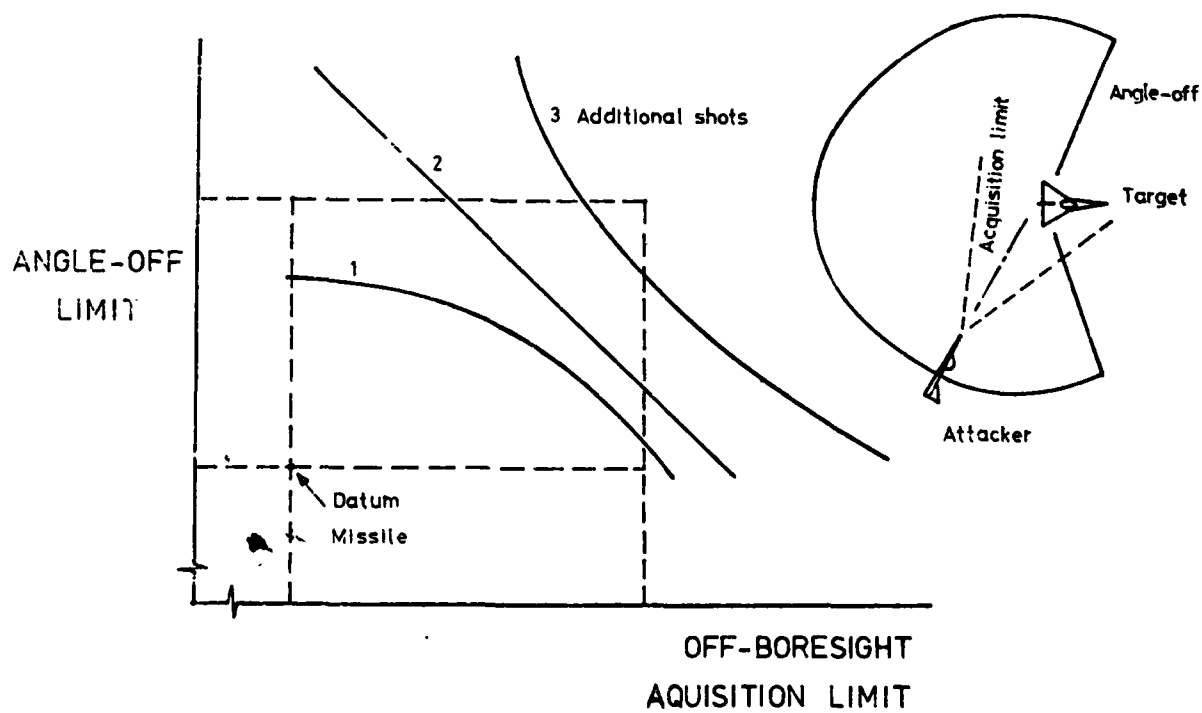
FIGURE 17. BACTAC 7 CORRELATION OF PERFORMANCE TERMSFIGURE 18. PARAMETRIC MISSILE VARIATIONS

FIGURE 19. PROS & CONS OF COMPUTERISED OPPONENT

FOR

- Fearless, tireless, merciless.
- Adapts to A/C and weapons
on both sides.
- Never exceeds limits.
- Takes only one pilot out of flying.
- Datum pilot of known capability,
within the family of pilots.
- Great training potential.
- Cost effective combat simulation.

AGAINST

- Continuous, perfect information.
- Deterministic, repeatable.
- Lacks flair and innovation.
- Only as clever as the program.
- Does not learn.

On balance - BACTAC is a combat-worthy opponent.

BACTAC

B.A.C. TACTICAL AIR COMBAT MODEL

- One-on-One Combat
- One-on-Many Interception (sequence)
- Many-on-Many Combat (20 a/c max.)

INTERACTIVE AIDED DESIGN SYSTEM FOR AIRCRAFT DYNAMIC CONTROL PROBLEMS

by

Dr. Wolfgang J. Kubbat
Dr. G. Oesterhelt
U. Korte
Messerschmitt, Bölkow, Blohm GmbH
Ottobrunn bei München
Federal Republic of Germany

SUMMARY

The paper describes a computer aided design system for control law design and system synthesis. A short description of the available methods (continuous - discrete, time domain-frequency domain) is followed by an illustration of the practical work. The designer has access to the huge program system via a graphical CRT display and a keyboard.

Selection of method (i.e. discrete vs. continuous complete vs. incomplete state feedback, optimal control vs. pole-placement etc.) is followed by a dialogue designer-computer with immediate results presented in numerical and graphical form (plots, print-outs).

Each result is stored and can be compared with any other one via dual plots. The system also allows for the input of disturbances like white or coloured noise, ramps, steps, sine-and cosine-combinations. No practical restriction for the number of state variables is present.

The paper concludes with an illustrating example for aircraft application.

PREFACE

With the advent of powerful digital computers, new tools have become available to the designer of feedback control system. Not only that the computing speed has increased unbelievably but new methods such as multivariable control and optimal control have become applicable.

At the same time, a new disease was caused among the control system engineers :

AMOK - Computing

Since it was so easy to do some more computer runs, the engineers (and others too!) got excited and did many, many more computer runs.

But the excitement was followed by a hang over. Huge piles of printed results had to be evaluated, thousands of results to be stored in the engineers' brain and then the "BEST" to be selected.

Since not all conditions and especially experience can be formulated into mathematical and numerical criteria, the human being has to stay in the design loop. On the other hand, the piles of printed matter do not offer a satisfactory solution.

Our solution is a dialogue between the system engineer and the computer via an interactive graphic display, a Computer Aided Design (CAD) for feedback control system. This, in most cases, cures also the amok-computing disease.

1. INTRODUCTION TO THE DIALOGUE : DESIGNER - COMPUTER GRAPHICS

In order to enable the engineer more than ever to gain access to the computer through programming languages, to express and modulate problems for the computer, the visual display with its high standard of information was chosen as an essential means of communication.

The centre of this engineer-computer process is therefore a graphical interactive display unit which is connected via a regenerating buffer to the main computer - at MBB we use for this an IBM 2250 station, - which is coupled via a channel to the IBM 370/165. A similar system with a MBB graphic 7 and a DEC VAX 11/780 is on the way. The designers' decision is inputted into the calculation and driving programs through an alphanumeric keyboard or via a light stick, by the touching and selection of graphical displayed elements. The computer puts out its result either graphically on the display screen or alternatively in the usual way on the lineprinter.

The graphical display serves here various purposes namely :

Computer Aided Design for Feedback Control Systems Design

- program control
- method selection
- parameter input
- influence on the computing process in the case of optimization programs for convergence improvements
- compression of optical information in the form of diagrams, lists and notifications, which enables the comparison of results from different decisions
- simulation of calculation results i.e. representation of the time histories of the state variables
- control and selection of simultaneous documentation programs
- instant indication of input errors and their correction

The designer can switch from one function of the graphical display unit, without delay to another significant one where optical aids can be used as a guide. The computer will check the validity of his decision, execute it and then through simulation the designer will receive a display instantly interpretable which enables further decisions.

The objections, that this process may lead to playing with the display and this in turn leads to unnecessary costs, can be countered by the following points :

- the design process will be speeded up remarkably as extensive use at MBB proves
- the grade of optimization is, depending on the designer's opinion of optimality - in many cases - greatly increased
- variation on purpose is one of the elements which increases the human capability of optimization
- only through compressed (optical) information display can decisions be arrived at, which not only result in permissible but optimal results
- the decision for a digital or analogue controller solution, which are realized through different pieces of hardware, and hence give a difference in cost, can be arrived at by direct comparison
- the gap between the control system designer, the mathematician and the data processing people is getting smaller.

2. AVAILABLE METHODS

On implementation of the various design methods for multi-variable control systems, a linear state description has been taken as a basis. Its relation to the frequency range is given via the standard operations: Calculation of the Eigenvalues and Eigenvectors of the system matrix.

For this the standard methods of the QR-algorithms after Francis were used with various shift techniques as well as the inverse power-method after Wielandt. In case of non-convergence other methods are available, but non-convergence usually is a signal of an unsuitable formulation of the problem. Almost all methods have been formulated so that from the Eigenvalue - Eigenvector analysis the best possible use can be made which leads to a considerable speed up of the computing.

The techniques for the control system design have been prepared in such a way that they can also be used for the observer design.

In principal there are 3 classes of programs to be differentiated which support the control design :

2.1 SERVICE PROGRAMS

Besides the self evident existing program variations from the sphere of linear Algebra, such as

- matrix inversion (symmetric, assymmetric, complex) or
- solution of linear equations (symmetric, real, complex) etc., to which also the above mentioned Eigenvalue/vector determination programs(hermitic, real, complex) belongs, can be added
- transition-/control matrix calculation which is being done via Eigenvalue analysis as well as via integration of matrix equations

- controllability checks, whereby partly, because of the considerably large systems the explicit setting up of the controllability matrix is avoided
- calculation of the observability index as well as checking on observability without setting up of the matrices concerned as above
- pole-zero calculation of any matrix transfer function of the open and closed loop system
- optimization of non-linear functions under non-linear constraints (Davidon, Fletcher-Powell)

These programs can be controlled by the individual user as well as automatically integrated into certain design programs.

2.2 FEEDBACK CONTROL LAW AND OBSERVER DESIGN

A chief distinction between digital (time discrete) and analogue (continuous) control systems can be made. Also a simulation of hybrid systems is possible with the availability of all the usual methods from both areas. On the design, one differentiates between control processes with limited control time and unlimited control time.

In the control process with limited control time, the control law is usually time dependent.

For digital systems the following control law design methods are available

- minimization of a quadratic performance index ("energy minimization")
 - with time dependent control and limited control time
 - with time independent control
 - without convergence acceleration for unlimited control time
 - with convergence acceleration utilising suitable E-function weighting of the time behaviour for limited control time
- Dead-Beat-Control with pre-specification of the transient behaviour by minimization of a quadratic performance criterion ("time minimization")
- pole-zero assignment for matrix transfer functions of the feedback system through minimization of rational vector functions
- incomplete state feedback through
 - introduction of a compensator system and minimization of a quadratic criterion respectively pole-zero assignment for the controlled system
 - introduction of a minimum compensator system for the optimal simulation of complete state feedback systems by the use of previous information or state variable derivatives
- Model-Following-Design via minimization of a quadratic performance criterion. This method of design is also well suited for the analysis and the design of
- parameter insensitive control systems
- observer design for incomplete state measurement
- optimization of state variables and controller design for deterministic disturbances (ramp, oscillations)
- optimization of state variables for stochastic disturbances (prescribed auto-correlation function)

The same design systems apply to analogue control systems with the exception of Dead-Beat-Control, whereby integral criterion replaces the summation criterion. Therefore, a direct comparison is possible. Some of these methods such as the design of a minimum compensator system with incomplete state feedback with respect to maintaining a similar transient behaviour as with the complete state variable feedback have been developed at MBB and published.

2.3 SIMULATION PROGRAMS

In order to analyse the controlled and uncontrolled systems several simulation analysis programs have been developed which analyse the state and control behaviour for deterministic systems as well as for systems with stochastic disturbances. The "Kalman-Buzy-Filtering" belongs under this heading although it could be considered as a control system design method as well.

Individually available are :

- Calculation of state and control variables
 - precisely through analytical integration and display of the Eigenforms with the support of the Eigenvalue/vector analysis
 - through numerical integration of differential equations
- generation of arbitrary coloured stationary noise from an autocorrelation function or its spectrum through the establishment of a set of differential equations with white noise as input
- trajectories of the state and control variables under coloured noise for controlled and uncontrolled systems
- Kalman-Buzy-Filtering and variance analysis of stationary disturbed linear processes
- interactive change of controller coefficients

A suitable combination of these programs with the service programs of chapter 2.1 enables an aimed analysis of the control system.

The list of the available methods given here cannot, because of the possibilities of variations, be complete. It, however, shows the variety of possibilities available.

3. ORGANISATION OF HANDLING

Here, two main points have to be differentiated :

On the one hand the handling of a complex program by the user requires an easily understood computing language formulated to support in a simple and flexible way all sensible operations required by a control engineer without the need for the designer to have special knowledge of data processing

On the other hand a complicated program structure requires data administration as well as the usage of dialogue languages.

Both problem areas shall be just shortly dealt with.

3.1 MBB's GRAPHIC MONITOR SYSTEM

The composition of the overall program system is based on the MBB developed Graphic Monitor System, a dialogue extension of the IBM-Operating System OS/MVS, respectively, with the aid of a graphic interactive program language GSP. The monitor permits an interactive way of working, in the approach to most operating functions such as compile, link, copy, update, file construction etc. and as well as the execution of several loading modules in sequence in one step. That means that many individual programs are put-on a disc library and only connected - linked - at the time of the execution of the computing operation, a process which happens in the classical way of programming once before every calculation, and then always in a pre-determined way.

The consequence, however, is that any thinkable combination and sequence of processes and simulation in one computing program have to be tested and programmed thoroughly - while with the help of the monitor during the work period only those programs which are to be used at that time are automatically linked.

In order to transfer data and information from one part of the program to the next, a data communication regime is established in the memory of the computer, and a data file with a flexible structure is built on a disc for every design example. The file retains and archives all the necessary data for a design example, as well as all the controllers gained through application of the design processes and analysis techniques, state variables and a storage name.

In case one likes to continue a design example at a later date the calling up of the program through its storage name will be sufficient. Per run, that means per work session, design examples of any number you choose can be dealt with in parallel, within every example any combination of design processes and analyses, every example with a maximum of 60 state variables and control inputs. The speeding up of the disc-computer-operation during the run was achieved by the development of access routines without the necessity of an intermediate buffer.

3.2 OPERATING CONTROLS

The user of the system referred to here as the design engineer, controls the computer run through 3 types of pictures which appear on the screen and which are :

- the control picture for the control of data transmission and selection of method

Picture 5 :

TIME DEPENDENT controller design allows the execution of the following processes:

- DEAD BEAT
- Control system design with finite performance index
 - discrete
 - continuous

As well as the above, there also belongs, from the practical point of view, the design of compensator systems, however, the system analyst will include them directly as a constant controller design, into the control picture to show that the controller of the system is constant.

If certain methods have been selected via the light stick, the control program calls up the necessary computing programs from a disc, links them together and presents them for data input in the computer.

The Input Picture

Dependent on the chosen design method, one of the 16 input pictures appears. Not all are shown here (picture 6-15).

By means of these pictures the parameters necessary for the control synthesis can be displayed (DISPLAY). In case, the data has been transmitted earlier it can be cleared (CLEAR) or new data can be entered via the keyboard (UPDATE) by choosing the parameter name with the light stick. All parameter names have been taken from the vocabulary of the design engineer to whom the method concerned is known. Input redundancy i.e. with the symmetric weighting matrices has been taken into consideration.

Through touching the option PRINT the inputted data together with the system data will be printed on the lineprinter.

The touching of (RECHNEN) CALCULATION initiates the computer programs which control the synthesis. If no notification of error is indicated, the display appears immediately.

The touching of CONTROL DISPLAY enables a jump back to method selection.

3.2.3 THE DISPLAY

After the controller has been designed by means of the chosen procedures and parameters, the state variables and controls will be determined and their trajectories or a linear combination will be displayed graphically after touching of the variable number (pictures 16-18). The scaling is done automatically, the limits of the data being written numerically, as well as the control error at the end of a pre-specified period of time.

One option enables, for constant control design to look at the time histories within the following period of time. Another option enables the labelling of the design result as "Optimal" and storage through touching of "NEW TRAJECTORY OPTIMUM". If at a later date however, the optimum behaviour for reasons of comparison is required it can be called up through the option of "OPTIMUM TRAJECTORY".

A documentation option which, of course, also appears on all the other pictures allows the print out of all the information gained so far. Apart from that, the picture, the diagrams and the text can be plotted automatically.

After the display, the input picture can be recalled (automatically the right one will appear) for the variation of the parameters or the control picture can be recalled for the purpose of varying the method and or the cessation of the method.

The illustrated organisation shows that the design engineer if he possesses knowledge of the possible methods, does not require further training, as all contact possibilities are feedback control orientated. He does not need any extensive documentation and he can find 'his' optimum method with optimum parameters in one way.

In the following some of the applied examples will be described.

4. APPLICATIONS

Since the CAD has been introduced many applications were found.

- Fighter Aircraft
- CCV F 104
- TRF

- RPV
- Helicopter
- Flutter Supression
- Vibration Isolation
- Missile Control

The number of users is still growing and on the other hand any new method coming up will be integrated in to the computer aided design system. It should be mentioned that successful flight tests, with control systems being designed as described, have already been conducted.

5.1 EXAMPLE

Out of many applications one example for an optimization of a multi-variable control system has been selected.

The control plant is a helicopter BO 105. The vehicle is characterized by the following main features.

- ° Non-linear behaviour
- ° Eight strongly coupled state variables, four controls with influence in several degrees of freedom

The control system design has been split into 2 parts. Part 1, is a non-linear trim computation.

Several trim points dependent on velocity and altitude have been defined. The system description (differential equations) has been linearised around the trim points. Different controllers have been designed each one optimized for one trim point. During practical flight tests a continuous interpolation between the different control laws takes place.

In order to illustrate our CAD the design of a controller for the BO 105 at an altitude of 1500 m and a flight speed of 27,8 m/s is given as an example.

At the given flight speed initial disturbances of 5 m/s in V_x and -5 m/s in V_z should be decreased quickly without any possible overshoot (limit at 10%) and with permissible control inputs (small feedback gains).

The results finally gained are shown in pictures 16-18. For comparison the behaviour of the uncontrolled plant is given within the pictures as well (starred lines). The respective state variables and controls are as follows.

- $x_1 = v_x$ = forward velocity in x - direction
- $x_2 = v_y$ = lateral velocity in y - direction
- $x_3 = v_z$ = vertical velocity in z - direction
- $x_4 = w_x$ = roll rate around x - axis
- $x_5 = w_y$ = pitch rate around y - axis
- $x_6 = w_z$ = yaw rate around z - axis
- $x_7 = \varphi$ = bank angle
- $x_8 = \vartheta$ = pitch angle
- $u_1 = \delta_o$ = collective pitch (mutual adjustment of all main rotor blades)
- $u_2 = \delta_c$ = cyclic blade adjustment roll
- $u_3 = \delta_s$ = cyclic blade (rotation) adjustment pitch
- $u_4 = \delta_{Hr}$ = blade angle of tail rotor

The result : v_z is quickly brought to zero as it is controlled directly via collective pitch.

v_x is slower, as the thrust vector has to be rotated first. (The helicopter pitches up to large attitudes) in order to reduce the speed via an enlargement of the thrust component in negative x-direction.

There are only small coupling effects in lateral movement
as can be seen : $v_{y \max} = -0.092 \text{ m/s}$

$\gamma_{\max} = 0.48^\circ$ respectively

The control variables remain far below the permissible limits.

Since for the pictures direct photographs from the CAD screen have been taken
the re-production contains the original German text as well as translation into English.

Storage Name

catalogue - erase file

generate a file

read data off cards according to file

check observability

check controllability

control design : time dependent, constant

calculation of transition- and control matrix

punching of time dependent - constant controller

calculation of poles and zeros

optimal control for incomplete continuous feedback

optimal control for incomplete discrete feedback

model following

time histories of state variables and control inputs

input and display of a deterministic disturbance

display of $Y = CA \cdot X + DA \cdot U$? YES/NO

transfer functions - continuous - discrete

Program End

Normal Version

Picture 1 : CAD Control

Generation of file for constant - time dependent controller

Number of File : 3

Blocksize : 0

Number of state variables : 4

Control picture

Picture 2

Calculation of transition- and control matrix

for sampling time $T =$

transition- and control matrix via integration? Yes No

Integration interval $DT =$

Picture 3

Control system design with pole placement

Control system design with quadratic performance index
discrete/continuous

Control system design with pole and zero placement

Control system design with pole placement for incomplete
feedback : DISCRETE

Control system design with pole placement for incomplete
state feedback : CONTINUOUS

Quadratic performance index for incomplete state feedback - DISCRETE

Quadratic performance index for incomplete state feedback - CONTINUOUS

Picture 4 : Constant Controller Design

- DEAD BEAT
- Control system design with finite performance index
 - .. discrete
 - .. continuous

Picture 5 : Time Dependent Controller Design

Time Dependent Controller Design ZEITABHÄNGIGER REGLERENTWURF

N	XS
1	0.00000
2	0.00000
3	0.0
4	0.0

UPDATE / CLEAR / DISPLAY

ZEITABHÄNGIGKEIT :

EXP - FUNKTION T=EXPONENT

= ANFANGSWERT XS
SOLLWERT XS

MATRIX G - DIAGONALE
EXP.G - DIAGONALE
MATRIX H - DIAGONALE
EXP.H - DIAGONALE
LAMBDA
ALPHA
SCHWITTENGE

*** PRINT ***
*** RECHNEN ***
*** STEUERTEIL ***

Picture 6

Control System Design with Pole Placement REGLERENTWURF MIT POLVORGABE GEMEINSCHTE POLE

N	REAL	N	IMAG
1	-0.000001	0.100000	
2	-0.000001	-0.100000	
3	-0.000000	-0.000002	
4	-0.000000	0.000002	

KONTINUIERLICH / DISKRET

UPDATE / CLEAR / DISPLAY

ANFANGSWERT XS
SOLLWERT XS

= GEMEINSCHTE POLE
SPIELVEKTOR
SCHWITTENGE

*** PRINT ***
*** RECHNEN ***
*** STEUERTEIL ***

Picture 7

Control System Design with Pole - Zero Placement
 REGLERENTWURF MIT NULLSTELLEN- UND POLVORGABE

CONTINUIERLICH / DISCRET UPDATE / CLEAR / DISPLAY ANFANGSWERT X0 SOLLWERT X0 ERRL. O. ITER. ANZAHL DER NULLSTELLENGLEICHUNGEN NZ SPALTENANZAHL DER SPIELMATRIX NP Vektor R Vektor T VORGESCHENE NULLSTELLEN NZ - VORGESCHENE POLE SPIELMATRIX SPALTE REGLER Vektor GEWUNSCHTES BEHARRUNGZEIT SCHRITTZAHL SCHRITTBREITE LÖSUNG DES GLEICHUNGSSYSTEMS MITTELS MINIMIERUNG INTEGRATION START- u. PUNKT. -N. *** PRINT *** RECHNEN *** STEUERBILD ***
--

Picture 8

Control System Design with Pole Placement
 (Augmented System)

REGLERENTWURF MIT POLVORGABE
 (ERWEITERTES SYSTEM)

CONTINUIERLICH UPDATE / CLEAR / DISPLAY ANFANGSWERT X0 GEWUNSCHTES POLE MATRIX P SPALTE EIGENWERTS VON D SPILVEKTOR SCHRITTZAHL SCHRITTBREITE *** PRINT *** *** RECHNEN *** *** STEUERBILD ***

Picture 9

Constant Controller Design
(Augmented System)

CONSTANT CONTROLLER DESIGN
(ERWEITERTES SYSTEM)

	DISCRET
	UPDATE / CLEAR / DISPLAY
	ANFANGSWERT 10
	MATRIX 0 - SPALTE
	- DIAGONALE
	MATRIX H - SPALTE
	- DIAGONALE
	MATRIX P SPALTE
	EIGENWERT VON D
	LAMBDA
	ALPHA
	SCHWERTZAH
	GENAUIGKEIT GENAUIGKEIT
	ANZAHL DER ITERATIONEN
	*** PRINT ***
	*** RECHNEN ***
	*** STEUERBILD ***

Picture 10

Pole - Zero Calculation

BERECHNUNG DER NULLSTELLEN UND POLE

	KONTINUUMLICH / DISCRET
	MIT / OHNE RESONANZ
	GESCHLOSSENEN / OFFENEN KREIS
	REGELN : ZIELWERT / IST
	ERWEITERTES SYSTEM
	VERTON H
	VERTON T LAENGE : H
	LAENGE : B
	NULLSTELLEN
	POLE
	UPDATE / CLEAR / DISPLAY
	*** PRINT *** RECHNEN *** STEUERBILD ***

Picture 11

Constant Controller Design - Discrete
Augmented System - Optimal Control

KONSTANTER REGLERENTWURF - DISKRET
ERWEITERTES SYSTEM - OPTIMALE REGELUNG

UPDATE / CLEAR / DISPLAY

ANFANGSWERT X0
SCHRITTZAHL

*** PRINT ***
*** RECHNEN ***
*** STEUERBILD ***

Picture 12

MODEL - FOLLOWING

KONTROLLIERUNG

UPDATE / CLEAR / DISPLAY

ANFANGSWERT X0
ANFANGSWERT XN
MATRIX G - SPALTE
- DIAGONALE
MATRIX H - SPALTE
- DIAGONALE

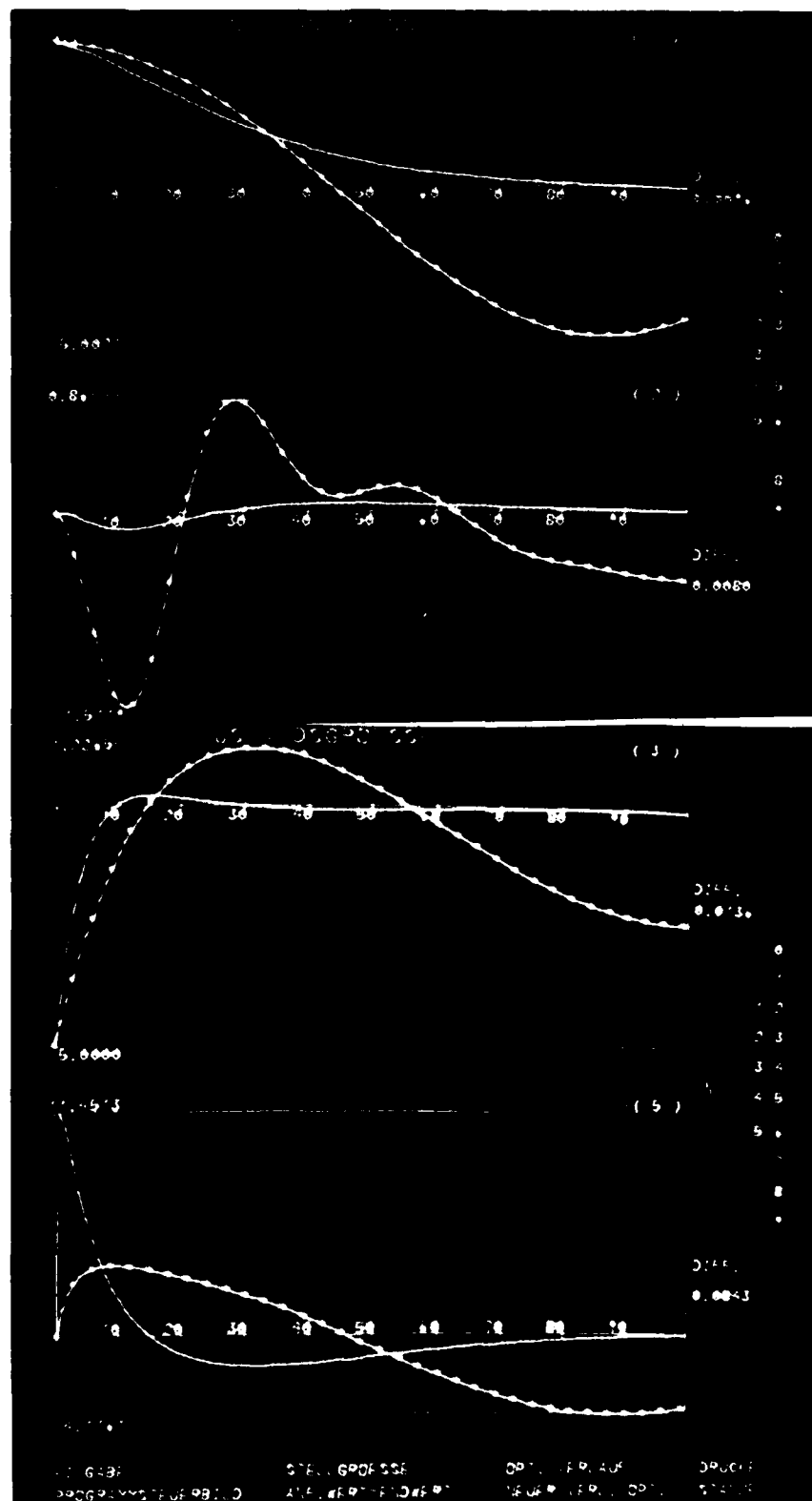
LAMBDA
ALPHA
SCHRITTZAHL
SCHRITTWEITE
MODEL - INPUT UN
INTES - SCHRITTWEITE

*** PRINT ***
*** RECHNEN ***
*** STEUERBILD ***

FP / GP / FN / GN FEHLEN

Picture 13

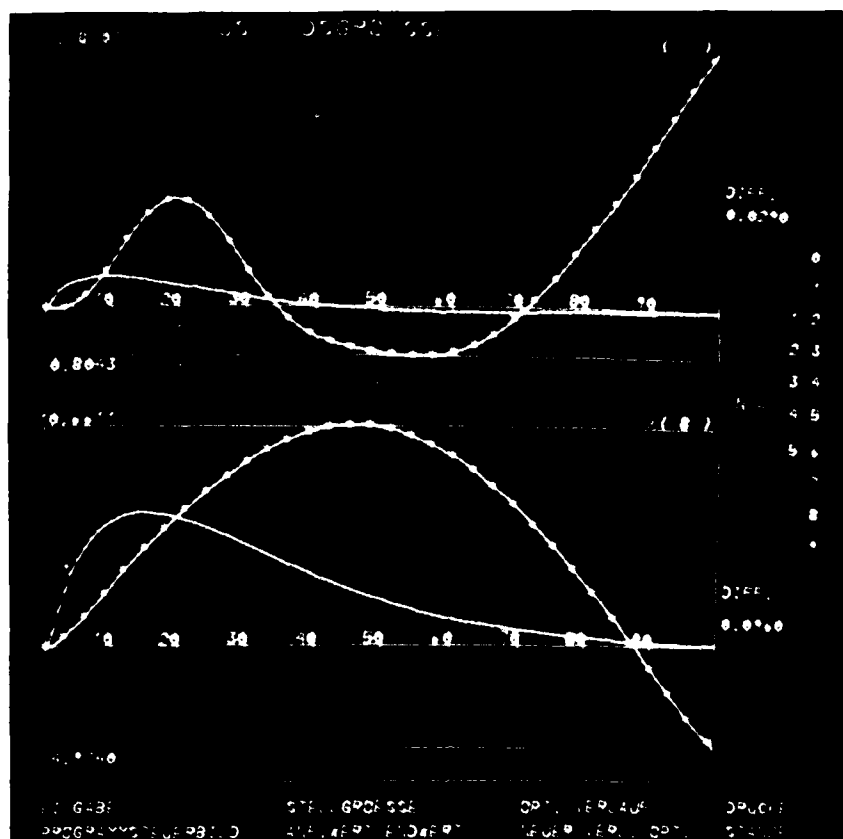
State Variable



input control variable opt. trajectory print
 progr. control pict. initial=final value new traj. optimal punch

Picture 16: B0 105 Discrete Optimal Control

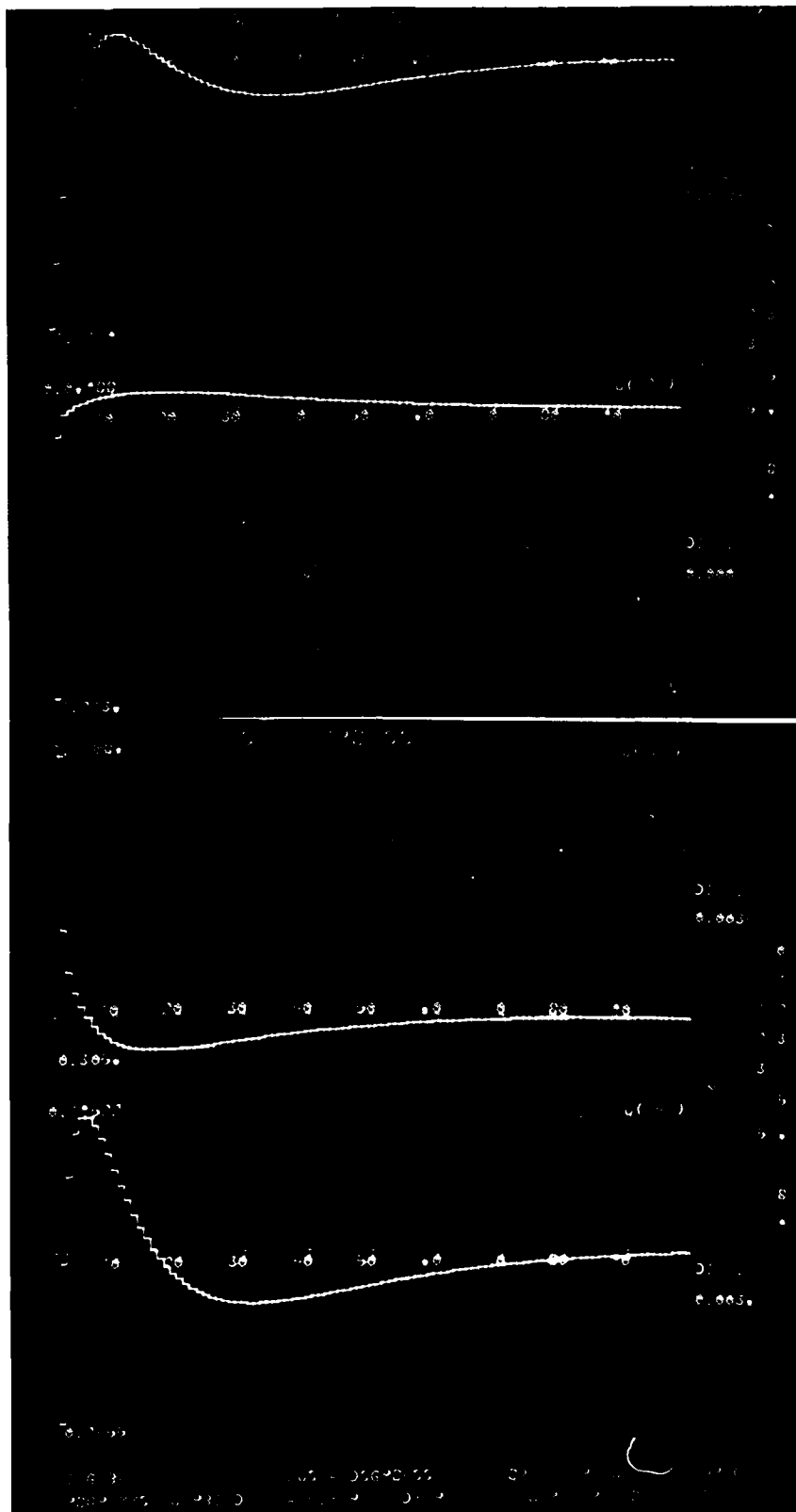
State Variable



input	control variable	opt. trajectory	print
progr. control pict.	initial=final value	new traj. optimal	punch

Picture 17: B0 105 Discrete Optimal Control

Control Variable



input	state variable	opt. trajectory	print
prog. control pict.	initial=final value	new traj. optimal	punch

Picture 18: B0 105 Discrete Optimal Control

THE USE OF ADVANCED COMPUTER TECHNIQUES IN FLIGHT TEST EVALUATIONS

by
Captain David P. Maunder

and
Mr. Robert E. Lee
6510 Test Wing/TEEEP
Air Force Flight Test Center (AFFTC)
Edwards AFB, California 93523

ABSTRACT

Advances in technology have completely restructured the flight test process. There have been marked improvements in test aircraft data acquisition systems, telemetry systems, test range capabilities, and data processing systems. Computers have played the major role in many of these advances.

The past decade has seen explosive growth in the capability to monitor and control flight testing. Much of this increase in capability stems from widespread use of digital computers to assimilate enormous quantities of data and quickly display results to the test team. Ground-based computer systems now provide the capability of processing large amounts of flight test data in real time, and near real time analytical calculations are commonplace.

An essential accessory of the flight test engineer of the past was the two-foot slide rule. Today, the slide rule has been replaced by the calculator and on-line access to large scale computers for flight test data processing. Test techniques and computer software have been developed to determine mathematical models of aircraft behavior and to determine compliance with performance, flying qualities and control system specification requirements.

Advances in digital circuitry and applications of airborne digital computers have resulted in dramatic changes in airborne instrumentation as well as in production aircraft subsystems. The airborne computer is being employed as both a primary control system and as a powerful test tool.

This paper examines the uses of advanced computer techniques in flight test evaluations at the AFFTC. Uses of the computer for real time mission control, integrated systems development, flutter testing, and postflight data analysis are emphasized.

INTRODUCTION

The large scale use of the digital computer in flight test evaluations of aircraft systems and subsystems has progressed rapidly over the past decade. Indeed, in today's world of complex, sophisticated, high performance aircraft much in the way of the design and implementation of a test program is centered around the capabilities of the computer. During the earlier days of flight testing, data processing and analysis by hand computation was the rule. This complemented the manual nature of data gathering via stopwatch and hand recorded information. Even with more automated recording devices such as the oscillograph and time correlated photographic records of flight instruments, test data for processing by a computer was, to a large extent, input manually. It remained for the development of high speed digital recording techniques to enable the flight test engineer to effectively utilize the tremendous mathematical processing capabilities of the computer.

The advent of Large Scale Integrated Circuitry and the microprocessor led to the development of lightweight, compact, flight-qualified data recording systems capable of recording hundreds of measurements at high sample rates. With this development, the data analyst was provided with an overwhelming quantity of data but not always with the necessary computational tools to analyze it efficiently. Test results were often analyzed utilizing only a fraction of the data available. A great deal of effort has been expended over the past decade in developing test techniques and analytical software to advance the state of the art in flight test evaluations. This development process continues today and the AFFTC employs state of the art computer techniques on all major test programs.

Today computers are found in a wide range of applications at the AFFTC: in ground tests, engineering simulations, preflight checkouts, airborne mission control, postflight and second generation data processing and analysis, and onboard the test aircraft as a tool for developing and evaluating new applications of digital technology in aircraft subsystems. This paper presents a broad overview of some of the present and planned applications of the computer in the developmental test and evaluation process at the AFFTC.

REAL TIME MISSION CONTROL

The key elements of a real time mission control capability are the airborne telemetry system, an extensive test range net linked via a microwave system, a ground-based computer system capable of processing large quantities of data, and displays which present critical information to the test engineer. Data from a variety of airborne and range instrumentation sources are now available at the AFFTC. This capability makes it practical to use

real time data for reasons other than safety-of-flight. Systems are now in use which markedly increase the efficiency of the test process. These improvements are brought about by real time answer-oriented software which allows an immediate assessment of significant test results (reference 1).

Real time answers are a necessity to accomplish a program safely in a reasonable time, especially for testing high performance aircraft where rapid decision-response time is critical and flight time is at a premium. An additional benefit of having answers at the conclusion of the flight is the enhanced interpretation of results during the postflight debrief when the events of the flight are fresh in the minds of the flightcrew and engineers. Final analysis is expedited when much of the data manipulation and working plot generation are accomplished during and immediately following the flight. Real time applications currently in use to support various test disciplines at the AFFTC are summarized below. A detailed functional description of the AFFTC system may be found in reference 2.

Avionic Systems Testing:

A unique and complex application of the real time system was used to evaluate the B-1 in the terrain following environment (reference 3). The test engineer was provided with displays showing the terrain profile of a test course at Edwards AFB and the aircraft flight profile above that course, as well as deviation from predictions. This application merges onboard telemetry data with range data from a number of sources. The flight test range space positioning and onboard navigation and control systems data are merged in the central computer to provide real time results. This analysis package is being expanded and additional test range instrumentation has been installed to support terrain following tests of the air launched cruise missile.

Flutter:

Flutter test engineers have been analyzing time histories of data for many years by using analog techniques during postflight analysis sessions. In flight analysis was often limited to strip chart recorder observations. Often the aircraft was equipped with an excitation system, and frequency sweeps were conducted to identify modal frequencies. The sweeps were followed by multiple frequency dwell/quick stop points to obtain damping. This method was often time consuming. If pilot induced control surface impulses were used, it was not uncommon for the engineer to observe a record in which closely spaced modes made it impossible to determine the modal characteristics of the single modes in real time.

The potential for flutter analysis capability in near real time resulted from the availability of spectral analyzers which used minicomputer technology to perform the fast Fourier transform. For the first time, flight test engineers had access to a dedicated system which could be used to make accurate real time analyses.

In 1972 the AFFTC acquired, and has subsequently developed a real time flutter analysis system (reference 4). A minicomputer-based time series analyzer and the associated analysis software are the heart of the system, which is used to apply digital time series analysis techniques to structural response data.

The AFFTC flutter test capability is designed to meet a broad range of requirements and is applicable during the testing of most types of aircraft. Further, since onboard excitation systems may or may not be installed, the system has an analysis capability for those cases where the input forcing function may not be measurable. Current test vehicles utilizing the AFFTC flutter facility span a range from the small air launched cruise missile to the KC-135 winglet test aircraft.

Aircraft Performance:

Achieving high quality airplane performance test results requires close attention to accurate engine thrust determination procedures, proper bookkeeping of secondary thrust and drags, incorporation of data from supporting wind tunnel and engine tests, accurate instrumentation, and the use of special maneuver techniques. These ingredients have been meshed together and are used with real time dynamic performance techniques to generate lift and drag with a significant reduction in test time. The methodology has proven particularly useful in obtaining drag at maneuvering lift conditions and at supersonic speeds where it is now possible to obtain data over a sufficiently large lift range to develop polar and lift curve slopes. Turnaround of final data is expedited for performance testing with much of the time-consuming data manipulations accomplished in real time. Real time analysis was utilized extensively during the F-16 and B-1 flight test programs.

Propulsion:

Real time techniques have been developed to achieve peak aircraft performance at maximum Mach number conditions by examining engine gas generator characteristics, inlet performance and variable inlet positions and manually changing variable geometry inlet positions to achieve desired performance. Variable geometry inlet schedule optimization testing is accomplished by monitoring critical inlet parameters. Engine performance is available in real time to expedite engine as well as airplane evaluation requirements.

Stability and Control:

Test techniques and real time software have been developed to determine compliance with flying qualities and control system specification requirements. Examples include

the calculation of damping ratios, maneuvering gradient crossplots, and roll performance parameters such as roll time constant and peak roll rates.

DATA ANALYSIS

There is a computer adage that states that computational requirements will expand to utilize the available capabilities. This has proven to be true in the area of flight test data analysis. The tremendous speed of the computer, coupled with the increased data acquisition capabilities have led to rapid delivery of classical test information and never-before-available analysis tools which are used in parameter identification applications, statistical analyses, power spectral density calculations, and for the evaluation of aerodynamic cross coupling, stall/spin characteristics, compressor face distortion characteristics and for dynamic performance analysis.

In recent years emphasis has been given to the increased use of modeling to define flight vehicle characteristics. This type of analysis employs the use of dynamic test maneuvers to generate the test data over a broad range of problem variables (model parameters) thus increasing the amount of data obtained at a particular point in the sky. The advantages and benefits of developing a mathematical description of an air vehicle's characteristics have long been recognized by the flight test community. They include:

1. Improved verification of performance criteria.
2. Improved dependability of estimating flight characteristics at untested flight conditions.
3. Enhanced system development and optimization of vehicle performance.
4. More accurately represented engineering and operational simulators, and
5. The reduction of the amount of flight test time required to adequately assess the flight characteristics of an air vehicle.

In some areas of testing, it is becoming recognized that this type of approach is the only practical way to obtain analytical results. This is particularly true in the analysis of complex systems with large numbers of variables. For example, optimizing the integration of a fire control system into the flight control system on the upcoming Advanced Fighter Technology Integrator F-16 (AFTI-16) test program will require the computer aided identification of numerous transfer functions from among the many flight vehicle and control system variables.

Several of the advanced computer oriented analysis tools currently in use and/or under development at the AFFTC are outlined below.

Parameter Identification:

Parameter identification is a discipline that provides tools for the efficient use of data in the estimation of constants appearing in mathematical models of physical phenomena. In general, model parameters may relate to aerodynamic, structural, performance, or other types of characteristics. The particular parameter identification technique which has been widely used at the AFFTC is the Modified Maximum Likelihood Estimator (MMLE). MMLE is a digital computer program which estimates the coefficients of a set of differential equations describing a dynamic system from recorded observations of its dynamic motion. Our experience with this method has been restricted to identification of aerodynamic parameters for linear mathematical models (reference 5).

Over the past several years this method had been applied on nine major test programs; X-24B, YF-16, YF-17, A-10, YC-14, YC-15, F-15, F-16 and B-1. The uniqueness of application at the AFFTC has been in its use as a primary analysis tool for developmental flight testing. The AFFTC has processed more than 1500 maneuvers using parameter identification techniques. Our successes have included the reduction and optimization of flight test requirements, improvement in our ability to verify performance criteria, enhanced system development and optimization of vehicle performance, and improvement in the dependability of measured flight characteristics which has also led to more accurately represented simulations. We are committed to the continued use and development of parameter identification techniques, and expect further improvements in flight testing will occur with the development of nonlinear model identification programs and broader applications.

Mission-Oriented Test Techniques:

New pilot-in-the-loop handling qualities test and evaluation techniques are in the development process at the AFFTC. These techniques are called System Identification From Tracking (SIFT) test techniques. Pilot-in-the-loop test data are obtained during precision tracking maneuvers using specially developed piloting techniques (references 6). From these data, flight control system transfer functions, aerodynamic transfer functions, and overall system transfer functions (aerodynamics plus flight control system) are identified using time series analysis computer software. These quantitative results are correlated with qualitative pilot ratings and comments to provide unique insights into pilot-in-the-loop handling qualities.

The SIFT techniques have been shown to be an effective tool for testing and evaluating pilot-in-the-loop handling qualities. These techniques were used during an evaluation of

a variable stability F-4C aircraft to demonstrate the existence of a previously unsuspected coupling from the lateral-directional axes into the pitch axis and to analyze data obtained during pilot-induced oscillations (PIO). Based on our present experience, quantitative results of the precision tracking data analysis correlate well with the qualitative pilot comments and ratings. This capability to directly correlate quantitative and qualitative results from the same test maneuver is a significant advantage of the SIFT techniques over traditional open-loop techniques.

The AFFTC is continuing the development of the SIFT test and evaluation techniques and is investigating their versatility as a flight test tool. These techniques will be expanded to support integrated flight/fire control system testing.

Dynamic Test Techniques:

A research program is underway at the AFFTC to further refine dynamic test techniques. The program acronym is DyMoTech, which stands for Dynamic Modeling Technique. The overall objective of DyMoTech is to develop dynamic flight test techniques as a potentially powerful tool for defining the performance characteristics of aircraft. Included under this is the objective to demonstrate the dynamic test techniques' ability to generate accurate aircraft performance compared with the results of conventional flight test techniques. The other major objectives are to define related airborne instrumentation system requirements and calibration and analysis procedures for dynamic maneuvers and to develop performance models and investigate improved modeling techniques including nonlinear parameter identification (reference 7).

Batch Processed Simulation:

Recently we have implemented a computer program at the AFFTC which provides quick access to a six degrees of freedom, nonlinear simulation capability. The program is structured similar to several real time simulation computer languages in that the user constructs a model by specifying component blocks and their interconnections. Standard components are available for aircraft equations of motion and most common flight control components. A great deal of flexibility is provided for entering aerodynamic data and in modeling nonlinear components. The program is engineer rather than programmer oriented so that a complete model may be formulated without the extensive setup time required for most simulations.

In addition to providing a nonreal time engineering simulation, the program can perform classical frequency domain analysis. This program is being used extensively to assess predicted flight characteristics, as an aid in modeling and analyzing nonlinear flight characteristics, to evaluate proposed flight control system changes, and even to generate simulated flight test data to check out other data analysis software. Current test program applications include evaluating cruise missile performance during terrain following flight and assessing the validity of simulator data for the B-52/KC-135 Weapon System Trainer.

System and Human Factors Analyses:

In addition to those analysis tools already mentioned, software programs have been developed at the AFFTC to:

1. Analyze ballistic trajectories from weapon delivery tests. Data from cinetheodolite trackers, gunsight camera and aircraft sensors are merged to analyze accuracy of the weapons delivery system and identify systematic errors from subsystem components.
2. Compile statistical records of maintenance actions for reliability and maintainability analysis and prediction of maintenance related life cycle costs.
3. Analyze and simulate lead computing optical sight performance to predict the accuracy and effectiveness of the aircraft/gun combination in air to air and air to ground roles.
4. Perform statistical analysis of such human responses as heartrate, eye movement, respiration, and skin response in order to quantify pilot workload during task oriented test maneuvers.

Interactive Graphics:

In most modeling problems the attainment of an optimum solution requires an iterative procedure between the human operator and the computer. This can be very time consuming when intermediate results must be hand manipulated. Generally, analytical results are most useful in a graphical form. The whole modeling process can be significantly speeded up if the computer is used to transform the data from the matrix of numbers it requires to the more useful pictorial form the human understands (and vice versa).

Within the past several years, a number of economical, "smart" graphics oriented computer terminals have appeared on the market. The AFFTC is presently in the process of integrating several graphics oriented terminals into our computer network. Some of these have significant offline computation and display capabilities. Already we are seeing significant reductions in manipulation of graphical data and we have only begun to utilize the full potential computer graphics has to offer for increasing the efficiency of communication between the engineer and the computer. Use of interactive graphics on a routine basis

promises to significantly improve the effectiveness of our present modeling techniques as well as hastening the introduction of new techniques as they become available

AIRCRAFT SUBSYSTEM DESIGN AND EVALUATION TRENDS

Advances in digital circuit technology are changing the character of aircraft subsystem design which will, in turn, have a major impact on the flight test process. The application of digital circuitry and programmable firmware to aircraft subsystems continues to increase. Some current and future applications to production subsystems and for special test purposes are described below (reference 8).

Displays:

The ability to solve complex problems in near real time and to generate symbology have allowed the development of highly sophisticated airborne standard dials and tapes which are providing information never before available to the pilot. The programmability of these computers allows the testing of a wide range of display variables before committing them to production software. Applications include flight directors, fire control/weapons delivery systems, and energy management systems.

Control Systems/Variable Stability:

The computer is being employed as both a primary control system and as augmentation to provide variable stability for aircraft. In both cases, the ability to replace hardware with programmable software allows the relatively easy evaluation of control laws and aircraft handling qualities. The variable stability concept can be combined with the display systems previously discussed to provide a powerful design and evaluation tool. Another combination is the airborne computer with a groundbased computer to provide remotely augmented capability for remotely piloted vehicles. In this application, the onboard computer acts as a system monitor, determining the validity of the signals received from the ground and as a backup control system in case of signal failure. This type of system is currently employed on the HiMAT (Highly Maneuverable Aircraft Technology) demonstrator test vehicle.

Integrated Flight/Fire Control Systems:

The potential benefits of subsystem digital integration are especially evident in the integrated flight/fire control system area. This integration consists of blending information from the fire control system with pilot inputs to the flight control system. The blending covers a spectrum from a manual weapon delivery mode to an automatic mode. In the latter case, the aircraft is controlled entirely by commands from the fire control system, within the authority of the flight control system. A high authority, redundant flight control system can be tailored to meet the varied requirements of different mission flight phases. It is evident that for such integrated systems, evaluation of the fire control and flight control systems must be accomplished concurrently.

The complex and interrelated performance characteristics of such a sophisticated system will require a parametric optimization that is too extensive to be accomplished solely through flight test. The practical solution for systems of this type is a flight test program complemented by an on-the-scene subsystem integration facility. The AFFTC plans to construct an integration facility to complement flight testing of digitally integrated subsystems. Avionics subsystem component development and integration involves several levels of simulation supplemented by flight tests, and the facility will support the total effort. Preliminary estimates indicate that use of the avionics integration facility will permit a reduction of in flight testing of future avionics systems of 30 percent, a considerable savings in time and resources.

Propulsion:

The use of digital fuel control systems will permit greater flexibility in determining airframe/propulsion interactions and in matching test data variables in flight to those obtained in ground based facilities. This eliminates the interpolation of results to match these two data sets. Digital engine fuel controls make it possible to greatly improve engine performance and enhance certain types of flight tests. As an example, software can be generated which will allow parameters such as fuel flow to be maintained constant during a maneuver, eliminating it as a variable.

FLIGHT TRAINING SIMULATOR DEVELOPMENT TESTING

Recent concerns over the resources required for flight training and the availability of petroleum have prompted the Air Force to look for a reduction in flying hours through the increased use of simulators for training and proficiency. The AFFTC became involved in the simulator effort to assist Using Commands and procuring agencies in developing and verifying the accuracy of their training simulators.

In the next several years, numerous (over a dozen identified to date) new simulators or major simulator modifications are planned. Some of these simulators will be major systems and will require a level of effort equivalent in some respects to that of a new aircraft development. As an illustration, two contractors are currently building prototypes of a B-52/KC-135 mission simulator and a competitive "flyoff" will be conducted.

The training simulator development and test activity is a logical extension of flight test disciplines in the areas of performance, flying qualities, systems, and human factors.

The AFFTC will assist in the development and verification of the simulator performance and flying qualities mathematical models as well as evaluating controls and displays.

Engineering simulators have long been a valuable adjunct to flight test programs. Because of the increase of initial developmental testing at the AFFTC, the availability of onsite piloted simulators for flight test envelope expansion and flight control system development has become a necessity. To meet the demands of future flight test programs, as well as the training simulator test requirements mentioned above, the AFFTC test simulator facility is being expanded and upgraded to an all-digital capability. The completed facility will be capable of supporting several test programs concurrently.

CONCLUSION

This paper has attempted to overview the numerous ways in which the computer is used as an aid in flight test evaluations. The computer has become an indispensable requirement in nearly all aspects of a test program. The driving factors have been the desire for a more complete analysis resulting ultimately in a better system for the user and in a reduction in the total cost of the developmental test and evaluation cycle through a reduction in program flight hours. Computers are aiding us significantly in achieving these goals.

REFERENCES

1. Adolph, C.E., "Flight Testing at the Air Force Flight Test Center: Yesterday, Today and Tomorrow", Proceedings of the Society of Flight Test Engineers Ninth Annual Symposium, Arlington, Texas, October 1978.
2. Johnson, C.O., and Sehnert, P.J., "The Automated Flight Test Data System", Paper 25, AGARD Symposium on Flight Test Techniques, AGARD-CP-223, Porz Wahn, Germany, October 1976.
3. Brinkley, C.W., Sharp, P.S., and Abrams, R., "B-1 Terrain Following", Proceedings of the Society of Flight Test Engineers Eighth Annual Symposium, Washington, D.C., August 1977.
4. Lenz, R.W., and McKeever, B., "Time Series Analysis in Flight Flutter Testing at the Air Force Flight Test Center: Concepts and Results", Paper 12, Flutter Testing Techniques Conference, NASA SP-415, Dryden Flight Research Center, Edwards, California, October 1975.
5. Maunder, D.P., "AFFTC Parameter Identification Experience", Paper to be presented to the AIAA Systems and Technology Meeting, New York, New York, 20-22 Aug 79.
6. Twisdale, T.T., and Ashhurst, T.A., "System Identification from Tracking, a New Technique for Handling Qualities Test and Evaluation (Initial Report)", AFFTC-TR-77-27, November 1977.
7. Hicks, J.W., Plews, L.D., and Rawlings, K., "Flight Test Technology Development: A Preview of DyMoTech", Proceedings of the Society of Flight Test Engineers Ninth Annual Symposium, Arlington, Texas, October 1978.
8. Lucero, F.N., and Adolph, C.E., "Overall Aircraft Systems Evaluation, Paper 14, AGARD Symposium on Flight Test Techniques, AGARD-CP-223, Porz Wahn, Germany, October 1976.

REPORT DOCUMENTATION PAGE

1. Recipient's Reference	2. Originator's Reference AGARD-CP-280	3. Further Reference ISBN 92-835-0256-6	4. Security Classification of Document UNCLASSIFIED
5. Originator Advisory Group for Aerospace Research and Development North Atlantic Treaty Organization 7 rue Ancelle, 92200 Neuilly sur Seine, France			
6. Title THE USE OF COMPUTERS AS A DESIGN TOOL			
7. Presented at the Flight Mechanics Panel Symposium on The Use of Computers as a Design Tool, held in Neubiberg, Germany, 3-6 September 1979.			
8. Author(s)/Editor(s) Various			9. Date January 1980
10. Author's/Editor's Address Various			11. Pages 460
12. Distribution Statement This document is distributed in accordance with AGARD policies and regulations, which are outlined on the Outside Back Cover of all AGARD publications.			
13. Keywords/Descriptors <div style="display: flex; justify-content: space-between;"> <div> Computer aided design Aerodynamics Structural analysis </div> <div> Aircraft engines Design Computers </div> </div>			
14. Abstract ↓ The proceedings consist of the papers presented at the FMP Symposium on "The Use of Computers as a Design Tool". Sessions were held on the topics of: specifications and assessments of requirements, computer-aided design and computer graphics, computational aerodynamics and design, structural analysis and design, propulsion and systems design. A comprehensive Technical Evaluation of the meeting appears in AGARD Advisory Report No.158.			

<p>AGARD Conference Proceedings No.280 Advisory Group for Aerospace Research and Development, NATO THE USE OF COMPUTERS AS A DESIGN TOOL Published January 1980 460 pages</p> <p>The proceedings consist of the papers presented at the FMP Symposium on "The Use of Computers as a Design Tool". Sessions were held on the topics of: specifications and assessments of requirements, computer-aided design and computer graphics, computational aerodynamics and design, structural analysis and design, propulsion and systems design. A comprehensive Technical Evaluation of the meeting appears in AGARD Advisory Report No.158.</p> <p>P.T.O.</p>	<p>AGARD-CP-280</p> <p>Computer aided design Aerodynamics Structural analysis Aircraft engines Design Computers</p>	<p>AGARD Conference Proceedings No.280 Advisory "Group for Aerospace Research and Development, NATO THE USE OF COMPUTERS AS A DESIGN TOOL Published January 1980 460 pages</p> <p>The proceedings consist of the papers presented at the FMP Symposium on "The Use of Computers as a Design Tool". Sessions were held on the topics of: specifications and assessments of requirements, computer-aided design and computer graphics, computational aerodynamics and design, structural analysis and design, propulsion and systems design. A comprehensive Technical Evaluation of the meeting appears in AGARD Advisory Report No.158.</p> <p>P.T.O.</p>	<p>AGARD-CP-280</p> <p>Computer aided design Aerodynamics Structural analysis Aircraft engines Design Computers</p>
<p>AGARD Conference Proceedings No.280 Advisory Group for Aerospace Research and Development, NATO THE USE OF COMPUTERS AS A DESIGN TOOL Published January 1980 460 pages</p> <p>The proceedings consist of the papers presented at the FMP Symposium on "The Use of Computers as a Design Tool". Sessions were held on the topics of: specifications and assessments of requirements, computer-aided design and computer graphics, computational aerodynamics and design, structural analysis and design, propulsion and systems design. A comprehensive Technical Evaluation of the meeting appears in AGARD Advisory Report No.158.</p> <p>P.T.O.</p>	<p>AGARD-CP-280</p> <p>Computer aided design Aerodynamics Structural analysis Aircraft engines Design Computers</p>	<p>AGARD Conference Proceedings No.280 Advisory Group for Aerospace Research and Development, NATO THE USE OF COMPUTERS AS A DESIGN TOOL Published January 1980 460 pages</p> <p>The proceedings consist of the papers presented at the FMP Symposium on "The Use of Computers as a Design Tool". Sessions were held on the topics of: specifications and assessments of requirements, computer-aided design and computer graphics, computational aerodynamics and design, structural analysis and design, propulsion and systems design. A comprehensive Technical Evaluation of the meeting appears in AGARD Advisory Report No.158.</p> <p>P.T.O.</p>	<p>AGARD-CP-280</p> <p>Computer aided design Aerodynamics Structural analysis Aircraft engines Design Computers</p>

<p>Papers presented at the Flight Mechanics Panel Symposium on The Use of Computers as a Design Tool, held in Neubiberg, Germany, 3-6 September 1979.</p> <p>ISBN 92-835-0256-6</p>	<p>Papers presented at the Flight Mechanics Panel Symposium on The Use of Computers as a Design Tool, held in Neubiberg, Germany, 3-6 September 1979.</p> <p>ISBN 92-835-0256-6</p>
<p>Papers presented at the Flight Mechanics Panel Symposium on The Use of Computers as a Design Tool, held in Neubiberg, Germany, 3-6 September 1979.</p> <p>ISBN 92-835-0256-6</p>	<p>Papers presented at the Flight Mechanics Panel Symposium on The Use of Computers as a Design Tool, held in Neubiberg, Germany, 3-6 September 1979.</p> <p>ISBN 92-835-0256-6</p>

B793
4

AGARD

NATO  OTAN

7 RUE ANCELLE · 92200 NEUILLY-SUR-SEINE
FRANCE

Telephone 745.08.10 · Telex 610176

**DISTRIBUTION OF UNCLASSIFIED
AGARD PUBLICATIONS**

AGARD does NOT hold stocks of AGARD publications at the above address for general distribution. Initial distribution of AGARD publications is made to AGARD Member Nations through the following National Distribution Centres. Further copies are sometimes available from these Centres, but if not may be purchased in Microfiche or Photocopy form from the Purchase Agencies listed below.

NATIONAL DISTRIBUTION CENTRES

BELGIUM

Coordonnateur AGARD - VSL
Etat-Major de la Force Aérienne
Quartier Reine Elisabeth
Rue d'Evere, 1140 Bruxelles

CANADA

Defence Science Information Services
Department of National Defence
Ottawa, Ontario K1A 0K2

DENMARK

Danish Defence Research Board
Østerbrogades Kaserne
Copenhagen Ø

FRANCE

O.N.E.R.A. (Direction)
29 Avenue de la Division Leclerc
92320 Châtillon sous Bagneux

GERMANY

Zentralstelle für Luft- und Raumfahrt-
dokumentation und -information
c/o Fachinformationzentrum Energie,
Physik, Mathematik GmbH
Kernforschungszentrum
7514 Eggenstein-Leopoldshafen 2

GREECE

Hellenic Air Force General Staff
Research and Development Directorate
Holargos, Athens

ICELAND

Director of Aviation
c/o Flugrad
Reykjavik

ITALY

Aeronautica Militare
Ufficio del Delegato Nazionale all'AGARD
3, Piazzale Adenauer
Roma/EUR

LUXEMBOURG

See Belgium

NETHERLANDS

Netherlands Delegation to AGARD
National Aerospace Laboratory, NLR
P.O. Box 126
2600 A.C. Delft

NORWAY

Norwegian Defence Research Establishment
Main Library
P.O. Box 25
N-2007 Kjeller

PORTUGAL

Direcção do Serviço de Material
da Força Aérea
Rua da Escola Politécnica 42
Lisboa
Attn: AGARD National Delegate

TURKEY

Department of Research and Development (ARGE)
Ministry of National Defence, Ankara

UNITED KINGDOM

Defence Research Information Centre
Station Square House
St. Mary Cray
Orpington, Kent BR5 3RE

UNITED STATES

National Aeronautics and Space Administration (NASA)
Langley Field, Virginia 23365
Attn: Report Distribution and Storage Unit

**THE UNITED STATES NATIONAL DISTRIBUTION CENTRE (NASA) DOES NOT HOLD
STOCKS OF AGARD PUBLICATIONS, AND APPLICATIONS FOR COPIES SHOULD BE MADE
DIRECT TO THE NATIONAL TECHNICAL INFORMATION SERVICE (NTIS) AT THE ADDRESS BELOW.**

PURCHASE AGENCIES

Microfiche or Photocopy

National Technical
Information Service (NTIS)
5285 Port Royal Road
Springfield
Virginia 22161, USA

Microfiche

Space Documentation Service
European Space Agency
10, rue Mario Nikis
75015 Paris, France

Microfiche

Technology Reports
Centre (DTI)
Station Square House
St. Mary Cray
Orpington, Kent BR5 3RF
England

Requests for microfiche or photocopies of AGARD documents should include the AGARD serial number, title, author or editor, and publication date. Requests to NTIS should include the NASA accession report number. Full bibliographical references and abstracts of AGARD publications are given in the following journals:

Scientific and Technical Aerospace Reports (STAR)
published by NASA Scientific and Technical
Information Facility
Post Office Box 8757
Baltimore/Washington International Airport
Maryland 21240; USA

Government Reports Announcements (GRA)
published by the National Technical
Information Services, Springfield
Virginia 22161, USA